Investigating the Role of Oncogenic KRAS G12 Mutations in Cell Signalling

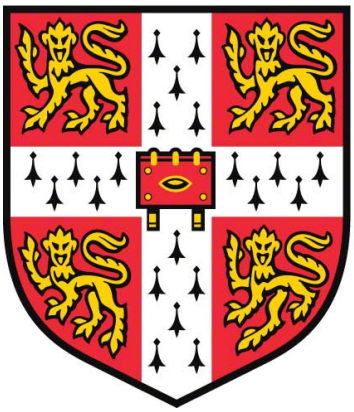

Khushali Patel

Murray Edwards College

University of Cambridge

May 2021

This thesis is submitted for the degree of Doctor of Philosophy

DECLARATION

This thesis is the result of my own work and includes nothing which is the outcome of work done in collaboration except as declared in the preface and specified in the text. It is not substantially the same as any work that has already been submitted before for any degree or other qualification except as declared in the preface and specified in the text. It does not exceed the prescribed word limit of 60,000 words for the School of Clinical Medicine Degree Committee.

Investigating the Role of Oncogenic KRAS G12 Mutations in Cell Signalling

Khushali Patel

Abstract

Cancer is a multistep process reflecting genetic alterations that drive progressive transformation of normal cells into highly proliferative malignant cells. Deregulation of cellular signalling is one of the key traits in cancer, allowing cells to breach anticancer defence mechanisms. The most frequently mutated oncogene in cancer is *KRAS,* encoding a small GTPase protein involved in controlling the activity of critical signalling pathways that regulate normal cellular proliferation, such as the PI3K and ERK pathways. The prevalence of different codon substitutions in the *KRAS* gene varies in different tissues. There is emerging evidence supporting the notion that different codon substitutions may trigger different biological effects. We hypothesise that different codon substitutions in KRAS can trigger different feedbacks and signalling dynamics that may result in varying fitness advantages in different tissues.

I use quantitative Western blotting and Modular Response Analysis with KRAS isogenic cell lines to characterise how KRAS substitutions at codon G12 perturb the topology and dynamics of the ERK signalling network as a first step to test this hypothesis. My work has identified two mutant-specific interactions in the ERK pathway: a MEK to RAF inhibition seen strongest in G12A, G12C and G12D cells, and a RAF to ERK activation (or loss of inhibition) seen in all mutants compared to WT. Antibody array data suggests the potential role of JNK and TYK2 in mediating these interactions, respectively, and thus my work has provided preliminary, albeit testable, hypotheses for elucidating the possible mechanisms responsible for this rewiring of the ERK pathway. My work has also identified the presence of a second BRAF form present only in the mutants with the strongest MEK to RAF inhibition. It appears this KRAS-mutant specific BRAF form is most likely a splice variant that has enhanced dimerisation capabilities with CRAF. RAF dimerisation is one mechanism via which RAF inhibitors fail to be effective in treating KRAS-mutant cancers. This exemplifies the importance of characterising the identity and role of this BRAF form, as it may have implications on development of mutant-specific therapies for KRAS-driven cancers.

ERK pathway activation can also regulate the transcription of many downstream targets. I have attempted to characterise KRAS-dependent gene expression changes with RNA sequencing data, with the aim of understanding key differences between mutant and WT KRAS cells and to also understand how the gene expression profiles change over time during the very early steps in oncogenesis. Preliminary data suggests mutant-specific differential gene transcription that may be linked to the RAF inhibition via MEK and/or the second BRAF form. My work currently does not explain the specific mechanisms behind the interactions identified with MRA, however, it does lay down the foundation and provides hypotheses that can be tested in the lab. Gaining mechanistic insight into the pathogenicity of cancer driver mutations and their differential role in different tissues is of fundamental importance to understand how different mutations shape the evolution of cancer clones during carcinogenesis and to design optimal targeted therapeutic strategies.

ACKNOWLEDGEMENTS

I would like to express my very sincere gratitude to Dr Alessandro Esposito for giving me the opportunity to complete this PhD under his guidance. He has been the most supportive, inspiring and understanding supervisor I could have asked for. I would also like to thank the members of both the Esposito and Venkitaraman labs for their friendship and support over the last 3.5 years. Special thanks to Suzan for being my first teacher in the lab and for all the support and help you have given me. Annie and Pablo – you guys have been such great friends and I'm going to miss you! I would also like a give a special thanks to Dr Ben Hall, who took me under his guidance during the first lockdown and has always been an incredible supervisor. I have learnt a great deal from both Ale and Ben, and I am grateful to have had such kind and inspiring supervisors.

I would like to thank mum, dad and Anmol for always believing in me and encouraging me. Mum, thank you for all the sacrifices you make and for always encouraging me. I am here because of you. Anmol, you are literally the best brother I could have ever asked for. You have always been there for me and I will forever be grateful for that. Dad, thank you for always supporting me. Lastly, I would like to thank Murray Edwards College for their support and the Medical Research Council for funding my PhD and providing me with this invaluable experience.

TABLE OF CONTENTS

LIST OF ABBREVIATIONS

Abbreviation	Definition
AP-1	Activating protein 1
ARF	ADP-ribosylation factor
ATF-2	Activating transcription factor 2
BAD	BCL2-antagonist of death
bFGF	Basic fibroblast growth factor
cAMP	Cyclic adenosine monophosphate
CD	Common docking
CDC42	Cell division control protein homolog 42
CDK	Cyclin dependent kinase
CFC	Cardio-facio-cutaneous syndrome
CM-AVM	Capillary malformation-arteriovenous malformation syndrome
CRBN	Cereblon
CRC	Colorectal cancer
CRD	Cysteine rich domain
CREB	Cyclic adenosine monophosphate (camp) response element-binding protein
CS	Costello syndrome
CTLA4	Cytotoxic T lymphocyte protein 4
DAG	Diacylglycerol
DH	Dbl homology
DNA	Deoxyribonucleic acid
DUSP	Dual-specificity phosphatase
EGF	Epidermal growth factor
EGFR	Epidermal growth factor receptor
EH	Eps15 homology
EMT	Epithelial-mesenchymal transition
EPR	Electron paramagnetic resonance
ER	Endoplasmic reticulum
ERF	ETS2 repressor factor
ERK	Extracellular signal regulated kinase
ETS1	ERK1/2 responsive transcription factor
FAK	Focal adhesion kinase
FBXW7	F-box/WD repeat-containing protein 7
FOLFOX	Folinic acid, fluorouracil and oxaliplatin
FOXO1	Forkhead-related transcription factor
FRS2a	FGF receptor substrate 2a
Ftase	Farnesyltransferase
FTIs	Ftase inhibitors
GAP	Gtpase-activating protein
GDP	Guanosine-5'-diphosphate

GEF	Guanine nucleotide exchange factor
GGTase	Geranylgeranyltransferase
GM-CSF	Granulocyte-macrophage colony-stimulating factor
GPCR	G-protein-coupled receptor
GppNHp	Guanosine-5'-[β,γ-imido]triphosphate
GRB2	Growth factor receptor-bound protein 2
GSEA	Gene set enrichment analysis
GSK3	Glycogen synthase kinase 3
GTP	Guanosine-5'-triphosphate
HNSCC	Head and neck squamous cell carcinoma
HPC	High performance computing
HPNE	Human pancreatic nestin-expressing
HRAS	Harvey rat sarcoma viral oncogene homolog
HSP27	Heat shock protein 27
hTERT	Human telomerase
HVR	Hypervariable region
ICMT	Isoprenylcysteine carboxyl methyltransferase
IEG	Immediate early gene
IGF-1	Insulin-like growth factor-1
IL-2	Interleukin-2
IP3	Inositol 1,4,5 trisphosphate
IRS1	Insulin receptor substrate 1
ITCH	E3 ubiquitin-protein ligase Itchy homolog
JAK/STAT	Janus kinase and signal transducer and activator of transcription
JNK	C-Jun amino terminal kinase
KRAS	Kirsten rat sarcoma viral oncogene homolog
KSR	Kinase suppressor of RAS
LS	Legius syndrome
LSCC	Lung squamous cell carcinoma
MAPK	Mitogen-activated protein kinase
MAPKK	Mitogen activated protein kinase kinase
MAPKKK	Mitogen activated protein kinase kinase kinase
MD	Molecular dynamics
MEF	Myocyte enhancer factor
MEK	Mitogen activated protein kinase kinase
MK2	MAPK-activated protein kinase 2
MP-1	MEK1 partner 1
MTORC	Mammalian target of rapamycin
NES	Nuclear export signal
NF1	Neurofibromatosis type 1
NFA	Negative feedback amplifier
NFKB	Nuclear factor kappa B
NMR	Nuclear magnetic resonance

NRAS	Neuroblastoma RAS viral (v-ras) oncogene homolog
NS	Noonan syndrome
NSCLC	Non-small cell lung cancer
NSML	Noonan Syndrome with Multiple Lentigines
NUP50	Nucleoporin-50
P-loop	Phosphate binding loop
PARP1	Poly(ADP-ribose) polymerase-1
PC12	Phaeochromocytoma
PD1	Programmed cell death protein-1
PDAC	Pancreatic ductal adenocarcinoma
PDGF	Platelet-derived growth factor
PDGFR	Platelet-derived growth factor
PDK1	Phosphoinositide-dependent kinase 1
PDX	Patient derived xenograft
PH	Pleckstrin homology
PHPLL	PH domain Leucine-rich repeat protein phosphatase
PI3K	Phosphoinositide 3-kinase
PIK3CA	Phosphatidylinositol-4,5-bisphosphate 3-kinase catalytic subunit alpha
PIP2	Phosphatidylinositol-4,5-bisphosphate
PIP3	Phosphatidylinositol-3,4,5-triphosphate
PKB	Protein kinase B. Also known as AKT.
PKC	Protein kinase C
PLCε	Phospholipase Cε
PLCγ	Phospholipase Cγ
PRAS40	Proline rich Akt substrate of 40 kDa
PROTAC	Proteolysis targeting chimera
PTB	Phosphotyrosine binding
PTEN	Phosphatase and tensin homologue
PTM	Post-translational modification
PTPN11	Protein tyrosine phosphatase non-receptor type 11
RA	RAS-association
RAB	Ras-associated binding
RAC1	Rac Family Small gtpase 1
RAD	RAS association domain
RAF	Rapidly accelerated fibrosarcoma
RAL	Ras-like
RAL	RAS-like
RalBD	Ral-binding domain
RALBP1	RAL-binding protein 1
RALGDS	RAL-guanine nucleotide dissociation stimulator
RalGEF	RAL-specific guanine nucleotide exchange factor
RALGPS	RAL/PH/SH3-binding GEFs
RAN	Ras-related nuclear protein

RAP	Ras-related protein
RAS	Rat sarcoma virus
RASGAP	Ras gtpase activating protein
RBD	RAS-binding domain
RCE1	RAS-converting enzyme
REPS1	RALBP1-associated Eps homology (EH) domain protein 1
RGL	Ral GDP dissociation stimulator-like
RHEB	Ras homolog enriched in brain
RHO-GAP	RHO gtpase activating protein
RHO	Ras homologous
RHOA	Ras homolog family member A
RLF	Ralgds-like factor
RNA	Ribonucleic acid
ROK	Rho-dependent kinase
RSK2	Ribosomal s6 kinase 2
RTK	Receptor tyrosine kinase
SAP1A	Synapse-associated protein 1a
SH2	Src homology 2
SHC	Src homology 2 domain containing transforming protein
SHP2	SRC homology region 2 domain-containing phosphatase-2
siRNA	Small interfering RNA
SOS	Son of Sevenless
SPRED1	Sprouty related evh1 domain containing 1
TGFβ	Transforming growth factor beta
TILs	Tumour infiltrating lymphocytes
TNF	Tumour necrosis factor
TP53	Tumour protein p53
VEGF	Vascular endothelial growth factor
VEGFR2	VEGF receptor 2
VHL	Von Hippel-Lindau
WT	Wild type

LIST OF FIGURES

LIST OF SUPPLEMENTARY FIGURES

LIST OF TABLES

1. Introduction

1.1 Deregulation of signalling in cancer cells

Cancer is a complex disease, arising from the multistep process of acquiring mutations over time, resulting in the progressive transformation of normal human cells into malignant ones. In a seminal paper entitled "The Hallmarks of Cancer", Hanahan and Weinberg (2000) have reviewed the cellular and molecular phenotypes underlying cancer. One of those characteristics is the ability of malignant cancer cells to grow without stimulation from external growth signals (Moses *et al.*, 1978; Kaplan, Anderson and Ozanne, 1982). Indeed, non-transformed cells require mitogenic growth signals for committing to proliferation (Ham and Walthall, 1981; Leof *et al.*, 1982; Westermark and Heldin, 1985; Goustin *et al.*, 1986). In physiological conditions, cells depend on molecular cues from the tissue microenvironment to maintain tissue homeostasis by balancing cell death, proliferation and differentiation (Walker, Mojares and Del Río Hernández, 2018). Transformed cells, however, overcome the need for mitogenic growth factors leading to the irreversible loss of homeostatic control. In some tumours, cells acquire the capability to synthesise growth factors thus establishing a positive autocrine feedback signalling loop where cells secrete growth factors to which they will respond (Walsh *et al.*, 1991). Cancer cells can also overexpress membrane receptors allowing cells to be hyper-responsive to normal levels of growth factors (Li, Huang and Peng, 2005; Akhtar *et al.*, 2014; L. Wang *et al.*, 2017). Other mechanisms of signalling deregulation include the acquired insensitivity of cancer cells to anti-growth signals (Amin *et al.*, 2015), and also the ability of these cells to evade cell death via apoptosis (Fernald and Kurokawa, 2013). Cell signalling pathways not only control cell fate decisions including cell growth, motility and apoptosis, but can also play a part in changing the tumour microenvironment to further aid the progression of cancer development (Sever and Brugge, 2015).

Growth factor signalling deregulation is not the only phenomenon that offsets the homeostatic balance to favour the uncontrolled growth of cancer cells. For instance, it is well known that malignant cancer cells acquire a limitless ability to replicate (Gobinda and Bolander, 1995; Kelland, 2007), can induce and sustain the development of new blood vessels (angiogenesis) (Warren, 1966; Nishida *et al.*, 2006), and have the capability of invading surrounding tissue and metastasizing to other parts of the body (Fidler and Kripke, 1977; Fares *et al.*, 2020). In more recent years, the capability of cancer cells to also re-programme metabolic processes (Phan, Yeung and Lee, 2014), and to evade or even hijack immune cells to enable neoplastic proliferation has been established (Vinay *et al.*, 2015). Moreover, the tumour microenvironment has a crucial role as a complex ecosystem comprising

different cancer clones playing different roles interacting with stroma, a picture more similar to a complex organ rather than a homogenous lump of cells (Hanahan and Weinberg, 2011). The key hallmarks of cancer are summarised in ***Figure 1.1*****.**

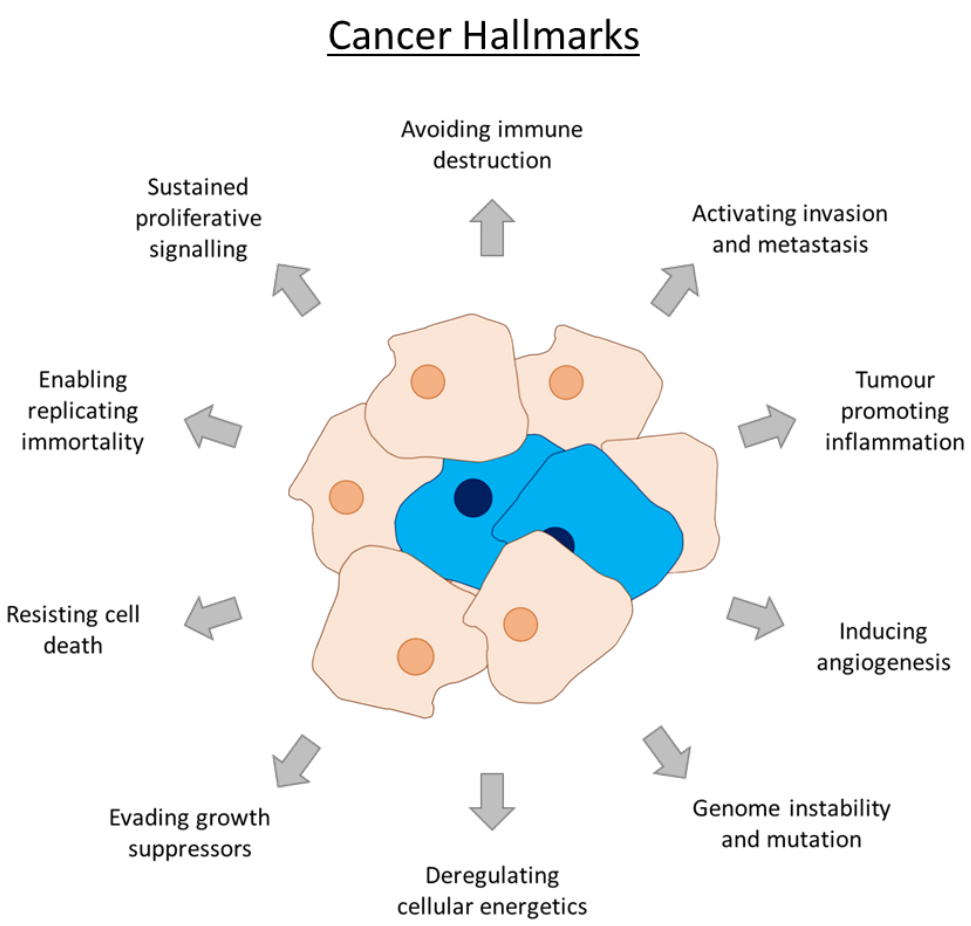

Figure 1.1. **Hallmarks of cancer.** Illustration of the acquired capabilities of tumour cells as outlined by Hanahan and Weinberg (2011). It is proposed that most, if not all, cancers acquire these capabilities through various mechanisms.

Depending on the tumour type, the genes and pathways mutated can vary greatly. Some pathways, such as the RAS (rat sarcoma virus) signalling pathway, are frequently mutated across many different types of cancers (Kan *et al.*, 2010). On the other hand, some pathways are more frequently altered in only specific tumour types, such as the oxidative stress response pathway in squamous cell carcinomas (Sanchez-Vega *et al.*, 2018). Commonly altered signalling pathways involved in tumorigenesis include the cell cycle, Hippo, myc, Notch, TGFβ, MAPK, PI3K, beta-catenin/WNT and p53 signalling pathways (Sever and Brugge, 2015). For simplicity, we refer to signalling pathways; however, biochemical pathways do not work in isolation and are interconnected, constituting in all effect a network of

biochemical reactions that processes information from within and outside the cells to trigger different transcriptional programmes and cellular functions. The frequencies of mutations within these pathways differ vastly between cancers (Sanchez-Vega *et al.*, 2018). The understanding of the mechanisms underpinning these alterations is thus of fundamental importance to develop more effective and personalised therapies and improve patient care.

A study that looked at data from The Cancer Genome Atlas (TCGA) from 3281 tumours across 12 tumour types showed that the most frequently mutated gene in the cohort was the *TP53* gene, with 42% of the samples having this mutation. This was followed by *PIK3CA* as the second most commonly mutated gene with more than 10% of samples having this mutation in most of the cancer types studied (Kandoth *et al.*, 2013). The *TP53* gene encodes the p53 protein, a tumour suppressor; missense mutations in this gene are prevalent across human cancers, resulting in the loss of tumour suppressive abilities such as the cell's ability to become senescent or apoptotic (Mantovani, Collavin and Del Sal, 2019). The *PIK3CA* gene encodes the p110α catalytic subunit of phosphatidylinositol 3-kinases (PI3Ks), a family of heterodimeric lipid kinases that regulate signalling pathways important for cancer cell survival (Samuels *et al.*, 2004). Activating mutations in *PIK3CA* have been identified in many different types of tumours, including colorectal, ovarian, breast and lung cancers (Ligresti *et al.*, 2009). Mutations in the *RAS* genes *KRAS, NRAS* and *HRAS* are also frequently found in human cancers and play essential roles in the control of cell proliferation, differentiation and survival (Prior, Lewis and Mattos, 2012). A detailed description of the RAS family – the topic of this thesis – follows in the next section.

1.2 The RAS family

1.2.1 Introduction to the RAS proteins

The RAS proteins are part of a larger RAS superfamily of GTPases, and this family of proteins consists of over 150 human members (Wennerberg, Rossman and Der, 2005). They share conserved structures and biochemical properties and act as molecular switches (Vetter and Wittinghofer, 2001). The RAS superfamily can be split into five branches based on their functional similarities: RAS proteins, RAS homologous (RHO) proteins, RAS-like proteins in brain (RAB), RAS-like nuclear (RAN) proteins and ADP-ribosylation factor (ARF) proteins (summarised in ***Figure 1.2***). The RAS subfamily also includes a number of RAS-related proteins in addition to the RAS proteins such as RAP, RAL and RHEB, all of which play roles in regulating signalling networks (Wennerberg, Rossman and Der, 2005). The RHO GTPases, of which the best studied are RHOA, RAC1 and CDC42, also control signal transduction of

several pathways and play a role in regulating the actin cytoskeleton and influencing cell polarity (Etienne-Manneville and Hall, 2002; Hodge and Ridley, 2016). The RAB GTPases form the largest subfamily within the RAS family, and members of this family are involved in regulating intracellular vesicular transport and trafficking proteins between organelles (Pereira-Leal and Seabra, 2001; Zerial and McBride, 2001). Members of the RAN family are predominantly involved in regulating nucleocytoplasmic transport of RNA and proteins, but also play a role in regulation of mitotic spindle assembly, DNA replication and nuclear envelope formation (Li, Cao and Zheng, 2003; Weis, 2003). Lastly, the ARF proteins are mainly involved in the regulation of membrane traffic and actin remodelling (Nie, Hirsch and Randazzo, 2003). This was a brief overview of the RAS superfamily, however, henceforth, the focus will be on the RAS proteins.

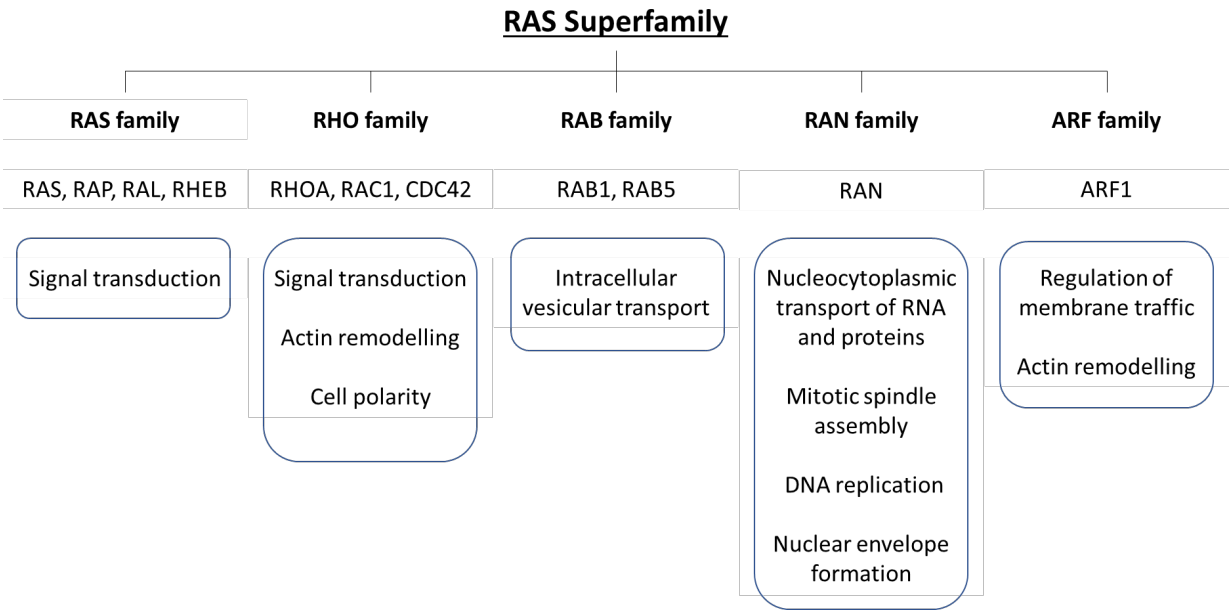

Figure 1.2. **RAS superfamily overview.** The superfamily is split into five branches according to functional similarities. A summary of the five families (RAS, RHO, RAB, RAN and ARF) is shown, along with examples of family members and their roles.

There are three human *RAS* genes encoding four RAS proteins: HRAS (Harvey rat sarcoma viral oncogene homolog), NRAS (neuroblastoma RAS viral (v-ras) oncogene homolog) and two isoforms of KRAS (Kirsten rat sarcoma viral oncogene homolog) (Ihle *et al.*, 2012; Hobbs, Der and Rossman, 2016). The two KRAS isoforms, KRAS4A and KRAS4B, arise from alternate RNA splicing of the fourth exon, hence the designated names (Tsai *et al.*, 2015). There is major variability between the different RAS proteins in the C-terminal region, which includes the hypervariable region (HVR) and the CAAX motif (Hancock, 2003). These regions are important for membrane association of RAS, which is essential for

its function (Willumsen *et al.*, 1984). Activating oncogenic mutations commonly occur in exons 1 or 2, therefore, both variants of KRAS are susceptible to becoming oncogenic (Tsai *et al.*, 2015). Despite this, KRAS4A has generally been understudied because it has been regarded as the less important splice variant. This may partly be because it has been shown in mice that although the *KRAS* gene is essential for normal mouse development, KRAS4A is dispensable in the presence of functional KRAS4B (Plowman *et al.*, 2003). However, the role of KRAS4A in cancer might be re-evaluated in the future considering recent indication of specificity of isoforms in signal transduction, metabolic rewiring and gene expression pattern dynamics (Newlaczyl, Coulson and Prior, 2017; Amendola *et al.*, 2019).

Members of the RAS GTPase family are important players in many signalling networks that connect different upstream signals to a large number of downstream effectors that are involved in controlling many cellular phenotypes including cell growth, migration, apoptosis, senescence and cytoskeletal changes (Rajalingam *et al.*, 2007). These networks are composed of many different signalling pathways that communicate with each other and are controlled by different sets of signals. The outcome of cellular responses are determined by the balance of network signalling as a result of crosstalk between pathways within these large networks (Matozaki, Nakanishi and Takai, 2000; Aksamitiene, Kiyatkin and Kholodenko, 2012). Due to the complexity of these networks, when certain pathways are altered in pathological situations, it becomes very difficult to understand how to treat these conditions; alteration in one pathway could mean multiple different pathways in a network are affected in ways not fully understood. For this reason, in order to develop therapeutic approaches that can restore the balance in signalling, it is crucial to understand signalling networks not only on their own, but also how they are embedded within larger networks (Fernández-Medarde and Santos, 2011).

One of the main pathways HRAS, NRAS and KRAS signal via is the mitogen-activated protein kinase (MAPK) pathway, which plays an essential role in controlling proliferation, differentiation and survival of cells (Guo *et al.*, 2020). Whereas cancers are caused by somatic mutations in components of this RAS/MAPK pathway, there are a group of developmental disorders, called the RASopathies, that are caused by germline mutations in the genes of this pathway. Whilst each RASopathy has a different phenotype, they have overlapping characteristics (e.g., craniofacial dysmorphology, cardiac malformations and neurocognitive impairment) due to the common dysregulation of the same pathway (Rauen, 2013).

The first RASopathy to be identified as a syndrome caused by a mutation in the MAPK pathway was Neurofibromatosis type 1 (NF1), which is caused by a loss-of-function mutation in the *NF1* gene that

encodes neurofibromin, a RASGAP, thus resulting in reduced RAS GTPase activity (Cawthon *et al.*, 1990; Viskochil *et al.*, 1990; Wallace *et al.*, 1990). Another RASopathy, Noonan Syndrome (NS), can be caused by activating mutations in a number of genes, with the most commonly mutated gene being *PTPN11* (Tartaglia *et al.*, 2001), followed by *SOS1* (Roberts *et al.*, 2007; Tartaglia *et al.*, 2007). Other genes include *KRAS* (Klein *et al.*, 2006), *NRAS* (Cirstea *et al.*, 2010), *RAF1* (Pandit *et al.*, 2007; Razzaque *et al.*, 2007), *SHOC2* (Cordeddu *et al.*, 2009) and *CBL* (Martinelli *et al.*, 2010; Niemeyer *et al.*, 2010), all of which harbour heterozygous germline mutations and encode components of the MAPK pathway.

Mutations in the *PTPN11* (Digilio *et al.*, 2002; Legius *et al.*, 2002) and *RAF1* (Pandit *et al.*, 2007) genes can also cause Noonan Syndrome with Multiple Lentigines (NSML). Inactivating mutations in the *RASA1* gene, which encodes a RASGAP like the *NF1* gene (p120-RASGAP in this case), cause the Capillary Malformation-Arteriovenous Malformation Syndrome (CM-AVM) (Eerola *et al.*, 2003). Some of the rarer disorders include Costello Syndrome (CS), which is caused by heterozygous activating mutations in *HRAS* (Aoki *et al.*, 2005) and Cardio-Facio-Cutaneous Syndrome (CFC), which can be caused by activating mutations in *BRAF*, *MAP2K1*/*MAP2K2* or *KRAS* (Niihori *et al.*, 2006; Rodriguez-viciana *et al.*, 2006). Finally, one of the relatively newer syndromes to be identified is Legius Syndrome (LS, also called NF-1 like syndrome), which is caused by heterozygous inactivating mutations in *SPRED1* (Brems *et al.*, 2007). Although all of these germline mutations are not necessarily oncogenic, due to the impact of these mutations on the MAPK pathway, many patients with a RASopathy also have an increased risk of cancer along with the developmental problems (Rauen, 2013).

1.3 Differences in structural and post-translational modifications of RAS proteins

HRAS, NRAS and *KRAS* genes vary in their sizes due to differences in the sizes of the introns, ranging from 4.5 kb to 50 kb (Silver, Nadeau and Klein, 1998); each RAS protein is encoded by four exons and an additional 5' non-coding exon (McGrath *et al.*, 1983). The encoded RAS proteins are small GTPases with a molecular weight of 21 kDa (Shih *et al.*, 1979; Gibbs *et al.*, 1984; McGrath *et al.*, 1984). The primary sequence between these RAS isoforms is highly similar, with an 82% to 90% amino acid sequence overlap (Hobbs, Der and Rossman, 2016). The N-terminus contains the G domain (also called the catalytic domain), which is involved in GTP binding and hydrolysis (Pai *et al.*, 1990). Within this G domain, there are specific regions (switch I and switch II) which change conformation depending on

whether RAS is bound to guanosine-5'-diphosphate (GDP) or guanosine-5'-triphosphate (GTP) and also play a big role in RAS binding to its effector proteins (Milburn *et al.*, 1990).

Within the 166 amino acid long G domain, there are two separate lobes: the effector lobe and the allosteric lobe (Buhrman *et al.*, 2011). All RAS isoforms have identical amino acid sequences from residues 1 to 86, which makes up the effector lobe, but there is only 90% sequence similarity in the allosteric lobe (Gorfe, Grant and McCammon, 2008). The effector lobe contains the catalytic machinery, which includes switch I and switch II, the phosphate binding loop (P-loop) and most of the nucleotide binding pocket. The effector lobe is named as such because it contains the protein-protein interaction sites with effectors. On the other hand, the allosteric lobe contains the membrane interacting portions, including the allosteric site, the allosteric switch components and the helix 4 which forms salt bridges with membrane phospholipids when RAS is GTP-bound (Buhrman *et al.*, 2011). The orientation of RAS at the membrane determines its interaction with effector proteins, thus impacting signalling downstream of RAS (Abankwa *et al.*, 2008). Also, variations in the amino acid sequence of the allosteric lobe alters RAS orientation at the plasma membrane, resulting in isoform-specific differential downstream signalling (Abankwa, Gorfe and Hancock, 2008).

Differences between the RAS isoforms have been in part attributed to differences in the C-terminal HVR domain (Wolfman, 2001). Changes at this site can alter the targeting of RAS isoforms to specific subcellular locations, thus resulting in distinct signals (Jaumot *et al.*, 2002; Hancock, 2003). Therefore, it is important to understand how the different RAS isoforms are distributed at the subcellular level and the impact this has on downstream signalling. In addition to the canonical view that RAS regulates signalling from the plasma membrane, it is now apparent that RAS can also bind to subcellular organelles such as the Golgi and the endoplasmic reticulum (ER), from where it can propagate downstream signalling (Choy *et al.*, 1999; Chiu *et al.*, 2002). For example, it has been shown that both KRAS4A and KRAS4B have polybasic sequences that favour the association of KRAS with acidic membrane regions, such as endosomal membranes, where 10-15% of total KRAS is found (Gelabert-Baldrich *et al.*, 2014).

RAS localisation is also sensitive to specific phospholipids (Prior and Hancock, 2012). At the plasma membrane, RAS proteins exist in a mixture of transient nanoclusters and freely diffusing monomers (Hancock and Parton, 2005; Plowman *et al.*, 2005). The formation of these nanoclusters is dependent on the interaction of specific phospholipids and cholesterol in the lipid bilayer with the C-terminal lipid anchor (comprised of the processed CAAX motif and two palmitic acid residues), the HVR and the

N-terminal catalytic domain of RAS (Rotblat *et al.*, 2004). The activity state of RAS also has an impact on the formation of nanoclusters, with RAS-GTP and RAS-GDP having been shown to segregate into separate clusters (Prior, Harding, *et al.*, 2001; Prior, Muncke, *et al.*, 2001). In addition, the different RAS isoforms undergo distinct posttranslational modifications which allow for selective lipid sorting and the formation of separate non-overlapping nanoclusters (Zhou, Gorfe and Hancock, 2021). The RAS isoform-specific modifications also allow for their differential localisation to distinct microdomains of the plasma membrane. For example, different PTMs impact the affinity of RAS to cholesterol in the plasma membrane, and certain membrane-bound scaffold proteins can also bind to specific RAS isoforms, thus allowing for unique microdomain interactions of RAS (Prior, Muncke, *et al.*, 2001; Hancock and Parton, 2005).

The HVR is a site in RAS proteins that is differentially lipid-modified (Van *et al.*, 2021). Whilst KRAS4A and NRAS are palmitoylated at a single amino acid within the HVR, HRAS harbours two palmitoylation sites (Hancock *et al.*, 1989; Hancock, Paterson and Marshall, 1990). Palmitoylation and depalmitoylation steps regulate RAS interaction with the plasma membrane, endomembranes and the cytosol, and therefore affect the functionality of RAS isoforms (Cox, Der and Philips, 2015). For example, palmitoylated HRAS and NRAS localise at the Golgi, whereas KRAS4B does not (Choy *et al.*, 1999; Apolloni *et al.*, 2000; Goodwin *et al.*, 2005). Furthermore, doubly-palmitoylated HRAS is distributed throughout the Golgi stacks but the singly-palmitoylated NRAS is asymmetrically distributed with enrichment within the *cis* Golgi compartment, and this differential localisation of HRAS and NRAS is determined by their different palmitoylation states (Lynch *et al.*, 2015).

Palmitoylation is not the only post-translational modification (PTM) that RAS proteins are subjected to. In fact, RAS proteins are cytosolic after translation and become associated with membranes through a series of different PTMs (Gutierrez *et al.*, 1989). These PTMs are initiated by the presence of the CAAX motif, which, as briefly mentioned earlier, is found at the C-terminus of all RAS proteins. The CAAX motif, which consists of a cysteine (C), two aliphatic residues (A) and any amino acid (X), lies to the C-terminal end of the HVR. The newly synthesised RAS protein is first farnesylated at the cysteine residue of the CAAX motif by the addition of a C15 farnesyl isoprenoid lipid, which is catalysed by the enzyme farnesyltransferase (Casey *et al.*, 1989; Hancock, Paterson and Marshall, 1990). Next, the -AAX amino acids are removed by proteolysis before methyl esterification takes place at the α carboxyl group of the new C-terminal prenylcysteine (Clarke *et al.*, 1988). These PTMs are thought to increase the hydrophobicity of the RAS protein, therefore enabling plasma membrane association (Clarke, 1992).

Whilst all RAS isoforms go through these initial modifications, further modifications such a palmitoylation may differ, as mentioned earlier. Whilst HRAS, NRAS and KRAS4A can be palmitoylated on one or two cysteines present in their respective HVRs (excluding the cysteine of the CAAX motif), KRAS4B does not have this additional cysteine and therefore cannot be palmitoylated. Instead, it has a polybasic domain consisting of six consecutive lysine residues, conferring it a positive charge that aids its association with the membrane (Hancock, Paterson and Marshall, 1990). KRAS4A on the other hand has a bipartite polybasic region (containing RLKK and KIKK motifs) along with a cysteine residue in the HVR that can be palmitoylated (Tsai *et al.*, 2015; Zhao *et al.*, 2015). Another unique aspect of KRAS4B is that it has a phosphorylation site (Ser181) in its HVR which acts as an electrostatic farnesyl switch, and upon phosphorylation by protein kinase C (PKC), promotes rapid dissociation from the plasma membrane allowing it to translocate to endomembranes (Ballester, Furth and Rosen, 1987; Bivona *et al.*, 2006). The removal of KRAS4B from the plasma membrane might be a mechanism to downregulate its signalling and PKC-driven phosphorylation of Ser181 in KRAS4B has also been shown to increase apoptosis in KRAS-mutated cancer cells (Bivona *et al.*, 2006). Novel approaches to restore PKC activity have been investigated as potential therapeutic strategies for cancer treatment (Tovell and Newton, 2021). Bivona and colleagues showed that bryostatin-1, a potent PKC agonist, inhibited the growth of transformed KRAS-mutant cells, both *in vitro* and *in vivo*, in a Ser181-dependent manner (Bivona *et al.*, 2006). Another group had also previously shown that bryostatin-1 was efficacious in a pancreatic tumour xenograft model (Mohammad *et al.*, 1998). Efforts have also been made to block the inhibitors of PKC activity, such as PH domain Leucine-rich repeat protein phosphatase (PHPLL) (Gao, Brognard and Newton, 2008; Sierecki *et al.*, 2010). However, as shown by Smith and colleagues, PHPLL also negatively regulates signalling via the AKT and ERK pathways and inhibiting PHPLL can have unwanted effects such as increased cell migration (Smith *et al.*, 2016).

There are other phosphorylation events in the different RAS isoforms that affect their functionality. For example, phosphorylation of HRAS at Tyr137 by the ABL tyrosine kinase leads to increased interaction with the downstream effector RAF, and a reduction in intrinsic GTP hydrolysis, both leading to increased downstream activation (Ting *et al.*, 2015). On the other hand, NRAS can be phosphorylated at Tyr32 by the SRC tyrosine kinase, but this leads to a reduction in downstream signalling because it decreases NRAS affinity to the RAS-binding domain (RBD) of RAF. It also increases affinity to GTPase-activating proteins (GAPs), which are proteins that bind to and stabilise RAS catalytic machinery and help to inactive RAS (Bunda *et al.*, 2014).

The expression and localisation of RAS is also regulated by ubiquitination. The RAS proteins can be differentially ubiquitinated, allowing for isoform-specific control of signalling (Jura *et al.*, 2006). For example, HRAS, but not KRAS4B, is modified by Lys63-linked diubiquitin chains, which leads to the stabilisation of HRAS to the endosomal membranes. The resulting smaller pool of HRAS at the plasma membrane results in less efficient activation of CRAF, as this occurs at the plasma membrane (Jura *et al.*, 2006). Whilst the ubiquitination of NRAS occurs in a manner similar to HRAS, KRAS4B can be monoubiquitinated at Lys147, which results in higher GTP loading and increased affinity to the downstream effectors RAF and PI3K (Sasaki *et al.*, 2011). Mono and/or diubiquitination of HRAS, NRAS and KRAS4A can also result in increased GTP loading (Sasaki *et al.*, 2011; Baker *et al.*, 2013). Hence, elucidating the mechanism, site and effects of ubiquitination in all isoforms may be beneficial in developing therapies against RAS isoform-specific mutant cancers.

Two other important post-translational modifications that occur in RAS proteins are acetylation and nitrosylation. Acetylation can modulate protein stability, subcellular localisation, protein-protein and protein-DNA interactions (Ahearn, Zhou and Philips, 2018; Narita, Weinert and Choudhary, 2019). KRAS4B is acetylated at Lys104 (Yang *et al.*, 2012), which is in loop 7 between the α3 and β5 regions of the protein, which lies outside the switch I and switch II domains that are important for RAS function (Milburn *et al.*, 1990). With molecular dynamics (MD) simulations, Yang and colleagues predict that this PTM affects the conformational stability of the switch II domain. This can explain the *in vitro* observation that Lys104 acetylation results in suppressed GEF-induced nucleotide exchange, as switch II plays a critical role in the ability of RAS proteins to interact with GEFs. Therefore, acetylation at Lys104 can result in an inhibition of transforming activity, but unlike other PTMs, it does not impact the subcellular localisation of KRAS4B (Yang *et al.*, 2012).

It was discovered many years ago that free radicals may play important roles in carcinogenesis by acting as tumour promotors, causing DNA damage or by modulating signalling pathways, and this prompted research into elucidating whether RAS proteins are modified by reactive free radicals (Halliwell and Aruoma, 1991; Lander *et al.*, 1995). It was discovered that RAS can be nitrosylated at Cys118, the most surface-exposed cysteine and a very highly conserved residue among the RAS isoforms. Cys118 has been shown to be a critical site of redox regulation of RAS and that nitrosylation at this site increases guanine nucleotide exchange and subsequently increases downstream signalling (Lander *et al.*, 1996).

As outlined thus far, the different RAS proteins undergo numerous different post-translational modifications, which result in changes to subcellular localisation, membrane association and signalling output amongst other effects. Some PTMs occur in all isoforms, whilst others only occur in specific isoforms, highlighting potential mechanisms that can be targeted for development of therapies against specific RAS-mutant cancers. Despite the vast knowledge about post-translational modifications of RAS proteins accrued in the past two decades, we are still far from fully understanding how specific PTMs are regulated, their role in carcinogenesis and their potential as targets for therapies. A more complete understanding of this would allow for the development of therapies that can precisely modulate the mechanisms behind these PTMs and potentially help treat RAS-mutant cancers more effectively (Ahearn *et al.*, 2012).

1.3.1 Regulation of RAS activation

RAS proteins are small GTPases, and they are involved in transducing extracellular signals to the nucleus via different signalling pathways (Molina and Adjei, 2006; Gimple and Wang, 2019). They act as molecular switches that can be turned on (when bound to GTP) and turned off (when bound to GDP) and play essential roles in the regulation of cell growth and differentiation (Skolnik and Margolis, 1994). It has been established for around 30 years now that external signals such as growth factors including epidermal growth factor (EGF) and platelet-derived growth factor (PDGF), can control the activity of RAS proteins (Satoh *et al.*, 1990). Growth factors are proteins that are involved in a variety of different roles and can induce tumourigenesis and promote epithelial-mesenchymal transition (EMT) (Tse and Kalluri, 2007; Domenico and Giordano, 2017), and both EGF and PDGF can regulate cell proliferation, differentiation and survival (Stoscheck and King, 1986; Huang *et al.*, 2017). These growth factors bind to their respective receptors (for example the EGF receptor (EGFR) and the PDGF receptor (PDGFR)), which are types of receptor tyrosine kinases (RTKs) (Ullrich and Schlessinger, 1990). RTKs have intrinsic tyrosine kinase activity which allows them to phosphorylate tyrosine residues on their substrates including phospholipase C gamma (PLCγ), RAF proteins and phosphatidylinositol 3-kinases (PI3Ks), and therefore are able to activate multiple downstream signalling pathways (Satoh *et al.*, 1990). RTKs play an important role in many different cellular processes and receptor activity is tightly controlled under normal physiological conditions. However, dysregulation of RTK signalling can lead to imbalance between cell proliferation and death, which can lead to cancer development (Du and Lovly, 2018).

Although certain discoveries related to RAS proteins and their functionality were made many years ago, much has been learned, or confirmed, since. For example, it was believed that the stimulation of EGFR by the binding of EGF to its extracellular ligand-binding domain results in the dimerisation of two monomeric ligand-bound EGFRs, which then allows for *trans*-autophosphorylation of multiple tyrosine residues on each other's intracellular kinase domains, initiating downstream signalling cascades (Schlessinger and Ullrich, 1992). This model is known as the 'ligand-induced dimerisation' model; however, more recent research has suggested a different mechanism of activation of EGFR. The newer 'flexible rotation model', proposed by Moriki and colleagues, suggests that EGFR dimers exist in a dormant state when not bound to a ligand (Moriki, Maruyama and Maruyama, 2001). Upon binding of the ligand to the extracellular domain, there is a rotation of the transmembrane domain that runs parallel through the plasma membrane, which causes a reorientation of the intracellular kinase domain from an inactive symmetric form to an active asymmetric form. This model is able to explain how in the absence of a ligand, oncogenic mutations are able to activate these receptors, without assuming that these mutations cause receptor dimerisation (Yu *et al.*, 2002; Zhang *et al.*, 2006). Despite much research being carried out on EGFR activation, the mechanism is not completely clear due to confounding results. For example, recent research has suggested that EGFR may in fact exist as a monomer and dimerise upon ligand-binding, therefore, supporting the older 'ligand-induced dimerisation' model instead (Yamashita *et al.*, 2015).

Different RTKs have been shown to be activated differently depending on the type of receptor and ligand. For example, there are three isoforms of PDGF, comprised of the individual A or B monomer that form a homodimer (AA or BB) or a heterodimer (AB). Two populations of PDGFR also exist, the B receptor (that binds only the BB dimer) and the A/B receptor (that binds all three dimers) (Hart *et al.*, 1988). The PDGF BB dimer binds two separate PDGFR molecules and this results in the dimerisation and stabilisation of the receptor dimer. It is suggested that the receptors exist in an equilibrium of monomers and dimers, with the monomer being favoured in the absence of ligand, and the dimer being favoured in optimal ligand concentration (Heldin *et al.*, 1989). The preferred binding specificities of the different receptor isoforms to the various forms of PDGF dimers may be a mechanism for expanding the diversity of signals generated due to the increase in the repertoire of receptor-ligand interactions and ultimately resulting in a change in signal functionality (Heldin *et al.*, 1988). RAS activation is also achieved by signalling via the insulin receptor, which is activated upon the binding of insulin to specific binding sites on the extracellular domain on the receptor (Ullrich and Schlessinger, 1990). The insulin receptor is comprised of two monomeric structures, each containing an extracellular α-subunit (containing the insulin binding sites), and a transmembrane β-subunit

(containing the kinase domain). The insulin receptor differs from other RTKs in that it exists as a covalent disulphide-linked dimer of the two αβ-subunit monomeric structures (αβ-S-S-αβ) (Boni-Schnetzler *et al.*, 1988).

Regardless of the mechanism of activation of the RTK, once specific tyrosine residues on the intracellular kinase domain of the receptor are phosphorylated, they can act as docking sites for effector proteins that have an SRC homology 2 (SH2) domain; these effector proteins can then bind the RTK and form heteromeric protein complexes that can activate downstream signalling (Moran *et al.*, 1990; Pawson *et al.*, 2001). The SH2 domain is a conserved region amongst a number of cytoplasmic signalling proteins, including PLCγ, RAS activating proteins and SRC-like tyrosine kinases. Many SH2-containing proteins also have another conserved SH3 domain, which plays a role in modulating protein interactions with the cytoskeleton and cellular membranes (Koch *et al.*, 1991). The growth factor receptor-bound protein 2 (GRB2) is an important adaptor protein involved in RAS signalling, and it plays an essential role in recruiting Son of Sevenless (SOS), a guanine nucleotide exchange factor (GEF), from the cytoplasm to the plasma membrane (Buday and Downward, 1993). GRB2 is able to do this because it contains both SH2 and SH3 domains; the SH2 domain allows it to bind to specific phospho-tyrosine residues on the EGFR, and the SH3 domains bind to SOS (Simon and Schreiber, 1995).

GEFs are a group of enzymes that activate G-proteins by accelerating the release of guanine nucleotides from the G-protein by several orders of magnitude (Quilliam *et al.*, 1995). There are a number of GEF families that regulate members of the different G-protein families, with individual GEFs having a certain specificity profile which is generally unique to each family (Cherfils and Chardin, 1999). For example, GEFs for RAS proteins have a CDC25 domain (Boriack-Sjodin *et al.*, 1998), GEFs for ARF proteins have a Sec7 domain (Cherfils *et al.*, 1998), and GEFs for RHO proteins have a Dbl-homology (DH) domain (Aghazadeh *et al.*, 1998). The mechanisms of GEF action involves a series of successive reversible steps which lead from a binary G-protein:nucleotide complex to a ternary G-protein:nucleotide:GEF complex to finally a binary G-protein:GEF complex that is stable in the absence of bound nucleotide. This reaction is reversed by the rebinding of a nucleotide, primarily GTP due to its higher molar concentration in the cytoplasm (Klebe *et al.*, 1995; Lenzen *et al.*, 1998). An illustration of this mechanism is shown in ***Figure 1.3***. The predominant GEF involved in RAS activation is SOS, which upon binding to RAS causes a conformational change in its switch regions and the P-loop; this causes the affinity of GDP to RAS to weaken and ultimately results in its release and replacement with GTP (Boriack-Sjodin *et al.*, 1998). The affinity of RAS to GDP and GTP does not differ, however, the intracellular concentration of GTP is approximately ten-fold higher than GDP, therefore

this results in an increase in GTP binding to RAS upon GDP displacement (Simanshu, Nissley and McCormick, 2017).

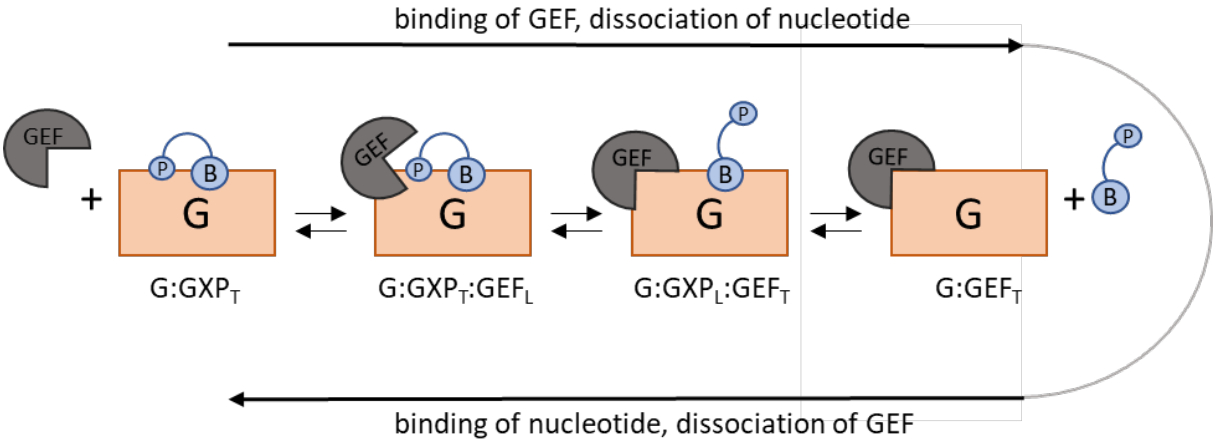

Figure 1.3. **The reversible exchange reaction of nucleotide displacement and loading.** The nucleotide (GTP or GDP) is depicted in blue. It interacts with the G-protein (e.g., KRAS) via its base (B) and phosphate (P) moieties. The GEF (grey), competes with the nucleotide and promotes nucleotide exchange. Subscript L and T refer to loose or tight interaction of the G-protein with the nucleotide and the GEF. This is a simplified illustration adapted from Bos, Rehmann and Wittinghofer (2007).

The first insight into the conformational differences between GTP-bound RAS and GDP-bound RAS structures was provided by the elucidation of the crystal structure of HRAS bound to guanosine-5'-[β,γ-imido]triphosphate (GppNHp), a non-hydrolysable GTP analogue (Pai *et al.*, 1989). From here on, for the purpose of discussing crystal structures, any reference to 'GTP-bound RAS' refers to a RAS protein in complex with a GTP-analogue, as that is how these crystal structures were determined. The GDP-bound crystal structure had been resolved a year earlier, and the resolution of the GTP-bound complex allowed for comparisons to be made to understand the differences between the inactive and active RAS complexes (De Vos *et al.*, 1988).

As shown by Milburn et al., (1990) and others, the structural differences observed are mainly confined to two segments of the RAS protein: the switch I and switch II regions within the G domain (Tong *et al.*, 1989; Krengel *et al.*, 1990). Compared to GDP-bound RAS, there are three prominent differences in the switch I domain of GTP-bound RAS. One difference is the breaking of hydrogen bonds between the side chains of Tyr32 and Tyr40, resulting in the side chain of Tyr32 now swinging out of the phosphate pocket and partially blocking the entrance of the guanine nucleotide pocket (Milburn *et al.*, 1990). Another difference is that the side chain of Thr35 coordinates with a Mg^{2+} ion and forms a hydrogen bond with the γ-phosphate of the GTP molecule, whilst in the GDP-bound form, this residue

points outwards away from the protein complex (Chung *et al.*, 1993). Lastly, the side chains of residues 36 and 38 were also shown to be very differently orientated compared to the GDP-bound complex; these extensive conformational differences illustrate the presence of the two different states of the molecular switch that RAS acts as (Milburn *et al.*, 1990).

Within the switch II region, which is comprised of residues 60 to 76 and corresponds to loop 4 and a following helix (α2), there are two main differences between the active and inactive RAS complexes (Milburn *et al.*, 1990; Quilliam *et al.*, 1996). Weak/disordered electron density is associated with the first part of the switch II region (residues 60 to 68), suggesting high flexibility in this portion of the protein (Buhrman, Wink and Mattos, 2007). The first key difference between both forms of RAS complexes is that in the GTP-bound form, residues 60 and 61 are in a position that allows them to form hydrogen bonds to the γ-phosphate of GTP, and the functional importance of residue 61 is reflected in the fact that it is one of the most common oncogenic mutation sites on RAS (Milburn *et al.*, 1990; Hobbs, Der and Rossman, 2016). The other key difference is the orientation of the α2 helix, which is positioned differently between the two complexes in respect to the rest of the molecule. Although only one residue from switch I (Thr35) and one or two residues from switch II (Gly60/Gln61) form bonds with the γ-phosphate of GTP, a conformational change is seen covering most of switch I and switch II regions, an area spanning 40Å. This suggests that the entire length of the switch region is conformationally linked; changes at one end would propagate to the other end of the region (Milburn *et al.*, 1990).

Since the initial discovery of these conformational changes, several research findings have confirmed and further elucidated the differences between GTP-bound and GDP-bound RAS, but also between different RAS isoforms (Spoerner *et al.*, 2001; Ford *et al.*, 2005, 2006; Lukman *et al.*, 2010; Lu *et al.*, 2016a; Matsumoto *et al.*, 2016). MD simulations have shown that there are significant differences in the dynamics of HRAS, NRAS and KRAS, and that these differences vary depending on the type of nucleotide bound. These simulations have also lead to the identification of several transient pockets on RAS structures that are difficult to observe in crystal structures (Gorfe, Grant and McCammon, 2008; Kapoor and Travesset, 2015). The increased flexibility at the switch regions observed in the active-RAS conformation is also supported by studies using nuclear magnetic resonance (NMR) and electron paramagnetic resonance (EPR) data that show increased flexibility in these regions in GTP-bound RAS (Farrar, Halkides and Singel, 1997; Ito *et al.*, 1997).

Once the conformation of RAS is altered by GTP-binding, the affinity of RAS proteins to their effector proteins increases, allowing them to bind to certain residues (amino acids 32 to 40) within the switch

I region; the specific residues involved in effector binding can differ depending on the effector protein (McCormick and Wittinghofer, 1996). These effector proteins can now be activated via various mechanisms such as stimulation of catalytic activity or release of auto-inhibition, and the transduction of downstream signalling can occur. A number of domains have been identified in effector proteins that mediate specific binding to RAS, including the RAS-binding domains (RBDs), Ral-binding domains (RalBDs) and RAS association domains (RADs) (Patel and Côté, 2013). The first effector protein of RAS to be identified was the serine/threonine protein kinase CRAF (also known as RAF-1) (Downward, Warne and Viciana, 1993; Wolfman *et al.*, 1993). CRAF contains an RBD comprising residues 55 to 132, allowing it to sufficiently bind GTP-bound RAS. Structural analysis has shown that the RBD of CRAF consists of a five-stranded β-sheet, a 12-residue α-helix, and an additional one-turn helix, and forms an inter-protein β-sheet between both proteins (Donald Emerson *et al.*, 1995). The topology of the RBD is very similar to that of ubiquitin and forms a tertiary fold structure, and this common ubiquitin-like binding domain is shared by all known downstream effectors of RAS (Nassar *et al.*, 1995).

A study investigating the interactions of CRAF and RAL-specific guanine nucleotide exchange factor (RalGEF) with RAS and the closely related RAP GTP-binding protein showed that residues 32 to 40 of RAS and RAP are responsible for the molecular recognition of effector proteins, but that residues outside of this region are responsible for the specificity of the interaction (Nassar *et al.*, 1996). RAS and RAP share 50% sequence homology and the region within switch I involved in effector binding (residues 32 to 40) is identical in both, therefore, it is not surprising that both proteins share effector proteins such as CRAF, RALGEF and PI3K (Nassar *et al.*, 1995). However, there is a difference in the affinity of effector binding, mediated in part by differences in the surface charges between the GTP-binding proteins and their effector proteins (Nassar *et al.*, 1996; Nakhaeizadeh *et al.*, 2016).

Whilst the binding of some effector proteins, such as RAF, is mediated primarily by the existence of a preformed binding domain, other effector proteins, such as PI3K, also undergo additional allosteric changes in order to be activated (Herrmann, Martin and Wittinghofer, 1995; Zhang, Jang and Nussinov, 2019). The switch I region of RAS forms critical interactions with PI3Kγ (an isoform of PI3K), similar to how it does with other effector proteins. However, RAS also makes essential interactions with PI3Kγ using its switch II region, unlike other effectors; this is probably due to a unique orientation of RAS with the RBD of PI3Kγ (Pacold *et al.*, 2000). The catalytic domain of PI3Kγ also interacts with switch II of RAS, which may contribute to a conformational change in PI3Kγ, leading to its activation. This data supports the notion of PI3Kγ activation requiring not only membrane association but also an allosteric change in structure (Walker *et al.*, 1999; Pacold *et al.*, 2000).

Once effector proteins are activated, they can propagate specific signals and mediate cellular responses and alter cell phenotypes (Rajalingam *et al.*, 2007). RAS-activated signalling pathways will be discussed in more detail in **Section 1.4**. As already mentioned, RAS proteins have intrinsic GTPase activity, albeit at very low levels (Barbacid, 1987; Moghadamchargari *et al.*, 2019). To inactive RAS signalling, RAS-GTP needs to be converted to RAS-GDP, and this is achieved by the binding of GTPase-activating proteins (GAPs) (Trahey and McCormick, 1987; Gideon *et al.*, 1992). The crystal structure of RAS bound to RASGAP shows that RASGAP stabilises the position of Gln61 of RAS, which is within the switch II domain. Gln61 is involved in coordinating the attacking water molecule required for hydrolysis by contacting one of the fluoride ions and an axial ligand derived from the incoming nucleophilic water molecule and thus stabilising the transition state (Scheffzek *et al.*, 1997). Binding of RASGAP also positions an Arg789, termed the 'arginine finger', into the phosphate binding site and further stabilises the transition state by neutralising the negative charge at the γ-phosphate (Scheffzek *et al.*, 1997; Resat *et al.*, 2001). Biochemical and mutational studies have shown that Gln61 mutations in RAS, which occur frequently in human tumours, abolish GAP-induced GTP hydrolysis, thus supporting this mechanism of catalysis (Zhang *et al.*, 1991).

1.4 Overview of the RAS signalling pathways

Interaction of RAS with several families of effector proteins results in the activation of multiple different signalling pathways (Faller and Rankin, 2015; Cuesta, Arévalo-Alameda and Castellano, 2021). The main effector pathways are discussed in this section (summarised in ***Figure 1.4***). These pathways include the ERK1/2 pathway, which is one of four mitogen-activated protein kinase (MAPK) pathways, and the other activated pathways include phosphatidylinositol 3-kinase (PI3K), RAL-guanine nucleotide dissociation stimulator (RALGDS) and phospholipase Cε (PLCε) pathways (Downward, 2003; Morrison, 2012).

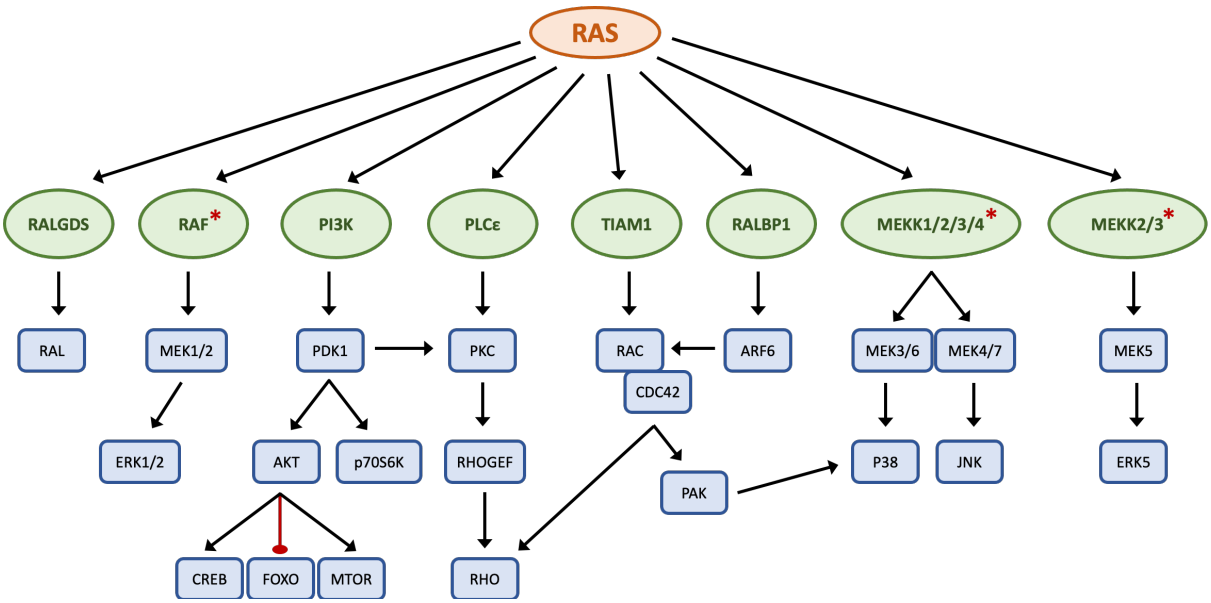

Figure 1.4. **Overview of main RAS signalling pathways.** Activated RAS interacts with many effector proteins that engage different downstream pathways. Through the regulation of these pathways, RAS proteins are able to regulate many cell functions including proliferation, migration and apoptosis. A summary of the pathways is shown here, with information derived from Cuesta *et al.,* (2021) and Faller and Rankin (2015). Black arrows indicate activation, red rounded arrows indicate inhibition. Red asterisks show the MAPK pathways, which are illustrated in further detail in ***Figure 1.5***.

The MAPK signalling pathways

Mitogen activated protein kinase (MAPK) pathways refer to a group of evolutionarily conserved signal transduction cascades that transduce extracellular signals to the nucleus and are involved in many normal cell functions including cell differentiation, proliferation, growth, migration, apoptosis and survival (Dhillon *et al.*, 2007). These pathways are comprised of three kinase modules: a mitogen activated protein kinase kinase kinase (MAPKKK) which phosphorylates and activates a mitogen activated protein kinase kinase (MAPKK), which finally phosphorylates and activates a MAPK (Schaeffer and Weber, 1999). The MAPK pathways can be split into three major subfamilies: the extracellular signal regulated kinase 1/2 (ERK1/2) family, which is mainly activated by growth factors, the c-Jun amino terminal kinase (JNK) family, which can be activated by growth, differentiation and stress factors, and finally the p38 MAP kinase family, which is mainly activated via stress factors (Krens, Spaink and Snaar-Jagalska, 2006). An additional non-canonical MAPK pathway, the ERK5 pathway, is also discussed in this section, and an overview of the pathways is presented in ***Figure 1.5.*** The ERK1/2 pathway is deregulated in around a third of all human cancers and is the most well-studied and characterised MAPK pathway (Dhillon *et al.*, 2007). The ERK1/2 pathway is the focus of my project, and hence will be discussed in considerable detail in **Section 1.5**.

The JNK signal transduction pathway has been implicated in multiple physiological processes, including cell survival and apoptosis. There are at least ten JNK isoforms, which are alternatively spliced and encoded by three genes, *JNK1, JNK2 and JNK3* (Gupta *et al.*, 1996). JNK is activated by dual phosphorylation of Thr183 and Tyr185 in the tripeptide motif Thr-Pro-Tyr by the MAPK kinases MKK4 and MKK7 (Dérijard *et al.*, 1994; Tournier *et al.*, 1997; Wang, Destrument and Tournier, 2007). Multiple isoforms of MKK4 and MKK7 exist that are biochemically distinct in terms of inducibility and basal activity. The upstream MAPKKKs responsible for activating MKK4/7 also differ, with MKK4 being primarily activated by environmental stress and MKK7 being activated by cytokines such as tumour necrosis factor (TNF) and interleukin-2 (IL-2). MKK4/7 also show significant differences in substrate specificity, with MKK4 preferentially phosphorylating Tyr185 and MKK7 showing a preference for Thr183, although both are dual specificity protein kinases (Lawler *et al.*, 1998). Activated JNK can bind to and phosphorylate its downstream targets, which include transcription factors part of the activating protein 1 (AP-1) family such as c-Jun and activating transcription factor 2 (ATF-2), and regulate cellular processes such as apoptosis, survival and tumour development (Whitmarsh and Davis, 1996; Davis, 2000).

Another major MAPK pathway that has been studied for many years is the p38 pathway. Mammalian p38 MAPK is activated by a variety of stress stimuli, including UV light, heat, osmotic shock and inflammatory cytokines such as TNF-α (Freshney *et al.*, 1994; Rouse *et al.*, 1994; Pietersma *et al.*, 1997). Interestingly, certain stimuli, such as insulin, can activate p38 signalling in one cell type but inhibit it in another cell type, adding to the complexity of p38 signalling (Heidenreich and Kummer, 1996; Sweeney *et al.*, 1999). There are four splice variants of p38 identified (p38α, p38β, p38γ and p38δ) and each of them have a Thr-Gly-Tyr dual phosphorylation motif. p38 is phosphorylated predominantly by the MAPKKs MKK3 and MKK6, and they can differentially activate p38β. Furthermore, MKK4 can also activate p38α and p38δ in specific cell types; taken together, these observations suggest that the activity of specific p38 isoforms can be controlled through the coactivation of different upstream regulators (Jiang *et al.*, 1997; Parker *et al.*, 1998). The first substrate of p38 to be identified was the MAPK-activated protein kinase 2 (MK2), which has been shown to activate many other downstream substrates such as small heat shock protein 27 (HSP27) and cyclic adenosine monophosphate (cAMP) response element-binding protein (CREB) (Stokoe *et al.*, 1992; Rouse *et al.*, 1994; Tan *et al.*, 1996). Transcription factors are another group of substrates that are activated by p38, and include targets like ATF-1/2/6, p53 and ETS transcription factor ELK1 (Tan *et al.*, 1996; Thuerauf *et al.*, 1998; Huang *et al.*, 1999). Activation of the p38 pathway plays a part in many

different biological processes, including inflammation, apoptosis, cell differentiation, senescence and tumour development (Zarubin and Han, 2005).

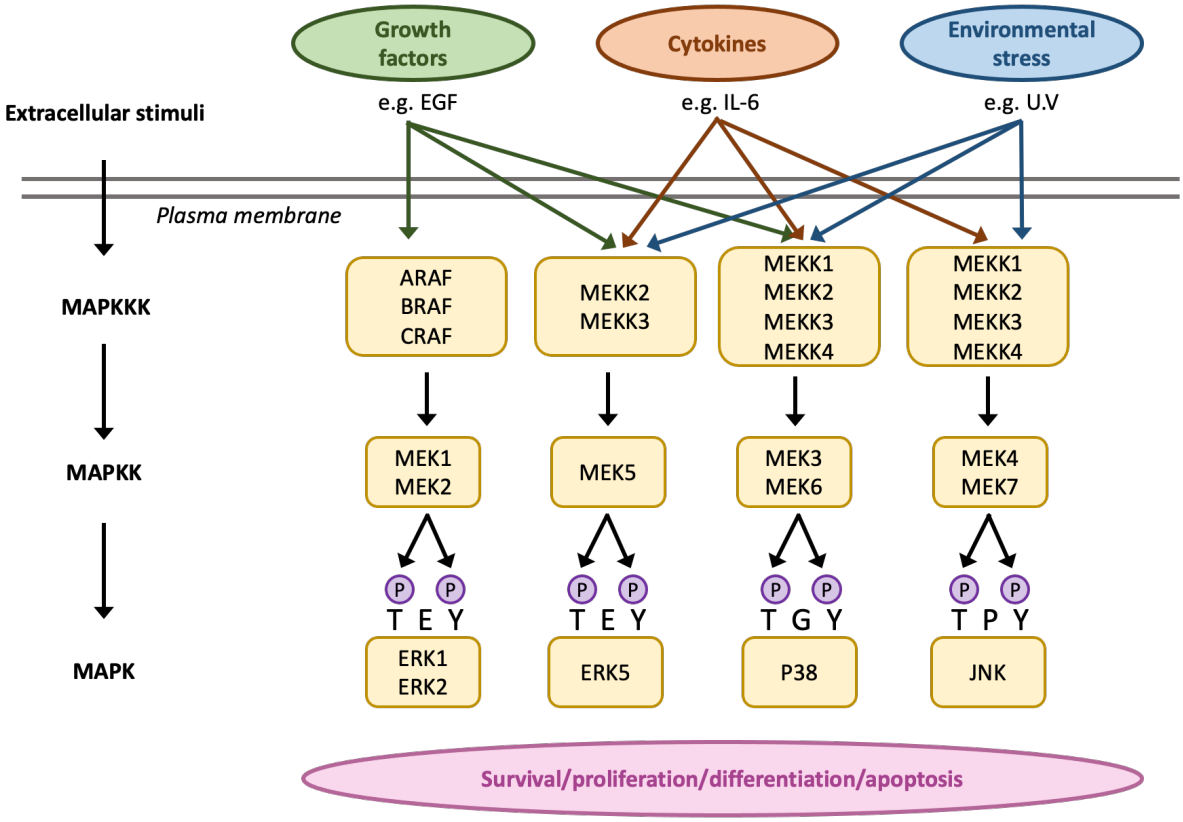

Figure 1.5. **Overview of the MAPK pathways.** Mammalian cells have four distinct MAPK pathways: the ERK1/2, p38, JNK and ERK5 pathways. Different stimulants activate the pathways, with each pathway regulating a number of different physiological responses. These pathways are comprised of three kinases modules, MAPKKK, MAPKK and MAPK. Please note MEKK is interchangeably used with MKK. Image adapted from Nithianandarajah-Jones *et al.,* (2012).

Lastly, a lesser understood and more recently discovered MAPK pathway is the ERK5 pathway. This pathway can be activated by a multitude of different growth factors such as epidermal growth factor (EGF), basic fibroblast growth factor (bFGF) and vascular endothelial growth factor (VEGF) (Kato *et al.*, 1998; Hayashi *et al.*, 2004; Kesavan *et al.*, 2004). It can also be activated by inflammatory cytokines such as interleukin-6 (IL-6) and osmotic and oxidative stress (Abe *et al.*, 1996; Carvajal-Vergara *et al.*, 2005). The MAPKKKs of this pathway that are activated by these stimuli are MEKK2 and MEKK3, which phosphorylate Ser311 and Thr315 of MEK5, which then activates ERK5 by phosphorylating the residues Thr219 and Tyr221 within a Thr-Glu-Tyr motif (Sun *et al.*, 2001; Mody *et al.*, 2003). Once activated, ERK5 can regulate a number of downstream transcription factors including members of the myocyte enhancer factor (MEF) family (MEF2A, C and D), c-Myc, CREB and synapse-associated protein

1a (Sap1a) (English *et al.*, 1998; Kamakura, Moriguchi and Nishida, 1999). ERK5 can also activate AKT via the VEGF receptor 2 (VEGFR2) and the PDGF receptor β (PDGFRβ), regulating cellular processes such as survival and apoptosis (Lennartsson *et al.*, 2010; Roberts *et al.*, 2010). ERK5 signalling plays a role in many different biological systems, and can regulate vascular smooth muscle cell migration and proliferation, facilitate neuronal cell survival and regulate cell proliferation and adhesion during carcinogenesis (Kato *et al.*, 1998; Liu *et al.*, 2003; Izawa *et al.*, 2007; Sawhney, Liu and Brattain, 2009).

The phosphatidylinositol 3-kinase (PI3K) pathway

The PI3K pathway is a commonly activated signalling pathway in human cancer (Samuels *et al.*, 2004; Fruman *et al.*, 2017). It plays an important role in connecting oncogenes and multiple receptor classes to essential cellular functions such as cell survival, motility and morphology (Vivanco and Sawyers, 2002; Bader *et al.*, 2005). The PI3Ks are members of a conserved family of lipid kinases that phosphorylate phosphatidylinositols and phosphoinositides (phosphorylated forms of phosphatidylinositols), resulting in the activation of many signalling pathways that regulate a diverse range of cellular functions. Intracellular signalling proteins are able to bind to and become activated by these phosphorylated lipids (Engelman, Luo and Cantley, 2006). The PI3Ks can be grouped into three classes (I-III) depending on sequence homology and substrate preference (Liu *et al.*, 2011).

The best characterised class of the PI3Ks is class I, which can be divided into classes Ia and Ib (Liu *et al.*, 2011). Class Ia PI3Ks are heterodimers composed of one of five regulatory subunit variants (p85α (which can be alternatively spliced to form p55α and p50α), p85β, and p55γ) and one of three catalytic subunits (p110α, p110β or p110δ) (Xu *et al.*, 2020). The regulatory subunit has two SH2 domains which allow for interaction with phosphorylated tyrosine residues on an RTK (or with adaptor proteins associated with receptors, such as insulin receptor substrate 1 (IRS1)) (Backer *et al.*, 1992; Zhou *et al.*, 1993). The regulatory subunit also interacts with the catalytic subunit keeping it in an inactive conformation in the cytoplasm, however, upon binding to an RTK, a conformational change relieves the inhibitory effect of the regulatory subunit on the catalytic subunit (Shoelson *et al.*, 1993; J. Yu *et al.*, 1998; Huang *et al.*, 2007). Once PI3K is near the membrane, the activated catalytic subunit is in close enough proximity to convert the membrane-bound phosphatidylinositol-4,5-bisphosphate (PIP_2) to phosphatidylinositol-3,4,5-triphosphate (PIP_3) (Whitman *et al.*, 1988; Koyasu, 2003). Class Ib enzymes are also heterodimers like class Ia enzymes, however, they have a p110γ catalytic subunit and a p101 regulatory subunit (Stoyanov *et al.*, 1995; Stephens *et al.*, 1997; Krugmann *et al.*, 1999). Furthermore, whilst class Ia enzymes are activated by RTKs, G-protein-coupled receptors (GPCRs) and

certain oncogenes such as RAS, class Ib enzymes are only activated by GPCRs (Bader *et al.*, 2005). Class II and III enzymes are less well-studied, and only have a catalytic subunit. The function of class II enzymes is not fully understood, whilst class III enzymes appear to play a role in regulating cell growth and also autophagy (Liu *et al.*, 2011).

One of the key downstream effectors of this pathway is protein kinase B (PKB), also called AKT. There are three isoforms: AKT1, AKT2 and AKT3, encoded by *PKBα, PKBβ,* and *PKBγ* (Nicholson and Anderson, 2002). AKT translocates to the plasma membrane which is mediated by the docking of a pleckstrin homology (PH) domain in its N-terminus to PIP_3 on the plasma membrane (Stokoe *et al.*, 1997). It is proposed that this causes a conformational change in AKT, resulting in the exposure of two critical phosphorylation sites, Thr308 in the activation loop and Ser473 in a hydrophobic region near the C-terminus (Alessi *et al.*, 1996; Andjelković *et al.*, 1997). Thr308 is phosphorylated by phosphoinositide-dependent kinase 1 (PDK1), whilst Ser473 is phosphorylated by mammalian target of rapamycin 2 (mTORC2); although phosphorylation of Thr308 is sufficient for AKT activation, maximal activity is achieved after phosphorylation of both sites (Scheid and Woodgett, 2001; Sarbassov *et al.*, 2005; He *et al.*, 2021).

Activated AKT phosphorylates a number of substrates either at the plasma membrane, cytosol or nucleus, including BCL2-antagonist of death (BAD), forkhead-related transcription factor (FOXO1) and glycogen synthase kinase 3 α/β (GSK3α/β) (Manning and Cantley, 2007; Franke, 2008). Many of these substrates have a consensus Arg-X-Arg-X-X-Ser/Thr motif, where X is any amino acid (Jaworski, Kluz and Trzepieciński, 1996). AKT inactivates many inhibitors of cell cycle progression, thus promoting processes involved in oncogenesis (Georgescu, 2010). One such target of AKT is proline rich Akt substrate of 40 kDa (PRAS40), a protein which binds to and inhibits mammalian target of rapamycin complex 1 (mTORC1), which is involved in protein synthesis and cell cycle progression (Sancak *et al.*, 2007; Szwed, Kim and Jacinto, 2021). AKT phosphorylates PRAS40 on Thr246 which leads to its dissociation from mTORC1, and thus activates it (Kovacina *et al.*, 2003; Haar *et al.*, 2007). A well characterised negative regulator of AKT activity is phosphatase and tensin homologue (PTEN) (Maehama and Dixon, 1998). PTEN is a phosphatase that acts as a direct antagonist of PI3K by catalysing the dephosphorylation of PIP_3 to PIP_2. Loss of PTEN results in AKT hyperphosphorylation and is found in many tumours (Haddadi *et al.*, 2018).

The RALGDS signalling pathway

RAS-like (RAL) GTPases were discovered more than thirty years ago by scientists trying to identify new members of the RAS family. RAL proteins share more than 50% homology with HRAS, NRAS and KRAS; they contain the GTP binding regions of RAS and also key amino acid residues including a C-terminal cysteine required for palmitic acid binding and subsequent anchoring to the plasma membrane (Chardin and Tavitian, 1986). RAL proteins are encoded for by two genes, *RALA* and *RALB,* located on human chromosomes 7 and 2, respectively (Rousseau-Merck *et al.*, 1988; Hsieh, Swaroop and Francke, 1990). Their encoded proteins share around 85% sequence identity, with the switch I and II regions being 100% identical, but with variation at the C-terminal HVR. This variation at the C-terminus allows for distinct subcellular membrane localisation and functions of the RAL proteins (Shipitsin and Feig, 2004).

RAL proteins are activated by RAL-guanine nucleotide exchange factors (RALGEFs) and this family of proteins includes RAL-guanine nucleotide dissociation stimulator (RALGDS), Ral GDP dissociation stimulator-like (RGL) and RalGDS-like factor (RLF) (Albright *et al.*, 1993; Murai *et al.*, 1997). These GEFs are able to bind to GTP-bound RAS via a RAS-association (RA) domain on the C-terminus, allowing RALGEFs to be recruited to the plasma membrane where RAL is also localised (Popovic *et al.*, 2016). GEFs are able to stimulate the exchange of GDP for GTP on RAL and therefore activate it (Gentry *et al.*, 2014). RALGEFs can also be indirectly activated by RAS, for example via the PI3K pathway. The N-terminus of PI3K-dependent kinase 1 (PDK1) is able to form a complex with the N-terminus of RALGDS upon EGF stimulation, relieving an autoinhibition of the catalytic domain of RALGDS (Tian *et al.*, 2002). RAL can also be activated in RAS-independent manners via a distinct group of GEFs: the RAL/PH/SH3-binding GEFs (RALGPS) (Rebhun, Chen and Quilliam, 2000; Ceriani *et al.*, 2007). This is achieved via calmodulin binding to RAL and also via an increase in intracellular Ca^{2+} levels (Hofer, Berdeaux and Martin, 1998; Clough, Sidhu and Bhullar, 2002).

The RAL proteins can interact with multiple downstream effector proteins and are involved in many different physiological processes (Yan and Theodorescu, 2018). The first effector protein of RAL to be identified was RAL-binding protein 1 (RALBP1), and it was shown that it contains a RAL-binding domain and that it binds specifically to active GTP-bound RAL-A. RALBP1 also contains a RHO-GTPase-activating protein (RHO-GAP) domain, allowing it to bind to cell division control protein homolog 42 (CDC42) (Cantor, Urano and Feig, 1995). CDC42 is a member of the RHO family of GTPases, a family of proteins known to regulate the actin cytoskeleton (Heasman and Ridley, 2008). CDC42

activates RAC, which then activates RHO, and all three of these proteins are able to regulate the polymerisation of actin to produce stress fibres, lamellipodia and filopodia, respectively. RALBP1, therefore, is able to regulate cell polarity, movement and division due to its RHO-GAP domain (Hall, 1992; Nobes and Hall, 1995). RALBP1 can also interact with REPS1 (RALBP1-associated Eps homology (EH) domain protein 1) and REPS2/POB1 (partner of RALBP1) proteins at the C-terminus distinct from the RAL-binding domain and the RHO-GAP domain. REPS1 and POB1 both contain Eps15 homology (EH) domains which are found on proteins involved in endocytosis (Yamaguchi *et al.*, 1997; Ikeda *et al.*, 1998). REPS1 can regulate receptor-mediated endocytosis by interacting with a RAB11-binding protein, RAB11-FIP2, via its EH domain. RAB11-binding proteins play a role in recycling endosomes, and RALBP1 is able to mediate regulation of endocytosis by interacting with REPS1 which interacts with RAB11-FIP2 (Cullis *et al.*, 2002).

RAL can also regulate exocytosis via its interaction with SEC5, another one of its effector proteins. SEC5 is a central component of the mammalian exocyst complex, which is a multiprotein complex involved in targeting of vesicles to the basolateral plasma membrane (Moskalenko *et al.*, 2002). The RAL proteins also regulate gene transcription and cellular transformation (Moghadam *et al.*, 2017). It has been shown that the RALGDS pathway plays a major role in RAS-dependent phosphorylation of c-Jun, a transcription factor that can regulate proliferation, differentiation and RAS-induced transformation (de Ruiter *et al.*, 2000). The authors showed that RLF, a RAS effector and also a RALGEF, was able to phosphorylate c-Jun upon RAS and RAL activation, thus regulating gene transcription and oncogenesis in this way. Another study has shown that RALGDS can also cooperate with activated RAF to induce transformation of cells, although the mechanism is unclear (White *et al.*, 1996).

The phosphoinositide-specific phospholipase Cε (PLCε) signalling pathway

The final major signalling pathway downstream of RAS is the PLCε pathway. There are six identified classes of PLC: PLCβ, PLCγ, PLCδ, PLCε, PLCζ and PLCη; they are enzymes that hydrolyse membrane phospholipids (phosphatidylinositol 4,5-bisphosphate (PIP_2)) to generate diacylglycerol (DAG) and inositol 1,4,5-trisphosphate (IP_3) (Rhee and Choi, 1992; Fukami *et al.*, 2010). DAG activates specific protein kinase C (PKC) isoforms and IP_3 binds to IP_3 receptors resulting in an increase in intracellular Ca^{2+} levels (Streb *et al.*, 1983; Huang, 1989). PLCε was identified as the isoform directly regulated by RAS. It contains two C-terminal RAS-binding domains (RA1 and RA2), via which RAS is able to bind and activate PLCε. It also contains an N-terminal GTP exchange factor (GRF CDC25) domain, the function

of which is not fully understood, however, it is thought to activate RAS and autoregulate its own PLC activity (Kelley *et al.*, 2001).

As PLCε regulates intracellular Ca^{2+} levels, it therefore may play a role in regulating many different biological processes that are controlled by calcium signalling. These processes include cell growth and transformation (Berridge, 1993). Furthermore, because PLCε also activates PKC, it follows that PLCε can regulate biological processes that are controlled by PKC activation. These include cell differentiation, migration and apoptosis (Reyland, 2009).

1.5 The ERK1/2 Pathway

The ERK1/2 (from here on referred to as ERK) pathway is the focus of my PhD research, and thus I will give a more in-depth review of this pathway. The ERK pathway was the first MAPK cascade to be identified as a downstream signalling pathway of RAS and over the last three decades much about it has been elucidated due to the immense amount of research output on this topic (Seger and Krebs, 1995; Dhillon *et al.*, 2007). The ERK pathway is activated in response to a number of different stimuli, including growth factors, hormones and cytokines. Upon binding of GTP to RAS, the serine/threonine protein kinase RAF is recruited to the membrane and subsequently activated. Three isoforms of RAF exist, ARAF, BRAF and CRAF (Cargnello and Roux, 2011).

The RAF proteins

The *CRAF* gene was the first human *RAF* gene to be identified and therefore has been intensively studied. CRAF was identified as the human cellular homologue of the acutely transforming murine retroviral oncogene product v-RAF, with ARAF and BRAF being discovered a few years after (Rapp *et al.*, 1983; Huleihel *et al.*, 1986; Beck *et al.*, 1987; Ikawa *et al.*, 1988). The mechanism of RAF activation is highly complex and involves membrane localisation, phosphorylation and dephosphorylation of certain residues, conformational changes, dimerisation and the binding of other proteins (Terrell and Morrison, 2019). The three RAF proteins share a common structure, with each containing three conserved regions, CR1 and CR2 at the N-terminus and CR3 at the C-terminus (Roskoski Jr, 2010). CR1 contains a RAS-binding domain (RBD) and a cysteine rich domain (CRD), both of which are required for recruitment of RAF to the membrane (Wellbrock, Karasarides and Marais, 2004). Binding of RAF to the plasma membrane is key to initiating the RAF activation process, however, simply binding of RAF to RAS-GTP does not stimulate RAF enzymatic activity as it has been shown that RAF can be activated

in a RAS-independent manner by artificially targeting it to the plasma membrane (Leevers, Paterson and Marshall, 1994; Stokoe *et al.*, 1994).

The initial contact of RAF with RAS is made via the RBD of RAF and the effector domain of RAS (Herrmann, Martin and Wittinghofer, 1995; Nassar *et al.*, 1995). The RBD of RAF was initially identified as an 81 amino acid residue region on the N-terminus of CRAF (which corresponds to a 77 amino acid region in ARAF) and RAS was shown to interact with it in a GTP-dependent manner (Vojtek, Hollenberg and Cooper, 1993). In addition to the RBD, the CRD of RAF also makes contact with RAS (Mott *et al.*, 1996). Williams and colleagues have shown that the CRD can interact with RAS with no preference for its nucleotide state, and that it can aide in membrane recruitment of RAF via interaction with the farnesyl groups of processed RAS (Williams *et al.*, 2000). The CRD can bind to RAS independently of RBD binding and is required for efficient RAS-RAF interaction. The CRD is also required for RAS-dependent activation of RAF and residues within the activator domain of RAS are critical for RAS-CRD interaction, thereby providing a possible explanation of the molecular basis of RAF activation by RAS (Hu *et al.*, 1995).

Further studies have also shown that RAF exists in an autoinhibited conformation, which is mediated in part by the binding of the CRD with the C-terminal catalytic domain of RAF, thereby supressing its kinase activity (Cutler Jr *et al.*, 1998; Chong and Guan, 2003; Tran and Frost, 2003; Tran, Wu and Frost, 2005). It has been shown that mutated RAS can activate CRAF by stimulating a conformational change from a closed 'inactive' conformation of RAF to an open 'active' conformation, hence supporting the notion that RAS plays an additional role in RAF activation other than membrane localisation (Terai and Matsuda, 2005). Another important role of the CRD of RAF is that it promotes the translocation of RAF to the membrane by interacting with phospholipids of the plasma membrane, therefore providing an additional means of membrane localisation (Ghosh *et al.*, 1994; Mott *et al.*, 1996). Lastly, although a lot of the early work on RAF was carried out with CRAF, the RBD and the CRD are highly conserved in all three RAF isoforms, and RAS also recruits ARAF and BRAF to the plasma membrane (Marais *et al.*, 1997; Wellbrock, Karasarides and Marais, 2004).

RAF activation also involves binding of other proteins, such as the adaptor protein 14-3-3. 14-3-3 proteins form dimers and they bind to phosphorylated serines within sequence-specific motifs (Muslin *et al.*, 1996). The RAF proteins contain two high-affinity 14-3-3 binding sites that are phosphorylation-dependent. One is in the CR2 region at the N-terminus (Ser365 of BRAF, Ser259 of CRAF, Ser214 of ARAF) and the other is after the kinase domain at the C-terminus (Ser729 of BRAF,

Ser621 of CRAF, Ser582 of ARAF) (Morrison *et al.*, 1993; Dougherty *et al.*, 2005; Daniel A. Ritt *et al.*, 2010). Both of these sites are phosphorylated in the inactive state of RAF when it is in its 'closed' conformation, and a proposed model is that 14-3-3 is not only required for the stabilisation of this inactive state via bivalent binding to both the N-terminus (phospho-Ser259) and the C-terminus (phospho-Ser621), but that it also stabilises the active conformation of CRAF once activated (Tzivion, Luo and Avruch, 1998) (see ***Figure 1.6***).

Upon binding of RAF to RAS at the plasma membrane, part of the 14-3-3 dimer is displaced from the CR2 site, thereby exposing the site to phosphatases and allowing for continued RAF activity (Rommel *et al.*, 1996; Roy *et al.*, 1998; Mcpherson *et al.*, 1999). Findings by Fischer and colleagues have suggested that prohibitin (PHB), a membrane chaperone, may be involved in displacing 14-3-3 from RAF (Fischer *et al.*, 2009). Displacement of 14-3-3 from Ser259 (of CRAF, which is the isoform that will be referred to in this section henceforth unless stated otherwise) causes a conformational change that exposes the kinase domain, and the 14-3-3 just displaced from Ser259 is free to either bind to Ser621 (within the CR3 of the kinase domain) (Morrison and Cutler, 1997), bind to unidentified phosphorylation sites at the N-terminus (Tzivion, Luo and Avruch, 1998) or bind to other adaptor proteins/be completely displaced from RAF (Fischer *et al.*, 2009), thereby stabilising the RAF open conformation and increasing RAF kinase activity.

Dimerisation of RAF proteins also plays a key role in their activation. It was first shown that RAS-independent CRAF dimerisation alone, without the need for any membrane localisation, was sufficient to activate CRAF and stimulate the ERK signalling cascade (Farrar, Alberola-lla and J, 1996). Studies later revealed that CRAF and BRAF dimers (hetero- and homodimers) can also form via RAS-dependent mechanisms, and that 14-3-3 proteins can play a role in this (Luo *et al.*, 1996; Weber *et al.*, 2001; Rushworth *et al.*, 2006). Interestingly, it has been demonstrated that BRAF can activate CRAF independently of its own kinase activity. Experiments have shown catalytically-impaired mutant BRAF being able to activate the ERK pathway, via both RAS-independent and RAS-dependent mechanisms, partly due to an enhanced ability to associate with CRAF (Garnett *et al.*, 2005; Heidorn *et al.*, 2010). Recent work by Morrison and colleagues has confirmed the importance of dimerisation in RAS-mediated RAF activity; they show that RAF dimerisation is a requirement for RAS-dependent RAF activation, and that RAF mutants also require this dimerisation unless they possess high catalytic activity. Furthermore, they also provide proof-of-principle evidence of an inhibitor of RAF dimerisation that suppresses RAF-dependent signalling (Freeman, Ritt and Morrison, 2013). This is significant

because many RAF inhibitors have failed in the past by promoting RAF dimerisation and paradoxically activating downstream ERK (Hatzivassiliou *et al.*, 2010; Heidorn *et al.*, 2010; Poulikakos *et al.*, 2011).

Regulation of CRAF activity also occurs via phosphorylation of several residues in addition to serines 259 and 621. For example, phosphorylation at Ser43 and Ser233 (and Ser259) inhibit CRAF activity. All three are targets of protein kinase A, a cyclic-AMP-dependent kinase, which induces hyperphosphorylation at these sites and reduces RAF activity (Dhillon *et al.*, 2002; Dumaz, Light and Marais, 2002). The mechanism of inhibition differs depending on which site of CRAF is phosphorylated. Ser43 phosphorylation seems to reduce the binding of CRAF to RAS by sterically hindering the interaction, and interestingly, phosphorylated Ser233 seems to be another 14-3-3 binding site, thus inhibiting RAF activity in a similar way to Ser259 phosphorylation as mentioned above (Wu *et al.*, 1993; Dumaz and Marais, 2003). Additionally, Ser259 can also be phosphorylated (and thus inhibited) by AKT (Zimmermann and Moelling, 1999).

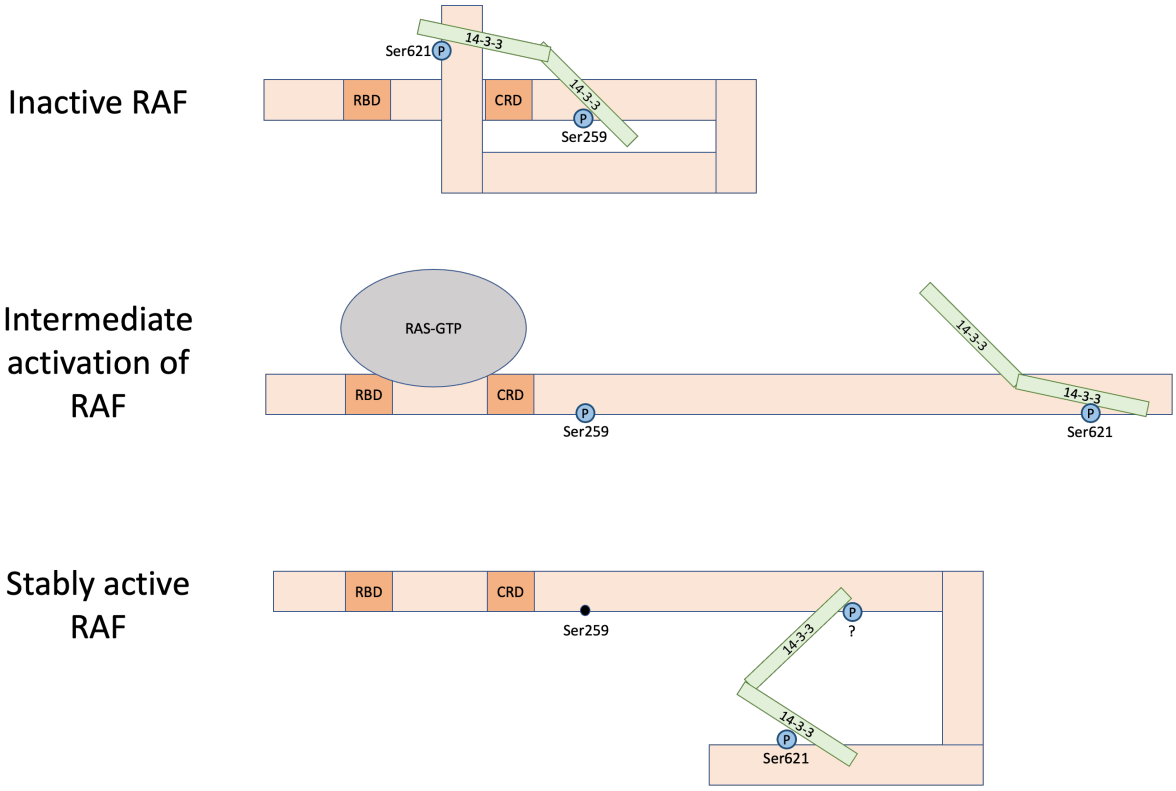

Figure 1.6. **A proposed model of RAF activation.** This model proposes that in the inactive state, a 14-3-3 dimer binds to both phosphorylated Ser259 at the N-terminus and phosphorylated Ser621 at the C-terminus and stabilises it in this conformation. Upon binding of RAF RBD and CRD to GTP-bound RAS, half of the 14-3-3 dimer is displaced from Ser259. Phosphorylation of further sites may occur and a conformational change allows the displaced 14-3-3 to bind to one the newly phosphorylated (unidentified) residues at the N-terminus and keep it in the open conformation. Image adapted from Tzivion, Luo and Avruch, (1998) and Fischer *et al.,* (2009).

CRAF can also be activated via phosphorylation of five key residues that are either within or flanking the kinase domain (Noble *et al.*, 2008). It has been difficult to precisely understand what phosphorylation at one of these sites, Ser621, accomplishes as it seems to play a role in both activating and inhibiting CRAF (Tzivion, Luo and Avruch, 1998). Four sites that must be phosphorylated for CRAF activation are Ser338, Tyr341, Thr491 and Ser494. Within the kinase domain, Thr491 and Ser494 fully inhibit CRAF activation when mutated (Barnard *et al.*, 1998; Chong, Lee and Guan, 2001). The residues Ser338 and Tyr341 are located at the N-terminal side of CR3; this segment is known as the N-region due to its negative charge, which is important for CRAF kinase activity (Mason *et al.*, 1999). Phosphorylation of Ser339 and Tyr340 also activates CRAF but there is conflicting evidence regarding whether these sites are critical for activation. There is evidence that mutations at these sites can either have no effect on CRAF activity, or that they can actually block activation (Fabian, Daar and Morrison, 1993; Marais *et al.*, 1995; Diaz *et al.*, 1997). These conflicting observations could be due to the use of different cell types and the possibility that CRAF activation is achieved via distinct molecular mechanisms in different types of cells. Furthermore, only a small proportion of the total CRAF pool is activated upon ligand stimulation, therefore issues with detection sensitivity could also provide false results (Hallberg, Rayter and Downward, 1994).

The five key phosphorylation sites for CRAF activation are conserved in ARAF, and overall ARAF activation is regulated in a similar manner to that of CRAF (Wellbrock, Karasarides and Marais, 2004). It has been shown that for CRAF and ARAF to achieve maximal activation, both GTP-bound RAS and phosphorylation of key tyrosine residues are necessary. On the other hand, BRAF can achieve strong activation upon stimulation by oncogenic RAS alone, and it also has a much higher basal activity level. Taken together, these observations suggest that BRAF might be the primary target of oncogenic RAS (Marais *et al.*, 1997). Furthermore, phylogenetic comparisons of all three RAF isoforms reveal that BRAF is the most similar to the RAF kinase homologues D-Raf (in *Drosophila*) and LIN-45 (in *Caenorhabditis elegans*). It is thus hypothesised that ARAF and CRAF might have evolved from BRAF (e.g., to carry out additional functions), and that BRAF is the prototypical RAF kinase (Desideri, Cavallo and Baccarini, 2015).

A key difference between CRAF and BRAF is that instead of a tyrosine residue at the equivalent position of Tyr341 on CRAF, BRAF has an aspartic acid (Asp448) (Marais *et al.*, 1997). Furthermore, although the activating Ser338 residue of CRAF is conserved in BRAF (Ser445), BRAF Ser445 is constitutively phosphorylated. BRAF does not require tyrosine phosphorylation for activation, and instead has an aspartic acid at key CRAF tyrosine residues. Replacing these acidic residues with

phenylalanine or alanine reduces BRAF activation by RAS, therefore it appears that these acidic residues regulate BRAF activity in some way. Substitutions at both Asp448 or Ser445 cause a decrease in BRAF basal activity, thus it seems as though both of these residues could be responsible for the relatively high basal activity of BRAF (Mason *et al.*, 1999).

Further differences between the RAF isoforms include differences in their binding affinities to RAS, how potently they are able to activate their downstream target mitogen activated protein kinase kinase 1/2 (MEK1/2) and the existence of splice variants. Weber and colleagues showed that compared to CRAF, ARAF has significantly lower binding affinity to HRAS and that HRAS is able to preferentially activate CRAF. This can be attributed to the exchange of an arginine to lysine at a key residue within the RBD (Arg59 in CRAF and Lys22 in ARAF) (Weber *et al.*, 2000). Because different RAS isoforms can localise to distinct membrane microdomains, the differential binding of different RAF isoforms to RAS can expose RAF proteins to distinct environments, which could affect their activity (Hancock, 2003). Different RAF isoforms are also able to differentially activate MEK1/2; with ARAF, CRAF and BRAF being the least to most potent activators, respectively. BRAF's strong MEK activation capability may be due to its higher basal kinase activity and also its ability to heterodimerise with MEK in the cytosol (Haling *et al.*, 2014). Another key difference between the RAF isoforms is that BRAF - contrary to ARAF and CRAF - is alternatively spliced, although recent research reveals that ARAF splice variants may exist (Barnier *et al.*, 1995; Rauch *et al.*, 2011). BRAF splice variants might have a key role in the work discussed in this thesis and, therefore, further details will be provided in **Chapter 3**.

Much insight has been gained into the specific roles of the different RAF isoforms from different knockout and transgenic mice models. Knockout studies of individual RAF isoforms have revealed the essential and non-overlapping roles these isoforms play in mice development, with most RAF knockout strains resulting in lethality (Leicht *et al.*, 2007). Pritchard and colleagues for example showed that *ARAF*-deficient mice had gastrointestinal and neurological defects and died within 21 days post-partum (Pritchard *et al.*, 1996). Another study showed that mice with a disrupted *BRAF* gene die during mid-gestation due to vascular defects (Wojnowski *et al.*, 1997). The same group also later showed that a mutation in the *CRAF* gene causes embryonic lethality, thus demonstrating that it is essential for mouse development (Wojnowski *et al.*, 1998). They also show that RAF signalling is critical for development beyond the blastocyst stage, but that there is a redundancy between the *CRAF* and *BRAF* genes until mid-gestation which allows for normal development if either gene is mutated (Wojnowski *et al.*, 2000). Other studies have also highlighted the critical roles of *CRAF* in counteracting

apoptosis (Mikula *et al.*, 2001), and *BRAF* in mediating the survival of embryonic sensory and motoneurons during development (Wiese *et al.*, 2001).

The role of the RAF isoforms in RAS-mediated oncogenesis has also been investigated in mouse models. Kern and colleagues have shown that ablation of *BRAF* causes a decrease in ERK activation and proliferation, which stops the onset and progression of RAS-driven epidermal tumours. In contrast, *CRAF* ablation triggers an ERK-independent increase in Rho-dependent kinase (ROK) signalling which, when combined with *BRAF* ablation, causes regression of established tumours (Kern *et al.*, 2013). In support of this, another study has shown that *CRAF* is critical for the development and maintenance of RAS-induced skin epidermis tumours and is required to restrain ROK signalling in the epidermis (Ehrenreiter *et al.*, 2009). In a study in adult mice, Blasco and colleagues have shown that whilst *CRAF* is critical for onset of RAS-driven NSCLC, *BRAF* ablation does not have any significant impact on tumour development, indicating a unique role of CRAF in mediating KRAS signalling (Blasco *et al.*, 2011). This is also supported by data published by Karreth and colleagues, who show that in a cancer mouse model, oncogenic KRAS-G12D signals via CRAF, which is essential for tumour initiation, whereas BRAF is dispensable (Karreth *et al.*, 2011).

MEK1/MEK2

Activated RAF propagates the signal by phosphorylating the two dual-specificity threonine/tyrosine kinases MEK1 and MEK2 (MAPK/ERK kinase 1/2), encoded by the *MAP2K1* and *MAP2K2* genes (Kyriakis *et al.*, 1992; Papin *et al.*, 1996; Yin *et al.*, 2002). MEK1 and MEK2, along with MKK3, MKK4, MKK6, MKK7 and MEK5 make up the current members of the mammalian MAPKK family (Nithianandarajah-Jones *et al.*, 2012). MEK1/2 proteins were first identified as activators of ERK1/2, and further studies revealed that MEK1/2 needed to be phosphorylated on specific serine residues in order to be activated (Ahn *et al.*, 1991; Gómez and Cohen, 1991; Zheng and Guan, 1993). MEK1/2 can also be activated via phosphorylation of common residues by MAPK kinase kinase (MEKK) independently of RAF, thus demonstrating the convergence of two independent kinases in regulating the activity of ERK1/2 (Gardner *et al.*, 1994). MEK1 and MEK2, which have molecular weights of ~45 kDa and ~46 kDa, respectively, share 85% sequence homology, with more than 90% similarity within their catalytic domains (Seger *et al.*, 1992; Xu *et al.*, 1997).

RAF phosphorylates MEK1 on Ser117/Ser221 and MEK2 on Ser222/Ser226, which are within a Ser-X-Ala-X-Ser/Thr motif conserved within the MAPKK family members (Alessi *et al.*, 1994; Lavoie and

Therrien, 2015). MEK1/2 proteins (from here on referred to as just MEK, unless specified otherwise) are composed of a large N-terminal regulatory region containing a nuclear export signal (NES), a short C-terminal region and a catalytic kinase domain (Fischmann *et al.*, 2009). The NES is important for the subcellular distribution of MEK as it allows it to be localised to the cytoplasm (Jaaro *et al.*, 1997). Similar to the NES sequences found in other proteins, the NES of MEK is rich in leucines which are critical for its activity. Mutations of specific leucine residues within the NES allow MEK to be evenly distributed throughout the cell rather than localise in the cytoplasm, indicating that without a functioning NES, MEK is able to freely diffuse through the nuclear membrane. MEK phosphorylation by RAF occurs in the cytoplasm, therefore cytoplasmic localisation of MEK plays a key role in the signal transduction of the ERK cascade (Fukuda *et al.*, 1996).

Other than simply transducing the signal from RAF to its downstream effector proteins, an additional role of MEK appears to be to convert graded signalling inputs into switch-like inputs. MEK phosphorylates only one residue of ERK (its downstream target) first, which is generally tyrosine but can sometimes be threonine, and these monophosphorylated ERK proteins are not active. Once a threshold of monophosphorylated ERK molecules has been reached, the second phosphorylation can occur, allowing for the rapid conversion from an inactive to an active state of ERK (Ferrell and Bhatt, 1997).

ERK1/ERK2

ERK1 and ERK2 are evolutionarily conserved proteins that are encoded by the *MAPK3* and *MAPK1* genes, respectively (Boulton *et al.*, 1991; Buscà, Pouysségur and Lenormand, 2016). ERK1 is activated by dual phosphorylation of Thr202 and Tyr204 and ERK2 is activated by phosphorylation of Thr183 and Tyr185; these sites are within a signature motif (Thr-X-Tyr) found in their activation segments (Payne *et al.*, 1991; Robbins and Cobb, 1992; Robbins *et al.*, 1993). It has been demonstrated that MEK phosphorylates the tyrosine residue first, dissociates from the mono-phosphorylated pY-ERK, then rebinds to and phosphorylates the threonine residue of the pY-ERK with high probability due to molecular crowding (Aoki *et al.*, 2011). Phosphorylation at these sites cause conformational changes that allow interaction with downstream substrates and increase the catalytic activity of ERK (Zhang *et al.*, 1994). ERK signalling can be inactivated by the removal of phosphate from the tyrosine residue, the threonine residue or both residues together. These sites can be dephosphorylated by protein serine/threonine phosphatases, protein tyrosine phosphatases and dual specificity phosphatases (Yao and Seger, 2004).

In addition to ERK1 and ERK2, splice variants of ERK also exist. For example, *MAPK3* can encode for ERK1c, which is a lower molecular weight ERK1 variant due to the introduction of a premature stop codon. Its expression levels are around 10% of that of ERK1 and it may play a unique role, which is not shared by ERK1, in cell-density induced Golgi fragmentation (Gonzalez *et al.*, 1992; Aebersold *et al.*, 2004). ERK can also be regulated via phosphorylation of additional residues. For example, phosphorylation of Ser244 and Ser246 within a Ser-Pro-Ser motif on ERK2 appears to facilitate its translocation to the nucleus by allowing ERK2 to bind to importin7, a nuclear translocating protein. This is important for ERK2 activity as some of its functions include the regulation of gene expression, amongst others that will be discussed later on (Chuderland, Konson and Seger, 2008). Another regulatory phosphorylation site is Thr188 within the activation loop of ERK2, which is autophosphorylated and has also been shown to promote nuclear localisation (Lorenz *et al.*, 2009). Phosphorylation at this site appears to play a role in cardiac hypertrophy by allowing ERK2 to phosphorylate nuclear targets known to cause it; this site is also unique in that it appears to integrate RAF-MEK signalling with G-protein-coupled receptor (GPCR)-initiated signalling to achieve this (Lorenz *et al.*, 2009; Ruppert *et al.*, 2013).

Differences between ERK1 and ERK2

ERK1 and ERK2 proteins have molecular weights of 44 kDa and 42 kDa, respectively, and they share a high degree of amino acid identity (around 90%). ERK2 has fewer residues just before the catalytic domain at the N-terminus, hence the lower molecular weight. Both proteins also appear to be activated by similar upstream stimuli, have comparable subcellular distribution patterns and share similar substrate recognition properties (Boulton *et al.*, 1991; Seger and Krebs, 1995). Due to these reasons, ERK1 and ERK2 were thought to be functionally redundant, however, numerous studies have since revealed critical functional differences between them. Genetic ablation of ERK2 results in embryonic lethality in early mouse development after the implantation stage, and ERK1 is unable to compensate for the loss of ERK2. This suggests that ERK2, but not ERK1, has a specific role in normal trophoblast development in mice (Saba-El-Leil *et al.*, 2003).

Pagès and colleagues have shown that, in contrast to ERK2, the loss of ERK1 is not lethal and mice with ERK1$^{-/-}$ are viable, fertile and normal size. This suggests that ERK1 may be dispensable and that ERK2 may be able to compensate for the loss of ERK1. However, loss of ERK1 does cause some non-lethal effects, such as deficits in thymocyte maturation. ERK1 plays a unique role in this as ERK2 is unable to compensate (Pagès *et al.*, 1999). Another example that shows isoform specificity is the role of ERK1 in

synaptic plasticity, where its ablation results in ERK2 activation in the brain and consequently behavioural and learning deficits in mice (Mazzucchelli *et al.*, 2002). Differences in cell cycle control have also been shown, with ERK2 (but not ERK1) knockdown interfering with cell cycle progression in hepatocytes and hepatocarcinoma cells *in vitro* and liver tumour growth *in vivo* (Frémin *et al.*, 2007; Bessard *et al.*, 2008). In other cell types such as fibroblasts, ERK1 ablation results in the enhanced activation of ERK2 and the consequent increase in cell proliferation (Vantaggiato *et al.*, 2006)

The numerous phenotypic differences outlined so far might depend on specific biochemical differences between ERK1 and ERK2. For example, Vantaggiato and colleagues have shown that the enhanced activity of ERK2 does not depend on changes in expression but on an increase in MEK-ERK2 complex formation upon ERK1 knockdown. This observation suggests that ERK1 might have higher affinity for MEK than ERK2 thus modulating ERK2-specific functions by displacing ERK2 from MEK (Vantaggiato *et al.*, 2006). Another biochemical property of ERKs critical to their function is the speed at which ERK1/2 can translocate to the nucleus and be retained in the nucleoplasm to exert transcriptional functions (Volmat *et al.*, 2001; Ando, Mizuno and Miyawaki, 2004; Costa *et al.*, 2006). Indeed, ERK1 shuttles through the nuclear membrane significantly slower than ERK2 because of differences in the N-terminal segment (residues 8-39 of ERK1). Differences in shuttling and relative dephosphorylation by phosphatases results in the slower ERK1 nuclear accumulation thus making ERK1, for example, less sensitive to serum stimulation (Marchi *et al.*, 2008).

Although there is ample evidence supporting clear isoform-specific roles of ERK1 and ERK2, more recent research suggests that they may in fact have redundant roles and that the more critical factor may be the total ERK levels. One such study in mice has shown that *ERK1 and ERK2* have redundant but kinase-dependent roles in hematopoietic progenitor functions (Chan, Gu and Neel, 2013). Buscà and colleagues used a novel approach to compare the evolution of *ERK1* and *ERK2* cloning sequences and protein expression levels across different vertebrates and found that both isoforms are functionally redundant and can act interchangeably in tetrapods (Buscà *et al.*, 2015). A recent in-depth review of current data on the ERK isoforms has suggested that ERK1 and ERK2 exhibit functional redundancy and that the total ERK quantity may be the critical factor in determining ERK function (Buscà, Pouysségur and Lenormand, 2016). Work published by Frémin and colleagues supports this hypothesis, as they have shown that the development of mouse placenta and embryo is strictly correlated with total ERK1/2 activity and not the presence of individual ERK isoforms (Frémin *et al.*, 2015).

Localisation and downstream effects of ERK1/2

In unstimulated cells, RAF, MEK and ERK proteins are localised in the cytoplasm, predominantly due to interactions with scaffolding/anchor proteins (Chuderland and Seger, 2005). Upon KRAS activation and the subsequent RAF and MEK activation, ERK proteins are released from their anchor proteins and are able to translocate to other compartments of the cell such as the nucleus, mitochondria, endosomes, Golgi apparatus and cytoskeletal elements (Yao and Seger, 2009). Not all of the kinase molecules get released from their anchors; for example, it has been shown that a portion of ERK molecules stay bound to one of their anchor proteins, PEA-15. This prevents ERK translocation to the nucleus and blocks its phosphorylation of ELK-1, a downstream nuclear transcription factor; PEA-15 also enforces cytoplasmic localisation of ERK due to the presence of a nuclear export sequence (NES) (Formstecher *et al.*, 2001).

A large portion of ERK molecules (around 50-70%) translocate to nucleus, where ERK can execute its nuclear effects (Chen, Sarnecki and Blenis, 1992). The main group of nuclear effectors regulated by ERK signalling are transcription factors, with one of the best studied being ELK-1. ERK phosphorylates ELK-1 which results in the induction of the immediate early gene (IEG) c-FOS, a protein important in the regulation of proliferation and differentiation (Marais, Wynne and Treisman, 1993; Cruzalegui, Cano and Treisman, 1999; Eferl and Wagner, 2003). Activated ERK is also able to modulate transcriptional suppression, for example, by phosphorylating and subsequently decreasing the repressive activity of ETS2 repressor factor (ERF), a transcriptional repressor (Sgouras *et al.*, 1995). ERK2 can impact nuclear processes by binding to DNA and by also activating PolyADP-ribose polymerase-1 (PARP1)) to modulate chromatin remodelling (Cohen-Armon *et al.*, 2007; Hu *et al.*, 2009). Furthermore, by phosphorylating nucleoporin-50 (NUP50), a key component of the nuclear core complex which is involved in the transportation of molecules across the nuclear membrane, ERK can regulate the nuclear translocation of other proteins (Kosako *et al.*, 2009).

ERK can also modulate mitochondrial functions, especially those associated with cell death. Under conditions of cellular stress, ERK appears to play a protective role by maintaining mitochondrial function (H. J. Lee *et al.*, 2004). A study has also shown that MEK and ERK are activated in cerebral cortical neurones upon exposure to hypoxia, and that this appears to protect these cells from hypoxic injury by the phosphorylation (and therefore inactivation) of the downstream pro-apoptotic protein BAD (Jin *et al.*, 2002). ERK molecules are also localised to the endosomes, which are intracellular membrane-bound compartments that transport signalling molecules bound to receptors; they play a

role in many cellular functions, including cell migration, intracellular signalling and intercellular communication (Miaczynska and Bar-Sagi, 2010). A scaffold protein involved in directing ERK proteins to endosomal vesicles is MEK1 partner 1 (MP-1), which only binds to MEK1 and ERK1, not MEK2 or ERK2. MP-1 enhances binding of ERK1 to MEK1 and increases ERK1 activation. It also operates in conjunction with another binding protein, termed p14, to direct ERK1 to the cytoplasmic surface of late endosomes (Wunderlich *et al.*, 2001). Finally, ERK molecules can also interact with the plasma membrane (via scaffold proteins such as paxillin), with cytoskeletal elements such as microtubules, and the Golgi apparatus (Reszka *et al.*, 1995; Ishibe *et al.*, 2003; Torii *et al.*, 2004; Boeckeler *et al.*, 2010).

Controlling ERK signal specificity

ERK signalling regulates numerous and often opposing biological processes. The depiction of ERK signalling as a linear cascade is in fact simplistic and could not explain the plasticity of this network. There are several mechanisms involved in modulating ERK signalling and allowing for tight control of signal specificity; including the control of duration and strength of signal, the involvement of scaffolding proteins, crosstalk between signalling pathways and the existence of multiple components at each level of the cascade (Wortzel and Seger, 2011). Specificity is also achieved by the ability of ERK to recognise and bind to specific docking sites on its substrates. Docking sites allow ERK to phosphorylate its phospho-acceptor sites (Ser/Thr-Pro being the minimum required recognition sequence) amongst the multiple potential phosphorylation sites on the substrate, and the position, arrangement, type and number of docking sites also impacts the affinity of a substrate for ERK (Fantz *et al.*, 2001). Two types of docking domains on ERK substrates include the D-domain and the DEF motif (Yang *et al.*, 1998; Jacobs *et al.*, 1999; Sheridan *et al.*, 2008). ERK contains a common docking (CD) domain (which includes key aspartate residues) via which it can bind to the D-domain on its substrates (Tanoue *et al.*, 2000; Zhou *et al.*, 2006). On the other hand, the DEF domain on substrates can form hydrophobic interactions with key leucine and tyrosine residues on ERK (T. Lee *et al.*, 2004).

One of the first mechanisms of signal specificity control to be elucidated was the role of signal duration. In phaeochromocytoma (PC12) cells, both epidermal growth factor (EGF) and nerve growth factor (NGF) could induce strong stimulation of ERK, but whilst EGF caused a transient response and resulted in cell proliferation, NGF caused a more sustained response and resulted in cell differentiation (Nguyen *et al.*, 1993). Cell differentiation also occurs when ERK activity is artificially prolonged upon EGF stimulation, supporting the notion that signal duration is key to controlling this, not just the

stimulus (Traverse *et al.*, 1994). In support of this, another study has shown that PDGF and basic fibroblast growth factor (bFGF), both of which induce sustained ERK signalling, are able to cause differentiation, whereas, insulin-like growth factor-1 (IGF-1), which only induces a transient response, does not trigger differentiation (Heasley and Johnson, 1992). More recently, it has been shown that sustained ERK signalling results in prolonged expression of certain transcription factors encoded by IEGs. Multiple signalling pathways positively regulate the induction of IEGs following exposure to extracellular stimuli, resulting in various cellular outcomes such as differentiation, proliferation and oncogenic transformation. Several of these IEG-encoded proteins contain an ERK docking site, allowing them to locally concentrate active ERK. These proteins can also act as ERK sensors as they can be post-translationally modified in a manner dependent on signal amplitude and duration, resulting in changes in the expression levels of these proteins (Murphy, MacKeigan and Blenis, 2004).

Another mechanism for controlling signal specificity is via the help of scaffolding proteins, which are proteins that interact with more than one protein in a signalling cascade. Scaffolding proteins bring target proteins within close proximity of each other, enabling them to induce faster kinetics, higher specificity, compartmentalisation and crosstalk between pathways (Good, Zalatan and Lim, 2011). They may also allow the same pathway to perform different functions in response to the same stimulus, for example, by recruiting different substrates. Examples of ERK-specific mammalian scaffolding proteins include MEK partner 1 (MP-1), kinase suppressor of RAS (KSR), β-arrestin and paxillin (Chuderland and Seger, 2005). Crosstalk between different pathways also plays a role in signal specificity, as multiple different pathways are able to modulate the activity of components at several tiers of the ERK cascade, usually via phosphorylation/dephosphorylation by kinases and phosphatases, respectively (Shaul and Seger, 2007). For example, MEK1 is a site for the convergence of integrin and growth factor induced signalling. PAK1, a downstream effector of the cell adhesion mediated-RAC1/CDC42 cascade, is able to phosphorylate MEK1 on Ser298, which not only appears to play a role in the control of cell adhesion and migration, but also in the efficient activation of MEK1 and subsequently ERK (Frost *et al.*, 1997; Slack-Davis *et al.*, 2003). Another group of kinases that are able to crosstalk with the ERK cascade are the cyclin dependent kinases (CDKs), a group of serine/threonine kinases involved in the regulation of cell cycle progression. CDK2 and CDK5 have been shown to phosphorylate MEK1 on Thr286 and Thr292, but unlike with PAK1, these phosphorylation events lead to an inhibition of MEK1 activity (Rossomando *et al.*, 1994; Sharma *et al.*, 2002; Tassin *et al.*, 2015).

Lastly, the presence of various isoforms at each tier of the signalling cascade plays an important role in determining signal specificity. The different proteins can have distinct functions and may be regulated differentially. For example, within the MAP3K tier, in addition to the RAF proteins discussed earlier, it also includes c-Mos, TPL2 and MEKK1, all of which can operate under distinct conditions (Rubinfeld and Seger, 2005). The predominant proteins within the MAP2K tier are MEK1 and MEK2, and although they are highly similar and mediate similar transcriptional and morphological responses, clear differences in their functions have been demonstrated. For example, knockout of MEK1 causes embryonic lethality in mice, whereas MEK2 knockout mice are viable and fertile (Mansour *et al.*, 1996; Giroux *et al.*, 1999; Bélanger *et al.*, 2003). Differences in interactions of MEK1 and MEK2 with different RAF isoforms and RAS have also been demonstrated. For example, RAS and CRAF can form complexes with only MEK1, not MEK2; another study has shown that CRAF can activate both MEKs whereas ARAF can only active MEK1 (Jelinek *et al.*, 1994; Wu *et al.*, 1996). Importantly, this can have an impact on cell cycle progression as the MEKs have differential effects on G_2/M arrest and the G_1/S phase of the cell cycle (Liu *et al.*, 2004; Ussar and Voss, 2004). Finally, within the MAPK tier, ERK1, ERK2 and alternatively spliced ERK variants exist, which can be distinctly regulated as already discussed earlier.

In conclusion, signal transduction pathways in general – and ERK signalling specifically - do not simply relay a signal from the plasma membrane to a subcellular compartment. Crosstalk and feedback between a multitude of enzymes permit the cell to robustly amplify molecular cues, integrate and process information from the extracellular and intracellular environments, and to coordinate the most appropriate responses and transcriptional programmes. To better understand how ERK signalling contributes to cell decision making during carcinogenesis, my work has focused on how ERK signalling is rewired in the context of different KRAS mutations, with the ultimate aim of linking this with cell fate decisions in future work.

Feedback regulation of the ERK pathway

In addition to the mechanisms discussed above, ERK signalling specificity is also highly controlled via numerous positive and negative feedback loops within the whole of the RTK-RAS-RAF-MEK-ERK pathway (Lake, Corrêa and Müller, 2016). In this section, I will summarise the key phosphorylation sites on the different components of this pathway, including important adaptor proteins. The key activatory phosphorylation sites have already been discussed (which are included in the summary shown in ***Figure 1.7***), therefore, this section will focus more on the inhibitory interactions. There are two main types of negative feedback loops in this pathway: direct posttranslational modification of

pathway components, which occur nearly instantaneously, and the induction of *de novo* gene expression and protein synthesis of inhibitors of the pathway, which can take relatively longer.

Direct feedback phosphorylation

Nearly all components of this pathway can be phosphorylated in a negative manner by ERK, with one being the growth factor receptors (Lake, Corrêa and Müller, 2016). Several studies have shown that ERK can phosphorylate EGFR on Thr669 (Northwood *et al.*, 1991; Takishima *et al.*, 1991), which is a conserved Ser/Thr phosphorylation site located in the juxtamembrane region of the receptor (Sato *et al.*, 2013). Sato and colleagues showed that Thr669 phosphorylation reduces the level of constitutive tyrosine phosphorylation, which appears to reduce the ability of the phosphorylated juxtamembrane region to transactive the other receptor of the dimer. They show that Thr669 phosphorylation is dependent on ERK activity, and thus provide an ERK-mediated mechanism of EGFR downregulation (Sato *et al.*, 2013). Interestingly, it has been shown that Thr669 phosphorylation can also inhibit EGFR downregulation, thereby increasing its activity (Li *et al.*, 2008).

There is also a negative feedback loop between ERK and the adaptor protein SOS1. It has been shown that ERK pathway activation results in the hyperphosphorylation of SOS1, and that this is prevented by MEK inhibition (Langlois *et al.*, 1995) and increased by ERK overexpression (Yachis *et al.*, 1994). It has further been shown *in vitro* that ERK phosphorylates SOS1 on multiple sites (Ser1132, Ser1167, Ser1178 and Ser1193) (Corbalan-Garcia *et al.*, 1996). Hyperphosphorylation of SOS1 results in disassociation of SOS1 from the adaptor proteins GRB2 and SHC (Src homology 2 domain containing transforming protein), and therefore disrupts its association with the RTK (Langlois *et al.*, 1995; Corbalan-Garcia *et al.*, 1996; Porfiri and Mccormick, 1996). ERK can also phosphorylate SOS1 via ribosomal s6 kinase 2 (RSK2), an ERK effector protein. The phosphorylated sites (Ser1134 and Ser1161) are different to the ones targeted directly by ERK and it has been shown that RSK2-mediated SOS1 phosphorylation allows 14-3-3 to bind which results in downregulation of ERK pathway activity (Saha *et al.*, 2012).

A negative feedback loop from ERK to FGF receptor substrate 2α (FRS2α) also exists. The FRS2 proteins (FRS2α and FRS2β) are adaptor proteins that bind to several different activated RTKs (including FGF and EGFR) via their phosphotyrosine binding (PTB) domains and they contain several tyrosine phosphorylation sites which allow them to bind to GRB2 (Kouhara, Hadari and Schilling, 1997). It has been shown that FRS2α can be phosphorylated on eight threonine residues (Thr132, Thr135, Thr138,

Thr376, Thr452, Thr455, Thr458 and Thr463) via an ERK-dependent feedback mechanism, and that phosphorylation of these residues results in reduced tyrosine phosphorylation of FRS2α and thereby reduced GRB2 association (Lax *et al.*, 2002; Wu, Chen and Ullrich, 2003).

In addition to the negative feedback interactions from ERK to adaptor proteins, ERK can also negatively regulate RAF and MEK. Ueki and colleagues provided the first evidence of CRAF being subjected to feedback phosphorylation; they showed that CRAF is hyperphosphorylated (which results in the downregulation of its activity) upon insulin treatment, and that this occurs in a delayed manner post-activation of CRAF, MEK and ERK. Furthermore, they show that ERK overexpression enhances the CRAF hyperphosphorylation, indicating an ERK-mediated negative feedback loop (Yachis *et al.*, 1994). Further studies have shown that pharmacological inhibition of ERK results in increased and more sustained CRAF activity (Alessi *et al.*, 1995; Weiss, Maga and Ramirez, 1998) and that hyperphosphorylation of CRAF results in reduced association with the plasma membrane, therefore indicating a possible mechanism of the negative feedback regulation of CRAF (Wartmann *et al.*, 1997). At least five residues on CRAF (Ser29, Ser289, Ser296, Ser301 and Ser642) have been identified as sites that can be directly phosphorylated by ERK. Phosphorylation at these sites reduces the ability of CRAF to bind to the plasma membrane and engage activated RAS, and also prevents sustained CRAF activity (Dougherty *et al.*, 2005). ERK can also negatively regulate BRAF via phosphorylation on four sites (Ser151, Thr401, Ser750 and Thr753) and mutational analysis suggests that this is due to disruption of BRAF dimerisation to CRAF (with Ser151 phosphorylation also inhibiting BRAF interaction with activated RAS) (Brummer *et al.*, 2003; Daniel A. Ritt *et al.*, 2010).

Another target of ERK-mediated negative feedback regulation is MEK. ERK has been shown to phosphorylate MEK1 at Thr292 and Thr386 in an inhibitory manner (Brunet, Pagès and Pouysségur, 1994; Coles and Shaw, 2002). Phosphorylation of Thr292 has been shown to interfere with the binding of MEK1 to ERK2 (Eblen *et al.*, 2004) and it has also been shown to inhibit its kinase activity (Rossomando *et al.*, 1994). Finally, direct negative feedback loops also exist between ERK and scaffold proteins such as KSR1. KSR1 interacts with RAF, MEK and ERK in the cytoplasm (Therrien *et al.*, 1996; Xing, Kornfeld and Muslin, 1997; Douville *et al.*, 1998; W. Yu *et al.*, 1998), and has been shown to translocate to the plasma membrane upon growth factor stimulation (Copeland *et al.*, 2001; Müller *et al.*, 2003). ERK1 associates with KSR1 in a RAS-dependent manner, and a number of residues on KSR1 (Thr260, Thr274, Ser320, Ser443 and Ser463) have been shown to be phosphorylated by ERK *in vitro* in cells stimulated with growth factors (Cacace *et al.*, 1999; Canal *et al.*, 2011). Disrupting the phosphorylation of these sites by ERK results in the increase and prolonged association of KSR1 to

BRAF (suggesting that KSR1 phosphorylation may disrupt the ternary KSR1-BRAF-MEK complex) and also promotes the dissociation of KSR1 from the plasma membrane, thus downregulating ERK signalling (Mckay, Ritt and Morrison, 2009).

Transcriptionally induced feedback mechanisms

ERK pathway activation can induce the transcription of dual-specificity phosphatases (DUSPs), which downregulate ERK pathway signalling by dephosphorylating activated ERK (Huang and Tan, 2012). It has been shown that FGF can induce the expression of DUSP6, and that this is blocked by MEK inhibition, suggesting an involvement of DUSP6 in pathway feedback regulation (Ekerot *et al.*, 2008). The upregulation of DUSP6 is mediated by the binding of ERK1/2 responsive transcription factor (ETS1) to the DUSP6 gene promoter, and it has also been shown that overexpression of DUSP6 (but not a phosphatase-dead mutant) reduces the level of EGF-stimulated phospho-ERK, indicating that ERK-induced DUSP6 expression results in negative feedback via ERK dephosphorylation (Ekerot *et al.*, 2008; Zhang *et al.*, 2010). Additionally, DUSPs may also potentially delay reactivation of ERK by anchoring inactive ERK in the nucleus or cytoplasm due to their restricted distribution (Karlsson *et al.*, 2004; Mandl, Slack and Keyse, 2005).

The SPROUTY proteins (encoded by the *SPRY* genes) are another group of transcriptionally induced inhibitors of ERK signalling (Casci, Vinós and Freeman, 1999; Guy *et al.*, 2009). There are four mammalian *SPRY* genes identified and their transcription can be induced by growth factor signalling (Ozaki *et al.*, 2001; Panagiotaki *et al.*, 2010). Several groups have shown that MEK inhibition can block RTK-induced expression of SPROUTY proteins, suggesting a role of ERK in feedback modulation via SPROUTY (Yang *et al.*, 2006; Jiang *et al.*, 2011; Sylvestersen *et al.*, 2011). SPROUTY proteins can interact with a number of different components of the ERK signalling pathway, including CRAF, BRAF and GRB2, but it is not always fully understood how these associations modulate signalling (Mason *et al.*, 2006). Hanafusa and colleagues showed that EGF or FGF stimulation results in SPROUTY1 and SPROUTY2 translocating to the plasma membrane, and that a conserved N-terminal tyrosine residue is also phosphorylated (Tyr53 on SPROUTY1 and Tyr55 on SPROUTY2). Phosphorylation at this site allows the SH2 domain of GRB2 to bind, thereby disrupting the interaction between GRB2 and the FGFR adaptor FR2, resulting in pathway inhibition (Hanafusa *et al.*, 2002). Others have reported that SPROUTY proteins may be able to inhibit RAS signalling via interaction with CRAF (Yusoff *et al.*, 2002; Sasaki *et al.*, 2003). Other possible mechanisms of ERK-mediated feedback regulation via SPROUTY have also

been reported, with the current data suggesting that SPROUTY can act on multiple nodes on the pathway in a cell- and context-dependent manner (Masoumi-Moghaddam, Amini and Morris, 2014).

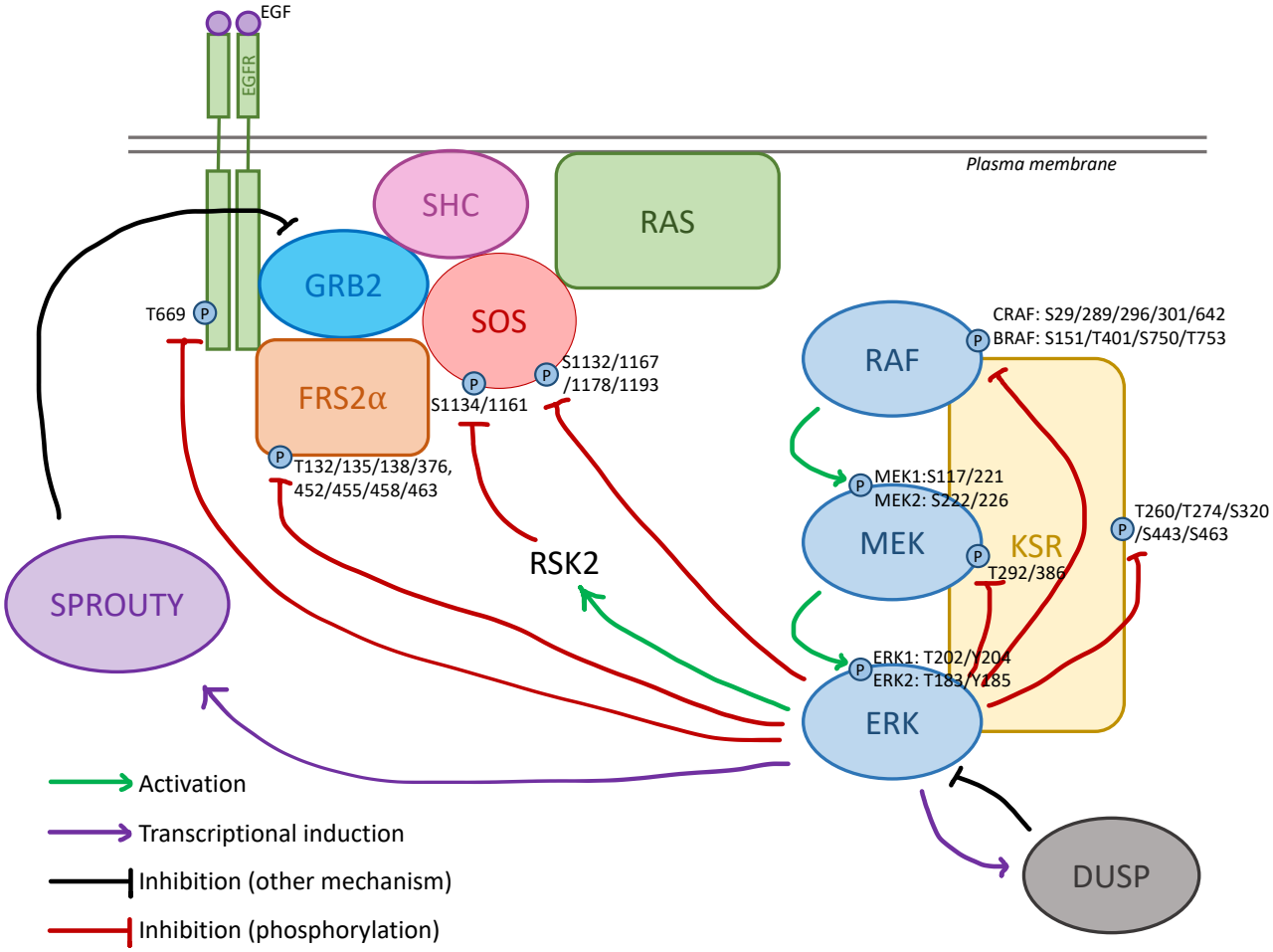

Figure 1.7. **ERK pathway feedback regulation.** Illustration showing the main activatory phosphorylations on the ERK pathway components and the negative feedback regulation in the larger network. The negative feedback loops include transcriptionally induced feedback regulators such as SPROUTY proteins and DUSPs and also direct phosphorylations by ERK on other proteins. The key inhibitory phosphorylation sites are labelled on each ERK target. Image adapted from Lake, Corrêa and Müller (2016).

Studies involving network analysis have helped increase the understanding of pathway signalling kinetics and the consequences of pathway rewiring on cell fate decisions. For example, Traverse and colleagues have shown that in PC12 cells, stimulation with EGF results in proliferation, whereas NGF causes differentiation (Traverse *et al.*, 1992). Network analysis via computer simulation has suggested that differential feedback regulation of the ERK cascade is the major determinant of these differences observed in PC12 cells (Brightman and Fell, 2000). This data has also been further supported by Santos and colleagues who utilised the Modular Response Analysis technique to show that a negative feedback loop from ERK to CRAF is present in cells stimulated with EGF, whereas there is a positive loop in cells stimulated with NGF (Santos, Verveer and Bastiaens, 2007). The role of negative feedback regulation in the ERK cascade has been studied further by other groups. For example, Sturm and colleagues utilised mathematical modelling and experimental validation to show that the ERK pathway has properties of a 'negative feedback amplifier' (NFA). An NFA confers the signalling cascade: robustness to change, increased output stability and characteristics of a graded response (as opposed to a switch-like one) (Sturm *et al.*, 2010). This negative-feedback-mediated robustness has also been demonstrated by further experimental work and mathematical network analysis (Fritsche-Guenther *et al.*, 2011).

Understanding feedback regulation is important for the development of therapies because inhibition of ERK pathway components can inhibit feedback loops, which can have critical effects on therapeutic response and drug resistance. In cells with mutations upstream of the cascade (such as within RTKs or RAS), negative feedback loops can reduce the activity of downstream MEK and ERK, however, inhibitors of MEK or RAF can weaken the negative feedback loops, resulting in increased MEK and ERK activity instead (Lake, Corrêa and Müller, 2016). Sturm and colleagues predicted this behaviour based on their proposed NFA model and also supported this with experimental data, showing that increasing U0126 (MEK inhibitor) concentration weakened the negative feedback and increased resistance to U0126. They showed that resistance persists until high enough inhibitor concentrations (that can fully inhibit ERK signalling) are used (Sturm *et al.*, 2010). Based on their modelling studies, they also suggested that inhibition of pathways outside of the NFA or inhibition of scaffold proteins would likely produce better drug responses, and this has been supported by a study in which *SPRY2* silencing improved the sensitivity of BRAF-mutant thyroid cancer cells to ERK pathway inhibition by ten-fold compared to control cells (Dultz *et al.*, 2013).

Negative feedback loops can also play a role in the development of resistance to ERK pathway inhibitors. Several studies have shown an association between activation of RTKs or RAS and resistance

to RAF inhibitors (Nazarian *et al.*, 2010; Yadav *et al.*, 2012; Nissan *et al.*, 2014). Activation of these upstream components of the ERK cascade combined with the relief of negative feedback can ultimately result in the increase of RAS-GTP-dependent RAF dimers, which are insensitive to RAF inhibition (Poulikakos *et al.*, 2010). Treatment with RAF inhibitors can also cause the activation of parallel pathways downstream of RTKs due to their increased activity as a result of the loss of negative feedback regulation on these receptors. For example, prolonged BRAF inhibition in melanoma cells can result in the upregulation of the insulin-like growth factor 1 receptor (IGF-1R) and increased activation of AKT (Villanueva *et al.*, 2010).

To conclude, multiple mechanisms of feedback regulation exist within the RTK-RAS-RAF-MEK-ERK pathway, enabling for the tight control of signalling dynamics. Network analysis has aided in increasing the understanding of how the ERK pathway can be rewired, and ***Figure 1.7*** summarises the key negative feedback regulations along with the activating interactions discussed earlier in the chapter. In order to develop more effective cancer therapies, it is of much importance to fully understand the role of feedback regulation due to its critical impact on the development of drug resistance.

1.6 RAS mutations in cancer and the current therapeutic landscape

1.6.1 Frequency of RAS mutations in cancer

There is a widespread prevalence of RAS mutations in human cancers, with mutations in RAS first being discovered more than thirty years ago and numerous studies having since validated mutated RAS as a driver of tumorigenesis (Hobbs, Der and Rossman, 2016; Jinesh *et al.*, 2018). When comparing the three RAS isoforms (KRAS4a and KRAS4b grouped together), *KRAS* is the most frequently mutated and is found in 75% of RAS-mutant cancers, followed by *NRAS* mutations in 17% of patients and *HRAS* mutations in 7% of patients (Prior, Hood and Hartley, 2020). The main cancers in which *KRAS* mutations are most common are pancreatic ductal adenocarcinoma (PDAC), colorectal cancer (CRC), and non-small cell lung cancer (NSCLC); and when looking at frequencies of mutations in these cancers, 91% of pancreatic cancers, 42% of colon cancers and 33% of lung cancers have a *KRAS* mutation. Also of significance, 27% of melanomas have an *NRAS* mutation (Simanshu, Nissley and McCormick, 2017). As supported by these statistics, there appears to be an isoform-specific role of RAS in different cancer types, and it has been shown experimentally in mouse models that HRAS and

NRAS are not required for growth and development, whereas KRAS appears to be essential (Umanoff *et al.*, 1995; Johnson *et al.*, 1997; Koera *et al.*, 1997; Esteban *et al.*, 2001).

Across the top three KRAS-driven cancers, 98% of KRAS-activating mutations are at codons 12, 13 and 61 with G12 codon substitutions being the most common KRAS mutations in human cancers (please note, for simplicity, one letter amino acid codes will be used when discussing RAS mutations). At codon 12, the G12D mutation is the most prevalent, followed by G12V and then G12C (Lu *et al.*, 2016b). Not only is there a cancer-specific difference in the mutational frequency of the RAS isoform, but also of the codon that is mutated. In addition, the substitutions at these codons also differ in a tissue-specific manner (Haigis, 2017; Cook *et al.*, 2021). It is not fully understood why there are these mutational frequency variabilities between different cancers, with the exception of the increased frequencies of G12C and G12V mutations in NSCLC being explained by a smoking-related mutational mechanism (the G:C to T:A transversion, which is responsible for these amino acid substitutions, is a known smoking-related mutation) (Nelson *et al.*, 1999; Ahrendt *et al.*, 2001).

Whilst tissue-dependent mutational landscapes are driven by tissue-specific mutagenic processes, mutational signatures alone cannot explain the frequency of codon substitutions. Notably, emerging evidence shows that both mutation and selective pressure drive the variation in distribution of *KRAS* driver mutations in different tissue types (Temko *et al.*, 2018). Specific *KRAS* mutations are more favoured by natural selection in specific tissue types, and these mutations correlate with worse clinical outcomes. A new picture is thus emerging whereby different codon substitutions result in distinct responses that can drive carcinogenesis only in permissive tissues (Ostrow *et al.*, 2016).

Several early studies have shown that specific codon substitutions in RAS can result in distinct biological manifestations such as altered transforming potential (Seeburg *et al.*, 1984; Pincus and Brandt-Rauf, 1985; Der, Finkel and Cooper, 1986). More recent work has also shown that different RAS mutants can have distinct transforming capabilities (Smith *et al.*, 2010; Stolze *et al.*, 2014). In addition to *in vitro* studies, genetically engineered mouse models and xenograft models have also been utilised to study the biological impact of different RAS mutations (Muñoz-Maldonado, Zimmer and Medová, 2019). For example, one study showed that whilst both KRAS G12V and G12D mutations generated tumours in nude mice, cells with the G12V mutation grew significantly quicker compared to those with the G12D mutation. Interestingly, they also showed that the G12V mutant interacts with CRAF and predominantly signals via the ERK pathway, whereas the G12D mutant signals via the PI3K/AKT, JNK, p38 and FAK (focal adhesion kinase) pathways and results in the development of less

aggressive tumours (Céspedes *et al.*, 2006). Another study, by Haigis and colleagues, looked at the impact of G12D mutations in KRAS and NRAS. They showed that mutant KRAS, but not NRAS, promotes hyperplastic growth in the colonic epithelium of mice (Haigis *et al.*, 2008). It has also been shown that the NRAS Q61R mutation results in decreased intrinsic GTPase activity and enhanced nucleotide binding compared to the NRAS G12D mutation, and that mice harbouring the Q61R mutation develop nevi more frequently than mice with the G12D mutation (Burd *et al.*, 2014). Collectively, these studies provide evidence of different RAS mutations resulting in distinct transforming potentials and that this can depend on not only the mutation, but also the RAS isoform and cell type.

The impact of RAS mutations on effector interactions and downstream signalling has also been studied. For example, Hunter and colleagues investigated the affinity of specific KRAS mutants for the RBD of CRAF, and found that G12A, G12C, G13D, Q61L and Q61H all displayed a 1.2 to 2.3-fold decrease in CRAF affinity compared to WT RAS, and that G12D, G12R and G12V showed even lower affinity (4.8 to 7.3-fold decrease) (Hunter *et al.*, 2015). Stolze and colleagues also found that in MCF10A breast cancer cells with ectopically expressed mutant KRAS, only the G13D mutant (and not the codon 12, 18, 61 or 117 mutants) promoted phosphorylation of both EGFR and p53. They suggest that this could explain the favourable outcome of patients with G13D-mutant colorectal cancer receiving anti-EGFR therapy compared to those patients with G12 mutations (Stolze *et al.*, 2014).

Different RAS mutations can also differentially impact the transcriptional, proteomic and metabolic profile of cells. Roberts and colleagues investigated the expression pattern of over 2000 genes in G12V-mutant HRAS and KRAS tumours *in vivo*, and found that 26 genes were differentially regulated between the KRAS G12V and HRAS G12V tumours, including genes involved in Notch signalling, cell motility, cytokinesis and angiogenesis (Roberts *et al.*, 2006). Quantitative analysis of the proteome and phosphoproteome of SW48 colorectal cancer cells harbouring specific KRAS mutations has also revealed that G12D and G12V-expressing cells have similar signatures that cluster together but are different to the G13D signature (Hammond *et al.*, 2015). Finally, Brunelli and colleagues characterised the metabolic profile of NSCLC cells overexpressing KRAS WT or KRAS G12D, G12C or G12V mutations and found that although many metabolites identified were common to all three mutants, each mutant also uniquely harboured a set of metabolites when compared to the WT cells (Brunelli *et al.*, 2014). These studies further reiterate the fact that the impact of a RAS mutation depends on multiple factors including the site of mutation, the specific amino acid substitution at that site and also the RAS isoform affected.

Another important issue to consider is the function of wild-type (WT) KRAS in tumourigenesis. Results from studies using mouse models suggest a tumour suppressive role of WT KRAS, as loss of the WT allele results in enhanced tumour progression (Zhang *et al.*, 2001; To *et al.*, 2013). However, it is not fully understood whether this is due to WT KRAS being a tumour suppressor, or whether its due to the WT:mutant ratio being critical. The resulting 'allelic imbalance' is seen frequently in tumours in mice and humans, and importantly, it may have an impact on cancer treatment (Burgess *et al.*, 2017). It is not known whether allelic imbalance is associated with specific alleles, however, it is feasible that the biochemical properties of different KRAS mutants may render KRAS differentially sensitive to regulation of its expression levels (Haigis, 2017).

Biochemistry of allele substitutions

The most common RAS mutations cluster around the nucleotide-binding pocket, with G12 and G13 being within the P-loop; as mentioned very early on in this chapter, the P-loop is part of the effector lobe of RAS (Buhrman *et al.*, 2011). Although right next to each other, these two sites have distinct effects on the biochemistry of RAS. Whilst G12 and G13 mutations decrease GTP hydrolysis (both intrinsic and GAP-induced), G13 mutations also increase the intrinsic rate of nucleotide exchange (Hunter *et al.*, 2015). X-ray crystallography data shows that the G13D mutation causes a change in the electrostatic charge distribution of the active site, which can explain this increased nucleotide exchange rate (Lu *et al.*, 2015). On the other hand, the structural explanation for the decrease in intrinsic GTP hydrolysis is less well-understood. Generation of electrostatic potential maps show that the backbone nitrogen atoms of both G12 and G13 contribute to charge stabilisation during hydrolysis, therefore, mutations at these sites could also have effects on the local electrostatic environment, resulting in the destabilisation of the transition state (Smith, Neel and Ikura, 2013; Hunter *et al.*, 2015). Stolze and colleagues characterised the GTPase activity of different KRAS mutants by determining the KRAS-GTP levels in MCF10A cells expressing different KRAS mutants. They found that KRAS G12D and G13D cells showed similar KRAS-GTP levels as WT KRAS, indicating similar GTPase activity levels. However, KRAS G12C, G12V and G13C mutants showed a 2- fold increase in GTP binding and Q61H showed a 5- to 6- fold increase. These results reveal the variable GTP binding properties amongst different KRAS mutants, which may result in different biological functions (Stolze *et al.*, 2014)

Another frequently mutated codon, Q61, is a site that is essential for GTP hydrolysis, and it is predicted that G12 and G13 mutations impact the ability of Q61 to coordinate the nucleophilic water molecule during hydrolysis, further resulting in transition state destabilisation (Hunter *et al.*, 2015). It follows

that mutations at Q61 would also impact hydrolysis rates, and in fact Q61L and Q61H mutants exhibit lower intrinsic GTP hydrolysis rates (Buhrman *et al.*, 2010). Regarding GAP-induced hydrolysis, structural work has shown that mutations at G12 and G13 create a steric hindrance that impact the formation of van der Waals interactions between KRAS and GAPs, thus reducing GAP-induced hydrolysis too (Scheffzek *et al.*, 1997). Der and colleagues analysed the kinetics of GTP hydrolysis and transforming potency in WT and 17 different HRAS Q61 mutants. They found that all mutants displayed an 8- to 10- fold lower GTP hydrolysis rate compared to WT HRAS. Interestingly, there was no correlation between hydrolysis rate and transformation, indicating that reduced GTP hydrolysis is not sufficient to activate RAS transforming potential (Der, Finkel and Cooper, 1986).

Lastly, the roles of less-frequently mutated codons, such as K117 and A146, differ slightly compared to those discussed above. K117 makes hydrophobic interactions with the guanine base and also forms a salt bridge with the carbonyl of G13, thus has a dual role of stabilising the nucleotide and promoting hydrolysis (Pai *et al.*, 1990). A146 appears to play a role in nucleotide specificity and mutations at this site result in a 1000-fold increase in nucleotide exchange (Feig and Cooper, 1988). In summary, common KRAS mutations can have different biochemistries which have an impact on GTP hydrolysis, nucleotide exchange or both.

Clinical impact of KRAS mutations

The prognostic value of KRAS mutations has been studied in different cancers, with the role of different alleles at specific codons also being investigated. The impact of a KRAS mutation on patient survival depends not only on the mutation that is present, but also the type of cancer. For example, in PDAC, it was found that patients with a G12D mutation had significantly worse overall survival compared to patients with G12V, G12R or wild-type (WT) KRAS. Having a G12D mutation was identified as an independent predictor for worse prognosis in patients either receiving or not receiving chemotherapy (Bournet *et al.*, 2016). Another study found that when compared with G12 mutations, patients with Q61 mutations had improved survival (Witkiewicz *et al.*, 2015). Huang and colleagues investigated overall survival in patients with different KRAS mutations, and found that it was lowest to highest in patients with G12V, G12R, G12D and finally WT KRAS, respectively (Huang *et al.*, 2015). Several other groups have investigated whether the presence or absence of KRAS mutations has an impact on patient survival, with most studies concluding that the presence of a KRAS mutation correlates with an adverse effect on patient survival (Kawesha *et al.*, 2000; Kim *et al.*, 2011; Ogura *et al.*, 2013; Rachakonda *et al.*, 2013; Shin *et al.*, 2013; Kwon *et al.*, 2015; Qian *et al.*, 2018).

In CRC, multiple studies with analyses of large cohorts of patient data have identified that G12 mutations (particularly G12V mutations), but not G13 mutations, are associated with worse survival (Font *et al.*, 2001; Imamura *et al.*, 2012; Jones *et al.*, 2017). Data from other studies show that mutations at A146 correlate with improved patient survival in comparison to patients with other mutations, and patients with Q61 mutations tend to exhibit poor overall survival (Janakiraman *et al.*, 2010; Taieb *et al.*, 2017). In contrast to this, it has been demonstrated that in patients with early stage NSCLC, those with G12C or G12V mutations did better than those with rarer G12 mutations, although having any type of KRAS mutation correlated with worse survival compared to those with WT KRAS (Izar *et al.*, 2014).

Understanding how different KRAS mutations impact patient survival is important because the mutational status of KRAS can be used to determine whether a patient would benefit from certain cancer treatments. For example, the standard first-line of treatment for CRC is a combination of folinic acid, fluorouracil, and oxaliplatin (FOLFOX), but having a KRAS mutation is a negative prognostic factor for progression-free survival, with G12D in particular being significantly associated with a poor prognosis (Zocche *et al.*, 2015). Another type of treatment for CRC is antibody-based inhibition of epidermal growth factor receptor (EGFR), such as cetuximab, and is given to patients who don't respond to other types of treatment (Jonker *et al.*, 2007). However, cetuximab is not effective in patients with a KRAS mutation at specific codons including 12, 13, 61 and 146, therefore, patients with certain KRAS mutations are excluded from receiving antibody-based EGFR inhibitor therapy (Karapetis *et al.*, 2008; Loupakis *et al.*, 2009; Douillard *et al.*, 2013; Allegra *et al.*, 2016).

1.7 The current therapeutic landscape

Over the last three decades, much effort has gone into developing RAS inhibitors. However, apart from one KRAS-G12C inhibitor being recently approved (Blair, 2021), no other effective RAS inhibitor has been approved, thus leading to the widely accepted notion that RAS is an 'undruggable' target. As RAS behaves like a molecular switch, alternating between an active GTP-bound state to an inactive GDP-bound state, with mutated RAS essentially being stuck in the active state, it followed that inhibiting this activated RAS would be a logical way to treat RAS-mutant cancers. Therefore, attempts to develop GTP-competitive inhibitors were made. However, these failed due to the affinity of GTP for RAS being in the picomolar range, therefore preventing inhibitors from being able to compete with it (Cox *et al.*, 2014). Failed efforts were also made in developing molecules that could act as GAPs for

mutant RAS (Stephen *et al.*, 2014). An additional hurdle in developing RAS inhibitors is the fact that there do not seem to be any deep hydrophobic pockets on its surface that can allow small molecules to tightly bind, although some potential binding sites have been identified using computational approaches (Buhrman *et al.*, 2011; Grant *et al.*, 2011).

Direct targeting of RAS

Despite the difficulties in targeting RAS, scientists have managed to develop several KRAS inhibitors, some of which are currently in clinical trials. Most success has been found with covalent inhibitors targeting the KRAS-G12C mutant because cysteines are naturally reactive; it is in fact a common strategy in drug discovery to covalently target active site cysteines (Gehringer and Laufer, 2019). As WT KRAS lacks a cysteine at codon 12, these inhibitors have the added advantage of being specific for the mutant KRAS only. Development of the first series of small molecules to target KRAS-G12C began after the discovery of a novel allosteric binding pocket beneath the effector binding switch II (termed the switch II pocket (S-IIP)). Binding of small molecule compounds to the S-IIP was shown to impair KRAS function via two distinct mechanisms, firstly, by altering its relative affinity to favour GDP over GTP, and secondly, by impairing its binding to RAF. It is important to note that these compounds only bind to KRAS-G12C in the GDP-bound state, therefore, KRAS is required to undergo hydrolysis first (Ostrem *et al.*, 2013). KRAS-G12C has the highest level of intrinsic GTPase activity compared to the other common KRAS mutants, therefore rendering it more vulnerable to treatment with these compounds (Hunter *et al.*, 2015).

The most potent compound in the first series of small molecules developed was called ‘compound 12’, and another group demonstrated that despite its promising *in vitro* properties, it was not very good at engaging KRAS-G12C, even at high concentrations and long incubation times. They developed a more potent compound, ARS-853, by making modifications to the linker and the hydrophobic binding pocket (Patricelli *et al.*, 2016). Further improvements have since been made by other groups, leading to the development of even more potent and selective compounds such ARS-1620 and AMG 510 (Janes *et al.*, 2018; Canon *et al.*, 2019). Another covalent KRAS-G12C inhibitor, MRTX849, was also recently discovered via a structure-based drug design approach (Hallin *et al.*, 2020). The first KRAS-G12C inhibitor to enter clinical trials was AMG 510; it showed promising results for NSCLC and the FDA had also granted a fast track designation to this drug (Amgen, 2019b, 2019a). Currently it is still undergoing clinical trial testing (trial identifier: NCT03600883), although the FDA has now granted it accelerated approval for the treatment of KRAS-G12C-mutated locally advanced or metastatic

NSCLC in adult patients (Blair, 2021; ClinicalTrials.gov, 2021a). A downside of these inhibitors is that because they only bind to KRAS-G12C when GDP-bound, there is a possibility of resistant mutations arising that could promote the exchange of GDP for GTP or could inhibit the GTPase activity of KRAS. Recently, however, molecules that can bind to both GDP-bound and GTP-bound state of RAS have been discovered. They bind to a novel switch II groove (S-IIG) next to the S-IIP, and this discovery provides proof-of-concept evidence that inhibitors can bind both states of RAS (Gentile *et al.*, 2017).

Although progress has been made in developing inhibitors for KRAS-G12C, it is much harder to do this for other mutants as they lack the reactive cysteine at the mutated codon. Therefore, scientists have tried targeting conserved ligand binding sites to reduce effector binding instead. For example, compound 3144 binds to Asp38, a conserved residue in the switch I segment of the RAS proteins, and inhibits RAS-effector interactions. However, toxicity and off-target activity of the compound was found *in vitro* and in mice, therefore, requiring the need for optimisation (Welsch *et al.*, 2017). Furthermore, targeting all isoforms of RAS may not be tolerated well as RAS is essential for normal signalling and it has been shown in mice that the deletion of all three isoforms results in embryonic lethality (Nakamura *et al.*, 2008).

In addition to the covalent inhibitors of RAS, efforts have also been made to develop PROTAC (proteolysis targeting chimera) therapies (Sun *et al.*, 2019) and RAS dimerisation inhibitors (O'Bryan, 2019). Although RAS proteins function as monomeric GTPases, there is accumulating evidence that RAS dimer formation can play a role in the activation of downstream effectors. For example, Inouye and colleagues found that artificial RAS dimer formation in a cell-free system was essential (although not sufficient) for the activation of CRAF (Inouye *et al.*, 2000). RAS dimers have also been observed in X-ray crystal structures (Güldenhaupt *et al.*, 2012; Spencer-Smith *et al.*, 2017). Efforts have therefore been made to inhibit RAS dimer formation as means to reduce RAS signalling. Spencer-Smith and colleagues isolated a monobody, NF1, that targets a region of RAS that overlaps with the proposed RAS dimerisation interface. NF1 expression in cells resulted in the disruption of RAS dimerisation, inhibition of RAF heterodimerisation and inhibition of both the ERK and PI3K/AKT pathways (Kovrigina, Galiakhmetov and Kovrigin, 2015; Spencer-Smith *et al.*, 2017).

The PROTAC technology is another approach that is being explored for the development of KRAS-mutant cancer therapy. PROTACs work by hijacking the ubiquitin-proteosome system to induce the degradation of the target protein (Pettersson and Crews, 2019). Zeng and colleagues designed a library of PROTACs and identified a lead compound that was able to engage with an E3 ligase substrate

receptor protein (cereblon (CRBN)), bind to overexpressed GFP-KRAS-G12C *in vitro*, induce dimerisation of CRBN with GFP-KRAS-G12C and ultimately degrade GFP-KRAS-G12C in a CRBN-dependent manner. However, it wasn't able to degrade endogenous KRAS-G12C, and the authors suggest that this is due to the inability of the PROTAC to poly-ubiquitinate endogenous KRAS (Zeng *et al.*, 2020). Bond and colleagues developed another PROTAC, LC-2, that was shown to be able to degrade endogenous KRAS-G12C via the recruitment of von Hippel-Lindau (VHL) E3 ligase, resulting in reduced ERK signalling (Bond *et al.*, 2020). Other groups have also developed PROTACs for the treatment of KRAS-mutant tumours, and although this is relatively new technology, PROTAC therapy appears to be very promising (Bery, Miller and Rabbitts, 2020; Röth *et al.*, 2020).

Indirect targeting of RAS

As targeting RAS directly is difficult, scientists have also started developing inhibitors for other proteins involved in RAS signalling (Mattingly, 2013). Normal activation of RAS involves multiple processes, including post-translational modification of RAS, nucleotide exchange, membrane localisation and effector binding (Gurung and Bhattacharjee, 2015). Therefore, efforts have been targeted towards altering some of these essential steps instead. For the targeting of nucleotide exchange, small-molecule inhibitors of the GEF protein Son of Sevenless (SOS) have been developed. One such inhibitor, BAY-293, was found to inhibit KRAS-SOS1 interaction at nanomolar concentrations. Unfortunately, BAY-293 was shown to inhibit the proliferation of WT KRAS cells more potently than the mutant KRAS cells. Interestingly, when used in conjunction with ARS-853 (KRAS-G12C inhibitor), synergistic growth-inhibitory effects were seen in KRAS-G12C cells (Hillig *et al.*, 2019). This suggests that SOS inhibitors may potentially be used with KRAS-G12C inhibitors as these inhibitors target GDP-bound KRAS, of which there would be a larger pool because SOS inhibitors inhibit the release of GDP.

Another mechanism for inhibiting nucleotide exchange is via inhibition of SRC homology region 2 domain-containing phosphatase-2 (SHP2), a non-receptor protein tyrosine phosphatase required for ERK pathway activation (Shi *et al.*, 2000). The function of SHP2 is not fully understood, but it appears to function as a scaffold protein by binding to and recruiting the GRB2/SOS1 complex to the plasma membrane, and therefore, increasing RAS nucleotide exchange (Dance *et al.*, 2008). A small allosteric inhibitor of SHP2, RMC-4550, was shown to decrease ERK signalling and cancer growth by disrupting GTP-loading of RAS. It had the most effect on KRAS-G12C cells compared to KRAS-G12D and KRAS-G12V cells (Nichols *et al.*, 2018). This highlights the importance of mutation-specific biochemical

properties and indicates that efficacy of SOS inhibitors may depend on guanine nucleotide exchange rate, as KRAS-G12C has the highest intrinsic GTPase activity compared to other mutants (Hunter *et al.*, 2015).

Targeting of key enzymes responsible for critical post-translational modifications of RAS proteins is another mechanism that has been explored. As mentioned early on in this chapter, there are three modification steps that allow RAS to bind to the plasma membrane, something which is required for RAS activity (Clarke, 1992). These steps are prenylation of the CAAX motif (by farnesyltransferase (FTase) or geranylgeranyltransferase (GGTase)) (Casey, 1992), removal of the terminal -AXX residues (by RAS-converting enzyme (RCE1)) (Hampton, Dore and Schmidt, 2018) and finally, methylation of the cysteine of the CAAX motif (by isoprenylcysteine carboxyl methyltransferase (ICMT)) (J. Yang *et al.*, 2011). FTase inhibitors (FTIs) do not seem to work well in KRAS-mutant cancer cells due to compensation by GGTase, however, HRAS-mutant cancer cells seem to be uniquely sensitive to FTIs (Whyte *et al.*, 1997). In support of this, tipifarnib, an FTI, has been shown to have robust anti-tumour activity in HRAS-mutant head and neck squamous cell carcinoma (HNSCC) and lung squamous cell carcinoma (LSCC). Tipifarnib is also currently in phase II clinical trials for the treatment of HRAS-mutant HNSCC and thyroid cancer (trial identifier: NCT02383927) (Kessler *et al.*, 2018; ClinicalTrials.gov, 2021k).

To overcome the functional redundancy of FTase and GGTase, inhibitors targeting the downstream RAS processing enzymes RCE1 and ICMT have been tested (Baines, Xu and Der, 2011). These enzymes are critical in KRAS-mutant cells but not in WT cells, as opposed to FTase, which is critical for both mutant and WT cells (which results in FTase inhibition being detrimental to all cells, not just the mutant cells). On the other hand, inhibition of RCE1 or ICMT would be expected to provide mutant selectivity and reduce non-targeted toxicity (T. Wang *et al.*, 2017). Unfortunately, much success has not been gained with RCE1 and ICMT inhibitors as of yet (Cox *et al.*, 2014). Some ICMT inhibitors appear to reduce proliferation only mildly (Judd *et al.*, 2011), although a recent inhibitor, UCM-1336, was shown to be able to impair membrane association of all RAS isoforms and decrease cell proliferation in KRAS-mutated cell lines with distinct mutations (Marín-Ramos *et al.*, 2019). Nevertheless, further work is required for effective therapeutic use.

Targeting the EGFR family

The EGFR family is upstream of RAS and the inhibition of these receptor tyrosine kinases has been explored for the treatment of RAS-mutant cancers (Downward, 2003). For example, Patricelli and colleagues have shown that treatment of KRAS-G12C cells with erlotinib, an EGFR inhibitor, results in significant time-dependent decrease in the pool of GTP-bound KRAS-G12C. Interestingly, they also show that treatment with ARS-853 (KRAS-G12C inhibitor that only binds the GDP-bound form) following treatment with erlotinib results in increased engagement between ARS-853 and KRAS-G12C, which makes sense as treatment with erlotinib is increasing the pool of GDP-bound KRAS-G12C (Patricelli *et al.*, 2016). However, despite EGFR inhibitors such as erlotinib and gefitinib being approved for the treatment of EGFR-mutant NSCLC, they are ineffective as monotherapy agents against KRAS-mutant NSCLC (Pao *et al.*, 2004; Linardou *et al.*, 2008; Mao *et al.*, 2010). Unfortunately, treatment with EGFR inhibitors can result in the upregulation of other EGFR family members such as ERBB2, ERBB3 and ERBB4 as a resistance mechanism (Moll *et al.*, 2018). However, it has been found that treatment with pan-ERBB inhibitors suppresses the formation of KRAS-driven lung tumours, and combination treatment with a MEK inhibitor appears to have an additional synergistic effect (Kruspig *et al.*, 2018).

RAF, MEK and ERK inhibitors

Currently there are BRAF-V600 kinase inhibitors such as vemurafenib and dabrafenib that are approved for the treatment of BRAF-V600 mutant metastatic melanoma (Karoulia *et al.*, 2017). However, these inhibitors, which are types of ATP-competitive inhibitors, cannot be used for RAS-mutant cancers, as they have been shown to paradoxically activate the ERK pathway (Heidorn *et al.*, 2010; Joseph *et al.*, 2010). They can do this by binding to WT RAF and causing RAF dimerisation, which allows for transduction of the activated signal (Hatzivassiliou *et al.*, 2010). The binding of RAF inhibitor to the ATP-binding site of one monomer of a RAF dimer inhibits the activity of the monomer it is bound to but activates the drug-free monomer. It has also been shown that this RAF-inhibitor mediated ERK pathway activation is dependent on RAS activity, and because RAS is not activated in BRAF-V600-mutated tumours, these inhibitors cause minimal transactivation of the ERK pathway in those tumours (Poulikakos *et al.*, 2010).

One approach explored to overcome ERK pathway activation in RAS-mutant cancers is the development of compounds that inhibit dimeric RAF with as much potency as monomeric RAF

(Durrant and Morrison, 2018). One example is LY3009120, a pan-RAF inhibitor that was found to inhibit RAF dimers in both RAF and RAS-mutant melanoma and CRC tumour cells *in vitro* and *in vivo*, whilst causing only minimal paradoxical ERK pathway activation in RAS-mutant cells (Peng *et al.*, 2015). Vakana and colleagues showed similar results in preclinical models of colorectal cancer (Vakana *et al.*, 2017). Unfortunately, a clinical trial of LY3009120 in patients with advanced/metastatic cancer was terminated in phase I due to lack of sufficient clinical efficacy (trial identifier: NCT02014116) (ClinicalTrials.gov, 2019). Compounds that inhibit the actual formation of RAF dimers have also been investigated. Examples include belvarafenib and LXH-254, which also appear to be beneficial in both RAF-mutant and RAS-mutant cancers (Kim *et al.*, 2019; Monaco *et al.*, 2019). Both compounds are currently in phase I clinical trials for RAS-mutant tumours, either alone or in combination therapy with another inhibitor (trial identifiers: NCT02405065, NCT03118817, NCT02607813) (ClinicalTrials.gov, 2021f, 2021g, 2021j).

Similar to RAF inhibitors, currently there are MEK inhibitors that have been approved for the treatment of BRAF-V600 mutant melanoma but not for RAS-mutant tumours, such as the allosteric inhibitors cobimetinib, trametinib and binimetinib (Grimaldi *et al.*, 2017). MEK inhibitors used as monotherapy against RAS-mutant tumours have found no improvement, and like RAF inhibitors, they also appear to induce pathway feedback loops, resulting in only modest efficacy in these tumours (Lito *et al.*, 2014; Carter *et al.*, 2016). Although single-agent MEK inhibitors have largely failed, there has been some success in NRAS-mutant melanomas (Ascierto *et al.*, 2013). Additionally, MEK inhibitors have shown some promising results when used in conjunction with RAF inhibitors, for example, one study showed that combined MEK and RAF inhibition results in synergistic efficacy in KRAS-mutant cells. They showed that MEK inhibition in these cells increases RAS-GTP levels and induces RAF dimerisation, and that this drug-induced RAF dimerisation and increase in RAS-GTP levels makes the cells more sensitive to RAF inhibition (Yen *et al.*, 2018). There are currently two phase I clinical trials investigating the efficacy of combination treatment of RAF and MEK inhibitors in RAS-mutant and BRAF-mutant tumours (trial identifiers: NCT03284502 and NCT02974725) (ClinicalTrials.gov, 2021h, 2021c). One MEK inhibitor, selumetinib, has been the first inhibitor to be approved by the FDA for the treatment of NF1 in paediatric patients (Dombi *et al.*, 2016; AstraZeneca.com, 2020; Gross *et al.*, 2020).

Development of ERK inhibitors lags behind MEK and RAF inhibitors, and currently there are no ERK inhibitors approved for clinical use (Samatar and Poulikakos, 2014; Liu *et al.*, 2018). Although some ERK inhibitors have shown promise *in vitro,* this has not always translated to *in vivo* success. For

example, MK-8353 is an ERK inhibitor that has dual functionality, it binds to and inhibits ERK1/2 and also causes a conformational change that prevents ERK1/2 from being phosphorylated by upstream kinases. This inhibitor was shown to inhibit proliferation of NRAS-mutant melanoma cells, but in phase I clinical trials, it had no antitumour effects in patients with either KRAS or NRAS mutations (Boga *et al.*, 2018; Moschos *et al.*, 2018). MK-8353 is however in clinical trials in combination with selumetinib (a MEK inhibitor) or pembrolizumab (an antibody treatment used for a number of cancers including melanoma and NSCLC) in patients with RAS mutations (trial identifiers: NCT03745989 and NCT02972034) (ClinicalTrials.gov, 2021l, 2021m). Another ERK inhibitor in clinical trials is LY-3214996; it showed promising results in *in vivo* KRAS cancer models and is currently in phase I clinical trials in patients with advanced and metastatic cancers (trial identifier: NCT02857270) (Bhagwat *et al.*, 2017; Pant *et al.*, 2019; ClinicalTrials.gov, 2021d).

Emerging therapeutics

In addition to the above therapies targeting different aspects of ERK signalling, there are several emerging therapies being investigated for the treatment for KRAS-mutant cancers. One such type of therapy is the use of small interfering RNA (siRNA) to target mutant KRAS, for example, a mutant-specific siRNA against KRAS-G12D is being investigated in combination with chemotherapy in phase I clinical trials in patients with PDAC, showing promising results (trial identifier: NCT01188785) (Golan *et al.*, 2015; ClinicalTrials.gov, 2021i). It is also in phase II trials in combination with gemcitabine and nab-paclitaxel (approved drugs for PDAC) in patients with KRAS-G12D PDAC (trial identifier: NCT01676259) (ClinicalTrials.gov, 2021b).

Another type of treatment being investigated is the inhibition of autophagy with hydroxychloroquine, which is FDA approved for the treatment of malaria (Sindhu *et al.*, 2021). It has been shown that autophagy is critical for pancreatic tumour growth, and inhibiting it leads to elevated DNA damage and a decrease in mitochondrial oxidative phosphorylation, which ultimately induces tumour regression in preclinical models (S. Yang *et al.*, 2011; Yang and Kimmelman, 2014). Results obtained from a clinical trial of hydroxychloroquine treatment in patients with PDAC showed limited efficacy (Wolpin *et al.*, 2014); however, when used in conjunction with other inhibitors of the ERK pathway, more promising results were obtained for the treatment of KRAS-mutant PDAC and NRAS-mutant melanoma. Combined treatment of hydroxychloroquine and trametinib, a MEK inhibitor, resulted in tumour regression in patient derived xenograft (PDX) models and treatment of hydroxychloroquine with ERK inhibition enhanced the ability of ERK inhibitors to mediate anti-tumour activity in

KRAS-driven PDAC (Bryant *et al.*, 2019; Kinsey *et al.*, 2019). With these promising results, hydroxychloroquine is currently undergoing phase I clinical trials in combination with trametinib for the treatment of patients with PDAC (trial identifier: NCT03825289) (ClinicalTrials.gov, 2021n).

Lastly, immunotherapy treatments including immune checkpoint inhibitors, adoptive cell therapy and cancer vaccines are all being investigated for the treatment of RAS-mutant cancers (Hoo, Siak and In, 2019). Tumours can evade detection by the immune system and suppress immune responses by activating negative regulatory pathways (also called checkpoints) by expressing specific antigens such as cytotoxic T lymphocyte protein 4 (CTLA4), programmed cell death protein-1 (PD1) and PD1 ligand (PDL1) on the cell surface (Chen and Mellman, 2017). CTLA4 is found on the surface of T cells, and it negatively regulates T cell activation. PD1 is also found on T cells, and it binds to one of its ligands, PDL1, which is found on many tumour cell surfaces. Upon binding of PDL1 with PD1, an inhibitory signal is generated that attenuates the activity of T cells (Houot *et al.*, 2015). Therefore, antibodies targeted against these antigens should augment the anti-tumour immune response. Currently, there are a number of antibody therapies approved by the FDA against these antigens, including ipilimumab (an anti-CTLA4 antibody) as a monotherapy for metastatic melanoma (Eggermont *et al.*, 2016), and ipilimumab in combination with nivolumab (an anti-PD1 antibody) for the treatment of NSCLC and melanoma (Wolchok *et al.*, 2017; Hellmann *et al.*, 2019).

Adoptive cell therapy involves engineering the immune system to recognise specific antigens present on KRAS-mutant-specific tumour cells. A study showed that a patient with metastatic CRC had regression in seven pulmonary metastatic lesions after being infused with their own KRAS-G12D-recognising CD8+ tumour infiltrating lymphocytes (TILs) that had been expanded *ex vivo* (Tran *et al.*, 2016). A third immunotherapeutic approach is the use of vaccines against RAS-mutant cancers. In patients with PDAC, intradermal injection of granulocyte–macrophage colony-stimulating factor (GM-CSF) with peptides from mutant RAS proteins stimulates dendritic cells and triggers a T cell response against these peptides, resulting in prolonged patient survival (Gjertsen *et al.*, 2001). A phase I/II clinical trial has looked at the effects of this type of vaccine, Targovax TG-01, with adjuvant gemcitabine chemotherapy in patients with PDAC and found that treated patients had an increased immune response and increased overall survival (trial identifier: NCT02261714) (Palmer *et al.*, 2017; ClinicalTrials.gov, 2021e).

In conclusion, although there is currently only one approved therapy specifically for RAS-mutant tumours, there is a lot of research being carried out in this area, with many different types of

therapeutics being investigated. The first approved therapy is a KRAS-G12C inhibitor, and hopefully therapies against other alleles will also soon be developed. It is likely that combination therapies will be the norm as opposed to monotherapies, as inhibition of the ERK pathway appears to induce feedback loops allowing RAS-mutant cells to circumvent these inhibitions; this is demonstrated by the success of combination treatments currently being investigated in clinical trials.

1.8 Aims

Despite the enormous efforts made in targeting RAS signalling in cancer, they have largely failed to translate into significant clinical benefits. The progress described entitles us to some optimism for the future, but progress might be hindered by the incomplete understanding of the mechanisms of pathogenicity of specific KRAS mutations in different tissues, and the plasticity of ERK signalling that often mediates resistance to therapies. The main aim of my project is thus to fill this gap in knowledge by investigating how different KRAS G12 mutations rewire signalling in mutant cells. Our hypothesis is that different mutations in KRAS, even at the same codon, result in different downstream signalling dynamics and, consequently, result in the activation of different transcriptional programmes that support distinct biological processes. This is supported by studies showing different biological impacts of different alleles at the same codon, for example, in NSCLC, patients with a KRAS-G12V or KRAS-G12C mutation have worse progression-free survival compared to patients with WT KRAS or other KRAS mutations (Ihle *et al.*, 2012). This is further supported by the fact that different KRAS alleles can confer different sensitivities to MEK1/2 inhibitors (Janakiraman *et al.*, 2010). A comparison of gene expression and proteomic profiles of different KRAS mutations also supports the notion that all KRAS mutants, even at the same codon, are not the same (Hammond *et al.*, 2015). Establishing the existence and characterising these differences may help us in understanding the causes of different mutational frequencies in different types of cancers and, hopefully, aid in the development of effective therapies. Indeed, signalling differences within the ERK pathway will almost certainly also involve the influence of other connected pathways, which is why it is important to understand the greater network of signalling pathways and how they may interact with and modulate the ERK pathway. These signalling differences could be the key to developing mutant-specific therapies resulting in more effective treatment against certain KRAS-mutant cancers.

I have used two isogenic colorectal cancer cell lines (LIM1215 and SW48) harbouring different KRAS mutations to study the signalling dynamics between different G12 mutants. These isogenic panels are ideal for understanding mutant-specific differences as the only variability within each cell line in a

panel is the mutation at codon 12; therefore, differences can confidently be attributed to the specific mutation. My work has also attempted to understand if differences in different codons induce distinct transcriptional programmes during early carcinogenesis that might mediate a fitness advantage to specific KRAS mutant cells. For this, I used a non-transformed doxycycline-inducible PDAC cell line (HPNE) that expresses a third mutant copy of KRAS upon treatment with doxycycline. RNA sequencing of these cells was carried out to uncover key transcriptional changes.

In the results chapters, I will discuss the steps taken to elucidate the rewiring of the ERK pathway in the context of different KRAS G12 mutants. I report two previously unreported interactions within this pathway that are specific to only G12A, G12C and G12D KRAS mutations. In addition, I discuss attempts made to elucidate the identity of an unknown BRAF form present only in these mutants. Finally, I also examine changes in gene transcriptional programmes between different KRAS mutants in both colorectal and pancreatic cancer cells. My results have enabled the formulation of testable hypotheses which inform the next steps to be taken to elucidate the mechanisms behind my observations.

2. Results Chapter I: Different KRAS G12 mutations distinctly rewire cellular signalling

2.1 Background

In the Introduction chapter, I have discussed how a stimulus is not just relayed from the extracellular space to the nucleus, but that a complex network of biochemical reactions transduce, amplify and process a stimulus integrating information from the environment to trigger an appropriate response. I have also presented evidence suggesting that different KRAS G12 mutants may trigger distinct responses by differentially rewiring downstream pathways. In this chapter, I illustrate experimental results aimed to first characterise different responses of two key pathways, the MAPK and PI3K pathways. The main aim of this chapter is, however, to characterise quantitatively, the effects of G12 mutations on the network topology of signalling cascades that could explain differences in signalling dynamics and, eventually, cell states.

Most of my work in this chapter has been carried out in the LIM1215 isogenic panel of colorectal carcinoma cells, which contain a heterozygous knock-in mutation of the desired activating mutation (G12A, G12C, G12D or G12V KRAS mutation) or the wild-type (WT) cell line with no KRAS mutation. All of the LIM1215 cell lines also contain a mutation in the *CTNNB1* gene, which encodes for β-catenin, a multifunctional protein involved in many physiological processes and known to play a role in a number of cancers, including colorectal cancer (Shang, Hua and Hu, 2017). Apart from the respective KRAS mutations, this panel of cell lines is essentially identical, making it an ideal tool to utilise for my experimental needs. Disregarding genetic changes occurring in cells naturally over time, differences observed between cell lines can be attributed confidently to specific KRAS mutations.

I have also used the SW48 isogenic panel of colorectal carcinoma cells with the exact same panel of KRAS G12 mutants. The key difference between the two isogenic panels is that the SW48 cells have additional mutations in the *EGFR* and the *FBXW7* genes, which encode for the epidermal growth factor receptor protein and F-box/WD repeat-containing protein 7, respectively. The mutation in EGFR is not ideal as it is directly involved in the ERK pathway, one of the pathways being studied in my project, and also because mutations in *EGFR* and *KRAS* typically do not co-occur, although more recent findings have contradicted this earlier observation (Marchetti *et al.*, 2005; Li *et al.*, 2014; Tsukumo, Naito and

Suzuki, 2020). FBXW7 is a critical tumour suppressor protein and is frequently deregulated in human cancers; its role and importance will be elaborated upon further in **Chapter 3**.

One approach I have established to investigate the differences in signalling between the KRAS G12 mutants is via a technique called Modular Response Analysis (MRA). This method was developed originally in 2002 by the Kholodenko lab and has been applied also to the investigation of MAPK signalling (Bruggeman *et al.*, 2002; Kholodenko *et al.*, 2002). For example, Santos and colleagues show that different growth factors (EGF and NGF) trigger distinct signalling dynamics (transient vs sustained) leading to either proliferation or differentiation in rat adrenal pheochromocytoma (PC-12) cells. With MRA, the authors showed that the different dynamics are caused by changes in MAPK network topologies related to the differential engagement of feedback mechanisms in the presence of EGF or NGF (Santos, Verveer and Bastiaens, 2007).

In MRA, specific nodes within a pathway of interest are systematically perturbed using RNA interference or small molecule inhibitors. The change in activity of each protein of interest (a 'module') is quantified, for example in our case by Western blots. The active state of each kinase is measured by determining the total percentage of phosphorylated protein in comparison to total protein levels. This change in activity of each module is termed as a 'global response coefficient'. These global response coefficients are then used to calculate numerical values that quantify the relationship of the modules to one another, termed as 'local response coefficients', and thus network topologies are generated ***(Figure 2.1)***.

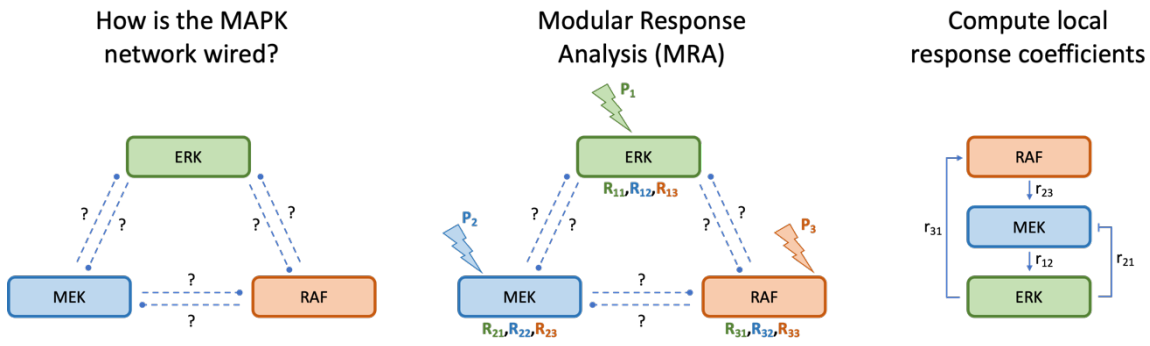

Figure 2.1. **Schematic representation of MRA.** Each module is systematically perturbed (Px), and the resulting change in activity of each module, the 'global response coefficient' (Rx), is calculated. The connectivity of each module to another is obtained by computing 'local response coefficients' (rx) via MATLAB code. The specific nodes in a pathway (in my case RAF, MEK and ERK) are perturbed systematically using siRNA or small molecule inhibitors. Quantitative Western blots are used to quantify the phosphorylated protein levels, which are normalised to total protein levels. A MATLAB code utilises these ratios to generate network topology maps. Image adapted from Santos, Verveer and Bastiaens (2007).

2.2 Characterising MAPK and PI3K signalling responses in different KRAS G12 mutants

I measured responses of the MAPK and PI3K pathways in LIM1215 cells to characterise signalling differences between the mutants and WT in response to EGF and insulin, the respective hormones primarily responsible for stimulation of these pathways. The 'active' levels of the proteins were calculated as the fraction of total protein that is phosphorylated. The cells were starved because serum contains many different growth factors and cytokines which can contribute to activation of cellular signalling pathways. By starving the cells, the aim was to bring down the levels of ERK and AKT to a basal level so that any responses observed would be more comparable between the cells.

2.2.1 EGF stimulation reveals mutant specific ERK responses

The ERK responses in starved cells are shown in ***Figure 2.2***. G12A, G12C and G12D cells clustered together in their ERK responses, which were lower compared to WT and G12V cells. All mutants responded less compared to WT, which is interesting as I would expect mutated KRAS to increase downstream signalling and therefore have higher levels of activated ERK. In contrast, AKT response was highest in G12A cells, although the error bars are very large, therefore, it is difficult to make confident conclusions. It is important to note that the responses are normalised to the cells not treated with EGF, therefore, differences in baseline levels between mutants can reflect in the peaks observed. WT cells have a lower baseline in the starved condition ***(Figure 2.4),*** which could explain the larger responses seen in WT cells. However, normalising to the non-stimulated cells is still an effective way to measure ERK and AKT responses as it gives an indication of response to EGF irrespective of basal levels. In the non-starved conditions (similar to the starved conditions), ERK and AKT responses peaked at 5 minutes of EGF treatment ***(Figure 2.3).*** WT had highest ERK response, followed by G12V. The other mutants clustered together, similarly to the responses observed in starved cells. AKT responses were similar to ERK, with a key difference being that responses were higher in G12V than WT; however, the data variance is quite large and therefore this is not conclusive. The responses were also more sustained when compared to starved cells. Nevertheless, WT and G12V cluster together, and G12A, G12C and G12D cluster together. An interesting observation is the increase in active ERK levels between 20 mins and 40 mins of EGF treatment in non-starved cells, possibly due to effects on signalling feedbacks by growth factors in serum. Please note the conclusions made in regards to the non-starved data is still preliminary as data from only two repeats is shown.

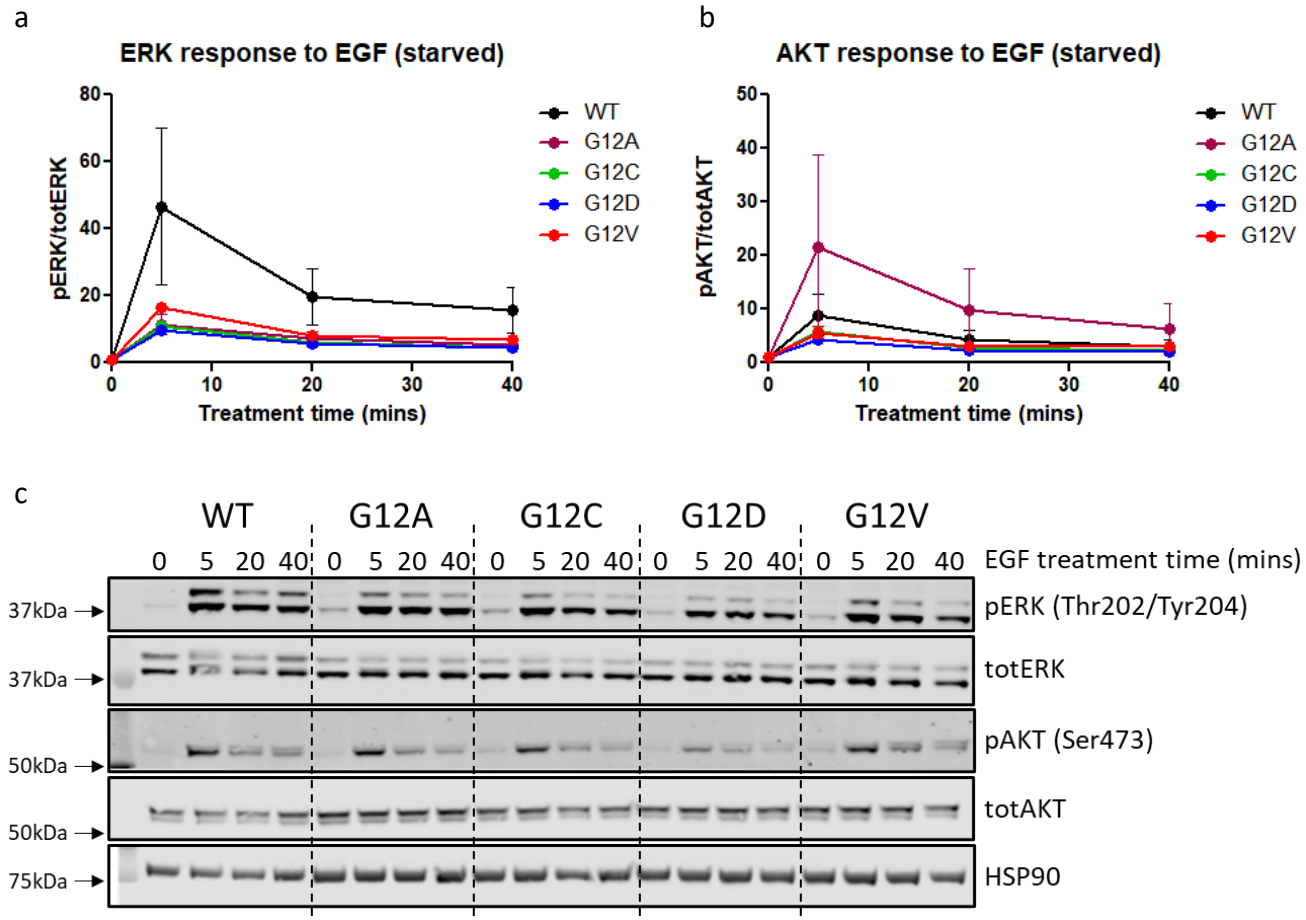

Figure 2.2. **ERK and AKT responses to EGF stimulation in starved LIM1215 cells.** Graphs and representative Western blots depicting the ERK and AKT responses of LIM1215 WT and mutant cells upon EGF stimulation (100ng/ml) for 0, 5, 20 and 40 minutes. ERK and AKT activity is measured as a phospho/total ratio and then normalised to the non-treated (0 minute EGF) sample. **a.** ERK response to EGF. **b.** AKT response to EGF. **c.** Representative Western blots of one repeat. Please note, pERK phosphorylation sites refer to the ERK1 sites. Mean values +/-SEM error bars plotted (n=3). Statistical analysis shows that differences in mean responses are insignificant between mutants.

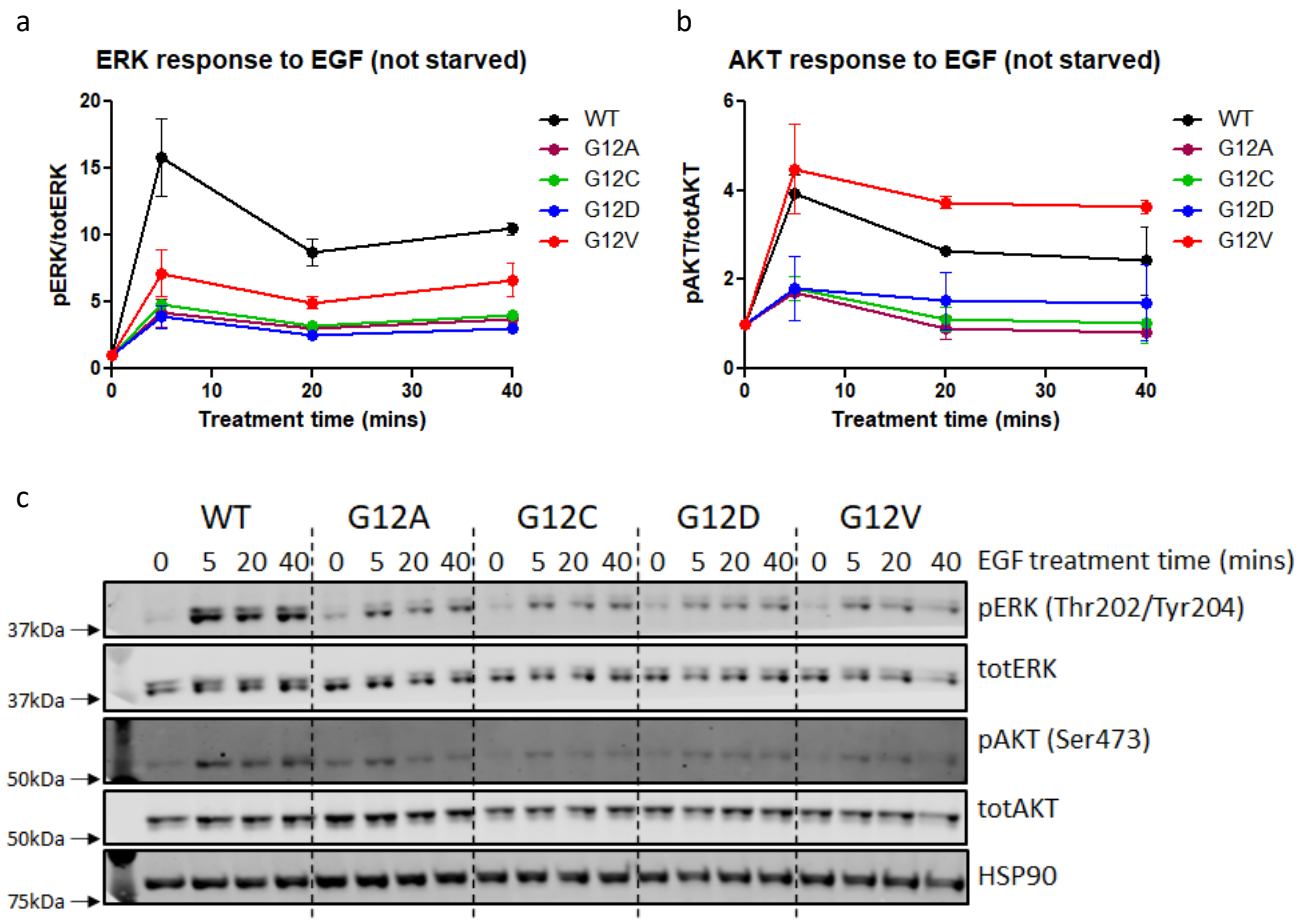

Figure 2.3. **ERK and AKT responses to EGF stimulation in non-starved LIM1215 cells**. Graphs and representative Western blots depicting the ERK and AKT responses of LIM1215 WT and mutant cells upon EGF stimulation (100ng/ml) for 0, 5, 20 and 40 minutes. ERK and AKT activity is measured as a phospho/total ratio and then normalised to the non-treated (0 minute EGF) sample. **a.** ERK response to EGF. **b.** AKT response to EGF. **c.** Representative Western blots of one repeat. Please note, pERK phosphorylation sites refer to the ERK1 sites. Mean values +/-SEM error bars plotted (n=2 due to technical issues). Statistical analysis not carried due to insufficient repeats.

When looking at the basal levels of ERK and AKT activity (with no EGF stimulation), the ERK levels in starved conditions are higher in mutants than in WT cells (***Figure 2.4***). This is not reflected in the non-starved cells to the same extent. In contrast, the AKT levels in mutant cells are generally similar to WT cells in both starved and non-starved conditions (with the exception of G12V cells that have a lower AKT level in non-starved conditions). All cells also have higher AKT levels in the starved conditions compared to the non-starved conditions.

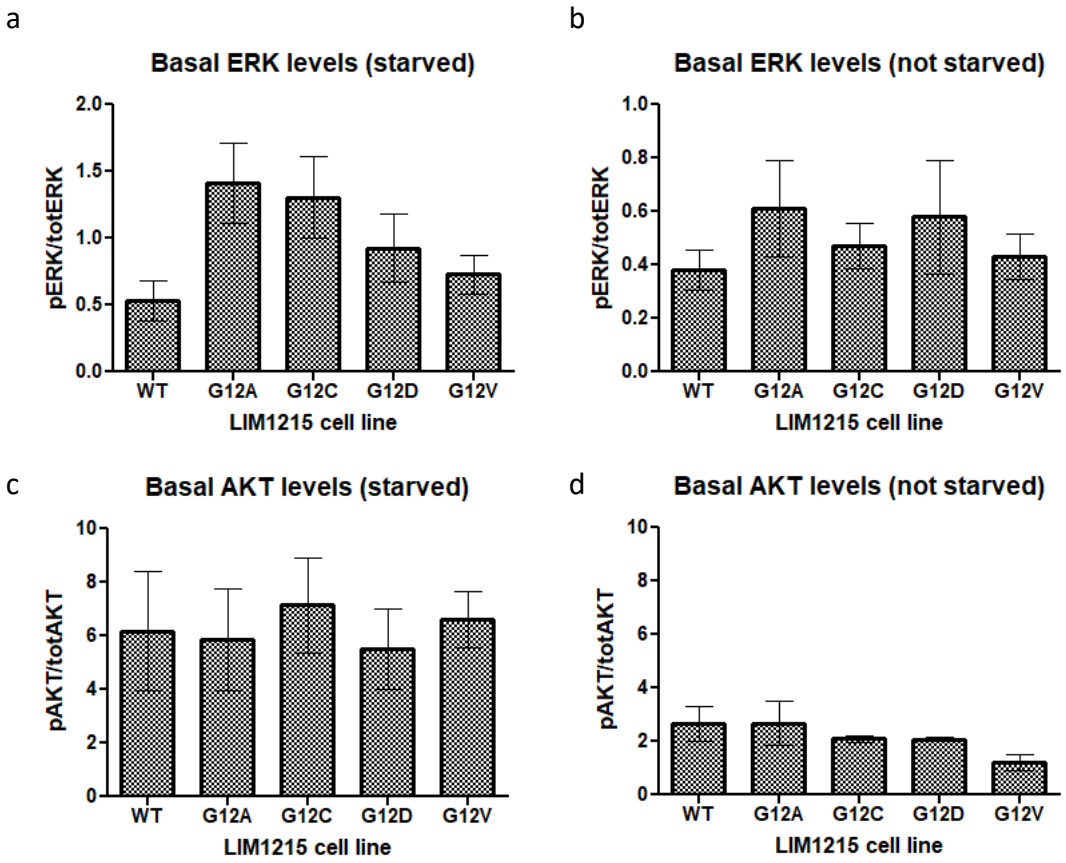

Figure 2.4. **Basal ERK and AKT levels in starved and non-starved conditions in LIM1215 cells.** Graphs depicting basal levels of ERK and AKT in LIM1215 WT and mutant cells with no EGF stimulation. ERK and AKT activity is measured as a phospho/total ratio. **a.** Basal ERK levels in starved cells. **b.** Basal ERK levels in non-starved cells. **c.** Basal AKT levels in starved cells. **d.** Basal AKT levels in non-starved cells. SEM error bars shown (n=3 for starved conditions; n=2 for non-starved conditions).

2.2.2 Insulin stimulation

Cells were treated with insulin as another way of understanding how the MAPK and PI3K pathways respond in cells harbouring different KRAS mutations. Insulin is a useful comparator with EGF because whilst both can activate RAS (Medema *et al.*, 1993), differences in how efficiently RAS is activated (Osterop *et al.*, 1993) and how RAS is desensitised to further activation (Klarlund, Cherniack and Czech, 1995; Waters *et al.*, 1996) have been reported between both stimulants. Therefore, it would be interesting to see how insulin treatment impacts MAPK and PI3K pathway activation in the presence of different KRAS mutations when compared to EGF treatment.

In contrast to the EGF stimulation responses, the responses in the starved and non-starved conditions to insulin varied more ***(Figure 2.5)***. The ERK responses in starved conditions were similar to those seen

with EGF stimulation, with WT responding the most, followed by G12V, and then G12A, G12C and G12D clustering together. In non-starved conditions, however, there were clear differences in ERK responses between the mutants and WT cells. 5 minutes after stimulation, WT cells exhibited a slight increase in pERK levels, whereas mutants show a drastic drop in pERK. At 20 and 40 minutes after stimulation, all cell lines behaved similarly. This is a very different response compared to the EGF treated cells.

Definite conclusions of the AKT responses in starved conditions cannot be made confidently due to high variability in the data. Interestingly, in non-starved conditions, G12V responds very differently to the other mutants. At 5 minutes treatment, WT has highest AKT response, with the mutants clustered together. However, at 20 and 40 minutes, G12V behaves similarly to WT, and it also peaks at 20 minutes rather than 5 minutes like the other cell lines. From the current data, it does look like WT and G12V have generally higher ERK and AKT responses to insulin treatment in starved and non-starved conditions.

To conclude this section, these experiments show that the MAPK and PI3K pathways respond to EGF and insulin to different extents in the presence of different KRAS G12 mutations and that although all of these mutants are supposedly constitutively active, they do not control downstream signalling in the exact same way. The MAPK pathway is the predominant pathway that KRAS signals via, and to further understand how signalling may be rewired in different mutants, I decided to utilise the MRA technique mentioned earlier to achieve this.

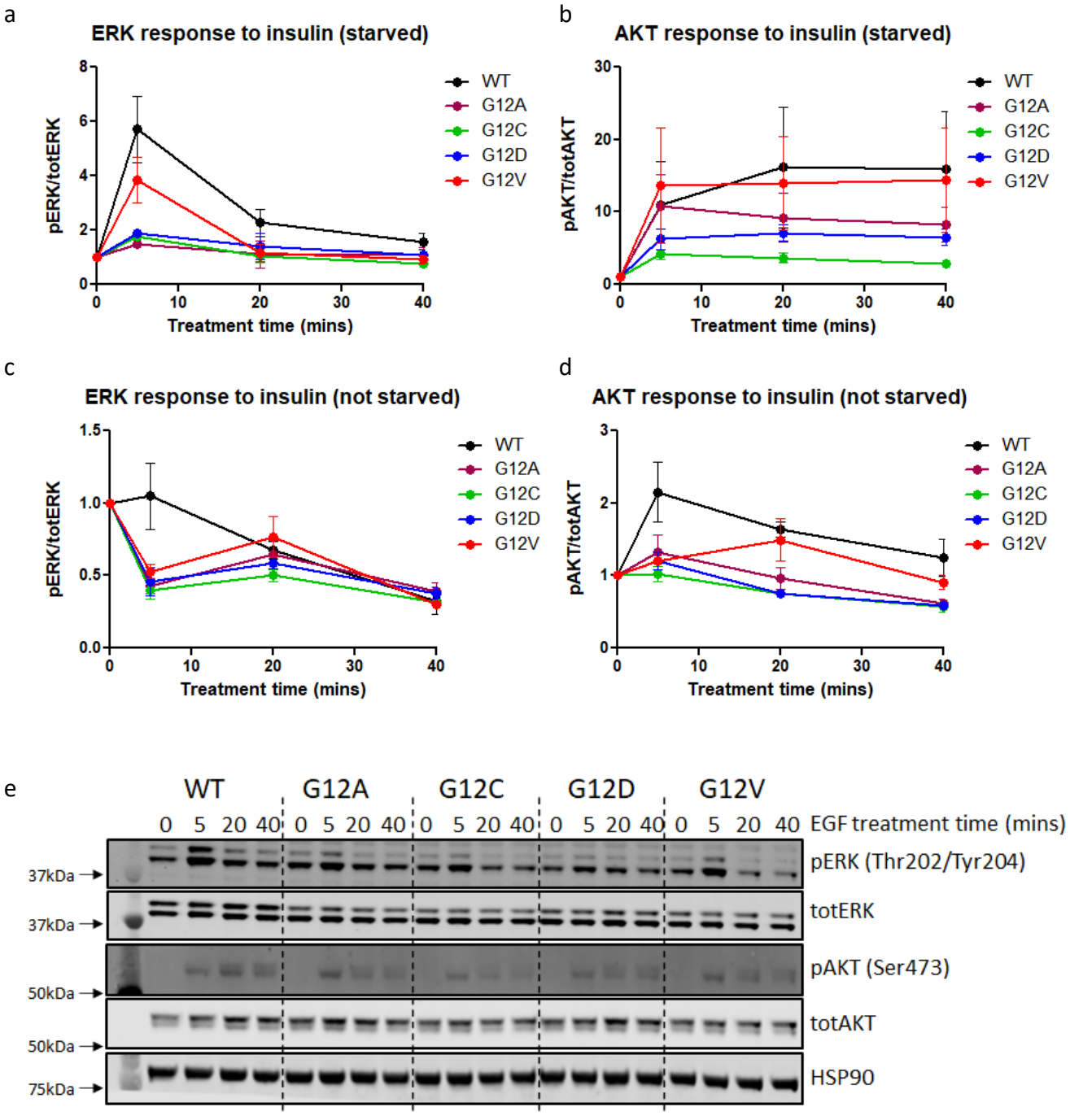

Figure 2.5. **ERK and AKT response to insulin stimulation in starved and non-starved LIM1215 cells.** Graphs depicting the ERK and AKT responses in LIM1215 WT and mutant cells upon insulin stimulation (10μg/ml) for 0, 5, 20 and 40 minutes. ERK and AKT activity is measured as a phospho/total ratio. **a.** ERK response in starved cells. **b.** AKT response in starved cells **c.** ERK response in non-starved cells **d.** AKT response in non-starved cells. **d.** Representative Western blots of one repeat. Please note, pERK phosphorylation sites refer to the ERK1 sites. Mean values +/-SEM error bars plotted (n=3). Statistical analysis shows that differences in mean responses are insignificant between mutants except for WT vs G12A, G12C and G12D mean responses at 5 minutes EGF in graph **a.**

2.3 Modular Response Analysis in LIM1215 cells

2.3.1 MRA optimisation in LIM1215 cells

To investigate if the differences in signalling dynamics depend on feedback mechanisms that reshape the network topology (i.e., the interactions between the nodes of the network) of MAPK signalling, I performed modular response analysis. I knocked down each of the nodes of the MAPK signalling pathway (RAFs, MEKs and ERKs) and then quantified node activities by the surrogate measurement of activating phosphorylations. Reliable and accurate topological interaction maps can be achieved with partial knockdown, as successfully demonstrated by Santos, Verveer and Bastiaens (2007). The knockdown needs to be enough to perturb protein activity whilst still allowing interaction between proteins of interest (termed as 'modules'). In WT cells, 10nM, 20nM, 30nM and 40nM siRNA concentrations were tested ***(Figure 2.6a)***. Percentage knockdown was calculated by quantifying proteins levels in samples treated with RAF, MEK or ERK siRNA and normalised to the respective control samples (treated with non-targeting (NT) siRNA). From the results, 10nM was chosen to test in all cell lines as it gave the closest knockdown to 60% and in some cases using higher concentrations was redundant. ***Figure 2.6b*** shows the knockdown levels in WT and all mutant cells when transfected with 10nM siRNA concentration. The protein levels were too low in some cases, so 5nM was also tested ***(Figure 2.6c)***. Protein levels were closer to the desired 40 to 60% knockdown when 5nM siRNA was transfected into the cells so that was the concentration decided upon for the MRA experiments.

Another requirement for accurate interaction maps is the need for a good ERK response with EGF treatment, and as shown in the above section, 100ng/ml EGF provides a robust response. Lastly, needing to perform Western blotting in the most quantitative and reproducible manner, I optimised the technique to ensure high reproducibility and that I operated in the linear range of detection, something often neglected. I used the Li-Cor gel imager system to avoid artefacts caused by densitometry analysis on developed films, and titrated protein loading for a given concentration of antibodies to establish a linear range of operation. This linear range has to be determined for both the target proteins and the loading control because reliable quantitative Western blots require mathematically correct normalisation.

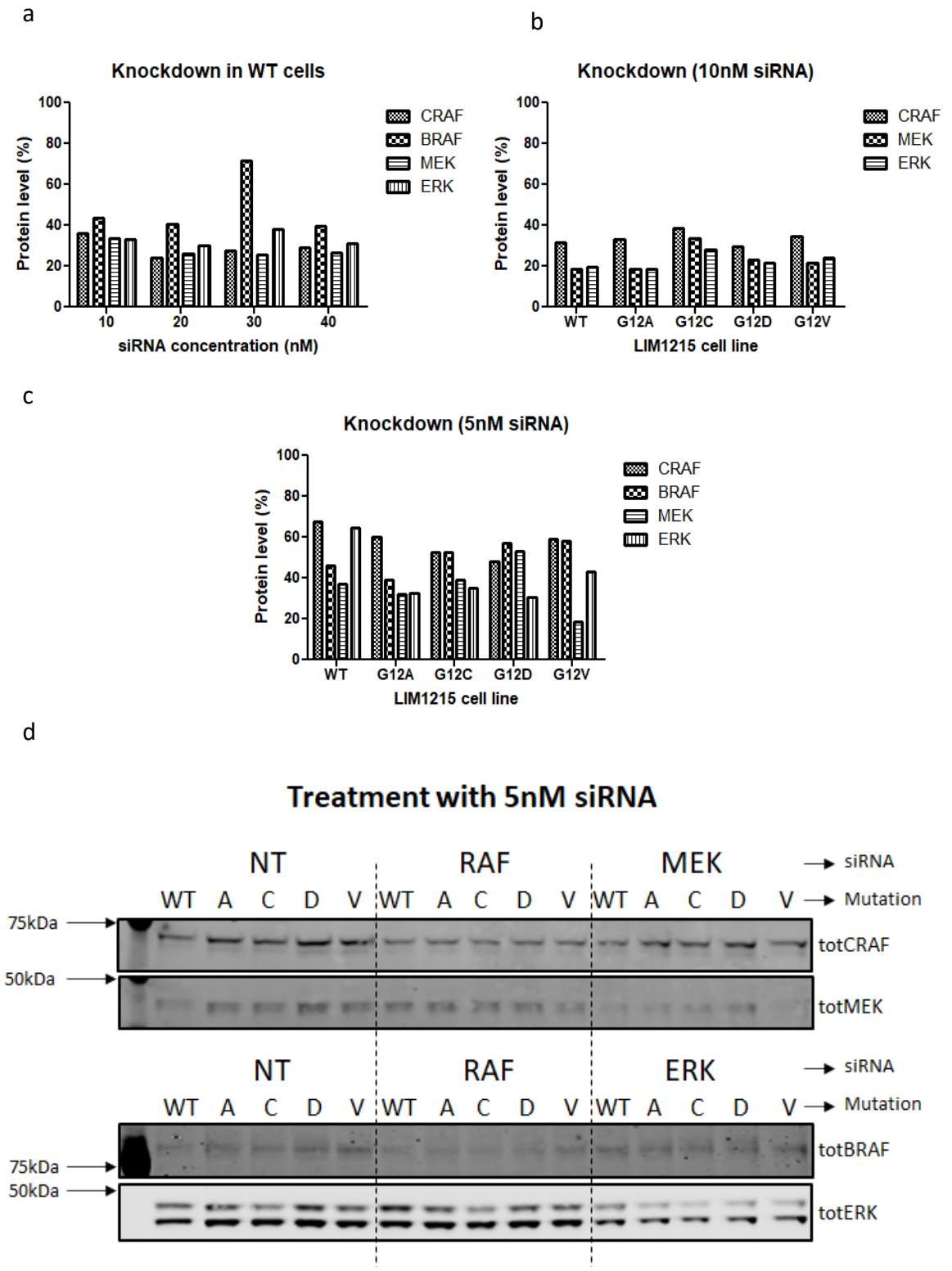

Figure 2.6. **Optimisation of knockdown efficiency in LIM1215 cells.** Graphs showing knockdown (as a percentage) in samples treated with RAF, MEK or ERK siRNA normalised to samples treated with non-targeting (NT) siRNA. All experiments repeated once (n=1). **a.** 10nM to 40nM tested in just WT cells. **b.** 10nM tested in WT and all mutants. There was no BRAF data due to poor quantification of bands. **c.** 5nM tested in WT and all mutants. **d.** Representative Western blots for 5nM knockdown shown.

The signals of pERK, totERK and β-actin (one of the possible loading controls) were quantified, titrating the amount of protein loaded onto the gel ***(Supplementary figure 2.1)***. This was followed by analysis of pERK, totERK, pMEK, totMEK, totBRAF, pCRAF and totCRaf against the REVERT™ Total Protein Stain as it was believed that the stain would be more accurate than using β-actin for normalisation. A range of linearity was confirmed and 15ug was chosen as the appropriate loading amount ***(Supplementary figure 2.2)***. However, after using the REVERT™ stain a few times, it became clear that it is not as reliable as β-actin for normalisation of protein loading between lanes and therefore only β-actin was used as a loading control.

2.3.2 MRA reveals mutant specific interactions within the ERK pathway

Having identified a robust protocol, I performed 5 repeats of MRA experiments on all of the LIM1215 cell lines with EGF treatment [100ng/ml] for 0, 5 and 20 minutes. ***Figure 2.7*** shows the knockdowns achieved, which were at optimal level for the purposes of MRA, and the mean responses of BRAF, CRAF, MEK and ERK. The individual responses are shown in ***Supplementary figure 2.3***. Despite the high standards employed in these experiments, responses were occasionally stronger in some repeats (especially at 5 mins EGF treatment, hence the large error bars in some cases). However, the timing and comparisons between mutants were highly reproducible.

As shown in ***Figure 2.7***, all responses were similar in trend in all cell lines for all proteins expect for BRAF in G12C where there was a transient response rather than an increasing sustained response. CRAF levels were also sustained, whilst MEK and ERK responses were transient with peaks at 5 mins. The ERK responses correlated with the EGF experiments done prior, with WT having the highest response, followed by G12V. Representative quantitative Western blots are presented in ***Figure 2.8***. Quantification of protein level was carried out using Image Studio software, and the resulting phospho/total ratios in all experimental conditions were inputted into a MATLAB code written by my supervisor Dr Alessandro Esposito. The complete set of maps can be found in ***Supplementary figure 2.4***, but the main ones of interest are shown in ***Figure 2.9***.

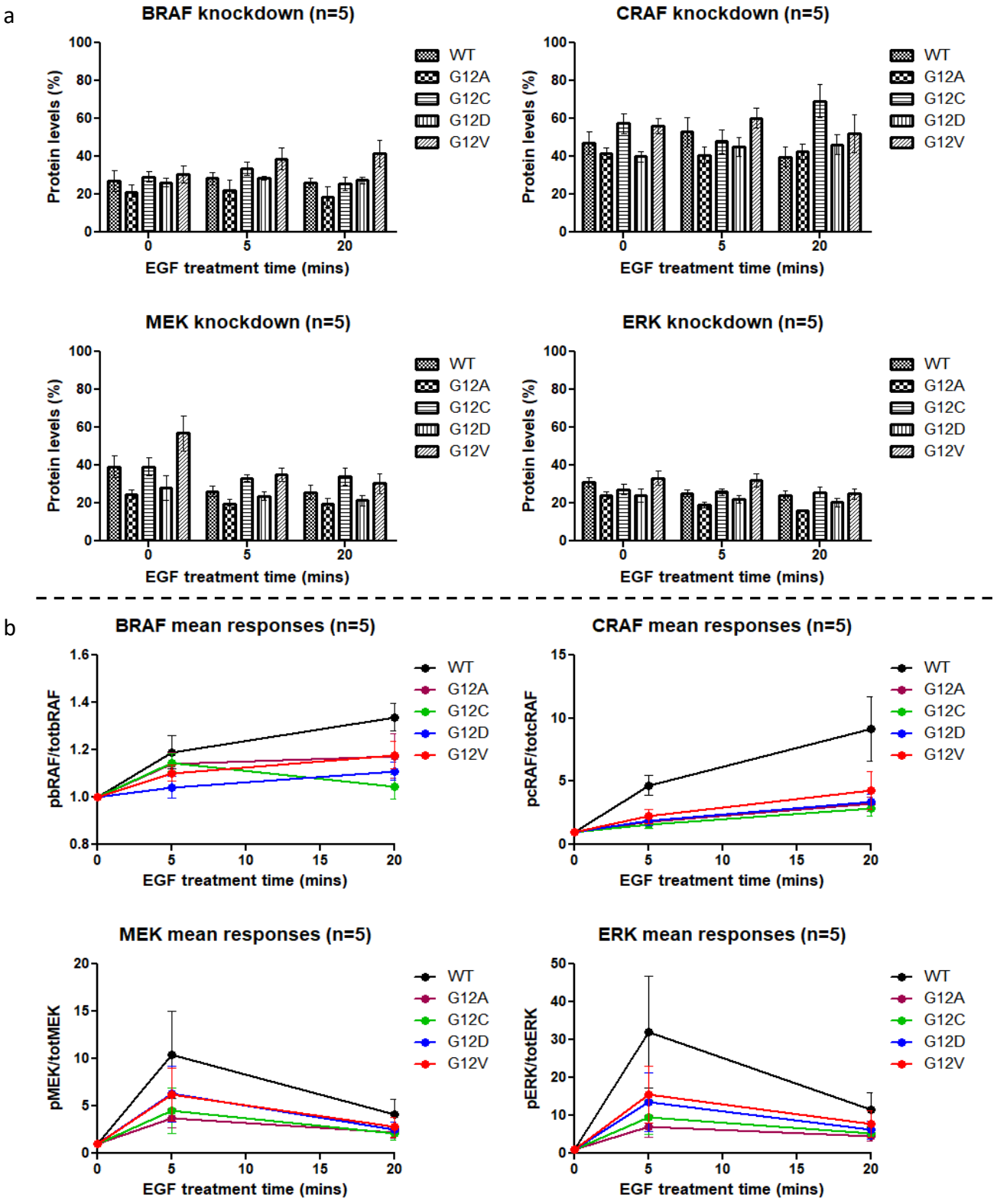

Figure 2.7. **MRA knockdowns achieved and mean responses. a.** Bar charts depicting knockdowns for BRAF, CRAF, MEK and ERK (n=5). Knockdowns (shown as a percentage) are calculated by quantifying total target protein levels in samples treated with RAF, MEK or ERK siRNA normalised to samples treated with non-targeting (NT) siRNA. **b.** Graphs depicting the BRAF, CRAF, MEK and ERK responses to 0, 5 and 20 mins EGF stimulation when treated with NT siRNA in the MRA experiments. Responses are normalised to samples with 0' EGF treatment (the non-treated cells). Means +/- SEM plotted (n=5).

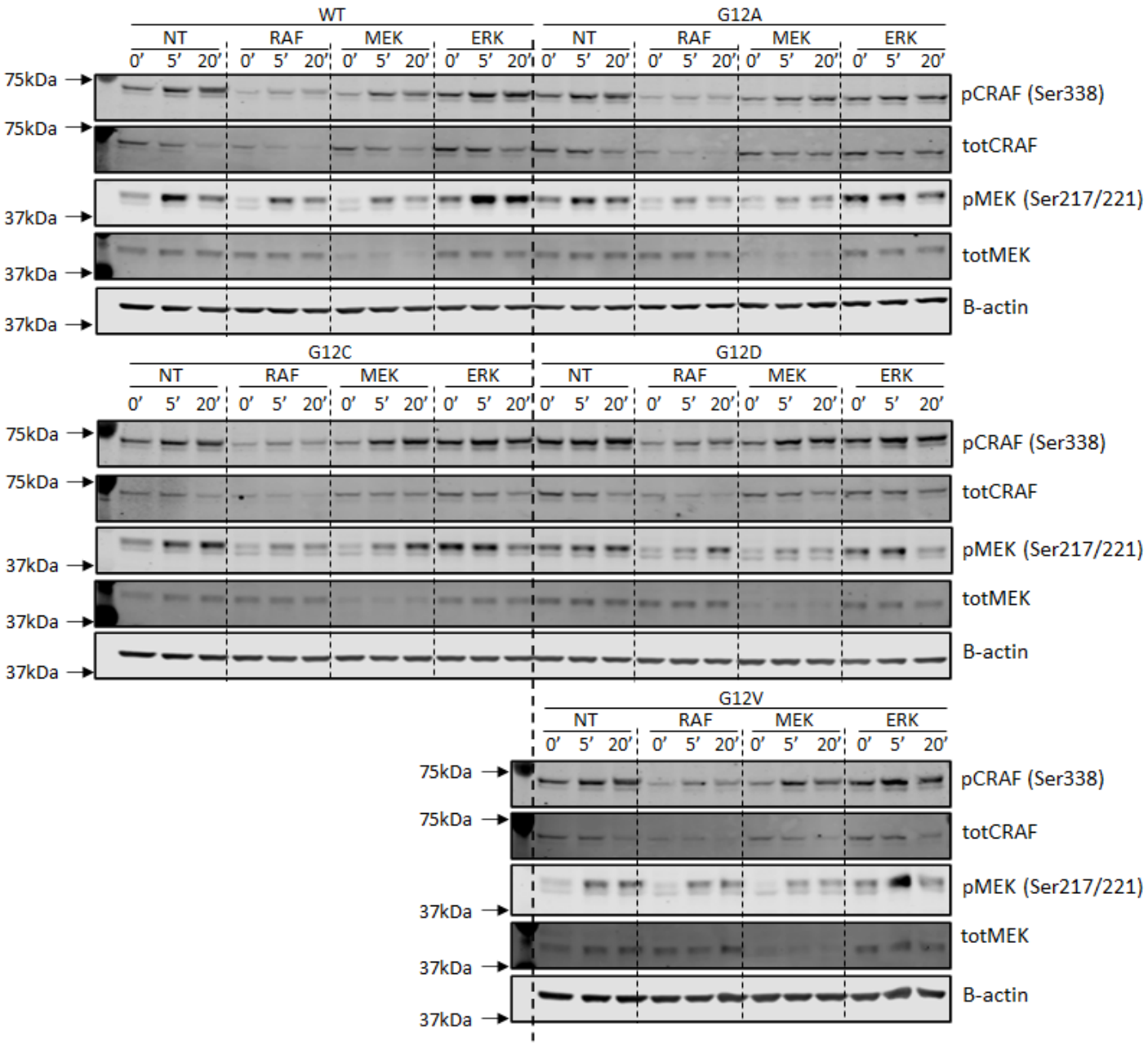

(figure legend on next page)

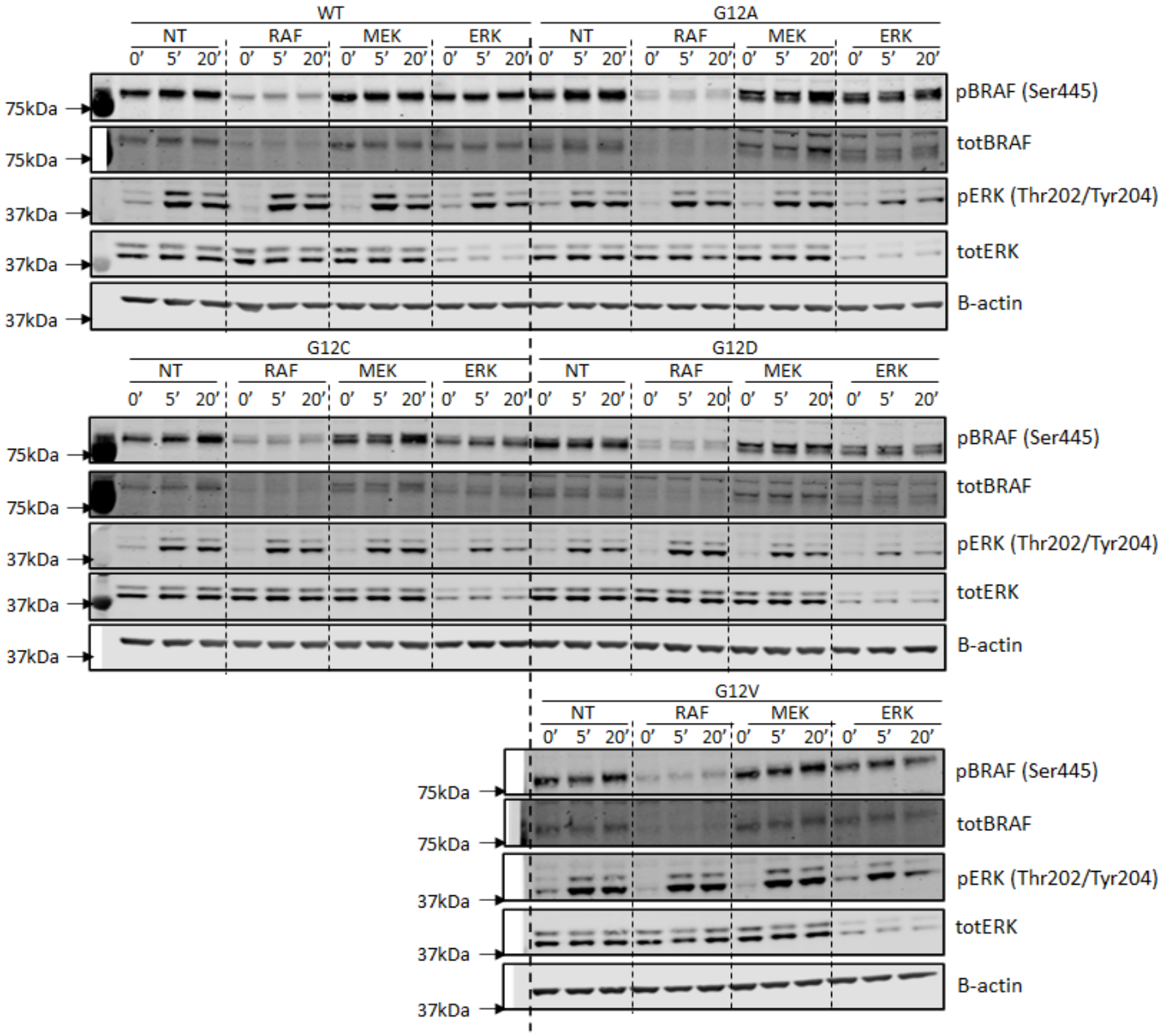

Figure 2.8. **Representative Western blots for MRA in LIM1215 cells.** Western blots from one repeat of MRA in LIM1215 cells showing pBRAF, totBRAF, pCRAF, totCRAF, pMEK, totMEK, pERK and totERK levels in WT and all mutant cells. Cells were treated with either non-targeting (NT), RAF, MEK or ERK siRNA, and 0,5 or 20 minutes of EGF (100ng/ml). Please note, pERK and pMEK phosphorylation sites refer to the ERK1 and MEK1 sites (n=5).

From the analysis of all topological maps shown in ***Supplementary figure 2.4***, we can infer two interesting observations that are summarised by the maps shown in ***Figure 2.9***. First, I observed a MEK to RAF negative feedback which is particularly prominent in G12D and almost absent in WT. To my knowledge, a negative feedback between MEK and RAF has not been reported in the literature. However, I note that MRA does not inform about the nature of the feedback, i.e., if the feedback is direct or - more likely in this case - mediated by other proteins.

Interestingly, this negative feedback is also seen, in a decreasing manner, in G12A, then G12C and the least in G12V ***(Supplementary figure 2.4)***. ***Figure 2.10*** shows the MEK to RAF interaction represented in a more visual way, showing the bootstrapped distribution of the feedback strengths. The x-axis shows the strength of the connection, with a positive number representing an activating interaction, and a negative number representing an inhibitory interaction. The y-axis shows the likelihood to find a given strength value across experiments. This graph shows more clearly the comparisons between the mutants and WT focusing solely on this particular interaction, with G12V clearly being more similar to WT than the other three mutants. Furthermore, as most of the distributions are rather tight and separated, especially when comparing G12A, G12C and G12D together with WT and G12V, it supports the fact that these differences are statistically significant. This data also supports the EGF treatment data shown earlier, where it was shown that the ERK responses were highest in WT followed by G12V, and then the other three mutants clustered together with even lower responses. The reduced ERK activation in G12A, G12C and G12D could be explained by this negative feedback seen most strongly in these three mutants.

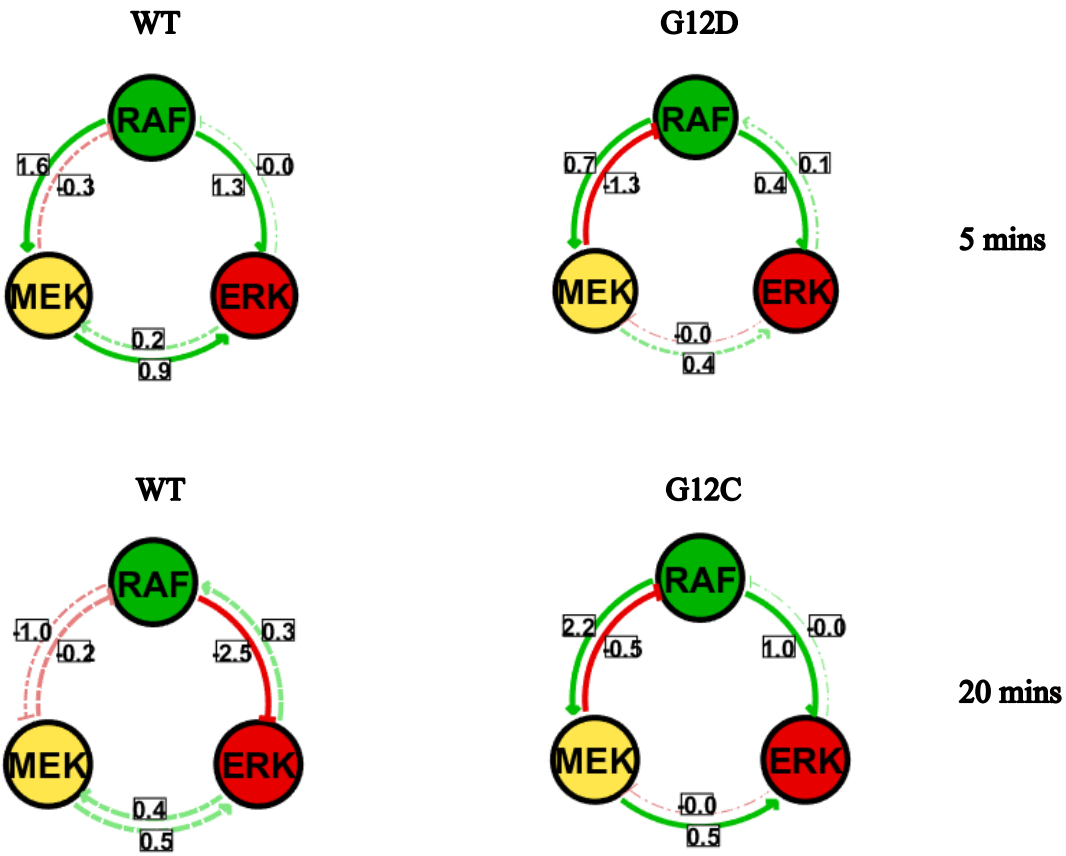

Figure 2.9. **Selected MRA maps.** Topological maps for WT and G12D with 5 mins EGF stimulation and WT and G12C with 20 mins EGF stimulation. The values represent the strength of the interaction between the 'nodes' of the pathway (RAF, MEK and ERK). A positive value indicates an activation and a negative value indicates an inhibition. The strength of the interaction is shown by the scale of the number (i.e., a larger positive value indicates a stronger activation). The colour and type of line also indicates the type of interaction (green arrow = activation, red blunt line = inhibition). Statistical analysis is done via bootstrapping and the thickness of the line connecting the nodes tells whether the connection is statistically significant (thick line = $p \leq 0.05$). The interactions between nodes represent both direct and indirect interactions.

The second robust observation is at 20 mins post EGF treatment when the ERK signalling returns to baseline. In WT cells, the well-characterised desensitisation of the pathway is determined by several negative feedback mechanisms, depicted in WT cells by MRA as an inhibitory interaction between RAF and ERK. In mutant cells, this negative feedback vanishes and, in some cells (e.g., G12C), appears to be a positive feedback. This negative feedback between RAF and ERK is the strongest in WT cells and decreases in G12D/V/A/C (in this order) ***(Supplementary figure 2.4)***. This could be due to loss of negative feedback, or activation of a positive feedback. Neither observations have been reported in literature, and the next step is to elucidate these mechanisms.

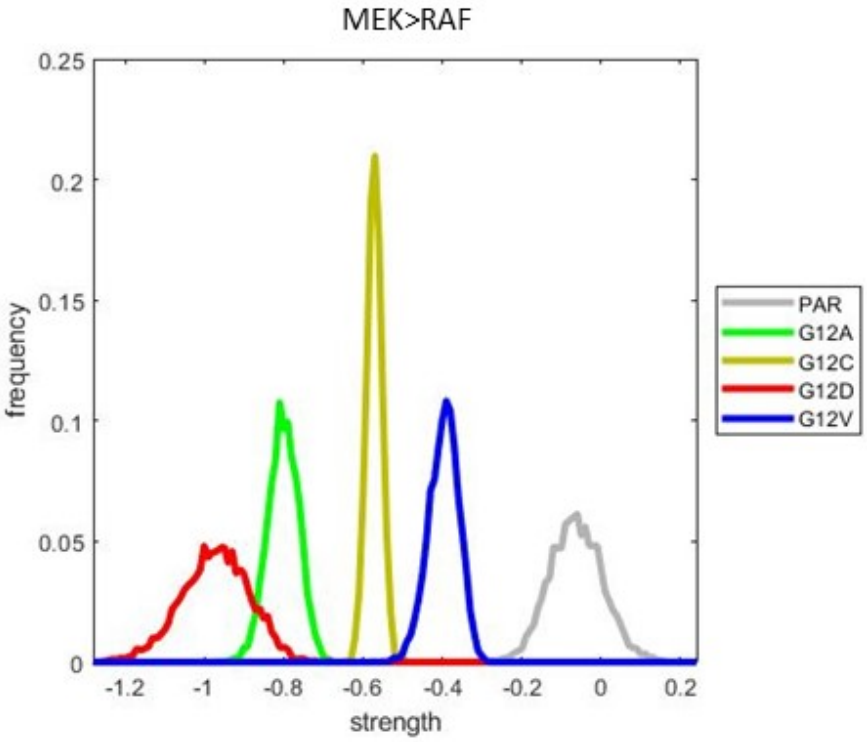

Figure 2.10. **MEK to RAF inhibition in G12D.** Graphical display showing the bootstrapped distribution of the MEK to RAF connection in WT (labelled as PAR for 'parental') and mutant cells with 5 minutes EGF treatment. The x-axis shows the strength of the connection (positive number represents an activating interaction, negative number represents an inhibitory interaction). The y-axis shows the likelihood of finding a given strength value across experiments.

Next, I generated heat maps from the raw quantification data (the ratio of phosphorylated/total levels of target proteins quantified from Western blots) that is inputted into the MATLAB code to see whether it reflects these two observations of interest. If indeed MEK inhibits RAF in G12D, then the phosphorylated fraction of RAF should increase upon treatment with MEK siRNA. ***Figure 2.11*** shows that the heat map for CRAF is in agreement with the generated MRA maps, however, for BRAF this is not the case. It should be noted that both BRAF and CRAF maps show a MEK to RAF inhibition at 5 minutes EGF. This possible disagreement in the data could be explained by the larger SEM values for BRAF due to the greater variation in phospho/total BRAF levels between the five repeats ***(Supplementary figure 2.5)***. Additionally, the total BRAF antibody used for the MRA experiments was acceptable but not very good, therefore, this could be a potential source for the larger variation. The heat map for the second observation also is in agreement with the maps generated; RAF siRNA should increase p/t ERK levels in WT but decrease it in G12C, and that is reflected in the raw data ***(Figure 2.11)***.

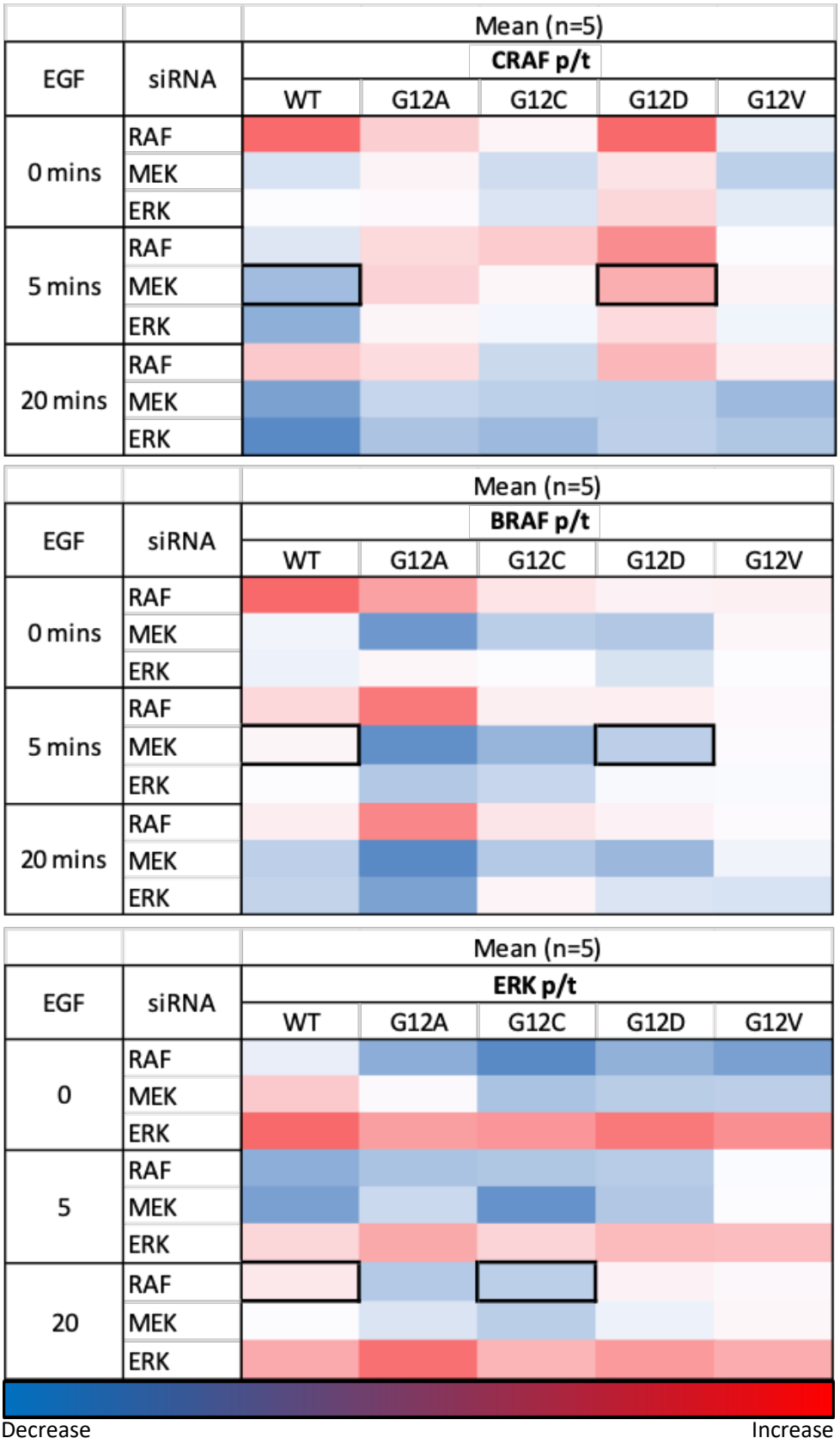

Figure 2.11. **Heat maps of raw MRA data.** Heat maps of BRAF, CRAF and ERK showing the increase and decrease in active protein levels with respective knockdown of RAF or MEK (n=5). The data is from the MRA raw quantification data from Western blots (which is used to generate the MRA maps). Scale bar: blue indicates decrease in active protein level, red indicates increase in active protein level

2.3.3 Validation of the MEK to RAF feedback

I hypothesised that AKT might be responsible for the MEK to RAF negative feedback because AKT is known to inhibit RAF (Zimmermann and Moelling, 1999). To test this hypothesis, I treated cells with an ATP-competitive inhibitor of AKT, afuresertib (2.5 μM for 2 hours). This resulted in a paradoxical increase in pAKT, which was not unexpected however, as hyper-phosphorylation of AKT at Tyr308 and Ser473 is a known effect of ATP-competitive AKT inhibitors (Okuzumi *et al.*, 2009; Yamaji *et al.*, 2017). To confirm AKT inhibition, therefore, I probed for a downstream effector of AKT, GSK3β. The data shown in ***Figure 2.12*** confirms that AKT is inhibited, at least in part, but whilst there is a slight increase in pCRAF levels in both WT and G12D, there is no difference in pBRAF levels, suggesting that AKT is not responsible for the RAF inhibition in G12D cells.

Another interesting observation from the Western blots of the MRA experiments was that there appears to be two BRAF populations present in G12A, G12C and G12D cells, but only one population present in WT and G12V. This is interesting because the data obtained thus far has shown WT and G12V behaving in a more similar manner in comparison to G12A, G12C and G12D cells. To my knowledge, the second BRAF protein form as visible in my Western blots at ~89kDa has not been formerly reported in human cells. Furthermore, the expression of the BRAF ~89kDa form increases with MEK knockdown suggesting that the apparent negative feedback we observe and the BRAF ~89kDa protein form might be causally linked. I wanted to test whether the increase in the top band of BRAF can be replicated with MEK inhibition rather than knockdown, therefore, in this experiment, I also inhibited MEK using the MEK inhibitor U0126.

I used both long (2μM U0126 for 46 hours) and short (20μM U0126 for 2 hours) treatment conditions. The short treatment did not alter BRAF expression, but the 2-days treatment resulted in the increase of BRAF and pBRAF immunostaining, recapitulating the MRA observations ***(Figure 2.12).*** Interestingly, the short UO126 treatment still seems to work as pMEK levels do increase in WT and, to a lesser extent, in G12D cells. This indicates that the mechanism responsible for the increase in the top BRAF band requires a certain amount of time. With 2 hours not being enough but 46 hours being sufficient, it appears transcriptional and/or translational changes may be involved. The characterization of the second BRAF band will be further described in **Chapter 3.**

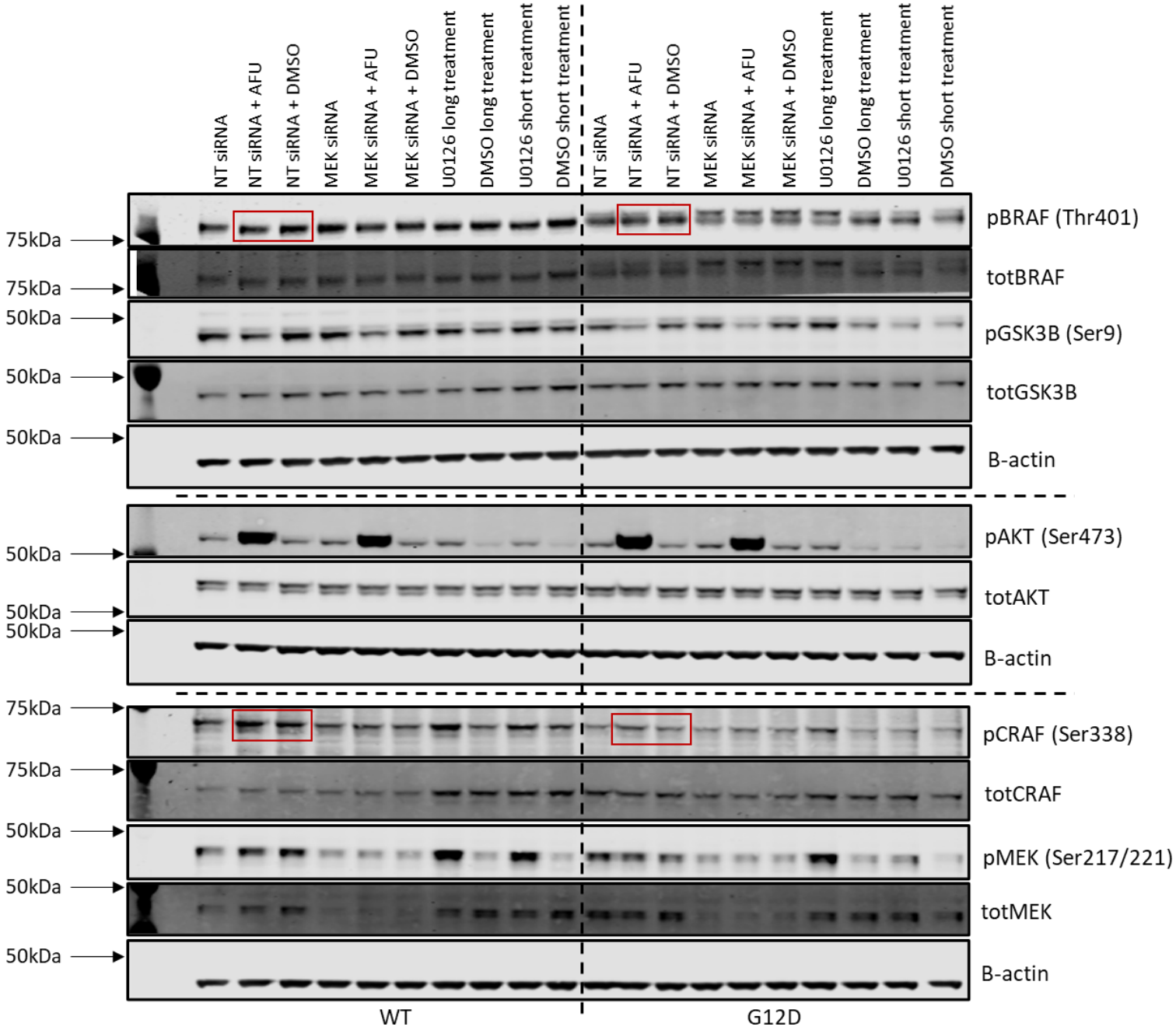

Figure 2.12. **Effects of AKT and MEK inhibition on RAF in LIM1215 WT and G12D cells.** Representative Western blots shown. U0126 'long' treatment refers to 2μM U0126 for 46 hours and 'short' treatment refers to 20μM U0126 for 2 hours. Cells were treated with either 5nM NT or MEK siRNA (for 29 hours). For AKT inhibition, 2.5μM afuresertib for 2 hours was added. No change in BRAF and CRAF activity with afuresertib treatment can be seen. Red boxes mark the afuresertib-treated and DMSO-treated lanes. With U0126 long treatment, appearance of higher molecular weight BRAF band increases. Please note, the pMEK phosphorylation sites correspond to MEK1 sites.

2.4 Antibody array

In order to investigate the mechanisms responsible for the two observations of interest from the LIM1215 MRA maps, I used an antibody array kit that detects phosphorylated proteins in five different signalling pathways: MAPK, AKT, JAK/STAT, NFκB, and TGFβ. I used this array specifically because RNA sequencing analysis of the LIM1215 cells indicated that genes involved in the inflammatory response of cells, including the NFκB signalling pathway, were upregulated in G12A, G12C and G12D cells (but not in G12V cells) in comparison to WT cells (see ***Figure 4.2***). This is interesting because again G12A, G12C and G12D appear to cluster together, this time in terms of transcriptional regulation. For the antibody array, the minimum conditions I wished to investigate were WT 5 mins EGF in comparison with G12D 5 mins EGF and WT 20 mins EGF in comparison with G12C 20 mins EGF as these are the conditions of interest from the MRA maps. The kit was an 8-sample kit, therefore, I also included WT, G12C and G12D 0 min EGF as controls and G12D 20 mins as a test sample. The full list of probed proteins and the targeted phosphorylation sites can be found in ***Supplementary figure 2.6***, and the sequencing results mentioned above will be discussed in detail in **Chapter 4**.

Each membrane contains duplicate spots for each target protein, and the data shown below is an average of the two spots. Negative control spots were used to subtract background noise. To account for unequal probing and different exposure times between membranes, they were normalised to a reference array (WT 0 min EGF) for each pathway. Each membrane has positive control (PC) spots which were used for this purpose (similar to using an internal loading control such as β-actin when running Western blots). The data for the 5 minute and 20 minute EGF samples have been normalised to the respective 0 min EGF samples and there are no error bars on the graphs as this experiment was only conducted once as an exploratory experiment.

2.4.1 Preliminary antibody array data suggests potential mediators of interactions revealed by MRA

When comparing the WT 5 min EGF sample with G12D 5 minute EGF sample, there are a number of differences in protein activation that are evident. The antibody arrays are shown in ***Supplementary figure 2.7*** and the graphs are shown in ***Figure 2.13.*** There appears the be an increase in phosphorylation of many proteins involved in the MAPK and the AKT pathways, which would be expected as KRAS predominantly signals via these two pathways. In contrast, a decrease in phosphorylation of many proteins of the NFκB and TGFβ pathways is seen, with the exception of

HDAC4, a histone deacetylase, which is activated. Proteins of the JAK/STAT pathway are largely unchanged between WT and G12D cells, except for a few such as EGFR, JAK1, SRC and STAT5, which are phosphorylated less in G12D cells. An in-depth literature review of those proteins that are differentially phosphorylated in G12D relative to WT cells did not reveal any obvious links to RAF inhibition via MEK. However, one of the differentially phosphorylated proteins from this array, c-Jun N-terminal kinase (JNK), may be of interest. As can be seen in ***Figure 2.13***, there is a larger amount of phosphorylated JNK in the G12D cells compared to the WT cells. MEK has been shown to activate JNK, and JNK has been shown to inhibit CRAF and BRAF (please see discussion chapter for further details), therefore, we can hypothesise that JNK may play a role in the MEK to RAF inhibition seen in KRAS G12D cells. However, this is extremely preliminary data, with no biological repeats or validation.

The second interaction of interest is that at 20 minutes EGF treatment, which is when the ERK signalling is shutting down in LIM1215 cells, and there is a RAF to ERK activation that is seen in G12C cells whereas in WT cells RAF is inhibiting ERK (which makes sense as a mechanism of reducing ERK signalling). To investigate the possible causes of this activation seen in G12C cells, the WT 20 minute EGF sample was compared with G12C 20 minute EGF sample (both normalised to their respective 0 minute EGF conditions). The array membranes are shown in ***Supplementary figure 2.8*** and as can be seen in the graphs in ***Figure 2.14,*** there are a number of proteins differentially phosphorylated between WT and G12C. Of these, TYK2, TAK1, TABK1, p38, AMPKα could be of potential interest based on their known interactions with ERK. TYK2 (tyrosine kinase 2) is particularly interesting because it is known to bind BRAF and has been shown to be required for full activation of ERK. Its phosphorylation is increased in G12C cells (see ***Figure 2.14c***), therefore, this increase may be causing the increase in pERK levels, which may be mediated in part by RAF (Carmo *et al.*, 2011).

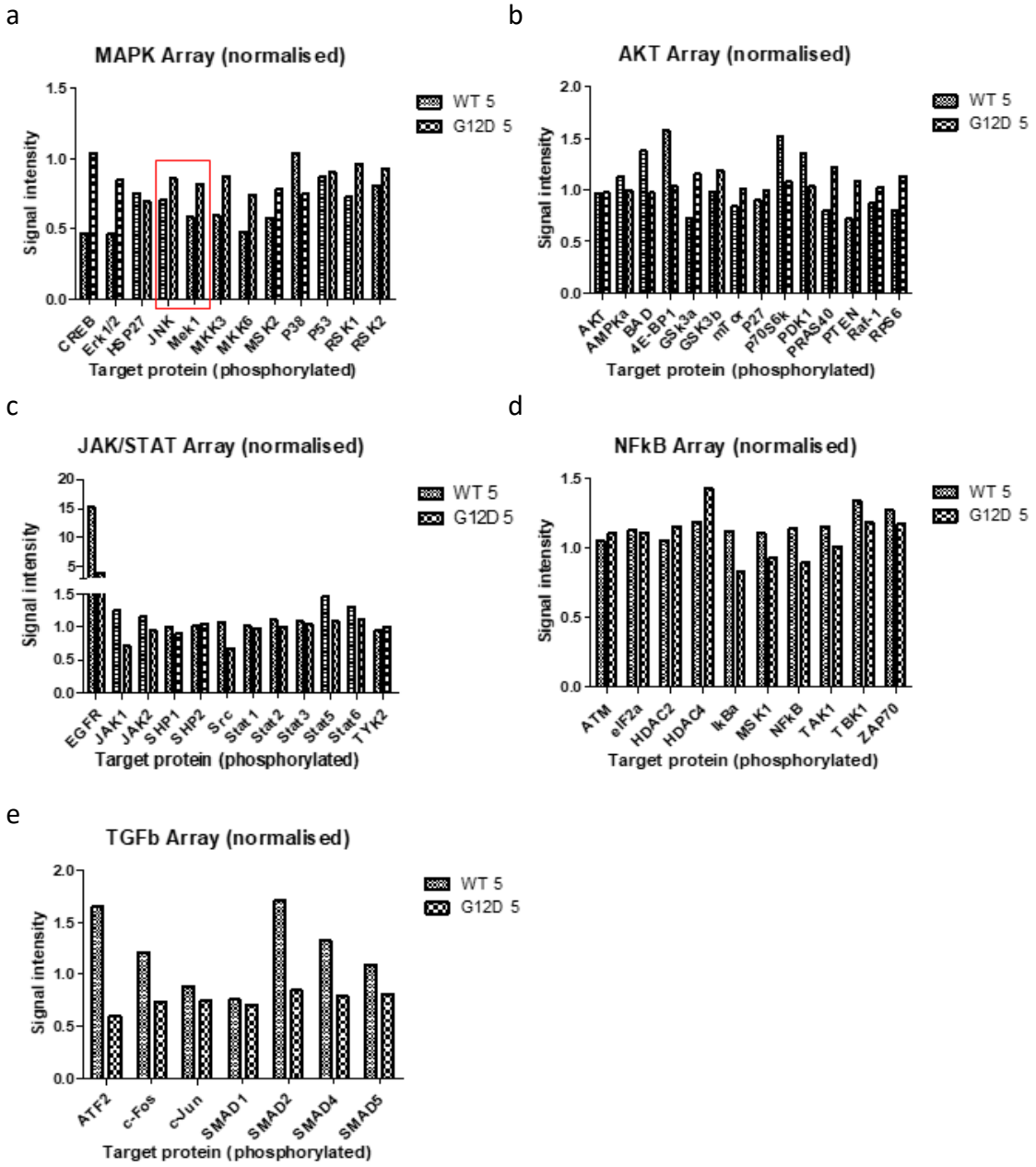

Figure 2.13. **Quantification of array spots for WT and G12D 5 minutes EGF samples.** Graphs depicting changes in phosphorylation of target proteins in LIM1215 WT 5 minutes EGF condition compared to G12D 5 minute EGF condition. **a.** MAPK array. **b.** AKT array. **c.** JAK/STAT array. **d.** NFκB array. **e.** TGFβ array. No error bars as only repeated once. Signal intensity is normalised to WT 0 minute and G12D 0 minute EGF conditions, respectively. Two measurements taken for each target, and background was subtracted using negative control spots on membranes. ImageJ (with an array plug-in) was used to quantify spots. Red box highlights the increase in JNK and MEK phosphorylation in G12D cells.

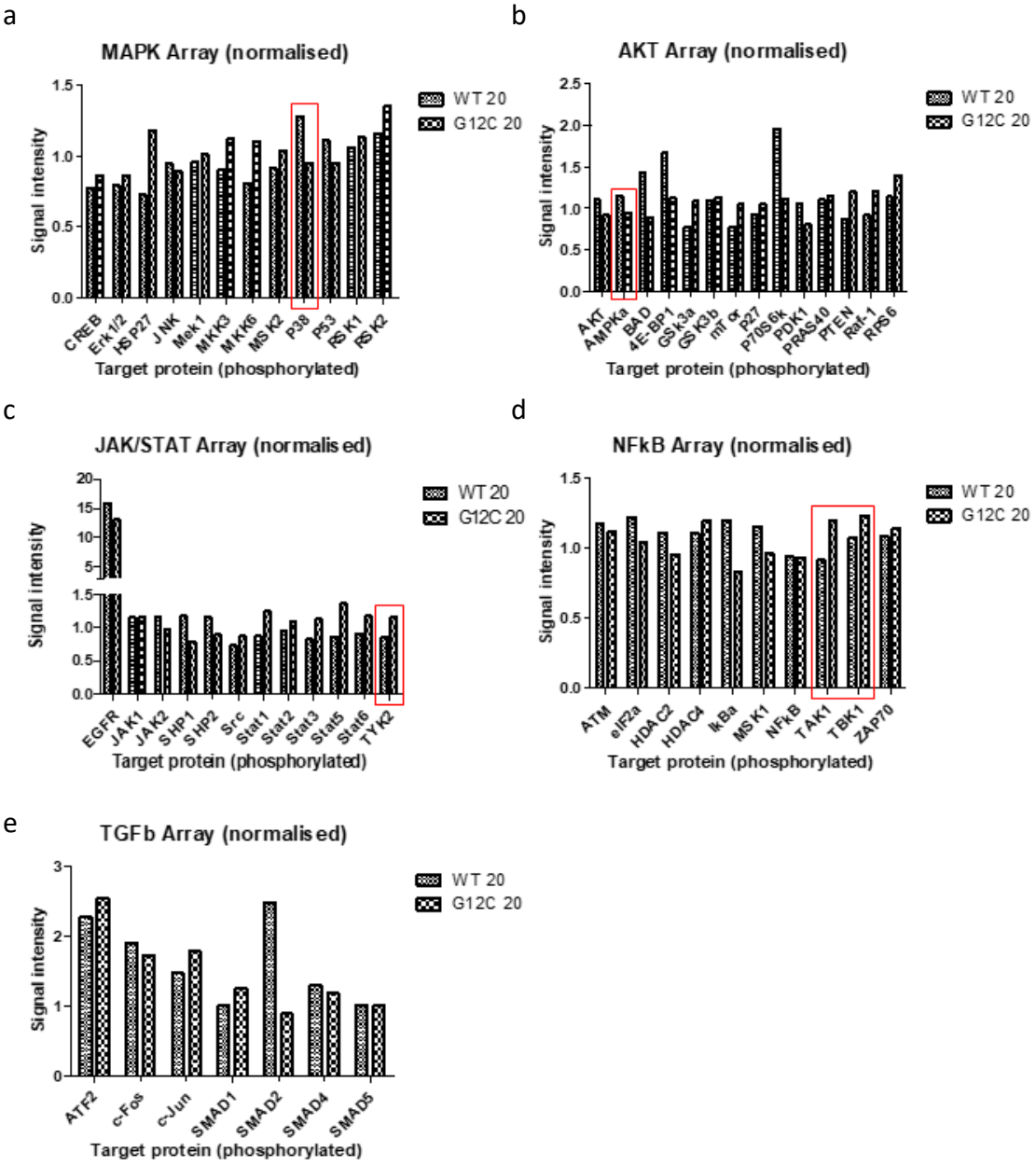

Figure 2.14. **Quantification of array spots for WT and G12C 20 minutes EGF samples.** Graphs depicting changes in phosphorylation of target proteins in LIM1215 WT 20 minutes EGF condition compared to G12C 20 minute EGF condition. **a.** MAPK array. **b.** AKT array. **c.** JAK/STAT array. **d.** NFκB array. **e.** TGFβ array. No error bars as only repeated once. Signal intensity is normalised to WT 0 minute and G12C 0 minute EGF conditions, respectively. Two measurements taken for each target, and background was subtracted using negative control spots on membranes. ImageJ (with an array plug-in) was used to quantify spots. Red boxes highlight key proteins of interest identified from literature review.

2.5 Modular Response Analysis in SW48 cells

2.5.1 MRA optimisation in SW48 cells

Initially, I attempted to generate MRA-based maps in SW48 cells but I had encountered issues in reproducibility of the knockdowns. This is why I have focused on the LIM1215 cell lines. However, for completeness, I report here the results obtained in this second SW48 isogenic panel of colorectal carcinoma cells (wild type (WT), G12A, G12C, G12D or G12V KRAS mutation) by Horizon Discovery. The cell line had been extensively characterised by the lab before the start of my project and, thus, was an ideal model system to use. As mentioned earlier, the key endogenous mutations in this cell line are in the *EGFR*, *FBXW7* and *CTNNB1* genes, which encode for the epidermal growth factor receptor, F-box/WD repeat-containing protein 7 and β-catenin, respectively.

Notably, the mutation within *EGFR* is not ideal as it is directly involved in the pathway being studied in this project and, usually, *KRAS* and *EGFR* mutations do not co-occur (although, as discussed earlier in this chapter, it has been shown that they are not mutually exclusive as previously thought). However, the SW48 isogenic panel of cell lines is still a valuable tool as any differences observed in signalling between these mutants can confidently be attributed to the specific G12 mutation.

An initial optimisation experiment was carried out prior to executing the MRA experiments to determine optimal siRNA concentration. I tested 5nM and 10nM pooled siRNA concentrations, and as shown in ***Figure 2.15****,* the knockdowns achieved were not very different between the two concentrations, with 5nM being sufficient in most cases. Therefore, to keep the conditions consistent with the MRA experiments in LIM1215 cells, 5nM was used.

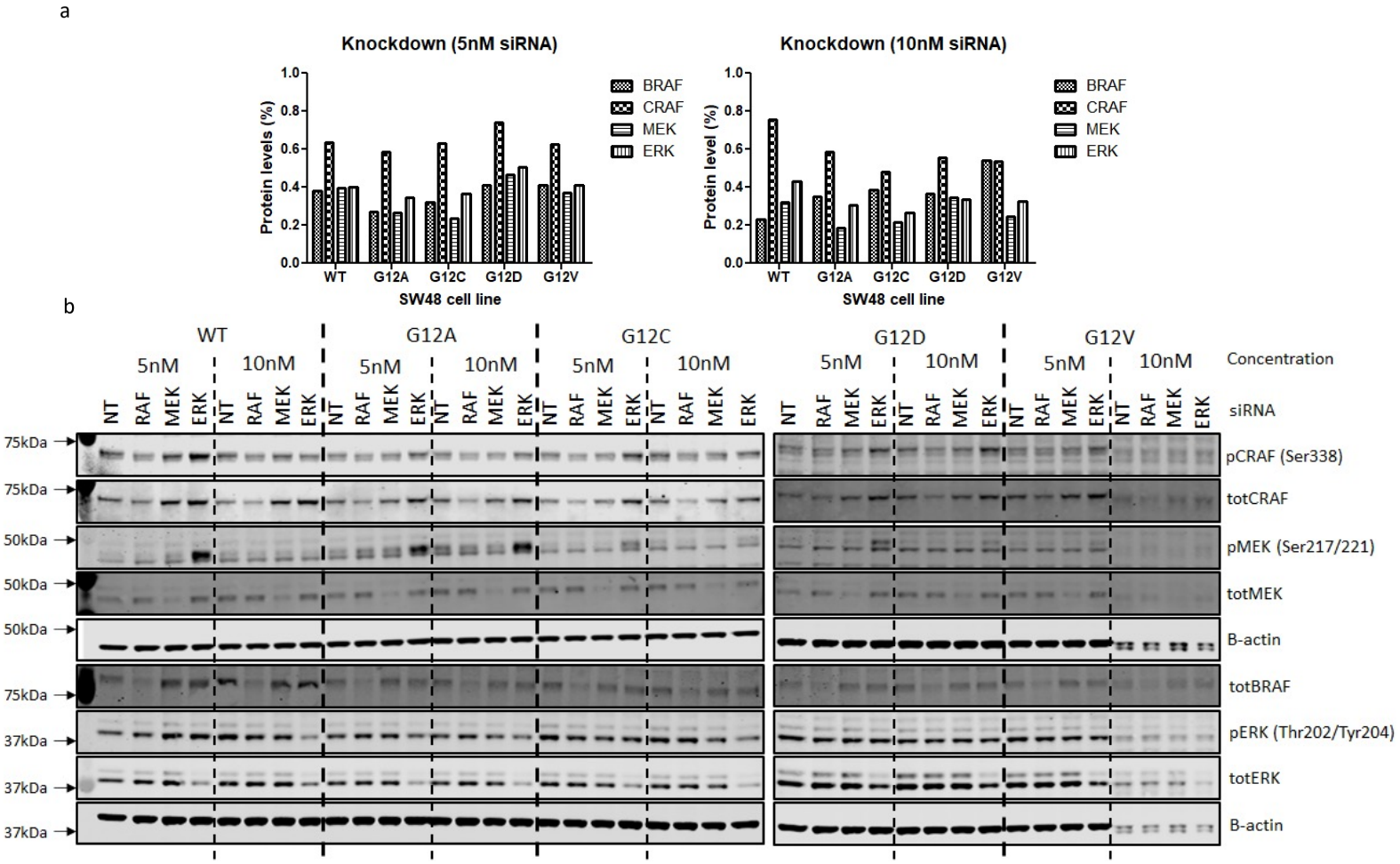

Figure 2.15. **Knockdown optimisation of BRAF, CRAF, MEK and ERK in SW48 cells. a.** Graphs showing the knockdowns achieved with 5nM and 10nM siRNA concentrations in SW48 WT and mutant cells. **b.** Western blots of BRAF, CRAF, MEK and ERK bands. No error bars as only n=1. Last four lanes look distorted due to technical problem with manufacture of gel. Please note pERK phosphorylations correspond to ERK1 sites.

2.5.2 MRA results in SW48 cells

As shown in ***Figure 2.16***, the knockdowns achieved for CRAF were not as low as desired, as the aim was to have a 40-60% knockdown. In hindsight, perhaps 10nM CRAF siRNA concentration should have been used, however, there were still clear perturbations in total CRAF levels and, therefore, this shouldn't impact the MRA results significantly. The knockdowns for BRAF, MEK and ERK were much better and the mean responses of BRAF, CRAF, MEK and ERK are shown in ***Figure 2.17***. Representative Western blots are shown in ***Figure 2.18***. In contrast to the LIM1215 cells, WT cells did not have the highest ERK responses. This could be attributed to the other mutations present in the SW48 cells (*EGFR* and *FBXW7*). The constitutive activation of EGFR coupled with the KRAS mutation may result in these cells rewiring pathway activation in a way not fully understood in this moment. FBXW7 is also linked to the RAF-MEK-ERK pathway, as it has been reported in literature that FBXW7 can recognise a specific phosphorylation site (Thr401) on BRAF and target it for proteasomal degradation (Hernandez *et al.*, 2016).

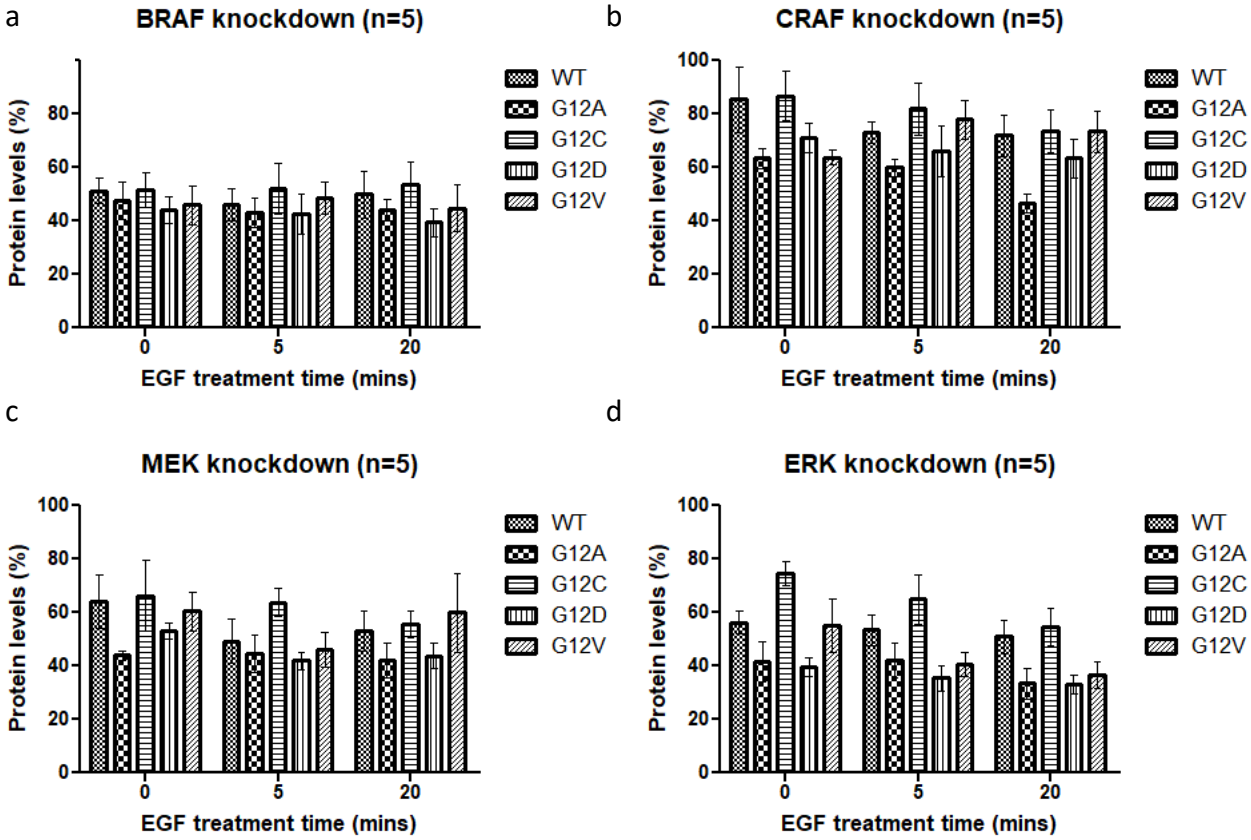

Figure 2.16. **MRA knockdowns achieved in SW48 cells**. Bar charts depicting mean knockdowns for: **a.** BRAF **b.** CRAF **c.** MEK and **d.** ERK in SW48 WT and mutant cells. Cells were treated with 5nM pooled RAF, MEK or ERK siRNA and normalised to cells treated with non-targeting siRNA. Means +/- SEM error bars plotted (n=5).

Many of the interactions within the generated MRA maps in the SW48 cells are not significant, as depicted by the dashed arrows connecting the nodes, therefore, it is difficult to make confident conclusions based on these maps ***(Supplementary figure 2.9)***. Furthermore, some of the values generated were unrealistically too large or too small, indicating a large variance in the data. One potential reason for these results may have been the fact that knockdowns were not achieved in every single sample in every repeat. Out of a total of 300 samples in the five repeats, 6 samples did not have any knockdown at all (although, when averaged across all repeats there is an overall knockdown). Therefore, because there is no perturbation of the targeted protein in those samples, this may naturally have an impact on the results. Also of significance, the SW48 cells in general appear to be more variable in their responses to siRNA treatment, as was observed in previous experimental data not shown in this thesis.

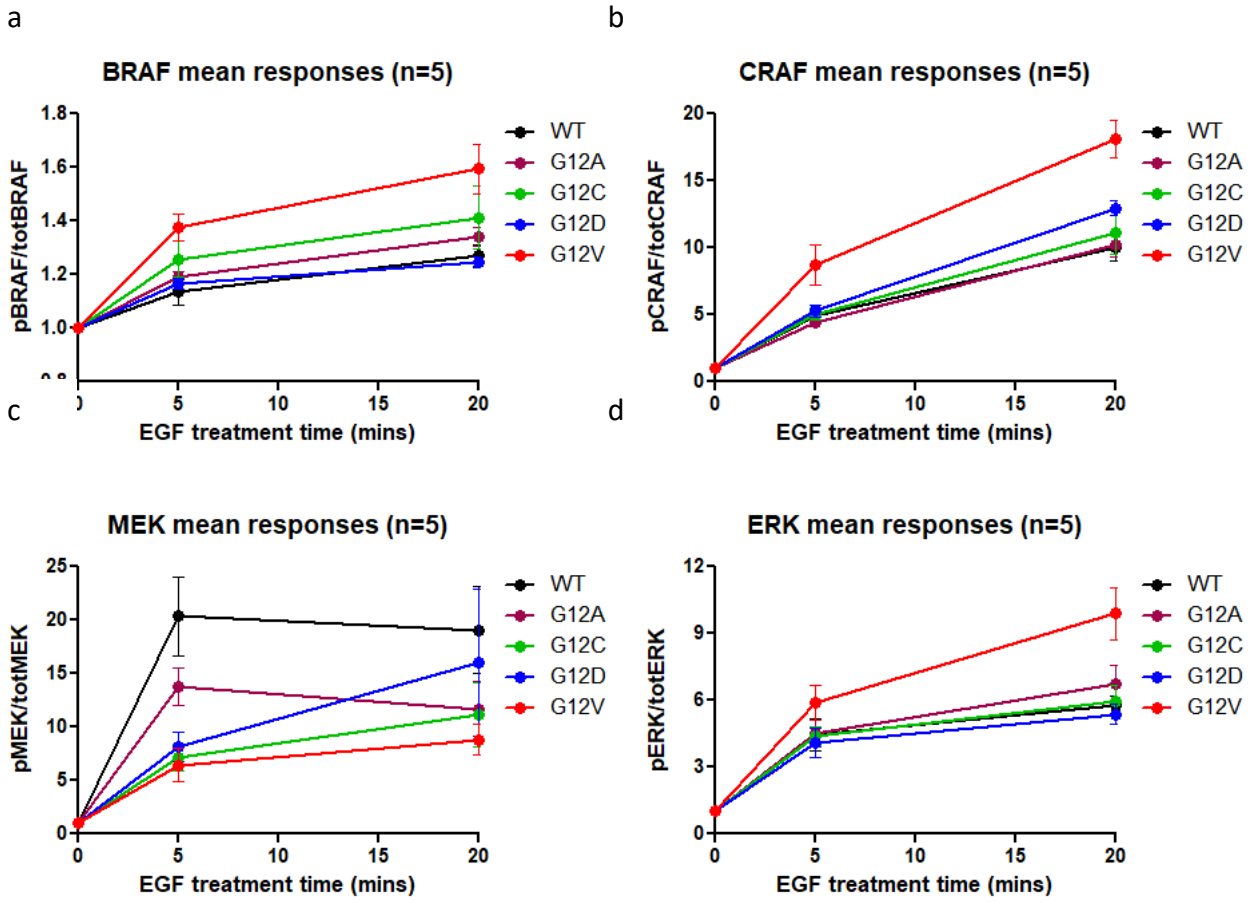

Figure 2.17. **MRA mean responses in SW48 cells**. Graphs depicting the mean responses of: **a.** BRAF **b.** CRAF **c.** MEK and **d.** ERK to 0, 5 and 20 mins EGF stimulation (100ng/ml) in SW48 WT and mutant cells for the MRA experiments. Means +/-SEM error bars plotted (n=5).

To overcome the issue of the failed knockdowns, I repeated these experiments twice more, but only in WT and G12D cells because in three of the original repeats, all knockdowns had been achieved to some extent in these cell lines. Therefore, the aim was to have five repeats for WT and G12D cells where all knockdowns have worked and that would have hopefully translated into more statistically robust MRA maps. Unfortunately, in one of the new repeats, again there was no knockdown in two samples and the maps generated from these repeats (three of the original and two new ones) were also not very statistically robust (data not shown). In hindsight, a higher siRNA concentration should have been used, even if it meant the conditions were slightly different between LIM1215 cells and SW48 cells; it is more important to have the desired knockdowns and not necessarily the same experimental conditions in this case.

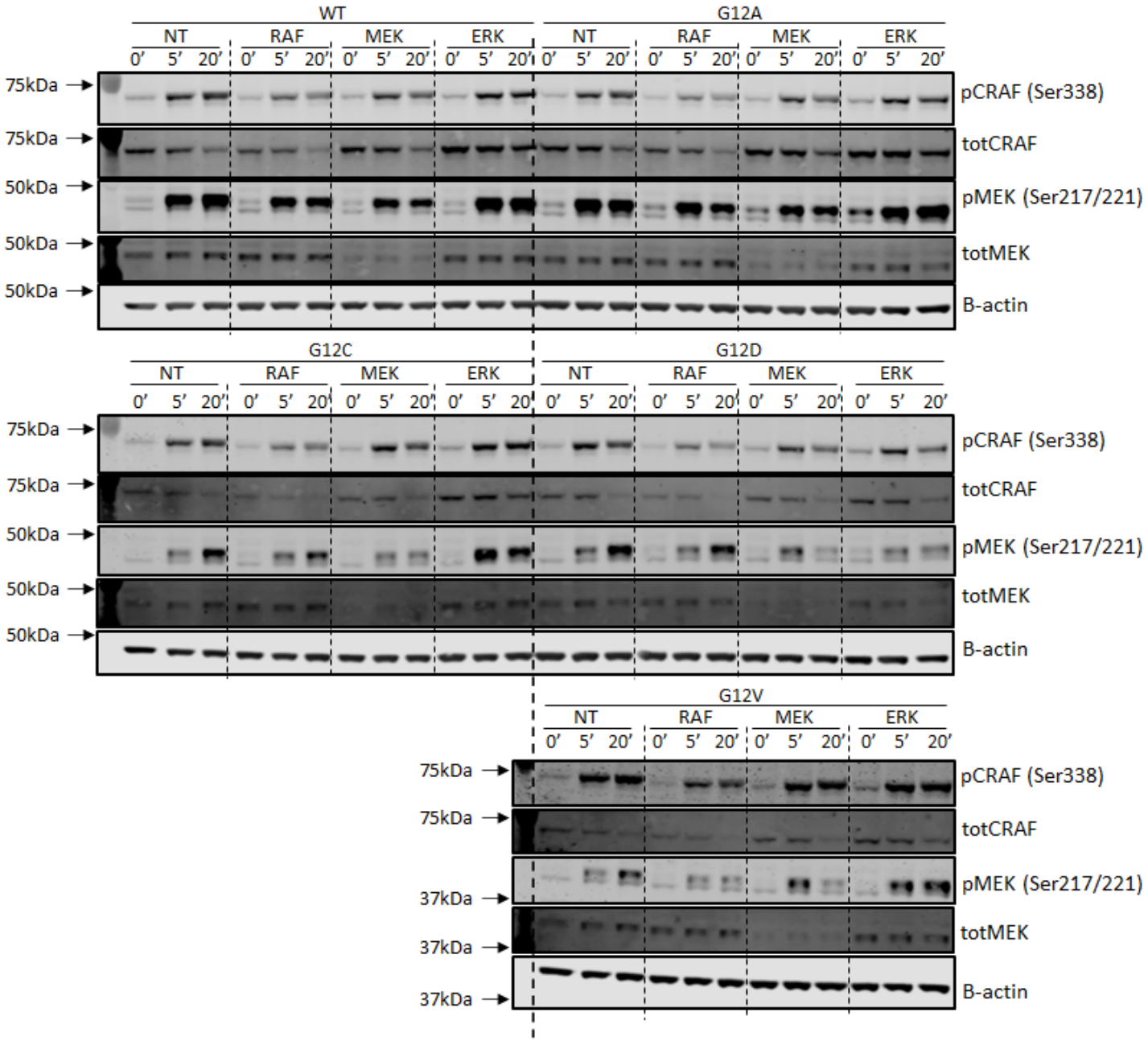

(figure legend on next page)

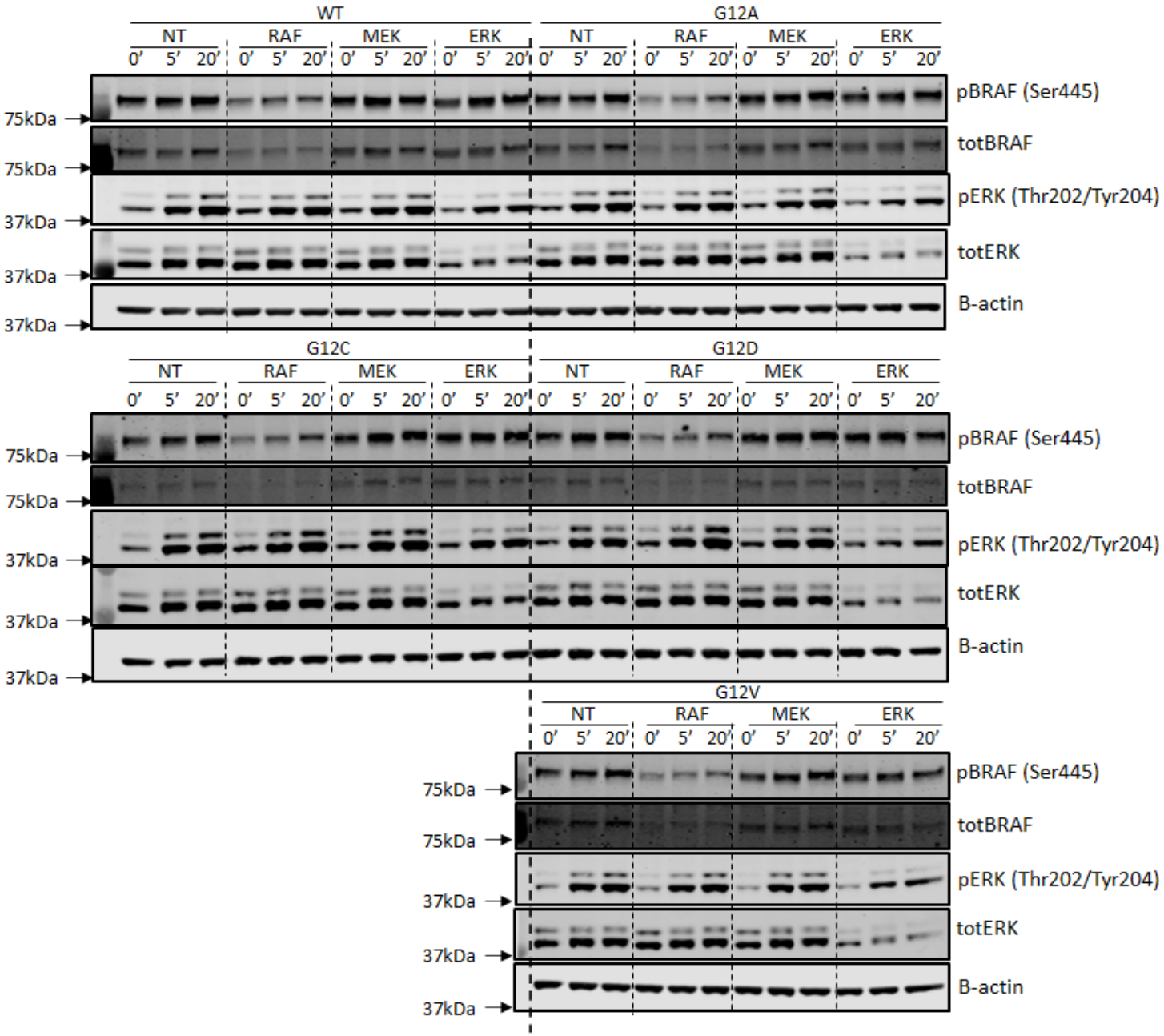

Figure 2.18. **Representative Western blots for MRA in SW48 cells.** Western blots from one repeat of MRA in SW48 cells showing pBRAF, totBRAF, pCRAF, totCRAF, pMEK, totMEK, pERK and totERK levels in WT and all mutant cells. Cells were treated with either non-targeting (NT), RAF, MEK or ERK siRNA, and 0,5 or 20 minutes of EGF (100ng/ml). Please note, pERK and pMEK phosphorylation sites refer to the ERK1 and MEK1 sites (n=5).

One interesting observation made was that with 20 minutes EGF stimulation there is a mobility shift in the BRAF and CRAF bands ***(Figure 2.18)***. It appears as if this shift is most pronounced with MEK or ERK knockdown, and in order to visualise the position of these bands in comparison to those in LIM1215 cells, lysates treated with MEK siRNA and 20 minutes EGF stimulation (from original MRA experiments) were run side-by-side on a gel ***(Figure 2.19).*** The mobility shift of the pBRAF bands was confirmed. It has been reported in literature that hyperphosphorylation of CRAF is a mechanism adopted by cells to downregulate RAF-MEK-ERK signalling (Dougherty *et al.*, 2005). This would explain this mobility shift at 20 minutes EGF for CRAF, and a similar mechanism may also be true for BRAF.

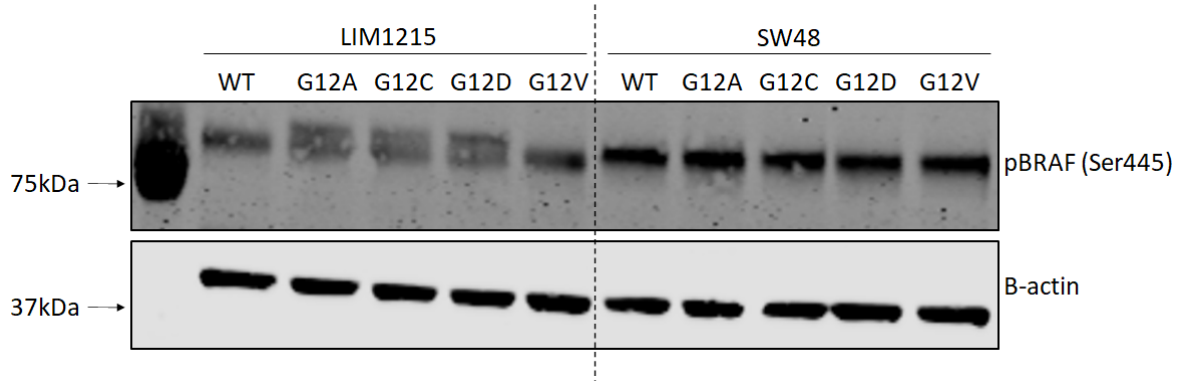

Figure 2.19. **Comparison of pBRAF bands in LIM1215 and SW48 cells.** Western blot showing the mobility shift of the pBRAF bands in LIM1215 cells compared to SW48 cells treated with MEK siRNA and 20 minutes EGF treatment. Samples treated with 20 minutes EGF were chosen because the mobility shift was most apparent in this condition. The samples run on this gel are from original MRA experiments (5th repeat of LIM1215 MRA and 2nd repeat of SW48 MRA experiments). MEK was not probed on this gel as knockdown has been established on the original MRA gels. ***Supplementary figure 2.10*** shows the MEK knockdowns in these samples.

2.6 EGF titration in SW48 and LIM1215 cells

It has been shown previously that ERK signalling dynamics can change with different growth factor concentrations (Ryu *et al.*, 2015). Another PhD student in the lab, Pablo Oriol Valls, has studied the impact of different EGF concentrations on ERK signalling in SW48 KRAS WT and G12D cells extensively at the single cell level ***(Figure 2.20)***. To build on this, I attempted to probe the ERK and PI3K pathways by titrating the EGF concentrations with the aim of observing changes in signalling dynamics in different KRAS mutant cells. I treated both LIM1215 and SW48 cells with EGF concentrations ranging from 0ng/ml to 200ng/ml for 5 minutes. In addition to probing for ERK and AKT, I also probed for BRAF due to the unknown MEK to RAF inhibition seen in MRA maps and the BRAF doublets seen in LIM1215 cells.

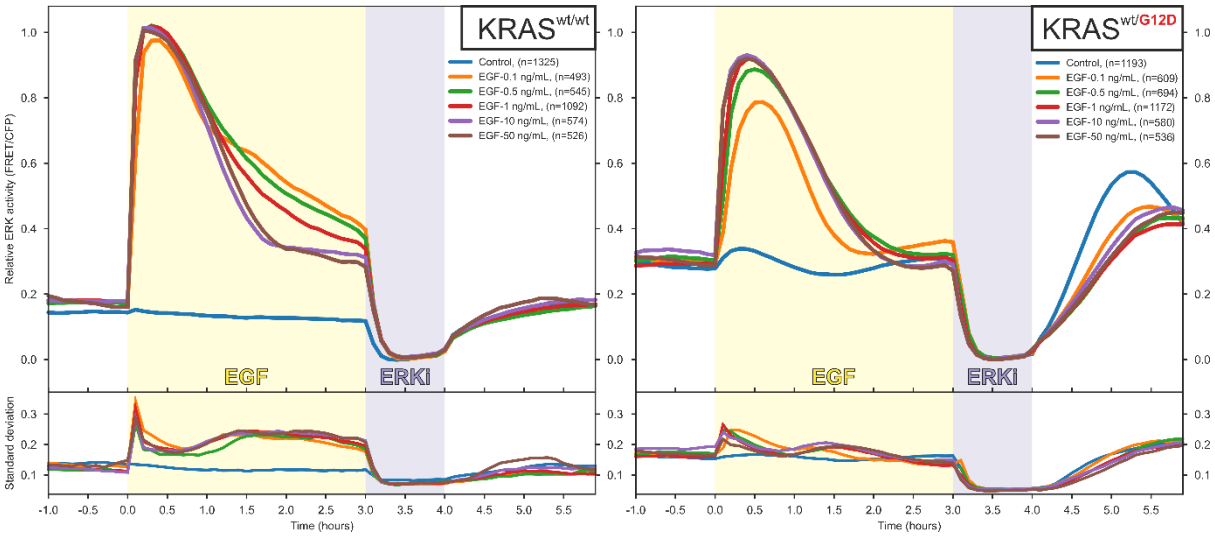

Figure 2.20. **Relative ERK activity in response to various EGF concentrations.** The signalling dynamics of ERK activity shown for SW48 KRAS WT and G12D cells using single cell data. Cells stably express an ERK FRET sensor which measures the ERK activity. Single cell data collected from 3 repeats (6 repeats for control and 1ng/ml EGF). Standard deviation shown at the bottom of the graphs. Data kindly provided by Pablo Oriol Valls.

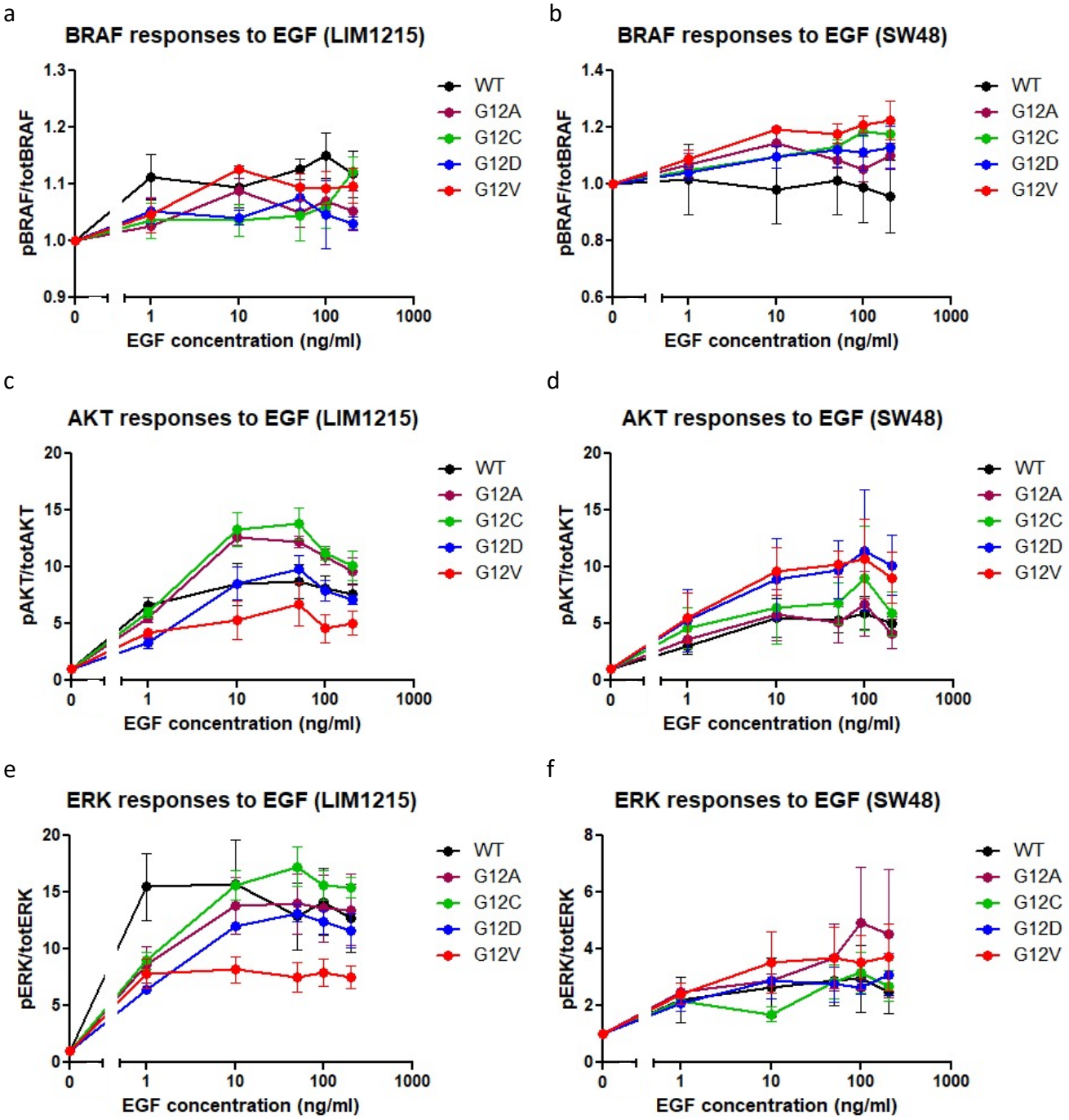

Figure 2.21. **Titration of EGF concentration in SW48 and LIM1215 cells.** Graphs showing mean BRAF, AKT and ERK responses in SW48 and LIM1215 cells in response to different EGF concentrations for 5 minutes. **a.** BRAF responses to EGF in LIM1215 cells. **b.** BRAF responses to EGF in SW48 cells. **c.** AKT responses to EGF in LIM1215 cells. **d.** AKT responses to EGF in SW48 cells. **e.** ERK responses to EGF in LIM1215 cells. **f.** ERK responses to EGF in SW48 cells. Means +/-SEM error bars plotted (n=3).

As can be seen in ***Figure 2.21***, the active BRAF levels are not significantly different in the different mutants in both LIM1215 and SW48 cells. AKT response in LIM1215 cells appeared to peak at 10ng/ml or 50ng/ml, with WT and mutants having similar trends. Interestingly, depending on which concentration is used, different mutants respond to different extents. For example, at 1ng/ml, the responses of all cell lines are relatively similar in comparison to other concentrations, and WT and G12D appear to have the largest and lowest responses, respectively. At 10ng/ml EGF however, not only do the responses vary more, the order of response across the mutants vary too, with G12A and G12C responding more now and G12V having the lowest response. When compared to SW48 cells, the trend is slightly different to LIM1215 cells in that instead of peaking at 10 or 50ng/ml, the peak is at 100ng/ml for all cell lines and it then dips at 200ng/ml. Unlike with the LIM1215 cells, there isn't much difference in the order of response of each mutant with different EGF concentrations; the same mutants appear to respond the most or least regardless of EGF concentration. However, it is important to note the error bars are large and overlapping, therefore, it is difficult to make conclusive remarks here.

The ERK responses in LIM1215 cells compared to SW48 cells are quite interesting because not only are the responses much more amplified in LIM1215 cells, but the trend of the responses is also very different. Whereas the responses appear to gradually increase with increasing EGF concentration in the SW48 cells, this is not the case in LIM1215 cells where the responses peak earlier and then appear to plateau out or even decrease slightly. The ERK response in SW48 cells also seem to become more variable between the cell lines with increasing EGF, but again, due to the large error bars it is difficult to conclude this confidently. Interestingly, in the LIM1215 cells, the trends for WT and G12V are similar to each other and different to the trends for G12A, G12C and G12D, which cluster together in their responses. In WT and G12V, the peak response of ERK occurs with 1ng/ml, and then the responses plateau out or decrease slightly with increasing EGF. In contrast, with the other three mutants, there is a more gradual increase in ERK response up to 50ng/ml EGF, after which responses plateau out. This is of potential interest as WT and G12V cells tend to cluster together in their responses to stimulants, as shown earlier in the EGF and insulin treatment experiments and the MRA maps, and G12A, G12C and G12D cells tend to cluster together separately.

2.7 Discussion

Over the years, it has become apparent that not all KRAS mutants are biochemically the same and can have different impacts on cell signalling dynamics (Stolze *et al.*, 2014; Hammond *et al.*, 2015; Mo, Coulson and Prior, 2018). Understanding these differences could be key to developing mutant-specific therapies. This is further supported by the fact that many inhibitors targeting signalling pathways fail due to the induction of feedback mechanisms, leading to drug-resistance (Chandarlapaty, 2012). Studies have also shown that the presence of specific KRAS mutations can determine response to therapy (Linardou *et al.*, 2008; De Roock *et al.*, 2010; Garassino *et al.*, 2011). Signalling pathways do not operate in isolation, but rather interact with many other pathways, forming a complex network which is difficult to fully understand (Sanchez-Vega *et al.*, 2018). Therefore, an increased understanding of network rewiring in the presence of different KRAS mutations may provide invaluable information for the development of newer, more effective therapies for KRAS-mutant cancers.

In this chapter, I have attempted to elucidate how signalling downstream of KRAS may be rewired in different KRAS mutant cells using the LIM1215 isogenic panel. By conducting initial experiments where WT and mutant KRAS colorectal cancer cells were treated with EGF or insulin, it became apparent that certain mutants clustered together in their responses to these stimuli. WT tended to have the highest ERK response, which is the opposite of what would be expected as mutant KRAS should be signalling more strongly via the ERK pathway compared to WT KRAS. We hypothesised that mutant cells might need to constrain ERK signalling to keep it within a 'sweet spot', as too much signalling may hinder cell survival by causing cell death or senescence (Sale, Balmanno and Cook, 2019). In LIM1215 cells, G12V cells generally appeared to have the second highest response, with G12A, G12C and G12D mutant cells clustering together and responding the least. Collectively, this data suggests that mutant cells do signal differently, and that G12V may behave in a more similar manner to WT than the other mutants.

Another observation made was that the basal ERK levels were much higher in mutants compared to WT cells. Tumour cells can be 'addicted' to RAS (Singh and Settleman, 2009; Singh *et al.*, 2009; Vivanco, 2014), and it is a possibility that the added stress of starvation may actually be upregulating basal active ERK levels in mutants because these cells may be addicted to KRAS and need ongoing pathway stimulation for survival. AKT levels were also much higher in starved conditions (in WT and all mutants) compared to non-starved conditions, which could also be due to similar mechanisms. One way to test this hypothesis is to 'turn off' KRAS activity in these cells and see if this impacts cell survival. An

increase in cell death would suggest addiction to KRAS.

To test the hypothesis that KRAS mutant cells might reshape downstream pathways to moderate MAPK signalling, I carried out Modular Response Analysis (MRA) experiments to map the ERK pathway in LIM1215 cells. MRA is a technique which has been utilised by multiple groups to study connections within signalling networks. For example, Hood and colleagues used MRA to characterise isoform-specific mutant RAS signalling in isogenic SW48 cell lines. They found that in the absence of growth factors, basal downstream signalling of oncogenic RAS is reduced and that growth factors are required very early on in the RAF activation process for pathway activation. Furthermore, they also show that there is differential coupling of the different RAS isoforms to the RAF-MEK-ERK and the PI3K pathways and that these differences are dependent on growth factor stimulation. They used mathematical modelling based on MRA to show that the core signalling networks are very similar between the different RAS isoforms, although KRAS was shown to be the most distinguished from the rest of the isoforms (Hood *et al.*, 2019).

Interesting work has also been published by Bluthgen and colleagues, who utilised MRA-based mathematical models to identify feedbacks and crosstalk between the ERK and PI3K pathways in colorectal cancer cells. They showed that the existence of a negative feedback loop from ERK to EGFR leads to ATK activation upon MEK inhibition and predicted that combined inhibition of both MEK and EGFR is required for prevention of AKT activation and tumour cell survival. Using a xenograft model, they demonstrated that combined inhibition blocks cell growth in both BRAF-mutant and KRAS-mutant tumour cells (Klinger *et al.*, 2013). They have also more recently used MRA to investigate the role of SHP2, a protein that has been shown to be involved in resistance to colorectal cancer therapy. They found that whilst ERK signalling requires SHP2, AKT signalling is only partially dependent on it (Dorel *et al.*, 2018). Bluthgen and colleagues have also found that ERK is differentially activated by oncogenic KRAS in colon cancer and intestinal epithelial cells, and using MRA they found that this cell type-dependent differential ERK activation is modulated by specific MEK to ERK feedforward and negative feedback interactions (Brandt *et al.*, 2019).

MRA has also been used to analyse signalling reactivation and drug resistance mechanisms following treatment with inhibitors. Kholodenko and colleagues showed that negative and positive feedback loops are not sufficient for the full reactivation of stead-state pathway signalling following drug inhibition. They demonstrate that drug inhibition-induced activation of pathway signalling can be achieved depending on specific network topologies and the dimerisation of the kinase targeted by the

inhibitor. These findings are useful in informing the combination of existing drugs and also the development of newer drugs that consider the topologies of the network being targeted in specific contexts (Kholodenko *et al.*, 2021). All of these studies collectively highlight the value of MRA as a tool for studying signalling dynamics. Network topologies generated via MRA in my work revealed the presence of an apparent mechanism that permits MEK to inhibit RAF during the initial acute phases of a stimulus. This inhibitory mechanism is the strongest in G12D cells, followed by G12A and G12C cells and the weakest in G12V and then WT cells. These results are consistent with our interpretation of LIM1215 mutant responses to EGF. RAF inhibition via MEK in a KRAS G12 mutation-specific manner has not been reported in literature, and whilst there are multiple published studies demonstrating network rewiring in different contexts, these have not specifically focused on the impact of different KRAS mutations at the same codon. Santos and colleagues reported differential rewiring of the ERK pathway depending on whether EGF or NGF was used to stimulate the cells, but they did not report a MEK to RAF negative feedback interaction. However, this may be because they used a different cell line (PC-12) and also did not investigate ERK rewiring in the presence of KRAS mutations (Santos, Verveer and Bastiaens, 2007).

Next, the phosphorylation levels of multiple protein targets involved in the MAPK, AKT, JAK/STAT, NFκB and TGFβ pathways were probed. One motivation for selecting this specific array was the fact that RNA sequencing analysis (which will be discussed in **Chapter 4**) indicated that genes within inflammatory pathways such as TNFα signalling via NFκB were upregulated in only G12A, G12C and G12D cells when compared to WT, whilst this was not the case with G12V cells. One of the differentially phosphorylated targets was c-Jun N-terminal kinase (JNK), a protein kinase that exhibits both pro-oncogenic and tumour suppressive roles, although the role of JNK in the tumour microenvironment is not well characterised (Tournier, 2013). It has been shown that JNK can hyper-phosphorylate BRAF and CRAF in an inhibitory manner which renders RAF unresponsive to upstream signalling (Ritt *et al.*, 2016). Another study has shown that JNK can phosphorylate CRAF on Ser259, which then enables 14-3-3 to bind and inhibit the migration of CRAF to the plasma membrane where it would normally interact with GTP-bound RAS and be activated itself. This phosphorylation of Ser259 also appears to be dependent on the presence of oncogenic KRAS, not WT KRAS. Furthermore, MEK can active JNK (Adler *et al.*, 2008). These observations suggest that in G12D cells, the increase in active JNK may be leading to increased inhibitory phosphorylation of RAF; furthermore, this may be mediated by MEK, because not only does MEK activate JNK, but the array data also shows an increase in pMEK in G12D cells.

It is important to note that this proposed mechanism is based on extremely preliminary data. The antibody array has only been repeated once, therefore, confident conclusions can only be made after repeating it at least twice more. Furthermore, the Adler *et al.*, (2008) paper demonstrating JNK activation by MEK has not been confirmed by any other published data. If JNK is shown to be differentially phosphorylated in two more repeats of the antibody array data, this hypothesis can be tested with knockdown or inhibitor studies. If blocking JNK activity reduces RAF activation and if MEK knockdown reduces JNK activity, then these observations would then be able to strengthen the hypothesis. The hypothesis would be strengthened even further if these observations are only seen in KRAS G12A, G12C and G12D cells but not in WT or G12V cells. The next goal would be to understand why and how JNK is differentially regulated in the presence of different KRAS G12 mutants.

The MRA data has also indicated that G12C (and other mutants to a lesser extent) might exhibit a stronger RAF to ERK activation loop which is consistent with the faster desensitisation seen in WT cells. MAPK signalling dynamics has profound effects on the transcriptional reprogramming of cells (Yang, Sharrocks and Whitmarsh, 2003; Nadal-Ribelles, 2019). The differences I observe might therefore have both implication in determining specific phenotypes but potentially also in the response to inhibitor therapy. Preliminary data obtained with an antibody array highlighted several possible candidates for explaining this loss of negative feedback, including TYK2, TAK1, TBK1, p38 and AMPKα. TYK2, a non-receptor tyrosine kinase involved in cytokine signalling and the regulation of the immune system, is a particularly strong candidate that has also been implicated in oncogenesis, although its precise role in the tumour progression is not fully understood (Übel *et al.*, 2013). TYK2 is known to be required for full ERK activation and to bind to BRAF, providing a plausible mechanism to explain our observations (Carmo *et al.*, 2011). The other four proteins identified are of less interest because a link with RAF is less clear from literature review. For example, TAK1 and TBK1 are involved in the activation of ERK and phosphorylation of these two proteins is increased in G12C cells in the array data (Zhou *et al.*, 2018; Qu *et al.*, 2019). P38 and AMPKα (the catalytic subunit of AMPK) are known to decrease ERK (and MEK) activity. P38 achieves ERK inhibition via the activation of protein phosphatases 1 and 2A (PP1 and PP2A). The reduction in p38 and AMPKα activity in G12C cells could therefore reduce ERK inhibition resulting in a net reactivation of ERK (Westermarck *et al.*, 2001; Kim *et al.*, 2012). As with the JNK hypothesis, the TYK data is very preliminary and needs to be validated.

It is important to note that there is some discrepancy between the MEK and ERK responses in the array data when compared to my previous experimental data. In previous experiments in LIM1215 cells, pERK and pMEK levels would always be highest in WT cells compared to the mutants. However,

in this data, the opposite is the case. The phosphorylation sites probed in all experiments are the same, so that is not an issue. Potential explanations for this difference could be the use of different reagents between experiments and differences in quantification (different quantification softwares and techniques used and the fact that other experiments show a ratio of phospho/total protein levels whereas in the antibody array only phospho levels are quantified). Furthermore, as mentioned earlier, this array has only been repeated once and unfortunately, due to lack of time, validation experiments have not been done yet. However, I can formulate very preliminary working hypotheses that JNK and TYK may potentially be involved in mediating the two interactions of interest revealed by the MRA data.

The majority of my experiments have been carried out with a stimulus of 100ng/ml EGF. This concentration was initially chosen because it is the concentration Santos and colleagues utilised to activate ERK signalling in PC-12 cells and successfully generate topological maps using MRA (Santos, Verveer and Bastiaens, 2007). Based on the methodology employed by another group, the concentration of the stimulus should generate sub-saturating responses (Hood *et al.*, 2019). I have shown that 100ng/ml EGF produces strong ERK and AKT responses in all of my cell lines, and although my data does not confirm that this concentration is not saturating, it would be unlikely that a saturating concentration results in such differing levels of ERK activation in the different mutants. I also tested the linearity of the ERK and PI3K pathways in response to a variety of EGF concentrations. EGF titration experiments illustrate how mutant LIM1215 and SW48 cells respond differently from wild-type cells both in ERK and PI3K pathways. This observation confirms my MRA results showing that network topologies, signalling dynamics and amplitude of responses are all altered by oncogenic mutations.

Several observations could not be generalised across different panels of cell lines and the specific molecular mechanisms underpinning these differences has eluded us so far. However, we have plausible working hypotheses that might permit us to discover novel mechanisms for oncogene-mediated signalling rewiring. Once validated, we would be able to investigate how common these mechanisms are in cancer. In **Chapter 3**, I illustrate my attempts to identify a BRAF protein form that might be a mediator of the differences shown and in **Chapter 4,** I show how oncogenic mutations impact the transcriptome of cells.

3. Results Chapter II: A distinct BRAF protein form might contribute to differences between specific G12 mutants

3.1 Background

In the previous chapter, it was mentioned that two populations of BRAF can be seen in specific LIM1215 KRAS G12 mutant cells. The appearance of this BRAF doublet is consistent in every experiment and is even more intriguing because it associates uniquely with G12A, G12C and G12D cells, which as discussed in **Chapter 2**, cluster together in their responses to EGF and in the MEK to RAF inhibition seen in LIM1215 cells. In this chapter, the efforts made to elucidate the identity of the second BRAF band are presented and discussed.

Amongst other hypotheses, one that I explore in this chapter is that the unknown second BRAF population may be a splice variant. The consensus *BRAF* transcript contains 18 exons translating into a 766 amino acid (~ 84.4kDa) protein. *BRAF* transcripts can be alternatively spliced resulting in multiple different BRAF splice variants (Hirschi and Kolligs, 2013). Some transcripts include known additional exons 8b and/or 9b translating into BRAF proteins with higher molecular weights (Hmitou *et al.*, 2007). There are also other exons such as 14, 15, 15b, 16b and 16c that are either deleted and/or inserted which all lead to truncated BRAF proteins due to the introduction of premature stop codons (Hirschi and Kolligs, 2013). The presence of exon 8b or exon 9b differentially regulates BRAF by decreasing or increasing its kinase and oncogenic activities, respectively (Papin *et al.*, 1998). These exons also interfere with the ability of the BRAF N-terminus to interact with the C-terminal kinase domain, with exon 8b increasing and exon 9b decreasing the binding between these domains (Hmitou *et al.*, 2007). Valluet and colleagues generated two conditional knockout mice of exons 8b and 9b in order to understand further the importance of BRAF splice variants. They found that constitutive deletion of either exon alone results in healthy and fertile mice with no developmental abnormalities, but that exon 9b (but not exon 8b) is required for hippocampal-dependent learning and memory (Valluet *et al.*, 2010).

Alternative splicing of BRAF can also play a role in the development of resistance to RAF inhibitors. For example, Vido and colleagues showed that RAF inhibitor treatment increased phosphorylation at

Ser729 on alternatively spliced BRAF V600E, resulting in drug resistance via enhanced association with MEK (Vido *et al.*, 2018). Of the many alternate splice variants of BRAF reported in literature and the NCBI database, those with an exon 9b would produce a BRAF protein of the molecular weight observed in my Western blots (see ***Figure 3.1***). Other hypotheses explored in this chapter include the possibility that the higher molecular weight BRAF population is a differentially phosphorylated or ubiquitinated variant of BRAF.

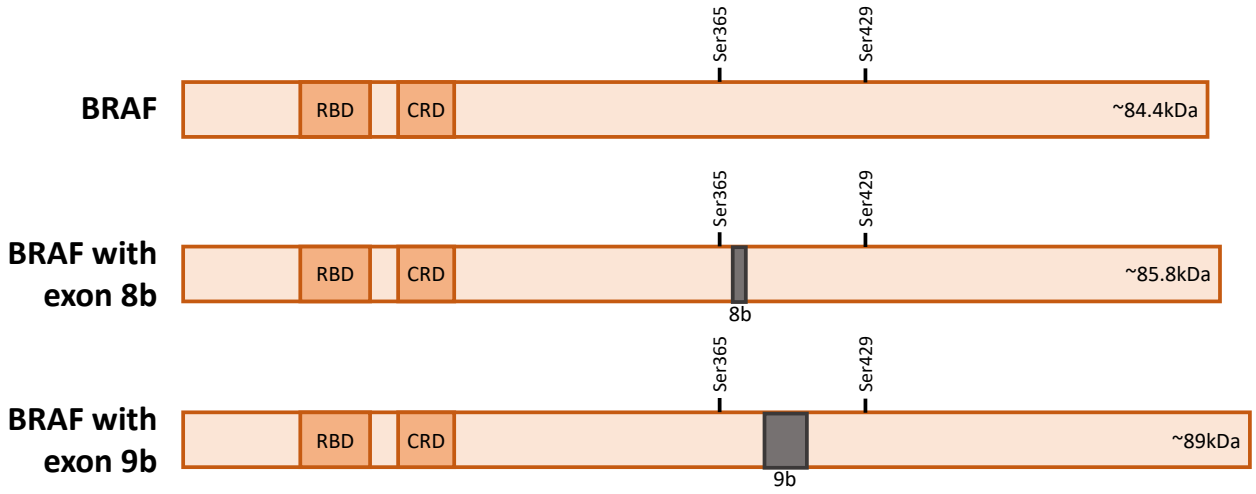

Figure 3.1. **Schematic diagram of BRAF splice variants with exon 8b and 9b insertions.** Insertion of exon 8b or 9b can interfere with the ability of the N-terminus to interact with the C-terminus via the involvement of two key residues, Ser365 and Ser429 (highlighted). Predicted molecular weights are also shown for each splice variant, with the exon 9b variant corresponding most closely with the molecular weight of the unknown BRAF band seen in my Western blots. Antibodies used in my work are able to detect these splice variants as these additional exons do not interfere with the antibody recognition sequence.

In this chapter, I also utilise another cell line in addition to the LIM1215 and SW48 cell lines. It is the human pancreatic nestin-expressing (HPNE) cells, which are pancreatic ductal epithelial cells that have been immortalised via the ectopic expression of the catalytic subunit of human telomerase (hTERT). These cells also express the HPV proteins E6 and E7 and the SV40 small t antigen (Lee *et al.*, 2003; Campbell *et al.*, 2007). These hTERT-HPNE E6/E7/st cells were purchased from ATCC and an additional myc-tagged KRAS copy (WT or mutant) has been inserted in-house by other members of the lab. An mCherry expressing cell line has also been engineered as a control. This cell line was utilised as a substitute cell line for LIM1215 in one of the experiments where knockdown of FBXW7 (a protein of interest) could not be achieved in LIM1215 cells.

3.2 Unknown higher molecular weight BRAF population increases with MEK knockdown/inhibition

In the previous experiments where the appearance of the top BRAF band was seen, all mutants were never on the same Western blot gel. Therefore, to visualise and compare the BRAF bands of WT and mutants together and to confirm that the additional band is definitely a higher molecular weight band, they were all run on the same gel. ***Figure 3.2*** confirms this, and it is also evident that the top band increases (and bottom band decreases) with MEK siRNA in G12A, G12C and G12D cells. This is interesting also because the MEK to RAF inhibition is seen in these mutants and, therefore, there could be a link between the top BRAF band and the inhibition seen in the MRA maps.

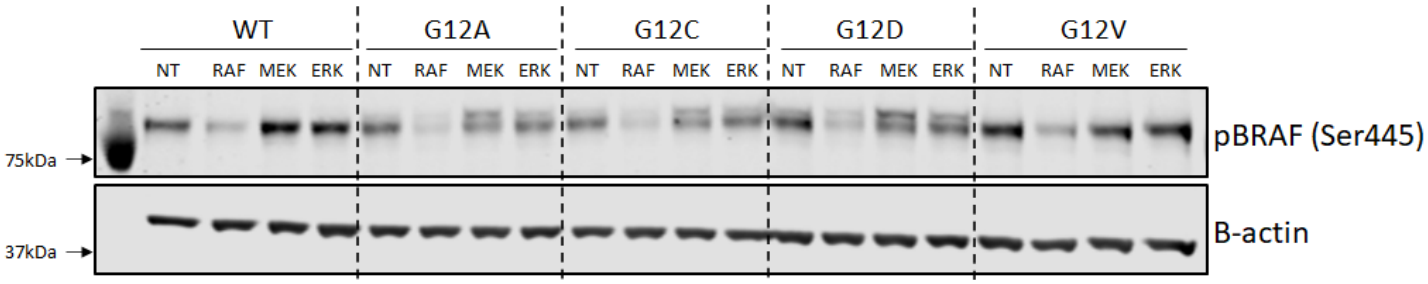

Figure 3.2. **Confirmation of top BRAF band in LIM1215 G12A, G12C and G12D cells.** Western blot showing pBRAF bands in LIM1215 WT and mutant cells on one gel. Gel also confirms increase in top BRAF band with MEK knockdown compared to cells treated with non-targeting siRNA.

As briefly mentioned in the previous chapter, these cells were also treated with the MEK inhibitor U0126 to see whether this also has an impact on the top BRAF band. Cells were treated with either 2µM U0126 for 46 hours ('long treatment') or 20µM U0126 for 2 hours ('short treatment'), then the cells were treated with EGF for 5 minutes prior to being harvested with cell lysis buffer (RIPA). As can be seen in ***Figure 3.3***, both short and long treatment of U0126 is sufficient for inhibition of MEK and ERK, demonstrated by the paradoxical hyperactivation of MEK and subsequent reduction in ERK phosphorylation. The paradoxical hyperactivation of MEK is similar to that seen with AKT upon treatment of afuresertib in the previous chapter and therefore is not a surprise. Inhibition of MEK and, therefore ERK, is demonstrated by the reduction in ERK phosphorylation.

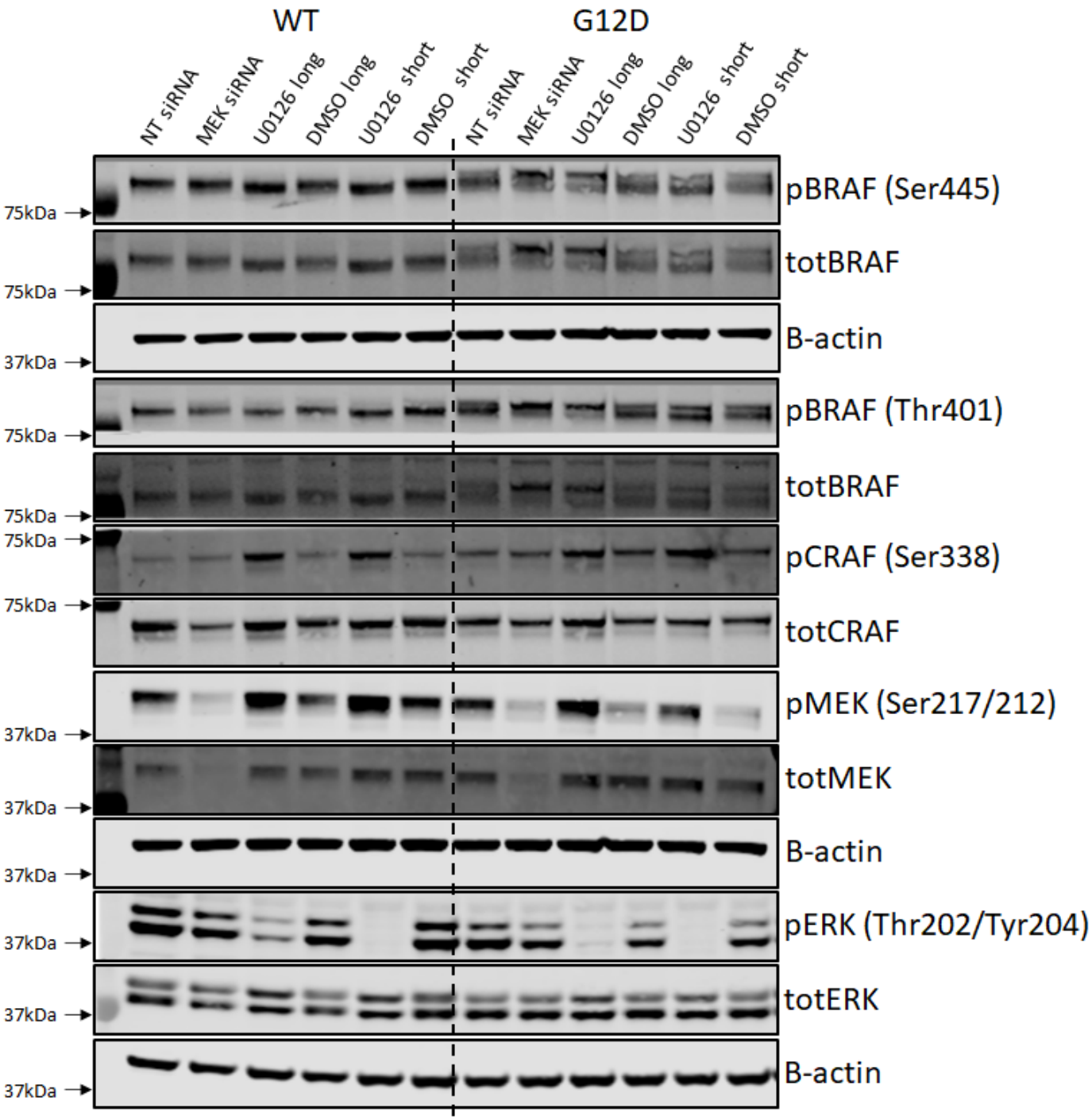

Figure 3.3. **Effect of U0126 treatment in LIM1215 WT and G12D cells.** Representative Western blot showing effects of long (2μM U0126 for 46 hours) and short (20μM U0126 for 2 hours) U0126 treatment time on activity of BRAF, CRAF, MEK and ERK. Two BRAF phosphorylation sites are probed: Ser445 because it is the standard measure of BRAF activation in my work, and Thr401 because it is an ERK-mediated phosphorylation site and FBXW7 recognition site. Please note the pMEK and pERK phosphorylations correspond to the MEK1 and ERK1 sites, respectively.

Despite the fact that short treatment of U0126 is sufficient for MEK inhibition, this does not translate to any effects on BRAF. Whereas long U0126 treatment results in an increase in the top BRAF band, short treatment does not have this effect. It is important to note that when treated with MEK siRNA, this is also for 46 hours. This suggests that whatever mechanism is responsible for the increase in the top BRAF band mediated by MEK knockdown or inhibition requires a certain amount of time to work.

Another interesting observation is that only U0126 treatment (long and short) increases CRAF phosphorylation in both WT and G12D cells, whereas MEK siRNA doesn't have this effect. On the other hand, the effects on BRAF differ depending on whether it is in WT or G12D cells. In G12D cells, only longer treatments such as with MEK siRNA or long U0126 treatment increases BRAF phosphorylation, specifically the top band. In WT cells, however, neither MEK siRNA nor U0126 treatment have any effect on BRAF phosphorylation, presumably due to the absence of the top BRAF band. These observations can be explained by the distinct effects of MEK siRNA and U0126 on pERK levels. ERK is known to inhibit BRAF and CRAF as part of a negative feedback loop, therefore, because MEK siRNA doesn't reduce ERK activity to the extent that U0126 does, the RAF inhibition by ERK is reduced in the samples treated with U0126 (Dougherty *et al.*, 2005; D. A. Ritt *et al.*, 2010). This would explain the U0126-induced increase in CRAF phosphorylation in both WT and G12D cells, which appears to be regulated by a ERK-mediated mechanism, and therefore is instead influenced predominantly by the phosphorylation levels of ERK rather than the treatment time of MEK knockdown or inhibition. In short, pCRAF levels appear to be influenced by pERK levels, and pBRAF levels appear to be influenced by total MEK levels.

Lastly, two different BRAF phosphorylation sites were probed for in this experiment, Ser445 and Thr401. Ser445 is the site probed in all other experiments as an indicator of BRAF activity, and Thr401 is an ERK-mediated inhibitory phosphorylation site (Mason *et al.*, 1999; Hernandez *et al.*, 2016). ***Figure 3.3*** shows that Thr401 phosphorylation levels are not affected by ERK phosphorylation levels and that the pattern of BRAF phosphorylation is also the same regardless of the phosphorylation site. Therefore, it appears that Thr401 phosphorylation is not involved in the top BRAF band, at least not via ERK.

3.3 Unknown BRAF population not due to additional phosphorylation

To test whether the top BRAF band is caused by increased phosphorylation on BRAF, the LIM1215 cells were harvested and treated with lambda phosphatase for 90 minutes to ensure all phosphate groups are removed. As can be seen by the lack of BRAF bands detected by pBRAF (Ser445) antibody in ***Figure 3.4***, the treatment successfully removed all phosphate groups (unfortunately, as no other phosphosites were probed, we cannot confirm the complete removal of all phosphosites except for the Ser445 ones). Total BRAF antibody did detect both bands, therefore, it can be concluded with somewhat confidence, that the second BRAF population is not caused by additional phosphorylation (at least not solely by phosphorylation).

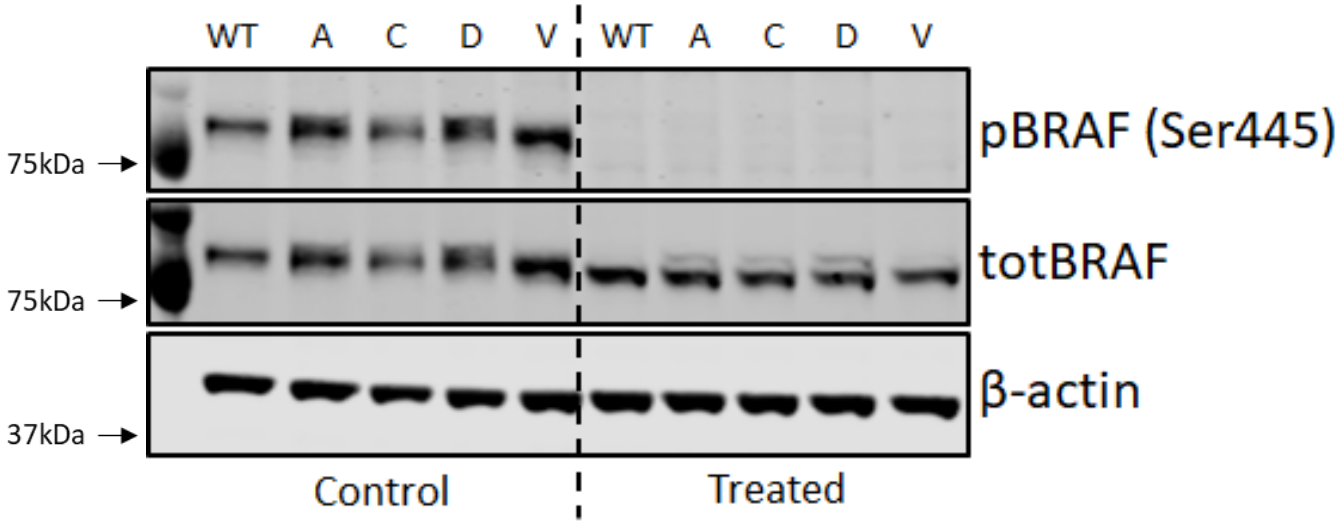

Figure 3.4. **Lambda phosphatase treatment of LIM1215 cells.** All KRAS G12 mutants and WT LIM1215 cells were treated with lambda phosphatase for 90 minutes resulting in all Ser445 phosphate groups being removed. Total BRAF antibody still detects top band. Representative Western blot shown (n=3).

3.4 Differential binding of myosin-9 and BRAF in different mutants

To identify the differences between the two BRAF populations, proteomics analysis was performed on the BRAF bands in LIM1215 WT and G12D cells with mass spectrometry. The cells were seeded in 15cm plates to ensure sufficient protein was collected to be able to pulldown enough BRAF via

immunoprecipitation (IP) and allow for good mass spectrometry reads. Cells were treated with either NT or MEK siRNA and 5 minutes or no EGF. The MEK siRNA and 5 minutes EGF treated samples were sent off for proteomics analysis as previous blots showed that MEK knockdown (and in some cases, 5 minutes EGF treatment) increases the expression of the top band. ***Figure 3.5b*** confirms the presence of the top BRAF band in the G12D sample. The proteomics analysis did not reveal any substantial differences in PTMs between WT and G12D cells that could explain the increased molecular weight of the second BRAF form ***(Supplementary figure 3.1)*.** Interestingly, a unique BRAF fragment with C-terminus GEFAAFK was detected. As we did not carry out quantitative proteomics (e.g., SILAC), we cannot determine the relative expression of this protein form between mutant and WT cells, but we note that it was detected in both cell lines (see **Section 3.7** for a discussion on splice variants). Another potentially interesting observation was that on the Coomassie stained gel, additional bands were present in the WT sample that were only very faintly visible in G12D cells ***(Figure 3.5a)***.

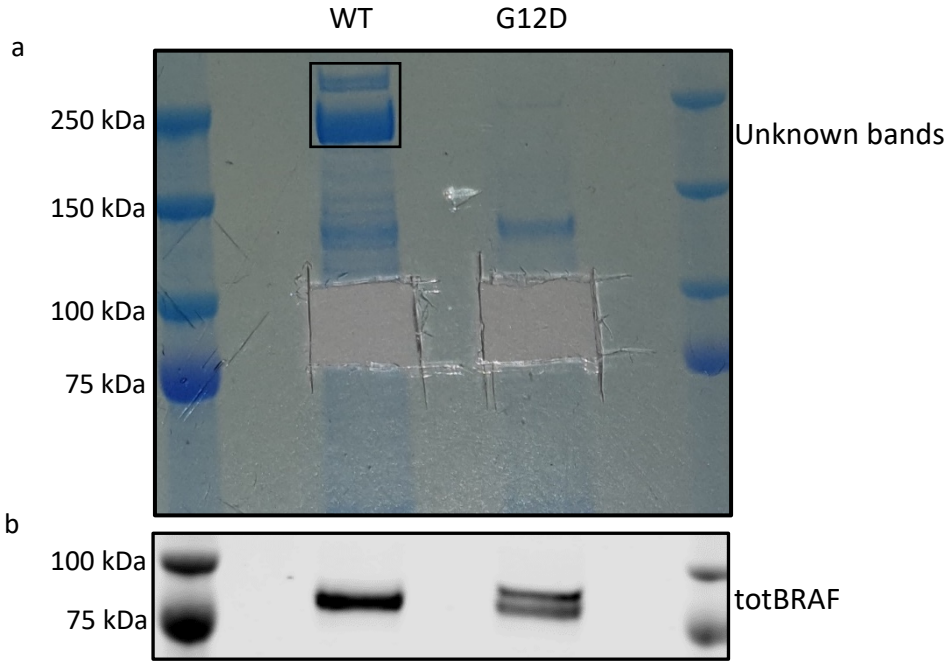

Figure 3.5. **BRAF immunoprecipitation in LIM1215 WT and G12D cells.** BRAF was immunoprecipitated using a total BRAF antibody. **a.** Coomassie stain of SDS-PAGE gel shown with BRAF bands cut out and sent for proteomics analysis. Appearance of unknown bands in WT cells is highlighted with black box. **b.** Western blot of input samples of same lysates confirming presence of top BRAF band in G12D cells. Samples: WT and G12D LIM1215 cells treated with MEK siRNA and 5 minutes EGF treatment.

To identify these unknown bands, BRAF IP was repeated in other lysates from the experiment (WT and G12D cells treated with MEK siRNA and no EGF treatment). Surprisingly, this time only one of these unknown bands was visible, and it was more prominent in G12D cells. The only difference between both sets of samples is that the previous ones were treated with 5 minutes EGF, whereas

these ones were not ***(Figure 3.6)***. This suggests that the expression of these unknown bands may potentially be regulated by EGF stimulation. Proteomics analysis of the unknown band in the G12D sample revealed this band to be myosin-9 (also called non-muscle myosin-IIA), which is encoded by the *MYH9* gene (see ***Supplementary figure 3.2*** for full list of peptides). To ensure myosin-9 is not just a contaminant, I queried it in the Contaminant Repository for Affinity Purification (CRAPome), where it was indicated that only 27 out of a total of 716 (~3.8%) experiments reported spectral counts of more than 150 (*Profile Detail for MYH9 | CRAPome*, 2022). In my data, the total spectral count for myosin-9 is 263, therefore, although it is possible, it is unlikely that myosin-9 is simply a contaminant in my sample.

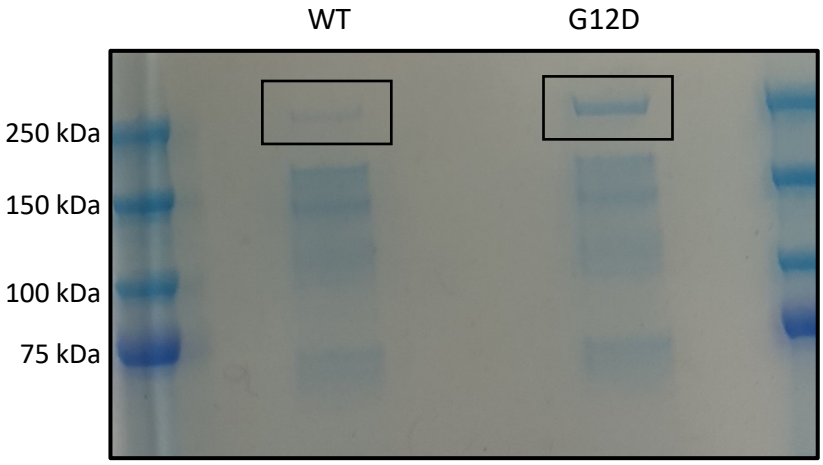

Figure 3.6. **BRAF immunoprecipitation repeated in LIM1215 WT and G12D cells.** BRAF was immunoprecipitated using a total BRAF antibody. Coomassie stain of Western blot showing more prominent unknown band in G12D cells (also present in WT cells at lower expression level). Samples: WT and G12D LIM1215 cells treated with MEK siRNA and no EGF treatment.

Differential BRAF:Myosin-9 binding dynamics in different mutants

Myosin-9 has been shown to promote growth and metastasis via the activation of the ERK and PI3K pathways in colorectal cancer cells (Wang *et al.*, 2019). The IP experiments were repeated this time in LIM1215 WT and all mutants, in order to observe differences in myosin-9 binding to BRAF in different KRAS mutant cells that have been treated with or without MEK siRNA and with or without EGF treatment ***(Figure 3.7)***. Another aim of this experiment was to observe whether changes in CRAF:BRAF dimerisation are involved in the regulation of the top BRAF band and whether this is linked to the binding of myosin-9 to BRAF. RAF heterodimerisation plays an important role in propagating ERK signalling and may be involved in the differential regulation of the top BRAF band (Rushworth *et al.*, 2006).

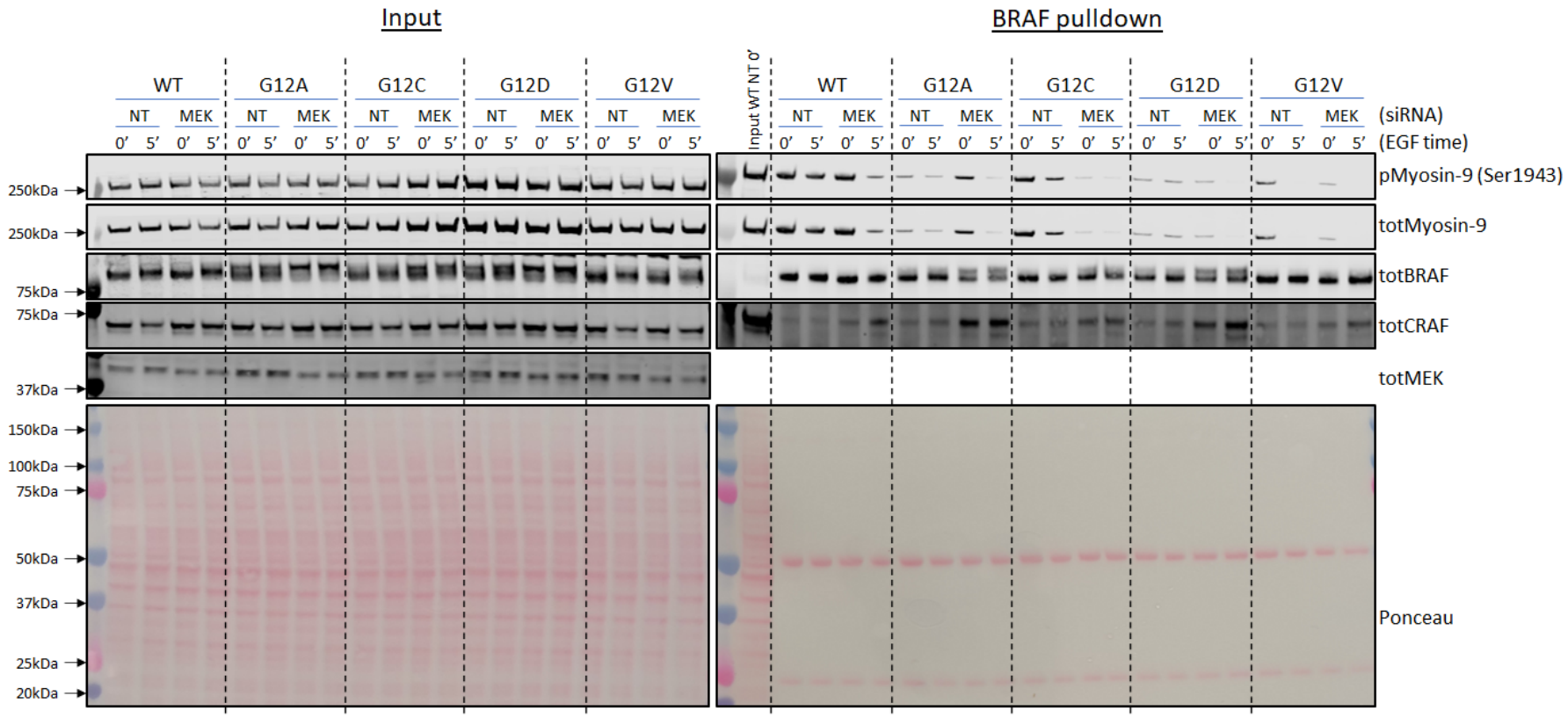

Figure 3.7. **BRAF immunoprecipitation repeated in LIM1215 WT and all mutants.** BRAF antibody was used to immunoprecipitate BRAF in LIM1215 WT and mutant cells. Western blot showing differential myosin-9 binding with BRAF in different LIM1215 mutants and the impact of EGF treatment and/or MEK knockdown on this. Gel also shows difference in CRAF:BRAF dimer formation in different conditions.

As this experiment has only been conducted once in all the cell lines, only preliminary conclusions can be made at this stage. It can be seen in ***Figure 3.7*** that there are differences in the binding of myosin-9 to BRAF in the different mutants and conditions. In all mutants and WT cells, both with or without MEK knockdown, there is a decrease in the amount of myosin-9 binding to BRAF upon EGF treatment, providing some support for the preliminary hypothesis that EGF may regulate this interaction. However, the switch in expression levels with EGF treatment seen in the previous IP experiment is not replicated here (where myosin-9 expression was higher in WT cells compared to G12D cells with 5 minutes EGF treatment but was lower with no EGF treatment). This highlights the need for further repeats to be carried out in order to make confident conclusions.

The impact of MEK knockdown varies depending on the mutant and whether it is combined with EGF treatment. When combined, this results in the greatest reduction in myosin-9 binding to BRAF in all mutants and WT cells, meaning that the reduction seen with EGF treatment is enhanced even further with MEK knockdown. With MEK knockdown alone (with no EGF treatment), whilst there is no impact on myosin-9 and BRAF interaction in WT and G12D cells, there is increased interaction in G12A cells and reduced interaction in G12C and G12V cells. These observations suggest that the binding of BRAF and myosin-9 may not only be regulated by EGF (and therefore, by the ERK pathway or another pathway downstream of EGFR), but that there may be a separate MEK-dependent regulation that is altered in different mutants in the absence of EGF treatment.

Looking at just the basal levels of binding with no EGF and no MEK knockdown, there are some differences in the level of myosin-9 binding to BRAF, with highest levels in WT, followed by G12C and G12V, and lowest binding in G12D and G12A. This is interesting because the MEK to RAF inhibition and the appearance of the top BRAF band is strongest in the mutants with the least BRAF:myosin-9 binding (G12D and G12A). Interestingly, despite these differences in binding of BRAF to myosin-9, the total levels present in the cells do not appear to differ in a correlative manner. There does seem to be higher levels in G12C and G12D in the input samples, however, judging by the gradual increase in the expression of both phospho-Myosin-9 and total-Myosin-9 levels across the membrane this appears to be due to uneven antibody staining. Only once this experiment has been repeated at least twice more, it will be possible to make confident conclusions. It should also be noted that this experiment lacks certain controls which should be included in the next repeats. These include a BRAF knockdown sample to confirm the specificity of the antibody, and a sample with no antibody, just the beads with the cell lysate (which should not generate any bands on the Western blot).

Association of CRAF:BRAF dimerisation with expression of unknown BRAF population

Figure 3.7 also shows that MEK knockdown leads to an increase in CRAF:BRAF dimer formation. Interestingly, the strongest dimerisation is seen in conditions with the most prominent top BRAF band, which is in G12D and G12A cells with MEK knockdown. This is also seen, to a lower extent, in the G12C cells with MEK knockdown, which in this case have a lower expression level of the top BRAF band. Therefore, it is possible that the expression level of the unknown BRAF population may be linked to BRAF:CRAF dimerisation. This is investigated further in **Section 3.5.**

Role of myosin-9 in ERK and PI3K pathway activation

To investigate the role of myosin-9 in ERK and PI3K pathway activation, LIM1215 WT and mutant cells were treated with 20nM pooled siRNA targeted against myosin-9. The concentration of the siRNA to use was optimised, with 20nM resulting in an acceptable ~85% knockdown, with any increase in siRNA concentration being effectively redundant ***(Figure 3.8)***.

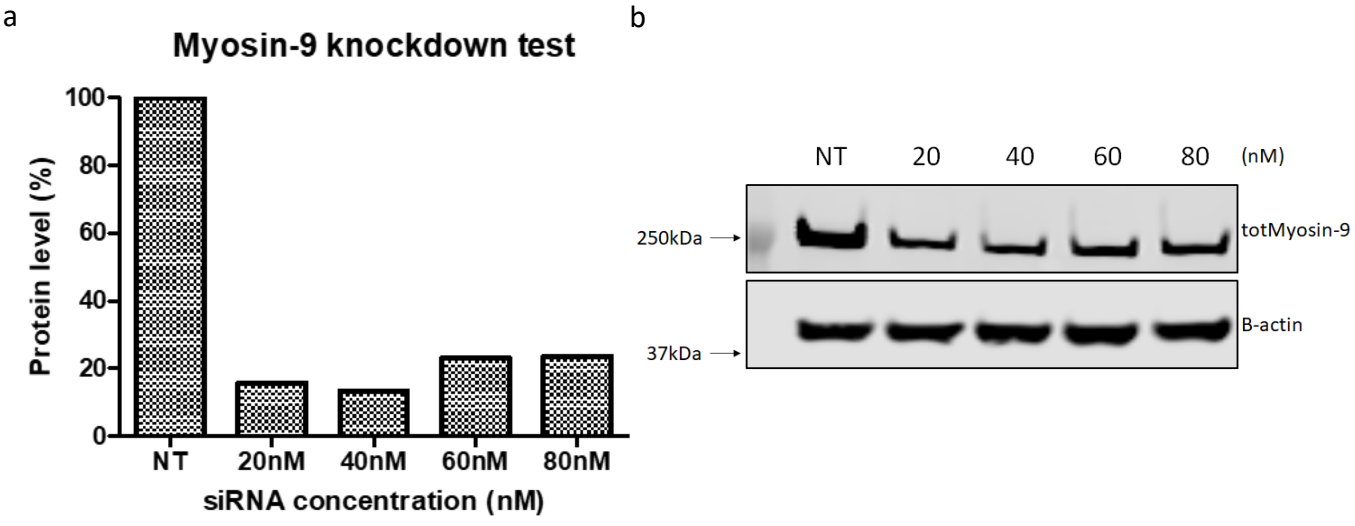

Figure 3.8. **Myosin-9 knockdown optimisation. a.** Graph and **b.** Western blot showing myosin-9 knockdowns achieved in LIM1215 WT cells with 20nM to 80nM myosin-9 siRNA concentrations compared to non-targeting (NT) siRNA. 80nM was used for the NT siRNA (n=1, therefore no error bars).

The aim of this experiment was to see whether knockdown of myosin-9 has any impact on ERK and AKT signalling and whether this is affected by EGF stimulation. A representative Western blot is shown in ***Figure 3.9,*** and although not as effective as in the optimisation experiment, 20nM siRNA definitely did result in a knockdown of myosin-9 levels in all cell lines, as can be seen in ***Figure 3.10a***.

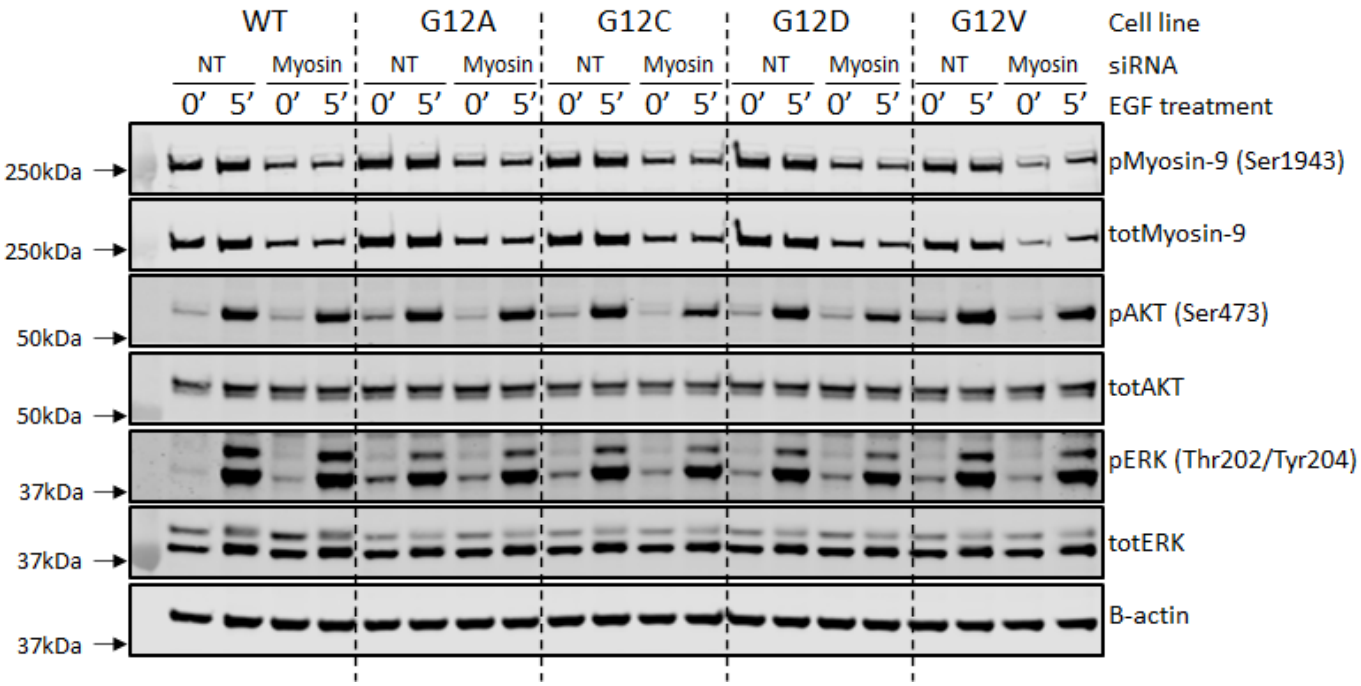

Figure 3.9. **Myosin-9 knockdown in LIM1215 cells.** Representative Western blot showing the impact of myosin-9 knockdown on ERK and AKT activation in WT and mutant cells (n=3). Please note this blot does not necessarily replicate exactly the data in ***Figure 3.10a*** due to variation between repeats. The pERK phosphorylations correspond to ERK1 sites.

As can be seen in ***Figure 3.10b***, the ERK responses in WT and mutant cells are in agreement with the responses to EGF seen in previous experiments, with WT having the highest ERK response, followed by G12V, and then the other three mutants. When the expression of myosin-9 is knocked down, this pattern in responses is still the same, however, in WT (and to a lesser extent in G12V cells), there is a reduction in ERK activity upon myosin-9 knockdown, whilst in the other mutants, there is no change. This suggests that in EGF-stimulated cells, myosin-9 plays a role in ERK activation in WT cells and possibly G12V cells, but not in G12A, G12C and G12D cells. When looking at the impact of myosin-9 knockdown on AKT responses in EGF-stimulated cells, there are no clear conclusions as the responses are all similar and generally more variable. This is also in line with results from previous experiments (see **Chapter 2).**

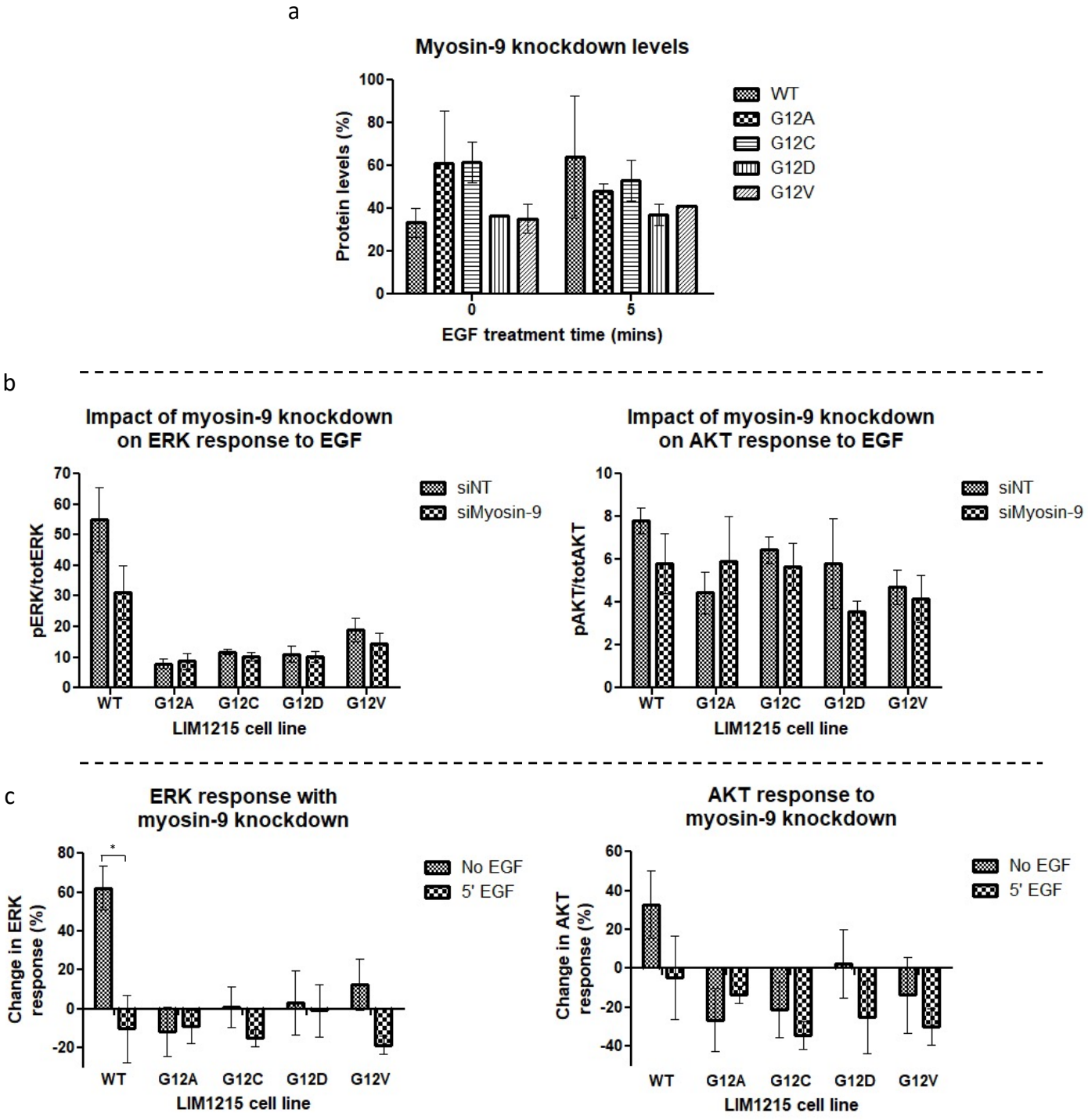

Figure 3.10. **Impact of myosin-9 knockdown on AKT and ERK in LIM1215 cells. a.** Graph showing knockdowns achieved. Large error bars for G12A no EGF and WT 5 minute EGF samples due to knockdown not working in one of the three repeats for those samples only. **b.** Graphs showing the impact of myosin-9 knockdown on ERK and AKT responses to 5 minutes EGF treatment. **c.** Graphs showing how the change in ERK and AKT activation upon myosin-9 knockdown is further influenced by EGF treatment. Means +/- SEM error bars plotted (n=3). Statistical analysis (unpaired t-test) carried out for data in **b** and **c**, *p-value* of ≤0.05 depicted with asterisk.

Whilst the above looks at the effect of myosin-9 knockdown in EGF treated cells, ***Figure 3.10c*** shows instead the impact of EGF treatment in myosin-9 knockdown cells, in terms of the change in the ERK and AKT responses when compared to NT siRNA treated cells. When comparing the unstimulated cells with EGF stimulated cells, the greatest difference in ERK response seen with myosin-9 knockdown is in WT and G12V cells. With no EGF stimulation, WT cells show a definite increase in ERK response when myosin-9 is knocked down, and although to a much lower extent, this is also seen in G12V cells. In contrast, in EGF-stimulated cells, the ERK responses decrease in WT and G12V cells when myosin-9 is knocked down. In G12A, G12C and G12D cells, the change in ERK activity upon myosin-9 knockdown in unstimulated cells is the opposite to WT and G12V cells, with ERK activity decreasing slightly, or not changing. With EGF treatment, there is no change in G12A and G12D cells, with a slight decrease in G12C cells. In these mutants, any changes seen are generally masked by the large error bars, therefore, it appears that there are generally no changes in ERK activity in the different conditions. Combined, this data suggests that the impact of myosin-9 on ERK signalling is not only different in different mutants but is also influenced by activation of pathways downstream of EGFR in WT and G12V cells.

Focusing on the AKT pathway now, in unstimulated cells, there is an increase in AKT activity upon myosin-9 knockdown only in WT cells, whilst this activity decreases (or doesn't change) in the other mutants. In EGF-stimulated cells, myosin-9 knockdown decreases AKT activity in WT and all mutant cells, but in G12A cells this is a lesser decrease compared to unstimulated cells.

3.5 CRAF dimerises with both BRAF protein forms

From the BRAF IP data, it is evident that CRAF:BRAF dimerisation increases with MEK knockdown in WT and all mutant cells, and the highest level of dimerisation is seen in G12A and G12D cells. These two mutants have the highest level of the BRAF top band present too, therefore, it is feasible that this unknown BRAF population is connected to the increase in CRAF:BRAF dimerisation. To test whether CRAF dimerises with both BRAF protein forms, CRAF was immunoprecipitated in LIM1215 WT and G12D cells. ***Figure 3.11*** *shows* that both BRAF protein forms are pulled down with the CRAF antibody in the G12D samples. An interesting observation is that the top BRAF band appears to interact with CRAF more strongly than the bottom band, and this may explain why CRAF:BRAF dimerisation is strongest in the mutants with the highest level of expression of the top BRAF band. To conclude this section, it appears that CRAF dimerises with both populations of BRAF, potentially more strongly with the unknown BRAF band.

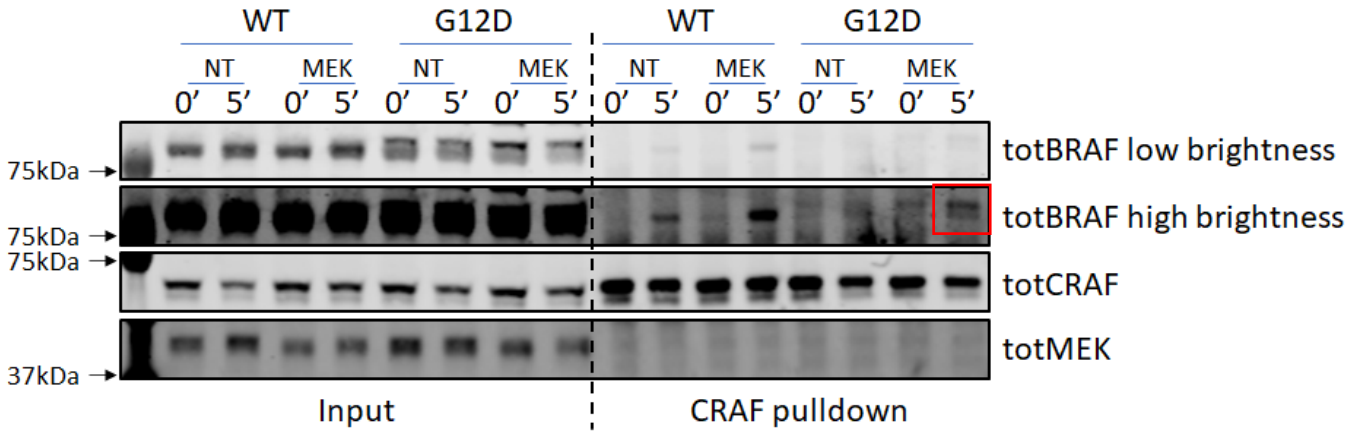

Figure 3.11. **CRAF:BRAF dimer formation.** CRAF antibody was used to immunoprecipitate CRAF in LIM1215 WT and G12D cells. Western blot showing CRAF:BRAF dimerisation levels in WT and G12D cells treated with NT or MEK siRNA and 0 or 5 minute EGF stimulation (100ng/ml). Red box shows CRAF dimerisation with both BRAF populations in G12D cells.

3.6 BRAF is not differentially ubiquitinated between WT and G12D cells

One key difference between the LIM1215 and the SW48 cell lines is that SW48 cells harbour an *FBXW7* mutation. The unknown higher molecular weight BRAF protein form may be comprised of BRAF proteins that have been ubiquitinated and targeted for degradation by FBXW7. Due to the *FBXW7* mutation in SW48 cells, the SCF complex may be faulty and therefore unable to target BRAF for degradation. The lack of the BRAF top band in LIM1215 WT and G12V cells could be then explained by differential regulation of FBXW7 in those backgrounds. Therefore, knockdown of FBXW7 in LIM1215 cells was attempted. If knockdown of FBXW7 decreased or abolished the top BRAF band, then it would suggest that FBXW7 plays a role in the existence of the unknown BRAF population.

A range of concentrations of pooled FBXW7 siRNA (purchased from Horizon discovery) was tested in LIM1215 WT cells, but unfortunately no knockdown was achieved ***(Figure 3.12a)***. The FBXW7 antibody appeared to be working well; there was no unspecific binding, and the bands were strong. The FBXW7 bands were also present on the correct part of the gel for the expected molecular weight of 69kDa. Therefore, it appeared that the problem was with the siRNA and not the antibody. New FBXW7 siRNA purchased from Qiagen was then used, but again no knockdown was achieved ***(Figure 3.12b)***.

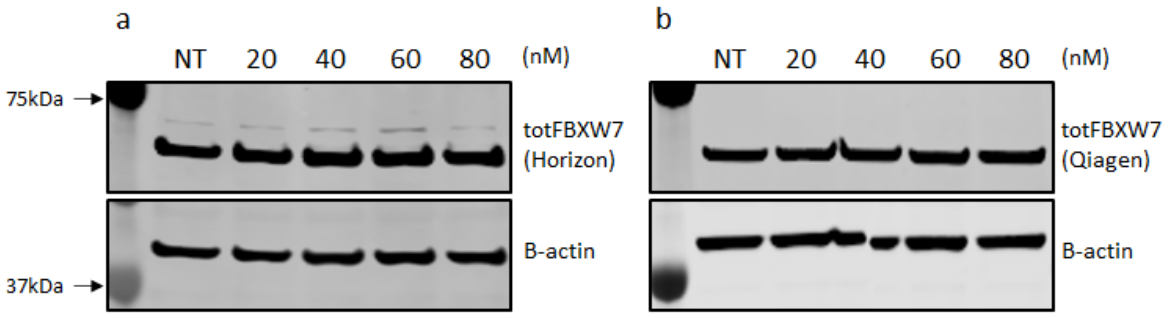

Figure 3.12. **FBXW7 knockdown test.** Different concentrations of pooled siRNA against FBXW7 was tested in LIM1215 WT cells but there was no knockdown. **a.** Using Horizon discovery siRNA. **b.** Using Qiagen siRNA. 80nM was used for the respective NT siRNA. The 40nM actin band in (b) is split in the middle due to a rip in the gel.

Lastly, siRNA knockdown was attempted in HPNE cells. The rationale behind this was the fact that a BRAF doublet can be seen in these cells too and it also doesn't have an FBXW7 mutation, therefore effectively making it a suitable substitute cell line to be used instead of the LIM1215 cells for the purpose of this experiment. In a separate experiment for a different project, HPNE cells were treated with doxycycline for up to 14 days to induce the expression of a third copy of either myc-tagged WT or mutant KRAS, or just mCherry. ***Figure 3.13*** shows the presence of the two BRAF populations in G12D and G12V cells, but not in WT and mCherry cells. The presence of the BRAF top band corelates with doxycycline treatment, therefore, it correlates with the overexpression of mutant KRAS. The presence of the BRAF top band in G12V cells is unexpected, but it suggests that perhaps its expression is linked to the level of oncogenic burden in a cell and not a specific mutation, at least in HPNE cells. The HPNE cells and LIM1215 cells are very different, with the former being a pancreatic cancer cell line and the latter being a colorectal cancer cell line. Furthermore, HPNEs are immortalised but not transformed, and they utilise a doxycycline-induced overexpression system, whereas the LIM1215 cells are already transformed and have a KRAS heterozygous knock-in mutation. Any of these differences may be responsible for the dissimilarity seen in G12V cells between these two cell lines.

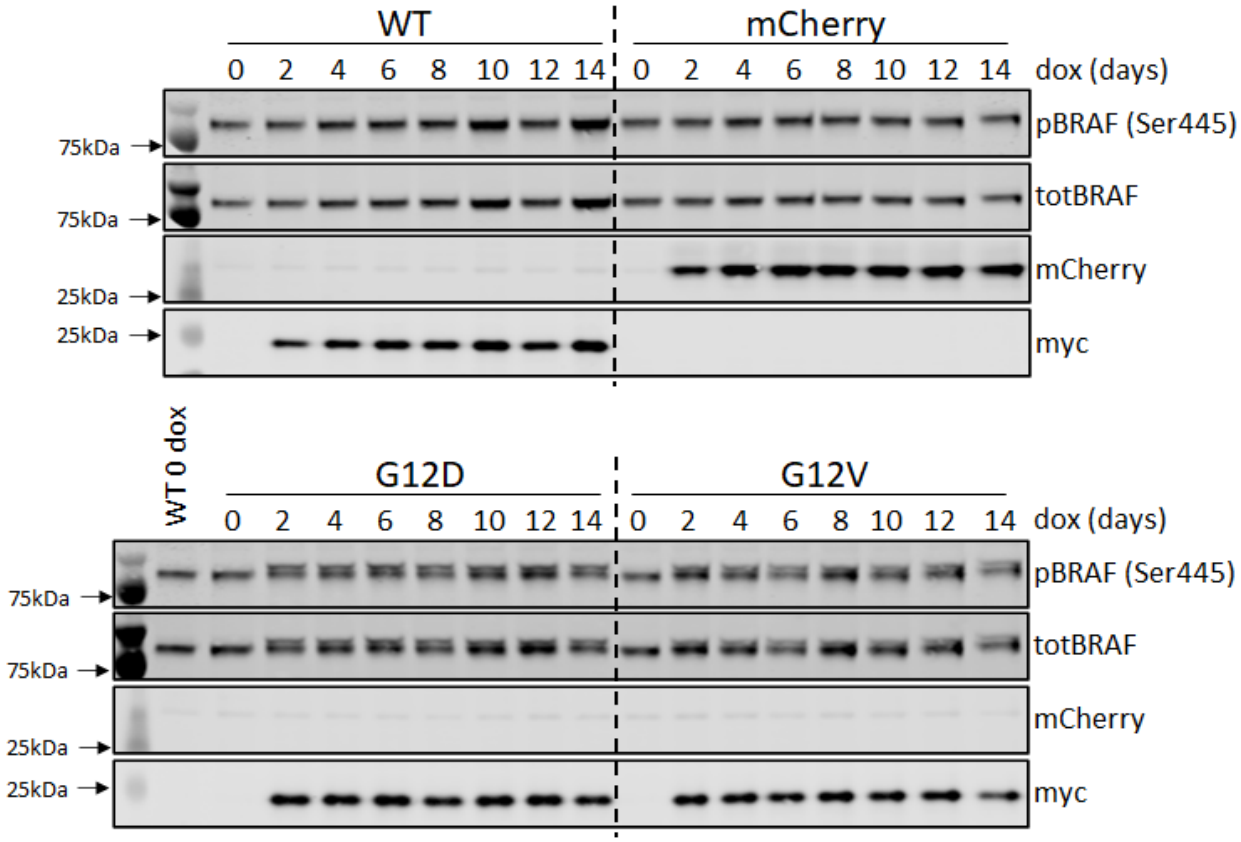

Figure 3.13. **BRAF expression in HPNE cells.** Expression of the third mutant copy of KRAS (myc-tagged) was induced with doxycycline treatment. The mCherry cell line expresses myc-tagged mCherry instead of KRAS. Western blot showing the presence of two BRAF populations in HPNE G12D and G12V cells but not in WT or mCherry-expressing cells.

Unfortunately, FBXW7 knockdown was also not achieved in HPNE cells using the Qiagen siRNA, as can be seen in ***Figure 3.14a***. I concluded that FBXW7 might be extremely difficult to knockdown. Before further proceeding in these experiments, I checked ubiquitination of BRAF in LIM1215 WT and G12D cells. As can be seen in ***Figure 3.14b***, there is no difference in ubiquitination of BRAF between WT and G12D cells. Therefore, I concluded that FBXW7 and ubiquitination might not explain the unidentified BRAF protein form.

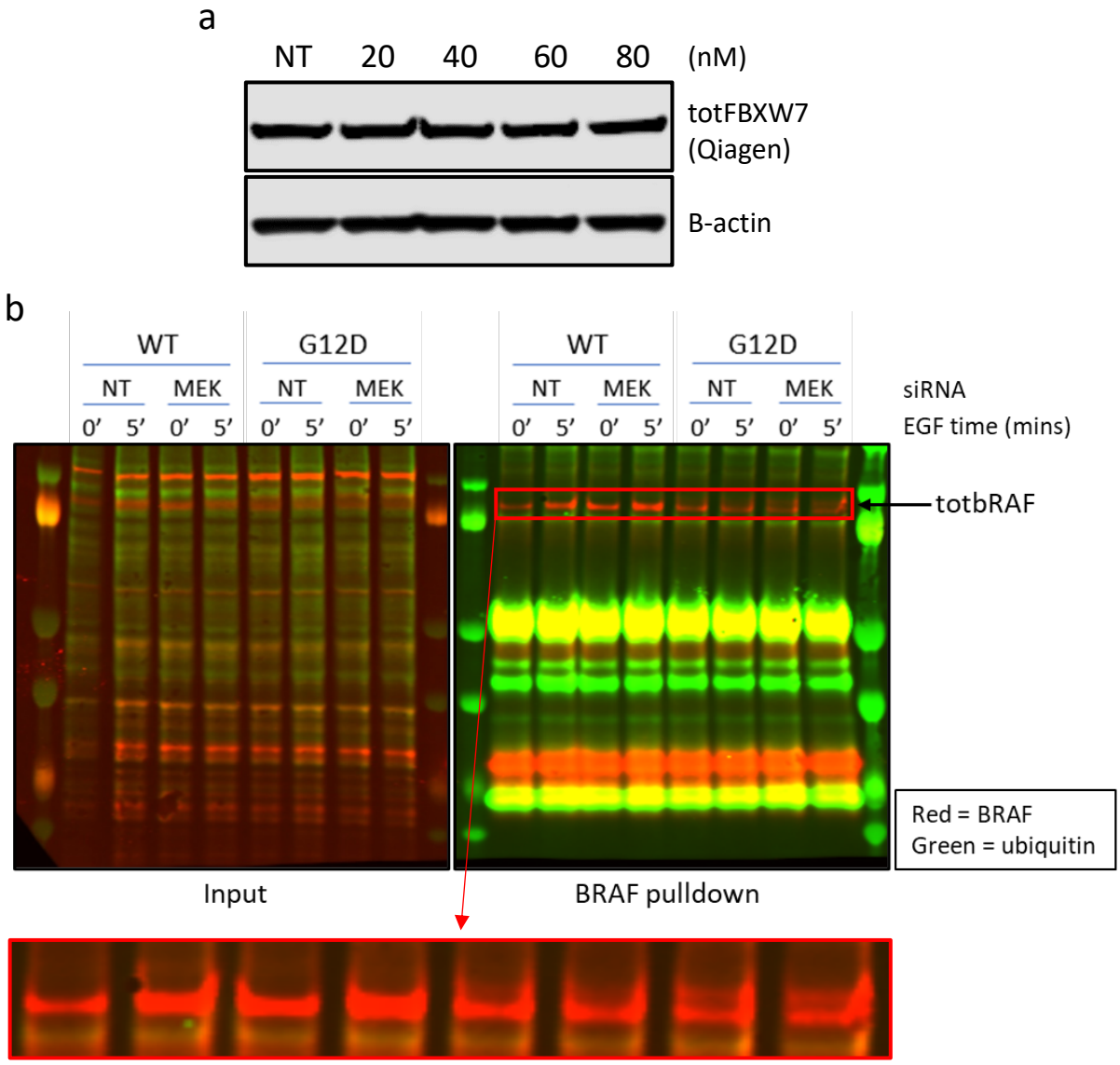

Figure 3.14. **Final FBXW7 knockdown test and ubiquitin blot. a.** Western blot showing the lack of knockdowns achieved in HPNE WT cells using different concentrations of pooled siRNA against FBXW7 (Qiagen). 80nM was used for the NT siRNA. **b.** No difference in ubiquitination between WT and G12D LIM1215 cells. A zoomed-in version with increased contrast of the BRAF bands is shown at the bottom.

3.7 Investigating BRAF splice variants

Next, the hypothesis that the second BRAF band may be a splice variant was tested by overexpressing FLAG-tagged BRAF in LIM1215 WT and G12D cells. The overexpressed BRAF cannot be spliced, therefore, if in G12D cells two bands of endogenous BRAF appear but only one band of the FLAG-tagged overexpressed BRAF appears, then that would strongly suggest that the second BRAF band is a splice variant. In contrast, if two bands of the overexpressed BRAF are seen, then that would rule out the possibility of the second band being a splice variant. Transfections were carried out using jetPRIME® transfection reagent, with FLAG-tagged BRAF being transfected in WT and G12D cells and mTurqouse-2 plasmid being transfected into additional cells to check transfection efficiency. The m-Turquise-2 samples were visualised using a Zoe fluorescent cell imager (Bio-Rad) and good transfection efficiency was determined ***(Supplementary figure 3.3)***. As can be seen in ***Figure 3.15***, BRAF was successfully overexpressed. Because of the high expression, I could not relate the expression of FLAG-BRAF to the endogenous BRAF expression in the same samples. However, only one FLAG-BRAF band is present. Therefore, this experiment is consistent with the hypothesis that a post-translational modification of the main BRAF isoform is most likely not responsible for the appearance of a second BRAF protein form, leaving the possibility that a splice variant is differentially regulated in different mutants.

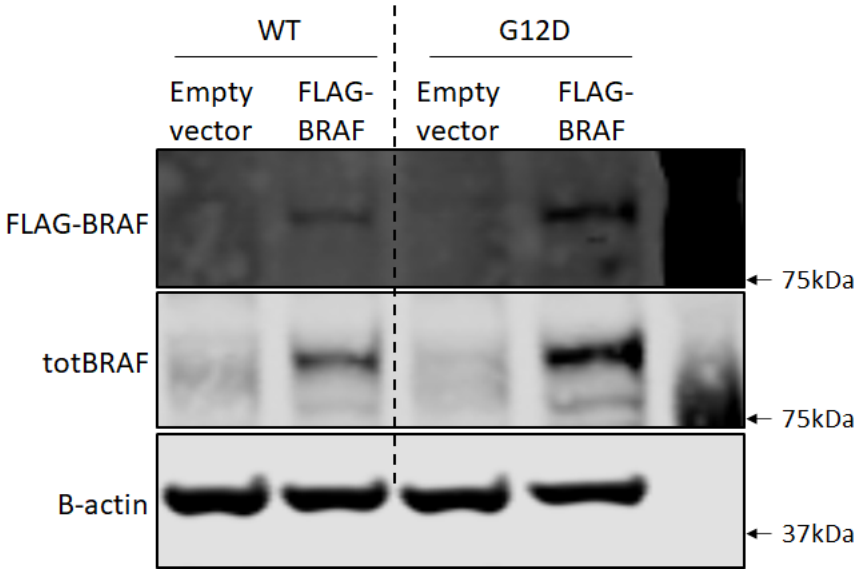

Figure 3.15. **BRAF overexpression.** Representative Western blot showing endogenous expression and FLAG-tagged overexpression of BRAF in LIM1215 WT and G12D cells (n=3). The presence of only one FLAG-BRAF band suggests a PTM is likely not the cause of the second BRAF form, and is probably a splice variant.

Proteomics analysis of LIM1215 WT and G12D cells has revealed the presence of a BRAF fragment with an altered C-terminus ending in GEFAAFK instead of GAFPVH. This data does not inform us of the prevalence of this alternate BRAF fragment in both cell lines, however, it is possible that the regulation of this additional fragment may differ between WT and G12D cells. When cross-referenced with the NCBI database of the mRNA transcripts of BRAF, out of the 16 BRAF transcripts deposited, 8 of them have this variant of the C-terminus. Of these 8 variants, only one is the correct molecular weight (~89kDa) that matches with the top BRAF band. The rest are all smaller or the same size as the reference BRAF (~84.4kDa). This variant (transcript 5 of the database) has an additional exon 9b, which is 120bp long and increases the molecular of BRAF by ~4.6kDa. The NCBI database also includes one BRAF variant with the reference C-terminus that also has this additional exon 9b and is also ~89kDa (transcript 4). Therefore, there are two transcripts from the database that could potentially be the second BRAF form in the LIM1215 cells.

There are a number of different BRAF splice variants that have been reported in literature. Of these, the only ones that are the correct molecular weight are ones with exon 9b present (Hmitou *et al.*, 2007). Analysing the sequences of transcripts 4 and 5 revealed that there is a unique PvuII restriction enzyme site which is only present in exon 9b, therefore, a simple test to check whether the top BRAF band is one of these splice variants is to do a restriction enzyme digest with PvuII. RNA was extracted from LIM1215 WT and G12D cell pellets, from which cDNA was synthesised via RT-PCR. Primers in exon 2, 6, 13 and 18 of BRAF were designed and exon 2-exon 18 and exon 6-exon 13 combinations were used to amplify nearly the whole of BRAF or a smaller section surrounding where exon 9b would be. Most of the DNA was run on an agarose gel without carrying out any further steps, but some was taken to perform the restriction enzyme digest using PvuII; the digested DNA was also run on the same gel ***(Figure 3.16)***.

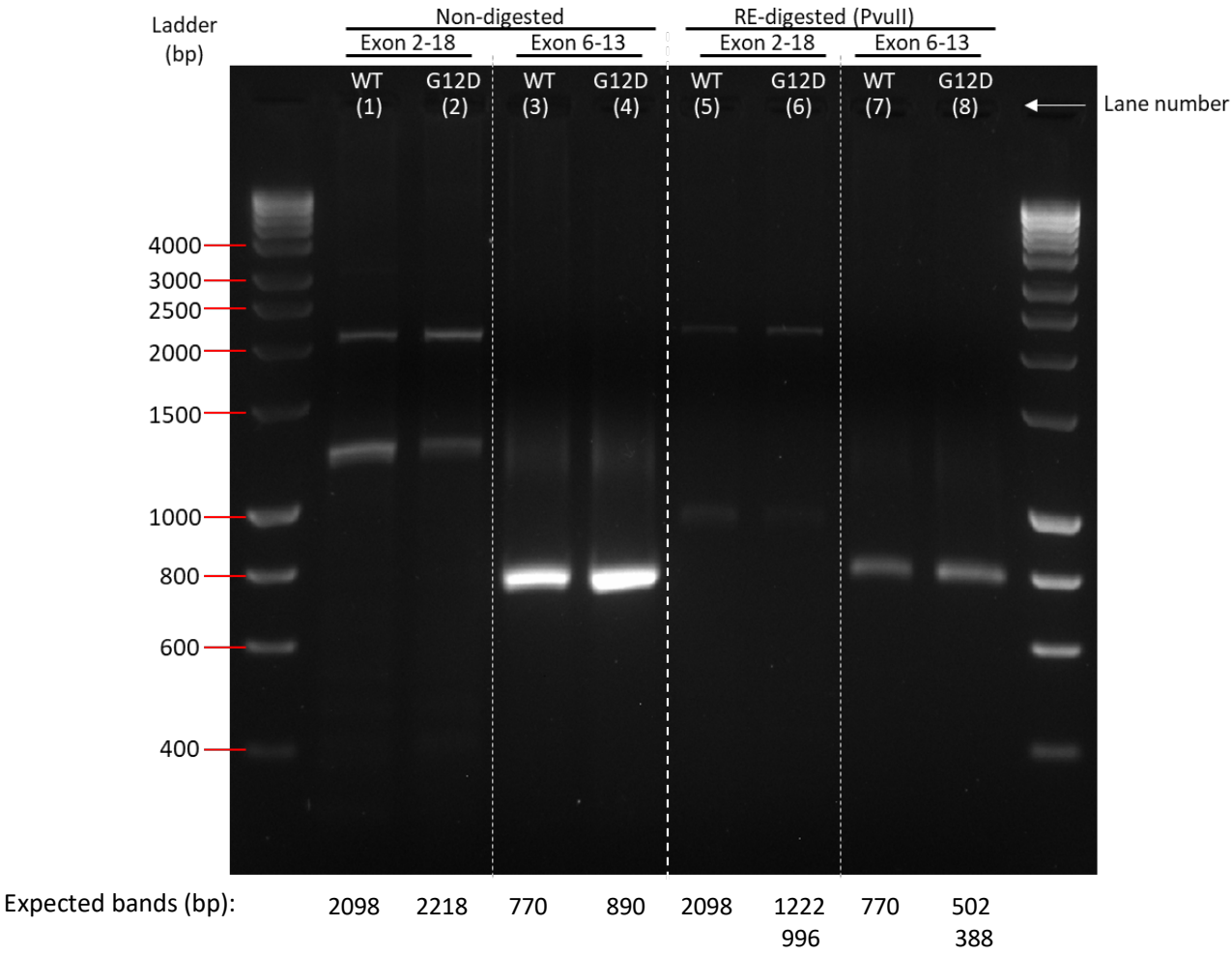

Figure 3.16. **Amplification and restriction enzyme digest of BRAF.** Parts of BRAF DNA extracted from LIM1215 WT and G12D cells were amplified using two sets of primers. A restriction enzyme (RE) digest was also carried out using PvuII because exon 9b has a PvuII recognition site.

As can be seen in ***Figure 3.16,*** there are no differences between WT and G12D cells. The non-digested and digested samples are loaded in lanes 1-4 and lanes 5-8, respectively. In lanes 1 and 2, the expected BRAF band in WT is 2098bp long and in G12D is 2218bp long (if exon 9b is present in G12D). Of course, due to the small difference in size and low separation for that segment size, it is a bit difficult to confidently say that there is no difference. However, in lanes 3 and 4, the bands are the same size and a difference of 120bp should be seen clearly. This data therefore does not appear to support the hypothesis that exon 9b is present in G12D cells. Furthermore, the RE digest also didn't produce the expected bands in the G12D samples, probably because the PvuII recognition site was not present.

An unexpected observation is the presence of the ~1300bp bands in lanes 1 and 2. To identify them, those bands were cut out and sent for sequencing after DNA extraction was carried out, and the same was done with the BRAF bands in those lanes to confirm the identity of those bands. The sequences

of the BRAF bands confirm the absence of exon 9b in G12D cells. The sequence of the unexpected bands were queried in BLASTn and matched with a gene encoding the basic helix-loop-helix family member E40 (BHLHE40), a protein involved in the control of circadian rhythm (Cho *et al.*, 2009). The query coverage however is only 24% between the sequence of the unexpected bands and the sequence of BHLHE40, of which there is 98% sequence similarity. There is also no similarity between the sequences on BRAF and the unexpected bands, and the BRAF primers do not bind the sequence of the unexpected bands with high fidelity, therefore, it has eluded us as to how the extra bands have appeared in the gel. Additional experiments are ongoing in the Esposito laboratory to identify the nature of this unidentified BRAF protein form, with most of our attempts focusing on the possibility it is a splice variant.

3.8 Discussion

In this chapter, I have investigated the identity and possible role of a second BRAF form present in specific KRAS mutant cells. As discussed in the introduction to this chapter, BRAF can be alternatively spliced (Hirschi and Kolligs, 2013). Alternative splicing of BRAF can have crucial effects on development of resistance to RAF inhibitor therapy (Vido *et al.*, 2018), and has also been shown to modulate the ability of BRAF to activate MEK (Hmitou *et al.*, 2007). Furthermore, it may also serve to function as an additional mechanism for oncogenic BRAF activation in certain cancers such as thyroid carcinomas (Baitei *et al.*, 2009).

My work has revealed the existence of two BRAF protein forms, with a higher molecular weight form being expressed only in specific LIM1215 mutants (G12A, G12C and G12D cells). This second BRAF form is present in all conditions tested (unstimulated and EGF-stimulated cells, with and without MEK knockdown/inhibition), with MEK knockdown (or MEK inhibitor treatment for 46 hours) increasing the expression level of the second form. MEK inhibitor treatment for 2 hours did not increase the expression of this BRAF form, suggesting that the mechanism responsible for increasing its expression requires longer than 2 hours (with 46 hours being sufficient).

Compatible BRAF splice variants that could potentially match the estimated molecular weight of the second form (a few kDa heavier) have been reported both in literature and RNA repositories, but their roles have not been well-characterised. The best splice variant options from literature and the NCBI database that would lead to a BRAF protein of the right size were identified as the ones with the addition of exon 9b, either with the putative GAFPVH C-terminus, or the alternative GEFAAFK C-terminus. Exon 9b is 40 amino acids long and the molecular weight of a splice variant with exon 9b is ~89kDa, thus matching the estimated molecular weight of the unknown BRAF population. Furthermore, mass spectrometry data revealed the presence of both alterative C-termini of BRAF, therefore, the second form could have either one of these C-termini. Although preliminary investigations have not confirmed the presence of exon 9b in LIM1215 G12D cells, experiments are ongoing in the Esposito lab with the focus on characterising the identity of this potential BRAF splice variant.

The LIM1215 mutants with the second BRAF form (G12A, G12C and G12D) are also those that exhibit the strongest MEK to RAF inhibition based on the MRA topological maps. Because of the strong correlation between the presence of the second BRAF band and the negative feedback, I hypothesised

that this BRAF protein form might be related to the MEK>RAF inhibitory mechanism. RAF can be phosphorylated in an inhibitory manner by AKT (Zimmermann and Moelling, 1999), however, testing the hypothesis that MEK is inhibiting RAF via AKT revealed that AKT is not playing a role in this unidentified mechanism. BRAF can also be inhibited via phosphorylation by ERK on Thr401 (D. A. Ritt *et al.*, 2010). However, my data shows that phosphorylation of Thr401 on BRAF is not modulated by different levels of phosphorylated ERK, thus indicating that ERK-mediated Thr401 phosphorylation is unlikely to be the cause of the BRAF inhibition. To further confirm this, the effect of ERK knockdown on BRAF-Thr401 phosphorylation could be tested.

In addition to Thr401 being an ERK-mediated inhibitory phosphorylation site, it is also part of a conserved FBXW7 recognition site (Mason *et al.*, 1999; Hernandez *et al.*, 2016). FBXW7 is an F-box protein family member and is the substrate recognition component of the Skp1-Cdc53/Cullin-F-box (SCF) protein complex. This protein complex is an E3-ubiquitin ligase that can regulate the turnover of target proteins by ubiquitinating them and triggering proteasomal degradation (Yeh, Bellon and Nicot, 2018). FBXW7 is of interest here because it has been shown to be involved in targeting BRAF for proteasomal degradation via ubiquitination (Yeh *et al.*, 2020)**.** The second BRAF form is not present in SW48 cells, and one of the key mutations within these cells is the inactivating mutation in *FBXW7*. Therefore, the hypothesis was formed that FBXW7 may be ubiquitinating BRAF in specific LIM1215 mutant cells, resulting in the second higher molecular weight population, and is unable to do so in the SW48 cells due to impaired FBXW7 activity. Although this would however not explain the absence of the second BRAF form in LIM1215 WT and G12V cells, it was a preliminary hypothesis which I tried to test experimentally. Unfortunately, I was unable to knockdown FBXW7 in both the LIM1215 and HPNE cell lines and therefore have not been able to rule out its involvement in ubiquitinating BRAF.

In order to check whether the second BRAF form is differentially ubiquitinated, I immunoprecipitated BRAF in LIM1215 WT and G12D cells and probed for ubiquitin. This was only repeated once, therefore, confident conclusions cannot be made, however, so far it appears that there is no difference in ubiquitination between WT and G12D cells. As it is difficult to observe the presence of ubiquitin on the Western blot, and an alternative test would be to immunoprecipitate ubiquitin and probe for BRAF. Increased expression of BRAF in G12D compared to WT cells would indicate increased ubiquitination in those cells. It is important to understand if BRAF is differentially ubiquitinated as it can have essential effects on ERK signalling (Fan *et al.*, 2020). It has been shown in melanoma cells that BRAF is ubiquitinated by E3 ubiquitin-protein ligase Itchy homolog (ITCH) in response to proinflammatory cytokines and that this disrupts 14-3-3 binding, ultimately causing sustained BRAF

activation and elevated MEK/ERK signalling (Yin *et al.*, 2019). It has also been shown that BRAF ubiquitination by the ubiquitin specific peptidase 28/F-box WD repeat-containing protein 7 (USP28/FBW7) complex targets it for degradation and acts as a negative regulator of the ERK pathway and that the loss of this process in many BRAF-mutant melanoma patients results in resistance to inhibitor therapy (Saei and Eichhorn, 2018). These studies highlight the importance of understanding whether differential BRAF ubiquitination is causing the expression of the second BRAF form in my work and, if so, what impact this has on its role.

Immunoprecipitation of BRAF had also revealed the presence of high molecular weight bands that mass spectrometry analysis indicated were myosin-9. This was, however, only repeated once and only in LIM1215 WT and G12D cells, therefore, we cannot confidently say that mysoin-9 was definitely present. Myosins are common artefactual contaminants of IPs detected by mass spectrometry (Mellacheruvu *et al.*, 2013), however, querying myosin-9 in the CRAPome database suggested it was unlikely to be purely just a contaminant in my samples due to the relatively high spectral count. Myosin-9 has previously been shown to activate the ERK and PI3K pathways in colorectal cancer cells and promote growth and metastasis (Wang *et al.*, 2019). To investigate whether myosin-9 differentially binds BRAF in the presence of different KRAS mutations, BRAF was immunoprecipitated in LIM1215 WT and mutant cells and a myosin-9 antibody was used to determine myosin-9:BRAF interaction. This was only repeated once, therefore, conclusions cannot be made confidently yet. However, this preliminary data suggests a possible role of EGF in the interaction of BRAF with myosin-9 with a separate MEK-dependent mechanism that is altered in different KRAS mutants. This needs to be repeated at least twice more to ascertain whether the data is reproducible.

To understand the role of myosin-9 further, siRNA was used to knockdown myosin-9 and the impact of this on AKT and ERK pathway activation was analysed in LIM1215 WT and mutant cells. Whilst the data suggests no role of AKT in the interaction between BRAF and myosin-9, there is evidence for a possible role of myosin-9 in regulating ERK activity which differs depending on the KRAS mutational status. It appears that myosin-9 may be involved in ERK activation only in WT and G12V cells, as knocking it down inhibits ERK activity. This effect is not seen in G12A, G12C and G12D cells. ***Figure 3.7*** shows that all mutants and WT cells express myosin-9 and exhibit myosin-9:BRAF binding, with this decreasing upon EGF treatment. However, there is no correlation between the amount of myosin-9 bound to BRAF and the decrease in ERK activity upon myosin-9 knockdown in WT and G12V mutant cells. Therefore, in this thesis, I prioritised work related to the role of the uncharacterised second BRAF protein form. However, myosin-9 and the second BRAF population might be somewhat linked. It is

possible that a key aspect to understand here is not whether there is a difference in binding, but how myosin-9 modulates BRAF differently in WT and G12V cells compared to the other mutants once bound. It is important to understand why myosin-9 knockdown is able to reduce ERK activity in WT and G12V cells, but is unable to do so in G12A, G12C and G12D cells; this is because the unknown BRAF population is only present in these three mutants, and therefore, this second BRAF population may be involved in the inability of myosin-9 knockdown to inhibit ERK activity in these cells. This is work that might be continued after the unidentified BRAF protein form is isolated and characterised. Further experiments to carry out include immunoprecipitating myosin-9 in all mutants and WT LIM1215 cells with and without AKT or ERK knockdown to see if AKT/ERK have an impact on myosin-9:BRAF binding in different mutants.

The BRAF immunoprecipitation data also showed the greatest CRAF:BRAF dimerisation in G12A and G12D cells, the two mutants with the strongest presence of the second BRAF form. This may suggest a possible link between the unknown BRAF form and CRAF:BRAF dimerisation, with CRAF appearing to bind to the unknown BRAF form more strongly than with the common BRAF form. CRAF was immunoprecipitation data indicated that the top unknown BRAF band interacted more strongly with CRAF than the bottom band, supporting the possibility of a link between the unknown BRAF population and CRAF dimerisation. This however was only repeated once and therefore the conclusions are extremely preliminary. It is important to understand whether there are any mutant-specific differences in the BRAF:CRAF dimerisation dynamics as RAF heterodimers have been shown to have distinct biochemical properties that can play an important role in the regulation of biological processes such as cellular transformation (Rushworth *et al.*, 2006).

In HPNE cells, WT and mCherry cells do not have the unknown BRAF form, whilst G12D and, unexpectedly, G12V cells do. The top BRAF band only appears upon doxycycline addition to HPNE cells, which induces the expression of the third KRAS copy (either WT or mutant). This suggests that the expression of the top band may be associated with the level of oncogenic burden, as this increases with the expression of the third KRAS copy. Oncogenic activity would realistically be different not only in different cell lines but also in different mutants within the same cell line, based on the fact that different RAS mutants display differing levels of oncogenic potential (Hobbs, Der and Rossman, 2016). One way this theory can be tested is by immunoprecipitating GTP-bound KRAS in different cell lines and seeing if there is a correlation between the level of active KRAS and expression of the second BRAF population.

In conclusion, my work has revealed a previously unknown mechanism that cells may adopt to suppress oncogenic KRAS signalling. Although I could not identify the specific protein involved, I have been able to provide testable hypotheses that the lab is working on. The results of my work in this section suggest that this BRAF form is likely to be a splice variant that affects CRAF:BRAF dimerisation, possibly with the involvement of post-translational modifications. The presence of this second BRAF form is very relevant to research underlying KRAS-driven oncogenesis due to it being linked so strongly to not only specific KRAS mutations in two different cancer cell lines (colorectal and pancreatic), but also because of its possible link to the apparent MEK to RAF inhibition seen in the MRA experiments. The absence of the second BRAF population in SW48 cells may potentially be explained by the presence of different mutations (such as the *FBXW7* mutation) in the cell line. However, this needs to be checked in multiple different cell lines next to see how common this unknown BRAF population actually is. Furthermore, many experiments in this chapter have only been carried out once, therefore, they need to be repeated and the data needs to be strengthened by doing the additional experiments suggested above. Characterisation of the role and identity of the second BRAF population is a top priority right now as it may tie in and explain not only the MEK>RAF inhibition, but also the clustering of ERK signalling dynamics between G12A, G12C and G12D vs WT and G12V cells.

4. Results Chapter III: RNA Sequencing of LIM1215 and HPNE cells

4.1 Background

In this chapter I provide a brief overview of computational work and transcriptomics experiments. The experimental work was significantly delayed by the COVID-19 pandemic and more analysis and validation will be carried out in the Esposito laboratory. To test the hypothesis that different KRAS mutant alleles can trigger biologically significant differences, we have carried out two large RNA-seq experiments. In one experiment, I looked at differential gene transcription in the LIM1215 WT and mutant cells in basal conditions with no EGF stimulation. This experiment was also designed to identify genes that might mediate the phenotypes illustrated in other experiments. To this aim, I also analysed transcriptomics data with a curated database called OmniPath to predict protein-protein interactions.

OmniPath is a database of molecular biology prior knowledge that combines data from over 100 resources and contains information on protein-protein and gene regulatory interactions, intercellular communication, enzyme-PTM relationships and protein complexes and protein annotations such as the function and localisation of proteins. There are multiple ways to use OmniPath, including via R/Bioconductor, Python and Cytoscape (Türei *et al.*, 2021). I have used OmniPath to generate potential interaction maps between proteins based on identified genes of interest from the RNA-seq data analysis of LIM1215 cells. There are specific parameters which can be modulated to make the search criteria more or less stringent, and upon running the code for the desired genes of interest, an interaction map is generated which can be further analysed in BioModelAnalyzer (BMA), an online biological modelling tool.

In this project, I have analysed RNA-seq data generated in the Esposito lab to investigate gene transcriptional changes in the context of different KRAS mutations. RNA-seq is a powerful, robust and adaptable technique for genome-wide analysis of differential transcription. There are many algorithms and pipelines that have been developed over the years, each with their pros and cons which need to be considered in order to avoid a high frequency of false-negative deregulated genes in the data analysis (Corchete *et al.*, 2020). Other techniques used for gene expression analysis include expression microarrays and quantitative polymerase chain reactions (qPCRs) (San Segundo-Val and Sanz-Lozano, 2016). Compared to microarray technology, there are a number of benefits of using

RNA-seq, including the ability to detect novel transcripts, single nucleotide variants and gene fusions, which arrays cannot detect (Wang, Gerstein and Snyder, 2009; Wilhelm and Landry, 2009). RNA-seq also demonstrates a broader dynamic range, allowing for the detection of more differentially expressed genes with higher fold-change (Zhao *et al.*, 2014). Furthermore, RNA-seq technology allows for increased specificity and sensitivity of detection, and is able to detect rare and low-abundance transcripts (Wang *et al.*, 2014; Li *et al.*, 2016).

The LIM1215 isogenic panel is an excellent tool that provides the opportunity to compare cells that differ from just a single heterozygous mutation. A limitation of this panel is that the LIM1215 cell line is a cancer cell line and the cells are propagating with the oncogenic mutation representing, at best, a model for chronic activation of different mutant KRAS alleles. Therefore, I used a panel of inducible, immortalised but non-transformed HPNE cell lines to test differences that specific mutants might cause during early oncogenesis. Each KRAS mutant cell line has an additional third copy of KRAS inserted, which is myc-tagged and doxycycline inducible. The mCherry HPNE cell line is used as a control and instead of a third KRAS copy, it has a doxycycline-induced mCherry gene inserted. The mCherry line provides a good control for overexpression of a protein and doxycycline treatment. Although we have also sequenced the HPNE WT KRAS cell line (which has a third WT copy of KRAS) as an additional control, the data for the WT cells is not yet processed from the High Performance Computing (HPC) cluster because of a technical fault on the server. Therefore, I could not include this additional control in the analysis shown in this chapter. Lastly, all cell lines have been periodically STR profiled, mycoplasma tested and individually genotyped by Sanger sequencing.

This chapter focuses on the data analysis I have carried out for my project. Having submitted a large number of samples, the workload for cell culturing was shared with Dr Suzan Ber (post-doctoral scientist in the Esposito laboratory) and Ms Annie Howitt (PhD student in the Esposito and Frezza laboratories, working on KRAS-induced metabolic alterations). The alignment to the reference genome and the computation of differential expression was performed by the collaborator Dr Shamith Samarajiwa, a computational biologist and group leader at the MRC Cancer Unit. The code I used to interrogate OmniPath was provided by Dr Ben Hall, co-supervisor of my PhD.

4.2 Enrichment of inflammatory pathway genes in LIM1215 G12A, G12C and G12D cells

In parallel to RNA sequencing of LIM1215 cells, we have also sequenced SW48 cells for a separate project. For each cell line, we decided to sequence five samples each. Rather than using identical conditions for each sample, we thawed two different vials with cells of different passages for each cell line. Cells were cultured for two weeks before the first batch was collected for sequencing and other batches were acquired after serial passaging. Six separate samples were collected, of which five were sent for RNA sequencing as illustrated in ***Figure 4.1***.

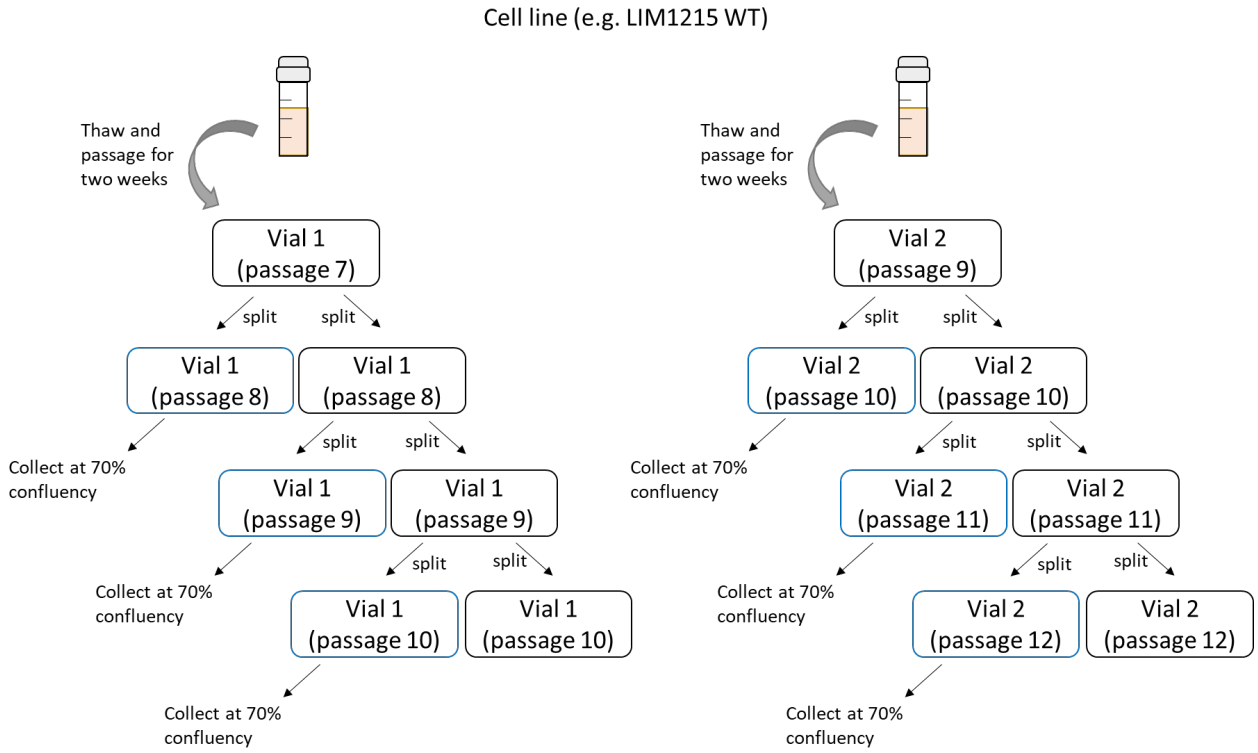

Figure 4.1. **Cell collection process for LIM1215 RNA sequencing.** Illustration showing the process of passaging and the collection of cells to be sent for RNA sequencing. In short, two vials of different passages were thawed and cultured simultaneously and cells were cultured for two weeks before collecting the first sample. Blue boxes indicate cells that were seeded for collection, black boxes indicate cells that were seeded for further passaging. Passages are given as an example.

This protocol was designed to ensure the RNA sequencing would capture the variability caused by standard culturing conditions and to minimise artefacts caused by passage and batch effects. Differential expression analysis was carried out with DESeq2, with each mutant being compared to WT. I used GSEAPreranked to run Gene Set Enrichment Analysis (GSEA) against my ranked list of genes

from the RNA-seq data to identify which gene sets are enriched in the mutants. My project primarily focused on LIM1215 cells, therefore, that is the data I report here. Analysis of the LIM1215 mutant cells showed an interesting pattern in G12A, G12C and G12D cells. In these mutants, there is an upregulation of two cancer hallmark gene sets, TNFα signalling via NFκB and the inflammatory response gene set (see ***Figure 4.2***). Interestingly, these are not upregulated in G12V. Therefore, I speculated that these pathways related to enriched genes could inform us on the MEK to RAF inhibition and/or the second BRAF protein form discussed in the previous chapters.

LIM1215 **UPREGULATED** pathways (mutant vs WT)	
G12A	**G12C**
HALLMARK_TNFA_SIGNALING_VIA_NFKB	**HALLMARK_TNFA_SIGNALING_VIA_NFKB**
HALLMARK_INFLAMMATORY_RESPONSE	HALLMARK_KRAS_SIGNALING_UP
HALLMARK_EPITHELIAL_MESENCHYMAL_TRANSITION	HALLMARK_WNT_BETA_CATENIN_SIGNALING
HALLMARK_KRAS_SIGNALING_UP	**HALLMARK_INFLAMMATORY_RESPONSE**
HALLMARK_COMPLEMENT	HALLMARK_COMPLEMENT
HALLMARK_APOPTOSIS	HALLMARK_HYPOXIA
HALLMARK_TGF_BETA_SIGNALING	HALLMARK_TGF_BETA_SIGNALING
HALLMARK_IL2_STAT5_SIGNALING	HALLMARK_P53_PATHWAY
HALLMARK_HYPOXIA	HALLMARK_UNFOLDED_PROTEIN_RESPONSE
HALLMARK_COAGULATION	HALLMARK_IL2_STAT5_SIGNALING
HALLMARK_WNT_BETA_CATENIN_SIGNALING	HALLMARK_ANDROGEN_RESPONSE
HALLMARK_ALLOGRAFT_REJECTION	HALLMARK_EPITHELIAL_MESENCHYMAL_TRANSITION
HALLMARK_P53_PATHWAY	HALLMARK_ALLOGRAFT_REJECTION
HALLMARK_UNFOLDED_PROTEIN_RESPONSE	HALLMARK_APOPTOSIS
HALLMARK_APICAL_JUNCTION	
HALLMARK_ESTROGEN_RESPONSE_EARLY	
G12D	**G12V**
HALLMARK_TNFA_SIGNALING_VIA_NFKB	HALLMARK_INTERFERON_ALPHA_RESPONSE
HALLMARK_UNFOLDED_PROTEIN_RESPONSE	HALLMARK_WNT_BETA_CATENIN_SIGNALING
HALLMARK_INFLAMMATORY_RESPONSE	HALLMARK_INTERFERON_GAMMA_RESPONSE
HALLMARK_P53_PATHWAY	
HALLMARK_KRAS_SIGNALING_UP	
HALLMARK_APOPTOSIS	

***Figure 4.2*. Enriched pathways in LIM1215 mutants.** List of upregulated pathways (gene sets) in LIM1215 G12A, G12C, G12D and G12V cells in comparison to KRAS WT cells. Gene sets are ranked according to the normalised enrichment score (NES). Only gene sets with a false discovery rate (FDR) of less than 25% and a nominal p value less than or equal to 0.05 are shown in the list. The gene sets highlighted in red are the top upregulated ones common in G12A, G12C and G12D cells, but not upregulated in G12V cells.

From these two enriched gene sets, the top four common enriched genes were identified (*SERPINE1*, *PHLDA1*, *EGR2* and *KLF9*), which were ranked according to the rank metric score for each gene. These genes were chosen by following three steps. Firstly, the top 10 enriched genes upregulated in G12A,

G12C and G12D cells (compared to WT cells) within these two gene sets were chosen. From these, only the genes that were enriched in all three mutant cells were selected (highlighted green in ***Figure 4.3***). Next, the genes that were most enriched across the three mutants were picked. *SERPINE1* and *PHLDA1* were both ranked 1st and 2nd in all mutants, respectively. The 3rd and 4th ranked genes were more difficult to choose as they differed between mutants, but *EGF2* and *KLF9* were the next most enriched across the mutants overall. Some genes that were highly ranked in one mutant but much lower in another were not chosen, for example *PCDH7*. These are highlighted in red in ***Figure 4.3***.

Top enriched genes
LIM1215 **UPREGULATED** pathways mutant vs WT

a

G12A				G12C				G12D			
NFKB		Inflammatory		NFKB		Inflammatory		NFKB		Inflammatory	
Gene	Rank	Gene	Rank	Gene	Rank	Gene	Rank	Gene	Rank	Gene	Rank
SERPINE1	2	SERPINE1	2	SERPINE1	7	SERPINE1	7	SERPINE1	3	SERPINE1	3
PHLDA1	89	PCDH7	109	PHLDA1	73	NOD2	216	PHLDA1	46	PCDH7	135
EGR2	119	HAS2	120	DUSP5	106	SLC1A2	244	PTGS2	48	HBEGF	143
KLF9	133	AXL	122	EGR2	110	EREG	261	EGR3	49	TIMP1	185
PLK2	176	TIMP1	183	PTGS2	129	LAMP3	267	EGR2	70	EREG	227
SLC16A6	179	SLC7A2	200	KLF9	145	TIMP1	272	KLF9	83	LCK	247
PTGS2	248	LCK	236	PLK2	201	ITGB8	281	HBEGF	143	AXL	329
DUSP5	249	ITGB8	272	AREG	330	PCDH7	329	SLC16A6	146	LAMP3	387
PMEPA1	261	CD70	302	HBEGF	341	HBEGF	341	EGR1	148	ITGA5	417
AREG	298	EREG	305	CXCL11	392	CXCL11	392	DUSP5	152	PLAUR	448

Top 10 enriched genes in both pathways. Common for all mutants is highlighted.

b

G12A			G12C			G12D		
Gene	Rank	Pathway	Gene	Rank	Pathway	Gene	Rank	Pathway
SERPINE1	2	Both	SERPINE1	7	Both	SERPINE1	3	Both
PHLDA1	89	NFKB	PHLDA1	73	NFKB	PHLDA1	46	NFKB
PCDH7	109	Inflammatory	DUSP5	106	NFKB	PTGS2	48	NFKB
EGR2	119	NFKB	EGR2	110	NFKB	EGR2	70	NFKB
KLF9	133	NFKB	PTGS2	129	NFKB	KLF9	83	NFKB
TIMP1	183	Inflammatory	KLF9	145	NFKB	PCDH7	135	Inflammatory
PTGS2	248	NFKB	EREG	261	Inflammatory	DUSP5	152	NFKB
DUSP5	249	NFKB	TIMP1	272	Inflammatory	TIMP1	185	Inflammatory
EREG	305	Inflammatory	PCDH7	329	Inflammatory	EREG	227	Inflammatory

List of common genes in rank order

c

G12A			G12C			G12D		
Gene	Rank	Pathway	Gene	Rank	Pathway	Gene	Rank	Pathway
SERPINE1	2	Both	SERPINE1	7	Both	SERPINE1	3	Both
PHLDA1	89	NFKB	PHLDA1	73	NFKB	PHLDA1	46	NFKB
EGR2	119	NFKB	EGR2	110	NFKB	EGR2	70	NFKB
KLF9	133	NFKB	KLF9	145	NFKB	KLF9	83	NFKB

Top 4 common genes

Figure 4.3. **Selection process for top upregulated enriched genes in LIM1215 G12A, G12C and G12D cells compared to WT. a.** The top 10 enriched genes within the TNFα signalling via NFκB and the inflammatory response gene sets were selected. **b.** Of those, only the genes enriched in all three mutants were chosen and ranked according to GSEA ranked list. **c.** Finally, the top four enriched genes across all three mutants (*SERPINE1*, *EGR2*, *KLF9* and *PHLDA1*) selected for further investigation. Genes highlighted in red indicate those that were highly ranked in certain mutants but not others, therefore, were not chosen.

The rationale for picking only four genes was to work with a small list of genes that could be investigated further to expand our understanding of their roles in signalling in these mutants. Although these genes are regulated by TNFα signalling via NFκB, it should be noted that they are also potential ERK signalling targets (Takeda *et al.*, 2001; Joo *et al.*, 2007; Bradley, Ruan and Oursler, 2008), and may be upregulated in KRAS mutant cells for this reason. However, this wouldn't explain why this is not the case in G12V cells, therefore, they are still interesting targets to investigate. These genes, along with a selection of other genes of interest such as *FBXW7*, *BRAF* and *MYH9* were queried in OmniPath. The aim was to try and find the shortest path between pairs of genes, and from all of the

different possible shortest paths, construct the smallest network possible. Smaller networks are easier to falsify and fewer assumptions are made that need to be tested.

Within OmniPath, there are different database options, and when running a command, it can be specified which database it should search, with the option of searching all databases. Combining databases maximises the information available for network building, however, it can mix processes that would not occur on the same timescale, potentially producing misleading networks. Iteratively testing different combinations and individual data sources can help control for this. For my selected genes, which happen to not be very well-characterised, I tested various combinations of databases and ultimately decided to search all databases together; this was required for the inclusion of all genes in the networks generated.

There are also other filters that I can choose to turn on or off to make the search more or less stringent which has an impact on the complexity of the networks generated. These include the option to exclude or include:

- Self-loops in a network (which can result in very long loops with multiple intermediary proteins, thus complicating the network)
- Reverse interactions between a pair of genes (only showing one path between a pair of proteins – the shortest)
- Interactions between intermediary proteins in a path
- Interactions that are ambiguous (where there is conflicting or missing information on (i) which is the source protein and which is the target protein, or (ii) whether the interaction is an activation or an inhibition).

This tool also allows for genes to be designated as 'hub genes', that is, the smallest network between the hub and genes of interest is considered, rather than all genes with one another. Additionally, genes can also be excluded from the search, for example, if a gene is knocked out in a cell line.

The script is opened and loaded in a tool called Visual Studio Code, and upon running a command, the generated network is saved as a BioModelAnalyzer (BMA) model that can directly be pasted onto BMA. With BMA, each interaction can be manually assessed because the sources of information for the interactions (such as PubMed IDs) are generally provided. If the manual assessment of the network informs that it is potentially misleading, alternate networks can also be generated. Lastly, BMA can also be used to test the effects of activating or inhibiting a specific protein on the other proteins in the generated network.

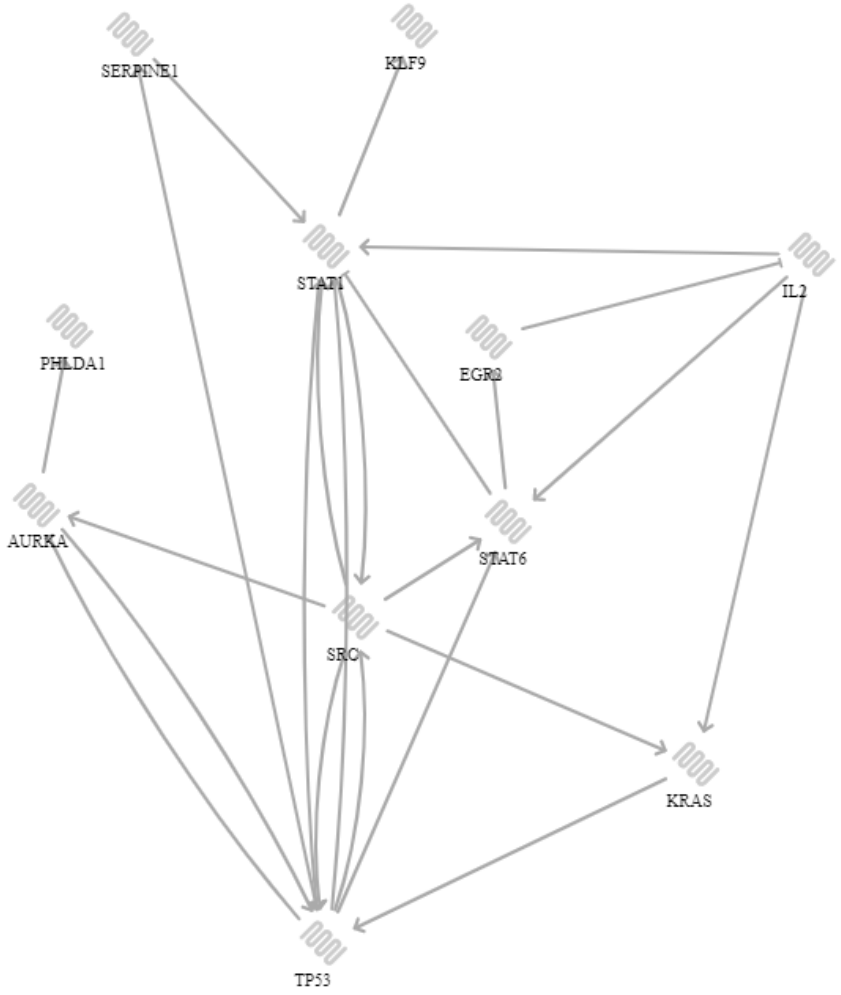

Figure 4.4. **Network generated using OmniPath for selected genes.** The network generated for the top enriched upregulated genes in LIM1215 G12A, G12C and G12D cells using OmniPath (*SERPINE1*, *EGR2*, *KLF9* and *PHLDA1*). Visual Studio Code was used to run the command that searches OmniPath, and BioModelAnalyser was used to generate the network.

Networks for the top enriched unregulated genes (*SERPINE1*, *EGR2*, *KLF9* and *PHLDA1*) were generated. Due to these genes being generally not well-characterised (i.e., there seems to be a relative lack of information on these genes), some of the filters had to be relaxed. Ultimately, a network was generated which included all of the supplied genes ***(Figure 4.4)***. The command specified that all OmniPath databases are searched, ambiguous interactions are included, reverse interactions between a pair of proteins are included and lastly, interactions between intermediary proteins are also included. Furthermore, KRAS was specified as a 'hub' gene, so all interactions involving KRAS are displayed. Each interaction in the network should be supported by references that support the

interaction. However, because of the relaxed filter settings, the database can lack citations for the interactions (as it includes the 'ambiguous' interactions that would be excluded with stricter search filters). To manually assess the interactions, I have checked the citations. It is important to remember that this network is generated from the use of all databases, therefore, interactions occurring at varying time scales are included. This emphasises the importance of checking the source of each interaction.

The network generated may potentially explain how *SERPINE1*, *EGR2*, *KLF9* and *PHLDA1* are upregulated in certain KRAS-mutant cell lines. According to the generated network ***(Figure 4.4)***, KRAS appears to have an "activatory" impact on p53. The evidence for this comes from a paper which shows that oncogenic KRAS can sensitise colorectal tumour cells to chemotherapeutic agents in a p53-dependent manner and promotes phosphorylation of p53 on Ser37 and Ser392 (De Bruijn *et al.*, 2010). Therefore, this apparent activatory interaction appears to reflect this PTM, and does not actually mean KRAS is activating p53. This highlights the need to confirm the predicted interactions shown on these networks by looking at the source of the data. It appears as though the effects of KRAS on the four genes/proteins of interest are mediated via p53. AURKA (aurora kinase A) is shown to be inhibited by p53 (via protein-protein interaction), and in turn it activates PHLDA1 (Sasai *et al.*, 2016). This "activation" is actually a phosphorylation, therefore, from a PTM perspective it would manifest as an activatory arrow. However, the reference paper shows that this phosphorylation actually degrades the protein (Johnson *et al.*, 2011). As there is no information on gene expression changes of PHLDA1 via AURKA, it is not known whether this interaction in the network is able to explain the upregulation of *PHLDA1* expression in the LIM1215 cells. According to this network, p53 can activate SRC, which is shown to activate AURKA, which in turn can activate PHLDA1. Therefore, this is an alternative pathway resulting in PHLDA1 activation. However, there is no reference confirming the activation of SRC by p53, although according to the OmniPath database this interaction is definitely not ambiguous (OmniPath.org, 2021b). This can occur if the data was supplied by a single high throughput study. The activation of aurora kinase A by SRC on the other hand is confirmed in literature (Mahankali *et al.*, 2015).

According to the generated network, p53 activates SERPINE1, and it has been shown experimentally that p53 can modulate SERPINE1 via miR-34a. miR-34a inhibits SERPINE1, and the interaction of p53 with miR-34a changes depending on the mutational status of p53. This ultimately results in an increase in SERPINE1 in the presence of mutant p53 (Akula, Ruvolo and McCubrey, 2020). In the LIM1215 cells, p53 is not mutated, however, KRAS does activate p53, as illustrated in this network. There may be

differences in the ability of KRAS to activate p53 in different LIM1215 KRAS mutant cell lines, which could manifest as changes in gene expression levels and protein-protein interactions. SERPINE1 can also activate STAT1, which is also supported by literature (Ji *et al.*, 2016). However, the interaction between STAT1 and KLF9 is less certain. The network shows an activation, however, there are no publications supporting this. Searching for the source in OmniPath reveals the database to be the DoRothEA (Discriminant Regulon Expression Analysis) database, which is a resource used to identify transcription factor-drug interactions in cancer. The interaction between p53 and STAT6 is also found in the DoRothEA database (Garcia-Alonso *et al.*, 2018). Therefore, although the network suggests STAT1 activates KLF9 and p53 activates STAT6, this needs to be confirmed experimentally because according to OmniPath, it is not known whether these interactions are activatory or inhibitory (OmniPath.org, 2021a, 2021c). Lastly, this network suggests STAT6 activates EGR2, and according to OmniPath, this is definitely an activation. However, the reference provided is 'Wang', and as no further information is given it is difficult to verify the connection.

OmniPath was also used to generate networks including BRAF, MEK, MYH9 and FBXW7 in combination with SERPINE1, PHLDA1, KLF9 or EGR2 to see if useful interactions can be revealed that could explain the RAF to MEK inhibition and/or the cause of the second BRAF population in these mutant cells. Of the networks generated, two showed interesting interactions. The network generated in ***Figure 4.5a*** suggests that SERPINE1 inhibits PLAT, which would normally activate PRKCE, which would then activate MYH9. SERPINE1 overexpression should therefore result in the inhibition of MYH9. However, when checking the references, although it can be confirmed that SERPINE1 inhibits PLAT, the interactions between PLAT, PRKCE and MYH9 are less certain due to lack of references confirming these interactions (Madison *et al.*, 1990). Although this network does not provide a solid mechanism of interaction between SERPINE1 and MYH9, it does however provide a testable hypothesis.

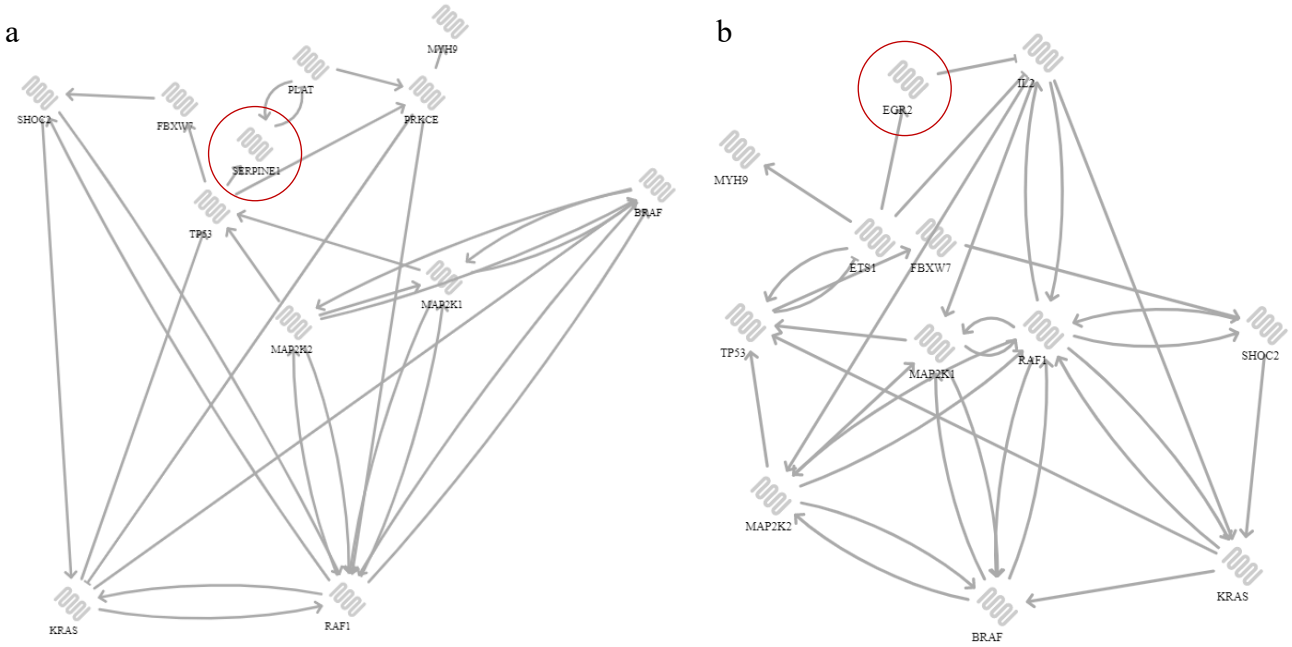

***Figure 4.5*. Networks generated using OmniPath for genes of interest.** Visual Studio Code was used to run the command that searches OmniPath, and BioModelAnalyser was used to generate the networks. The red circles highlight the genes probed along with BRAF, MYH9, MAP2K1, MAP2K2, FBXW7 and KRAS as the hub. **a.** The network generated for showing potential role of SERPINE1 on MYH9. **b.** Network showing potential role of EGR2 on BRAF.

The second network ***(Figure 4.5b)***, shows that overexpressed EGR2 would inhibit IL2, which would inhibit KRAS and ultimately lead BRAF and CRAF inhibition. This could potentially explain a mechanism for RAF inhibition in the LIM1215 G12A, G12C and G12D cells. However, the problem is that although OmniPath suggests that these interactions are 'consensus' interactions (which means that they have manually been checked), it is difficult to find literature supporting this. It is important to reiterate here that the RNA-seq samples were not treated with EGF, whereas the MEK to RAF inhibition and the appearance of the second BRAF population both occur in cells treated differently (with EGF and/or MEK siRNA).

To conclude this section, OmniPath has been a useful tool to understand the impact overexpression of certain genes may have on other targets and potential mechanisms behind the overexpression of the upregulated genes have been proposed. It has enabled the formulation of hypotheses that can be

tested not only experimentally, but also computationally, for example, the information gained from using this tool can also be used to re-analyse the RNA-seq data to identify further targets.

4.3 KRAS mutant-specific differential gene regulation in early steps of carcinogenesis

The protocol used for the sample preparation of HPNE cells was similar to that described in ***Figure 4.1*** for LIM1215 cells with five samples submitted for sequencing. The only difference was that only a single vial was thawed (see 'Materials and Methods' for a detailed protocol). The expression of the third KRAS copy is induced via the addition of doxycycline, and four time points were chosen for doxycycline treatment. The aim was to see how early changes in gene transcription post-transformation alter between different KRAS mutants. In addition to the mutants studied thus far, G12R is also included in this experiment as this mutation is uniquely prevalent in pancreatic cancer as it occurs in around 20% of PDAC, but only in around 1% of lung and colorectal cancers. There is also evidence that G12R is functionally distinct from G12V and G12D mutations in PDAC (Hobbs *et al.*, 2020). Therefore, it would be interesting to see what the differences in gene expression are between G12R cells and the other mutants in pancreatic cancer cells.

Within each cell line (mCherry, G12A, G12C, G12D, G12R and G12V), GSEA analysis shows which gene sets are differentially regulated at 2 days, 7 days and 14 days post-induction of mutant KRAS expression (or mCherry for the control). A limitation of using mCherry as a control is that any gene expression changes due to KRAS overexpression are not accounted for. The top three enriched gene sets (and the top three genes within each gene set) in each cell line are shown in ***Figure 4.6***. Data is shown for 2 days, 7 days and 14 days of doxycycline treatment. The mCherry control samples show changes to very few genes, but cells expressing mutant KRAS show larger changes and to a significantly larger gene set (tens vs hundreds), showing that the main difference between control cells and mutant cells is in fact the presence of the mutant allele. Mutant cell lines exhibit an upregulation in genes involved in TNFα signalling via NFκB when compared to uninduced cells. Notably, this gene set is also upregulated in mCherry cells although to a much lower extent, showing that although the expression of these genes is altered by doxycycline, oncogenic KRAS has a much larger impact.

Upregulated gene sets

Cell line	2 days				7 days				14 days			
	Gene set	Top enriched genes			Gene set	Top enriched genes			Gene set	Top enriched genes		
mCherry	HALLMARK_TNFA_SIGNALING_VIA_NFKB	EGR1	ATF3	IFIH1	HALLMARK_INTERFERON_GAMMA_RESPONSE	MX1	IRF7	HERC6	HALLMARK_INTERFERON_ALPHA_RESPONSE	MX1	HERC6	IFIH1
	HALLMARK_INTERFERON_GAMMA_RESPONSE	MX1	HERC6	IRF7	HALLMARK_INTERFERON_ALPHA_RESPONSE	MX1	IRF7	HERC6	HALLMARK_INTERFERON_GAMMA_RESPONSE	OAS2	MX1	HERC6
	HALLMARK_INTERFERON_ALPHA_RESPONSE	MX1	HERC6	IRF7	HALLMARK_TNFA_SIGNALING_VIA_NFKB	EGR1	BIRC3	ATF3	HALLMARK_TNFA_SIGNALING_VIA_NFKB	IFIH1	EGR1	ATF3
G12A	HALLMARK_MYC_TARGETS_V2	HK2	EXOSC5	BYSL	HALLMARK_TNFA_SIGNALING_VIA_NFKB	AREG	G0S2	IL1B	HALLMARK_TNFA_SIGNALING_VIA_NFKB	AREG	KLF4	G0S2
	HALLMARK_OXIDATIVE_PHOSPHORYLATION	SLC25A4	NDUFB6	SURF1	HALLMARK_CHOLESTEROL_HOMEOSTASIS	TRIB3	TM7SF2	PLAUR	HALLMARK_ANGIOGENESIS	PRG2	STC1	TIMP1
	HALLMARK_MYC_TARGETS_V1	ODC1	H2AZ1	PRDX4	HALLMARK_ANGIOGENESIS	STC1	PRG2	TIMP1	HALLMARK_KRAS_SIGNALING_UP	KLF4	G0S2	PRDM1
G12C	HALLMARK_KRAS_SIGNALING_UP	TMEM158	DUSP6	GALNT3	HALLMARK_TNFA_SIGNALING_VIA_NFKB	AREG	RELB	IL1B	HALLMARK_KRAS_SIGNALING_UP	G0S2	IL1B	TMEM158
	HALLMARK_TNFA_SIGNALING_VIA_NFKB	AREG	RELB	MAFF	HALLMARK_KRAS_SIGNALING_UP	DUSP6	IL1B	GALNT3	HALLMARK_TNFA_SIGNALING_VIA_NFKB	G0S2	AREG	IL1B
	HALLMARK_UV_RESPONSE_UP	AQP3	FOS	ICAM1	HALLMARK_UNFOLDED_PROTEIN_RESPONSE	DNAJC3	CHAC1	DNAJB9	HALLMARK_INFLAMMATORY_RESPONSE	IL1B	P2RY2	HAS2
G12D	HALLMARK_TNFA_SIGNALING_VIA_NFKB	FOS	AREG	PTGS2	HALLMARK_TNFA_SIGNALING_VIA_NFKB	G0S2	AREG	CXCL3	HALLMARK_TNFA_SIGNALING_VIA_NFKB	AREG	G0S2	KYNU
	HALLMARK_MTORC1_SIGNALING	TRIB3	STC1	HK2	HALLMARK_KRAS_SIGNALING_UP	G0S2	DUSP6	PTGS2	HALLMARK_INFLAMMATORY_RESPONSE	F3	GCH1	IL2RB
	HALLMARK_UV_RESPONSE_UP	FOS	ICAM1	ASNS	HALLMARK_INFLAMMATORY_RESPONSE	F3	IL1B	IL2RB	HALLMARK_UV_RESPONSE_UP	FOS	GCH1	GPX3
G12R	HALLMARK_XENOBIOTIC_METABOLISM	GCH1	JUP	UPP1	HALLMARK_TNFA_SIGNALING_VIA_NFKB	AREG	G0S2	EGR1	HALLMARK_TNFA_SIGNALING_VIA_NFKB	G0S2	AREG	SERPINB2
	HALLMARK_P53_PATHWAY	PITPNC1	UPP1	TRIB3	HALLMARK_KRAS_SIGNALING_UP	G0S2	PRDM1	SPRY2	HALLMARK_KRAS_SIGNALING_UP	G0S2	GPNMB	GALNT3
	HALLMARK_DNA_REPAIR	POLD4	POLR2H	SURF1	HALLMARK_CHOLESTEROL_HOMEOSTASIS	CXCL16	TRIB3	TM7SF2	HALLMARK_UNFOLDED_PROTEIN_RESPONSE	DNAJC3	DNAJB9	HSPA5
G12V	HALLMARK_TNFA_SIGNALING_VIA_NFKB	EGR1	FOS	AREG	HALLMARK_TNFA_SIGNALING_VIA_NFKB	FOS	EGR1	AREG	HALLMARK_TNFA_SIGNALING_VIA_NFKB	AREG	G0S2	EGR1
	HALLMARK_CHOLESTEROL_HOMEOSTASIS	CXCL16	TM7SF2	TRIB3	HALLMARK_CHOLESTEROL_HOMEOSTASIS	TRIB3	TM7SF2	CXCL16	HALLMARK_KRAS_SIGNALING_UP	G0S2	GALNT3	PRDM1
	HALLMARK_UV_RESPONSE_UP	FOS	ICAM1	FOSB	HALLMARK_ANGIOGENESIS	PRG2	STC1	TIMP1	HALLMARK_MTORC1_SIGNALING	STC1	ITGB2	NIBAN1

Downregulated gene sets

Cell line	2 days dox				7 days dox				14 days dox			
	Gene set	Top enriched genes			Gene set	Top enriched genes			Gene set	Top enriched genes		
mCherry	HALLMARK_MYC_TARGETS_V1	PSMC6	DEK	ABCE1	HALLMARK_MYC_TARGETS_V1	SSBP1	SNRPD2	VBP1	HALLMARK_MYC_TARGETS_V2	IPO4	SRM	EXOSC5
	HALLMARK_E2F_TARGETS	ING3	TIPIN	PNN	HALLMARK_OXIDATIVE_PHOSPHORYLATION	NDUFA5	UQCRB	COX17	HALLMARK_APICAL_JUNCTION	PTPRC	ITGA9	RHOF
	HALLMARK_OXIDATIVE_PHOSPHORYLATION	UQCRB	NDUFA5	DLD	HALLMARK_E2F_TARGETS	SMC6	ING3	SPC25	HALLMARK_HEDGEHOG_SIGNALING	L1CAM	HEY1	TLE3
G12A	HALLMARK_UV_RESPONSE_DN	CACNA1A	FBLN5	KIT	HALLMARK_E2F_TARGETS	PLK4	POLD3	WEE1	HALLMARK_E2F_TARGETS	PLK4	RFC3	GINS1
	HALLMARK_EPITHELIAL_MESENCHYMAL_TRANSITION	FBLN5	LAMA1	SNTB1	HALLMARK_MYC_TARGETS_V1	U2AF1	TYMS	CTPS1	HALLMARK_PROTEIN_SECRETION	SCAMP1	KRT18	ANP32E
	HALLMARK_KRAS_SIGNALING_DN	DLK2	MSH5	CELSR2	HALLMARK_G2M_CHECKPOINT	PLK4	CDK1	KIF15	HALLMARK_G2M_CHECKPOINT	PLK4	CKS2	HMMR
G12C	HALLMARK_EPITHELIAL_MESENCHYMAL_TRANSITION	MEST	COL4A1	WNT5A	HALLMARK_E2F_TARGETS	UNG	E2F8	MCM3	HALLMARK_EPITHELIAL_MESENCHYMAL_TRANSITION	MEST	RHOB	COL4A1
	HALLMARK_UV_RESPONSE_DN	IGF1R	COL3A1	COL1A2	HALLMARK_EPITHELIAL_MESENCHYMAL_TRANSITION	RHOB	NID2	FBLN5	HALLMARK_MYOGENESIS	COL4A2	DTNA	GADD45B
	HALLMARK_HEDGEHOG_SIGNALING	MYH9	ETS2	DPYSL2	HALLMARK_MYC_TARGETS_V2	UNG	MCM4	DCTPP1	HALLMARK_KRAS_SIGNALING_DN	MX1	TGFB2	GDNF
G12D	HALLMARK_EPITHELIAL_MESENCHYMAL_TRANSITION	MEST	WNT5A	THBS1	HALLMARK_EPITHELIAL_MESENCHYMAL_TRANSITION	MEST	WNT5A	COL4A1	HALLMARK_E2F_TARGETS	MMS22L	BARD1	PAN2
	HALLMARK_E2F_TARGETS	UNG	E2F8	PRKDC	HALLMARK_E2F_TARGETS	CDKN1A	E2F8	PCNA	HALLMARK_EPITHELIAL_MESENCHYMAL_TRANSITION	MEST	WNT5A	DCN
	HALLMARK_UV_RESPONSE_DN	FZD2	COL1A1	SNAI2	HALLMARK_MYOGENESIS	COL4A2	COL1A1	COL3A1	HALLMARK_G2M_CHECKPOINT	DMD	E2F2	BARD1
G12R	HALLMARK_UV_RESPONSE_DN	RASA2	ACVR2A	INPP4B	HALLMARK_E2F_TARGETS	HMMR	ATAD2	USP1	HALLMARK_EPITHELIAL_MESENCHYMAL_TRANSITION	MEST	LOXL1	LRRC15
	HALLMARK_G2M_CHECKPOINT	STAG1	KIF11	POLQ	HALLMARK_G2M_CHECKPOINT	DMD	NDC80	CUL5	HALLMARK_KRAS_SIGNALING_DN	SYNPO	NPY4R	NRIP2
	HALLMARK_PROTEIN_SECRETION	VPS4B	DNM1L	ABCA1	HALLMARK_MITOTIC_SPINDLE	FGD4	NDC80	BCL2L11	HALLMARK_APICAL_SURFACE	SHROOM2	PCSK9	THY1
G12V	HALLMARK_EPITHELIAL_MESENCHYMAL_TRANSITION	MEST	COL4A1	WNT5A	HALLMARK_MYC_TARGETS_V1	SSB	NOLC1	RPL22	HALLMARK_EPITHELIAL_MESENCHYMAL_TRANSITION	MEST	GAS1	LOXL1
	HALLMARK_UV_RESPONSE_DN	KIT	COL11A1	DMAC2L	HALLMARK_E2F_TARGETS	HMGB2	NOLC1	PNN	HALLMARK_NOTCH_SIGNALING	WNT5A	FZD7	LFNG
	HALLMARK_APICAL_SURFACE	PCSK9	CRYBG1	GAS1	HALLMARK_EPITHELIAL_MESENCHYMAL_TRANSITION	IGFBP3	MEST	OXTR	HALLMARK_MYOGENESIS	COL6A2	COL3A1	SSPN

Figure 4.6. **Differentially upregulated and downregulated genes in HPNE cells upon expression of mutant KRAS.** Tables showing the top three upregulated and downregulated gene sets (and the top three genes within these gene sets) in HPNE mCherry, G21A, G12C, G12D, G12R and G12V cells treated with doxycycline for 2, 7 or 14 days compared to cells not treated with doxycycline. Gene sets (and the top genes within each gene set) have been ranked by GSEA according to normalised enrichment score.

More importantly, all mutant cell lines exhibit an upregulation in genes involved in KRAS pathway activation, confirming the validity of the analysis. HPNE G12D cells exhibit the largest changes to the most genes. Preliminary analysis shows that the main difference between mutant cells is not if a gene is differentially regulated, but the extent of the differential expression between mutant cells. However, I observed also more distinctive features in individual mutants. For example, only in G12R cells there is an upregulation of genes involved in DNA repair and the p53 pathway very early on post-transformation, suggesting a unique mechanism of the G12R mutation in PDAC development. The G12R mutation is also unique in that genes involved in epithelial-mesenchymal transition (EMT) are not downregulated very early on post-transformation, whereas they are in all of the other mutants. EMT is a biological process that allows cells to have enhanced migratory capabilities, elevated resistance to apoptosis and invasiveness (Kalluri and Weinberg, 2009). Increased EMT in G12R relative to other KRAS mutants may be a potentially important mechanism of PDAC development that sets the G12R mutation apart from the other mutations. Another interesting observation is the upregulation of genes involved in the inflammatory response only in G12D and G12C cells (although this is seen earlier in G12D mutant cells). As G12D is the most common PDAC KRAS mutation, this difference in gene regulation may be important in understanding the cause of different frequencies of KRAS mutations in PDAC.

4.4 Discussion

In this chapter, I have attempted to characterise gene transcriptional changes in the context of different KRAS mutations. RNA-seq analysis of the LIM1215 cells revealed enrichment of genes within the TNFα via NFκB and inflammatory response pathways only in LIM1215 G12A, G12C and G12D cells. In an effort to understand why this is the case and whether differential expression of these genes is involved in the inhibition of RAF via MEK or the presence of the second BRAF form, I utilised a database of molecular biology interactions to generate potential interaction maps between proteins (and genes) of interest. These networks helped propose mechanisms of upregulation of certain genes and also possible interactions that could explain RAF inhibition in these cells, thereby allowing for the formulation of testable hypotheses.

One downside of my data is that I had to use very relaxed settings on OmniPath in order to generate my networks, as stricter settings eliminated some of my genes of interest. This meant that more ambiguous interactions between genes/proteins were included that potentially lacked strong supporting evidence in literature. The settings needed to be relaxed because of lack of information on

my selected genes of interest. These relaxed settings made it very important to manually check each citation provided by OmniPath to make sure the interactions were true. Another downside of the data from the LIM1215 RNA-seq analysis is that the LIM1215 cell line is a transformed cancer cell line (Whitehead *et al.*, 1985), and thus it is likely that over time genetic instability arises that can translate into cell line heterogeneity. Cell line evolution can occur due to positive clonal selection that is sensitive to cell culture conditions, and these genetic changes can be associated with differential gene activation which may skew the RNA-seq analysis (Ben-David *et al.*, 2018). However, as an isogenic panel is used, it can be assumed that any evolutionary genetic changes accumulated would be similar across the panel and therefore comparisons should still be able to be made confidently between mutants. Furthermore, the LIM1215 RNA-seq data also has its strengths, such as the fact that five individual repeats per sample were sequenced for strong statistical analysis and to account for clonal differences, and a sequencing depth of 20 million reads per sample was employed which is a good minimum threshold for effective differential expression analysis (Ching, Huang and Garmire, 2014; Lamarre *et al.*, 2018). RNA-sequencing is also a very strong technique for profiling of the transcriptome, being highly specific and sensitive and being able to detect novel transcripts (Wang, Gerstein and Snyder, 2009; Kukurba and Montgomery, 2015).

My work is not the first time mutant RAS driven gene expression has been studied. Multiple labs have investigated gene transcription changes driven by oncogenic RAS. In one study, Loboda and colleagues identified a RAS pathway signature consisting of 147 genes via the integrated analysis of internal datasets and literature data. Their aim was to develop a gene expression signature that could predict RAS pathway dependence in pre-clinical cancer models and human tumours. They related this signature to KRAS mutational status and drug response data in pre-clinical and clinical datasets and found that compared to looking at just the KRAS mutational status, the RAS pathway signature was a superior method not only for predicting pathway dependence but also predicting the response to PI3K and AKT inhibitors (Loboda *et al.*, 2010). Another group utilised TCGA datasets to investigate the relationship between RAS mutational status and mRNA expression. Their findings revealed a potential adaptive response during tumour evolution that is dependent on cellular context and the mutational status of proximal genes in the RAS pathway, and that the cell contextual differences may influence alternative resistance mechanisms to therapeutic inhibitors (Stephens *et al.*, 2017).

Zhang and colleagues analysed the gene expression profiles of 156 KRAS mutant lung cancer samples and were able to identify 41 predictive genes that may be molecular markers for identifying KRAS mutations. The gene expression profiles of KRAS positive and KRAS negative samples were

downloaded from the publicly available Gene Expression Omnibus (GEO) database, and the expression levels of 978 representative genes from Broad Institute Human L1000 landmark were measured. The genes were first ranked using an algorithm based on relevance with mutation samples and also redundancy amongst genes (the top ranked genes had high association with KRAS mutation status and low redundancy with other genes). They then used another algorithm to identify the final 41 predictive genes (Zhang *et al.*, 2020). Although in this study only the G12C KRAS mutation was considered, this methodology may be useful for identifying differentially expressed genes in a KRAS mutant-specific manner using our LIM1215 RNA-seq data.

Gene expression analysis has also been carried out to investigate the impact of therapeutic drugs on the transcriptional profile of the KRAS signalling pathway in PDAC patients. Oliverious and colleagues explored the interactions of paclitaxel (a conventional chemotherapeutic drug) and taxane SB-T-1216 (an experimental drug) with the RAS pathway in *in vitro* and *in vivo* PDAC models in order to identify predictive biomarkers or targets. Although they were unable to identify targets on the transcriptional level for further pre-clinical testing, this study did highlight that *in vitro* cell models differ in the basal transcriptional profile of the RAS signalling pathway (Oliverius *et al.*, 2019). This is something that we already know, but it does reiterate the need for my work to be repeated in other cell lines/cancer models to ensure observations are reproducible and not limited to just one cell line.

Although my work on the LIM1215 cell line is preliminary, it adds value to what is already known regarding RAS mutation related transcriptional changes in different cancer models. However, the LIM1215 cells are cancer cells that are already transformed and chronically propagate signalling downstream of KRAS, and because we wished to also understand the gene transcriptional profiles in the different KRAS mutations and how they change over time post-transformation, the HPNE cell line was used for this purpose. The HPNE cell line is a non-transformed doxycycline-inducible isogenic panel that allows for the control of induction of transformation. Initial RNA-seq data analysis suggests differential expression of gene sets that not only vary across mutants but also within the same mutant over time post-transformation (for example, G12R cells appear to have distinct gene regulation very early on post-transformation compared to the other mutants).

Due to time constraints, the RNA-seq analysis of the HPNE cells is very preliminary in this thesis. Currently, there is a list of gene sets and a list of the topmost enriched upregulated and downregulated genes, and to determine which genes may be interesting to study further (for example, via the use of OmniPath and BMA), a strategy needs to be in place. This strategy will depend on the aim of the

analysis. For example, the current analysis is a good start for understanding KRAS mutant-specific gene transcription changes over time upon expression of the mutant KRAS form, but it doesn't give much insight into the level of up or downregulation. Narrowing down the current list of genes to those that have the largest change in expression from day 0 to day 14 may help identify genes of interest to investigate further. Genes that are also specifically enriched in only G12R for example could also be investigated to help understand why the G12R mutation is so prevalent specifically in PDAC (Hobbs *et al.*, 2020). Genes that are enriched specifically only in the LIM1215 and HPNE mutants with the second BRAF population would also be of interest. OmniPath could then be utilised to help understand the signalling networks involving these genes/proteins. Lastly, commonly enriched genes between the same mutants but different cell lines could also be of interest, however, this is not ideal in my work as the experimental set up is so different between both the LIM1215 and HPNE RNA-seq experiments. Furthermore, one is a colorectal and the other is a pancreatic cancer cell line. ***Supplementary figure 4.1*** shows the most enriched upregulated genes for both LIM1215 and HPNE cell lines in a visual way and as can be seen, the mutants do not share any common genes. This could be explained by the fact that both cell lines were not subjected to the same experimental protocols. Furthermore, one is an overexpression system and the other isn't, which is likely to add variation between the cell lines. Future work could involve comparing gene expression changes between cell lines from the same cancer type and mutation either using publicly available datasets or conducting further RNA-seq experiments.

In conclusion, both RNA-seq datasets have provided preliminary hypotheses that can now be validated in the lab with experimental work and further transcriptomics and/or computational work. OmniPath is a continuously growing database of protein-protein and gene regulatory interactions (Türei, Korcsmáros and Saez-Rodriguez, 2016; Ceccarelli *et al.*, 2020), and is a useful tool that has its pros and cons. By understanding it better and fine-tuning the process of probing this substantial database, it can be a very strong and informative tool. I have presented relatively early-stage results in this thesis, which we can now build on.

5. Overall discussion

KRAS is one of the most commonly mutated oncogenes in human cancers, with activating mutations being most prevalent in pancreatic, lung and colorectal carcinomas (Simanshu, Nissley and McCormick, 2017). Within KRAS, there are hotspots with a high frequency of mutations occurring at those sites, with codon 12 being the most mutated. Cancer-specific differences in mutational frequency of the RAS isoforms and the specific mutations is observed, and it is not fully understood why this is the case.

Different allele substitutions at these hotspots can lend KRAS differential oncogenic capabilities, for example by altering cell signalling, thus suggesting that all KRAS mutants are not equal (Hobbs, Der and Rossman, 2016; Haigis, 2017). My work isn't the first to look at mutation-specific signalling and what the mechanism behind it could be. All KRAS G12 mutations are activating, so why is it that different mutants behave differently? Many groups have tried to elucidate this by investigating the role of different KRAS mutations on phenotypical consequences such as the impact on transforming potential, GDP/GTP binding, anchorage-independent growth and migration and also biochemical effects such as activation of different signalling pathways downstream of RAS (Muñoz-Maldonado, Zimmer and Medová, 2019). For example, early studies showed that specific codon substitutions in RAS resulted in altered transforming potential (Seeburg *et al.*, 1984; Pincus and Brandt-Rauf, 1985; Der, Finkel and Cooper, 1986), with more recent work also supporting this (Smith *et al.*, 2010; Stolze *et al.*, 2014). Another group found that the affinity of KRAS to the RBD of CRAF was affected by the specific mutation present on KRAS (Hunter *et al.*, 2015).

Different RAS mutations have also been shown to impact the transcriptional, proteomic and metabolic profile of a cell. For example, Hammond and colleagues carried out quantitative analysis of the proteome and phosphoproteome in SW48 cells harbouring specific KRAS mutations and found that G12D and G12V mutant cells have similar signatures that cluster together and are different to the G13D signature (Hammond *et al.*, 2015). Studies have also looked at the impact of specific RAS mutations in different RAS isoforms. Roberts and colleagues found a number of genes involved in Notch signalling, cell motility and cytokinesis that were differentially regulated between KRAS G12V tumours and HRAS G12V tumours (Roberts *et al.*, 2006).

My work has focussed on elucidating differences in KRAS mutant-specific downstream signalling, rather than primarily characterising phenotypic differences. Other groups have investigated the role

of different RAS isoforms or specific RAS mutations in the activation of downstream signalling pathways. Rosseland and colleagues compared the ability of HRAS G12V and KRAS G12V to preferentially activate the ERK or PI3K pathways and differentially control cell survival and growth. Interestingly, they found that whilst both HRAS and KRAS mediated PI3K-induced survival, HRAS was the major mediator of ERK-induced proliferation and survival, revealing that different RAS isoforms harbouring the same mutation can distinctly activate these pathways (Rosseland *et al.*, 2008). In contrast, a more recent study found no differences in ERK phosphorylation in MCF10A cells expressing low levels of various KRAS G12 and G13 mutants (Stolze *et al.*, 2014). This suggests that not only the cell type, but also level of expression of mutant RAS plays a role in its ability to activate downstream signalling pathways.

Despite the high frequency of KRAS mutations in cancer, until recently, there were currently no approved therapies. A lot of progress has been made in the last decade, however, it might be hindered by the incomplete understanding of not only the complexity, but also the plasticity of ERK signalling. My work has attempted to fill this gap by trying to elucidate further how signalling downstream of KRAS is rewired in the context of different G12 mutations.

The ERK pathway is differentially rewired in a KRAS-dependent manner

Initial studies of ERK pathway activation revealed interesting mutant-specific behaviours. Firstly, all mutants (G12A, G12C, G12D and G12V) activate the ERK pathway to a lower extent compared to WT KRAS. We hypothesise that this may be a survival mechanism adopted by transformed cells with an excessive oncogenic burden that would otherwise act to trigger cell death or senescence. This is supported by research showing that there is a precise level of active ERK that is optimal for cell survival and proliferation, and ERK signalling outside of this 'sweet spot' can result in senescence or cell death (Sale, Balmanno and Cook, 2019). The second interesting observation is that G12V cells cluster more with WT cells by having a higher ERK response compared to G12A, G12C and G12D cells.

To understand how the ERK pathway is rewired, I utilised Modular Response Analysis (MRA), a technique which has successfully been used in the past to study the rewiring of the ERK pathway in response to different stimuli. Santos and colleagues investigated how the MAPK network influences signal specificity in PC-12 cells upon treatment with either NGF or EGF. They found that depending on the growth factor, the network exhibited either a positive or negative feedback, resulting in differential cell fate dynamics (Santos, Verveer and Bastiaens, 2007). The protocol used in my work

has followed (and optimised) the protocol used in this work. Similar siRNAs and antibodies were used, with my work taking it a step further and also probing for CRAF in addition to BRAF (CRAF was not probed in Santos' work). Furthermore, my work also produced better knockdowns.

MRA has also been utilised by other groups to study not only ERK signalling dynamics downstream of KRAS, but also other RAS isoforms, with different studies employing slightly different and modified experimental techniques. For example, Hood and colleagues characterised isoform-specific mutant RAS signalling in a panel of isogenic SW48 cell lines harbouring either WT RAS or G12V RAS, and they found that the different RAS isoforms exhibited differential coupling to the ERK and PI3K pathways and that these differences were dependent on growth factor stimulation. They used mathematical modelling based on MRA to show that the core signalling network of KRAS was the most distinguished from the rest of the RAS isoforms. One difference in the experimental approach in this work is that instead of siRNA, they used pharmacological inhibitors (Hood *et al.*, 2019).

MRA has also been used to understand rewiring of the broader RAS network. Bluthgen and colleagues used MRA-based mathematical models to identify crosstalk and feedbacks between the PI3K and ERK pathways in colorectal cancer cells (Klinger *et al.*, 2013), and have also more recently used MRA to investigate the role of SHP2, a protein that has been implicated in resistance to colon cancer therapy, in RAS signalling (Dorel *et al.*, 2018). They also found that ERK activation is cell-type dependent, and using MRA, they found that this is due to specific MEK to ERK feedforward and feedback mechanisms (Brandt *et al.*, 2019). Finally, Kholodenko and colleagues utilised MRA to analyse drug resistance mechanisms following inhibitor treatment and found that network topologies and kinase dimerisation both played a role in inhibitor-induced pathway activation (Kholodenko *et al.*, 2021).

Interestingly, most of these studies used inhibitors rather than siRNAs. Although both may be used for the purpose of perturbating the activity of a target protein, a benefit of siRNA is that it reduces total protein levels, whereas inhibitors do not. Therefore, the use of siRNA impacts not only the activity but also other activity-independent interactions of the target protein with other proteins, whilst inhibitors target activity-dependent interactions (Weiss, Taylor and Shokat, 2007). As MRA is used to elucidate network topologies, it makes sense to use a method of perturbation which impacts both activity and any other potential role of the target protein in order to not miss unknown interactions. Furthermore, siRNAs specifically degrade the target mRNA, whereas inhibitors can have more off-target effects (Kumar *et al.*, 2008; Wynn *et al.*, 2011). Although siRNAs can also have off-target effects due to the presence of short stretches of sequence homology in non-coding regions of DNA or the RNA of other

structurally distinct classes of proteins, this can be minimised by using pooled siRNA and good negative controls (both of which I have done in my work). One reason for using inhibitors however is the ease of use and faster action compared to siRNAs which take relatively longer to work (Weiss, Taylor and Shokat, 2007).

My MRA work revealed two previously unreported interactions that are differentially rewired in the different mutants. A RAF inhibition via MEK is observed in a manner that correlates with the ERK responses, with the strongest inhibition seen in the mutants with the lowest ERK activity. This provides a potential mechanism that could explain the reduced ERK activity in certain KRAS mutant cells. To understand how MEK inhibits RAF, antibody array data revealed the possible role of c-Jun N-terminal kinase (JNK). MEK has been shown to activate JNK, which in turn has been shown to inhibit RAF (Adler *et al.*, 2008; Ritt *et al.*, 2016). JNK is upregulated in LIM1215 G12D cells compared to WT cells, and thus this data provides a logical testable hypothesis for the inhibition of RAF via MEK in G12D mutant cells. However, this data is extremely preliminary, and needs to be repeated at least twice more to strengthen this hypothesis. If JNK is confirmed to be differentially phosphorylated in more repeats of the array, then further experiments can be carried out to confirm this. For example, if inhibiting JNK results in RAF inhibition and MEK knockdown reduces JNK activity, then this would support the hypothesis. Observing this in only G12A, G12C and G12D cells but not in WT or G12V cells, preferable across several cell lines, would strengthen the data even further.

The second unreported interaction is observed when ERK signalling is shutting down. This is a loss of RAF to ERK inhibition, or the presence of a RAF to ERK activation, depending on the mutant. In WT cells, RAF inhibits ERK, which could explain the relatively fast desensitisation of ERK signalling seen in these cells. It is also possible that mutants that have a MEK to RAF inhibition do not require the RAF to ERK activation later on, as is seen in G12D cells, perhaps because ERK signalling is already at an optimal level in the first place. This exemplifies how KRAS-dependent rewiring of one part of the signalling pathway can influence the interaction of other proteins within the pathway. My work also proposes a potential mediator of the RAF to ERK activation, which is seen the strongest in G12C cells. Antibody array data suggests that tyrosine kinase 2 (TYK2) could be responsible, as it is upregulated in G12C cells and has been shown to bind to BRAF and activate ERK (Carmo *et al.*, 2011). Again, this data is preliminary, and the array experiment needs to be repeated to strengthen this hypothesis, but both JNK and TYK2 are proteins of interest that will now be validated in the Esposito lab.

Overall, the MRA work presented in this chapter is of good quality, with 5 repeats being carried out.

The protocols used for the MRA experiments have been significantly optimised to achieve the desired knockdowns and reproducibility required for the generation of robust network topologies. A weakness in this project arises from the array experiments, which need to be repeated further to strengthen the preliminary hypotheses I have presented here.

An unidentified BRAF form is present in specific KRAS-mutant cells

My work has revealed the presence of a second unidentified BRAF form in only LIM1215 G12A, G12C and G12D cells, the same mutants that cluster together in both the ERK responses and the presence of the MEK to RAF inhibition. This BRAF form is also present in another cell line (HPNE), and I explored many hypotheses to identify it. Due to its expression being specific to certain KRAS mutations, identifying it could aid in increasing the understanding of KRAS-mediated oncogenesis. Proteomics analysis failed to elucidate any post-translational modifications that could explain the increased molecular weight of the second BRAF form, although it did reveal the presence of a secondary BRAF population with the alternative GEFAAFK C-terminus instead of the putative GAFPVH.

BRAF transcripts can be alternatively spliced to produce BRAF splice variants of various molecular weights (Hirschi and Kolligs, 2013). The inclusion of exons 8b and/or 9b are particularly interesting because they result in the formation of higher molecular weight BRAF proteins (Hmitou *et al.*, 2007), whereas the inclusion of exons 14, 15, 15b, 16b and 16c for example result in the formation of truncated BRAF forms that are of lower molecular weight (Hirschi and Kolligs, 2013). An extensive review of literature and the NCBI database for BRAF mRNA transcripts identified two potential splice variants that could explain the size of the unknown BRAF form seen in my work. Both potential splice variants have an additional 120bp exon 9b present, with one having the GAFPVH C-terminus and another having a variation (GEFAAFK) at the C-terminus. In theory, the variant C-terminus may allow for differential regulation of BRAF between WT and G12D cells via a currently unknown mechanism, resulting in the expression of the second BRAF form only in G12D. However, it is the expression of exon 9b that would account for the increase in the molecular weight of BRAF. It has been shown that the presence of exon 9b can differentially regulate BRAF by increasing its kinase and oncogenic activities (Papin *et al.*, 1998). It has also been shown that exon 9b, along with exon 8b, can interfere with the ability of the N-terminus of BRAF to interact with its C-terminal kinase domain, with exon 9b decreasing this interaction (Hmitou *et al.*, 2007). It is clear that the presence of exon 9b can have a crucial impact on BRAF biology, and therefore, it is important to confirm or rule out whether this exon is present in the second BRAF population seen in my work. Although currently I present preliminary

data that does not show the presence of exon 9b in G12D cells, experiments are ongoing in the lab with the focus on identifying this BRAF population.

My data suggests that the expression of this second BRAF form may be modulated via transcriptional regulation rather than posttranslational modifications. This is based on the observation that short term (2 hours) MEK inhibitor treatment does not induce the expression of the top BRAF band, whereas 46 hours is sufficient. Of course, this does not, however, rule out a role of PTMs. Furthermore, I present data supporting a potential role of myosin-9 in regulating ERK activity in only LIM1215 WT and G12V cells, which do not have this second BRAF form present. Mysoin-9 has been shown to modulate ERK and AKT pathways in colorectal cancer cells, but my work adds a layer of complexity by identifying a KRAS-mutant and BRAF specific role in this (Wang *et al.*, 2019).

I also present data that supports a link between the second BRAF population and CRAF:BRAF dimerisation as the level of dimerisation seen is strongest in the mutants with the highest expression of the second BRAF form. RAF dimerisation plays a key role in ERK pathway activation (Freeman, Ritt and Morrison, 2013). In addition, it is also one of the known causes of RAF inhibitors failing to work clinically (Hatzivassiliou *et al.*, 2010). If the presence of the second BRAF population enables for high levels of RAF dimerisation in a KRAS-mutant specific manner, then it is vital to understand this further in order to be able to develop more effective mutant-specific therapies.

Overall, the data from my work suggests that most likely this KRAS-mutant specific BRAF form is a splice variant and that it increases CRAF:BRAF dimerisation. However, as the data currently stands, it is quite preliminary. Most experiments have only been repeated once due to lack of time, and therefore, the next step would be to repeat them. To confirm a potential role of myosin-9 in the appearance of the second BRAF form, mysosin-9 can be immunoprecipitated in WT and mutant cells with or without ERK/AKT knockdown to see if BRAF:myosin-9 binding is altered in different mutants and whether this is influenced by ERK or AKT. Proteomics analysis can also be repeated but modified for specifically identifying PTMs; there are many modification-specific proteomics strategies that can be employed for the characterisation of PTMs using enrichment techniques (Zhao and Jensen, 2009). One of the PTMs investigated in my work is ubiquitination, and I have not yet been able to confidently rule out ubiquitination as a differential PTM on BRAF. One experiment to do next would be to immunoprecipitate ubiquitin in LIM1215 WT and G12D cells and probe for BRAF. If the second BRAF population is a result on additional ubiquitination, then two BRAF bands should appear in the G12D samples on a Western blot. Lastly, to investigate the splice variant hypothesis further, RNA-sequencing

targeted specifically for detecting splice variants can be utilised (Mertes *et al.*, 2021). All in all, my work has enabled the formation of hypotheses that have partly been tested, but further work is required to elucidate the identity of this second BRAF form.

Impact of KRAS mutations on gene transcriptional regulation

ERK pathway activation can modulate the transcriptional regulation of many target genes, which is also influenced by the kinetics of the signal. For example, the strength and duration of ERK signalling can be interpreted by immediate early gene (IEG) products such as the AP-1 family member c-FOS to direct distinct cell phenotypes such as proliferation (Murphy *et al.*, 2002; Murphy and Blenis, 2006). Many groups have studied RAS-driven differential gene expression in cancer cells. For example, Stephens and colleagues utilised TCGA datasets to study the relationship between RAS mutations and mRNA expression (Stephens *et al.*, 2017). Another group was able to identify key predictive genes that could be used as markers to identify KRAS mutations in lung cancer (Zhang *et al.*, 2020). We hypothesise that not only do different KRAS mutations differentially regulate the gene transcriptional profile of a cancer cell, but that these mutations also distinctly influence gene expression patterns in the very early steps of oncogenesis. This is supported by data published by Loboda and colleagues, who found that there is a potential adaptive response during tumour evolution which is not only dependent on the mutational status of proximal genes in the RAS pathway, but also on the cell type (Loboda *et al.*, 2010).

In this thesis, I present preliminary RNA sequencing data in LIM1215 and HPNE cells. Gene set enrichment analysis revealed the upregulation of genes involved in TNFα signalling via NFκB and the inflammatory response in only LIM1215 G12A, G12C and G12D cells (and not G12V cells) when compared to WT. This provides a hypothesis potentially linking the gene regulation changes in these mutants to the second BRAF form and the MEK to RAF inhibition. Computational methods also provide testable hypotheses for the cause of the upregulation of specific genes. Similarly, RNA sequencing of HPNE cells 2, 7 and 14 days post-induction of mutant KRAS suggests differential expression of gene sets that not only vary between mutants but also over time within the same mutant cell line. In particular, G12R cells appear to harbour unique gene transcriptional changes very early on post-transformation, which is interesting as this mutation is present at a high frequency only in pancreatic cancer (Hobbs *et al.*, 2020).

My work on mutant-specific transcriptional regulation is preliminary and there are some weaknesses

in my data. Firstly, the OmniPath settings used for generating networks needed to be very relaxed in order to include all of my genes of interest. This can potentially allow for more uncertain interactions to be included, and therefore, can result in misleading/incorrect network generation. Secondly, the gene selection process from the HPNE data is not the most well-defined and a more articulated strategy needs to be employed to select real genes of interest to investigate further. However, some strengths include the fact that a good number of sample repeats (five) and read depth (20 million per sample) were used, allowing for good differential expression analysis (Wang, Gerstein and Snyder, 2009; Kukurba and Montgomery, 2015).

Future directions

My work has enabled the formation of logical hypotheses which will now be tested in the Esposito lab. We recognise that characterising the identify and role of the unknown BRAF form is most likely the key to understanding the other phenotypes observed.

To build on my work, two other experiments that could be carried out include (i) investigating ERK signalling in a 3D cell culture system and (ii) correlating oncogenic burden to cell phenotype. I have already invested some effort in preparation for these experiments, however, due to lack of time they did not materialise. The rationale for understanding ERK signalling dynamics in 3D cultured cells is that it is more physiologically relevant, and it has also been shown that ERK signalling dynamics are altered between 2D and 3D cultured cells (Botta *et al.*, 2012). Secondly, understanding how levels of oncogenic signalling correlates with cell fate decisions would build on what is already known, that is that ERK signalling needs to be kept within a critical window for optimal proliferation (Sale, Balmanno and Cook, 2019). An extension of this would be understanding which levels of oncogenic KRAS activity correlate with cell phenotypes such as senescence, proliferation and apoptosis. In this way, we may uncover new ways to target specific KRAS-mutant cancers based on the oncogenic burden of each mutation and the impact of this on cell fate. For example, ways of increasing KRAS activity to induce cell death may be an option for specific KRAS-mutant cancer therapy in the future.

To conclude, my work has uncovered interesting changes in ERK signalling dynamics in different KRAS G12 mutants that may benefit the current understanding of RAS-mediated oncogenesis. This is potentially linked to the expression of a second unknown BRAF form and to changes in gene transcriptional regulation. Finally, to elucidate the mechanisms behind my observations, my work has provided valid, albeit preliminary, hypotheses that will be tested in the Esposito lab.

6. Material and Methods

Cell culture conditions

Passaging

SW48 cells (derived from colorectal adenocarcinoma, Dukes Type C Grade IV; obtained from Horizon Discovery) were cultured in RPMI 1640 medium with GlutaMAX and HEPES-10 supplemented with 10% foetal bovine serum (FBS) (both purchased from Gibco). LIM1215 cells (derived from colorectal carcinoma; obtained from Horizon Discovery) were cultured in RPMI 1640 medium with GlutaMAX and HEPES-10 (Gibco) supplemented with 10% FBS, 1µg/ml insulin (Sigma) and 1µg/ml hydrocortisone (Sigma). hTERT-HPNE E6/E7/st cells (derived from pancreatic ductal epithelial cells; obtained from ATCC) were cultured in low glucose DMEM (1g/L) with pyruvate, no glutamine and no phenol red (Thermo Fisher Scientific), supplemented with 25% M3:Base F medium (INCELL), 10ng/ml human EGF (Sigma), 5% FBS, 2mM glutamine (Gibco), 750ng/ml puromycin (Sigma), and 1% penicillin/streptomycin (Sigma; 10,000 units of penicillin and 10mg of streptomycin per ml in 0.9% NaCl). For RNA sequencing experiment, 150µg/ml hygromycin (InvitroGen) was also added to the media. A list of the cell lines used in this project is provided in ***Table 6.1*** in the **Appendix (Chapter 8)**.

SW48, LIM1215 and HPNE cells were cultured as a monolayer in a humidified atmosphere with 5% CO_2 at 37°C and passaged every 3 to 5 days. At 70-80% confluency, they were washed twice with phosphate buffered saline (PBS), trypsinised (0.05% Trypsin-EDTA, from Gibco), inactivated with pre-warmed media, filtered (with Sysmex/Partec CellTrics 50µm filters; purchased from Wolf Laboratories LTD) and plated into new sterile flasks. All cell lines were authenticated via STR profiling and mycoplasma tested via either an ELISA-based capture method (R&D) or a qPCR method (PhoenixDX) regularly (both at the CRUK-CI).

Seeding

Cells in culture were treated as outlined above up to the filtering step. 10µl of media containing the cells was mixed with 10µl of Trypan blue stain (Invitrogen). This solution was inserted into Countess™ cell counting chamber slides (Invitrogen) and cells were counted using Countess™ Automated Cell Counter (Invitrogen). For all experiments using SW48 cells, 1.5 million cells were seeded per well in a 6-well plate (Eppendorf). Pre-warmed fresh media (with 10% FBS) was added to make up the total

volume per well to 2ml. For all experiments using LIM1215 cells, except for IP experiments, cells were seeded in the same way but only 750,000 cells per well. For IP experiments, 11.3 million cells were seeded in 15cm^2 dishes, and 20ml of pre-warmed media was added. For all experiments using HPNE cells, 300,000 cells were seeded in 6-well plates. The specific seeding protocol for the RNA-seq experiment is described later.

siRNA transfection

All siRNA transfections were carried out using Dharmafect Transfection Reagent 1 from Dharmacon (now Horizon Discovery). MEK1/2, ERK1/2, CRAF, BRAF and non-targeting (NT) siRNAs were also purchased from Dharmacon. The siRNAs were pooled together so that cells were transfected with a combination of four different siRNAs. For MEK and ERK knockdown, this was two siRNAs against MEK-1 and MEK-2 and two against ERK-1 and ERK-2. For RAF knockdown, two against CRAF and two against BRAF were used. Only one NT siRNA was used. The total concentration of siRNA used was the same.
The required amount of pooled siRNA was added to serum-free media (same as the media used to culture the cells but without any FBS) and solutions were pipetted gently to mix. A transfection reagent master mix was made comprising 190µl serum-free media and 10µl Dharmafect transfection reagent per well. These solutions were incubated for 5 mins at room temperature and then the appropriate amount of master mix was added to each siRNA solution and incubated for 20 minutes at room temperature. FBXW7 and myosin-9 siRNA (already pooled) were also purchased from Horizon Discovery. Another set of FBXW7 siRNA (4 individual ones that I pooled together) were purchased from Qiagen.

Media from the wells of each 6-well plate with seeded cells was aspirated using an aspirator pump (BVC Professional Vacuubrand) and the wells were washed with sterile PBS. Pre-warmed media (with 10% FBS) was added to the wells, enough so that once the transfection reagent solution was added the total volume would be 2ml per well. Once the transfection solution had been incubated with the siRNAs for 20 mins, the appropriate volume was added to each well respectively.

siRNA target	Target sequence	Catalogue number	Supplier
MEK1	CCAUGCUGCUGGCGUCUAA	J-003571-06 -0002	Horizon Discovery
MEK1	GAGGUUCUCUGGAUCAAGU	J-003571-07 -0002	Horizon Discovery
MEK2	CGACAGCGCAUGCAGGAAC	J-003573-08 -0002	Horizon Discovery

MEK2	UCUUUGAACUCCUGGACUA	J-003573-11 -0002	Horizon Discovery
ERK1	GGUGUGCUCUGCUUAUGAU	J-003555-13- 0002	Horizon Discovery
ERK1	ACACCAACCUCUCGUACAU	J-003555-14- 0002	Horizon Discovery
ERK2	GACCGGAUGUUAACCUUUA	J-003592-07- 0002	Horizon Discovery
ERK2	CCUGCGACCUUAAGAUUUG	J-003592-08- 0002	Horizon Discovery
BRAF	CAUGAAGACCUCACAGUAA	J-003460-12- 0002	Horizon Discovery
BRAF	UCAGUAAGGUACGGAGUAA	J-003460-13- 0002	Horizon Discovery
CRAF	ACAGAGAGAUUCAAGCUAU	J-003601-13- 0002	Horizon Discovery
CRAF	CAAAGAACAUCAUCCAUAG	J-003601-15- 0002	Horizon Discovery
Non-targeting Pool	UGGUUUACAUGUCGACUAA, UGGUUUACAUGUUGUGUGA, UGGUUUACAUGUUUUCUGA, UGGUUUACAUGUUUUCCUA	D-001810-10-05	Horizon Discovery
Myosin-9 SMARTPool	GUAUCAAUGUGACCGAUUU, CAAAGGAGCCCUGGCGUUA, GGAGGAACGCCGAGCAGUA, CGAAGCGGGUGAAAGCAAA	L-007668-00-0005	Horizon Discovery
FBXW7 SMARTPool	CAACAACGACGCCGAAUUA, GGAGUUGUGUGGCGGAUCA, GUGAGUGGAUCUCUUGAUA, GGGCACCAGUCGUUAACAA	L-004264-00-0005	Horizon Discovery
FBXW7 FlexiTube	CTGGAGGCGAGGAGAACTCAA, CTCATTGATAGTTGTGAACCA, AAACATATGATGCAAGTGATA, CCCTAAAGAGTTGGCACTCTA	1027416	Qiagen
Negative control	AATTCTCCGAACGTGTCACGT	1027417	Qiagen

Table 5.1. **Information regarding the siRNAs used.** All siRNAs used in my work have been listed in this table, including the target sequences, catalogue numbers and suppliers.

Cell starvation

Media was aspirated from the wells and each well was washed once with sterile PBS. This was aspirated and 2ml pre-warmed fresh media supplemented with only 1% FBS (starvation media) was added. Cells were incubated in starvation media for 16 hours overnight.

EGF treatment and cell harvesting

Human EGF stock (E9644) was purchased from Sigma-Aldrich. The required concentration of EGF solution was prepared either in starvation media if cells had been starved overnight, or in regular 10% FBS media if they had not been starved. Cells were removed from incubator, media was aspirated and 2ml of EGF solution was added. Cells were put back into the incubator for required amount of time and then removed and put straight onto ice. EGF solution was aspirated and wells were washed with ice cold PBS and aspirated. 50µl of RIPA buffer (containing 300mM NaCl, 1% NP-40 (IGEPAL), 0.5% sodium deoxycholate, 0.1% SDS (sodium dodecyl sulphate), 50mM Tris-HCL pH 8.0, ultrapure water, protease inhibitors (complete EDTA-free, Roche), 10% phosphatase inhibitor cocktail 2 (P5276, Sigma-Aldrich) and 10% phosphatase inhibitor cocktail 3 (P0044, Sigma-Aldrich)) was added to each well. Cells were scraped using disposable cell scrapers (Fisher Scientific) and collected and dispensed into 1.5ml tubes (Eppendorf) and kept on ice.

MRA protocol

All steps were carried out according to how they have been outlined above (seeding, siRNA transfection, starving and then EGF treatment and harvesting). The following timepoints were followed as an example:

Day 1 at 12pm – seed cells
Day 2 at 12pm – transfect cells with siRNA
Day 3 at 5pm – starve cells
Day 4 at 9am – treat with EGF for 0,5 or 20 minutes then harvest cells

The MATLAB code used for MRA analysis was written by my supervisor Dr Alessandro Esposito. Please contact him at ae275@cam.ac.uk for access.

Insulin treatment and harvesting

Human insulin stock (I9278-5ML) was purchased from Sigma-Aldrich. The protocol followed was the same as with the EGF treatment, except 10µg/ml was added for treatment and no insulin was added to the starvation media.

Inhibitor treatment

The protocol followed was the same as the MRA treatment protocol, with some exceptions. On day 2, instead of siRNA transfection, 2µM U0126 (Sigma Aldrich) was added. On day 3, starvation media contained 2µM U0126. During harvesting, the 'short' treatment cells were treated with 20µM U0126 or 2.5µM Afuresertib (Stratech) for 2 hours prior to EGF treatment. EGF treatment media also contained the respective inhibitor at the concentration already used.

Plasmid transfection

FLAG-tagged BRAF, mTurqoise2 and the empty vector pcDNA3.1 were purchased from Addgene and JetPrime transfection reagent (purchased from VWR International) was used to transfect the plasmids into LIM1215 cells. Briefly, 750,000 LIM1215 cells were seeded in each well of a 6-well plate. The next day, 260µl of JetPrime buffer was added to 3µg of plasmid DNA in a 1.5ml Eppendorf tube, vortexed for 10 seconds and centrifuged briefly. 8µl of JetPrime transfection reagent was added, and samples were vortexed and centrifuged again. Samples were incubated at room temperature for 10 minutes, then added to 2ml of media, all of which was added to the respective well. Media was replaced after 4 hours and cells were harvested with RIPA lysis buffer 48 hours post-transfection.

Western blot techniques

Lysate preparation

Once cells had been collected into tubes as outlined above, they were kept on ice for 1 hour and vortexed every 15 minutes using a vortex mixer (Scientific Laboratories Supplies). Next, the cells were centrifuged (Eppendorf) at 13,200 rotations per minute (rpm) at 4°C for 30 minutes. The supernatant was collected and placed into new 1.5ml tubes and kept on ice.

Quantification of protein concentration

The protein concentration of the lysates was determined with the bicinchoninic acid (BCA) assay using the Pierce™ BCA Protein Assay Kit from Thermo Fisher Scientific. The required volume of BCA dye was made up by mixing 50 parts of Bicinchoninic Acid Solution (Solution A) with 1 part of Copper (II) Sulphate Solution (Solution B). 1µl of lysate was diluted in ultrapure water up to 20µl per well on a 96-well plate. Standards were made up using the 2mg/ml BSA stock that comes with the kit. 180µl of BCA dye was added to each well and the plate was incubated at 37°C for 30 minutes. The plate was allowed to cool down to room temperature and absorbance was measured at 562nm using a plate reader (TECAN). All lysate absorbance values were measured in duplicate wells and the average was taken. Protein concentration was calculated from the absorbance value of the lysates in comparison to those of the protein standard.

Sodium dodecyl sulphate - polyacrylamide gel electrophoresis (SDS-PAGE)

The cell lysates were mixed with 1x NuPage™ LDS sample loading buffer (containing the reducing agent dithiothreitol (80mM, DTT)) and boiled at 70°C for 10 minutes to denature the proteins. The gel apparatus was rinsed with deionised water and assembled with the NuPage™ 4-12% Bis-Tris midi or 3-8% Tris-Acetate (TA) midi gels (Invitrogen). 1x running buffer was prepared with deionised water using either NuPage™ MOPS SDS or TA SDS running buffer (Invitrogen). After removal of the comb from the pre-cast gels, wells were flushed with running buffer and the required amount of sample was loaded. Dual colour (Bio-Rad) was used for the protein ladder. The tanks were filled with running buffer and the gels were run at 125V, 400mA, 100W for 1hr 35mins.

Protein transfer and staining

Proteins were transferred onto 0.45µm nitrocellulose membranes (GE Healthcare Life Sciences) by wet transfer at 20V, 40mA at 4°C for 16 hours overnight. Transfer buffer consisted of 20% methanol, 1x NuPage™ transfer buffer (Invitrogen) and deionised water. Once transfer was complete, the membranes were stained with Ponceau S stain (Sigma Life Sciences) to confirm protein transfer. For some experiments, REVERT™ Total Protein Stain was used for normalisation of protein loading instead of probing for housekeeping proteins. The protocol was followed as outlined in the Li-Cor manual for this stain.

Antibody probing and imaging

Membranes were blocked in blocking buffer for 1 hour at room temperature prior to incubation with primary antibody solution. 5% milk, 1% milk or 5% BSA (bovine serum albumin) in Tris-buffered saline with 0.1% Tween-20 (TBST) was used. In later experiments, blocking buffer was filtered using a funnel and tissue. All primary antibodies used in my project are listed in ***Table 5.2***. Membranes were incubated with primary antibody at 4°C overnight for 16 hours. Then, membranes were washed with wash buffer (1x TBST) four times for 5 minutes each time.

Secondary antibody (IRDye-680 or IRDye-800, Li-Cor) was diluted 1:5000 in Li-Cor Odyssey blocking buffer (TBS). This product was replaced with the Li-Cor Intercept blocking buffer in 2019. Membranes were incubated with secondary antibody in the dark for 1 hour at room temperature and then washed four times for 5 minutes. Membranes were then imaged using the Li-Cor Odyssey CLx scanner. Membranes were scanned using the lowest quality setting (recommended by Li-Cor), auto intensity and resolution of 169µm. Quantification of protein levels was achieved by following the Li-Cor manual on band quantification (Image Studio was used for this).

Antibody	Species	Concentration	Dilution buffer (TBST)	Supplier	Catalogue number
pERK (Thr202/Tyr204)	Mouse	1:1000	5% milk	CST	#9106S
totERK	Rabbit	1:1000	5% milk	CST	#4695S
pMEK (Ser217/221)	Rabbit	1:1000	5% milk	CST	#9154S
totMEK	Mouse	1:1000	5% milk	CST	#4694S
pCRAF (Ser338)	Rabbit	1:1000	5% BSA	CST	#9427S
totCRAF	Mouse	1:1000	5% BSA	CST	#12552S
totCRAF*	Mouse	-	-	Santa Cruz	#sc-7267
pBRAF (Thr401)	Rabbit	1:800	1% milk	Abcam	#ab68215
pBRAF (Ser445)	Rabbit	1:800	1% milk	CST	#2696S
totBRAF	Rabbit	1:800	1% milk	CST	#9433S
totbRAF*	Mouse	-	-	Santa Cruz	#sc-5284
pAKT (Ser473)	Rabbit	1:1000	5% BSA	CST	#4060S
totAKT	Mouse	1:1000	5% BSA	CST	#2920S

pGSK3B (Ser9)	Rabbit	1:1000	5% BSA	CST	#9336
totGSK3B	Mouse	1:1000	5% BSA	CST	#9832
pMyosin-9 (Ser1943)	Mouse	1:1000	5% BSA	Thermo Fisher Scientific	#MA5-27764
totMyosin-9	Rabbit	1:1000	5% BSA	Abcam	#ab238131
HSP90	Rabbit	1:1000	5% BSA	Thermo Fisher Scientific	#4877
Actin	Mouse	1:20,000	5% milk	Merck	#A5441
FK2 ubiquitin	Mouse	1:1000	5% BSA	Enzo Life Sciences	#PW8810
FLAG-M2	Mouse	1:1000	5% milk	Merck	#F1804
FBXW7	Rabbit	1:1000	5% BSA	Abcam	#ab109617
mCherry	Rabbit	1:1000	5% BSA	Takara Bio	#632496
Anti-myc tag	Mouse	1:1000	5% BSA	Merck	#05-726

* only used for immunoprecipitation

Table 5.2. **Information regarding the antibodies used.** All antibodies used in my work have been listed in this table, including the target phosphorylation sites, species of origin, dilution ratios, dilution buffers, suppliers and catalogue numbers. The pERK and pMEK phosphorylations correspond to ERK1 and MEK1 sites.

Antibody array

LIM1215 cells were treated in the same way as described for the MRA samples. Samples were collected and stored at -80°C until required. Human Phosphorylation Multi-Pathway Profiling Array C55 was purchased from RayBiotech (8 sample kit). All reagents were supplied with the kit. The kit protocol was followed, with the exception of RIPA lysis buffer (same as with MRA experiments) being used for cell lysis instead of the supplied lysis buffer. All incubations were done with gentle shaking. Briefly, antibody array membranes were incubated in blocking buffer for 30 minutes at room temperature. Membranes were then incubated with sample overnight at 4°C. Next morning, samples were aspirated, and membranes were washed 5 times for 5 minutes at room temperature, incubated with a detection antibody cocktail overnight at 4°C and this was aspirated the next morning. Membranes were washed in the same way again, incubated with diluted HRP-anti-rabbit IgG for 2 hours at room temperature and then washed again. They were transferred print-side up onto a tissue paper first to remove excess wash buffer and then placed quickly onto a plastic sheet. Detection buffer

was then pipetted onto the membranes gently and incubated for 2 minutes at room temperature (without shaking). Immediately after, another plastic sheet was placed on top. Membranes were imaged using the Bio-Rad ChemiDoc Imaging system and images were taken with multiple exposure times. The antibody array signals were quantified using ImageJ with an array plug-in. Positive control spots were used for normalising all membranes to a reference membrane and negative control spots were used for background subtraction.

Lambda phosphatase treatment

LIM1215 cells (750,000) were seeded into each well of a 6-well plate and harvested after 48 hours by lysing cells with RIPA buffer without the phosphatase inhibitors. Regular RIPA was used for control samples. Lysates were processed in the same way as described above. For lambda phosphatase treatment, volume of lysate for 100µg of protein was used, and 5µl of 10x NEBuffer for Protein MetalloPhosphatases (PMP), 5µl of 10mM $MnCl_2$, 1µl of lambda protein phosphatase and ultrapure water was added to get a final volume of 50µl. This was heated at 30°C for 90 minutes. Control samples were diluted with normal RIPA buffer and prepared as usual to load on an SDS-PAGE gel.

Immunoprecipitation

Same protocol as for MRA was followed, but with cell number and media/reagent volumes scaled up. 11.3 million LIM1215 cells were seeded in 15cm^2 dishes. All volumes were multiplied by 10 (media, siRNA, transfection reagent). Cells were lysed with 700µl immunoprecipitation (IP) lysis buffer (containing 137mN NaCl, 1% NP-40 (IGEPAL), 20mM Tris-HCL pH 8.0, 10% glycerol, 2mM Ethylenediaminetetraacetic acid (EDTA), ultrapure water, protease inhibitors (complete EDTA-free, Roche), 10% phosphatase inhibitor cocktail 2 (P5276, Sigma-Aldrich) and 10% phosphatase inhibitor cocktail 3 (P0044, Sigma-Aldrich). Lysates were processed in same way as MRA samples. The Dynabeads Protein G Immunoprecipitation Kit (purchased from Thermo Fisher Scientific) was used for BRAF or CRAF IP. Manufacturer's protocol was followed, and all incubations were done with rotation. Briefly, 50µg of protein was removed for the input. Between 600-3000µg of protein was used for IP. 50µl of magnetic beads were mixed with 5µg of antibody (BRAF sc-5284 and CRAF sc-7267, both purchased from Santa Cruz) and 200µl of binding and washing buffer and tubes were incubated for 1 hour at 4°C. 15µl of beads were added to lysate and also incubated for 1 hour at 4℃. Blocked lysate and beads-antibody complex were incubated together overnight at 4℃. Next morning, supernatant was removed, and beads-antibody-antigen complex was washed 3 times with 200µl wash buffer. The

antibody-antigen complex was eluted with 20µl elution buffer. 6.5µl of 4x sample loading buffer (with 80mM DTT) was added, sample was heated for 10 minutes at 70℃, beads were removed with magnet and sample was loaded onto SDS-PAGE gel.

Mass spectrometry

The SDS-PAGE protocol followed was the same as described earlier, with the exception that the gel was run for 2 hours and 15 mins. The gel was then incubated with Instant Blue (Expedeon) on a shaker (Stuart Microtitre plate shaker) at 200 rpm for 1 hour at room temperature. Then it was incubated at 4°C for 16 hours without shaking. Area of interest was cut with sterile scalpel, placed in Eppendorf tubes with 50µl ultrapure water and kept in 4°C prior to sending for mass spectrometry analysis to the Cambridge Centre for Proteomics. Samples were trypsin-digested. Charge state deconvolution and deisotoping were not performed. All MS/MS samples were analysed using Mascot (Matrix Science, London, UK; version 2.6.2). Mascot was set up to search the cRAP_20190401.fasta; CCP_UniProt_homo_sapiens_proteome_20180409.fasta; P523_Ber_20190619 database (unknown version, 93733 entries) assuming the digestion enzyme trypsin. Mascot was searched with a fragment ion mass tolerance of 0.100 Da and a parent ion tolerance of 20 PPM. Scaffold (version Scaffold_4.9.0, Proteome Software Inc., Portland, OR) was used to validate MS/MS based peptide and protein identifications. Peptide identifications were accepted if they could be established at greater than 95.0% probability by the Peptide Prophet algorithm (Keller, A et al Anal. Chem. 2002;74(20):5383-92) with Scaffold delta-mass correction. Protein identifications were accepted if they could be established at greater than 95.0% probability and contained at least 2 identified peptides. Protein probabilities were assigned by the Protein Prophet algorithm (Nesvizhskii, Al et al Anal. Chem. 2003;75(17):4646-58). Proteins that contained similar peptides and could not be differentiated based on MS/MS analysis alone were grouped to satisfy the principles of parsimony. Proteins sharing significant peptide evidence were grouped into clusters.

RNA extraction from LIM1215 cells

LIM1215 cell pellets (3 million cells) were collected, washed in PBS once, and stored at -80°C until RNA extraction. The RNeasy Plus Mini Kit (from Qiagen) was used and the manufacturer's protocol was followed. All centrifugation steps were done at 10,000 rpm. Briefly, cell pellets were vortexed for 30 seconds and transferred to a gDNA Eliminator spin column placed in a collection tube. Tubes were centrifuged for 30 seconds. 1 volume of 70% ethanol was added to the flow-through and mixed by

pipetting. Sample was transferred to an RNase spin column placed in a collection tube and centrifuged for 15 seconds. Flow-through was discarded, 700µl of Buffer RW1 was added to the column and centrifuged for 15 seconds. Flow-through was discarded, and 500µl of Buffer RPE was added to the column and centrifuged for 15 seconds. This step was repeated but with 2 minutes centrifugation. After removing flow-through, columns were centrifuged again for 1 minute to discard excess buffer. Column was placed in a new 1.5ml Eppendorf collection tube. 50µl ultrapure water was added to the centre of the column membrane and left to sit for 1 minute. Tubes were centrifuged for 1 minute, and this step was repeated with the RNA eluate. RNA concentration was determined with nanodrop measurements (using NanoDrop ONE from Thermo Fisher Scientific).

cDNA synthesis

The FastGene Scriptase II cDNA Synthesis Kit (purchased from Geneflow Ltd) was used to synthesise cDNA from the extracted RNA. The manufacturer's protocol was followed. Briefly, 2.5µg RNA was mixed with 1µl oligo dT primer, 1µl of random hexamer and 2µl of dNTP. Sterile ultrapure water was added to make up a total volume of 12.5µl. Samples were heated at 65℃ for 5 minutes in a heat block, then quickly chilled on ice. 4µl of 5x scriptase II buffer, 2µl of 0.1M DTT and 0.5µl of RNase inhibitor was added to each sample and heated at 25℃ for 2 minutes, then chilled on ice. Next, 1µl of FastGene scriptase II was added to each sample and heated at 42℃ for 50 minutes, then 70℃ for 15 minutes. cDNA was stored at -80℃ until further requirement.

PCR reactions

The AccuPrime Pfx DNA polymerase kit (purchased from Invitrogen) was used to amplify BRAF transcripts. Per reaction, 1µl of DNA polymerase, 5µl of 10x buffer, 1.5µl of forward primer and 1.5µl of reverse primer, 5µl of cDNA and 36µl of ultrapure water was combined in a 0.2ml PCR tube. The Peltier Thermal Cycler was used for PCR reactions. The reaction settings are shown in ***Table 5.3*** and primers are listed in ***Table 5.4***.

Step	Temp	Time	
1	94°C	2 min	
2	94°C	15s	Repeat 30x
3	58°C	30s	
4	68°C	2m15s or 55s	
5	68°C	10 min	
6	16°C	Infinite	

Table 5.3. **PCR reaction settings.** The PCR steps (with temperature and time settings) used in my work is described in this table. Elongation time at 68°C (step 4) was adjusted depending on size of transcript to be amplified.

Primer name	Sequence (5'-3')	Corresponding BRAF bases
Exon_2_FWD	GACAAATTTGGTGGGGAGCA	422-441
Exon_6_FWD	TCACCAGCGTTGTAGTACAGA	1030-1050
Exon_13_RVS	GTTGTGGCTTTGTGGAATAGC	1779-1799
Exon_18_RVS	CAGGAAACGCACCATATCCC	2500-2519

Table 5.4**. Primer sequences.** The list of primers used for amplification of BRAF transcripts, along with their sequences and corresponding BRAF bases is shown in this table.

The PCR product was cleaned up using the QIAquick PCR Purification Kit (from Qiagen). The manufacturer's protocol was followed. All centrifugation steps were carried out at 13,000 rpm in a conventional table-top centrifuge at room temperature. In brief, 5 volumes of Buffer PB was added to 1 volume of PCR reaction mixture. Sample was applied to the QIAquick column and centrifuged for 60 seconds. Flow was discarded, 750µl of Buffer PE was added to the column and centrifuged for 60 seconds. After removing flow-through, columns were spun again to remove excess buffer. Column was transferred to a clean 1.5ml Eppendorf tube and 50µl of ultrapure water was added to the membrane. This was allowed to sit for 1 minute and then centrifuged for 1 minute. This step was repeated with the flow-through.

Restriction enzyme digest

PvuII-HF restriction enzyme was purchased from New England Biolabs. 5µl of PCR product was mixed with 2µl of 10x CutSmart buffer, 1µl of PvuII-HF and 42µl of ultrapure water. The mixture was heated

at 37℃ for 15 minutes. 1x DNA gel loading dye (Thermo Fisher Scientific) was added to each sample prior to loading onto gel.

Agarose gel electrophoresis

3g of agarose (Geneflow) was added to 200ml of 1xTBE buffer and microwaved until fully dissolved to make a 1.5% agarose solution. Solution was allowed to cool down slightly for 5 minutes and then poured into a gel tray with the well comb in place. 1x SYBR safe DNA gel stain (Invitrogen) was added to the solution in the tray with a pipette and mixed around quickly. The gel was allowed to set for 30 minutes until it was completely solidified. Gel was placed into the electrophoresis unit (purchased from Nippon Genetics) and 1xTBE buffer was added until it covered the gel. Hyperladder 1kb (Meridian Bioscience) was added to the first and last wells and 1x DNA gel loading dye was added to each sample prior to loading onto gel. The gel was run at 50V until dye line was approximately 75% of the way down (~3 hours). The gel was imaged using the Bio-Rad GelDoc XR+ Imager.

Gel extraction

Gel was placed on a blue light transilluminator (Safe Imager 2.0, Invitrogen) to visualise bands which were cut out and placed into clean 1.5ml Eppendorf tubes using a sterile scalpel. The QIAquick Gel Extraction Kit (from Qiagen) was used to purify the DNA from the gel. All centrifugation steps were carried out at 13,000 rpm. Briefly, the gel slice was weighed, and 3 volumes of Buffer QG was added to 1 volume of gel. This was incubated at 50℃ for 10 minutes and vortexed every few minutes (until gel slice was completely dissolved). 1 gel volume of isopropanol was added to the sample and mixed by pipetting. The sample was then added to a QIAquick spin column placed in a 2ml collection tube and centrifuged for 1 minute. The flow-through was discarded, 500µl of Buffer QG was added to the column and the tube was centrifuged for 1 minute. Flow-through was discarded, 750µl of Buffer PE was added, tube was allowed to sit for 5 minutes and then centrifuged for 1 minute. Flow-through was discarded and the tube was centrifuged again to remove excess buffer, and 50µl ultrapure water was used to elute the DNA as described previously. If required, DNA samples were sent off for sequencing to Source Bioscience (Cambridge).

RNA sequencing procedures

LIM1215 cells

Two vials of cells of different passages were thawed and passaged for 2 weeks before sample preparation and 5 samples across three batches were used for RNA sequencing. Briefly, 750,000 cells were seeded into 6cm^2 dishes and three days later (~70% confluency), dishes were placed on ice, cells were washed with ice cold 1x PBS and collected by scraping with 1ml PBS and transferring into 1.5ml Eppendorf tubes. Samples were centrifuged at 1000 rpm for 3 minutes at 4°C, PBS was removed and cell pellets were kept at -80℃ until shipment. Isolation of total RNA, library preparation and sequencing (20 million reads per sample) was performed by BGI.

HPNE cells

One vial of each cell line was thawed two weeks before sample preparation and 5 samples across 5 batches were used for RNA sequencing. Cells were maintained in HPNE media either with or without doxycycline prior to seeding into 6cm^2 dishes 7 days before harvesting. On the day of harvesting, the dishes were placed on ice in the fume hood and cells were first washed with ice cold 1x PBS. 400µl of Trizol was added to each dish, and the cells were scraped and transferred into 1.5ml Eppendorf tubes. Tubes were kept at -80°*C until RNA extraction.*

*To extract the RNA, samples were thawed and 80*µl of chloroform was added to the tubes. The tubes were vigorously shaken, then allowed to sit for 3 minutes at room temperature. Tubes were centrifuged at 10,000 *x g* for 18 minutes at 4°C. The top aqueous phase containing the RNA was carefully removed with a pipette and transferred to a new sterile RNase-free tube. An equal volume of 100% RNA-free ethanol was slowly added, and the sample was loaded into an RNeasy column placed within a collection tube (from the Qiagen RNeasy Plus Mini Kit) and centrifuged for 30 seconds at 8,000 *x g* at room temperature. The flow-through was discarded, 700µl of buffer RW1 was added and tubes were centrifuged for 30 seconds at 8,000 *x g*. 70µl of RDD was added to 10µl of DNase and this was pipetted onto the membrane. After allowing it to sit for 15 minutes, 700µl of buffer RW1 was added and tubes were centrifuged for 30 seconds at 8,000 *x g*. Columns were transferred to new tubes, 500µl of buffer RPE was added and tubes were centrifuged (30 seconds, 8,000 *x g*). This step was repeated but with centrifugation for 2 minutes, and then tubes were centrifuged once more to remove excess buffer. Columns were transferred to new 1.5ml Eppendorf tubes and 50µl of

RNase-free water was added to the membrane. Samples were allowed to sit for 2 minutes at room temperature and then centrifuged (1 minute, 8,000 *x g*) to elute the RNA. This step was repeated with the eluate. Samples were stored at -80°C until shipment. Library preparation and sequencing (20 million reads per sample) was performed by BGI.

Data analysis

Differential expression data was generated by Dr Shamith Samarajiwa. Gene set enrichment analysis was performed using the DeSeq2 files with GSEA pre-ranked tool for the LIM1215 dataset and the standard tool for the HPNE dataset. In both cases, the following settings were used: 1000 permutations, no collapse of database and 'gene set' for permutation type. Genes were tested for enrichment in the Hallmarks gene set of the Molecular Signature Database v7.4 (MSigDB). Only gene sets with a nominal p-value of less than 0.05 and an FDR of less than 0.25 were considered.

OmniPath settings

Commands were run on Visual Studio Code, which was installed with the Ionide extension. Scripts have been written by Dr Ben Hall and can be found at https://github.com/hallba/Z3Tutorials. The commands I used to generate networks specified that:

- All OmniPath databases are searched
- Ambiguous interactions are included
- Reverse interactions between a pair of proteins are included
- Interactions between intermediary proteins are also included
- KRAS is specified as a 'hub' gene, so all interactions involving KRAS are displayed

7. Supplementary figures

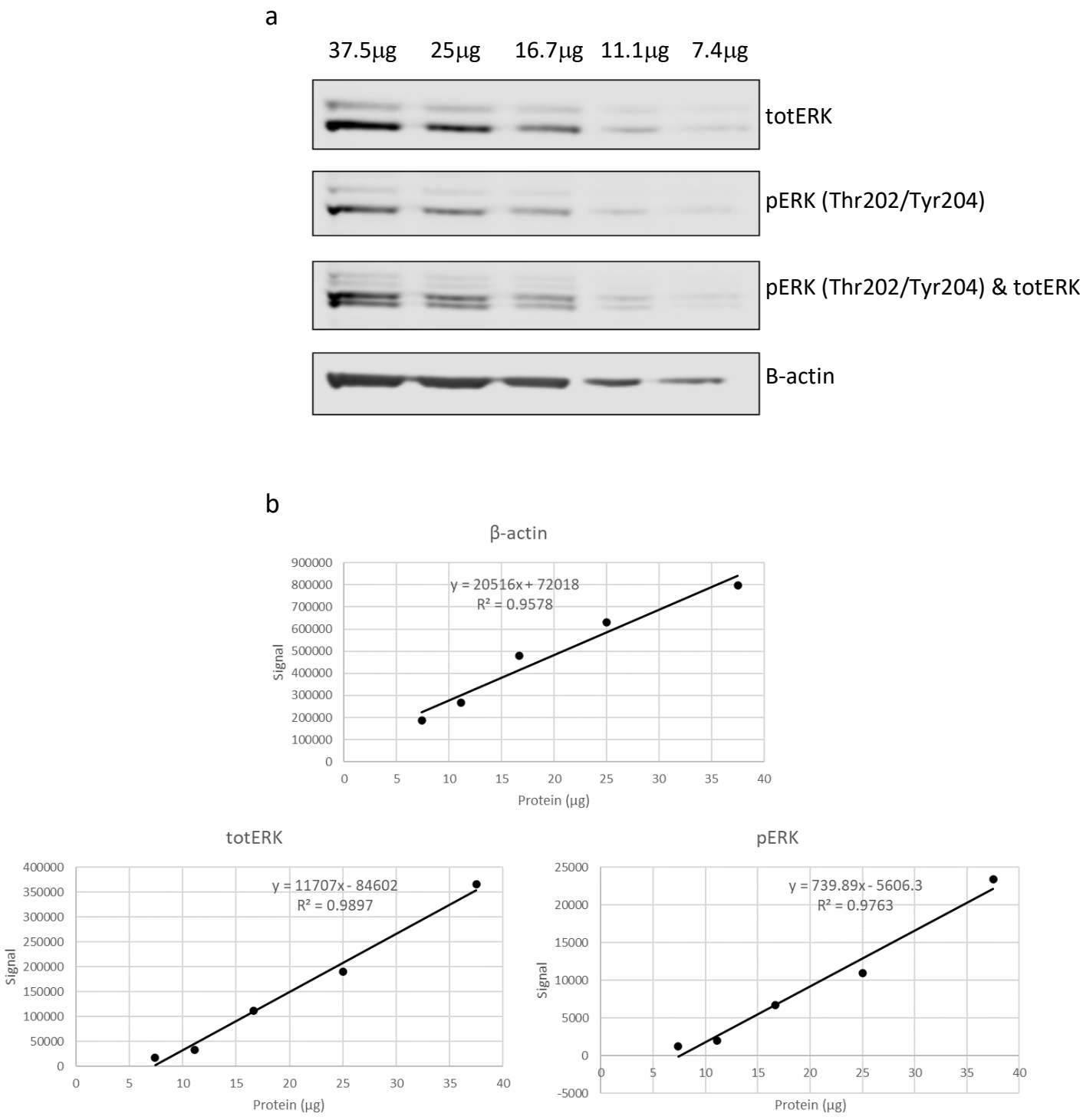

Supplementary figure 2.1. **Testing linear range of loading for ERK. a.** Western blots showing pERK, totERK and β-actin levels detected when a range of protein sample was loaded. Please not the pERK phosphorylations correspond to ERK1 sites. **b.** Graphs showing the quantifications of pERK, totERK and β-actin levels and confirming linear range of loading.

a

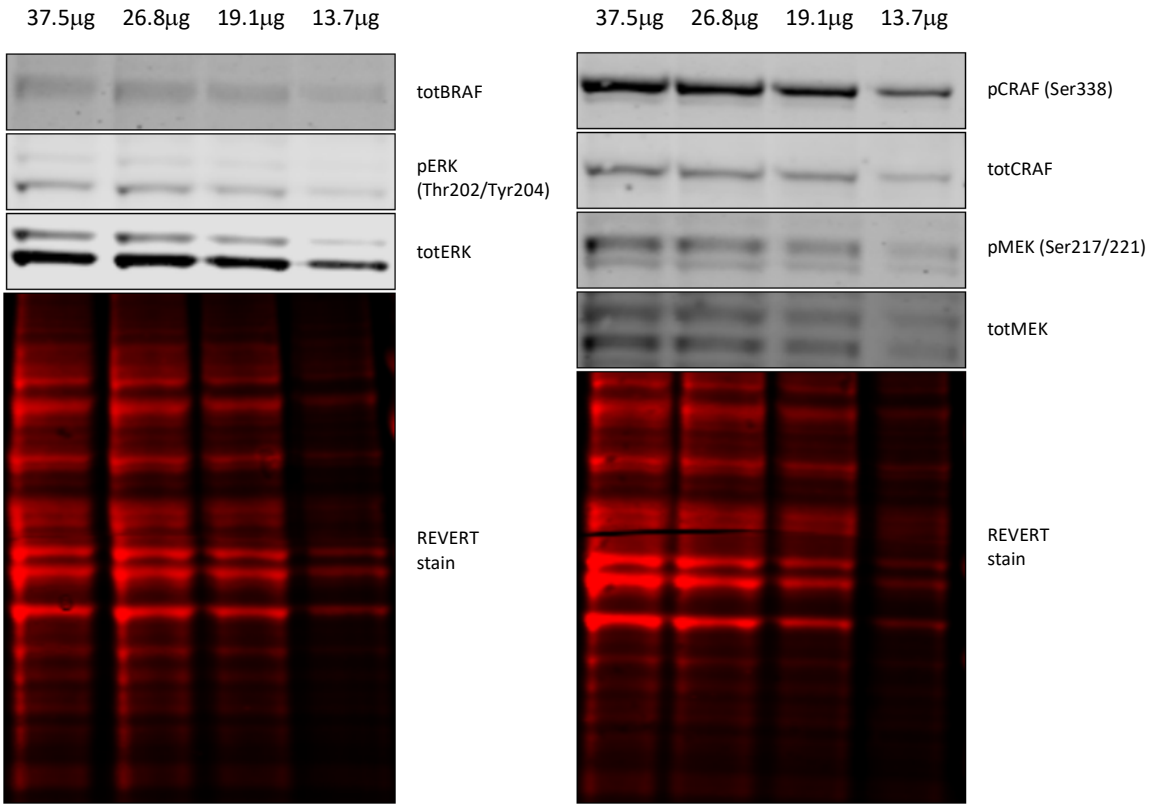

(figure continued on next page)

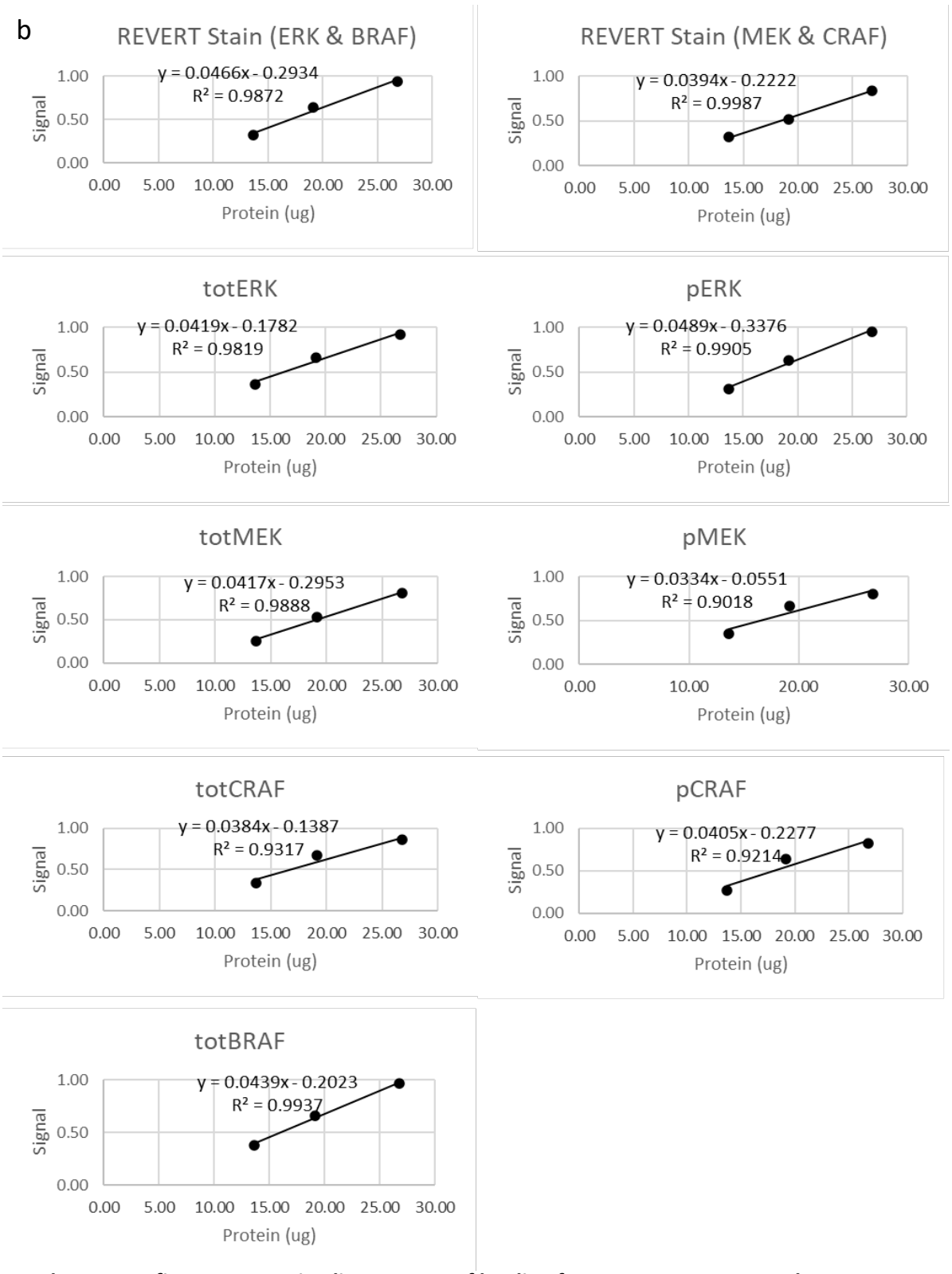

Supplementary figure 2.2. **Testing linear range of loading for BRAF, CRAF, MEK and ERK. a.** Western blots showing pERK, totERK, pMEK, totMEK, pCRAF, totCRAF, totBRAF and REVERT stain detection upon loading a range of protein sample. There was missing pBRAF data due to technical issues. Please not the pERK and pMEK phosphorylations correspond to the ERK1 and MEK1 sites. **b.** Graphs showing the quantifications of the respective protein levels and the REVERT stain and confirming linear range of loading.

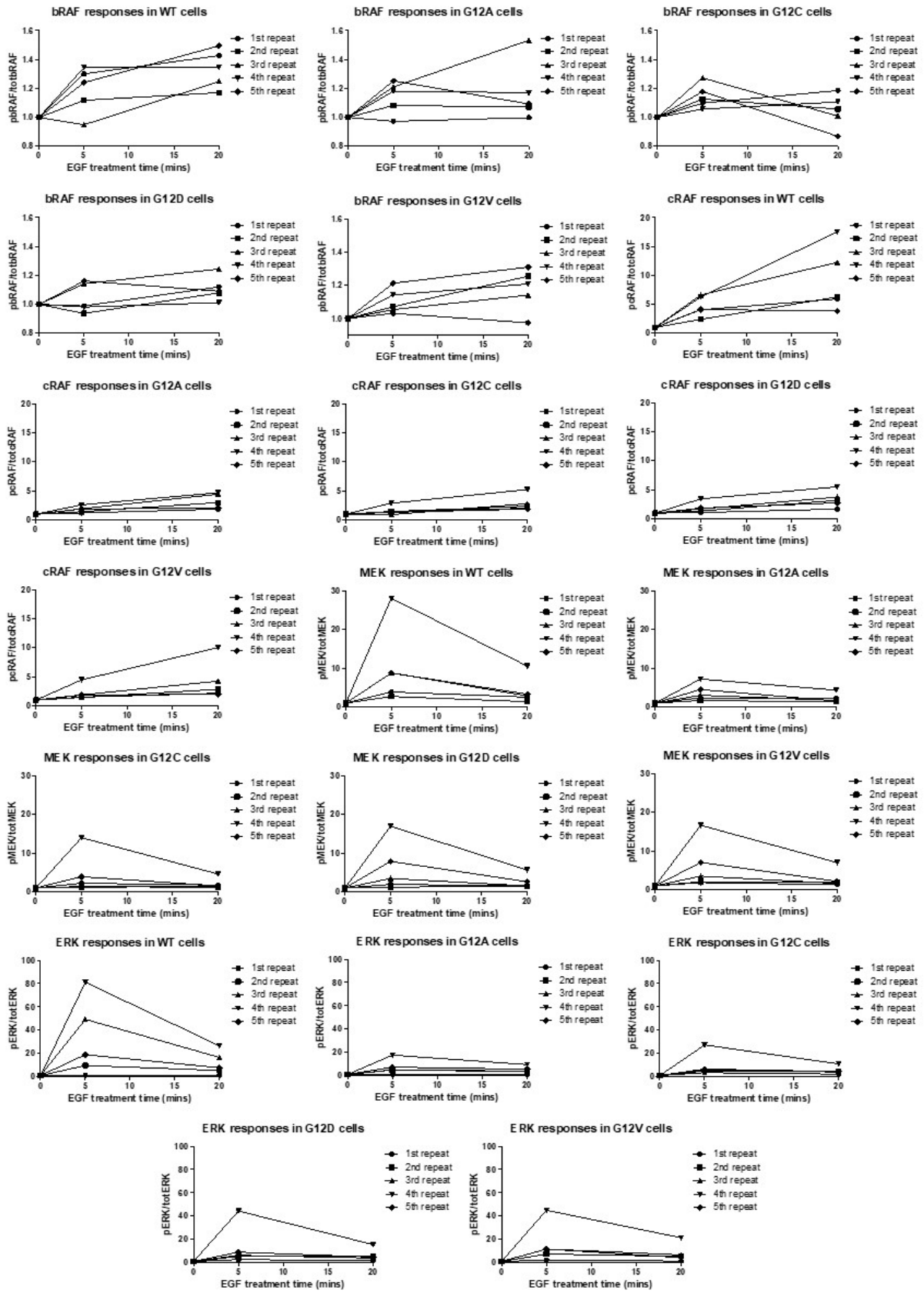

Supplementary figure 2.3. **MRA responses in LIM1215 cells.** Graphs showing the five individual BRAF, CRAF, MEK and ERK responses to 0, 5 and 20 minutes EGF stimulation (100ng/ml) in LIM1215 WT, G12A, G12C, G12D and G12V cells. Responses determined by calculating phosphorylated/total protein levels and normalising the 5 and 20 minute EGF samples to the 0 minute EGF samples.

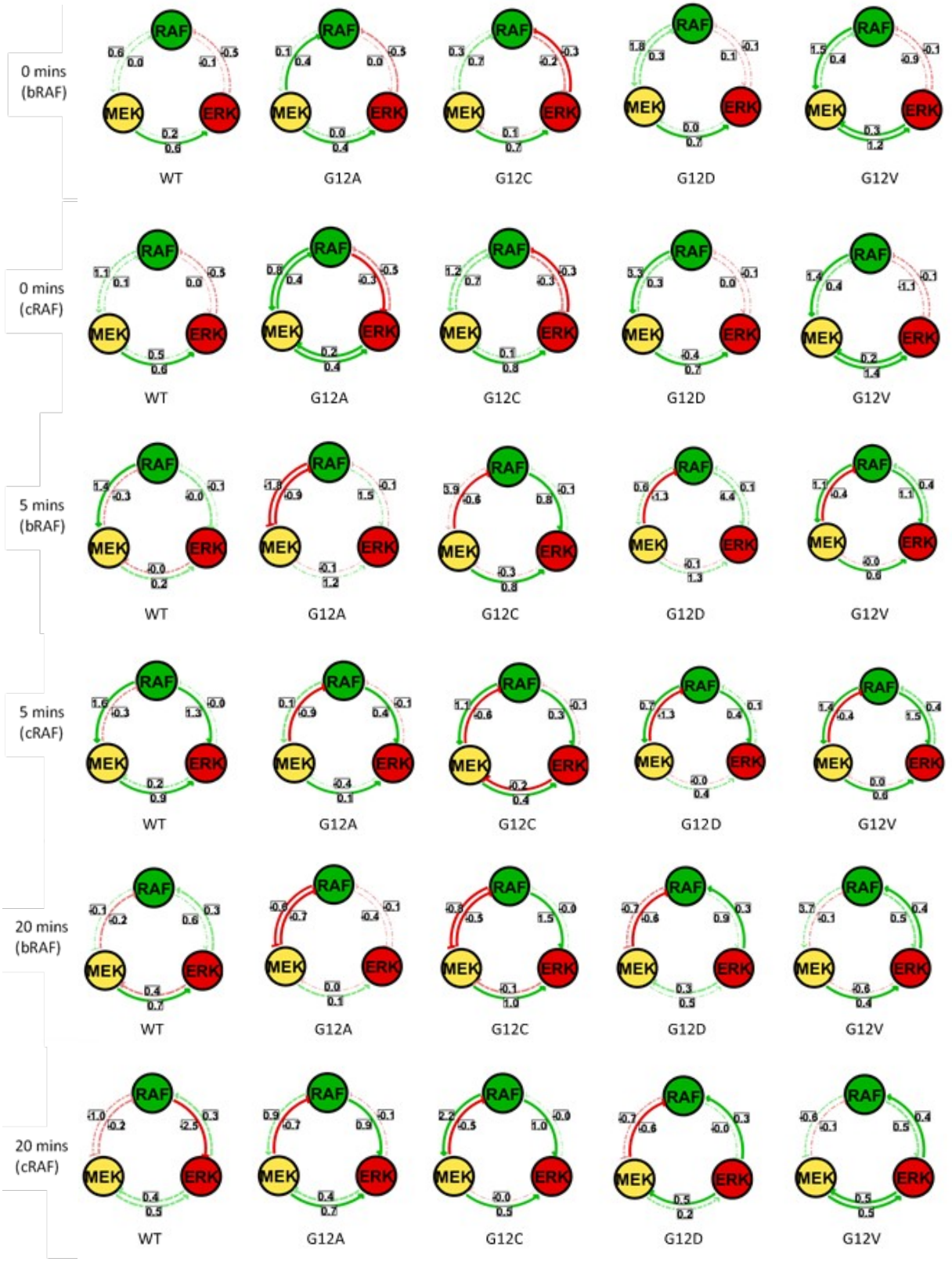

Supplementary figure 2.4. **Topological maps from MRA in LIM1215 cells.** Complete set of maps shown from MRA in LIM1215 cells generated by a MATLAB code. The maps have been separated by BRAF and CRAF (n=5). the arrows connecting the nodes (RAF, MEK and ERK) determine type of interaction: red means inhibitory and green means activatory. These interactions may be either direct or indirect. Thick lines represent statistically significant interactions ($p \leq 0.05$), dashed lines represent statistically insignificant interactions ($p > 0.05$). Statistical analysis done via bootstrapping.

BRAF		Standard error of mean														
		WT			G12A			G12C			G12D			G12V		
0'		Antibody probing														
		bRAF	MEK	ERK	bRAF	MEK	ERK	bRAF	MEK	ERK	bRAF	MEK	ERK	bRAF	MEK	ERK
Tranfection conditions	NT	2.05628	0.207034	0.004507	3.145035	0.222028	0.006752	1.329947	0.273585	0.000991	1.870707	0.150236	0.000688	0.912869	0.137693	0.000656
	RAF	16.8947	0.080397	0.006557	12.73884	0.099942	0.006562	2.004927	0.101602	0.000514	2.48317	0.061526	0.000385	1.052686	0.195483	0.000405
	MEK	1.255108	0.150655	0.013534	1.775294	0.250662	0.009481	1.336353	0.289852	0.000968	1.322347	0.291654	0.000387	0.687038	0.301669	0.000749
	ERK	1.628624	0.301916	0.017761	5.220682	0.427247	0.018421	2.120178	0.439082	0.002261	1.918116	0.310754	0.001658	0.676708	0.435193	0.00356
5'		Antibody probing														
		bRAF	MEK	ERK	bRAF	MEK	ERK	bRAF	MEK	ERK	bRAF	MEK	ERK	bRAF	MEK	ERK
Tranfection conditions	NT	1.866321	1.051427	0.020903	3.954119	0.382742	0.003761	1.847796	0.72975	0.012053	2.175061	0.378227	0.006164	0.967155	0.724482	0.010966
	RAF	5.485655	0.66754	0.008747	20.34837	0.209495	0.005582	3.330375	0.360578	0.009486	3.317035	0.165377	0.006084	1.05575	0.549037	0.011832
	MEK	2.541611	1.352498	0.012017	2.064748	0.838393	0.007216	1.450036	0.991465	0.00664	1.815384	0.722758	0.006006	0.784963	1.494634	0.013854
	ERK	2.503138	1.080706	0.027726	4.272324	0.443455	0.020346	1.803404	0.573382	0.020449	2.205426	0.325979	0.014508	0.858845	0.697808	0.027485
20'		Antibody probing														
		bRAF	MEK	ERK	bRAF	MEK	ERK	bRAF	MEK	ERK	bRAF	MEK	ERK	bRAF	MEK	ERK
Tranfection conditions	NT	2.490707	0.357966	0.00427	5.450548	0.26704	0.004813	1.419238	0.369685	0.005544	2.373526	0.201535	0.003418	0.905804	0.283352	0.0054
	RAF	3.734091	0.401467	0.015527	20.21179	0.15296	0.006585	1.503738	0.240628	0.006172	3.345296	0.21532	0.006225	0.778822	0.360181	0.006765
	MEK	1.836007	0.968534	0.010524	2.901474	0.769885	0.007893	1.292622	1.124129	0.005408	1.870537	0.587041	0.00319	0.867204	1.265074	0.005293
	ERK	2.012887	0.696844	0.011502	3.827239	0.283159	0.031749	2.651423	0.301617	0.014883	2.376391	0.160735	0.00857	0.636003	0.443137	0.012801

(figure legend on next page)

CRAF		Standard error of mean														
		WT			G12A			G12C			G12D			G12V		
0'		Antibody probing														
		cRAF	MEK	ERK	cRAF	MEK	ERK	bRAF	MEK	ERK	cRAF	MEK	ERK	cRAF	MEK	ERK
Tranfection conditions	NT	0.192881	0.207034	0.004507	0.19217	0.222028	0.006752	0.217021	0.273585	0.000991	0.12054	0.150236	0.000688	0.07133	0.137693	0.000656
	RAF	0.569965	0.080397	0.006557	0.266983	0.099942	0.006562	0.299666	0.101602	0.000514	0.413655	0.061526	0.000385	0.064379	0.195483	0.000405
	MEK	0.202902	0.150655	0.013534	0.213423	0.250662	0.009481	0.213412	0.289852	0.000968	0.20292	0.291654	0.000387	0.051488	0.301669	0.000749
	ERK	0.2184	0.301916	0.017761	0.193743	0.427247	0.018421	0.162891	0.439082	0.002261	0.168753	0.310754	0.001658	0.060083	0.435193	0.00356
5'		Antibody probing														
		cRAF	MEK	ERK	cRAF	MEK	ERK	bRAF	MEK	ERK	cRAF	MEK	ERK	cRAF	MEK	ERK
Tranfection conditions	NT	0.789266	1.051427	0.020903	0.378709	0.382742	0.003761	0.272027	0.72975	0.012053	0.224874	0.378227	0.006164	0.143169	0.724482	0.010966
	RAF	0.564291	0.66754	0.008747	0.458672	0.209495	0.005582	0.349568	0.360578	0.009486	0.485443	0.165377	0.006084	0.139544	0.549037	0.011832
	MEK	0.660172	1.352498	0.012017	0.524517	0.838393	0.007216	0.276723	0.991465	0.00664	0.40154	0.722758	0.006006	0.114973	1.494634	0.013854
	ERK	0.560156	1.080706	0.027726	0.334993	0.443455	0.020346	0.201731	0.573382	0.020449	0.239521	0.325979	0.014508	0.12784	0.697808	0.027485
20'		Antibody probing														
		cRAF	MEK	ERK	cRAF	MEK	ERK	bRAF	MEK	ERK	cRAF	MEK	ERK	cRAF	MEK	ERK
Tranfection conditions	NT	1.243014	0.357966	0.00427	0.351712	0.26704	0.004813	0.337729	0.369685	0.005544	0.295968	0.201535	0.003418	0.391144	0.283352	0.0054
	RAF	1.773714	0.401467	0.015527	0.59165	0.15296	0.006585	0.290384	0.240628	0.006172	0.644541	0.21532	0.006225	0.448385	0.360181	0.006765
	MEK	0.808415	0.968534	0.010524	0.51029	0.769885	0.007893	0.440956	1.124129	0.005408	0.376912	0.587041	0.00319	0.15115	1.265074	0.005293
	ERK	0.58151	0.696844	0.011502	0.444875	0.283159	0.031749	0.235988	0.301617	0.014883	0.34153	0.160735	0.00857	0.166412	0.443137	0.012801

Supplementary figure 2.5. **Large variation in BRAF quantification data in LIM1215 MRA experiments.** Table showing the large SEM values for BRAF compared to CRAF. This is likely due to the total BRAF antibody used which was not very good. The fainter BRAF bands with high background noise in the Western blots are likely to be quantified less accurately compared to the stronger CRAF bands with less background noise.

ARRAY 1 (MAPK Pathway)

		A	B	C	D	E	F	G	H
Each antibody is spotted in duplicate vertically	1	POS	POS	NEG	NEG	IC	CREB (S133)	ERK1 (T202/Y204) ERK2 (Y185/Y187)	IC
	2								
	3	IC	HSP27 (S82)	JNK (T183)	MEK (S217/221)	MKK3 (S189)	MMK6 (S207)	MSK2 (S360	IC
	4								
	5	p38 (T180/Y182)	P53 (S15)	IC	RSK1 (S380)	RSK2 (S386)	NEG	NEG	POS
	6								

ARRAY 2 (AKT Pathway)

		A	B	C	D	E	F	G	H
Each antibody is spotted in duplicate vertically	1	POS	POS	NEG	NEG	AKT (S473)	AMPKa (T172)	BAD (S112)	4E-BP1 (T36)
	2								
	3	IC	GSK3a (S21)	GSK3b (S9)	mTOR (S2448)	p27 (T198)	IC	P70S6K (T421/S424)	PDK1 (S241)
	4								
	5	PRAS40 (T246)	PTEN (S380)	RAF-1 (S301)	RPS6 (S235/236)	IC	IC	NEG	POS
	6								

ARRAY 3 (JAK/STAT Pathway)

		A	B	C	D	E	F	G	H
Each antibody is spotted in duplicate vertically	1	POS	POS	NEG	EGFR (Ser1070)	JAK1 (Tyr1022)	JAK2 (Tyr1007/1008)	SHP1 (Ser591)	SHP2 (Tyr542)
	2								
	3	Src (Tyr419)	Stat1 (Ser727)	Stat2 (Tyr689)	Stat3 (Tyr705)	Stat5 (Tyr694)	Stat6 (Tyr641)	TYK2 (Tyr1054)	POS
	4								

ARRAY 4 (NFkB Pathway)

		A	B	C	D	E	F	G	H
Each antibody is spotted in duplicate vertically	1	POS	POS	NEG	NEG	ATM (S1981)	eIF2a (S51)	HDAC2 (S394)	HDAC4 (S632)
	2								
	3	IkBa (S32)	MSK1 (S376)	NFkB (S536)	IC	TAK1 (S412)	TBK1 (S172)	ZAP70 (Y292)	POS
	4								

ARRAY 5 (TGFb Pathway)

		A	B	C	D	E	F	G	H
Each antibody is spotted in duplicate vertically	1	POS	POS	NEG	NEG	ATF2 (T69/71)	C-Fos (T232)	c-Jun (S73)	SMAD1 (S463/465)
	2								
	3	SMAD2(S245/250/255)	SMAD4 (T277)	SMAD5 (S463/465)	IC	NEG	NEG	NEG	POS
	4								

POS = Positive Control Spot
NEG = Negative Control Spot
IC = Internal Control Spot (for RayBiotech's use only)

Supplementary figure 2.6. **Antibody array information**. Tables depicting the target proteins, the phosphorylation sites on each target protein and the layout of the arrays. Taken from array manual.

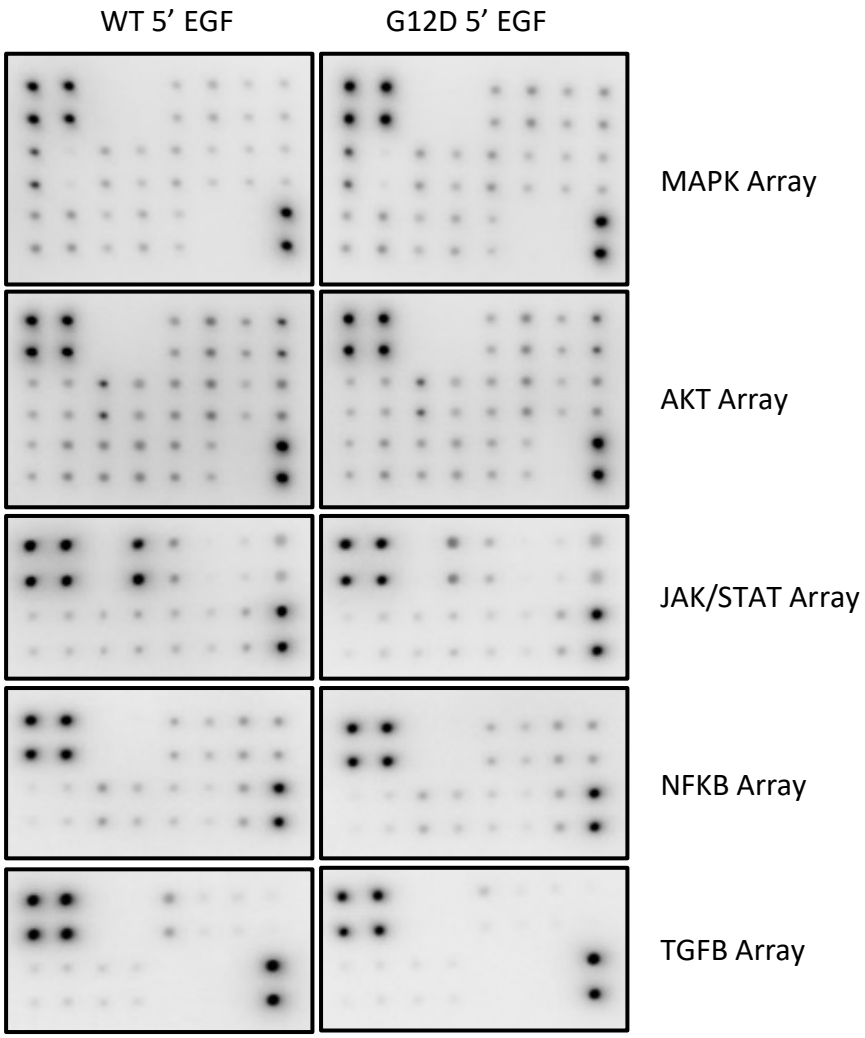

Supplementary figure 2.7. **Array membranes for WT and G12D 5 minutes EGF treated samples.** Images of the five array membranes (MAPK, AKT, JAK/STAT, NFκB and TGFβ) for WT 5 minute EGF and G12D 5 minute EGF conditions. The array membranes were scanned using a chemiluminescence imaging system and the spots were quantified using ImageJ with an array plug-in.

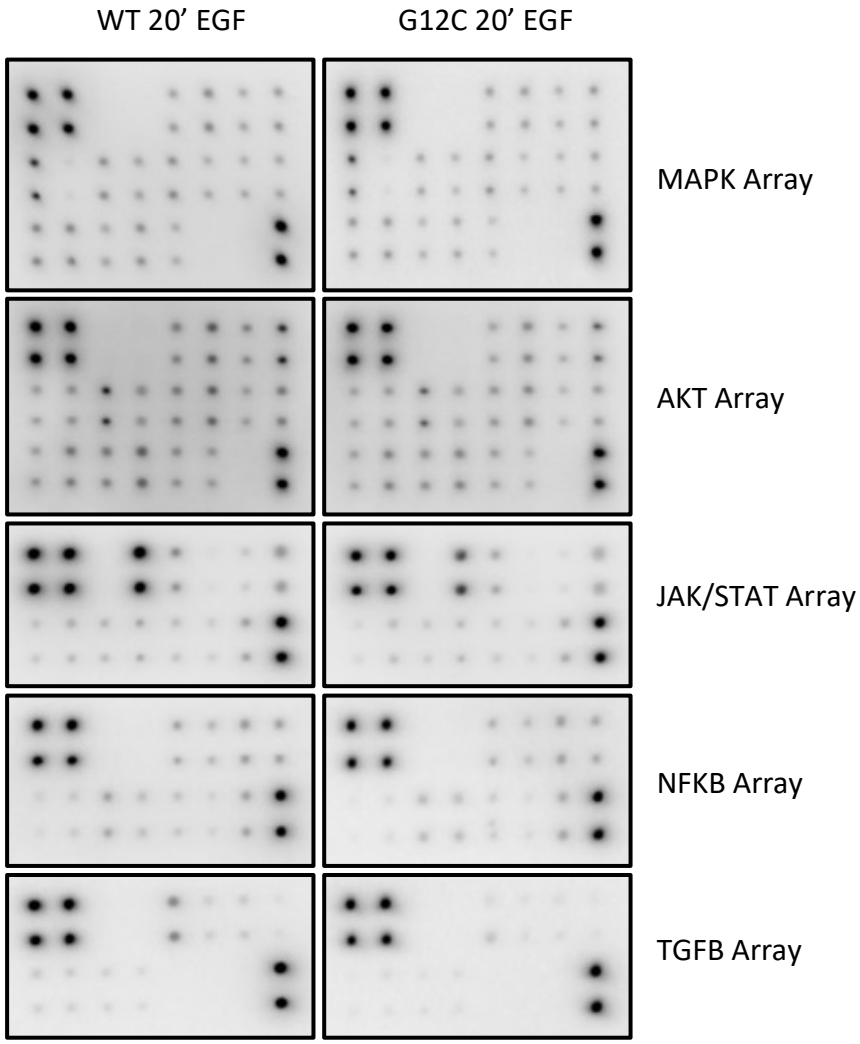

Supplementary figure 2.8. **Array membranes for WT and G12C 20 minutes EGF treated samples.** Images of the five array membranes (MAPK, AKT, JAK/STAT, NFκB and TGFβ) for WT 20 minute EGF and G12C 20 minute EGF conditions. The array membranes were scanned using a chemiluminescence imaging system and the spots were quantified using ImageJ with an array plug-in.

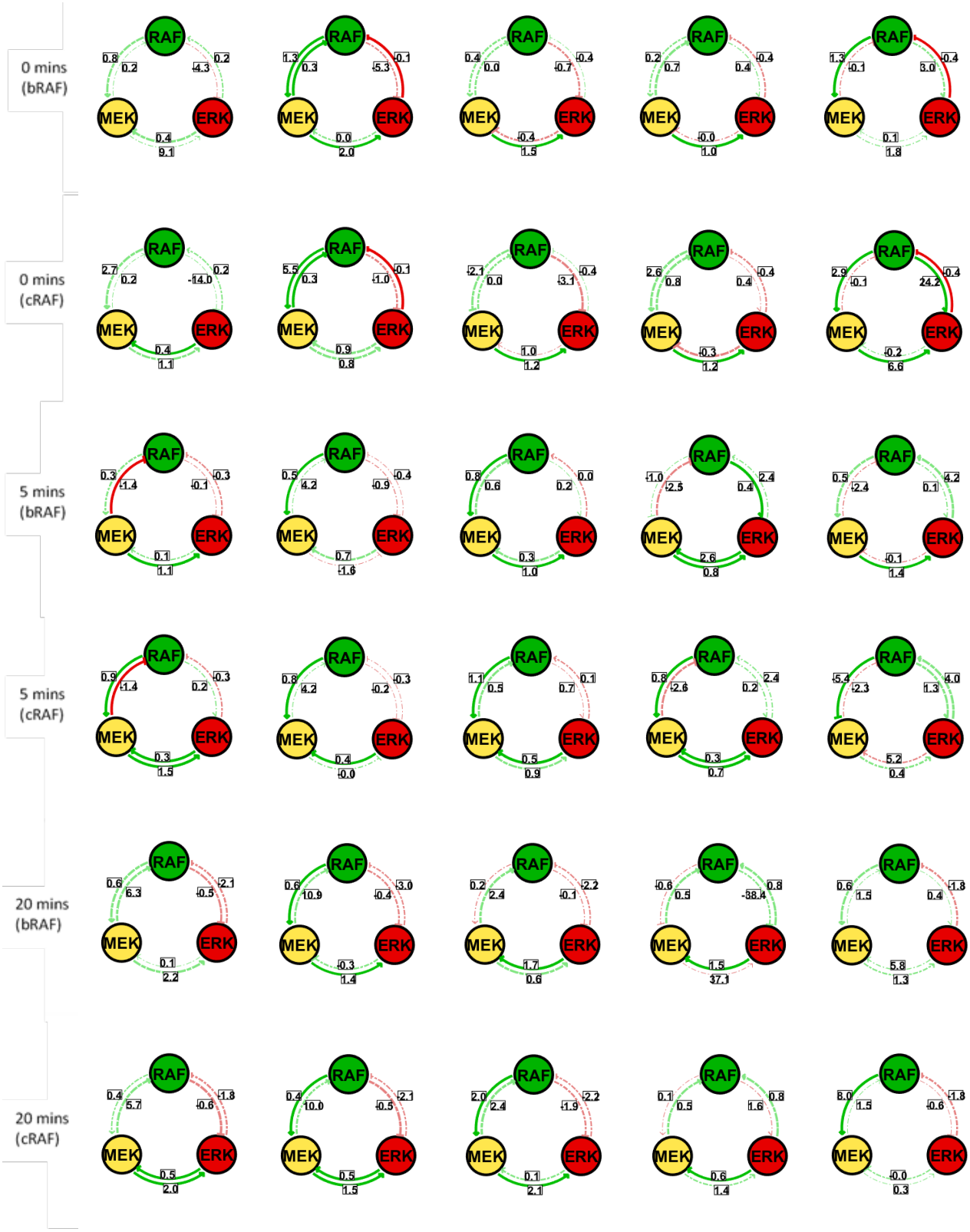

Supplementary figure 2.9. **Topological maps from MRA in SW48 cells.** Complete set of maps shown from MRA in SW48 cells generated by a MATLAB code. The maps have been separated by BRAF and CRAF (n=5). the arrows connecting the nodes (RAF, MEK and ERK) determine type of interaction: red means inhibitory and green means activatory. These interactions may be either direct or indirect. Thick lines represent statistically significant interactions ($p \leq 0.05$), dashed lines represent statistically insignificant interactions ($p > 0.05$). Statistical analysis done via bootstrapping.

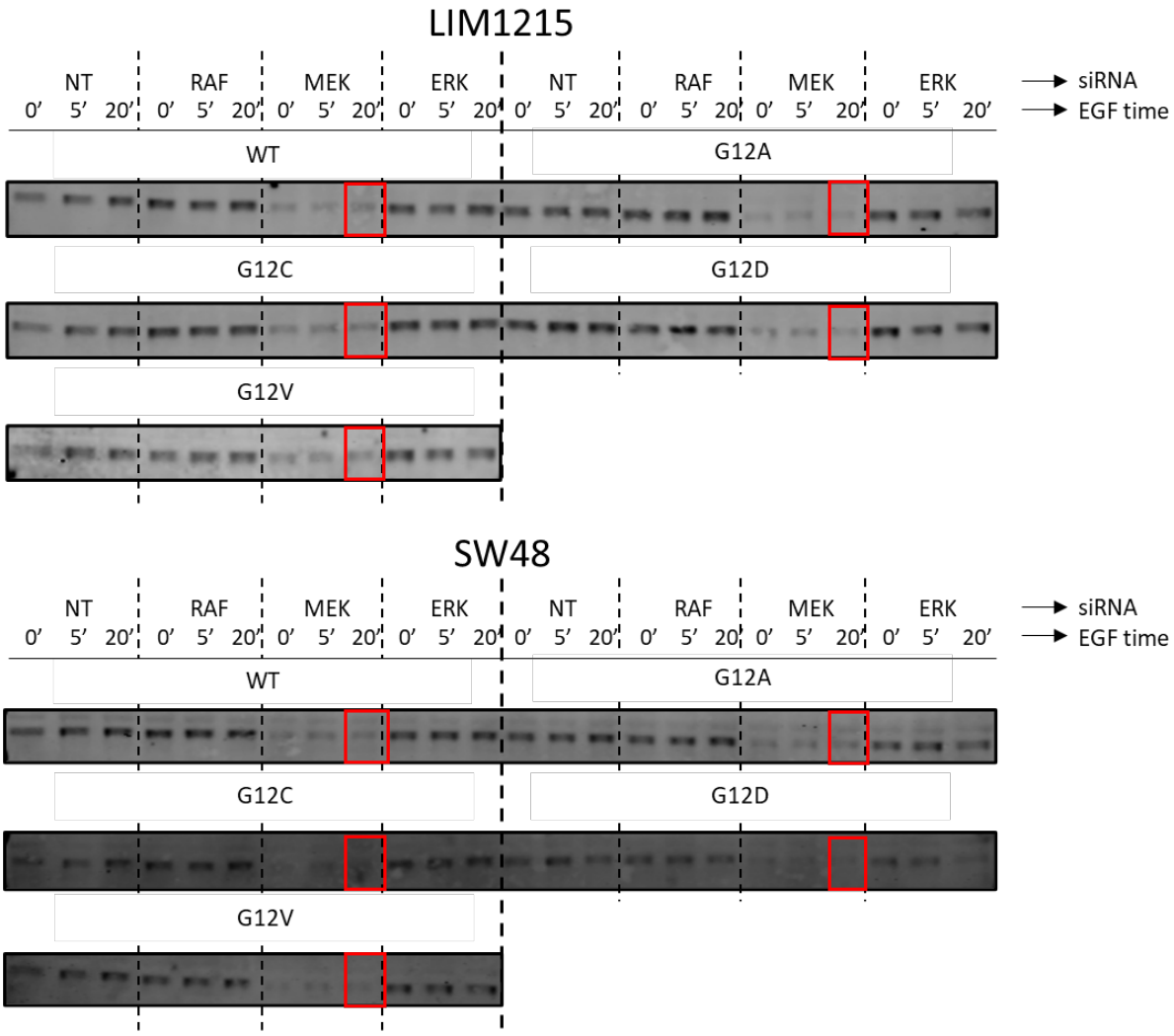

Supplementary figure 2.10. **MEK knockdown in LIM1215 and SW48 samples**. Samples are from the 2nd repeat of LIM1215 MRA and the 2nd repeat of SW48 MRA experiments. The highlighted samples are the ones ran on a gel together in ***Figure 2.19*** to confirm presence or absence of top BRAF band.

a

Summary of all BRAF fragments detected

Sequence Coverage	Protein	Accession	Category	Bio Sample	MS/MS Sa...	Prob	%Spec	#Pep	#Uni...	#Spec	%Cov	m.w.
	Serine/threo...	BRAF_HUMAN	Uncategoriz...	G12D		100%	0.45%	6	8	30	30%	84 kDa
	Serine/threo...	BRAF_HUMAN	Uncategoriz...	WT		100%	0.45%	12	14	37	41%	84 kDa
	Serine/threo...	H7C560_HU...	Uncategoriz...	G12D		100%	0.36%	1	2	24	40%	42 kDa
	Serine/threo...	H7C560_HU...	Uncategoriz...	WT		100%	0.29%	1	1	24	38%	42 kDa

b

G12D BRAF full length – 84kDa

Valid	...	Sequence	Prob	Masc...	Masc...	Masco...	NTT	Modifications	Observed	Actual Mass	Charge	Delta ...	Delta ...	Rete...	Intensity	TIC	Start	Stop	# Ot...	Other Prot...	Spectrum ID
☑	1.0	(K)LTQEHIEALLDK(F)	100%	47.7	43.3	34.7	2		470.59	1,408.76	3	-0.0011	-0.76	1940		759500	56	67	0		File: 'Y:\CORE\R...
☑	1.0	(K)SPQKPIVR(V)	99%	30.7	32.5	18.2	2		462.78	923.55	2	-0.00046	-0.50	1250		1691000	151	158	0		File: 'Y:\CORE\R...
☑	1.0	(R)GLIPECCAVYR(I)	100%	44.2	43.1	35.3	2	Carbamidomethyl...	669.32	1,336.63	2	-0.00057	-0.43	2020		514700	189	199	0		File: 'Y:\CORE\R...
☑	1.0	(R)SSSAPNVHINTIEPVNIDDLIR(D)	100%	63.8	48.2	30.3	2		802.09	2,403.24	3	-0.0027	-1.1	2320		1911000	363	384	0		File: 'Y:\CORE\R...
☑	1.0	(R)GDGGSTTGLSATPPASLPGSLTNVK(	100%	60.4	48.1	12.9	2		762.39	2,284.15	3	-0.0054	-2.4	2160		1456000	390	414	0		File: 'Y:\CORE\R...
☑	1.0	(R)GDGGSTTGLSATPPASLPGSLTNVK(	98%	43.5	48.0	0.0	2		1,143.08	2,284.15	2	-0.0029	-1.3	2160		625700	390	414	0		File: 'Y:\CORE\R...
☑	0.9	(R)RDSSDDWEIPDGQITVGQR(I)	100%	50.8	46.5	1.6	2	Phospho_STY (+80)	752.00	2,252.97	3	-0.00038	-0.17	2220		1888000	444	462	1	H7C560_HU...	File: 'Y:\CORE\R...
☑	0.9	(R)RDSSDDWEIPDGQITVGQR(I)	99%	35.0	47.5	2.3	2	Deamidated (+1)...	725.34	2,173.00	3	0.00032	0.15	2100		216400	444	462	1	H7C560_HU...	File: 'Y:\CORE\R...
☑	0.9	(R)IGSGSFGTVYK(G)	100%	82.0	41.3	70.8	2		558.29	1,114.57	2	-0.00080	-0.72	1830		2225000	463	473	1	H7C560_HU...	File: 'Y:\CORE\R...
☑	0.9	(K)WHGDVAVK(M)	98%	31.9	37.7	12.7	2		456.24	910.47	2	-0.0012	-1.3	1450		219400	476	483	1	H7C560_HU...	File: 'Y:\CORE\R...
☑	0.9	(K)MLNVTAPTPQQLQAFK(N)	100%	81.5	46.1	25.7	2	Oxidation (+16)	901.97	1,801.93	2	-0.0097	-5.4	2180		517500	484	499	1	H7C560_HU...	File: 'Y:\CORE\R...
☑	0.9	(K)MLNVTAPTPQQLQAFK(N)	99%	34.9	46.0	13.1	2	Oxidation (+16)	601.65	1,801.94	3	0.0010	0.56	2180		164400	484	499	1	H7C560_HU...	File: 'Y:\CORE\R...
☑	0.9	(R)QTAQGMDYLHAK(S)	100%	53.8	43.2	45.8	2		454.89	1,361.64	3	-0.00056	-0.41	1620		2231000	559	570	1	H7C560_HU...	File: 'Y:\CORE\R...
☑	0.9	(R)QTAQGMDYLHAK(S)	100%	42.2	42.7	26.1	2	Oxidation (+16)	460.22	1,377.63	3	-0.00082	-0.60	1450		3922000	559	570	1	H7C560_HU...	File: 'Y:\CORE\R...
☑	0.9	(R)DLKSNNIFLHEDLTVK(I)	100%	52.6	46.2	37.5	2		629.34	1,884.99	3	-0.00092	-0.49	2040		505200	576	591	1	H7C560_HU...	File: 'Y:\CORE\R...
☑	0.9	(R)DLKSNNIFLHEDLTVK(I)	99%	29.8	46.2	23.7	2		472.26	1,884.99	4	-0.0012	-0.61	2040		782400	576	591	1	H7C560_HU...	File: 'Y:\CORE\R...
☑	0.9	(K)SNNIFLHEDLTVK(I)	100%	48.4	44.9	37.1	2		510.60	1,528.79	3	-0.00051	-0.33	1990		1802000	579	591	1	H7C560_HU...	File: 'Y:\CORE\R...
☑	0.9	(K)SNNIFLHEDLTVK(I)	100%	44.4	44.9	3.2	2	Deamidated (+1)	510.93	1,529.77	3	-0.00022	-0.15	2110		467900	579	591	1	H7C560_HU...	File: 'Y:\CORE\R...
☑	0.9	(K)SNNIFLHEDLTVK(I)	100%	60.1	44.9	44.1	2		765.40	1,528.79	2	-0.00098	-0.64	1990		285800	579	591	1	H7C560_HU...	File: 'Y:\CORE\R...
☑	0.9	(K)IGDFGLATVK(S)	100%	63.6	39.1	53.6	2		510.79	1,019.57	2	0.000098	0.096	2090		1042000	592	601	1	H7C560_HU...	File: 'Y:\CORE\R...
☑	0.9	(R)DQIIFMVGR(G)	100%	52.7	42.0	33.0	2	Oxidation (+16)	547.79	1,093.56	2	-0.00098	-0.89	2170		664900	663	671	1	H7C560_HU...	File: 'Y:\CORE\R...
☑	0.9	(R)GYLSPDLSK(V)	100%	47.2	39.0	41.3	2		490.26	978.50	2	-0.00026	-0.27	1850		9992000	672	680	1	H7C560_HU...	File: 'Y:\CORE\R...
☑	0.9	(R)SASEPSLNR(A)	100%	43.0	39.8	6.2	2		480.74	959.47	2	-0.00034	-0.36	1430		377700	727	735	1	H7C560_HU...	File: 'Y:\CORE\R...
☑	0.9	(R)SASEPSLNR(A)	98%	30.5	39.6	0.0	2		480.74	959.47	2	-0.00010	-0.11	1410		213600	727	735	1	H7C560_HU...	File: 'Y:\CORE\R...
☑	0.9	(R)SASEPSLNR(A)	98%	32.6	38.1	7.5	2	Phospho_STY (+80)	520.72	1,039.43	2	-0.000...	-0.051	1570		2515000	727	735	1	H7C560_HU...	File: 'Y:\CORE\R...
☑	0.9	(R)AGFQTEDFSLYACASPK(T)	100%	106.0	45.8	96.6	2	Carbamidomethyl...	946.43	1,890.84	2	-0.0015	-0.78	2250		2034000	736	752	1	H7C560_HU...	File: 'Y:\CORE\R...
☑	0.9	(R)AGFQTEDFSLYACASPK(T)	100%	77.2	45.7	68.1	2	Carbamidomethyl...	631.29	1,890.84	3	-0.0035	-1.8	2250		400200	736	752	1	H7C560_HU...	File: 'Y:\CORE\R...
☑	0.9	(R)AGFQTEDFSLYACASPK(T)	100%	45.3	45.4	31.4	2	Deamidated (+1)...	946.92	1,891.83	2	-0.0014	-0.71	2280		55530	736	752	1	H7C560_HU...	File: 'Y:\CORE\R...
☑	1.0	(K)TPIQAGGYGAFPVH(-)	100%	62.2	43.7	53.0	2		707.86	1,413.70	2	-0.00044	-0.31	2090		308600	753	766	0		File: 'Y:\CORE\R...
☑	1.0	(K)TPIQAGGYGAFPVH(-)	100%	46.8	43.7	39.7	2	Deamidated (+1)	708.35	1,414.69	2	-0.0018	-1.3	2130		143000	753	766	0		File: 'Y:\CORE\R...

WT BRAF full length – 84kDa

Valid	...	Sequence	Prob	Masc...	Masc...	Masco...	NTT	Modifications	Observed	Actual Mass	Charge	Delta ...	Delta ...	Rete...	Intensity	TIC	Start	Stop	# Ot...	Other Prot...	Spectrum ID
☑	1.0	(K)LTQEHIEALLDK(F)	100%	45.1	43.5	32.3	2		470.59	1,408.76	3	-0.00017	-0.12	1960		3018000	56	67	0		File: 'Y:\CORE\R...
☑	1.0	(K)FGGEHNPPSIYLEAYEEYTSK(L)	100%	55.1	48.2	49.5	2		811.04	2,430.10	3	-0.0054	-2.2	2290		679600	68	88	0		File: 'Y:\CORE\R...
☑	1.0	(K)SPQKPIVR(V)	99%	36.3	32.5	22.6	2		462.78	923.55	2	-0.00082	-0.89	1270		4644000	151	158	0		File: 'Y:\CORE\R...
☑	1.0	(R)GLIPECCAVYR(I)	100%	58.8	43.1	51.6	2	Carbamidomethyl...	669.32	1,336.63	2	-0.00081	-0.61	2040		3194000	189	199	0		File: 'Y:\CORE\R...
☑	1.0	(R)KTFPTLAFCDFCR(K)	100%	39.0	45.2	30.1	2	Carbamidomethyl...	571.60	1,711.78	3	-0.0016	-0.92	2410		109300	240	252	0		File: 'Y:\CORE\R...
☑	1.0	(R)KLLFQGFR(C)	99%	32.5	36.1	5.1	2		504.80	1,007.59	2	0.000058	0.058	2040		652500	253	260	0		File: 'Y:\CORE\R...
☑	1.0	(K)FFEHMPIPQEEASLAETALTSGSSPS	99%	44.4	51.7	26.5	2		1,151.57	4,602.26	4	0.024	5.3	2350		963900	294	338	0		File: 'Y:\CORE\R...
☑	1.0	(R)DRSSSAPNVHINTIEPVNIDDLIR(D	100%	35.6	49.7	0.0	2	Phospho_STY (+80)	689.59	2,754.34	4	0.0011	0.41	2400		386900	361	384	0		File: 'Y:\CORE\R...
☑	1.0	(R)SSSAPNVHINTIEPVNIDDLIR(D)	100%	76.8	48.2	31.3	2		802.09	2,403.24	3	-0.0014	-0.58	2330		3147000	363	384	0		File: 'Y:\CORE\R...
☑	1.0	(R)SSSAPNVHINTIEPVNIDDLIR(D)	100%	58.9	48.4	7.7	2	Deamidated (+1)	802.42	2,404.23	3	0.0021	0.86	2370		536400	363	384	0		File: 'Y:\CORE\R...
☑	1.0	(R)DQGFRGDGGSTTGLSATPPASLPGS	100%	84.0	49.9	15.3	2		963.48	2,887.43	3	-0.0038	-1.3	2160		3132000	385	414	0		File: 'Y:\CORE\R...
☑	1.0	(R)GDGGSTTGLSATPPASLPGSLTNVK(	100%	85.6	48.1	20.4	2		1,143.08	2,284.15	2	-0.0070	-3.1	2180		2009000	390	414	0		File: 'Y:\CORE\R...
☑	1.0	(R)GDGGSTTGLSATPPASLPGSLTNVK(	100%	54.1	48.0	12.2	2		762.39	2,284.15	3	-0.0030	-1.3	2180		7894000	390	414	0		File: 'Y:\CORE\R...
☑	0.9	(R)RDSSDDWEIPDGQITVGQR(I)	100%	53.0	46.5	0.0	2	Phospho_STY (+80)	752.00	2,252.97	3	-0.0013	-0.57	2230		3925000	444	462	1	H7C560_HU...	File: 'Y:\CORE\R...
☑	0.9	(R)RDSSDDWEIPDGQITVGQR(I)	100%	68.6	46.5	2.2	2	Phospho_STY (+80)	1,127.49	2,252.97	2	-0.0027	-1.2	2230		1533000	444	462	1	H7C560_HU...	File: 'Y:\CORE\R...
☑	0.9	(R)IGSGSFGTVYK(G)	100%	81.1	41.3	69.0	2		558.29	1,114.56	2	-0.0019	-1.7	1840		4754000	463	473	1	H7C560_HU...	File: 'Y:\CORE\R...
☑	0.9	(K)MLNVTAPTPQQLQAFK(N)	100%	77.0	46.0	18.7	2	Oxidation (+16)	901.98	1,801.94	2	-0.00070	-0.39	2200		2646000	484	499	1	H7C560_HU...	File: 'Y:\CORE\R...
☑	0.9	(K)MLNVTAPTPQQLQAFK(N)	100%	49.0	46.1	13.2	2	Oxidation (+16)	601.65	1,801.93	3	-0.0051	-2.8	2200		1573000	484	499	1	H7C560_HU...	File: 'Y:\CORE\R...
☑	0.9	(R)QTAQGMDYLHAK(S)	100%	76.5	43.2	68.1	2		681.83	1,361.64	2	-0.00058	-0.43	1630		269300	559	570	1	H7C560_HU...	File: 'Y:\CORE\R...
☑	0.9	(R)QTAQGMDYLHAK(S)	100%	49.0	42.7	29.9	2	Oxidation (+16)	460.22	1,377.63	3	-0.00073	-0.53	1460		9508000	559	570	1	H7C560_HU...	File: 'Y:\CORE\R...
☑	0.9	(R)QTAQGMDYLHAK(S)	100%	48.6	43.2	40.8	2		454.89	1,361.64	3	-0.00035	-0.26	1630		8704000	559	570	1	H7C560_HU...	File: 'Y:\CORE\R...
☑	0.9	(R)DLKSNNIFLHEDLTVK(I)	100%	54.9	46.2	42.6	2		472.26	1,884.99	4	-0.00091	-0.48	2060		1451000	576	591	1	H7C560_HU...	File: 'Y:\CORE\R...
☑	0.9	(R)DLKSNNIFLHEDLTVK(I)	100%	49.2	46.2	35.6	2		629.34	1,884.99	3	-0.0015	-0.77	2060		1314000	576	591	1	H7C560_HU...	File: 'Y:\CORE\R...
☑	0.9	(K)SNNIFLHEDLTVK(I)	100%	81.2	44.9	65.7	2		765.40	1,528.79	2	-0.00086	-0.56	2000		1625000	579	591	1	H7C560_HU...	File: 'Y:\CORE\R...
☑	0.9	(K)SNNIFLHEDLTVK(I)	100%	56.2	44.9	45.7	2		510.60	1,528.79	3	-0.0021	-1.4	2000		8679000	579	591	1	H7C560_HU...	File: 'Y:\CORE\R...
☑	0.9	(K)SNNIFLHEDLTVK(I)	100%	50.9	44.9	3.4	2	Deamidated (+1)	510.93	1,529.77	3	0.000046	0.030	2130		2551000	579	591	1	H7C560_HU...	File: 'Y:\CORE\R...
☑	0.9	(K)IGDFGLATVK(S)	100%	60.8	39.1	51.6	2		510.79	1,019.56	2	-0.00064	-0.63	2110		4447000	592	601	1	H7C560_HU...	File: 'Y:\CORE\R...
☑	0.9	(R)DQIIFMVGR(G)	100%	48.9	41.3	18.0	2		539.79	1,077.56	2	-0.00046	-0.43	2350		1547000	663	671	1	H7C560_HU...	File: 'Y:\CORE\R...
☑	0.9	(R)DQIIFMVGR(G)	99%	35.9	42.0	21.6	2	Oxidation (+16)	547.79	1,093.56	2	-0.00062	-0.56	2180		2012000	663	671	1	H7C560_HU...	File: 'Y:\CORE\R...
☑	0.9	(R)GYLSPDLSK(V)	100%	37.6	39.0	32.7	2		490.26	978.50	2	-0.00020	-0.21	1860		3.635E7	672	680	1	H7C560_HU...	File: 'Y:\CORE\R...
☑	0.9	(R)SASEPSLNR(A)	100%	59.1	39.8	14.8	2		480.74	959.47	2	-0.00040	-0.42	1420		3802000	727	735	1	H7C560_HU...	File: 'Y:\CORE\R...
☑	0.9	(R)SASEPSLNR(A)	99%	38.4	39.6	7.3	2		480.74	959.47	2	0.00022	0.23	1450		489400	727	735	1	H7C560_HU...	File: 'Y:\CORE\R...
☑	0.9	(R)SASEPSLNR(A)	99%	32.0	38.1	5.8	2	Phospho_STY (+80)	520.72	1,039.43	2	-0.000...	-0.051	1570		3021000	727	735	1	H7C560_HU...	File: 'Y:\CORE\R...
☑	0.9	(R)AGFQTEDFSLYACASPK(T)	100%	114.0	45.8	101.2	2	Carbamidomethyl...	946.43	1,890.84	2	-0.0011	-0.58	2250		1999000	736	752	1	H7C560_HU...	File: 'Y:\CORE\R...
☑	0.9	(R)AGFQTEDFSLYACASPK(T)	100%	75.2	45.7	61.5	2	Carbamidomethyl...	631.29	1,890.84	3	-0.0037	-2.0	2260		843700	736	752	1	H7C560_HU...	File: 'Y:\CORE\R...
☑	0.9	(R)AGFQTEDFSLYACASPK(T)	100%	54.4	44.3	20.8	2	Carbamidomethyl...	986.41	1,970.81	2	-0.0042	-2.1	2420		539700	736	752	1	H7C560_HU...	File: 'Y:\CORE\R...
☑	1.0	(K)TPIQAGGYGAFPVH(-)	100%	89.6	43.8	82.3	2		707.86	1,413.70	2	-0.0017	-1.2	2100		2251000	753	766	0		File: 'Y:\CORE\R...

(figure continued on next page)

G12D BRAF fragment (C-terminal GEFAAFK) – 42kDa

Valid	...	Sequence	Prob	Masc...	Masc...	Masco...	NTT	Modifications	Observed	Actual Mass	Charge	Delta ...	Delta ...	Rete...	Intensity	TIC	Start	Stop	# Ot...	Other Prot...	Spectrum ID
☑	0.1	(R)RDSSDDWEIPDGQITVGQR(I)	100%	50.8	46.5	1.6	2	Phospho_STY (+80)	752.00	2,252.97	3	-0.00038	-0.17	2220		1888000	52	70	2	P523,BRAF_...	File: 'Y:\CORE\R...
☑	0.1	(R)RDSSDDWEIPDGQITVGQR(I)	99%	35.0	47.5	2.3	2	Deamidated (+1)...	725.34	2,173.00	3	0.00032	0.15	2100		216400	52	70	2	P523,BRAF_...	File: 'Y:\CORE\R...
☑	0.1	(R)IGSGSFGTVYK(G)	100%	82.0	41.3	70.8	2		558.29	1,114.57	2	-0.00080	-0.72	1830		2225000	71	81	2	P523,BRAF_...	File: 'Y:\CORE\R...
☑	0.1	(K)WHGDVAVK(M)	98%	31.9	37.7	12.7	2		456.24	910.47	2	-0.0012	-1.3	1450		219400	84	91	2	P523,BRAF_...	File: 'Y:\CORE\R...
☑	0.1	(K)MLNVTAPTPQQLQAFK(N)	100%	81.5	46.1	25.7	2	Oxidation (+16)	901.97	1,801.93	2	-0.0097	-5.4	2180		517500	92	107	2	P523,BRAF_...	File: 'Y:\CORE\R...
☑	0.1	(K)MLNVTAPTPQQLQAFK(N)	99%	34.9	46.0	13.1	2	Oxidation (+16)	601.65	1,801.94	3	0.0010	0.56	2180		164400	92	107	2	P523,BRAF_...	File: 'Y:\CORE\R...
☑	0.1	(R)QTAQGMDYLHAK(S)	100%	53.8	43.2	45.8	2		454.89	1,361.64	3	-0.00056	-0.41	1620		2231000	167	178	2	P523,BRAF_...	File: 'Y:\CORE\R...
☑	0.1	(R)QTAQGMDYLHAK(S)	100%	42.2	42.7	26.1	2	Oxidation (+16)	460.22	1,377.63	3	-0.00082	-0.60	1450		3922000	167	178	2	P523,BRAF_...	File: 'Y:\CORE\R...
☑	0.1	(R)DLKSNNIFLHEDLTVK(I)	100%	52.6	46.2	37.5	2		629.34	1,884.99	3	-0.00092	-0.49	2040		505200	184	199	2	P523,BRAF_...	File: 'Y:\CORE\R...
☑	0.1	(R)DLKSNNIFLHEDLTVK(I)	99%	29.8	46.2	23.7	2		472.26	1,884.99	4	-0.0012	-0.61	2040		782400	184	199	2	P523,BRAF_...	File: 'Y:\CORE\R...
☑	0.1	(K)SNNIFLHEDLTVK(I)	100%	48.4	44.9	37.1	2		510.60	1,528.79	3	-0.00051	-0.33	1990		1802000	187	199	2	P523,BRAF_...	File: 'Y:\CORE\R...
☑	0.1	(K)SNNIFLHEDLTVK(I)	100%	44.4	44.9	3.2	2	Deamidated (+1)	510.93	1,529.77	3	-0.00022	-0.15	2110		467900	187	199	2	P523,BRAF_...	File: 'Y:\CORE\R...
☑	0.1	(K)SNNIFLHEDLTVK(I)	100%	60.1	44.9	44.1	2		765.40	1,528.79	2	-0.00098	-0.64	1990		285800	187	199	2	P523,BRAF_...	File: 'Y:\CORE\R...
☑	0.1	(K)IGDFGLATVK(S)	100%	63.6	39.1	53.6	2		510.79	1,019.57	2	0.000098	0.096	2090		1042000	200	209	2	P523,BRAF_...	File: 'Y:\CORE\R...
☑	0.1	(R)DQIIFMVGR(G)	100%	52.7	42.0	33.0	2	Oxidation (+16)	547.79	1,093.56	2	-0.00098	-0.89	2170		664900	271	279	2	P523,BRAF_...	File: 'Y:\CORE\R...
☑	0.1	(R)GYLSPDLSK(V)	100%	47.2	39.0	41.3	2		490.26	978.50	2	-0.00026	-0.27	1850		9992000	280	288	2	P523,BRAF_...	File: 'Y:\CORE\R...
☑	0.1	(R)SASEPSLNR(A)	100%	43.0	39.8	6.2	2		480.74	959.47	2	-0.00034	-0.36	1430		377700	335	343	2	P523,BRAF_...	File: 'Y:\CORE\R...
☑	0.1	(R)SASEPSLNR(A)	98%	30.5	39.6	0.0	2		480.74	959.47	2	-0.00010	-0.11	1410		213600	335	343	2	P523,BRAF_...	File: 'Y:\CORE\R...
☑	0.1	(R)SASEPSLNR(A)	98%	32.6	38.1	7.5	2	Phospho_STY (+80)	520.72	1,039.43	2	-0.000...	-0.051	1570		2515000	335	343	2	P523,BRAF_...	File: 'Y:\CORE\R...
☑	0.1	(R)AGFQTEDFSLYACASPK(T)	100%	106.0	45.8	96.6	2	Carbamidomethyl...	946.43	1,890.84	2	-0.0015	-0.78	2250		2034000	344	360	2	P523,BRAF_...	File: 'Y:\CORE\R...
☑	0.1	(R)AGFQTEDFSLYACASPK(T)	100%	77.2	45.7	68.1	2	Carbamidomethyl...	631.29	1,890.84	3	-0.0035	-1.8	2250		400200	344	360	2	P523,BRAF_...	File: 'Y:\CORE\R...
☑	0.1	(R)AGFQTEDFSLYACASPK(T)	100%	45.3	45.4	31.4	2	Deamidated (+1)...	946.92	1,891.83	2	-0.0014	-0.71	2280		55530	344	360	2	P523,BRAF_...	File: 'Y:\CORE\R...
☑	1.0	(K)TPIQAGGYGEFAAFK(-)	100%	80.1	44.6	68.1	2		778.89	1,555.77	2	-0.00094	-0.61	2200		1372000	361	375	0		File: 'Y:\CORE\R...
☑	1.0	(K)TPIQAGGYGEFAAFK(-)	100%	76.3	44.4	61.6	2	Deamidated (+1)	779.38	1,556.75	2	-0.0020	-1.3	2240		226900	361	375	0		File: 'Y:\CORE\R...

WT BRAF fragment (C-terminal GEFAAFK) – 42kDa

Valid	...	Sequence	Prob	Masc...	Masc...	Masco...	NTT	Modifications	Observed	Actual Mass	Charge	Delta ...	Delta ...	Rete...	Intensity	TIC	Start	Stop	# Ot...	Other Prot...	Spectrum ID
☑	0.1	(R)RDSSDDWEIPDGQITVGQR(I)	100%	53.0	46.5	0.0	2	Phospho_STY (+80)	752.00	2,252.97	3	-0.0013	-0.57	2230		3925000	52	70	2	P523,BRAF_...	File: 'Y:\CORE\R...
☑	0.1	(R)RDSSDDWEIPDGQITVGQR(I)	100%	68.6	46.5	2.2	2	Phospho_STY (+80)	1,127.49	2,252.97	2	-0.0027	-1.2	2230		1533000	52	70	2	P523,BRAF_...	File: 'Y:\CORE\R...
☑	0.1	(R)IGSGSFGTVYK(G)	100%	81.1	41.3	69.0	2		558.29	1,114.56	2	-0.0019	-1.7	1840		4754000	71	81	2	P523,BRAF_...	File: 'Y:\CORE\R...
☑	0.1	(K)MLNVTAPTPQQLQAFK(N)	100%	77.0	46.0	18.7	2	Oxidation (+16)	901.98	1,801.94	2	-0.00070	-0.39	2200		2646000	92	107	2	P523,BRAF_...	File: 'Y:\CORE\R...
☑	0.1	(K)MLNVTAPTPQQLQAFK(N)	100%	49.0	46.1	13.2	2	Oxidation (+16)	601.65	1,801.93	3	-0.0051	-2.8	2200		1573000	92	107	2	P523,BRAF_...	File: 'Y:\CORE\R...
☑	0.1	(R)QTAQGMDYLHAK(S)	100%	76.5	43.2	68.1	2		681.83	1,361.64	2	-0.00058	-0.43	1630		269300	167	178	2	P523,BRAF_...	File: 'Y:\CORE\R...
☑	0.1	(R)QTAQGMDYLHAK(S)	100%	49.0	42.7	29.9	2	Oxidation (+16)	460.22	1,377.63	3	-0.00073	-0.53	1460		9508000	167	178	2	P523,BRAF_...	File: 'Y:\CORE\R...
☑	0.1	(R)QTAQGMDYLHAK(S)	100%	48.6	43.2	40.8	2		454.89	1,361.64	3	-0.00035	-0.26	1630		8704000	167	178	2	P523,BRAF_...	File: 'Y:\CORE\R...
☑	0.1	(R)DLKSNNIFLHEDLTVK(I)	100%	54.9	46.2	42.6	2		472.26	1,884.99	4	-0.00091	-0.48	2060		1451000	184	199	2	P523,BRAF_...	File: 'Y:\CORE\R...
☑	0.1	(R)DLKSNNIFLHEDLTVK(I)	100%	49.2	46.2	35.6	2		629.34	1,884.99	3	-0.0015	-0.77	2060		1314000	184	199	2	P523,BRAF_...	File: 'Y:\CORE\R...
☑	0.1	(K)SNNIFLHEDLTVK(I)	100%	81.2	44.9	65.7	2		765.40	1,528.79	2	-0.00086	-0.56	2000		1625000	187	199	2	P523,BRAF_...	File: 'Y:\CORE\R...
☑	0.1	(K)SNNIFLHEDLTVK(I)	100%	56.2	44.9	45.7	2		510.60	1,528.79	3	-0.0021	-1.4	2000		8679000	187	199	2	P523,BRAF_...	File: 'Y:\CORE\R...
☑	0.1	(K)SNNIFLHEDLTVK(I)	100%	50.9	44.9	3.4	2	Deamidated (+1)	510.93	1,529.77	3	0.000046	0.030	2130		2551000	187	199	2	P523,BRAF_...	File: 'Y:\CORE\R...
☑	0.1	(K)IGDFGLATVK(S)	100%	60.8	39.1	51.6	2		510.79	1,019.56	2	-0.00064	-0.63	2110		4447000	200	209	2	P523,BRAF_...	File: 'Y:\CORE\R...
☑	0.1	(R)DQIIFMVGR(G)	100%	48.9	41.3	18.0	2		539.79	1,077.56	2	-0.00046	-0.43	2350		1547000	271	279	2	P523,BRAF_...	File: 'Y:\CORE\R...
☑	0.1	(R)DQIIFMVGR(G)	99%	35.9	42.0	21.6	2	Oxidation (+16)	547.79	1,093.56	2	-0.00062	-0.56	2180		2012000	271	279	2	P523,BRAF_...	File: 'Y:\CORE\R...
☑	0.1	(R)GYLSPDLSK(V)	100%	37.6	39.0	32.7	2		490.26	978.50	2	-0.00020	-0.21	1860		3.635E7	280	288	2	P523,BRAF_...	File: 'Y:\CORE\R...
☑	0.1	(R)SASEPSLNR(A)	100%	59.1	39.8	14.8	2		480.74	959.47	2	-0.00040	-0.42	1420		3802000	335	343	2	P523,BRAF_...	File: 'Y:\CORE\R...
☑	0.1	(R)SASEPSLNR(A)	99%	38.4	39.6	7.3	2		480.74	959.47	2	0.00022	0.23	1450		489400	335	343	2	P523,BRAF_...	File: 'Y:\CORE\R...
☑	0.1	(R)SASEPSLNR(A)	99%	32.0	38.1	5.8	2	Phospho_STY (+80)	520.72	1,039.43	2	-0.000...	-0.051	1570		3021000	335	343	2	P523,BRAF_...	File: 'Y:\CORE\R...
☑	0.1	(R)AGFQTEDFSLYACASPK(T)	100%	114.0	45.8	101.2	2	Carbamidomethyl...	946.43	1,890.84	2	-0.0011	-0.58	2250		1999000	344	360	2	P523,BRAF_...	File: 'Y:\CORE\R...
☑	0.1	(R)AGFQTEDFSLYACASPK(T)	100%	75.2	45.7	61.5	2	Carbamidomethyl...	631.29	1,890.84	3	-0.0037	-2.0	2260		843700	344	360	2	P523,BRAF_...	File: 'Y:\CORE\R...
☑	0.1	(R)AGFQTEDFSLYACASPK(T)	100%	54.4	44.3	20.8	2	Carbamidomethyl...	986.41	1,970.81	2	-0.0042	-2.1	2420		539700	344	360	2	P523,BRAF_...	File: 'Y:\CORE\R...
☑	1.0	(K)TPIQAGGYGEFAAFK(-)	100%	78.8	44.6	63.1	2		778.89	1,555.76	2	-0.0023	-1.5	2210		9677000	361	375	0		File: 'Y:\CORE\R...

Supplementary figure 3.1. **Mass spectrometry analysis data of BRAF in LIM1215 WT and G12D cells.** **a.** Summary of the BRAF fragments detected (the truncated 42kDa fragments end in the alternative GEFAAFK C-terminus). **b.** List of peptides detected in WT and G12D samples (full form and truncated BRAF). Modifications are also shown.

Valid	...	Sequence	Prob	Masc...	Masc...	Masc...	NTT	Modifications	Observed	Actual Mass	Charge	Delta ...	Delta ...	Rete...	Intensity	TIC	Start	Stop	# Ot...	Other Prot...	Spectrum ID
☑	1.0	(K)SGFEPASL(K)	99%	38.6	41.9	7.8	2		404.20	806.38	2	0.00032	0.39	2370		1062000	39	46	0		File: "Z:\CORE\R...
☑	1.0	(K)SGFEPASLK(E)	100%	52.3	45.1	29.0	2		468.25	934.48	2	-0.00026	-0.28	2020		1.061E7	39	47	0		File: "Z:\CORE\R...
☑	1.0	(L)KEEVGEEAIVEL(V)	100%	57.6	47.6	11.3	2		672.85	1,343.68	2	-0.0019	-1.4	2340		5016000	47	58	0		File: "Z:\CORE\R...
☑	1.0	(L)KEEVGEEAIVELVENGK(K)	100%	143.5	47.1	8.0	2		936.48	1,870.95	2	0.00090	0.48	2420		4646000	47	63	0		File: "Z:\CORE\R...
☑	1.0	(L)KEEVGEEAIVELVENGK(K)	100%	74.3	47.2	9.5	2		624.66	1,870.95	3	-0.00034	-0.18	2420		2.734E7	47	63	0		File: "Z:\CORE\R...
☑	1.0	(L)KEEVGEEAIVELVENGK(K)	100%	69.9	47.4	45.0	2	Deamidated (+1)	624.99	1,871.93	3	-0.0024	-1.3	2350		1657000	47	63	0		File: "Z:\CORE\R...
☑	1.0	(L)KEEVGEEAIVELVENGK(K)	100%	38.7	47.1	0.0	2		624.66	1,870.96	3	0.0039	2.1	2450		766600	47	63	0		File: "Z:\CORE\R...
☑	1.0	(K)VKVNKDDIQK(M)	100%	43.2	46.0	9.5	2		396.23	1,185.67	3	-0.00038	-0.32	1500		433700	65	74	0		File: "Z:\CORE\R...
☑	1.0	(K)VKVNKDDIQK(M)	100%	39.3	46.0	8.4	2		396.23	1,185.67	3	-0.0012	-1.0	1480		2444000	65	74	0		File: "Z:\CORE\R...
☑	1.0	(K)VNKDDIQK(M)	99%	51.6	46.4	6.0	2		480.26	958.51	2	-0.00072	-0.75	1380		1078000	67	74	0		File: "Z:\CORE\R...
☑	1.0	(K)VNKDDIQK(M)	99%	51.4	46.4	12.7	2		480.26	958.51	2	-0.00030	-0.31	1410		715900	67	74	0		File: "Z:\CORE\R...
☑	1.0	(F)SKVEDMAEL(T)	100%	49.7	45.9	17.2	2		511.25	1,020.48	2	-0.00034	-0.33	2110		4526000	81	89	5	P35580,P35...	File: "Z:\CORE\R...
☑	0.6	(L)TCLNEASVL(H)	99%	36.6	46.0	18.8	2	Carbamidomethyl...	503.75	1,005.48	2	-0.00030	-0.29	2330		3.755E7	90	98	6	P35580,P35...	File: "Z:\CORE\R...
☑	0.6	(L)TCLNEASVL(H)	99%	34.7	46.0	21.7	2	Carbamidomethyl...	503.75	1,005.48	2	-0.00060	-0.59	2350		2170000	90	98	6	P35580,P35...	File: "Z:\CORE\R...
☑	1.0	(Y)SEEIVEMY(K)	99%	33.8	44.6	11.5	2	Oxidation (+16)	508.22	1,014.42	2	-0.00048	-0.47	2150		5058000	131	138	0		File: "Z:\CORE\R...
☑	1.0	(K)KRHEMPPHIY(A)	99%	33.1	47.1	16.5	2		436.56	1,306.66	3	0.0014	1.0	1910		3605000	142	151	5	P35580,P35...	File: "Z:\CORE\R...
☑	1.0	(K)RHEMPPHIY(A)	100%	31.4	47.3	19.5	2		393.86	1,178.57	3	-0.00050	-0.42	1880		3089000	143	151	5	P35580,P35...	File: "Z:\CORE\R...
☑	1.0	(K)RHEMPPHIY(A)	99%	28.8	47.3	16.7	2		393.86	1,178.57	3	-0.00020	-0.17	1900		3522000	143	151	5	P35580,P35...	File: "Z:\CORE\R...
☑	1.0	(R)HEMPPHIY(A)	99%	39.1	45.7	20.9	2		512.24	1,022.46	2	-0.00062	-0.61	1950		4942000	144	151	5	P35580,P35...	File: "Z:\CORE\R...
☑	1.0	(R)HEMPPHIY(A)	99%	38.9	46.4	26.5	2	Oxidation (+16)	520.24	1,038.46	2	-0.00056	-0.54	1800		2.648E7	144	151	5	P35580,P35...	File: "Z:\CORE\R...
☑	1.0	(R)HEMPPHIY(A)	99%	38.1	45.7	21.0	2		512.24	1,022.46	2	-0.00050	-0.49	1910		1.429E7	144	151	5	P35580,P35...	File: "Z:\CORE\R...
☑	1.0	(R)HEMPPHIY(A)	98%	40.5	45.9	24.4	2		512.24	1,022.46	2	-0.0020	-1.9	1890		795700	144	151	5	P35580,P35...	File: "Z:\CORE\R...
☑	1.0	(Y)AITDTAYR(S)	99%	49.3	44.9	32.8	2		455.74	909.46	2	0.00024	0.26	1750		2730000	152	159	0		File: "Z:\CORE\R...
☑	1.0	(K)KDQGELER(Q)	99%	62.1	46.2	22.7	2		487.75	973.48	2	-0.00048	-0.49	1420		2400000	202	209	0		File: "Z:\CORE\R...
☑	0.6	(L)QANPILEAF(G)	99%	39.5	46.5	19.1	2		501.77	1,001.52	2	0.00014	0.14	2470		1.734E7	213	221	1	Q7Z406-6	File: "Z:\CORE\R...
☑	1.0	(Y)LLSGAGEHL(K)	95%	34.9	42.2	26.0	2		448.74	895.47	2	-0.0024	-2.7	2050		6.23E7	280	288	0		File: "Z:\CORE\R...
☑	1.0	(L)SGAGEHLK(T)	99%	48.5	38.4	27.2	2		399.71	797.40	2	-0.00058	-0.73	1380		3175000	282	289	5	P35580,P35...	File: "Z:\CORE\R...
☑	1.0	(L)SGAGEHLK(T)	99%	46.3	38.4	26.4	2		399.71	797.40	2	-0.00034	-0.43	1360		2331000	282	289	5	P35580,P35...	File: "Z:\CORE\R...
☑	1.0	(R)FLSNGHVTIPGQQDK(D)	100%	57.1	47.2	4.1	2		547.62	1,639.83	3	-0.0021	-1.3	2010		2.257E7	302	316	0		File: "Z:\CORE\R...
☑	1.0	(R)FLSNGHVTIPGQQDK(D)	100%	92.9	47.2	17.2	2		820.92	1,639.83	2	-0.00018	-0.11	2010		7697000	302	316	0		File: "Z:\CORE\R...
☑	1.0	(R)FLSNGHVTIPGQQDK(D)	100%	44.2	47.2	7.7	2		547.62	1,639.83	3	-0.00086	-0.52	2030		7664000	302	316	0		File: "Z:\CORE\R...
☑	1.0	(R)FLSNGHVTIPGQQDK(D)	100%	39.9	47.5	7.7	2	Deamidated (+1)	547.94	1,640.81	3	-0.0035	-2.1	2060		5231000	302	316	0		File: "Z:\CORE\R...
☑	1.0	(R)FLSNGHVTIPGQQDK(D)	100%	59.0	47.4	9.6	2	Deamidated (+1)	821.42	1,640.82	2	0.0035	2.1	2060		2034000	302	316	0		File: "Z:\CORE\R...
☑	1.0	(F)LSNGHVTIPGQQDK(D)	100%	73.2	47.5	22.4	2		747.39	1,492.76	2	-0.00076	-0.51	1770		1907000	303	316	0		File: "Z:\CORE\R...
☑	1.0	(F)LSNGHVTIPGQQDK(D)	100%	66.2	47.8	23.9	2	Deamidated (+1)	747.88	1,493.75	2	0.00046	0.31	1840		1233000	303	316	0		File: "Z:\CORE\R...
☑	1.0	(F)LSNGHVTIPGQQDK(D)	100%	41.9	47.8	14.9	2	Deamidated (+1)	498.92	1,493.75	3	0.0017	1.1	1840		4991000	303	316	0		File: "Z:\CORE\R...
☑	1.0	(F)LSNGHVTIPGQQDK(D)	100%	38.2	47.5	6.1	2		498.59	1,492.76	3	-0.0010	-0.69	1770		8356000	303	316	0		File: "Z:\CORE\R...
☑	1.0	(F)LSNGHVTIPGQQDK(D)	100%	37.2	47.8	9.3	2	Deamidated (+1)	498.92	1,493.75	3	-0.0011	-0.77	1820		6957000	303	316	0		File: "Z:\CORE\R...
☑	1.0	(F)LSNGHVTIPGQQDK(D)	96%	32.2	47.4	0.8	2		498.59	1,492.76	3	-0.0035	-2.4	1790		1040000	303	316	0		File: "Z:\CORE\R...
☑	1.0	(L)SNGHVTIPGQQDK(D)	100%	39.5	48.0	16.3	2		460.90	1,379.68	3	-0.00095	-0.69	1660		8372000	304	316	0		File: "Z:\CORE\R...
☑	1.0	(L)SNGHVTIPGQQDK(D)	100%	33.9	48.1	16.2	2	Deamidated (+1)	461.23	1,380.66	3	-0.00015	-0.11	1720		5049000	304	316	0		File: "Z:\CORE\R...
☑	1.0	(L)SNGHVTIPGQQDK(D)	100%	43.3	48.0	16.9	2		690.85	1,379.68	2	-0.00040	-0.29	1660		739600	304	316	0		File: "Z:\CORE\R...
☑	1.0	(K)DMFQETMEAMR(I)	100%	48.4	45.5	10.2	2	Oxidation (+16), ...	718.78	1,435.54	2	-0.00081	-0.56	1750		405600	317	327	0		File: "Z:\CORE\R...
☑	1.0	(K)DMFQETMEAMR(I)	100%	55.3	45.4	33.6	2	Oxidation (+16), ...	710.78	1,419.55	2	-0.0020	-1.4	2010		5921000	317	327	0		File: "Z:\CORE\R...
☑	1.0	(K)DMFQETMEAMR(I)	100%	52.4	45.5	19.2	2	Oxidation (+16), ...	718.78	1,435.54	2	-0.000...	-0.047	1710		1968000	317	327	0		File: "Z:\CORE\R...
☑	1.0	(K)DMFQETMEAMR(I)	100%	46.4	45.4	9.9	2	Oxidation (+16), ...	718.78	1,435.54	2	-0.00093	-0.65	1730		584000	317	327	0		File: "Z:\CORE\R...
☑	1.0	(K)DMFQETMEAMR(I)	100%	46.2	45.6	18.8	2	Oxidation (+16), ...	710.78	1,419.55	2	-0.00051	-0.36	1940		3741000	317	327	0		File: "Z:\CORE\R...
☑	1.0	(K)ERNTDQASMPDNTAAQK(V)	100%	45.6	47.9	7.4	2		626.29	1,875.84	3	-0.0026	-1.4	1530		640900	357	373	0		File: "Z:\CORE\R...
☑	1.0	(R)NTDQASMPDNTAAQK(V)	100%	70.5	47.6	8.4	2		531.24	1,590.69	3	-0.00045	-0.28	1590		3159000	359	373	0		File: "Z:\CORE\R...
☑	1.0	(R)NTDQASMPDNTAAQK(V)	100%	115.0	47.4	15.9	2	Oxidation (+16)	804.35	1,606.69	2	-0.0025	-1.6	1590		2312000	359	373	0		File: "Z:\CORE\R...
☑	1.0	(R)NTDQASMPDNTAAQK(V)	100%	102.4	47.4	15.4	2	Oxidation (+16)	804.35	1,606.69	2	-0.0012	-0.72	1410		2637000	359	373	0		File: "Z:\CORE\R...
☑	1.0	(R)NTDQASMPDNTAAQK(V)	100%	55.9	47.3	4.6	2	Oxidation (+16)	536.57	1,606.69	3	-0.00038	-0.24	1390		6714000	359	373	0		File: "Z:\CORE\R...
☑	1.0	(R)NTDQASMPDNTAAQK(V)	100%	97.5	47.7	10.2	2		796.35	1,590.69	2	-0.0021	-1.3	1600		822800	359	373	0		File: "Z:\CORE\R...
☑	1.0	(R)NTDQASMPDNTAAQK(V)	100%	71.3	47.3	12.3	2	Oxidation (+16)	804.35	1,606.69	2	-0.0027	-1.7	1430		400100	359	373	0		File: "Z:\CORE\R...
☑	1.0	(R)NTDQASMPDNTAAQK(V)	100%	51.4	47.4	3.5	2	Deamidated (+1)	796.85	1,591.68	2	-0.0011	-0.70	1670		367500	359	373	0		File: "Z:\CORE\R...
☑	1.0	(R)NTDQASMPDNTAAQK(V)	100%	59.8	47.1	5.8	2	Deamidated (+1)...	804.85	1,607.68	2	0.0025	1.6	1450		354500	359	373	0		File: "Z:\CORE\R...
☑	1.0	(R)NTDQASMPDNTAAQK(V)	99%	69.3	47.3	6.8	2	Deamidated (+1)...	804.85	1,607.69	2	0.016	9.8	1380		182900	359	373	0		File: "Z:\CORE\R...
☑	1.0	(R)NTDQASMPDNTAAQK(V)	99%	43.8	47.3	0.0	2	Oxidation (+16)	804.35	1,606.69	2	-0.0027	-1.7	1470		162500	359	373	0		File: "Z:\CORE\R...
☑	1.0	(R)NTDQASMPDNTAAQK(V)	97%	53.8	47.7	3.6	2	Deamidated (+1)	796.86	1,591.70	2	0.017	11	1580		151100	359	373	0		File: "Z:\CORE\R...
☑	1.0	(L)IEKPAGPPGIL(A)	100%	50.0	43.6	35.0	2		546.33	1,090.64	2	0.00016	0.14	2250		1.43E7	515	525	0		File: "Z:\CORE\R...
☑	1.0	(K)VMQEQGTHPK(F)	100%	62.1	47.5	41.2	2		577.78	1,153.55	2	-0.00050	-0.43	1380		439700	546	555	0		File: "Z:\CORE\R...
☑	1.0	(K)VMQEQGTHPK(F)	100%	54.5	47.0	30.1	2	Oxidation (+16)	585.78	1,169.55	2	-0.00056	-0.48	1280		6478000	546	555	0		File: "Z:\CORE\R...
☑	1.0	(K)VMQEQGTHPK(F)	100%	41.5	47.6	32.5	2		385.53	1,153.55	3	-0.00092	-0.80	1380		1.346E7	546	555	0		File: "Z:\CORE\R...
☑	1.0	(K)VMQEQGTHPK(F)	100%	36.5	47.0	24.8	2	Oxidation (+16)	390.86	1,169.55	3	-0.00082	-0.70	1280		2.91E7	546	555	0		File: "Z:\CORE\R...
☑	1.0	(K)VMQEQGTHPK(F)	100%	36.6	47.6	27.2	2		385.53	1,153.55	3	-0.00092	-0.80	1400		687900	546	555	0		File: "Z:\CORE\R...
☑	1.0	(K)VMQEQGTHPK(F)	100%	41.8	47.0	23.1	2	Oxidation (+16)	585.78	1,169.55	2	-0.00044	-0.37	1300		195400	546	555	0		File: "Z:\CORE\R...
☑	1.0	(L)RNTNPNFVR(C)	98%	34.1	47.4	5.6	2		559.30	1,116.58	2	-0.00042	-0.38	1650		9531000	662	670	5	P35580,P35...	File: "Z:\CORE\R...
☑	1.0	(R)NTNPNFVR(C)	99%	48.0	46.4	30.7	2		481.25	960.48	2	-0.00010	-0.11	1790		1.159E7	663	670	5	P35580,P35...	File: "Z:\CORE\R...
☑	1.0	(R)NTNPNFVR(C)	99%	48.0	46.4	30.7	2		481.25	960.48	2	-0.00058	-0.61	1770		1.071E7	663	670	5	P35580,P35...	File: "Z:\CORE\R...
☑	1.0	(R)CIIPNMEK(K)	98%	38.2	46.8	14.8	2	Carbamidomethyl...	505.76	1,009.50	2	0.00024	0.24	1690		4.25E7	671	678	5	P35580,P35...	File: "Z:\CORE\R...
☑	0.6	(R)CNGVLEGIR(I)	100%	58.8	46.7	38.0	2	Carbamidomethyl...	509.26	1,016.51	2	-0.00044	-0.43	2070		6.518E7	694	702	6	P35580,P35...	File: "Z:\CORE\R...
☑	0.6	(R)CNGVLEGIR(I)	100%	57.9	46.4	42.5	2	Carbamidomethyl...	509.75	1,017.49	2	-0.00075	-0.74	2140		3610000	694	702	6	P35580,P35...	File: "Z:\CORE\R...
☑	0.6	(R)CNGVLEGIR(I)	100%	63.5	46.4	47.2	2	Carbamidomethyl...	509.75	1,017.49	2	-0.0015	-1.4	2120		3396000	694	702	6	P35580,P35...	File: "Z:\CORE\R...
☑	0.6	(R)CNGVLEGIR(I)	100%	57.0	46.8	36.3	2	Carbamidomethyl...	509.26	1,016.51	2	0.00012	0.12	2090		5476000	694	702	6	P35580,P35...	File: "Z:\CORE\R...
☑	1.0	(Y)EILTPNSIPK(G)	97%	34.1	45.0	20.9	2	Deamidated (+1)	556.81	1,111.61	2	0.00068	0.61	2170		5206000	722	731	0		File: "Z:\CORE\R...
☑	1.0	(R)AGVLAHLEEER(D)	100%	46.1	47.3	31.6	2		408.55	1,222.63	3	-0.00097	-0.79	2080		5257000	765	775	5	P35580,P35...	File: "Z:\CORE\R...
☑	1.0	(R)AGVLAHLEEER(D)	99%	54.0	47.4	40.2	2		612.32	1,222.63	2	-0.0047	-3.9	2080		1711000	765	775	5	P35580,P35...	File: "Z:\CORE\R...
☑	1.0	(R)QEEEMMAK(E)	99%	75.3	43.9	22.0	2		498.21	994.41	2	-0.00042	-0.42	1630		2721000	843	850	0		File: "Z:\CORE\R...
☑	1.0	(R)QEEEMMAK(E)	98%	34.9	43.8	19.1	2	Oxidation (+16), ...	514.21	1,026.40	2	0.00011	0.11	1260		377500	843	850	0		File: "Z:\CORE\R...
☑	1.0	(R)QEEEMMAKEEELVK(V)	100%	46.4	47.8	33.5	2	Oxidation (+16), ...	585.60	1,753.77	3	-0.0026	-1.5	1700		1584000	843	856	0		File: "Z:\CORE\R...
☑	1.0	(R)QEEEMMAKEEELVK(V)	97%	38.5	47.9	1.9	2	Deamidated (+1)...	580.60	1,738.78	3	0.016	9.0	1860		1380000	843	856	0		File: "Z:\CORE\R...
☑	1.0	(L)QLQEQLQAETEL(C)	100%	61.4	47.5	23.3	2		715.36	1,428.71	2	-0.0016	-1.1	2340		1.178E7	884	895	0		File: "Z:\CORE\R...
☑	1.0	(L)QAETELCAEAEEL(R)	100%	54.2	47.3	26.9	2	Carbamidomethyl...	746.83	1,491.64	2	-0.0026	-1.7	2350		3564000	890	902	0		File: "Z:\CORE\R...
☑	1.0	(L)QAETELCAEAEELR(A)	100%	99.9	48.0	80.3	2	Carbamidomethyl...	824.88	1,647.74	2	-0.0028	-1.7	2150		7931000	890	903	0		File: "Z:\CORE\R...
☑	1.0	(L)QAETELCAEAEELR(A)	100%	58.5	48.0	37.2	2	Carbamidomethyl...	550.25	1,647.74	3	-0.0023	-1.4	2160		3959000	890	903	0		File: "Z:\CORE\R...
☑	1.0	(L)CAEAEELR(A)	99%	52.4	44.8	7.1	2	Carbamidomethyl...	489.22	976.43	2	-0.00036	-0.36	1660		5189000	896	903	0		File: "Z:\CORE\R...
☑	1.0	(K)KQELEEICHDL(E)	100%	57.5	47.7	34.5	2	Carbamidomethyl...	707.34	1,412.66	2	-0.0017	-1.2	2100		3398000	910	920	0		File: "Z:\CORE\R...
☑	1.0	(K)QELEEICHDLEAR(V)	100%	64.2	48.0	44.6	2	Carbamidomethyl...	547.92	1,640.75	3	-0.00062	-0.38	2160		1.46E7	911	923	0		File: "Z:\CORE\R...
☑	1.0	(K)QELEEICHDLEAR(V)	100%	86.5	48.0	64.5	2	Carbamidomethyl...	821.38	1,640.74	2	-0.0019	-1.2	2160		1864000	911	923	0		File: "Z:\CORE\R...
☑	1.0	(K)KLEEEQIIL(E)	99%	44.4	45.8	0.4	2		557.82	1,113.63	2	0.0011	1.0	2360		7517000	975	983	0		File: "Z:\CORE\R...
☑	1.0	(K)LEEEQIILEDQNCK(L)	100%	107.2	48.1	0.0	2	Carbamidomethyl...	880.92	1,759.83	2	-0.0019	-1.1	2140		1.451E7	976	989	0		File: "Z:\CORE\R...
☑	1.0	(K)LEEEQIILEDQNCK(L)	100%	55.4	48.1	7.6	2	Carbamidomethyl...	587.62	1,759.83	3	-0.0017	-0.95	2140		6643000	976	989	0		File: "Z:\CORE\R...
☑	1.0	(K)LEEEQIILEDQNCK(L)	100%	60.6	48.2	0.0	2	Carbamidomethyl...	880.92	1,759.83	2	0.00090	0.51	2160		698300	976	989	0		File: "Z:\CORE\R...
☑	1.0	(F)TTNLTEEEEK(S)	100%	64.1	47.0	42.7	2		597.28	1,192.55	2	-0.00020	-0.17	1610		5219000	1005	1014	0		File: "Z:\CORE\R...
☑	1.0	(F)TTNLTEEEEK(S)	100%	51.2	47.0	32.2	2		597.28	1,192.55	2	-0.00044	-0.37	1630		435700	1005	1014	0		File: "Z:\CORE\R...
☑	1.0	(K)NKHEAMITDLEER(L)	100%	62.2	47.9	53.0	2	Oxidation (+16)	534.59	1,600.75	3	0.000057	0.036	1750		4240000	1023	1035	0		File: "Z:\CORE\R...
☑	1.0	(K)NKHEAMITDLEER(L)	100%	47.6	47.9	36.9	2	Oxidation (+16)	534.59	1,600.75	3	-0.00069	-0.43	1770		2674000	1023	1035	0		File: "Z:\CORE\R...
☑	1.0	(K)NKHEAMITDLEER(L)	100%	52.4	47.8	36.1	2		529.26	1,584.75	3	-0.0035	-2.2	1910		8834000	1023	1035	0		File: "Z:\CORE\R...
☑	1.0	(K)NKHEAMITDLEER(L)	100%	34.8	47.7	17.7	2		397.20	1,584.76	4	-0.0013	-0.83	1910		4059000	1023	1035	0		File: "Z:\CORE\R...
☑	1.0	(K)NKHEAMITDLEER(L)	100%	34.2	47.9	18.1	2	Oxidation (+16)	401.20	1,600.75	4	-0.000...	-0.018	1770		2699000	1023	1035	0		File: "Z:\CORE\R...
☑	1.0	(K)NKHEAMITDLEER(L)	100%	28.8	47.9	13.9	2	Oxidation (+16)	401.20	1,600.75	4	-0.000...	-0.018	1750		2293000	1023	1035	0		File: "Z:\CORE\R...
☑	1.0	(K)NKHEAMITDLEER(L)	97%	55.2	47.8	42.7	2	Deamidated (+1)	793.89	1,585.76	2	0.022	14	1910		2356000	1023	1035	0		File: "Z:\CORE\R...
☑	1.0	(K)HEAMITDLEER(L)	100%	81.9	47.3	63.8	2		672.32	1,342.62	2	-0.00072	-0.54	2020		3942000	1025	1035	0		File: "Z:\CORE\R...
☑	1.0	(K)HEAMITDLEER(L)	100%	71.8	47.1	58.0	2	Oxidation (+16)	680.31	1,358.61	2	0.00056	0.41	1850		3135000	1025	1035	0		File: "Z:\CORE\R...
☑	1.0	(K)HEAMITDLEER(L)	100%	70.1	47.2	52.8	2		672.32	1,342.62	2	0.00050	0.37	2040		1077000	1025	1035	0		File: "Z:\CORE\R...
☑	1.0	(K)HEAMITDLEER(L)	100%	68.5	47.3	54.0	2	Oxidation (+16)	680.31	1,358.61	2	-0.0015	-1.1	1870		4486000	1025	1035	0		File: "Z:\CORE\R...
☑	1.0	(K)HEAMITDLEER(L)	100%	42.2	47.3	30.0	2	Oxidation (+16)	453.88	1,358.61	3	-0.0012	-0.88	1860		6175000	1025	1035	0		File: "Z:\CORE\R...

(figure continued on next page)

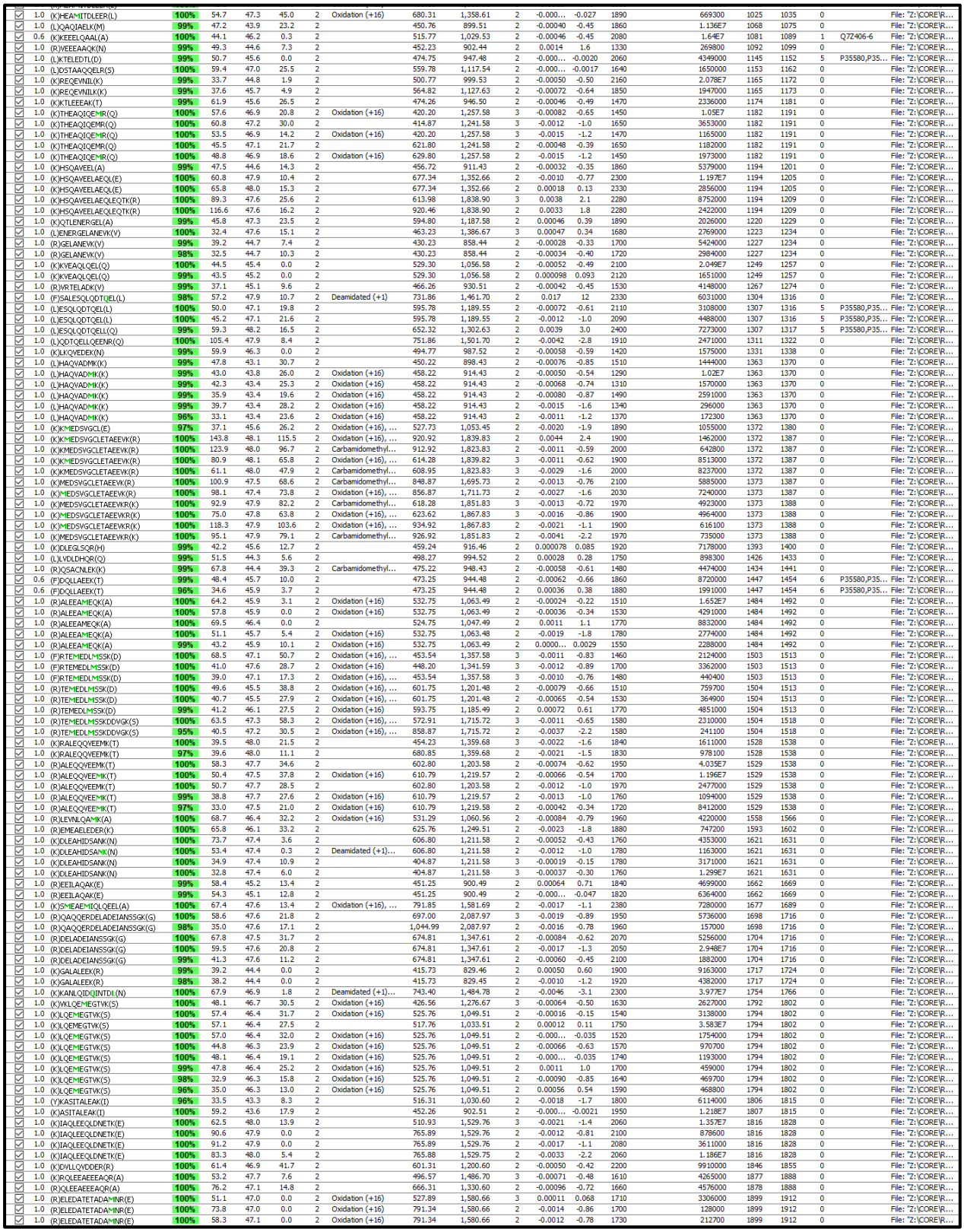

	1.0	(K)HEAMITDLEER(L)	100%	54.7	47.3	45.0	2	Oxidation (+16)	680.31	1,358.61	2	-0.000…	-0.027	1890	669300	1025	1035	0		File: "Z:\CORE\R…
	1.0	(L)QAQIAELK(M)	99%	47.2	43.9	23.2	2		450.76	899.51	2	-0.00040	-0.45	1860	1.136E7	1068	1075	0		File: "Z:\CORE\R…
	0.6	(K)KEEELQAAL(A)	100%	44.1	46.2	0.3	2		515.77	1,029.53	2	-0.00046	-0.45	2080	1.64E7	1081	1089	1	Q7Z406-6	File: "Z:\CORE\R…
	1.0	(R)VEEEAAQK(N)	99%	49.3	44.6	7.3	2		452.23	902.44	2	0.0014	1.6	1330	269800	1092	1099	0		File: "Z:\CORE\R…
	1.0	(L)KTELEDTL(D)	99%	50.7	45.6	0.0	2		474.75	947.48	2	-0.000…	-0.0020	2060	4349000	1145	1152	5	P35580,P35…	File: "Z:\CORE\R…
	1.0	(L)STAAQQELR(S)	100%	59.4	47.0	25.5	2		559.78	1,117.54	2	-0.000…	-0.0017	1640	1650000	1153	1162	0		File: "Z:\CORE\R…
	1.0	(K)REQEVNILK(K)	99%	33.7	44.8	1.9	2		500.77	999.53	2	-0.00050	-0.50	2160	2.078E7	1165	1172	0		File: "Z:\CORE\R…
	1.0	(K)REQEVNILK(K)	99%	37.6	45.7	4.9	2		564.82	1,127.63	2	-0.00072	-0.64	1850	1947000	1165	1173	0		File: "Z:\CORE\R…
	1.0	(K)KTLEEEAK(T)	99%	61.9	45.6	26.5	2		474.26	946.50	2	-0.00046	-0.49	1470	2336000	1174	1181	0		File: "Z:\CORE\R…
	1.0	(K)THEAQIQEMR(Q)	100%	57.6	46.9	20.8	2	Oxidation (+16)	420.20	1,257.58	3	-0.00082	-0.65	1450	1.05E7	1182	1191	0		File: "Z:\CORE\R…
	1.0	(K)THEAQIQEMR(Q)	100%	60.8	47.2	30.0	2		414.87	1,241.58	3	-0.0012	-1.0	1650	3653000	1182	1191	0		File: "Z:\CORE\R…
	1.0	(K)THEAQIQEMR(Q)	100%	53.5	46.9	14.2	2	Oxidation (+16)	420.20	1,257.58	3	-0.0015	-1.2	1470	1165000	1182	1191	0		File: "Z:\CORE\R…
	1.0	(K)THEAQIQEMR(Q)	100%	45.5	47.1	21.7	2		621.80	1,241.58	2	-0.00048	-0.39	1650	1182000	1182	1191	0		File: "Z:\CORE\R…
	1.0	(K)THEAQIQEMR(Q)	100%	48.8	46.9	18.6	2	Oxidation (+16)	629.80	1,257.58	2	-0.0015	-1.2	1450	1973000	1182	1191	0		File: "Z:\CORE\R…
	1.0	(K)HSQAVEEL(A)	99%	47.5	44.6	14.3	2		456.72	911.43	2	-0.00032	-0.35	1860	5379000	1194	1201	0		File: "Z:\CORE\R…
	1.0	(K)HSQAVEELAEQL(E)	100%	60.8	47.9	10.4	2		677.34	1,352.66	2	-0.0010	-0.77	2300	1.197E7	1194	1205	0		File: "Z:\CORE\R…
	1.0	(K)HSQAVEELAEQL(E)	100%	65.8	48.0	15.3	2		677.34	1,352.66	2	0.00018	0.13	2330	2856000	1194	1205	0		File: "Z:\CORE\R…
	1.0	(K)HSQAVEELAEQLEQTK(R)	100%	89.3	47.6	25.6	2		613.98	1,838.90	3	0.0038	2.1	2280	8752000	1194	1209	0		File: "Z:\CORE\R…
	1.0	(K)HSQAVEELAEQLEQTK(R)	100%	116.6	47.6	16.2	2		920.46	1,838.90	2	0.0033	1.8	2280	2422000	1194	1209	0		File: "Z:\CORE\R…
	1.0	(K)QTLENERGEL(A)	99%	45.8	47.3	23.5	2		594.80	1,187.58	2	0.00046	0.39	1890	2026000	1220	1229	0		File: "Z:\CORE\R…
	1.0	(L)ENERGELANEVK(V)	100%	32.4	47.6	15.1	2		463.23	1,386.67	3	0.00047	0.34	1680	2769000	1223	1234	0		File: "Z:\CORE\R…
	1.0	(R)GELANEVK(V)	99%	39.2	44.7	7.4	2		430.23	858.44	2	-0.00028	-0.33	1700	5424000	1227	1234	0		File: "Z:\CORE\R…
	1.0	(R)GELANEVK(V)	98%	32.5	44.7	10.3	2		430.23	858.44	2	-0.00034	-0.40	1720	2984000	1227	1234	0		File: "Z:\CORE\R…
	1.0	(K)KVEAQLQEL(Q)	100%	44.5	45.4	0.0	2		529.30	1,056.58	2	-0.00052	-0.49	2100	2.049E7	1249	1257	0		File: "Z:\CORE\R…
	1.0	(K)KVEAQLQEL(Q)	99%	43.5	45.2	0.0	2		529.30	1,056.58	2	0.000098	0.093	2120	1651000	1249	1257	0		File: "Z:\CORE\R…
	1.0	(R)VRTELADK(V)	99%	37.1	45.1	9.6	2		466.26	930.51	2	-0.00042	-0.45	1530	4148000	1267	1274	0		File: "Z:\CORE\R…
	1.0	(F)SALESQLQDTQEL(L)	98%	57.2	47.9	10.7	2	Deamidated (+1)	731.86	1,461.70	2	0.017	12	2330	6031000	1304	1316	0		File: "Z:\CORE\R…
	1.0	(L)ESQLQDTQEL(L)	100%	50.0	47.1	19.8	2		595.78	1,189.55	2	-0.00072	-0.61	2110	3108000	1307	1316	5	P35580,P35…	File: "Z:\CORE\R…
	1.0	(L)ESQLQDTQEL(L)	100%	45.2	47.1	21.6	2		595.78	1,189.55	2	-0.0012	-1.0	2090	4488000	1307	1316	5	P35580,P35…	File: "Z:\CORE\R…
	1.0	(L)ESQLQDTQELL(Q)	99%	59.3	48.2	16.5	2		652.32	1,302.63	2	0.0039	3.0	2400	7273000	1307	1317	5	P35580,P35…	File: "Z:\CORE\R…
	1.0	(L)QDTQELLQEENR(Q)	100%	105.4	47.9	8.4	2		751.86	1,501.70	2	-0.0042	-2.8	1910	2471000	1311	1322	0		File: "Z:\CORE\R…
	1.0	(K)LKQVEDEK(N)	99%	59.9	46.3	0.0	2		494.77	987.52	2	-0.00058	-0.59	1420	1575000	1331	1338	0		File: "Z:\CORE\R…
	1.0	(L)HAQVADMK(K)	99%	47.8	43.1	30.7	2		450.22	898.43	2	-0.00076	-0.85	1510	1444000	1363	1370	0		File: "Z:\CORE\R…
	1.0	(L)HAQVADMK(K)	99%	43.0	43.8	26.0	2	Oxidation (+16)	458.22	914.43	2	-0.00050	-0.54	1290	1.02E7	1363	1370	0		File: "Z:\CORE\R…
	1.0	(L)HAQVADMK(K)	99%	42.3	43.4	25.3	2	Oxidation (+16)	458.22	914.43	2	-0.00068	-0.74	1310	1570000	1363	1370	0		File: "Z:\CORE\R…
	1.0	(L)HAQVADMK(K)	99%	35.9	43.4	19.6	2	Oxidation (+16)	458.22	914.43	2	-0.00080	-0.87	1490	2591000	1363	1370	0		File: "Z:\CORE\R…
	1.0	(L)HAQVADMK(K)	99%	39.7	43.4	28.2	2	Oxidation (+16)	458.22	914.43	2	-0.0015	-1.6	1340	296000	1363	1370	0		File: "Z:\CORE\R…
	1.0	(L)HAQVADMK(K)	96%	33.1	43.4	23.6	2	Oxidation (+16)	458.22	914.43	2	-0.0011	-1.2	1370	172300	1363	1370	0		File: "Z:\CORE\R…
	1.0	(K)KMEDSVGCLE(E)	97%	37.1	45.6	26.2	2	Oxidation (+16), …	527.73	1,053.45	2	-0.0020	-1.9	1890	1055000	1372	1380	0		File: "Z:\CORE\R…
	1.0	(K)KMEDSVGCLETAEEVK(R)	100%	143.8	48.1	115.5	2	Oxidation (+16), …	920.92	1,839.83	2	0.0044	2.4	1900	1462000	1372	1387	0		File: "Z:\CORE\R…
	1.0	(K)KMEDSVGCLETAEEVK(R)	100%	123.9	48.0	96.7	2	Carbamidomethyl…	912.92	1,823.83	2	-0.0011	-0.59	2000	642800	1372	1387	0		File: "Z:\CORE\R…
	1.0	(K)KMEDSVGCLETAEEVK(R)	100%	80.9	48.1	65.8	2	Oxidation (+16), …	614.28	1,839.82	3	-0.0011	-0.62	1900	8513000	1372	1387	0		File: "Z:\CORE\R…
	1.0	(K)KMEDSVGCLETAEEVK(R)	100%	61.1	48.0	47.9	2	Carbamidomethyl…	608.95	1,823.83	3	-0.0029	-1.6	2000	8237000	1372	1387	0		File: "Z:\CORE\R…
	1.0	(K)MEDSVGCLETAEEVK(R)	100%	100.9	47.5	68.6	2	Carbamidomethyl…	848.87	1,695.73	2	-0.0013	-0.76	2100	5885000	1373	1387	0		File: "Z:\CORE\R…
	1.0	(K)MEDSVGCLETAEEVK(R)	100%	98.1	47.4	73.8	2	Oxidation (+16), …	856.87	1,711.73	2	-0.0027	-1.6	2030	7240000	1373	1387	0		File: "Z:\CORE\R…
	1.0	(K)MEDSVGCLETAEEVKR(K)	100%	92.9	47.9	82.2	2	Carbamidomethyl…	618.28	1,851.83	3	-0.0013	-0.72	1970	4923000	1373	1388	0		File: "Z:\CORE\R…
	1.0	(K)MEDSVGCLETAEEVKR(K)	100%	75.0	47.8	63.8	2	Oxidation (+16), …	623.62	1,867.83	3	-0.0016	-0.86	1900	4964000	1373	1388	0		File: "Z:\CORE\R…
	1.0	(K)MEDSVGCLETAEEVKR(K)	100%	118.3	47.9	103.6	2	Oxidation (+16), …	934.92	1,867.83	2	-0.0021	-1.1	1900	616100	1373	1388	0		File: "Z:\CORE\R…
	1.0	(K)MEDSVGCLETAEEVKR(K)	100%	95.1	47.9	79.1	2	Carbamidomethyl…	926.92	1,851.83	2	-0.0041	-2.2	1970	735000	1373	1388	0		File: "Z:\CORE\R…
	1.0	(K)DLEGLSQR(H)	99%	42.2	45.6	12.7	2		459.24	916.46	2	0.000078	0.085	1920	7178000	1393	1400	0		File: "Z:\CORE\R…
	1.0	(L)LVDLDHQR(Q)	99%	51.5	44.3	5.6	2		498.27	994.52	2	0.00028	0.28	1750	898300	1426	1433	0		File: "Z:\CORE\R…
	1.0	(R)QSACNLEK(K)	99%	67.8	44.4	39.3	2	Carbamidomethyl…	475.22	948.43	2	-0.00058	-0.61	1480	4474000	1434	1441	0		File: "Z:\CORE\R…
	0.6	(F)DQLLAEEK(T)	99%	48.4	45.7	10.0	2		473.25	944.48	2	-0.00062	-0.66	1860	8720000	1447	1454	6	P35580,P35…	File: "Z:\CORE\R…
	0.6	(F)DQLLAEEK(T)	96%	34.6	45.9	3.7	2		473.25	944.48	2	0.00036	0.38	1880	1991000	1447	1454	6	P35580,P35…	File: "Z:\CORE\R…
	1.0	(R)ALEEAMEQK(A)	100%	64.2	45.9	3.1	2	Oxidation (+16)	532.75	1,063.49	2	-0.00024	-0.22	1510	1.652E7	1484	1492	0		File: "Z:\CORE\R…
	1.0	(R)ALEEAMEQK(A)	100%	57.8	45.9	0.0	2	Oxidation (+16)	532.75	1,063.49	2	-0.00036	-0.34	1530	4291000	1484	1492	0		File: "Z:\CORE\R…
	1.0	(R)ALEEAMEQK(A)	100%	69.5	46.4	0.0	2		524.75	1,047.49	2	0.0011	1.1	1770	8832000	1484	1492	0		File: "Z:\CORE\R…
	1.0	(R)ALEEAMEQK(A)	100%	51.1	45.7	5.4	2	Oxidation (+16)	532.75	1,063.48	2	-0.0019	-1.8	1780	2774000	1484	1492	0		File: "Z:\CORE\R…
	1.0	(R)ALEEAMEQK(A)	99%	43.2	45.9	10.1	2	Oxidation (+16)	532.75	1,063.49	2	0.0000…	0.0029	1550	2288000	1484	1492	0		File: "Z:\CORE\R…
	1.0	(F)RTEMEDLMSSK(D)	100%	68.5	47.1	50.7	2	Oxidation (+16), …	453.54	1,357.58	3	-0.0011	-0.83	1460	2124000	1503	1513	0		File: "Z:\CORE\R…
	1.0	(F)RTEMEDLMSSK(D)	100%	41.0	47.6	28.7	2	Oxidation (+16)	448.20	1,341.59	3	-0.0012	-0.89	1700	3362000	1503	1513	0		File: "Z:\CORE\R…
	1.0	(F)RTEMEDLMSSK(D)	100%	39.0	47.1	17.3	2	Oxidation (+16), …	453.54	1,357.58	3	-0.0010	-0.76	1480	440400	1503	1513	0		File: "Z:\CORE\R…
	1.0	(R)TEMEDLMSSK(D)	100%	49.6	45.5	38.8	2	Oxidation (+16), …	601.75	1,201.48	2	-0.00079	-0.66	1510	759700	1504	1513	0		File: "Z:\CORE\R…
	1.0	(R)TEMEDLMSSK(D)	100%	40.7	45.5	27.9	2	Oxidation (+16), …	601.75	1,201.48	2	-0.00065	-0.54	1530	364900	1504	1513	0		File: "Z:\CORE\R…
	1.0	(R)TEMEDLMSSK(D)	99%	41.2	46.1	27.5	2	Oxidation (+16)	593.75	1,185.49	2	0.00072	0.61	1770	4851000	1504	1513	0		File: "Z:\CORE\R…
	1.0	(R)TEMEDLMSSKDDWGK(S)	100%	63.5	47.3	58.3	2	Oxidation (+16), …	572.91	1,715.72	3	-0.0011	-0.65	1580	2310000	1504	1518	0		File: "Z:\CORE\R…
	1.0	(R)TEMEDLMSSKDDWGK(S)	95%	40.5	47.2	30.5	2	Oxidation (+16), …	858.87	1,715.72	2	-0.0037	-2.2	1580	241100	1504	1518	0		File: "Z:\CORE\R…
	1.0	(K)RALEQQVEEMK(T)	100%	39.5	48.0	21.5	2		454.23	1,359.68	3	-0.0022	-1.6	1840	1611000	1528	1538	0		File: "Z:\CORE\R…
	1.0	(K)RALEQQVEEMK(T)	97%	39.6	48.0	11.1	2		680.85	1,359.68	2	-0.0021	-1.5	1830	978100	1528	1538	0		File: "Z:\CORE\R…
	1.0	(R)ALEQQVEEMK(T)	100%	58.3	47.7	34.6	2		602.80	1,203.58	2	-0.00074	-0.62	1950	4.035E7	1529	1538	0		File: "Z:\CORE\R…
	1.0	(R)ALEQQVEEMK(T)	100%	50.4	47.5	37.8	2	Oxidation (+16)	610.79	1,219.57	2	-0.00066	-0.54	1700	1.196E7	1529	1538	0		File: "Z:\CORE\R…
	1.0	(R)ALEQQVEEMK(T)	100%	50.7	47.7	28.5	2		602.80	1,203.58	2	-0.0012	-1.0	1970	2477000	1529	1538	0		File: "Z:\CORE\R…
	1.0	(R)ALEQQVEEMK(T)	99%	38.8	47.7	27.6	2	Oxidation (+16)	610.79	1,219.57	2	-0.0013	-1.0	1760	1094000	1529	1538	0		File: "Z:\CORE\R…
	1.0	(R)ALEQQVEEMK(T)	97%	33.0	47.5	21.0	2	Oxidation (+16)	610.79	1,219.58	2	-0.00042	-0.34	1720	8412000	1529	1538	0		File: "Z:\CORE\R…
	1.0	(R)LEVNLQAMIK(A)	100%	68.7	46.4	32.2	2	Oxidation (+16)	531.29	1,060.56	2	-0.00084	-0.79	1960	4220000	1558	1566	0		File: "Z:\CORE\R…
	1.0	(R)EMEAELEDER(K)	100%	65.8	46.1	33.2	2		625.76	1,249.51	2	-0.0023	-1.8	1880	747200	1593	1602	0		File: "Z:\CORE\R…
	1.0	(K)DLEAHIDSANK(N)	100%	73.7	47.4	3.6	2		606.80	1,211.58	2	-0.00052	-0.43	1760	4353000	1621	1631	0		File: "Z:\CORE\R…
	1.0	(K)DLEAHIDSANK(N)	100%	53.4	47.4	0.3	2	Deamidated (+1)…	606.80	1,211.58	2	-0.0012	-1.0	1780	1163000	1621	1631	0		File: "Z:\CORE\R…
	1.0	(K)DLEAHIDSANK(N)	100%	34.9	47.4	10.9	2		404.87	1,211.58	3	-0.00019	-0.15	1780	3171000	1621	1631	0		File: "Z:\CORE\R…
	1.0	(K)DLEAHIDSANK(N)	100%	32.8	47.4	6.0	2		404.87	1,211.58	3	-0.00037	-0.30	1760	1.299E7	1621	1631	0		File: "Z:\CORE\R…
	1.0	(R)EEILAQAK(E)	99%	58.4	45.2	13.4	2		451.25	900.49	2	0.00064	0.71	1840	4699000	1662	1669	0		File: "Z:\CORE\R…
	1.0	(R)EEILAQAK(E)	99%	54.3	45.1	12.8	2		451.25	900.49	2	-0.000…	-0.047	1820	6364000	1662	1669	0		File: "Z:\CORE\R…
	1.0	(K)SMEAEMIQLQEEL(A)	100%	67.4	47.6	13.4	2	Oxidation (+16), …	791.85	1,581.69	2	-0.0017	-1.1	2380	7280000	1677	1689	0		File: "Z:\CORE\R…
	1.0	(R)QAQQERDELADEIANSSGK(G)	100%	58.6	47.6	21.8	2		697.00	2,087.97	3	-0.0019	-0.89	1950	5736000	1698	1716	0		File: "Z:\CORE\R…
	1.0	(R)QAQQERDELADEIANSSGK(G)	98%	35.0	47.6	17.1	2		1,044.99	2,087.97	2	-0.0016	-0.78	1960	157000	1698	1716	0		File: "Z:\CORE\R…
	1.0	(R)DELADEIANSSGK(G)	100%	67.8	47.5	31.7	2		674.81	1,347.61	2	-0.00084	-0.62	2070	5256000	1704	1716	0		File: "Z:\CORE\R…
	1.0	(R)DELADEIANSSGK(G)	100%	59.5	47.6	20.8	2		674.81	1,347.61	2	-0.0017	-1.3	2050	2.948E7	1704	1716	0		File: "Z:\CORE\R…
	1.0	(R)DELADEIANSSGK(G)	99%	41.3	47.6	11.2	2		674.81	1,347.61	2	-0.00060	-0.45	2100	1882000	1704	1716	0		File: "Z:\CORE\R…
	1.0	(K)GALALEEK(R)	99%	39.2	44.4	0.0	2		415.73	829.46	2	0.00050	0.60	1900	9163000	1717	1724	0		File: "Z:\CORE\R…
	1.0	(K)GALALEEK(R)	98%	38.2	44.4	0.0	2		415.73	829.45	2	-0.0010	-1.2	1920	4382000	1717	1724	0		File: "Z:\CORE\R…
	1.0	(K)KANLQIDQINTDL(N)	100%	67.9	46.9	1.8	2	Deamidated (+1)…	743.40	1,484.78	2	-0.0046	-3.1	2300	3.977E7	1754	1766	0		File: "Z:\CORE\R…
	1.0	(K)VKLQEMEGTVK(S)	100%	48.1	46.7	30.5	2	Oxidation (+16)	426.56	1,276.67	3	-0.00064	-0.50	1630	2627000	1792	1802	0		File: "Z:\CORE\R…
	1.0	(K)LQEMEGTVK(S)	100%	57.4	46.4	31.7	2	Oxidation (+16)	525.76	1,049.51	2	-0.00016	-0.15	1540	3138000	1794	1802	0		File: "Z:\CORE\R…
	1.0	(K)LQEMEGTVK(S)	100%	57.1	46.4	27.5	2		517.76	1,033.51	2	0.00012	0.11	1750	3.583E7	1794	1802	0		File: "Z:\CORE\R…
	1.0	(K)LQEMEGTVK(S)	100%	57.0	46.4	32.0	2	Oxidation (+16)	525.76	1,049.51	2	-0.000…	-0.035	1520	1754000	1794	1802	0		File: "Z:\CORE\R…
	1.0	(K)LQEMEGTVK(S)	100%	44.8	46.3	23.9	2	Oxidation (+16)	525.76	1,049.51	2	-0.00066	-0.63	1570	970700	1794	1802	0		File: "Z:\CORE\R…
	1.0	(K)LQEMEGTVK(S)	100%	48.1	46.4	19.1	2	Oxidation (+16)	525.76	1,049.51	2	-0.000…	-0.035	1740	1193000	1794	1802	0		File: "Z:\CORE\R…
	1.0	(K)LQEMEGTVK(S)	99%	47.8	46.4	25.2	2	Oxidation (+16)	525.76	1,049.51	2	0.0011	1.0	1700	459000	1794	1802	0		File: "Z:\CORE\R…
	1.0	(K)LQEMEGTVK(S)	98%	32.9	46.3	15.8	2	Oxidation (+16)	525.76	1,049.51	2	-0.00090	-0.85	1640	469700	1794	1802	0		File: "Z:\CORE\R…
	1.0	(K)LQEMEGTVK(S)	96%	35.0	46.3	13.0	2	Oxidation (+16)	525.76	1,049.51	2	0.00056	0.54	1590	468800	1794	1802	0		File: "Z:\CORE\R…
	1.0	(Y)KASITALEAK(I)	96%	33.5	43.3	8.3	2		516.31	1,030.60	2	-0.0018	-1.7	1800	6114000	1806	1815	0		File: "Z:\CORE\R…
	1.0	(K)ASITALEAK(I)	100%	59.2	43.6	17.9	2		452.26	902.51	2	-0.000…	-0.0021	1950	1.218E7	1807	1815	0		File: "Z:\CORE\R…
	1.0	(K)IAQLEEQLDNETK(E)	100%	62.5	48.0	13.9	2		510.93	1,529.76	3	-0.0021	-1.4	2060	1.357E7	1816	1828	0		File: "Z:\CORE\R…
	1.0	(K)IAQLEEQLDNETK(E)	100%	90.6	47.9	0.0	2		765.89	1,529.76	2	-0.0012	-0.81	2100	878600	1816	1828	0		File: "Z:\CORE\R…
	1.0	(K)IAQLEEQLDNETK(E)	100%	91.2	47.9	0.0	2		765.89	1,529.76	2	-0.0017	-1.1	2080	3611000	1816	1828	0		File: "Z:\CORE\R…
	1.0	(K)IAQLEEQLDNETK(E)	100%	83.3	48.0	5.4	2		765.88	1,529.75	2	-0.0033	-2.2	2060	1.186E7	1816	1828	0		File: "Z:\CORE\R…
	1.0	(K)DVLLQVDDER(R)	100%	61.4	46.9	41.7	2		601.31	1,200.60	2	-0.00050	-0.42	2200	9910000	1846	1855	0		File: "Z:\CORE\R…
	1.0	(K)RQLEEAEEEEAQR(A)	100%	53.2	47.7	7.6	2		496.57	1,486.70	3	-0.00071	-0.48	1610	4265000	1877	1888	0		File: "Z:\CORE\R…
	1.0	(R)QLEEAEEEEAQR(A)	100%	76.2	47.1	14.8	2		666.31	1,330.60	2	-0.00096	-0.72	1660	4576000	1878	1888	0		File: "Z:\CORE\R…
	1.0	(R)ELEDATETADAMNR(E)	100%	51.1	47.0	0.0	2	Oxidation (+16)	527.89	1,580.66	3	0.00011	0.068	1710	3306000	1899	1912	0		File: "Z:\CORE\R…
	1.0	(R)ELEDATETADAMNR(E)	100%	73.8	47.0	0.0	2	Oxidation (+16)	791.34	1,580.66	2	-0.0014	-0.86	1700	128000	1899	1912	0		File: "Z:\CORE\R…
	1.0	(R)ELEDATETADAMNR(E)	100%	58.3	47.1	0.0	2	Oxidation (+16)	791.34	1,580.66	2	-0.0012	-0.78	1730	212700	1899	1912	0		File: "Z:\CORE\R…

Supplementary figure 3.2. **Mass spectrometry analysis data of myosin-9 in LIM1215 G12D cells.** List of peptides detected in the G12D sample with the high molecular weight unknown band. It was identified as mysoin-9, and modifications are also shown.

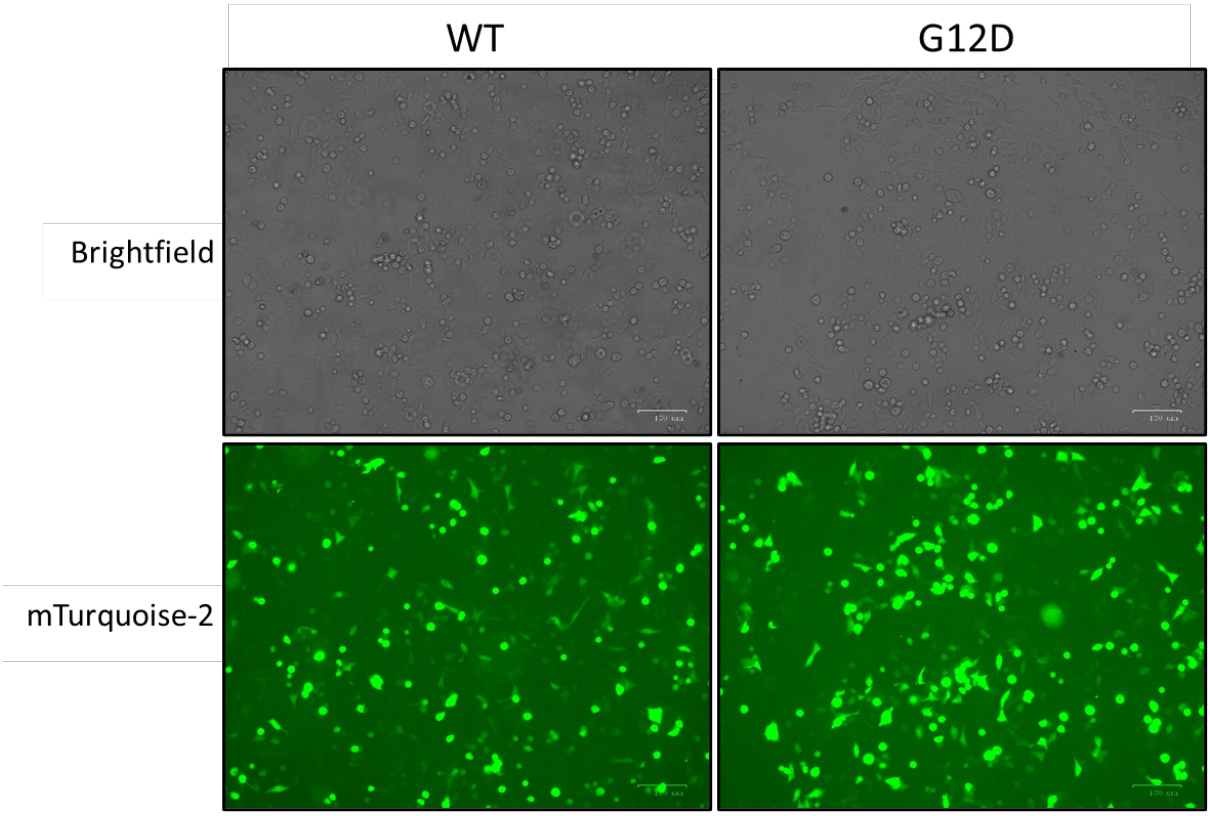

Supplementary figure 3.3. **BRAF overexpression in LIM1215 WT and G12D cells.** LIM1215 WT and G12D cells were transfected with mTourquise-2 plasmid (alongside FLAG-tagged BRAF) to visualise transfection efficiency.

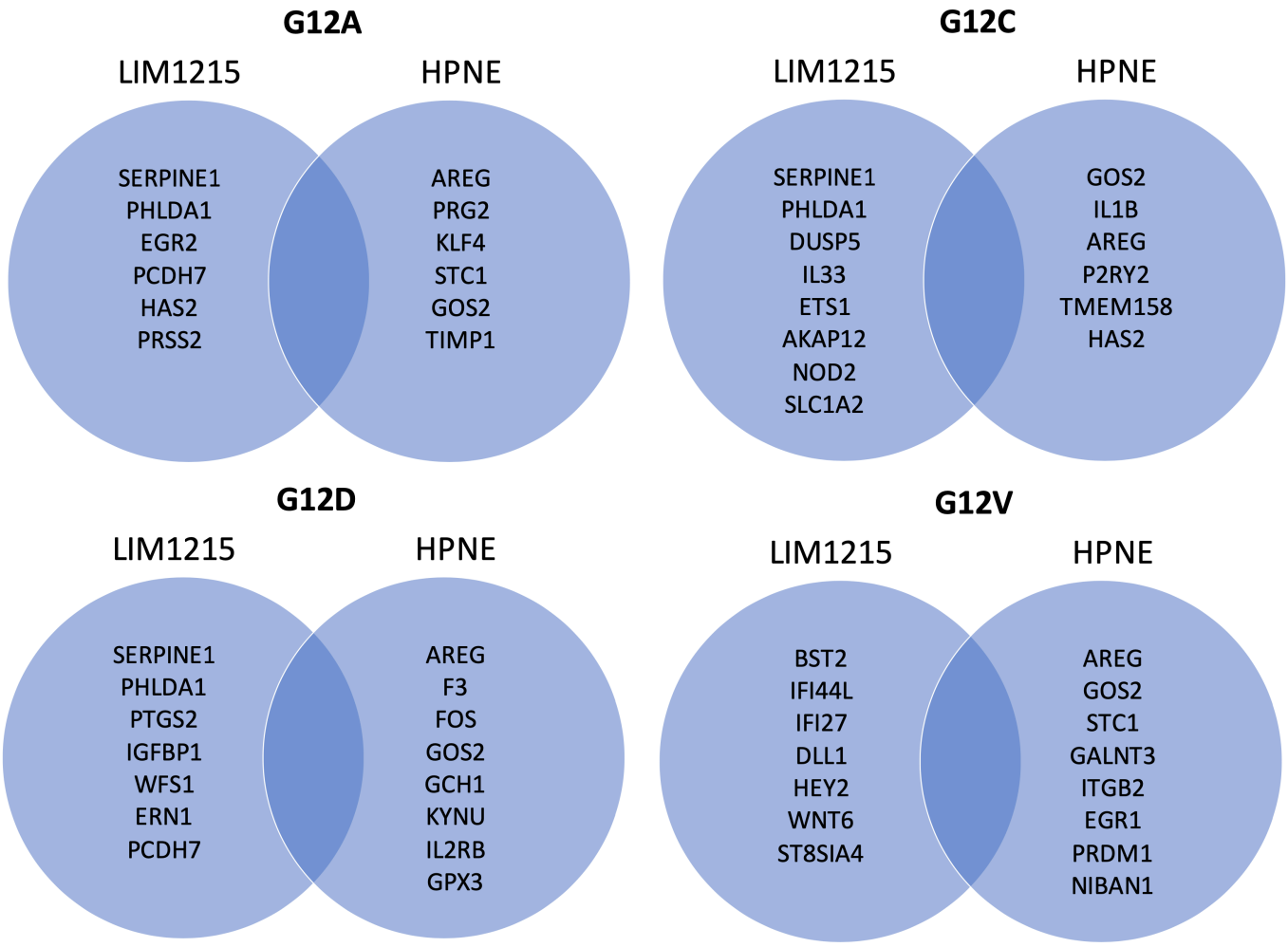

Supplementary figure 4.1. **Comparison of differentially expressed genes between LIM1215 and HPNE mutants.** Venn diagrams comparing the differential regulation of the top three genes from the top three upregulated pathways (ranked by GSEA according to normalised enrichment score) in LIM1215 and HPNE G12A, G12C, G12D and G12V cells. No genes are shared, likely due to a number of reasons: they are different cancer cell lines, one is an overexpression system and the other is not, and the data was obtained from completely different experimental set-ups with different aims.

8. Appendix

Cell line		Tissue of origin	Key endogenous mutations	Supplier
LIM1215	WT	Colon	CTNNB1	Horizon Discovery
	G12A			
	G12C			
	G12D			
	G12V			
SW48	WT	Colon	CTNNB1 FBXW7 EGFR	Horizon Discovery
	G12A			
	G12C			
	G12D			
	G12V			
hTERT-HPNE E6/E7/st	WT*	Pancreas		ATCC
	G12A*			
	G12C*			
	G12D*			
	G12V*			
	G12R*			
	mCherry*			

*the additional doxycycline-inducible myc-tagged copy of KRAS (or mCherry) gene added in-house via lentiviral transfection

Table 6.1. **List of cell lines used.** The cell lines used in my project, along with tissue of origin, key mutations and supplier, are shown in this table. LIM1215 and SW48 cells have heterozygous knock-in mutations of KRAS. HPNE cells have a third copy introduced in-house.

9. Bibliography

Abankwa, D. *et al.* (2008) 'A novel switch region regulates H-ras membrane orientation and signal output', *EMBO Journal*, 27(5), pp. 727–735. doi: 10.1038/emboj.2008.10.

Abankwa, D., Gorfe, A. A. and Hancock, J. F. (2008) 'Mechanisms of Ras membrane organization and signalling: Ras on a rocker', *Cell Cycle*, 7(17), pp. 2667–2673. doi: 10.4161/cc.7.17.6596.

Abe, J. I. *et al.* (1996) 'Big mitogen-activated protein kinase 1 (BMK1) is a redox-sensitive kinase', *Journal of Biological Chemistry*. Â© 1996 ASBMB. Currently published by Elsevier Inc; originally published by American Society for Biochemistry and Molecular Biology., 271(28), pp. 16586–16590. doi: 10.1074/jbc.271.28.16586.

Adler, V. *et al.* (2008) 'Site-specific phosphorylation of raf in cells containing oncogenic ras-p21 is likely mediated by jun-N-terminal kinase', *Annals of Clinical and Laboratory Science*, 38(1), pp. 47–56.

Aebersold, D. M. *et al.* (2004) 'Extracellular Signal-Regulated Kinase 1c (ERK1c), a Novel 42-Kilodalton ERK, Demonstrates Unique Modes of Regulation, Localization, and Function', *Molecular and Cellular Biology*, 24(22), pp. 10000–10015. doi: 10.1128/mcb.24.22.10000-10015.2004.

Aghazadeh, B. *et al.* (1998) 'Structure and mutagenesis of the Dbl homology domain', *Nature Structural Biology*, 5(12), pp. 1098–1107. doi: 10.1038/4209.

Ahearn, I. M. *et al.* (2012) 'Regulating the regulator: Post-translational modification of RAS', *Nature Reviews Molecular Cell Biology*. Nature Publishing Group, 13(1), pp. 39–51. doi: 10.1038/nrm3255.

Ahearn, I., Zhou, M. and Philips, M. R. (2018) 'Posttranslational Modifications of RAS Proteins', *Cold Spring Harbor perspectives in medicine*, 8(11), pp. 1–17. doi: 10.1101/cshperspect.a031484.

Ahn, N. G. *et al.* (1991) 'Multiple components in an epidermal growth factor-stimulated protein kinase cascade: In vitro activation of a myelin basic protein/microtubule-associated protein 2 kinase', *Journal of Biological Chemistry*, 266(7), pp. 4220–4227. doi: 10.1016/S0021-9258(20)64310-1.

Ahrendt, S. A. *et al.* (2001) 'Cigarette smoking is strongly associated with mutation of the K-ras gene in patients with primary adenocarcinoma of the lung', *Cancer*, 92(6), pp. 1525–1530. doi: 10.1002/1097-0142(20010915)92:6<1525::AID-CNCR1478>3.0.CO;2-H.

Akhtar, M. J. *et al.* (2014) 'Targeted anticancer therapy: Overexpressed receptors and nanotechnology', *Clinica Chimica Acta*. Elsevier B.V., 436, pp. 78–92. doi: 10.1016/j.cca.2014.05.004.

Aksamitiene, E., Kiyatkin, A. and Kholodenko, B. N. (2012) 'Cross-talk between mitogenic Ras/MAPK and survival PI3K/Akt pathways: a fine balance', *Biochemical Society Transactions*, 40(1), pp. 139–146. doi: 10.1042/BST20110609.

Akula, S. M., Ruvolo, P. P. and McCubrey, J. A. (2020) 'TP53/miR-34a-associated signaling targets SERPINE1 expression in human pancreatic cancer', *Aging*, 12(3), pp. 2777–2797. doi: 10.18632/aging.102776.

Albright, C. F. *et al.* (1993) 'Characterization of a guanine nucleotide dissociation stimulator for a ras-related GTPase', *EMBO Journal*, 12(1), pp. 339–347. doi: 10.1002/j.1460-2075.1993.tb05662.x.

Alessi, D. R. *et al.* (1994) 'Identification of the sites in MAP kinase kinase-1 phosphorylated by p74(raf-1)', *EMBO Journal*, 13(7), pp. 1610–1619. doi: 10.1002/j.1460-2075.1994.tb06424.x.

Alessi, D. R. *et al.* (1995) 'PD 098059 is a specific inhibitor of the activation of mitogen-activated protein kinase kinase in vitro and in vivo', *Journal of Biological Chemistry*. Â© 1995 ASBMB. Currently published by Elsevier Inc; originally published by American Society for Biochemistry and Molecular Biology., 270(46), pp. 27489–27494. doi: 10.1074/jbc.270.46.27489.

Alessi, D. R. *et al.* (1996) 'Mechanism of activation of protein kinase B by insulin and IGF-1', *EMBO Journal*, 15(23), pp. 6541–6551. doi: 10.1002/j.1460-2075.1996.tb01045.x.

Allegra, C. J. *et al.* (2016) 'Extended RAS gene mutation testing in metastatic colorectal carcinoma to predict response to anti-epidermal growth factor receptor monoclonal antibody therapy: American society of clinical oncology provisional clinical opinion update 2015', *Journal of Clinical Oncology*, 34(2), pp. 179–185. doi: 10.1200/JCO.2015.63.9674.

Amendola, C. R. *et al.* (2019) 'KRAS4A directly regulates hexokinase 1', *Nature*. Springer US, 576(7787), pp. 482–486. doi: 10.1038/s41586-019-1832-9.

Amgen (2019a) *Amgen Announces New Clinical Data Evaluating Novel Investigational KRAS(G12C) Inhibitor In Larger Patient Group At WCLC 2019*. Available at: https://www.amgen.com/newsroom/press-releases/2019/09/amgen-announces-new-clinical-data-evaluating-novel-investigational-krasg12c-inhibitor-in-larger-patient-group-at-wclc-2019 (Accessed: 4 April 2021).

Amgen (2019b) *Amgen Announces New Clinical Data Evaluating Novel Investigational KRAS(G12C) Inhibitor In Patients With Solid Tumors At ESMO 2019*. Available at: https://www.amgen.com/newsroom/press-releases/2019/09/amgen-announces-new-clinical-data-evaluating-novel-investigational-krasg12c-inhibitor-in-patients-with-solid-tumors-at-esmo-2019

(Accessed: 4 April 2021).

Amin, A. R. M. R. *et al.* (2015) 'Evasion of anti-growth signaling: A key step in tumorigenesis and potential target for treatment and prophylaxis by natural compounds', *Seminars in Cancer Biology*. Elsevier Ltd, 35 Suppl, pp. S55–S77. doi: 10.1016/j.semcancer.2015.02.005.

Andjelković, M. *et al.* (1997) 'Role of translocation in the activation and function of protein kinase B', *Journal of Biological Chemistry*. Â© 1997 ASBMB. Currently published by Elsevier Inc; originally published by American Society for Biochemistry and Molecular Biology., 272(50), pp. 31515–31524. doi: 10.1074/jbc.272.50.31515.

Ando, R., Mizuno, H. and Miyawaki, A. (2004) 'Regulated fast nucleocytoplasmic shuttling observed by reversible protein highlighting', *Science*, 306(5700), pp. 1370–1373. doi: 10.1126/science.1102506.

Aoki, K. *et al.* (2011) 'Processive phosphorylation of ERK MAP kinase in mammalian cells', *Proceedings of the National Academy of Sciences of the United States of America*, 108(31), pp. 12675–12680. doi: 10.1073/pnas.1104030108.

Aoki, Y. *et al.* (2005) 'Germline mutations in HRAS proto-oncogene cause Costello syndrome', *Nature Genetics*, 37(10), pp. 1038–1040. doi: 10.1038/ng1641.

Apolloni, A. *et al.* (2000) 'H-ras but Not K-ras Traffics to the Plasma Membrane through the Exocytic Pathway', *Molecular and Cellular Biology*, 20(7), pp. 2475–2487. doi: 10.1128/mcb.20.7.2475-2487.2000.

Ascierto, P. A. *et al.* (2013) 'MEK162 for patients with advanced melanoma harbouring NRAS or Val600 BRAF mutations: A non-randomised, open-label phase 2 study', *The Lancet Oncology*. Elsevier Ltd, 14(3), pp. 249–256. doi: 10.1016/S1470-2045(13)70024-X.

AstraZeneca.com (2020) *Koselugo (selumetinib) approved in US for paediatric patients with neurofibromatosis type 1 plexiform neurofibromas*. Available at: https://www.astrazeneca.com/media-centre/press-releases/2020/koselugo-selumetinib-approved-in-us-for-paediatric-patients-with-neurofibromatosis-type-1-plexiform-neurofibromas.html (Accessed: 5 December 2021).

Backer, J. M. *et al.* (1992) 'Phosphatidylinositol 3'-kinase is activated by association with IRS-1 during insulin stimulation', *EMBO Journal*, 11(9), pp. 3469–3479. doi: 10.1002/j.1460-2075.1992.tb05426.x.

Bader, A. G. *et al.* (2005) 'Oncogenic PI3K deregulates transcription and translation', *Nature Reviews Cancer*, 5(12), pp. 921–929. doi: 10.1038/nrc1753.

Baines, A. T., Xu, D. and Der, C. J. (2011) 'Inhibition of Ras for cancer treatment: the search continues', *Future Med Chem*, 3(14), pp. 1787–1808. doi: 10.4155/fmc.11.121.Inhibition.

Baitei, E. Y. *et al.* (2009) 'Aberrant BRAF splicing as an alternative mechanism for oncogenic B-Raf activation in thyroid carcinoma', *Journal of Pathology*, 217(5), pp. 707–715. doi: 10.1002/path.

Baker, R. *et al.* (2013) 'Differences in the regulation of K-Ras and H-Ras isoforms by monoubiquitination', *Journal of Biological Chemistry*, 288(52), pp. 36856–36862. doi: 10.1074/jbc.C113.525691.

Ballester, R., Furth, M. E. and Rosen, O. M. (1987) 'Phorbol ester- and protein kinase C-mediated phosphorylation of the cellular Kirsten ras gene product.', *Journal of Biological Chemistry*, 262(6), pp. 2688–2695. doi: 10.1016/S0021-9258(18)61562-5.

Barbacid, M. (1987) 'ras GENES', *Annual Review of Biochemistry*, 56, pp. 779–827.

Barnard, D. *et al.* (1998) 'Oncogenes, growth factors and phorbol esters regulate Raf-1 through common mechanisms', *Oncogene*, 17(12), pp. 1539–1547. doi: 10.1038/sj.onc.1202061.

Barnier, J. V. *et al.* (1995) 'The mouse B-raf gene encodes multiple protein isoforms with tissue-specific expression', *Journal of Biological Chemistry*, 270(40), pp. 23381–23389. doi: 10.1074/jbc.270.40.23381.

Beck, T. W. *et al.* (1987) 'The complete coding sequence of the human A-raf-1 oncogene and transforming activity of a human A-raf carrying retrovirus', *Nucleic Acids Research*, 15(2), pp. 595–609.

Bélanger, L.-F. *et al.* (2003) 'Mek2 Is Dispensable for Mouse Growth and Development', *Molecular and Cellular Biology*, 23(14), pp. 4778–4787. doi: 10.1128/mcb.23.14.4778-4787.2003.

Ben-David, U. *et al.* (2018) 'Genetic and transcriptional evolution alters cancer cell line drug response', *Nature*. Springer US, 560(7718), pp. 325–330. doi: 10.1038/s41586-018-0409-3.

Berridge, M. J. (1993) 'Inositol Trisphosphate and Calcium Signalling', *Nature*, 361(6410), pp. 315–325. doi: 10.1530/eje.0.130s0004.

Bery, N., Miller, A. and Rabbitts, T. (2020) 'A potent KRAS macromolecule degrader specifically targeting tumours with mutant KRAS', *Nature Communications*. Springer US, 11(1), p. 3233. doi: 10.1038/s41467-020-17022-w.

Bessard, A. *et al.* (2008) 'RNAi-mediated ERK2 knockdown inhibits growth of tumor cells in vitro and in vivo', *Oncogene*, 27(40), pp. 5315–5325. doi: 10.1038/onc.2008.163.

Bhagwat, S. V *et al.* (2017) 'Discovery of LY3214996, a selective and novel ERK1/2 inhibitor with potent antitumor activities in cancer models with MAPK pathway alterations [abstract].', *Cancer Research*, 77(Suppl. 13), p. 4973. doi: 10.1158/1538-7445.AM2017-4973.

Bivona, T. G. *et al.* (2006) 'PKC regulates a farnesyl-electrostatic switch on K-Ras that promotes its association with Bcl-XL on mitochondria and induces apoptosis', *Molecular Cell*, 21(4), pp. 481–493. doi: 10.1016/j.molcel.2006.01.012.

Blair, H. A. (2021) 'Sotorasib: First Approval', *Drugs*. Springer International Publishing, 81(13), pp. 1573–1579. doi: 10.1007/s40265-021-01574-2.

Blasco, R. B. *et al.* (2011) 'c-Raf, but Not B-Raf, Is Essential for Development of K-Ras Oncogene-Driven Non-Small Cell Lung Carcinoma', *Cancer Cell*, 19(5), pp. 652–663. doi: 10.1016/j.ccr.2011.04.002.

Boeckeler, K. *et al.* (2010) 'Manipulating signal delivery - Plasma-membrane ERK activation in aPKC-dependent migration', *Journal of Cell Science*, 123(16), pp. 2725–2732. doi: 10.1242/jcs.062299.

Boga, S. B. *et al.* (2018) 'MK-8353: Discovery of an Orally Bioavailable Dual Mechanism ERK Inhibitor for Oncology', *ACS Medicinal Chemistry Letters*, 9(7), pp. 761–767. doi: 10.1021/acsmedchemlett.8b00220.

Bond, M. J. *et al.* (2020) 'Targeted Degradation of Oncogenic KRASG12C by VHL-Recruiting PROTACs', *ACS Central Science*, 6(8), pp. 1367–1375. doi: 10.1021/acscentsci.0c00411.

Boni-Schnetzler, M. *et al.* (1988) 'Ligand-dependent intersubunit association within the insulin receptor complex activates its intrinsic kinase activity', *Journal of Biological Chemistry*, 263(14), pp. 6822–6828. doi: 10.1016/S0021-9258(18)68717-4.

Boriack-Sjodin, P. A. *et al.* (1998) 'The structural basis of the activation of Ras by Sos', *Nature*, 394(6691), pp. 337–343. doi: 10.1038/28548.

Botta, G. P. *et al.* (2012) 'Constitutive K-RasG12D Activation of ERK2 Specifically Regulates 3D Invasion of Human Pancreatic Cancer Cells via MMP-1', *Molecular Cancer Research*, 10(2), pp. 183–196. doi: 10.1158/1541-7786.MCR-11-0399.

Boulton, T. G. *et al.* (1991) 'ERKs: A family of protein-serine/threonine kinases that are activated and tyrosine phosphorylated in response to insulin and NGF', *Cell*, 65(4), pp. 663–675. doi: 10.1016/0092-8674(91)90098-J.

Bournet, B. *et al.* (2016) 'KRAS G12D Mutation Subtype Is A Prognostic Factor for Advanced

Pancreatic Adenocarcinoma', *Clinical and Translational Gastroenterology*. Nature Publishing Group, 7(3), p. e157. doi: 10.1038/ctg.2016.18.

Bradley, E. W., Ruan, M. M. and Oursler, M. J. (2008) 'Novel pro-survival functions of the kruppel-like transcription factor Egr2 in promotion of macrophage colony-stimulating factor-mediated osteoclast survival downstream of the MEK/ERK pathway', *Journal of Biological Chemistry*. Â© 2008 ASBMB. Currently published by Elsevier Inc; originally published by American Society for Biochemistry and Molecular Biology., 283(12), pp. 8055–8064. doi: 10.1074/jbc.M709500200.

Brandt, R. *et al.* (2019) 'Cell type-dependent differential activation of ERK by oncogenic KRAS in colon cancer and intestinal epithelium', *Nature Communications*. Springer US, 10(1), p. 2919. doi: 10.1038/s41467-019-10954-y.

Brems, H. *et al.* (2007) 'Germline loss-of-function mutations in SPRED1 cause a neurofibromatosis 1 – like phenotype', *Nature Genetics*, 39(9), pp. 1120–1126. doi: 10.1038/ng2113.

Brightman, F. A. and Fell, D. A. (2000) 'Differential feedback regulation of the MAPK cascade underlies the quantitative differences in EGF and NGF signalling in PC12 cells', *FEBS Letters*, 482(3), pp. 169–174. doi: 10.1016/S0014-5793(00)02037-8.

Bruggeman, F. J. *et al.* (2002) 'Modular response analysis of cellular regulatory networks.', *J Theor Biol*, 218(4), pp. 507–520. doi: 10.1006/yjtbi.3096.

De Bruijn, M. T. *et al.* (2010) 'Oncogenic KRAS sensitises colorectal tumour cells to chemotherapy by p53-dependent induction of Noxa', *British Journal of Cancer*. Nature Publishing Group, 102(8), pp. 1254–1264. doi: 10.1038/sj.bjc.6605633.

Brummer, T. *et al.* (2003) 'Identification of novel ERK-mediated feedback phosphorylation sites at the C-terminus of B-Raf', *Oncogene*, 22(55), pp. 8823–8834. doi: 10.1038/sj.onc.1207185.

Brunelli, L. *et al.* (2014) 'Capturing the metabolomic diversity of KRAS mutants in non-small-cell lung cancer cells', *Oncotarget*, 5(13), pp. 4722–4731. doi: 10.18632/oncotarget.1958.

Brunet, A., Pagès, G. and Pouysségur, J. (1994) 'Growth factor-stimulated MAP kinase induces rapid retrophosphorylation and inhibition of MAP kinase kinase (MEK1)', *FEBS Letters*, 346(2–3), pp. 299–303.

Bryant, K. L. *et al.* (2019) 'Combination of ERK and autophagy inhibition as a treatment approach for pancreatic cancer', *Nature Medicine*. Springer US, 25(April). doi: 10.1038/s41591-019-0368-8.

Buday, L. and Downward, J. (1993) 'Epidermal growth factor regulates p21ras through the formation

of a complex of receptor, Grb2 adapter protein, and Sos nucleotide exchange factor', *Cell*, 73(3), pp. 611–620. doi: 10.1016/0092-8674(93)90146-H.

Buhrman, G. *et al.* (2010) 'Allosteric modulation of Ras positions Q61 for a direct role in catalysis', *Proceedings of the National Academy of Sciences of the United States of America*, 107(11), pp. 4931–4936. doi: 10.1073/pnas.0912226107.

Buhrman, G. *et al.* (2011) 'Analysis of binding site hot spots on the surface of Ras GTPase', *Journal of Molecular Biology*. Elsevier Ltd, 413(4), pp. 773–789. doi: 10.1016/j.jmb.2011.09.011.

Buhrman, G., Wink, G. and Mattos, C. (2007) 'Transformation Efficiency of RasQ61 Mutants Linked to Structural Features of the Switch Regions in the Presence of Raf', *Structure*, 15(12), pp. 1618–1629. doi: 10.1016/j.str.2007.10.011.

Bunda, S. *et al.* (2014) 'Src promotes GTPase activity of Ras via tyrosine 32 phosphorylation', *Proceedings of the National Academy of Sciences of the United States of America*, 111(36), pp. E3785–E3794. doi: 10.1073/pnas.1406559111.

Burd, C. E. *et al.* (2014) 'Mutation-Specific RAS Oncogenicity Explains NRAS Codon 61 Selection in Melanoma', *Cancer Discovery*, 4(12), pp. 1418–1429. doi: 10.1158/2159-8290.CD-14-0729.

Burgess, M. R. *et al.* (2017) 'KRAS Allelic Imbalance Enhances Fitness and Modulates MAP Kinase Dependence in Cancer', *Cell*. Elsevier, 168(5), pp. 817-829.e15. doi: 10.1016/j.cell.2017.01.020.

Buscà, R. *et al.* (2015) 'ERK1 and ERK2 present functional redundancy in tetrapods despite higher evolution rate of ERK1', *BMC Evolutionary Biology*. BMC Evolutionary Biology, 15(1), p. 179. doi: 10.1186/s12862-015-0450-x.

Buscà, R., Pouysségur, J. and Lenormand, P. (2016) 'ERK1 and ERK2 map kinases: Specific roles or functional redundancy?', *Frontiers in Cell and Developmental Biology*, 4(JUN), pp. 1–23. doi: 10.3389/fcell.2016.00053.

Cacace, A. M. *et al.* (1999) 'Identification of constitutive and ras-inducible phosphorylation sites of KSR: implications for 14-3-3 binding, mitogen-activated protein kinase binding, and KSR overexpression', *Molecular and Cellular Biology*, 19(1), pp. 229–240.

Campbell, P. M. *et al.* (2007) 'K-Ras promotes growth transformation and invasion of immortalized human pancreatic cells by raf and phosphatidylinositol 3-kinase signaling', *Cancer Research*, 67(5), pp. 2098–2106. doi: 10.1158/0008-5472.CAN-06-3752.

Canal, F. *et al.* (2011) 'Compartmentalization of the MAPK scaffold protein KSR1 modulates synaptic

plasticity in hippocampal neurons', *FASEB Journal*, 25(7), pp. 2362–2372. doi: 10.1096/fj.10-173153.

Canon, J. *et al.* (2019) 'The clinical KRAS(G12C) inhibitor AMG 510 drives anti-tumour immunity', *Nature*. Springer US, 575(7781), pp. 217–223. doi: 10.1038/s41586-019-1694-1.

Cantor, S. B., Urano, T. and Feig, L. A. (1995) 'Identification and characterization of Ral-binding protein 1, a potential downstream target of Ral GTPases.', *Molecular and Cellular Biology*, 15(8), pp. 4578–4584. doi: 10.1128/mcb.15.8.4578.

Cargnello, M. and Roux, P. P. (2011) 'Activation and Function of the MAPKs and Their Substrates, the MAPK-Activated Protein Kinases', *Microbiology and Molecular Biology Reviews*, 75(1), pp. 50–83. doi: 10.1128/mmbr.00031-10.

Carmo, C. R. *et al.* (2011) 'A novel requirement for Janus Kinases as mediators of drug resistance induced by fibroblast growth factor-2 in human cancer cells', *PLoS ONE*, 6(5). doi: 10.1371/journal.pone.0019861.

Carter, C. A. *et al.* (2016) 'Selumetinib with and without erlotinib in KRAS mutant and KRAS wild-type advanced nonsmall-cell lung cancer', *Annals of Oncology*, 27(4), pp. 693–699. doi: 10.1093/annonc/mdw008.

Carvajal-Vergara, X. *et al.* (2005) 'Multifunctional role of Erk5 in multiple myeloma', *Blood*, 105(11), pp. 4492–4499. doi: 10.1182/blood-2004-08-2985.

Casci, T., Vinós, J. and Freeman, M. (1999) 'Sprouty, an intracellular inhibitor of Ras signaling', *Cell*, 96(5), pp. 655–665. doi: 10.1016/S0092-8674(00)80576-0.

Casey, P. J. *et al.* (1989) 'P21Ras Is Modified By a Farnesyl Isoprenoid', *Proceedings of the National Academy of Sciences of the United States of America*, 86(21), pp. 8323–8327. doi: 10.1073/pnas.86.21.8323.

Casey, P. J. (1992) 'Biochemistry of protein prenylation', *Journal of Lipid Research*. Â© 1992 ASBMB. Currently published by Elsevier Inc; originally published by American Society for Biochemistry and Molecular Biology., 33(12), pp. 1731–1740. doi: 10.1016/S0022-2275(20)41331-8.

Cawthon, R. M. *et al.* (1990) 'Identification and Characterization of Transcripts from the Neurofibromatosis 1 Region : The Sequence and Genomic Structure of EVIZ and Mapping of Other Transcripts', *Genomics*, 7(4), pp. 555–565.

Ceccarelli, F. *et al.* (2020) 'Bringing data from curated pathway resources to Cytoscape with OmniPath', *Bioinformatics*, 36(8), pp. 2632–2633. doi: 10.1093/bioinformatics/btz968.

Ceriani, M. *et al.* (2007) 'Functional analysis of RalGPS2, a murine guanine nucleotide exchange factor for RalA GTPase', *Experimental Cell Research*, 313(11), pp. 2293–2307. doi: 10.1016/j.yexcr.2007.03.016.

Céspedes, M. V. *et al.* (2006) 'K-ras Asp12 mutant neither interacts with Raf, nor signals through Erk and is less tumorigenic than K-ras Val12', *Carcinogenesis*, 27(11), pp. 2190–2200. doi: 10.1093/carcin/bgl063.

Chan, G., Gu, S. and Neel, B. G. (2013) 'Erk1 and Erk2 are required for maintenance of hematopoietic stem cells and adult hematopoiesis', *Blood*, 121(18), pp. 3594–3598. doi: 10.1182/blood-2012-12-476200.

Chandarlapaty, S. (2012) 'Negative feedback and adaptive resistance to the targeted therapy of cancer', *Cancer Discovery*, 2(4), pp. 311–319. doi: 10.1158/2159-8290.CD-12-0018.Negative.

Chardin, P. and Tavitian, A. (1986) 'The ral gene: a new ras related gene isolated by the use of a synthetic probe.', *The EMBO journal*, 5(9), pp. 2203–2208. doi: 10.1002/j.1460-2075.1986.tb04485.x.

Chen, D. S. and Mellman, I. (2017) 'Elements of cancer immunity and the cancer-immune set point', *Nature*, 541(7637), pp. 321–330. doi: 10.1038/nature21349.

Chen, R. H., Sarnecki, C. and Blenis, J. (1992) 'Nuclear localization and regulation of erk- and rsk-encoded protein kinases.', *Molecular and Cellular Biology*, 12(3), pp. 915–927. doi: 10.1128/mcb.12.3.915.

Cherfils, J. *et al.* (1998) 'Structure of the Sec7 domain of the Arf exchange factor ARNO', *Nature*, 392, pp. 101–105.

Cherfils, J. and Chardin, P. (1999) 'GEFs: Structural basis for their activation of small GTP-binding proteins', *Trends in Biochemical Sciences*, 24(8), pp. 306–311. doi: 10.1016/S0968-0004(99)01429-2.

Ching, T., Huang, S. and Garmire, L. X. (2014) 'Power analysis and sample size estimation for RNA-Seq differential expression', *RNA*, 20(11), pp. 1684–1696. doi: 10.1261/rna.046011.114.

Chiu, V. K. *et al.* (2002) 'Ras signalling on the endoplasmic reticulum and the Golgi', *Nature Cell Biology*, 4(5), pp. 343–350. doi: 10.1038/ncb783.

Cho, Y. *et al.* (2009) 'The Basic Helix-Loop-Helix Proteins Differentiated Embryo Chondrocyte (DEC) 1 and DEC2 Function as Corepressors of Retinoid X Receptors', *Molecular Pharmacology*, 76(6), pp. 1360–1369. doi: 10.1124/mol.109.057000.

Chong, H. and Guan, K. (2003) 'Regulation of Raf through Phosphorylation and N Terminus-C

Terminus Interaction', *Journal of Biological Chemistry*. Â© 2003 ASBMB. Currently published by Elsevier Inc; originally published by American Society for Biochemistry and Molecular Biology., 278(38), pp. 36269–36276. doi: 10.1074/jbc.M212803200.

Chong, H., Lee, J. and Guan, K. L. (2001) 'Positive and negative regulation of Raf kinase activity and function by phosphorylation', *EMBO Journal*, 20(14), pp. 3716–3727. doi: 10.1093/emboj/20.14.3716.

Choy, E. *et al.* (1999) 'Endomembrane trafficking of ras: The CAAX motif targets proteins to the ER and Golgi', *Cell*, 98(1), pp. 69–80. doi: 10.1016/S0092-8674(00)80607-8.

Chuderland, D., Konson, A. and Seger, R. (2008) 'Identification and Characterization of a General Nuclear Translocation Signal in Signaling Proteins', *Molecular Cell*, 31(6), pp. 850–861. doi: 10.1016/j.molcel.2008.08.007.

Chuderland, D. and Seger, R. (2005) 'Protein-protein interactions in the regulation of the extracellular signal-regulated kinase', *Molecular Biotechnology*, 29(1), pp. 57–74. doi: 10.1385/MB:29:1:57.

Chung, H. *et al.* (1993) 'Probing the role of loop 2 in Ras function with unnatural amino acids', *PNAS*, 90(November), pp. 10145–10149.

Cirstea, I. C. *et al.* (2010) 'A restricted spectrum of NRAS mutations causes Noonan syndrome', *Nature Genetics*. Nature Publishing Group, 42(1), pp. 27–29. doi: 10.1038/ng.497.

Clarke, S. *et al.* (1988) 'Posttranslational modification of the Ha-ras oncogene protein: Evidence for a third class of protein carboxyl methyltransferases', *Proceedings of the National Academy of Sciences of the United States of America*, 85(13), pp. 4643–4647. doi: 10.1073/pnas.85.13.4643.

Clarke, S. (1992) 'Protein isoprenylation and methylation at carboxyl-terminal cysteine residues', *Annual Review of Biochemistry*, 61, pp. 355–386. doi: 10.1146/annurev.bi.61.070192.002035.

ClinicalTrials.gov (2019) *A Study of LY3009120 in Participants With Advanced Cancer or Cancer That Has Spread to Other Parts of Their Body*. Available at: https://clinicaltrials.gov/ct2/show/NCT02014116 (Accessed: 11 November 2021).

ClinicalTrials.gov (2021a) *A Phase 1/2, Study Evaluating the Safety, Tolerability, PK and Efficacy of AMG 510 in Subjects With Solid Tumors With a Specific KRAS Mutation (CodeBreak 100)*. Available at: https://clinicaltrials.gov/ct2/show/NCT03600883 (Accessed: 4 April 2021).

ClinicalTrials.gov (2021b) *A Phase 2 Study of siG12D LODER in Combination With Chemotherapy in*

Patients With Locally Advanced Pancreatic Cancer. Available at: https://clinicaltrials.gov/ct2/show/NCT01676259 (Accessed: 7 April 2021).

ClinicalTrials.gov (2021c) *A Phase Ib Study of LXH254-centric Combinations in NSCLC or Melanoma*. Available at: https://clinicaltrials.gov/ct2/show/NCT02974725 (Accessed: 7 April 2021).

ClinicalTrials.gov (2021d) *A Study of LY3214996 Administered Alone or in Combination With Other Agents in Participants With Advanced/Metastatic Cancer*. Available at: https://clinicaltrials.gov/ct2/show/NCT02857270 (Accessed: 7 April 2021).

ClinicalTrials.gov (2021e) *Antigen-specific Cancer Immunotherapy (TG01) and Gemcitabine as Adjuvant Therapy in Resected Pancreatic Cancer*. Available at: https://clinicaltrials.gov/ct2/show/NCT02261714 (Accessed: 7 April 2021).

ClinicalTrials.gov (2021f) *Clinical Trial to Evaluate Safety, Tolerability and Pharmacokinetics and Anti-tumor Activity of HM95573*. Available at: https://clinicaltrials.gov/ct2/show/NCT02405065 (Accessed: 6 April 2021).

ClinicalTrials.gov (2021g) *Expansion Study to Evaluate the Efficacy and Safety of HM95573 in BRAF, KRAS or NRAS Mutant Solid Cancers*. Available at: https://clinicaltrials.gov/ct2/show/NCT03118817 (Accessed: 6 April 2021).

ClinicalTrials.gov (2021h) *HM95573 in Combination With Either Cobimetinib or Cetuximab in Patients With Locally Advanced or Metastatic Solid Tumors*. Available at: https://clinicaltrials.gov/ct2/show/NCT03284502 (Accessed: 7 April 2021).

ClinicalTrials.gov (2021i) *Phase I - Escalating Dose Study of siG12D LODER (Local Drug EluteR) in Patients With Locally Advanced Adenocarcinoma of the Pancreas, and a Single Dose Study of siG12D LODER (Local Drug EluteR) in Patients With Non-operable Adenocarcinoma of the Pancreas*. Available at: https://clinicaltrials.gov/ct2/show/NCT01188785 (Accessed: 7 April 2021).

ClinicalTrials.gov (2021j) *Phase I Study of LXH254 in Patients With Advanced Solid Tumors Haboring MAPK Pathway Alterations*. Available at: https://clinicaltrials.gov/ct2/show/NCT02607813 (Accessed: 6 April 2021).

ClinicalTrials.gov (2021k) *Phase II Study of Tipifarnib in Squamous Head and Neck Cancer With HRAS Mutations*. Available at: https://clinicaltrials.gov/ct2/show/NCT02383927 (Accessed: 6 April 2021).

ClinicalTrials.gov (2021l) *Study of MK-8353 + Selumetinib in Advanced/Metastatic Solid Tumors (MK-8353-014)*. Available at: https://clinicaltrials.gov/ct2/show/NCT03745989 (Accessed: 7 April 2021).

ClinicalTrials.gov (2021m) *Study of MK-8353 in Combination With Pembrolizumab (MK-3475) in Participants With Advanced Malignancies (MK-8353-013)*. Available at: https://clinicaltrials.gov/ct2/show/NCT02972034 (Accessed: 7 April 2021).

ClinicalTrials.gov (2021n) *Trametinib and Hydroxychloroquine in Treating Patients With Pancreatic Cancer*. Available at: https://clinicaltrials.gov/ct2/show/NCT03825289 (Accessed: 7 April 2021).

Clough, R. R., Sidhu, R. S. and Bhullar, R. P. (2002) 'Calmodulin binds RalA and RalB and is required for the thrombin-induced activation of Ral in human platelets.', *The Journal of biological chemistry*. Â© 2002 ASBMB. Currently published by Elsevier Inc; originally published by American Society for Biochemistry and Molecular Biology., 277(32), pp. 28972–28980. doi: 10.1074/jbc.M201504200.

Cohen-Armon, M. *et al.* (2007) 'DNA-Independent PARP-1 Activation by Phosphorylated ERK2 Increases Elk1 Activity: A Link to Histone Acetylation', *Molecular Cell*, 25(2), pp. 297–308. doi: 10.1016/j.molcel.2006.12.012.

Coles, L. C. and Shaw, P. E. (2002) 'PAK1 primes MEK1 for phosphorylation by Raf-1 kinase during cross-cascade activation of the ERK pathway', *Oncogene*, 21(14), pp. 2236–2244. doi: 10.1038/sj/onc/1205302.

Cook, J. H. *et al.* (2021) 'The origins and genetic interactions of KRAS mutations are allele- and tissue-specific', *Nature Communications*. Springer US, 12(1). doi: 10.1038/s41467-021-22125-z.

Copeland, T. *et al.* (2001) 'C-TAK1 regulates Ras signaling by phosphorylating the MAPK scaffold, KSR1', *Molecular Cell*, 8(5), pp. 983–993.

Corbalan-Garcia, S. *et al.* (1996) 'Identification of the mitogen-activated protein kinase phosphorylation sites on human Sos1 that regulate interaction with Grb2', *Molecular and Cellular Biology*, 16(10), pp. 5674–5682.

Corchete, L. A. *et al.* (2020) 'Systematic comparison and assessment of RNA-seq procedures for gene expression quantitative analysis', *Scientific Reports*. Nature Publishing Group UK, 10(1), p. 19737. doi: 10.1038/s41598-020-76881-x.

Cordeddu, V. *et al.* (2009) 'Mutation of SHOC2 promotes aberrant protein N-myristoylation and causes Noonan-like syndrome with loose anagen hair', *Nature Genetics*. Nature Publishing Group, 41(9), pp. 1022–1026. doi: 10.1038/ng.425.

Costa, M. *et al.* (2006) 'Dynamic regulation of ERK2 nuclear translocation and mobility in living cells', *Journal of Cell Science*, 119(23), pp. 4952–4963. doi: 10.1242/jcs.03272.

Cox, A. D. *et al.* (2014) 'Drugging the undruggable RAS: Mission Possible?', *Nature Reviews Drug Discovery*. Nature Publishing Group, 13(11), pp. 828–851. doi: 10.1038/nrd4389.

Cox, A. D., Der, C. J. and Philips, M. R. (2015) 'Targeting RAS membrane association: Back to the future for anti-RAS drug discovery?', *Clinical Cancer Research*, 21(8), pp. 1819–1827. doi: 10.1158/1078-0432.CCR-14-3214.

Cruzalegui, F. H., Cano, E. and Treisman, R. (1999) 'ERK activation induces phosphorylation of Elk-1 at multiple S/T-P motifs to high stoichiometry', *Oncogene*, 18(56), pp. 7948–7957. doi: 10.1038/sj.onc.1203362.

Cuesta, C., Arévalo-Alameda, C. and Castellano, E. (2021) 'The importance of being PI3K in the RAS signaling network', *Genes*, 12(7), p. 1094. doi: 10.3390/genes12071094.

Cullis, D. N. *et al.* (2002) 'Rab11-FIP2, an adaptor protein connecting cellular components involved in internalization and recycling of epidermal growth factor receptors', *Journal of Biological Chemistry*. Â© 2002 ASBMB. Currently published by Elsevier Inc; originally published by American Society for Biochemistry and Molecular Biology., 277(51), pp. 49158–49166. doi: 10.1074/jbc.M206316200.

Cutler Jr, R. E. *et al.* (1998) 'Autoregulation of the Raf-1 serine threonine kinase', *PNAS*, 95(16), pp. 9214–9219.

Dance, M. *et al.* (2008) 'The molecular functions of Shp2 in the Ras/Mitogen-activated protein kinase (ERK1/2) pathway', *Cellular Signalling*, 20(3), pp. 453–459. doi: 10.1016/j.cellsig.2007.10.002.

Davis, R. J. (2000) 'Signal transduction by the JNK group of MAP kinases', *Cell*, 103(2), pp. 239–252. doi: 10.1016/S0092-8674(00)00116-1.

Der, C. J., Finkel, T. and Cooper, G. M. (1986) 'Biological and biochemical properties of human rasH genes mutated at codon 61', *Cell*, 44(1), pp. 167–176. doi: 10.1016/0092-8674(86)90495-2.

Dérijard, B. *et al.* (1994) 'JNK1: A protein kinase stimulated by UV light and Ha-Ras that binds and phosphorylates the c-Jun activation domain', *Cell*, 76(6), pp. 1025–1037. doi: 10.1016/0092-8674(94)90380-8.

Desideri, E., Cavallo, A. L. and Baccarini, M. (2015) 'Alike but Different: RAF Paralogs and Their Signaling Outputs', *Cell*. Elsevier Inc., 161(5), pp. 967–970. doi: 10.1016/j.cell.2015.04.045.

Dhillon, A. S. *et al.* (2002) 'Cyclic AMP-Dependent Kinase Regulates Raf-1 Kinase Mainly by Phosphorylation of Serine 259', *Molecular and Cellular Biology*, 22(10), pp. 3237–3246. doi: 10.1128/mcb.22.10.3237-3246.2002.

Dhillon, A. S. *et al.* (2007) 'MAP kinase signalling pathways in cancer', *Oncogene*. doi: 10.1038/sj.onc.1210421.

Diaz, B. *et al.* (1997) 'Phosphorylation of Raf-1 serine 338-serine 339 is an essential regulatory event for Ras-dependent activation and biological signaling.', *Molecular and Cellular Biology*, 17(8), pp. 4509–4516. doi: 10.1128/mcb.17.8.4509.

Digilio, M. C. *et al.* (2002) 'Grouping of Multiple-Lentigines / LEOPARD and Noonan Syndromes on the PTPN11 Gene', *American Journal of Human Genetics*, 71(2), pp. 389–394.

Dombi, E. *et al.* (2016) 'Activity of Selumetinib in Neurofibromatosis Type 1–Related Plexiform Neurofibromas', *New England Journal of Medicine*, 375(26), pp. 2550–2560. doi: 10.1056/nejmoa1605943.

Domenico, M. Di and Giordano, A. (2017) 'Signal transduction growth factors: the effective governance of transcription and cellular adhesion in cancer invasion', *Oncotarget*, 8(22), pp. 36869–36884. doi: 10.1109/TASC.2016.2531580.

Donald Emerson, S. *et al.* (1995) 'Solution Structure of the Ras-Binding Domain of c-Raf-1 and Identification of Its Ras Interaction Surface', *Biochemistry*, 34(21), pp. 6911–6918. doi: 10.1021/bi00021a001.

Dorel, M. *et al.* (2018) 'Modelling signalling networks from perturbation data', *Bioinformatics*, 34(23), pp. 4079–4086. doi: 10.1093/bioinformatics/bty473.

Dougherty, M. K. *et al.* (2005) 'Regulation of Raf-1 by direct feedback phosphorylation', *Molecular Cell*, 17(2), pp. 215–224. doi: 10.1016/j.molcel.2004.11.055.

Douillard, J.-Y. *et al.* (2013) 'Panitumumab–FOLFOX4 Treatment and RAS Mutations in Colorectal Cancer', *New England Journal of Medicine*, 369(11), pp. 1023–1034. doi: 10.1056/nejmoa1305275.

Douville, E. M. *et al.* (1998) 'Murine Ksr interacts with MEK and inhibits Ras-induced transformation', *Current Biology*, 8(1), pp. 46–55.

Downward, J. (2003) 'Targeting RAS signalling pathways in cancer therapy', *Nature Reviews Cancer*, 3(1), pp. 11–22. doi: 10.1038/nrc969.

Downward, J., Warne, P. H. and Viciana, P. R. (1993) 'Direct interaction of Ras and the amino-terminal region of Raf-1 in vitro', *Nature*, 364(July), pp. 352–355.

Du, Z. and Lovly, C. M. (2018) 'Mechanisms of receptor tyrosine kinase activation in cancer', *Molecular Cancer*. Molecular Cancer, 17(58), pp. 1–13.

Dultz, L. A. *et al.* (2013) 'Clinical and therapeutic implications of Sprouty2 feedback dysregulation in BRAF V600E-mutation-positive papillary thyroid cancer', *Surgery (United States)*. Mosby, Inc., 154(6), pp. 1239–1245. doi: 10.1016/j.surg.2013.06.024.

Dumaz, N., Light, Y. and Marais, R. (2002) 'Cyclic AMP Blocks Cell Growth through Raf-1-Dependent and Raf-1-Independent Mechanisms', *Molecular and Cellular Biology*, 22(11), pp. 3717–3728. doi: 10.1128/mcb.22.11.3717-3728.2002.

Dumaz, N. and Marais, R. (2003) 'Protein kinase A blocks Raf-1 activity by stimulating 14-3-3 binding and blocking Raf-1 interaction with Ras', *Journal of Biological Chemistry*. Â© 2003 ASBMB. Currently published by Elsevier Inc; originally published by American Society for Biochemistry and Molecular Biology., 278(32), pp. 29819–29823. doi: 10.1074/jbc.C300182200.

Durrant, D. E. and Morrison, D. K. (2018) 'Targeting the Raf kinases in human cancer: The Raf dimer dilemma', *British Journal of Cancer*. Nature Publishing Group, 118(1), pp. 3–8. doi: 10.1038/bjc.2017.399.

Eblen, S. T. *et al.* (2004) 'Mitogen-activated protein kinase feedback phosphorylation regulates MEK1 complex formation and activation during cellular adhesion', *Molecular and Cellular Biology*, 24(6), pp. 2308–2317. doi: 10.1128/MCB.24.6.2308.

Eerola, I. *et al.* (2003) 'Capillary Malformation–Arteriovenous Malformation, a New Clinical and Genetic Disorder Caused by RASA1 Mutations', *The American Journal of Human Genetics*, 73(6), pp. 1240–1249.

Eferl, R. and Wagner, E. F. (2003) 'AP-1: A double-edged sword in tumorigenesis', *Nature Reviews Cancer*, 3(11), pp. 859–868. doi: 10.1038/nrc1209.

Eggermont, A. M. M. *et al.* (2016) 'Prolonged Survival in Stage III Melanoma with Ipilimumab Adjuvant Therapy', *New England Journal of Medicine*, 375(19), pp. 1845–1855. doi: 10.1056/NEJMoa1611299.Prolonged.

Ehrenreiter, K. *et al.* (2009) 'Raf-1 Addiction in Ras-Induced Skin Carcinogenesis', *Cancer Cell*. Elsevier Ltd, 16(2), pp. 149–160. doi: 10.1016/j.ccr.2009.06.008.

Ekerot, M. *et al.* (2008) 'Negative-feedback regulation of FGF signalling by DUSP6/MKP-3 is driven by ERK1/2 and mediated by Ets factor binding to a conserved site within the DUSP6/MKP-3 gene promoter', *Biochemical Journal*, 412(2), pp. 287–298. doi: 10.1042/BJ20071512.

Engelman, J. A., Luo, J. and Cantley, L. C. (2006) 'The evolution of phosphatidylinositol 3-kinases as regulators of growth and metabolism', *Nature Reviews Genetics*, 7(8), pp. 606–619. doi:

10.1038/nrg1879.

English, J. M. *et al.* (1998) 'Identification of substrates and regulators of the mitogen-activated protein kinase ERK5 using chimeric protein kinases', *Journal of Biological Chemistry*. Â© 1998 ASBMB. Currently published by Elsevier Inc; originally published by American Society for Biochemistry and Molecular Biology., 273(7), pp. 3854–3860. doi: 10.1074/jbc.273.7.3854.

Esteban, L. M. *et al.* (2001) 'Targeted Genomic Disruption of H- ras and N- ras , Individually or in Combination , Reveals the Dispensability of Both Loci for Mouse Growth and Development Targeted Genomic Disruption of H- ras and N- ras , Individually or in Combination , Reveals the Di', 21(5), pp. 1444–1452. doi: 10.1128/MCB.21.5.1444.

Etienne-Manneville, S. and Hall, A. (2002) 'Rho GTPases in cell biology', *Nature*, 420(6916), pp. 629–635. doi: 10.1016/j.febslet.2008.04.039.

Fabian, J. R., Daar, I. O. and Morrison, D. K. (1993) 'Critical tyrosine residues regulate the enzymatic and biological activity of Raf-1 kinase.', *Molecular and Cellular Biology*, 13(11), pp. 7170–7179. doi: 10.1128/mcb.13.11.7170.

Faller, D. V and Rankin, A. M. (2015) 'RAS signaling networks', in Thiagalingam, S. (ed.) *Systems Biology of Cancer*. Cambridge: Cambridge University Press, pp. 183–192. doi: DOI: 10.1017/CBO9780511979811.013.

Fan, Q. *et al.* (2020) 'The ubiquitin system: Orchestrating cellular signals in non-small-cell lung cancer', *Cellular and Molecular Biology Letters*. Cellular & Molecular Biology Letters, 25(1), pp. 1–19. doi: 10.1186/s11658-019-0193-6.

Fantz, D. A. *et al.* (2001) 'Docking Sites on Substrate Proteins Direct Extracellular Signal-regulated Kinase to Phosphorylate Specific Residues', *Journal of Biological Chemistry*. Â© 2001 ASBMB. Currently published by Elsevier Inc; originally published by American Society for Biochemistry and Molecular Biology., 276(29), pp. 27256–27265. doi: 10.1074/jbc.M102512200.

Fares, J. *et al.* (2020) 'Molecular principles of metastasis: a hallmark of cancer revisited', *Signal Transduction and Targeted Therapy*. Springer US, 5(1), p. 28. doi: 10.1038/s41392-020-0134-x.

Farrar, C. T., Halkides, C. J. and Singel, D. J. (1997) 'The frozen solution structure of p21 ras determined by ESEEM spectroscopy reveals weak coordination of Thr35 to the active site metal ion', *Structure*, 5(8), pp. 1055–1066. doi: 10.1016/S0969-2126(97)00257-8.

Farrar, M. A., Alberola-lla, J. and J, R. M. P. (1996) 'Activation of the Raf-1 kinase cascade by coumermycin-induced dimerization', *Nature*, 383(6596), pp. 178–181.

Feig, L. A. and Cooper, G. M. (1988) 'Relationship among guanine nucleotide exchange, GTP hydrolysis, and transforming potential of mutated ras proteins.', *Molecular and Cellular Biology*, 8(6), pp. 2472–2478. doi: 10.1128/mcb.8.6.2472.

Fernald, K. and Kurokawa, M. (2013) 'Evading apoptosis in cancer', *Trends in cell biology*, 23(12), pp. 620–633. doi: 10.1016/j.tcb.2013.07.006.Evading.

Fernández-Medarde, A. and Santos, E. (2011) 'Ras in cancer and developmental diseases', *Genes and Cancer*, 2(3), pp. 344–358. doi: 10.1177/1947601911411084.

Ferrell, J. E. and Bhatt, R. R. (1997) 'Mechanistic studies of the dual phosphorylation of mitogen-activated protein kinase', *Journal of Biological Chemistry*. Â© 1997 ASBMB. Currently published by Elsevier Inc; originally published by American Society for Biochemistry and Molecular Biology., 272(30), pp. 19008–19016. doi: 10.1074/jbc.272.30.19008.

Fidler, I. J. and Kripke, M. L. (1977) 'Metastasis results from preexisting variant cells within a malignant tumor', *Science*, 197(4306), pp. 893–895. doi: 10.1126/science.887927.

Fischer, A. *et al.* (2009) 'Regulation of RAF activity by 14-3-3 proteins: RAF kinases associate functionally with both homo- and heterodimeric forms of 14-3-3 proteins', *Journal of Biological Chemistry*. Â© 2009 ASBMB. Currently published by Elsevier Inc; originally published by American Society for Biochemistry and Molecular Biology., 284(5), pp. 3183–3194. doi: 10.1074/jbc.M804795200.

Fischmann, T. O. *et al.* (2009) 'Crystal structures of MEK1 binary and ternary complexes with nucleotides and inhibitors', *Biochemistry*, 48(12), pp. 2661–2674. doi: 10.1021/bi801898e.

Font, A. *et al.* (2001) 'Kirsten ras mutations in patients with colorectal cancer: the "RASCAL II" study', *British Journal of Cancer*, 85(5), pp. 692–696.

Ford, B. *et al.* (2005) 'Structure of the G60A mutant of Ras: Implications for the dominant negative effect', *Journal of Biological Chemistry*. Â© 2005 ASBMB. Currently published by Elsevier Inc; originally published by American Society for Biochemistry and Molecular Biology., 280(27), pp. 25697–25705. doi: 10.1074/jbc.M502240200.

Ford, B. *et al.* (2006) 'Structure of a transient intermediate for GTP hydrolysis by Ras', *Structure*, 14(3), pp. 427–436. doi: 10.1016/j.str.2005.12.010.

Formstecher, E. *et al.* (2001) 'PEA-15 Mediates Cytoplasmic Sequestration of ERK MAP Kinase', *Developmental Cell*, 1(2), pp. 239–250. doi: 10.1016/S1534-5807(01)00035-1.

Franke, T. F. (2008) 'PI3K/Akt: Getting it right matters', *Oncogene*, 27(50), pp. 6473–6488. doi: 10.1038/onc.2008.313.

Freeman, A. K., Ritt, D. A. and Morrison, D. K. (2013) 'Effects of Raf Dimerization and Its Inhibition on Normal and Disease-Associated Raf Signaling', *Molecular Cell*. Elsevier Inc., 49(4), pp. 751–758. doi: 10.1016/j.molcel.2012.12.018.

Frémin, C. *et al.* (2007) 'ERK2 but not ERK1 plays a key role in hepatocyte replication: An RNAi-mediated ERK2 knockdown approach in wild-type and ERK1 null hepatocytes', *Hepatology*, 45(4), pp. 1035–1045. doi: 10.1002/hep.21551.

Frémin, C. *et al.* (2015) 'Functional redundancy of ERK1 and ERK2 MAP kinases during development', *Cell Reports*, 12(6), pp. 913–921. doi: 10.1016/j.celrep.2015.07.011.

Freshney, N. W. *et al.* (1994) 'Interleukin-1 activates a novel protein kinase cascade that results in the phosphorylation of hsp27', *Cell*, 78(6), pp. 1039–1049. doi: 10.1016/0092-8674(94)90278-X.

Fritsche-Guenther, R. *et al.* (2011) 'Strong negative feedback from Erk to Raf confers robustness to MAPK signalling', *Molecular Systems Biology*, 7(489), pp. 1–13. doi: 10.1038/msb.2011.27.

Frost, J. A. *et al.* (1997) 'Cross-cascade activation of ERKs and ternary complex factors by Rho family proteins', *EMBO Journal*, 16(21), pp. 6426–6438. doi: 10.1093/emboj/16.21.6426.

Fruman, D. A. *et al.* (2017) 'The PI3K Pathway in Human Disease', *Cell*, 170(4), pp. 605–635. doi: 10.1016/j.cell.2017.07.029.

Fukami, K. *et al.* (2010) 'Phospholipase C is a key enzyme regulating intracellular calcium and modulating the phosphoinositide balance', *Progress in Lipid Research*. Elsevier Ltd, 49(4), pp. 429–437. doi: 10.1016/j.plipres.2010.06.001.

Fukuda, M. *et al.* (1996) 'Cytoplasmic localization of mitogen-activated protein kinase kinase directed by its NH2-terminal, leucine-rich short amino acid sequence, which acts as a nuclear export signal', *Journal of Biological Chemistry*. Â© 1996 ASBMB. Currently published by Elsevier Inc; originally published by American Society for Biochemistry and Molecular Biology., 271(33), pp. 20024–20028. doi: 10.1074/jbc.271.33.20024.

Gao, T., Brognard, J. and Newton, A. C. (2008) 'The Phosphatase PHLPP Controls the Cellular Levels of Protein Kinase C', *Journal of Biological Chemistry*. Â© 2008 ASBMB. Currently published by Elsevier Inc; originally published by American Society for Biochemistry and Molecular Biology., 283(10), pp. 6300–6311. doi: 10.1074/jbc.M707319200.

Garassino, M. C. *et al.* (2011) 'Different types of K-Ras mutations could affect drug sensitivity and tumour behaviour in non-small-cell lung cancer', *Annals of Oncology*, 22(1), pp. 235–237. doi: 10.1093/annonc/mdq680.

Garcia-Alonso, L. *et al.* (2018) 'Transcription factor activities enhance markers of drug sensitivity in cancer', *Cancer Research*, 78(3), pp. 769–780. doi: 10.1158/0008-5472.CAN-17-1679.

Gardner, A. M. *et al.* (1994) 'MEK-1 phosphorylation by MEK kinase, Raf, and mitogen-activated protein kinase: Analysis of phosphopeptides and regulation of activity', *Molecular Biology of the Cell*, 5(2), pp. 193–201. doi: 10.1091/mbc.5.2.193.

Garnett, M. J. *et al.* (2005) 'Wild-type and mutant B-RAF activate C-RAF through distinct mechanisms involving heterodimerization', *Molecular Cell*, 20(6), pp. 963–969. doi: 10.1016/j.molcel.2005.10.022.

Gehringer, M. and Laufer, S. A. (2019) 'Emerging and Re-Emerging Warheads for Targeted Covalent Inhibitors: Applications in Medicinal Chemistry and Chemical Biology', *Journal of Medicinal Chemistry*, 62(12), pp. 5673–5724. doi: 10.1021/acs.jmedchem.8b01153.

Gelabert-Baldrich, M. *et al.* (2014) 'Dynamics of KRas on endosomes: Involvement of acidic phospholipids in its association', *FASEB Journal*, 28(7), pp. 3023–3037. doi: 10.1096/fj.13-241158.

Gentile, D. R. *et al.* (2017) 'Ras Binder Induces a Modified Switch-II Pocket in GTP and GDP States', *Cell Chemical Biology*. Elsevier Ltd., 24(12), pp. 1455-1466.e14. doi: 10.1016/j.chembiol.2017.08.025.

Gentry, L. R. *et al.* (2014) 'Ral small GTPase signaling and oncogenesis: More than just 15 minutes of fame', *Biochimica et Biophysica Acta - Molecular Cell Research*. Elsevier B.V., 1843(12), pp. 2976–2988. doi: 10.1016/j.bbamcr.2014.09.004.

Georgescu, M. M. (2010) 'Pten tumor suppressor network in PI3K-Akt pathway control', *Genes and Cancer*, 1(12), pp. 1170–1177. doi: 10.1177/1947601911407325.

Ghosh, S. *et al.* (1994) 'The cysteine-rich region of raf-1 kinase contains zinc, translocates to liposomes, and is adjacent to a segment that binds GTP-ras', *Journal of Biological Chemistry*, 269(13), pp. 10000–10007. doi: 10.1016/s0021-9258(17)36981-8.

Gibbs, J. B. *et al.* (1984) 'Intrinsic GTPase activity distinguishes normal and oncogenic ras p21 molecules', *Proceedings of the National Academy of Sciences of the United States of America*, 81(18), pp. 5704–5708. doi: 10.1073/pnas.81.18.5704.

Gideon, P. *et al.* (1992) 'Mutational and kinetic analyses of the GTPase-activating protein (GAP)-p21

interaction: the C-terminal domain of GAP is not sufficient for full activity', *Molecular and Cellular Biology*, 12(5), pp. 2050–2056. doi: 10.1128/mcb.12.5.2050-2056.1992.

Gimple, R. C. and Wang, X. (2019) 'RAS: Striking at the Core of the Oncogenic Circuitry', *Frontiers in Oncology*, 9(September), pp. 1–16. doi: 10.3389/fonc.2019.00965.

Giroux, S. *et al.* (1999) 'Embryonic death of Mek1-deficient mice reveals a role for this kinase in angiogenesis in the labyrinthine region of the placenta', *Current Biology*, 9(7), pp. 369–376. doi: 10.1016/S0960-9822(99)80164-X.

Gjertsen, M. K. *et al.* (2001) 'Intradermal ras peptide vaccination with granulocyte-macrophage colony-stimulating factor as adjuvant: Clinical and immunological responses in patients with pancreatic adenocarcinoma', *International Journal of Cancer*, 92(3), pp. 441–450. doi: 10.1002/ijc.1205.

Gobinda, S. and Bolander, M. E. (1995) 'Telomeres, Telomerase, and Cancer', *Science*, 268(5214), pp. 1115–1117.

Golan, T. *et al.* (2015) 'RNAi therapy targeting KRAS in combination with chemotherapy for locally advanced pancreatic cancer patients', *Oncotarget*, 6(27), pp. 24560–24570. doi: 10.18632/oncotarget.4183.

Gómez, N. and Cohen, P. (1991) 'Dissection of the protein kinase cascade by which nerve growth factor activates MAP kinases', *Nature*, 353(6340), pp. 170–173. doi: 10.1038/353170a0.

Gonzalez, F. A. *et al.* (1992) 'Heterogeneous expression of four MAP kinase isoforms in human tissues', *FEBS Letters*, 304(2–3), pp. 170–178. doi: 10.1016/0014-5793(92)80612-K.

Good, M. C., Zalatan, J. G. and Lim, W. A. (2011) 'Scaffold proteins: hubs for controlling the flow of cellular information', *Science (New York, N.Y.)*, 332(6030), pp. 680–686. doi: 10.1126/science.1198701.

Goodwin, J. S. *et al.* (2005) 'Depalmitoylated Ras traffics to and from the Golgi complex via a nonvesicular pathway', *Journal of Cell Biology*, 170(2), pp. 261–272. doi: 10.1083/jcb.200502063.

Gorfe, A. A., Grant, B. J. and McCammon, J. A. (2008) 'Mapping the Nucleotide and Isoform-Dependent Structural and Dynamical Features of Ras Proteins', *Structure*, 16(6), pp. 885–896. doi: 10.1016/j.str.2008.03.009.

Goustin, A. S. *et al.* (1986) 'Growth Factors and Cancer', *Cancer Research*, 46(3), pp. 1015–1029.

Grant, B. J. *et al.* (2011) 'Novel allosteric sites on ras for lead generation', *PLoS ONE*, 6(10), pp. 1–10.

doi: 10.1371/journal.pone.0025711.

Grimaldi, A. M. *et al.* (2017) 'MEK Inhibitors in the Treatment of Metastatic Melanoma and Solid Tumors', *American Journal of Clinical Dermatology*. Springer International Publishing, 18(6), pp. 745–754. doi: 10.1007/s40257-017-0292-y.

Gross, A. M. *et al.* (2020) 'Selumetinib in Children with Inoperable Plexiform Neurofibromas', *New England Journal of Medicine*, 382(15), pp. 1430–1442. doi: 10.1056/nejmoa1912735.

Güldenhaupt, J. *et al.* (2012) 'N-Ras forms dimers at POPC membranes', *Biophysical Journal*, 103(7), pp. 1585–1593. doi: 10.1016/j.bpj.2012.08.043.

Guo, Y. *et al.* (2020) 'ERK/MAPK signalling pathway and tumorigenesis (Review)', *Experimental and Therapeutic Medicine*, 19(3), pp. 1997–2007. doi: 10.3892/etm.2020.8454.

Gupta, S. *et al.* (1996) 'Selective interaction of JNK protein kinase isoforms with transcription factors', *EMBO Journal*, 15(11), pp. 2760–2770. doi: 10.1002/j.1460-2075.1996.tb00636.x.

Gurung, A. and Bhattacharjee, A. (2015) 'Significance of Ras Signaling in Cancer and Strategies for its Control', *Oncology & Hematology Review (US)*, 11(2), pp. 147–152. doi: 10.17925/OHR.2015.11.02.147.

Gutierrez, L. *et al.* (1989) 'Post-translational processing of p21(ras) is two-step and involve carboxyl-methylation and carboxy-terminal proteolysis', *EMBO Journal*, 8(4), pp. 1093–1098. doi: 10.1002/j.1460-2075.1989.tb03478.x.

Guy, G. R. *et al.* (2009) 'Sprouty proteins: modified modulators, matchmakers or missing links?', *Journal of Endocrinology*, 203(2), pp. 191–202. doi: 10.1677/JOE-09-0110.

Haar, E. Vander *et al.* (2007) 'Insulin signalling to mTOR mediated by the Akt/PKB substrate PRAS40', *Nature Cell Biology*, 9(3), pp. 316–323. doi: 10.1038/ncb1547.

Haddadi, N. *et al.* (2018) 'PTEN/PTENP1: "Regulating the regulator of RTK-dependent PI3K/Akt signalling", new targets for cancer therapy', *Molecular Cancer*. Molecular Cancer, 17(1), pp. 1–14. doi: 10.1186/s12943-018-0803-3.

Haigis, K. M. *et al.* (2008) 'Differential effects of oncogenic K-Ras and N-Ras on proliferation, differentiation and tumor progression in the colon', *Nature Genetics*, 40(5), pp. 600–608. doi: 10.1038/ng.115.

Haigis, K. M. (2017) 'KRAS Alleles: The Devil Is in the Detail', *Trends in Cancer*. Elsevier Inc., 3(10), pp. 686–697. doi: 10.1016/j.trecan.2017.08.006.

Haling, J. R. *et al.* (2014) 'Structure of the BRAF-MEK Complex Reveals a Kinase Activity Independent Role for BRAF in MAPK Signaling', *Cancer Cell*. Elsevier Inc., 26(3), pp. 402–413. doi: 10.1016/j.ccr.2014.07.007.

Hall, A. (1992) 'Ras-related GTPases and the cytoskeleton', *Molecular Biology of the Cell*, 3(5), pp. 475–479. doi: 10.1091/mbc.3.5.475.

Hallberg, B., Rayter, S. I. and Downward, J. (1994) 'Interaction of Ras and Raf in intact mammalian cells upon extracellular stimulation', *Journal of Biological Chemistry*. © 1994 ASBMB. Currently published by Elsevier Inc; originally published by American Society for Biochemistry and Molecular Biology., 269(6), pp. 3913–3916. doi: 10.1016/s0021-9258(17)41718-2.

Hallin, J. *et al.* (2020) 'The KRASG12C inhibitor MRTX849 provides insight toward therapeutic susceptibility of KRAS-mutant cancers in mouse models and patients', *Cancer Discovery*, 10(1), pp. 54–71. doi: 10.1158/2159-8290.CD-19-1167.

Halliwell, B. and Aruoma, O. I. (1991) 'DNA damage by oxygen-derived species Its mechanism and measurement in mammalian systems', *FEBS Letters*, 281(1–2), pp. 9–19. doi: 10.1016/0014-5793(91)80347-6.

Ham, R. G. and Walthall, B. E. N. J. (1981) 'Multiplication of human diploid fibroblasts in a synthetic medium supplemented with EGF, insulin, and dexamethasone', *Experimental Cell Research*, 134(2), pp. 303–311.

Hammond, D. E. *et al.* (2015) 'Differential reprogramming of isogenic colorectal cancer cells by distinct activating KRAS mutations', *Journal of Proteome Research*, 14(3), pp. 1535–1546. doi: 10.1021/pr501191a.

Hampton, S. E., Dore, T. M. and Schmidt, W. K. (2018) 'Rce1: mechanism and inhibition', *Critical Reviews in Biochemistry and Molecular Biology*, 53(2), pp. 157–174. doi: 10.1080/10409238.2018.1431606.Rce1.

Hanafusa, H. *et al.* (2002) 'Sprouty1 and Sprouty2 provide a control mechanism for the Ras/MAPK signalling pathway', *Nature Cell Biology*, 4(11), pp. 850–858. doi: 10.1038/ncb867.

Hanahan, D. and Weinberg, R. A. (2000) 'The hallmarks of cancer.', *Cell*, 100(1), pp. 57–70. doi: 10.1007/s00262-010-0968-0.

Hanahan, D. and Weinberg, R. A. (2011) 'Hallmarks of cancer: The next generation', *Cell*. doi: 10.1016/j.cell.2011.02.013.

Hancock, J. F. *et al.* (1989) 'All ras proteins are polyisoprenylated but only some are palmitoylated', *Cell*, 57(7), pp. 1167–1177. doi: 10.1016/0092-8674(89)90054-8.

Hancock, J. F. (2003) 'Ras proteins: Different signals from different locations', *Nature Reviews Molecular Cell Biology*, 4(5), pp. 373–384. doi: 10.1038/nrm1105.

Hancock, J. F. and Parton, R. G. (2005) 'Ras plasma membrane signalling platforms', *Biochemical Journal*, 389(1), pp. 1–11. doi: 10.1042/BJ20050231.

Hancock, J. F., Paterson, H. and Marshall, C. J. (1990) 'A polybasic domain or palmitoylation is required in addition to the CAAX motif to localize p21ras to the plasma membrane', *Cell*, 63(1), pp. 133–139. doi: 10.1016/0092-8674(90)90294-O.

Hart, C. E. *et al.* (1988) 'Two classes of PDGF receptor recognize different isoforms of PDGF', *Science*, 240(4858), pp. 1529–1531. doi: 10.1126/science.2836952.

Hatzivassiliou, G. *et al.* (2010) 'RAF inhibitors prime wild-type RAF to activate the MAPK pathway and enhance growth', *Nature*. Nature Publishing Group, 464(7287), pp. 431–435. doi: 10.1038/nature08833.

Hayashi, M. *et al.* (2004) 'Targeted deletion of BMK1/ERK5 in adult mice perturbs vascular integrity and leads to endothelial failure', *Journal of Clinical Investigation*, 113(8), pp. 1138–1148. doi: 10.1172/JCI200419890.

He, J. *et al.* (2021) 'Full Activation of Kinase Protein Kinase B by Phosphoinositide-Dependent Protein Kinase-1 and Mammalian Target of Rapamycin Complex 2 Is Required for Early Natural Killer Cell Development and Survival', *Frontiers in Immunology*, 11(February), pp. 1–13. doi: 10.3389/fimmu.2020.617404.

Heasley, L. E. and Johnson, G. L. (1992) 'The β-PDGF receptor induces neuronal differentiation of PC12 cells', *Molecular Biology of the Cell*, 3(5), pp. 545–553. doi: 10.1091/mbc.3.5.545.

Heasman, S. J. and Ridley, A. J. (2008) 'Mammalian Rho GTPases: New insights into their functions from in vivo studies', *Nature Reviews Molecular Cell Biology*, 9(9), pp. 690–701. doi: 10.1038/nrm2476.

Heidenreich, K. A. and Kummer, J. L. (1996) 'Inhibition of p38 mitogen-activated protein kinase by insulin in cultured fetal neurons', *Journal of Biological Chemistry*. Â© 1996 ASBMB. Currently published by Elsevier Inc; originally published by American Society for Biochemistry and Molecular Biology., 271(17), pp. 9891–9894. doi: 10.1074/jbc.271.17.9891.

Heidorn, S. J. *et al.* (2010) 'Kinase-Dead BRAF and Oncogenic RAS Cooperate to Drive Tumor Progression through CRAF', *Cell*. Elsevier Ltd, 140(2), pp. 209–221. doi: 10.1016/j.cell.2009.12.040.

Heldin, C. H. *et al.* (1988) 'Binding of different dimeric forms of PDGF to human fibroblasts: evidence for two separate receptor types.', *The EMBO journal*, 7(5), pp. 1387–1393. doi: 10.1002/j.1460-2075.1988.tb02955.x.

Heldin, C. H. *et al.* (1989) 'Dimerization of B-type platelet-derived growth factor receptors occurs after ligand binding and is closely associated with receptor kinase activation', *Journal of Biological Chemistry*, 264(15), pp. 8905–8912. doi: 10.1016/S0021-9258(18)81879-8.

Hellmann, M. D. *et al.* (2019) 'Nivolumab plus Ipilimumab in Advanced Non–Small-Cell Lung Cancer', *New England Journal of Medicine*, 381(21), pp. 2020–2031. doi: 10.1056/nejmoa1910231.

Hernandez, M. A. *et al.* (2016) 'Regulation of BRAF protein stability by a negative feedback loop involving the MEK-ERK pathway but not the FBXW7 tumour suppressor', *Cellular Signalling*. The Authors, 28(6), pp. 561–571. doi: 10.1016/j.cellsig.2016.02.009.

Herrmann, C., Martin, G. A. and Wittinghofer, A. (1995) 'Quantitative Analysis of the Complex between p21ras and the Ras-binding Domain of the Human Raf-1 Protein Kinase', *Journal of Biological Chemistry*, 270(7), pp. 2901–2905.

Hillig, R. C. *et al.* (2019) 'Discovery of potent SOS1 inhibitors that block RAS activation via disruption of the RAS–SOS1 interaction', *Proceedings of the National Academy of Sciences of the United States of America*, 116(7), pp. 2551–2560. doi: 10.1073/pnas.1812963116.

Hirschi, B. and Kolligs, F. T. (2013) 'Alternative splicing of BRAF transcripts and characterization of C-terminally truncated B-Raf isoforms in colorectal cancer', *International Journal of Cancer*, 133(3), pp. 590–596. doi: 10.1002/ijc.28061.

Hmitou, I. *et al.* (2007) 'Differential Regulation of B-Raf Isoforms by Phosphorylation and Autoinhibitory Mechanisms', *Molecular and Cellular Biology*, 27(1), pp. 31–43. doi: 10.1128/mcb.01265-06.

Hobbs, G. A. *et al.* (2020) 'Atypical KRAS G12R mutant is impaired in PI3K signaling and macropinocytosis in pancreatic cancer', *Cancer Discovery*, 10(1), pp. 104–123. doi: 10.1158/2159-8290.CD-19-1006.

Hobbs, G. A., Der, C. J. and Rossman, K. L. (2016) 'RAS isoforms and mutations in cancer at a glance', *Journal of Cell Science*, 129(7), pp. 1287–1292. doi: 10.1242/jcs.182873.

Hodge, R. G. and Ridley, A. J. (2016) 'Regulating Rho GTPases and their regulators', *Nature Reviews Molecular Cell Biology*. Nature Publishing Group, 17(8), pp. 496–510. doi: 10.1038/nrm.2016.67.

Hofer, F., Berdeaux, R. and Martin, G. S. (1998) 'Ras-independent activation of Ral by a Ca2+-dependent pathway', *Current Biology*, 8(14), pp. 839–844. doi: 10.1016/s0960-9822(98)70327-6.

Hoo, W. P. Y., Siak, P. Y. and In, L. L. A. (2019) 'Overview of Current Immunotherapies Targeting Mutated KRAS Cancers.', *Current topics in medicinal chemistry*. United Arab Emirates, 19(23), pp. 2158–2175. doi: 10.2174/1568026619666190904163524.

Hood, F. E. *et al.* (2019) 'Isoform-specific Ras signaling is growth factor dependent', *Molecular Biology of the Cell*, 30(9), pp. 1108–1117. doi: 10.1091/mbc.E18-10-0676.

Houot, R. *et al.* (2015) 'T-cell-based immunotherapy: Adoptive cell transfer and checkpoint inhibition', *Cancer Immunology Research*, 3(10), pp. 1115–1122. doi: 10.1158/2326-6066.CIR-15-0190.

Hsieh, C. L., Swaroop, A. and Francke, U. (1990) 'Chromosomal localization and cDNA sequence of human ralB, a GTP binding protein', *Somatic Cell and Molecular Genetics*, 16(4), pp. 407–410. doi: 10.1007/BF01232469.

Hu, C. D. *et al.* (1995) 'Cysteine-rich region of Raf-1 interacts with activator domain of post-translationally modified Ha-Ras', *Journal of Biological Chemistry*. Â© 1995 ASBMB. Currently published by Elsevier Inc; originally published by American Society for Biochemistry and Molecular Biology., 270(51), pp. 30274–30277. doi: 10.1074/jbc.270.51.30274.

Hu, S. *et al.* (2009) 'Profiling the Human Protein-DNA Interactome Reveals ERK2 as a Transcriptional Repressor of Interferon Signaling', *Cell*. Elsevier Ltd, 139(3), pp. 610–622. doi: 10.1016/j.cell.2009.08.037.

Huang, C. *et al.* (1999) 'p38 kinase mediates UV-induced phosphorylation of p53 protein at serine 389', *Journal of Biological Chemistry*. Â© 1999 ASBMB. Currently published by Elsevier Inc; originally published by American Society for Biochemistry and Molecular Biology., 274(18), pp. 12229–12235. doi: 10.1074/jbc.274.18.12229.

Huang, C. H. *et al.* (2007) 'The structure of a human p110α/p85α complex elucidates the effects of oncogenic PI3Kα mutations', *Science*, 318(5857), pp. 1744–1748. doi: 10.1126/science.1150799.

Huang, C. and Tan, T. (2012) 'DUSPs, to MAP kinases and beyond', *Cell and Bioscience*, 2(1), p. 24.

Huang, F. *et al.* (2017) 'PDGF signaling in cancer progression', *International Journal of Clinical and*

Experimental Medicine, 10(7), pp. 9918–9929.

Huang, J. *et al.* (2015) 'Variant profiling of candidate genes in pancreatic ductal adenocarcinoma', *Clinical Chemistry*, 61(11), pp. 1408–1416. doi: 10.1373/clinchem.2015.238543.

Huang, K. P. (1989) 'The mechanism of protein kinase C activation', *Trends in Neurosciences*, 12(11), pp. 425–432. doi: 10.1016/0166-2236(89)90091-X.

Huleihel, M. *et al.* (1986) 'Characterization of murine A-raf, a new oncogene related to the v-raf oncogene.', *Molecular and Cellular Biology*, 6(7), pp. 2655–2662. doi: 10.1128/mcb.6.7.2655.

Hunter, J. C. *et al.* (2015) 'Biochemical and Structural Analysis of Common Cancer-Associated KRAS Mutations', *Molecular Cancer Research*, 13(9), pp. 1325–1335. Available at: http://mcr.aacrjournals.org/content/13/9/1325.abstract.

Ihle, N. T. *et al.* (2012) 'Effect of KRAS oncogene substitutions on protein behavior: Implications for signaling and clinical outcome', *Journal of the National Cancer Institute*, 104(3), pp. 228–239. doi: 10.1093/jnci/djr523.

Ikawa, S. *et al.* (1988) 'B-raf, a new member of the raf family, is activated by DNA rearrangement.', *Molecular and Cellular Biology*, 8(6), pp. 2651–2654. doi: 10.1128/mcb.8.6.2651.

Ikeda, M. *et al.* (1998) 'Identification and characterization of a novel protein interacting with Ral-binding protein 1, a putative effector protein of Ral', *Journal of Biological Chemistry*. Â© 1998 ASBMB. Currently published by Elsevier Inc; originally published by American Society for Biochemistry and Molecular Biology., 273(2), pp. 814–821. doi: 10.1074/jbc.273.2.814.

Imamura, Y. *et al.* (2012) 'Specific mutations in KRAS codons 12 and 13, and patient prognosis in 1075 BRAF wild-type colorectal cancers', *Clinical Cancer Research*, 18(17), pp. 4753–4763. doi: 10.1158/1078-0432.CCR-11-3210.

Inouye, K. *et al.* (2000) 'Formation of the Ras dimer is essential for Raf-1 activation', *Journal of Biological Chemistry*. Â© 2000 ASBMB. Currently published by Elsevier Inc; originally published by American Society for Biochemistry and Molecular Biology., 275(6), pp. 3737–3740. doi: 10.1074/jbc.275.6.3737.

Ishibe, S. *et al.* (2003) 'Phosphorylation-dependent paxillin-ERK association mediates hepatocyte growth factor-stimulated epithelial morphogenesis', *Molecular Cell*, 12(5), pp. 1275–1285. doi: 10.1016/S1097-2765(03)00406-4.

Ito, Y. *et al.* (1997) 'Regional polysterism in the GTP-bound form of the human c-Ha-Ras protein',

Biochemistry, 36(30), pp. 9109–9119. doi: 10.1021/bi970296u.

Izar, B. *et al.* (2014) 'The prognostic impact of KRAS, its codon and amino acid specific mutations, on survival in resected stage i lung adenocarcinoma', *Journal of Thoracic Oncology*. International Association for the Study of Lung Cancer, 9(9), pp. 1363–1369. doi: 10.1097/JTO.0000000000000266.

Izawa, Y. *et al.* (2007) 'Big mitogen-activated protein kinase 1 (BMK1)/extracellular signal regulated kinase 5 (ERK5) is involved in platelet-derived growth factor (PDGF)-induced vascular smooth muscle cell migration', *Hypertension Research*, 30(11), pp. 1107–1117. doi: 10.1291/hypres.30.1107.

Jaaro, H. *et al.* (1997) 'Nuclear translocation of mitogen-activated protein kinase kinase (MEK1) in response to mitogenic stimulation', *Proceedings of the National Academy of Sciences of the United States of America*, 94(8), pp. 3742–3747. doi: 10.1073/pnas.94.8.3742.

Jacobs, D. *et al.* (1999) 'Multiple docking sites on substrate proteins form a modular system that mediates recognition by ERK MAP kinase', *Genes and Development*, 13(2), pp. 163–175. doi: 10.1101/gad.13.2.163.

Janakiraman, M. *et al.* (2010) 'Genomic and biological characterization of exon 4 KRAS mutations in human cancer', *Cancer Research*, 70(14), pp. 5901–5911. doi: 10.1158/0008-5472.CAN-10-0192.

Janes, M. R. *et al.* (2018) 'Targeting KRAS Mutant Cancers with a Covalent G12C-Specific Inhibitor', *Cell*, 172(3), pp. 578-589.e17. doi: 10.1016/j.cell.2018.01.006.

Jaumot, M. *et al.* (2002) 'The linker domain of the Ha-Ras hypervariable region regulates interactions with exchange factors, Raf-1 and phosphoinositide 3-kinase', *Journal of Biological Chemistry*. Â© 2002 ASBMB. Currently published by Elsevier Inc; originally published by American Society for Biochemistry and Molecular Biology., 277(1), pp. 272–278. doi: 10.1074/jbc.M108423200.

Jaworski, J., Kluz, R. and Trzepieciński, T. (1996) 'Molecular basis for the substrate specificity of protein kinase B; comparison with MAPKAP kinase-1 and p70 S6 kinase', *FEBS Letters*, 399(6), pp. 333–338. doi: 10.17531/ein.2016.2.15.

Jelinek, T. *et al.* (1994) 'RAS and RAF-1 form a signalling complex with MEK-1 but not MEK-2.', *Molecular and Cellular Biology*, 14(12), pp. 8212–8218. doi: 10.1128/mcb.14.12.8212.

Ji, Y. *et al.* (2016) 'Pharmacological Targeting of Plasminogen Activator Inhibitor-1 Decreases Vascular Smooth Muscle Cell Migration and Neointima Formation', *Arteriosclerosis, Thrombosis, and Vascular Biology*, 36(11), pp. 2167–2175. doi: 10.1161/ATVBAHA.116.308344.

Jiang, Y. *et al.* (1997) 'Characterization of the structure and function of the fourth member of p38 group mitogen-activated protein kinases, p38δ', *Journal of Biological Chemistry*. Â© 1997 ASBMB. Currently published by Elsevier Inc; originally published by American Society for Biochemistry and Molecular Biology., 272(48), pp. 30122–30128. doi: 10.1074/jbc.272.48.30122.

Jiang, Z. L. *et al.* (2011) 'Fibroblast growth factor-2 regulation of Sprouty and NR4A genes in bovine ovarian granulosa cells', *Journal of Cellular Physiology*, 226(7), pp. 1820–1827. doi: 10.1002/jcp.22509.

Jin, K. *et al.* (2002) 'MEK and ERK protect-hypoxic cortical neurons via phosphorylation of Bad', *Journal of Neurochemistry*, 80(1), pp. 119–125. doi: 10.1046/j.0022-3042.2001.00678.x.

Jinesh, G. G. *et al.* (2018) 'Molecular genetics and cellular events of K-Ras-driven tumorigenesis', *Oncogene*. Nature Publishing Group, 37(7), pp. 839–846. doi: 10.1038/onc.2017.377.

Johnson, E. O. *et al.* (2011) 'PHLDA1 is a crucial negative regulator and effector of Aurora A kinase in breast cancer', *Journal of Cell Science*, 124(16), pp. 2711–2722. doi: 10.1242/jcs.084970.

Johnson, L. *et al.* (1997) 'K-ras is an essential gene in the mouse with partial functional overlap with N-ras', *Genes and Development*, 11(19), pp. 2468–2481. doi: 10.1101/gad.11.19.2468.

Jones, R. P. *et al.* (2017) 'Specific mutations in KRAS codon 12 are associated with worse overall survival in patients with advanced and recurrent colorectal cancer', *British Journal of Cancer*. Nature Publishing Group, 116(7), pp. 923–929. doi: 10.1038/bjc.2017.37.

Jonker, D. J. *et al.* (2007) 'Cetuximab for the Treatment of Colorectal Cancer', *New England Journal of Medicine*, 357(20), pp. 2040–2048. Available at: www.nejm.org.

Joo, J. H. *et al.* (2007) 'Farnesol-Induced Apoptosis in Human Lung Carcinoma Cells Is Coupled to the Endoplasmic Reticulum Stress Response', *Cancer Research*. American Association for Cancer Research, 67(16), pp. 7929–7936. doi: 10.1158/0008-5472.CAN-07-0931.

Joseph, E. W. *et al.* (2010) 'The RAF inhibitor PLX4032 inhibits ERK signaling and tumor cell proliferation in a V600E BRAF-selective manner', *Proceedings of the National Academy of Sciences of the United States of America*, 107(33), pp. 14903–14908. doi: 10.1073/pnas.1008990107.

Judd, W. R. *et al.* (2011) 'Discovery and SAR of methylated tetrahydropyranyl derivatives as inhibitors of isoprenylcysteine carboxyl methyltransferase (ICMT)', *Journal of Medicinal Chemistry*, 54(14), pp. 5031–5047. doi: 10.1021/jm200249a.

Jura, N. *et al.* (2006) 'Differential modification of Ras proteins by ubiquitination', *Molecular Cell*,

21(5), pp. 679–687. doi: 10.1016/j.molcel.2006.02.011.

Kalluri, R. and Weinberg, R. A. (2009) 'The basics of epithelial-mesenchymal transition', *The Journal of clinical investigation*. American Society for Clinical Investigation, 119(6), pp. 1420–1428. doi: 10.1172/JCI39104.

Kamakura, S., Moriguchi, T. and Nishida, E. (1999) 'Activation of the protein kinase ERK5/BMK1 by receptor tyrosine kinases. Identification and characterization of a signaling pathway to the nucleus', *Journal of Biological Chemistry*. Â© 1999 ASBMB. Currently published by Elsevier Inc; originally published by American Society for Biochemistry and Molecular Biology., 274(37), pp. 26563–26571. doi: 10.1074/jbc.274.37.26563.

Kan, Z. *et al.* (2010) 'Diverse somatic mutation patterns and pathway alterations in human cancers', *Nature*, 466(7308), pp. 869–873. doi: 10.1038/nature09208.

Kandoth, C. *et al.* (2013) 'Mutational landscape and significance across 12 major cancer types', *Nature*. Nature Publishing Group, 502(7471), pp. 333–339. doi: 10.1038/nature12634.

Kaplan, P. L., Anderson, M. and Ozanne, B. (1982) 'Transforming growth factor(s) production enables cells to grow in the absence of serum: An autocrine system', *Proceedings of the National Academy of Sciences of the United States of America*, 79(2), pp. 485–489. doi: 10.1073/pnas.79.2.485.

Kapoor, A. and Travesset, A. (2015) 'Differential dynamics of RAS isoforms in GDP- and GTP-bound states', *Proteins: Structure, Function and Bioinformatics*, 83(6), pp. 1091–1106. doi: 10.1002/prot.24805.

Karapetis, C. S. *et al.* (2008) 'K-ras Mutations and Benefit from Cetuximab in Advanced Colorectal Cancer', *New England Journal of Medicine*, 359(17), pp. 1757–1765.

Karlsson, M. *et al.* (2004) 'Both nuclear-cytoplasmic shuttling of the dual specificity phosphatase MKP-3 and its ability to anchor MAP kinase in the cytoplasm are mediated by a conserved nuclear export signal', *Journal of Biological Chemistry*. Â© 2004 ASBMB. Currently published by Elsevier Inc; originally published by American Society for Biochemistry and Molecular Biology., 279(40), pp. 41882–41891. doi: 10.1074/jbc.M406720200.

Karoulia, Z. *et al.* (2017) 'An integrated model of RAF inhibitor action predicts inhibitor activity against oncogenic BRAF signaling', *Cancer Cell*, 30(3), pp. 485–498. doi: 10.1016/j.ccell.2016.06.024.An.

Karreth, F. A. *et al.* (2011) 'C-Raf is required for the initiation of lung cancer by K-Ras(G12D)', *Cancer Discovery*, 1(2), pp. 128–136. doi: 10.1158/2159-8290.CD-10-0044.

Kato, Y. *et al.* (1998) 'Bmk1/Erk5 is required for cell proliferation induced by epidermal growth factor', *Nature*, 395(6703), pp. 713–716. doi: 10.1038/246170a0.

Kawesha, A. *et al.* (2000) 'K-ras oncogene subtype mutations are associated with survival but not expression of p53, p16(INK4A), p21(WAF-1), cyclin D1, ERBB-2 and ERBB-3 in resected pancreatic ductal adenocarcinoma', *International Journal of Cancer*, 89(6), pp. 469–474. doi: 10.1002/1097-0215(20001120)89:6<469::AID-IJC1>3.0.CO;2-L.

Kelland, L. (2007) 'Targeting the limitless replicative potential of cancer: The telomerase/telomere pathway', *Clinical Cancer Research*, 13(17), pp. 4960–4963. doi: 10.1158/1078-0432.CCR-07-0422.

Kelley, G. G. *et al.* (2001) 'Phospholipase Cε: A novel Ras effector', *EMBO Journal*, 20(4), pp. 743–754. doi: 10.1093/emboj/20.4.743.

Kern, F. *et al.* (2013) 'Essential, non-redundant roles of B-Raf and Raf-1 in Ras-driven skin tumorigenesis', *Oncogene*. Nature Publishing Group, 32(19), pp. 2483–2492. doi: 10.1038/onc.2012.254.

Kesavan, K. *et al.* (2004) 'MEKK2 Regulates the Coordinate Activation of ERK5 and JNK in Response to FGF-2 in Fibroblasts', *Journal of Cellular Physiology*, 199(1), pp. 140–148. doi: 10.1002/jcp.10457.

Kessler, L. *et al.* (2018) 'Tipifarnib is highly active in HRAS mutant lung squamous carcinoma tumor models [abstract]', *Cancer Research*, 78(13 Supplement), p. 4917. doi: 10.1158/1538-7445.AM2018-4917.

Kholodenko, B. N. *et al.* (2002) 'Untangling the wires: A strategy to trace functional interactions in signaling and gene networks', *Proceedings of the National Academy of Sciences*, 99(20), pp. 12841–6. doi: 10.1073/pnas.192442699.

Kholodenko, B. N. *et al.* (2021) 'A systematic analysis of signaling reactivation and drug resistance', *Cell Reports*. ElsevierCompany., 35(8), p. 109157. doi: 10.1016/j.celrep.2021.109157.

Kim, H. S. *et al.* (2012) 'Berberine-induced AMPK activation inhibits the metastatic potential of melanoma cells via reduction of ERK activity and COX-2 protein expression', *Biochemical Pharmacology*. Elsevier Inc., 83(3), pp. 385–394. doi: 10.1016/j.bcp.2011.11.008.

Kim, S. T. *et al.* (2011) 'Impact of KRAS mutations on clinical outcomes in pancreatic cancer patients treated with first-line gemcitabine-based chemotherapy', *Molecular Cancer Therapeutics*, 10(10), pp. 1993–1999. doi: 10.1158/1535-7163.MCT-11-0269.

Kim, T. W. *et al.* (2019) 'Belvarafenib, a novel pan-RAF inhibitor, in solid tumor patients harboring

BRAF, KRAS, or NRAS mutations: Phase I study', *Journal of Clinical Oncology*. Wolters Kluwer, 37(15_suppl), p. 3000. doi: 10.1200/JCO.2019.37.15_suppl.3000.

Kinsey, C. G. *et al.* (2019) 'Protective autophagy elicited by RAF→MEK→ERK inhibition suggests a treatment strategy for RAS-driven cancers', *Nature Medicine*. Springer US, 25(April). doi: 10.1038/s41591-019-0367-9.

Klarlund, J. K., Cherniack, A. D. and Czech, M. P. (1995) 'Divergent mechanisms for homologous desensitization of p21ras by insulin and growth factors', *Journal of Biological Chemistry*. Â© 1995 ASBMB. Currently published by Elsevier Inc; originally published by American Society for Biochemistry and Molecular Biology., 270(40), pp. 23421–23428. doi: 10.1074/jbc.270.40.23421.

Klebe, C. *et al.* (1995) 'The Kinetic Mechanism of Ran-Nucleotide Exchange Catalyzed by RCC1', *Biochemistry*, 34(39), pp. 12543–12552. doi: 10.1021/bi00039a008.

Klein, C. *et al.* (2006) 'Germline KRAS mutations cause Noonan syndrome', *Nature Genetics*, 38(3), pp. 331–337. doi: 10.1038/ng1748.

Klinger, B. *et al.* (2013) 'Network quantification of EGFR signaling unveils potential for targeted combination therapy', *Molecular Systems Biology*, 9(673), pp. 1–14. doi: 10.1038/msb.2013.29.

Koch, C. A. *et al.* (1991) 'SH2 and SH3 domains: Elements that control interactions of cytoplasmic signaling proteins', *Science*, 252(5006), pp. 668–674. doi: 10.1126/science.1708916.

Koera, K. *et al.* (1997) 'K-Ras is essential for the development of the mouse embryo', *Oncogene*, 15(10), pp. 1151–1159. doi: 10.1038/sj.onc.1201284.

Kosako, H. *et al.* (2009) 'Phosphoproteomics reveals new ERK MAP kinase targets and links ERK to nucleoporin-mediated nuclear transport', *Nature Structural and Molecular Biology*. Nature Publishing Group, 16(10), pp. 1026–1035. doi: 10.1038/nsmb.1656.

Kouhara, H., Hadari, Y. R. and Schilling, J. (1997) 'A lipid-anchored Grb2-binding protein that links FGF-receptor activation to the Ras/MAPK signaling pathway', *Cell*, 89(5), pp. 693–702.

Kovacina, K. S. *et al.* (2003) 'Identification of a proline-rich Akt substrate as a 14-3-3 binding partner', *Journal of Biological Chemistry*. Â© 2003 ASBMB. Currently published by Elsevier Inc; originally published by American Society for Biochemistry and Molecular Biology., 278(12), pp. 10189–10194. doi: 10.1074/jbc.M210837200.

Kovrigina, E. A., Galiakhmetov, A. R. and Kovrigin, E. L. (2015) 'The Ras G Domain Lacks the Intrinsic Propensity to Form Dimers', *Biophysical Journal*. Biophysical Society, 109(5), pp. 1000–1008. doi:

10.1016/j.bpj.2015.07.020.

Koyasu, S. (2003) 'The role of PI3K in immune cells', *Nature Immunology*, 4, pp. 313–319.

Krengel, U. *et al.* (1990) 'Three-Dimensional Structures of H-ras p21 Mutants : Molecular Basis for Their Inability to Function As Signal Switch Molecules', *Cell*, 62, pp. 539–548.

Krens, S. F. G., Spaink, H. P. and Snaar-Jagalska, B. E. (2006) 'Functions of the MAPK family in vertebrate-development', *FEBS Letters*, 580(21), pp. 4984–4990. doi: 10.1016/j.febslet.2006.08.025.

Krugmann, S. *et al.* (1999) 'Characterizing the interactions between the two subunits of the p101/p110γ/phosphoinositide 3-kinase and their role in the activation of this enzyme by G(βγ) subunits', *Journal of Biological Chemistry*. Â© 1999 ASBMB. Currently published by Elsevier Inc; originally published by American Society for Biochemistry and Molecular Biology., 274(24), pp. 17152–17158. doi: 10.1074/jbc.274.24.17152.

Kruspig, B. *et al.* (2018) 'The ERBB network facilitates KRAS-driven lung tumorigenesis', *bioRxiv*, 2565(June). doi: 10.1101/290700.

Kukurba, K. R. and Montgomery, S. B. (2015) 'RNA Sequencing and Analysis', *Cold Spring Harbor Protocols*, 11, pp. 951–969. doi: 10.1201/b11351-11.

Kumar, N. *et al.* (2008) 'Multipathway model enables prediction of kinase inhibitor cross-talk effects on migration of Her2-overexpressing mammary epithelial cells', *Molecular Pharmacology*, 73(6), pp. 1668–1678. doi: 10.1124/mol.107.043794.

Kwon, M. J. *et al.* (2015) 'Low Frequency of KRAS Mutation in Pancreatic Ductal Adenocarcinomas in Korean Patients and Its Prognostic Value', *Pancreas*, 44(3), pp. 484–492. Available at: https://journals.lww.com/pancreasjournal/Fulltext/2015/04000/Low_Frequency_of_KRAS_Mutation_in_Pancreatic.20.aspx.

Kyriakis, J. M. *et al.* (1992) 'Raf-1 activates MAP kinase-kinase', *Nature*, 358, pp. 417–421.

Lake, D., Corrêa, S. A. L. and Müller, J. (2016) 'Negative feedback regulation of the ERK1/2 MAPK pathway', *Cellular and Molecular Life Sciences*, 73(23), pp. 4397–4413. doi: 10.1007/s00018-016-2297-8.

Lamarre, S. *et al.* (2018) 'Optimization of an RNA-seq differential gene expression analysis depending on biological replicate number and library size', *Frontiers in Plant Science*, 9(108), pp. 1–18. doi: 10.3389/fpls.2018.00108.

Lander, H. M. *et al.* (1995) 'P21Ras As a Common Signaling Target of Reactive Free Radicals and

Cellular Redox Stress', *Journal of Biological Chemistry*, 270(36), pp. 21195–21198. doi: 10.1074/jbc.270.36.21195.

Lander, H. M. *et al.* (1996) 'Redox regulation of cell signalling', *Nature*, 381(May), pp. 380–381.

Langlois, W. J. *et al.* (1995) 'Negative Feedback Regulation and Desensitization of Insulin- and Epidermal Growth Factor-stimulated p21ras Activation', *Journal of Biological Chemistry*. Â© 1995 ASBMB. Currently published by Elsevier Inc; originally published by American Society for Biochemistry and Molecular Biology., 270(43), pp. 25320–25323. doi: 10.1074/jbc.270.43.25320.

Lavoie, H. and Therrien, M. (2015) 'Regulation of RAF protein kinases in ERK signalling', *Nature Reviews Molecular Cell Biology*. Nature Publishing Group, 16(5), pp. 281–298. doi: 10.1038/nrm3979.

Lawler, S. *et al.* (1998) 'Synergistic activation of SAPK1/JNK1 by two MAP kinase kinases in vitro', *Current Biology*, 8(25), pp. 1387–1391. doi: 10.1016/s0960-9822(98)00019-0.

Lax, I. *et al.* (2002) 'The docking protein FRS2alpha controls a MAP kinase-mediated negative feedback mechanism for signaling by FGF receptors', *Molecular Cell*, 10(4), pp. 709–719.

Lee, H. J. *et al.* (2004) 'Mitogen-activated protein kinase/extracellular signal-regulated kinase attenuates 3-hydroxykynurenine-induced neuronal cell death', *Journal of Neurochemistry*, 88(3), pp. 647–656. doi: 10.1111/j.1471-4159.2004.02191.x.

Lee, K. . *et al.* (2003) 'Immortalization with telomerase of the Nestin-positive cells of the human pancreas', *Biochemical and Biophysical Research Communications*, 301(4), pp. 1038–1044. doi: 10.1016/S0006-291X(03)00086-X.

Lee, T. *et al.* (2004) 'Docking motif interactions in MAP kinases revealed by hydrogen exchange mass spectrometry', *Bardwell and Thorner*, 14(1), pp. 43–55. Available at: http://www.molecule.org/cgi/.

Leevers, S. J., Paterson, H. F. and Marshall, C. J. (1994) 'Requirement for Ras in Raf activation is overcome by targeting Raf to the plasma membrane', *Nature*, 369(6479), pp. 411–414. doi: 10.1038/369411a0.

Legius, E. *et al.* (2002) 'PTPN11 mutations in LEOPARD syndrome', *Journal of Medical Genetics*, 39(8), pp. 571–574.

Leicht, D. T. *et al.* (2007) 'Raf Kinases: Function, Regulation and Role in Human Cancer', *Biochimica et Biophysica Acta*, 1773(8), pp. 1196–1212. doi: 10.1016/j.bbi.2008.05.010.

Lennartsson, J. *et al.* (2010) 'Erk 5 is necessary for sustained PDGF-induced Akt phosphorylation and inhibition of apoptosis', *Cellular Signalling*. Elsevier Inc., 22(6), pp. 955–960. doi:

10.1016/j.cellsig.2010.01.020.

Lenzen, C. *et al.* (1998) 'Kinetic analysis by fluorescence of the interaction between Ras and the catalytic domain of the guanine nucleotide exchange factor Cdc25(Mm)', *Biochemistry*, 37(20), pp. 7420–7430. doi: 10.1021/bi972621j.

Leof, E. B. *et al.* (1982) 'Epidermal growth factor (EGF) and somatomedin C regulate G1 progression in competent BALB/c-3T3 cells', *Experimental Cell Research*, 141(1), pp. 107–115.

Li, H.-Y., Cao, K. and Zheng, Y. (2003) 'Ran in the spindle checkpoint: a new function for a versatile GTPase', *Trends in Cell Biology*, 13(11), pp. 553–557. doi: 10.1016/j.tcb.2003.09.001.

Li, J. *et al.* (2016) 'Comparison of microarray and RNA-Seq analysis of mRNA expression in dermal mesenchymal stem cells', *Biotechnology Letters*. Springer Netherlands, 38(1), pp. 33–41. doi: 10.1007/s10529-015-1963-5.

Li, S. *et al.* (2014) 'Coexistence of EGFR with KRAS, or BRAF, or PIK3CA somatic mutations in lung cancer: A comprehensive mutation profiling from 5125 Chinese cohorts', *British Journal of Cancer*, 110(11), pp. 2812–2820. doi: 10.1038/bjc.2014.210.

Li, S., Huang, S. and Peng, S.-B. (2005) 'Overexpression of G protein-coupled receptors in cancer cells: Involvement in tumor progression', *Int J Oncol*. Eli Lilly and Company, Lilly Corporate Center, Indianapolis, IN 46285, USA. li_shuyu_dan@lilly.com null, 27(5), pp. 1329–1338. doi: 10.3892/ijo.27.5.1329.

Li, X. *et al.* (2008) 'ERK-dependent threonine phosphorylation of EGF receptor modulates receptor downregulation and signaling', *Cellular Signalling*, 20(11), pp. 2145–2155. doi: 10.1016/j.cellsig.2008.08.006.

Ligresti, G. *et al.* (2009) 'PIK3CA mutations in human solid tumors Role in sensitivity to various therapeutic approaches', 8(9), pp. 1352–1358.

Linardou, H. *et al.* (2008) 'Assessment of somatic k-RAS mutations as a mechanism associated with resistance to EGFR-targeted agents: a systematic review and meta-analysis of studies in advanced non-small-cell lung cancer and metastatic colorectal cancer', *The Lancet Oncology*, 9(10), pp. 962–972. doi: 10.1016/S1470-2045(08)70206-7.

Lito, P. *et al.* (2014) 'Disruption of CRAF-Mediated MEK activation is required for effective mek inhibition in KRAS mutant tumors', *Cancer Cell*. Elsevier Inc., 25(5), pp. 697–710. doi: 10.1016/j.ccr.2014.03.011.

Liu, F. *et al.* (2018) 'Targeting ERK, an Achilles' Heel of the MAPK pathway, in cancer therapy', *Acta Pharmaceutica Sinica B*. Elsevier B.V. doi: 10.1016/j.apsb.2018.01.008.

Liu, L. *et al.* (2003) 'ERK5 activation of MEF2-mediated gene expression plays a critical role in BDNF-promoted survival of developing but not mature cortical neurons', *Proceedings of the National Academy of Sciences of the United States of America*, 100(14), pp. 8532–8537. doi: 10.1073/pnas.1332804100.

Liu, P. *et al.* (2011) 'Targeting the phosphoinositide 3-kinase (PI3K) pathway in cancer', *Nature Reviews Drug Discovery*, 8(8), pp. 627–644. doi: 10.1038/nrd2926.Targeting.

Liu, X. *et al.* (2004) 'The MAP kinase pathway is required for entry into mitosis and cell survival', *Oncogene*, 23(3), pp. 763–776. doi: 10.1038/sj.onc.1207188.

Loboda, A. *et al.* (2010) 'A gene expression signature of RAS pathway dependence predicts response to PI3K and RAS pathway inhibitors and expands the population of RAS pathway activated tumors', *BMC Medical Genomics*, 3(26), pp. 1–11. doi: 10.1186/1755-8794-3-26.

Lorenz, K. *et al.* (2009) 'A new type of ERK1/2 autophosphorylation causes cardiac hypertrophy', *Nature Medicine*, 15(1), pp. 75–83. doi: 10.1038/nm.1893.

Loupakis, F. *et al.* (2009) 'KRAS codon 61, 146 and BRAF mutations predict resistance to cetuximab plus irinotecan in KRAS codon 12 and 13 wild-type metastatic colorectal cancer', *British Journal of Cancer*. Nature Publishing Group, 101(4), pp. 715–721. doi: 10.1038/sj.bjc.6605177.

Lu, J. *et al.* (2015) 'Structural dataset for the fast-exchanging KRAS G13D', *Data in Brief*. Elsevier, 5, pp. 572–578. doi: 10.1016/j.dib.2015.10.001.

Lu, S. *et al.* (2016a) 'The Structural Basis of Oncogenic Mutations G12, G13 and Q61 in Small GTPase K-Ras4B', *Scientific Reports*. Nature Publishing Group, 6(February), pp. 1–15. doi: 10.1038/srep21949.

Lu, S. *et al.* (2016b) 'The Structural Basis of Oncogenic Mutations G12, G13 and Q61 in Small GTPase K-Ras4B', *Scientific Reports*. Nature Publishing Group, 6(February), pp. 1–15. doi: 10.1038/srep21949.

Lukman, S. *et al.* (2010) 'The distinct conformational dynamics of K-Ras and H-Ras A59G', *PLoS Computational Biology*, 6(9), pp. 4–12. doi: 10.1371/journal.pcbi.1000922.

Luo, Z. *et al.* (1996) 'Oligomerization activates c-Raf-1 through a Ras-dependent mechanism', *Nature*, 383(6596), pp. 181–185.

Lynch, S. J. *et al.* (2015) 'The Differential palmitoylation states of N-Ras and H-Ras determine their distinct golgi subcompartment localizations', *Journal of Cellular Physiology*, 230(3), pp. 610–619. doi: 10.1002/jcp.24779.

Madison, E. L. *et al.* (1990) 'Amino acid residues that affect interaction of tissue-type plasminogen activator with plasminogen activator inhibitor 1', *Proceedings of the National Academy of Sciences of the United States of America*, 87(9), pp. 3530–3533. doi: 10.1073/pnas.87.9.3530.

Maehama, T. and Dixon, J. E. (1998) 'The tumor suppressor, PTEN/MMAC1, dephosphorylates the lipid second messenger, phosphatidylinositol 3,4,5-trisphosphate', *Journal of Biological Chemistry*. © 1998 ASBMB. Currently published by Elsevier Inc; originally published by American Society for Biochemistry and Molecular Biology., 273(22), pp. 13375–13378. doi: 10.1074/jbc.273.22.13375.

Mahankali, M. *et al.* (2015) 'A non-mitotic role for Aurora kinase A as a direct activator of cell migration upon interaction with PLD, FAK and Src', *Journal of Cell Science*, 128(3), pp. 516–526. doi: 10.1242/jcs.157339.

Mandl, M., Slack, D. N. and Keyse, S. M. (2005) 'Specific inactivation and nuclear anchoring of extracellular signal-regulated kinase 2 by the inducible dual-specificity protein phosphatase DUSP5', *Molecular and Cellular Biology*, 25(5), pp. 1830–1845. doi: 10.1128/mcb.25.5.1830-1845.2005.

Manning, B. D. and Cantley, L. C. (2007) 'AKT/PKB Signaling: Navigating Downstream', *Cell*, 129(7), pp. 1261–1274. doi: 10.1016/j.cell.2007.06.009.

Mansour, S. J. *et al.* (1996) 'Constitutively active mitogen-activated protein kinase kinase 1 (MAPKK1) and MAPKK2 mediate similar transcriptional and morphological responses', *Cell Growth and Differentiation*, 7(2), pp. 243–250.

Mantovani, F., Collavin, L. and Del Sal, G. (2019) 'Mutant p53 as a guardian of the cancer cell', *Cell Death and Differentiation*. Springer US, 26(2), pp. 199–212. doi: 10.1038/s41418-018-0246-9.

Mao, C. *et al.* (2010) 'KRAS mutations and resistance to EGFR-TKIs treatment in patients with non-small cell lung cancer: A meta-analysis of 22 studies', *Lung Cancer*. Elsevier Ireland Ltd, 69(3), pp. 272–278. doi: 10.1016/j.lungcan.2009.11.020.

Marais, R. *et al.* (1995) 'Ras recruits Raf-1 to the plasma membrane far activation by tyrosine phosphorylation', *EMBO Journal*, 14(13), pp. 3136–3145. doi: 10.1002/j.1460-2075.1995.tb07316.x.

Marais, R. *et al.* (1997) 'Differential regulation of Raf-1, A-Raf, and B-Raf by oncogenic Ras and tyrosine kinases', *Journal of Biological Chemistry*. Â© 1997 ASBMB. Currently published by Elsevier Inc; originally published by American Society for Biochemistry and Molecular Biology., 272(7), pp.

4378–4383. doi: 10.1074/jbc.272.7.4378.

Marais, R., Wynne, J. and Treisman, R. (1993) 'The SRF accessory protein Elk-1 contains a growth factor-regulated transcriptional activation domain', *Cell*, 73(2), pp. 381–393. doi: 10.1016/0092-8674(93)90237-K.

Marchetti, A. *et al.* (2005) 'EGFR mutations in non-small-cell lung cancer: Analysis of a large series of cases and development of a rapid and sensitive method for diagnostic screening with potential implications on pharmacologic treatment', *Journal of Clinical Oncology*, 23(4), pp. 857–865. doi: 10.1200/JCO.2005.08.043.

Marchi, M. *et al.* (2008) 'The N-terminal domain of ERK1 accounts for the functional differences with ERK2', *PLoS ONE*, 3(12). doi: 10.1371/journal.pone.0003873.

Marín-Ramos, N. I. *et al.* (2019) 'A Potent Isoprenylcysteine Carboxylmethyltransferase (ICMT) Inhibitor Improves Survival in Ras-Driven Acute Myeloid Leukemia', *Journal of Medicinal Chemistry*, 62(13), pp. 6035–6046. doi: 10.1021/acs.jmedchem.9b00145.

Martinelli, S. *et al.* (2010) 'Heterozygous Germline Mutations in the CBL Tumor-Suppressor Gene Cause a Noonan Syndrome-like Phenotype', *The American Journal of Human Genetics*. The American Society of Human Genetics, 87(2), pp. 250–257. doi: 10.1016/j.ajhg.2010.06.015.

Mason, C. S. *et al.* (1999) 'Serine and tyrosine phosphorylations cooperate in Raf-1, but not B-Raf activation', *EMBO Journal*, 18(8), pp. 2137–2148. doi: 10.1093/emboj/18.8.2137.

Mason, J. M. *et al.* (2006) 'Sprouty proteins: multifaceted negative-feedback regulators of receptor tyrosine kinase signaling', *Trends in Cell Biology*, 16(1), pp. 45–54.

Masoumi-Moghaddam, S., Amini, A. and Morris, D. L. (2014) 'The developing story of Sprouty and cancer', *Cancer and Metastasis Reviews*, 33(2–3), pp. 695–720. doi: 10.1007/s10555-014-9497-1.

Matozaki, T., Nakanishi, H. and Takai, Y. (2000) 'Small G-protein networks: Their crosstalk and signal cascades', *Cellular Signalling*, 12(8), pp. 515–524. doi: 10.1016/S0898-6568(00)00102-9.

Matsumoto, S. *et al.* (2016) 'Molecular Mechanism for Conformational Dynamics of Ras·GTP Elucidated from In-Situ Structural Transition in Crystal', *Scientific Reports*. Nature Publishing Group, 6(April), pp. 1–12. doi: 10.1038/srep25931.

Mattingly, R. R. (2013) 'Activated Ras as a Therapeutic Target: Constraints on Directly Targeting Ras Isoforms and Wild-Type versus Mutated Proteins', *ISRN Oncology*, 2013, pp. 1–14. doi: 10.1155/2013/536529.

Mazzucchelli, C. *et al.* (2002) 'Knockout of ERK1 MAP kinase enhances synaptic plasticity in the striatum and facilitates striatal-mediated learning and memory', *Neuron*, 34(5), pp. 807–820. doi: 10.1016/S0896-6273(02)00716-X.

McCormick, F. and Wittinghofer, A. (1996) 'Interactions between ras proteins and their effectors', *Current Opinion in Biotechnology*, 7(4), pp. 449–456. doi: 10.1016/S0958-1669(96)80123-6.

McGrath, J. P. *et al.* (1983) 'Structure and organization of the human Ki-ras proto-oncogene and a related processed pseudogene', *Nature*, 304(5926), pp. 501–506.

McGrath, J. P. *et al.* (1984) 'Comparative biochemical properties of normal and activated human ras p21 protein', *Nature*, 310(5979), pp. 644–649. doi: 10.1038/310644a0.

Mckay, M. M., Ritt, D. A. and Morrison, D. K. (2009) 'Signaling dynamics of the KSR1 scaffold complex', *PNAS*, 106(27), pp. 11022–11027.

Mcpherson, R. A. *et al.* (1999) 'Interactions of c-Raf-1 with phosphatidylserine and 14-3-3', *Oncogene*, 18(26), pp. 3862–3869.

Medema, R. H. *et al.* (1993) 'Ras activation by insulin and epidermal growth factor through enhanced exchange of guanine nucleotides on p21ras', *Molecular and Cellular Biology*, 13(1), pp. 155–162. doi: 10.1128/mcb.13.1.155-162.1993.

Mellacheruvu, D. *et al.* (2013) 'The CRAPome: a Contaminant Repository for Affinity Purification Mass Spectrometry Data', *Nature Methods*, 10(8), pp. 730–736. doi: 10.1038/nmeth.2557.The.

Mertes, C. *et al.* (2021) 'Detection of aberrant splicing events in RNA-seq data using FRASER', *Nature Communications*. Springer US, 12(1), pp. 1–13. doi: 10.1038/s41467-020-20573-7.

Miaczynska, M. and Bar-Sagi, D. (2010) 'Signaling endosomes: Seeing is believing', *Current Opinion in Cell Biology*. Elsevier Ltd, 22(4), pp. 535–540. doi: 10.1016/j.ceb.2010.05.007.

Mikula, M. *et al.* (2001) 'Embryonic lethality and fetal liver apoptosis in mice lacking the c-raf-1 gene', *The EMBO journal*, 20(8), pp. 1952–1962.

Milburn, M. V. *et al.* (1990) 'Molecular switch for signal transduction: Structural differences between active and inactive forms of protooncogenic ras proteins', *Science*, 247(4945), pp. 939–945. doi: 10.1126/science.2406906.

Mo, S. P., Coulson, J. M. and Prior, I. A. (2018) 'RAS variant signalling', *Biochemical Society Transactions*, 46(5), pp. 1325–1332. doi: 10.1042/BST20180173.

Mody, N. *et al.* (2003) 'An analysis of the phosphorylation and activation of extracellular-signal-regulated protein kinase 5 (ERK5) by mitogen-activated protein kinase kinase 5 (MKK5) in vitro', *Biochemical Journal*, 372(2), pp. 567–575. doi: 10.1042/BJ20030193.

Moghadam, A. R. *et al.* (2017) 'Ral signaling pathway in health and cancer', *Cancer Medicine*, 6(12), pp. 2998–3013. doi: 10.1002/cam4.1105.

Moghadamchargari, Z. *et al.* (2019) 'Intrinsic GTPase Activity of K-RAS Monitored by Native Mass Spectrometry', *Biochemistry*, 58(31), pp. 3396–3405. doi: 10.1021/acs.biochem.9b00532.

Mohammad, R. M. *et al.* (1998) 'Establishment of a Human Pancreatic Tumor Xenograft Model: Potential Application for Preclinical Evaluation of Novel Therapeutic Agents', *Pancreas*, 16(1), pp. 19–25.

Molina, J. R. and Adjei, A. A. (2006) 'The Ras/Raf/MAPK Pathway', *Journal of Thoracic Oncology*. International Association for the Study of Lung Cancer, 1(1), pp. 7–9. doi: 10.1016/s1556-0864(15)31506-9.

Moll, H. P. *et al.* (2018) 'Afatinib restrains K-RAS-driven lung tumorigenesis', *Science Translational Medicine*, 10(44), pp. 1–13. doi: 10.1126/scitranslmed.aao2301.

Monaco, K.-A. *et al.* (2019) 'RAF inhibitor LXH254 effectively inhibits B-and-CRAF, but not ARAF [abstract]', *Cancer Research*, 79(Suppl. 13), p. LB-114 LP-LB-114. doi: 10.1158/1538-7445.AM2019-LB-114.

Moran, M. F. *et al.* (1990) 'Src homology region 2 domains direct protein-protein interactions in signal transduction', *Proceedings of the National Academy of Sciences of the United States of America*, 87(21), pp. 8622–8626.

Moriki, T., Maruyama, H. and Maruyama, I. N. (2001) 'Activation of preformed EGF receptor dimers by ligand-induced rotation of the transmembrane domain', *Journal of Molecular Biology*, 311(5), pp. 1011–1026. doi: 10.1006/jmbi.2001.4923.

Morrison, D. K. *et al.* (1993) 'Identification of the Major Phosphorylation Sites of the Raf-1 Kinase', *The Journal of Biological Chemistry*, 268(23), pp. 17309–17316. doi: 10.1016/S0021-9258(19)85336-X.

Morrison, D. K. (2012) 'MAP kinase pathways', *Cold Spring Harbor Perspectives in Biology*, 4(11), pp. 1–5. doi: 10.1101/cshperspect.a011254.

Morrison, D. K. and Cutler, R. E. (1997) 'The complexity of Raf-1 regulation', *Current opinion in Cell*

Biology, 9, pp. 174–179.

Moschos, S. J. *et al.* (2018) 'Development of MK-8353, an orally administered ERK1/2 inhibitor, in patients with advanced solid tumors', *JCI insight*, 3(4). doi: 10.1172/jci.insight.92352.

Moses, H. L. *et al.* (1978) 'Mechanism of Growth Arrest of Chemically Transformed Cells in Culture', *Cancer Research*, 38(9), pp. 2807–2812.

Moskalenko, S. *et al.* (2002) 'The exocyst is a Ral effector complex', *Nature Cell Biology*, 4(1), pp. 66–72. doi: 10.1038/ncb728.

Mott, H. R. *et al.* (1996) 'The solution structure of the Raf-1 cysteine-rich domain: A novel Ras and phospholipid binding site', *Proceedings of the National Academy of Sciences of the United States of America*, 93(16), pp. 8312–8317. doi: 10.1073/pnas.93.16.8312.

Müller, J. *et al.* (2003) 'Functional analysis of C-TAK1 substrate binding and identification of PKP2 as a new C-TAK1 substrate', *EMBO Journal*, 22(17), pp. 4431–4442.

Muñoz-Maldonado, C., Zimmer, Y. and Medová, M. (2019) 'A Comparative Analysis of Individual RAS Mutations in Cancer Biology', *Frontiers in Oncology*, 9(1088), pp. 1–22. doi: 10.3389/fonc.2019.01088.

Murai, H. *et al.* (1997) 'Characterization of Ral GDP dissociation stimulator-like (RGL) activities to regulate c-fos promoter and the GDP/GTP exchange of ral', *Journal of Biological Chemistry*. Â© 1997 ASBMB. Currently published by Elsevier Inc; originally published by American Society for Biochemistry and Molecular Biology., 272(16), pp. 10483–10490. doi: 10.1074/jbc.272.16.10483.

Murphy, L. O. *et al.* (2002) 'Molecular, interpretation of ERK signal duration by immediate early gene products', *Nature Cell Biology*, 4(8), pp. 556–564. doi: 10.1038/ncb822.

Murphy, L. O. and Blenis, J. (2006) 'MAPK signal specificity: the right place at the right time', *Trends in Biochemical Sciences*, 31(5), pp. 268–275. doi: 10.1016/j.tibs.2006.03.009.

Murphy, L. O., MacKeigan, J. P. and Blenis, J. (2004) 'A Network of Immediate Early Gene Products Propagates Subtle Differences in Mitogen-Activated Protein Kinase Signal Amplitude and Duration', *Molecular and Cellular Biology*, 24(1), pp. 144–153. doi: 10.1128/mcb.24.1.144-153.2004.

Muslin, A. J. *et al.* (1996) 'Interaction of 14-3-3 with signaling proteins is mediated by the recognition of phosphoserine', *Cell*, 84(6), pp. 889–897. doi: 10.1016/S0092-8674(00)81067-3.

Nadal-Ribelles, M. (2019) 'Shaping the Transcriptional Landscape through MAPK Signaling', in Solé, C. (ed.) *Gene Expression and Control*. Rijeka: IntechOpen, p. Ch. 2. doi: 10.5772/intechopen.80634.

Nakamura, K. *et al.* (2008) 'Partial functional overlap of the three ras genes in mouse embryonic development', *Oncogene*, 27(21), pp. 2961–2968. doi: 10.1038/sj.onc.1210956.

Nakhaeizadeh, H. *et al.* (2016) 'The RAS-effector interface: Isoform-specific differences in the effector binding regions', *PLoS ONE*, 11(12), pp. 1–20. doi: 10.1371/journal.pone.0167145.

Narita, T., Weinert, B. T. and Choudhary, C. (2019) 'Functions and mechanisms of non-histone protein acetylation', *Nature Reviews Molecular Cell Biology*. Springer US, 20(3), pp. 156–174. doi: 10.1038/s41580-018-0081-3.

Nassar, N. *et al.* (1995) 'The 2.2 Å crystal structure of the Ras-binding domain of the serine/threonine kinase c-Raf1 in complex with RaplA and a GTP analogue', *Nature*, 375(6532), pp. 554–560. doi: 10.1038/375554a0.

Nassar, N. *et al.* (1996) 'Ras/Rap effector specificity determined by charge reversal', 3(8), pp. 723–729.

Nazarian, R. *et al.* (2010) 'Melanomas acquire resistance to B-RAF(V600E) inhibition by RTK or N-RAS upregulation', *Nature*. Nature Publishing Group, 468(7326), pp. 973–977. doi: 10.1038/nature09626.

Nelson, H. H. *et al.* (1999) 'Implications and prognostic value of K-ras mutation for early-stage lung cancer in women', *Journal of the National Cancer Institute*, 91(23), pp. 2032–2038. doi: 10.1093/jnci/91.23.2032.

Newlaczyl, A. U., Coulson, J. M. and Prior, I. A. (2017) 'Quantification of spatiotemporal patterns of Ras isoform expression during development', *Scientific Reports*. Nature Publishing Group, 7(January), pp. 1–7. doi: 10.1038/srep41297.

Nguyen, T. T. *et al.* (1993) 'Co-regulation of the mitogen-activated protein kinase, extracellular signal-regulated kinase 1, and the 90-kDa ribosomal S6 kinase in PC12 cells. Distinct effects of the neurotrophic factor, nerve growth factor, and the mitogenic factor, epidermal growth ', *Journal of Biological Chemistry*, 268(13), pp. 9803–9810. doi: 10.1016/s0021-9258(18)98418-8.

Nichols, R. J. *et al.* (2018) 'RAS nucleotide cycling underlies the SHP2 phosphatase dependence of mutant BRAF-, NF1- and RAS-driven cancers', *Nature Cell Biology*, 20(9), pp. 1064–1073. doi: 10.1038/s41556-018-0169-1.RAS.

Nicholson, K. M. and Anderson, N. G. (2002) 'The protein kinase B/Akt signalling pathway in human malignancy', *Cellular Signalling*, 14(5), pp. 381–395. doi: 10.1016/S0898-6568(01)00271-6.

Nie, Z., Hirsch, D. S. and Randazzo, P. A. (2003) 'Arf and its many interactors', *Current Opinion in Cell*

Biology, 15(4), pp. 396–404. doi: 10.1016/S0955-0674(03)00071-1.

Niemeyer, C. M. *et al.* (2010) 'Germline CBL mutations cause developmental abnormalities and predispose to juvenile myelomonocytic leukemia', *Nature Genetics*. Nature Publishing Group, 42(9), pp. 794–800. doi: 10.1038/ng.641.

Niihori, T. *et al.* (2006) 'Germline KRAS and BRAF mutations in cardio-facio-cutaneous syndrome', *Nature Genetics*, 38(3), pp. 294–296. doi: 10.1038/ng1749.

Nishida, N. *et al.* (2006) 'Angiogenesis in cancer', *Vascular Health and Risk Management*, 2(3), pp. 213–219. doi: 10.2147/vhrm.2006.2.3.213.

Nissan, M. H. *et al.* (2014) 'Loss of NF1 in cutaneous melanoma is associated with RAS activation and MEK dependence', *Cancer Research*, 74(8), pp. 2340–2350. doi: 10.1158/0008-5472.CAN-13-2625.

Nithianandarajah-Jones, G. N. *et al.* (2012) 'ERK5: Structure, regulation and function', *Cellular Signalling*. Elsevier Inc., 24(11), pp. 2187–2196. doi: 10.1016/j.cellsig.2012.07.007.

Nobes, C. D. and Hall, A. (1995) 'Rho, Rac, and Cdc42 GTPases regulate the assembly of multimolecular focal complexes associated with actin stress fibers, lamellipodia, and filopodia', *Cell*, 81(1), pp. 53–62. doi: 10.1016/0092-8674(95)90370-4.

Noble, C. *et al.* (2008) 'CRAF Autophosphorylation of Serine 621 Is Required to Prevent Its Proteasome-Mediated Degradation', *Molecular Cell*, 31(6), pp. 862–872. doi: 10.1016/j.molcel.2008.08.026.

Northwood, I. C. *et al.* (1991) 'Isolation and characterization of two growth factor-stimulated protein kinases that phosphorylate the epidermal growth factor receptor at threonine 669', *Journal of Biological Chemistry*, 266(23), pp. 15266–15276. doi: 10.1016/S0021-9258(18)98612-6.

O'Bryan, J. P. (2019) 'Pharmacological targeting of RAS: Recent success with direct inhibitors', *Pharmacological Research*, 139, pp. 503–511. doi: 10.1016/j.phrs.2018.10.021.

Ogura, T. *et al.* (2013) 'Prognostic value of K-ras mutation status and subtypes in endoscopic ultrasound-guided fine-needle aspiration specimens from patients with unresectable pancreatic cancer', *Journal of Gastroenterology*, 48(5), pp. 640–646. doi: 10.1007/s00535-012-0664-2.

Okuzumi, T. *et al.* (2009) 'Inhibitor hijacking of Akt activation', *Nature Chemical Biology*, 5(7), pp. 484–493. doi: 10.1038/nchembio.183.

Oliverius, M. *et al.* (2019) 'KRAS pathway expression changes in pancreatic cancer models by conventional and experimental taxanes', *Mutagenesis*, 34(5–6), pp. 403–411. doi:

10.1093/mutage/gez021.

OmniPath.org (2021a) *OmniPath (KLF9)*. Available at: https://omnipathdb.org/interactions?datasets=omnipath,pathwayextra,kinaseextra,ligrecextra,tfregulons,mirnatarget&fields=sources,references&genesymbols=1&partners=KLF9 (Accessed: 11 May 2021).

OmniPath.org (2021b) *OmniPath (SRC)*. Available at: https://omnipathdb.org/interactions?datasets=omnipath,pathwayextra,kinaseextra,ligrecextra,tfregulons,mirnatarget&fields=sources,references&genesymbols=1&partners=SRC (Accessed: 10 May 2021).

OmniPath.org (2021c) *OmniPath (STAT6)*. Available at: https://omnipathdb.org/interactions?datasets=omnipath,pathwayextra,kinaseextra,ligrecextra,tfregulons,mirnatarget&fields=sources,references&genesymbols=1&partners=STAT6 (Accessed: 11 May 2021).

Osterop, A. P. *et al.* (1993) 'Epidermal-growth-factor receptors generate Ras.GTP more efficiently than insulin receptors', *European Journal of Biochemistry*, 212(2), pp. 477–482. doi: 10.1111/j.1432-1033.1993.tb17684.x.

Ostrem, J. M. *et al.* (2013) 'K-Ras(G12C) inhibitors allosterically control GTP affinity and effector interactions', *Nature*. Nature Publishing Group, 503(7477), pp. 548–551. doi: 10.1038/nature12796.

Ostrow, S. L. *et al.* (2016) 'Variation in KRAS driver substitution distributions between tumor types is determined by both mutation and natural selection', *Scientific Reports*. Nature Publishing Group, 6(February), pp. 1–11. doi: 10.1038/srep21927.

Ozaki, K. *et al.* (2001) 'ERK pathway positively regulates the expression of Sprouty genes', *Biochemical and Biophysical Research Communications*, 285(5), pp. 1084–1088. doi: 10.1006/bbrc.2001.5295.

Pacold, M. E. *et al.* (2000) 'Crystal Structure and Functional Analysis of Ras Binding to Its Effector Phosphoinositide 3-Kinase γ', *Cell*, 103(6), pp. 931–944. doi: 10.1016/S0092-8674(00)00196-3.

Pagès, G. *et al.* (1999) 'Defective thymocyte maturation in p44 MAP kinase (Erk 1) knockout mice', *Science*, 286(5443), pp. 1374–1377. doi: 10.1126/science.286.5443.1374.

Pai, E. F. *et al.* (1989) 'Structure of the guanine-nucleotide-binding domain of the Ha-ras oncogene product p21 in the triphosphate conformation', *Nature*, 341(6239), pp. 209–214. doi: 10.1038/341209a0.

Pai, E. F. *et al.* (1990) 'Refined crystal structure of the triphosphate conformation of H-ras p21 at 1.35 Å resolution: Implications for the mechanism of GTP hydrolysis', *EMBO Journal*, 9(8), pp. 2351–2359. doi: 10.1002/j.1460-2075.1990.tb07409.x.

Palmer, D. H. *et al.* (2017) 'A phase I/II trial of TG01/GM-CSF and gemcitabine as adjuvant therapy for treating patients with resected RAS-mutant adenocarcinoma of the pancreas.', *Journal of Clinical Oncology*. Wolters Kluwer, 35(Suppl. 15), p. 4119. doi: 10.1200/JCO.2017.35.15_suppl.4119.

Panagiotaki, N. *et al.* (2010) 'Characterisation of a new regulator of BDNF signalling, Sprouty3, involved in axonal morphogenesis in vivo', *Development*, 137(23), pp. 4005–4015. doi: 10.1242/dev.053173.

Pandit, B. *et al.* (2007) 'Gain-of-function RAF1 mutations cause Noonan and LEOPARD syndromes with hypertrophic cardiomyopathy', *Nature Genetics*, 39(8), pp. 1007–1012. doi: 10.1038/ng2073.

Pant, S. *et al.* (2019) 'A phase I dose escalation (DE) study of ERK inhibitor, L Y3214996, in advanced (adv) cancer (CA) patients (pts) [abstract].', *Journal of Clinical Oncology*. Wolters Kluwer, 37(Suppl. 15), p. 3001. doi: 10.1200/JCO.2019.37.15_suppl.3001.

Pao, W. *et al.* (2004) 'EGF receptor gene mutations are common in lung cancers from "never smokers" and are associated with sensitivity of tumors to gefitinib and erlotinib', *Proceedings of the National Academy of Sciences of the United States of America*, 101(36), pp. 13306–13311. doi: 10.1073/pnas.0405220101.

Papin, C. *et al.* (1996) 'Identification of signalling proteins interacting with B-Raf in the yeast two-hybrid system', *Oncogene*, 12(10), pp. 2213–2221.

Papin, C. *et al.* (1998) 'Modulation of Kinase Activity and Oncogenic Properties by Alternative Splicing Reveals a Novel Regulatory Mechanism for B-Raf', *Journal of Biological Chemistry*, 273(38), pp. 24939–24947. doi: 10.1074/jbc.273.38.24939.

Parker, C. G. *et al.* (1998) 'Identification of stathmin as a novel substrate for p38 delta', *Biochemical and Biophysical Research Communications*, 249(3), pp. 791–796. doi: 10.1006/bbrc.1998.9250.

Patel, M. and Côté, J.-F. (2013) 'Ras GTPases' interaction with effector domains: Breaking the families' barrier.', *Communicative & integrative biology*, 6(4), p. e24298. Available at: http://www.tandfonline.com/doi/abs/10.4161/cib.24298#aHR0cDovL3d3dy50YW5kZm9ubGluZS5jb20vZG9pL3BkZi8xMC40MTYxL2NpYi4yNDI5OEBAQDA=.

Patricelli, M. P. *et al.* (2016) 'Selective inhibition of oncogenic KRAS output with small molecules targeting the inactive state', *Cancer Discovery*, 6(3), pp. 316–329. doi: 10.1158/2159-8290.CD-15-

1105.

Pawson, T. *et al.* (2001) 'SH2 domains , interaction modules and cellular wiring', *Trends in Cell Biology*, 11(12), pp. 504–511.

Payne, D. M. *et al.* (1991) 'Identification of the regulatory phosphorylation sites in pp42/mitogen-activated protein kinase (MAP kinase)', *EMBO Journal*, 10(4), pp. 885–892. doi: 10.1002/j.1460-2075.1991.tb08021.x.

Peng, S. Bin *et al.* (2015) 'Inhibition of RAF Isoforms and Active Dimers by LY3009120 Leads to Anti-tumor Activities in RAS or BRAF Mutant Cancers', *Cancer Cell*. Elsevier Inc., 28(3), pp. 384–398. doi: 10.1016/j.ccell.2015.08.002.

Pereira-Leal, J. B. and Seabra, M. C. (2001) 'Evolution of the Rab family of small GTP-binding proteins', *Journal of Molecular Biology*, 313(4), pp. 889–901. doi: 10.1006/jmbi.2001.5072.

Pettersson, M. and Crews, C. M. (2019) 'PROteolysis TArgeting Chimeras (PROTACs) — Past, present and future', *Drug Discovery Today: Technologies*. Elsevier Ltd, 31, pp. 15–27. doi: 10.1016/j.ddtec.2019.01.002.

Phan, L. M., Yeung, S. C. J. and Lee, M. H. (2014) 'Cancer metabolic reprogramming: importance, main features, and potentials for precise targeted anti-cancer therapies', *Cancer Biology and Medicine*, 11(1), pp. 1–19. doi: 10.7497/j.issn.2095-3941.2014.01.001.

Pietersma, A. *et al.* (1997) 'P38 mitogen activated protein kinase regulates endothelial VCAM-1 expression at the post-transcriptional level', *Biochemical and Biophysical Research Communications*, 230(1), pp. 44–48. doi: 10.1006/bbrc.1996.5886.

Pincus, M. R. and Brandt-Rauf, P. W. (1985) 'Structural effects of substitutions on the p21 proteins', *PNAS*, 82(11), pp. 3596–3600. doi: 10.1073/pnas.82.11.3596.

Plowman, S. J. *et al.* (2003) 'While K- ras Is Essential for Mouse Development , Expression of the K-ras 4A Splice Variant Is Dispensable', *Molecular and Cellular Biology*, 23(24), pp. 9245–9250. doi: 10.1128/MCB.23.24.9245.

Plowman, S. J. *et al.* (2005) 'H-ras, K-ras, and inner plasma membrane raft proteins operate in nanoclusters with differential dependence on the actin cytoskeleton', *PNAS*, 102(43), pp. 15500–15505.

Popovic, M. *et al.* (2016) 'The structure of the Guanine Nucleotide Exchange Factor Rlf in complex with the small G-protein Ral identifies conformational intermediates of the exchange reaction and

the basis for the selectivity', *Journal of Structural Biology*. Elsevier Inc., 193(2), pp. 106–114. doi: 10.1016/j.jsb.2015.12.006.

Porfiri, E. and Mccormick, F. (1996) 'Regulation of epidermal growth factor receptor signaling by phosphorylation of the ras exchange factor hSOS1', *Journal of Biological Chemistry*. Â© 1996 ASBMB. Currently published by Elsevier Inc; originally published by American Society for Biochemistry and Molecular Biology., 271(10), pp. 5871–5877. doi: 10.1074/jbc.271.10.5871.

Poulikakos, P. I. *et al.* (2010) 'RAF inhibitors transactivate RAF dimers and ERK signalling in cells with wild-type BRAF', *Nature*. Nature Publishing Group, 464(7287), pp. 427–430. doi: 10.1038/nature08902.

Poulikakos, P. I. *et al.* (2011) 'RAF inhibitor resistance is mediated by dimerization of aberrantly spliced BRAF(V600E)', *Nature*. Nature Publishing Group, 480(7377), pp. 387–390. doi: 10.1038/nature10662.

Prior, I. A., Muncke, C., *et al.* (2001) 'Direct visualization of Ras proteins in spatially distinct cell surface microdomains', *Journal of Cell Biology*, 160(2), pp. 165–170. doi: 10.1083/jcb.200209091.

Prior, I. A., Harding, A., *et al.* (2001) 'GTP-dependent segregation of H-ras from lipid rafts is required for biological activity', *Nature Cell Biology*, 3(4), pp. 386–375.

Prior, I. A. and Hancock, J. F. (2012) 'Ras trafficking, localization and compartmentalized signalling', *Seminars in Cell and Developmental Biology*, 23(2), pp. 145–153. doi: 10.1016/j.semcdb.2011.09.002.Ras.

Prior, I. A., Hood, F. E. and Hartley, J. L. (2020) 'The frequency of ras mutations in cancer', *Cancer Research*, 80(14), pp. 2669–2974. doi: 10.1158/0008-5472.CAN-19-3682.

Prior, I. a, Lewis, P. D. and Mattos, C. (2012) 'A comprehensive survey of Ras mutations in cancer', *Cancer Research*, 72(10), pp. 2457–2467. doi: 10.1158/0008-5472.CAN-11-2612.A.

Pritchard, C. A. *et al.* (1996) 'Post-natal lethality and neurological and gastrointestinal defects in mice with targeted disruption of the A-Raf protein kinase gene', *Current Biology*, 6(5), pp. 614–617.

Profile Detail for MYH9 | CRAPome (2022). Available at: https://reprint-apms.org/?q=geneprofiledetail/MYH9/human/2.0/singleStep (Accessed: 6 March 2022).

Qian, Z. R. *et al.* (2018) 'Association of Alterations in Main Driver Genes With Outcomes of Patients With Resected Pancreatic Ductal Adenocarcinoma', *JAMA Oncology*, 4(3), p. e173420. doi: 10.1001/jamaoncol.2017.3420.

Qu, H. *et al.* (2019) 'Blocking TBK1 alleviated radiation-induced pulmonary fibrosis and epithelial-mesenchymal transition through Akt-Erk inactivation', *Experimental and Molecular Medicine*. Springer US, 51(4). doi: 10.1038/s12276-019-0240-4.

Quilliam, L. A. *et al.* (1995) 'Guanine nucleotide exchange factors: activators of the Ras superfamily of proteins', *Bioessays*, 17(5), pp. 395–404.

Quilliam, L. A. *et al.* (1996) 'Involvement of the switch 2 domain of Ras in its interaction with guanine nucleotide exchange factors', *Journal of Biological Chemistry*. © 1996 ASBMB. Currently published by Elsevier Inc; originally published by American Society for Biochemistry and Molecular Biology., 271(19), pp. 11076–11082. doi: 10.1074/jbc.271.19.11076.

Rachakonda, P. S. *et al.* (2013) 'Somatic Mutations in Exocrine Pancreatic Tumors: Association with Patient Survival', *PLoS ONE*, 8(4). doi: 10.1371/journal.pone.0060870.

Rajalingam, K. *et al.* (2007) 'Ras oncogenes and their downstream targets', *Biochimica et Biophysica Acta - Molecular Cell Research*, 1773(8), pp. 1177–1195. doi: 10.1016/j.bbamcr.2007.01.012.

Rapp, U. R. *et al.* (1983) 'Structure and biological activity of v-raf, a unique oncogene transduced by a retrovirus', *Proceedings of the National Academy of Sciences of the United States of America*, 80(14 I), pp. 4218–4222. doi: 10.1073/pnas.80.14.4218.

Rauch, J. *et al.* (2011) 'c-Myc regulates RNA splicing of the A-Raf kinase and its activation of the ERK pathway', *Cancer Research*, 71(13), pp. 4664–4674. doi: 10.1158/0008-5472.CAN-10-4447.

Rauen, K. A. (2013) 'The RASopathies', *Annu Rev Genomics Hum Genet*, 14(1), pp. 355–369. doi: 10.1146/annurev-genom-091212-153523.The.

Razzaque, M. A. *et al.* (2007) 'Germline gain-of-function mutations in RAF1 cause Noonan syndrome', *nature ge*, 39(8), pp. 1013–1017. doi: 10.1038/ng2078.

Rebhun, J. F., Chen, H. and Quilliam, L. A. (2000) 'Identification and characterization of a new family of guanine nucleotide exchange factors for the Ras-related GTPase Ral', *Journal of Biological Chemistry*. Â© 2000 ASBMB. Currently published by Elsevier Inc; originally published by American Society for Biochemistry and Molecular Biology., 275(18), pp. 13406–13410. doi: 10.1074/jbc.C000085200.

Resat, H. *et al.* (2001) 'The arginine finger of RasGap helps Gln-61 align the nucleophilic water in GAP-stimulated hydrolysis of GTP', *Proceedings of the National Academy of Sciences of the United States of America*, 98(11), pp. 6033–6038. doi: 10.1073/pnas.091506998.

Reszka, A. A. *et al.* (1995) 'Association of mitogen-activated protein kinase with the microtubule cytoskeleton', *Proceedings of the National Academy of Sciences of the United States of America*, 92(19), pp. 8881–8885. doi: 10.1073/pnas.92.19.8881.

Reyland, M. E. (2009) 'Protein kinase C isoforms: Multi-functional regulators of cell life and death', *Front Biosci (Landmark Ed)*, 14, pp. 2386–99.

Rhee, S. G. and Choi, K. D. (1992) 'Regulation of inositol phospholipid-specific phospholipase C isozymes', *Journal of Biological Chemistry*. Â© 1992 ASBMB. Currently published by Elsevier Inc; originally published by American Society for Biochemistry and Molecular Biology., 267(18), pp. 12393–12396. doi: 10.1016/s0021-9258(18)42284-3.

Ritt, Daniel A. *et al.* (2010) 'Impact of Feedback Phosphorylation and Raf Heterodimerization on Normal and Mutant B-Raf Signaling', *Molecular and Cellular Biology*, 30(3), pp. 806–819. doi: 10.1128/mcb.00569-09.

Ritt, D. A. *et al.* (2010) 'Impact of Feedback Phosphorylation and Raf Heterodimerization on Normal and Mutant B-Raf Signaling', *Molecular and Cellular Biology*, 30(3), pp. 806–819. doi: 10.1128/MCB.00569-09.

Ritt, D. A. *et al.* (2016) 'Inhibition of Ras/Raf/MEK/ERK Pathway Signaling by a Stress-Induced Phospho-Regulatory Circuit', *Molecular Cell*, 64(5), pp. 875–887. doi: 10.1016/j.molcel.2016.10.029.

Robbins, D. J. *et al.* (1993) 'Regulation and properties of extracellular signal-regulated protein kinases 1 and 2 in Vitro', *Journal of the American Society of Nephrology*, 4(5), pp. 1104–1110. doi: 10.1016/S0021-9258(18)53507-9.

Robbins, D. J. and Cobb, M. H. (1992) 'Extracellular signal-regulated kinases 2 autophosphorylates on a subset of peptides phosphorylated in intact cells in response to insulin and nerve growth factor: Analysis by peptide mapping', *Molecular Biology of the Cell*, 3(3), pp. 299–308. doi: 10.1091/mbc.3.3.299.

Roberts, A. E. *et al.* (2007) 'Germline gain-of-function mutations in SOS1 cause Noonan syndrome', *Nature Genetics*, 39(1), pp. 70–74. doi: 10.1038/ng1926.

Roberts, M. L. *et al.* (2006) 'Microarray analysis of the differential transformation mediated by Kirsten and Harvey Ras oncogenes in a human colorectal adenocarcinoma cell line', *International Journal of Cancer*, 118(3), pp. 616–627. doi: 10.1002/ijc.21386.

Roberts, O. L. *et al.* (2010) 'ERK5 is required for VEGF-mediated survival and tubular morphogenesis of primary human microvascular endothelial cells', *Journal of Cell Science*, 123(19), p. 3413. doi:

10.1242/jcs.080663.

Rodriguez-viciana, P. *et al.* (2006) 'Germline Mutations in Genes Within the MAPK Pathway Cause Cardio-facio-cutaneous Syndrome', *Science*, 311(5765), pp. 1287–1290.

Rommel, C. *et al.* (1996) 'Activated Ras displaces 14-3-3 protein from the amino terminus of c-Raf-1', *Oncogene*. England, 12(3), pp. 609–619.

De Roock, W. *et al.* (2010) 'Association of KRAS p.G13D Mutation With Outcome in Patients With Chemotherapy-Refractory Metastatic Colorectal Cancer Treated With Cetuximab', *JAMA*, 304(16), pp. 1812–1820.

Roskoski Jr, R. (2010) 'RAF protein-serine/threonine kinases: Structure and regulation', *Biochemical and Biophysical Research Communications*. Elsevier Inc., 399(3), pp. 313–317. doi: 10.1016/j.bbrc.2010.07.092.

Rosseland, C. M. *et al.* (2008) 'Distinct functions of H-Ras and K-Ras in proliferation and survival of primary hepatocytes due to selective activation of ERK and PI3K', *Journal of Cellular Physiology*, 215(3), pp. 818–826. doi: 10.1002/jcp.21367.

Rossomando, A. J. *et al.* (1994) 'Mitogen-activated protein kinase kinase 1 (MKK1) is negatively regulated by threonine phosphorylation.', *Molecular and Cellular Biology*, 14(3), pp. 1594–1602. doi: 10.1128/mcb.14.3.1594.

Rotblat, B. *et al.* (2004) 'Three Separable Domains Regulate GTP-Dependent Association of H-ras with the Plasma Membrane', *Molecular and Cellular Biology*, 24(15), pp. 6799–6810. doi: 10.1128/MCB.24.15.6799.

Röth, S. *et al.* (2020) 'Targeting Endogenous K-RAS for Degradation through the Affinity-Directed Protein Missile System', *Cell Chemical Biology*, 27(9), pp. 1151-1163.e6. doi: 10.1016/j.chembiol.2020.06.012.

Rouse, J. *et al.* (1994) 'A novel kinase cascade triggered by stress and heat shock that stimulates MAPKAP kinase-2 and phosphorylation of the small heat shock proteins', *Cell*, 78(6), pp. 1027–1037. doi: 10.1016/0092-8674(94)90277-1.

Rousseau-Merck, M. F. *et al.* (1988) 'The ras-related ral gene maps to chromosome 7p15-22', *Human Genetics*, 79(2), pp. 132–136. doi: 10.1007/BF00280551.

Roy, S. *et al.* (1998) '14-3-3 Facilitates Ras-Dependent Raf-1 Activation In Vitro and In Vivo', *Molecular and Cellular Biology*, 18(7), pp. 3947–3955. doi: 10.1128/mcb.18.7.3947.

Rubinfeld, H. and Seger, R. (2005) 'The ERK cascade', *Molecular Biotechnology*, 31, pp. 151–174.

de Ruiter, N. D. *et al.* (2000) 'Ras-Dependent Regulation of c-Jun Phosphorylation Is Mediated by the Ral Guanine Nucleotide Exchange Factor-Ral Pathway', *Molecular and Cellular Biology*, 20(22), pp. 8480–8488. doi: 10.1128/mcb.20.22.8480-8488.2000.

Ruppert, C. *et al.* (2013) 'Interference with ERK Thr188 phosphorylation impairs pathological but not physiological cardiac hypertrophy', *Proceedings of the National Academy of Sciences of the United States of America*, 110(18), pp. 7440–7445. doi: 10.1073/pnas.1221999110.

Rushworth, L. K. *et al.* (2006) 'Regulation and Role of Raf-1/B-Raf Heterodimerization', *Molecular and Cellular Biology*, 26(6), pp. 2262–2272. doi: 10.1128/mcb.26.6.2262-2272.2006.

Ryu, H. *et al.* (2015) 'Frequency modulation of ERK activation dynamics rewires cell fate', *Molecular Systems Biology*, 11(11), pp. 838–838. doi: 10.15252/msb.20156458.

Saba-El-Leil, M. K. *et al.* (2003) 'An essential function of the mitogen-activated protein kinase Erk2 in mouse trophoblast development', *EMBO Reports*, 4(10), pp. 964–968. doi: 10.1038/sj.embor.embor939.

Saei, A. and Eichhorn, P. J. A. (2018) 'Ubiquitination and adaptive responses to BRAF inhibitors in Melanoma', *Molecular and Cellular Oncology*. Taylor & Francis, 5(5), p. e1497862. doi: 10.1080/23723556.2018.1497862.

Saha, M. *et al.* (2012) 'RSK phosphorylates SOS1 creating 14-3-3-docking sites and negatively regulating MAPK activation', *Biochemical Journal*, 447(1), pp. 159–166. doi: 10.1042/BJ20120938.

Sale, M. J., Balmanno, K. and Cook, S. J. (2019) 'Resistance to ERK1/2 pathway inhibitors; sweet spots, fitness deficits and drug addiction', *Cancer Drug Resistance*, 2(2), pp. 365–380. doi: 10.20517/cdr.2019.14.

Samatar, A. A. and Poulikakos, P. I. (2014) 'Targeting RAS-ERK signalling in cancer: Promises and challenges', *Nature Reviews Drug Discovery*. Nature Publishing Group, 13, pp. 928–942. doi: 10.1038/nrd4281.

Samuels, Y. *et al.* (2004) 'High Frequency of Mutations of the PIK3CA Gene in Human Cancers', *Science*, 304(5670), p. 554. doi: 10.1126/science.1096502.

San Segundo-Val, I. and Sanz-Lozano, C. S. (2016) 'Introduction to the Gene Expression Analysis', in Isidoro García, M. (ed.) *Molecular Genetics of Asthma*. New York, NY: Springer New York, pp. 29–43. doi: 10.1007/978-1-4939-3652-6_3.

Sancak, Y. *et al.* (2007) 'PRAS40 Is an Insulin-Regulated Inhibitor of the mTORC1 Protein Kinase', *Molecular Cell*, 25(6), pp. 903–915. doi: 10.1016/j.molcel.2007.03.003.

Sanchez-Vega, F. *et al.* (2018) 'Oncogenic Signaling Pathways in The Cancer Genome Atlas', *Cell*, 173(2), pp. 321-337.e10. doi: 10.1016/j.cell.2018.03.035.

Santos, S. D. M., Verveer, P. J. and Bastiaens, P. I. H. (2007) 'Growth factor-induced MAPK network topology shapes Erk response determining PC-12 cell fate', *Nature Cell Biology*, 9(3), pp. 324–330. doi: 10.1038/ncb1543.

Sarbassov, D. D. *et al.* (2005) 'Phosphorylation and regulation of Akt/PKB by the rictor-mTOR complex', *Science*, 307(5712), pp. 1098–1101. doi: 10.1126/science.1106148.

Sasai, K. *et al.* (2016) 'Functional significance of Aurora kinases-p53 protein family interactions in cancer', *Frontiers in Oncology*, 6(NOV). doi: 10.3389/fonc.2016.00247.

Sasaki, A. *et al.* (2003) 'Mammalian Sprouty4 suppresses Ras-independent ERK activation by binding to Raf1', *Nature Cell Biology*, 5(5), pp. 427–432. doi: 10.1038/ncb978.

Sasaki, A. T. *et al.* (2011) 'Ubiquitination of K-Ras enhances activation and facilitates binding to select downstream effectors', *Science Signaling*, 4(163), pp. 1–10. doi: 10.1126/scisignal.2001518.

Sato, K. *et al.* (2013) 'Inverse correlation between Thr-669 and constitutive tyrosine phosphorylation in the asymmetric epidermal growth factor receptor dimer conformation', *Cancer Science*, 104(10), pp. 1315–1322. doi: 10.1111/cas.12225.

Satoh, T. *et al.* (1990) 'Accumulation of p21(ras)·GTP in response to stimulation with epidermal growth factor and oncogene products with tyrosine kinase activity', *Proceedings of the National Academy of Sciences of the United States of America*, 87(20), pp. 7926–7929. doi: 10.1073/pnas.87.20.7926.

Sawhney, R. S., Liu, W. and Brattain, M. G. (2009) 'A novel role of ERK5 in integrin-mediated cell adhesion and motility in cancer cells via FAK signaling', *Journal of Cellular Physiology*, 219(1), pp. 152–161. doi: 10.1002/jcp.21662.

Schaeffer, H. J. and Weber, M. J. (1999) 'Mitogen-Activated Protein Kinases: Specific Messages from Ubiquitous Messengers', *Molecular and Cellular Biology*, 19(4), pp. 2435–2444. doi: 10.1128/MCB.19.4.2435.

Scheffzek, K. *et al.* (1997) 'The Ras-RasGAP complex: Structural basis for GTPase activation and its loss in oncogenic ras mutants', *Science*, 277(5324), pp. 333–338. doi: 10.1126/science.277.5324.333.

Scheid, M. P. and Woodgett, J. R. (2001) 'PKB/AKT: Functional insights from genetic models', *Nature Reviews Molecular Cell Biology*, 2(10), pp. 760–768. doi: 10.1038/35096067.

Schlessinger, J. and Ullrich, A. (1992) 'Growth factor signaling by receptor tyrosine kinases', *Neuron*, 9(3), pp. 383–391. doi: 10.1016/0896-6273(92)90177-F.

Seeburg, P. H. *et al.* (1984) 'Biological properties of human c-Ha-ras1 genes mutated at codon 12', *Nature*, 312(5989), pp. 71–75.

Seger, R. *et al.* (1992) 'Purification and characterization of mitogen-activated protein kinase activator(s) from epidermal growth factor-stimulated A431 cells', *Journal of Biological Chemistry*, 267(20), pp. 14373–14381. doi: 10.1016/s0021-9258(19)49722-6.

Seger, R. and Krebs, E. G. (1995) 'The MAPK signaling cascade', *The FASEB Journal*, 9(9), pp. 726–735. doi: 10.1096/fasebj.9.9.7601337.

Sever, R. and Brugge, J. S. (2015) 'Signal transduction in cancer', *Cold Spring Harbor Perspectives in Medicine*, 5(4). doi: 10.1101/cshperspect.a006098.

Sgouras, D. N. *et al.* (1995) 'ERF: An ETS domain protein with strong transcriptional repressor activity, can suppress ets-associated tumorigenesis and is regulated by phosphorylation during cell cycle and mitogenic stimulation', *EMBO Journal*, 14(19), pp. 4781–4793. doi: 10.1002/j.1460-2075.1995.tb00160.x.

Shang, S., Hua, F. and Hu, Z. W. (2017) 'The regulation of β-catenin activity and function in cancer: Therapeutic opportunities', *Oncotarget*, 8(20), pp. 33972–33989. doi: 10.18632/oncotarget.15687.

Sharma, P. *et al.* (2002) 'Phosphorylation of MEK1 by cdk5/p35 down-regulates the mitogen-activated protein kinase pathway', *Journal of Biological Chemistry*. Â© 2002 ASBMB. Currently published by Elsevier Inc; originally published by American Society for Biochemistry and Molecular Biology., 277(1), pp. 528–534. doi: 10.1074/jbc.M109324200.

Shaul, Y. D. and Seger, R. (2007) 'The MEK/ERK cascade: From signaling specificity to diverse functions', *Biochimica et Biophysica Acta - Molecular Cell Research*, 1773(8), pp. 1213–1226. doi: 10.1016/j.bbamcr.2006.10.005.

Sheridan, D. L. *et al.* (2008) 'Substrate discrimination among mitogen-activated protein kinases through distinct docking sequence motifs', *Journal of Biological Chemistry*. Â© 2008 ASBMB. Currently published by Elsevier Inc; originally published by American Society for Biochemistry and Molecular Biology., 283(28), pp. 19511–19520. doi: 10.1074/jbc.M801074200.

Shi, Z.-Q. *et al.* (2000) 'Molecular Mechanism for the Shp-2 Tyrosine Phosphatase Function in Promoting Growth Factor Stimulation of Erk Activity', *Molecular and Cellular Biology*, 20(5), pp. 1526–1536. doi: 10.1128/mcb.20.5.1526-1536.2000.

Shih, T. Y. *et al.* (1979) 'Identification of a sarcoma virus-coded phosphoprotein in nonproducer cells transformed by Kirsten or Harvey murine sarcoma virus', *Virology*, 96(1), pp. 64–79. doi: 10.1016/0042-6822(79)90173-9.

Shin, S. H. *et al.* (2013) 'Genetic alterations of K-ras, p53, c-erbB-2, and DPC4 in pancreatic ductal adenocarcinoma and their correlation with patient survival.', *Pancreas*. United States, 42(2), pp. 216–222. doi: 10.1097/MPA.0b013e31825b6ab0.

Shipitsin, M. and Feig, L. A. (2004) 'RalA but Not RalB Enhances Polarized Delivery of Membrane Proteins to the Basolateral Surface of Epithelial Cells', *Molecular and Cellular Biology*, 24(13), pp. 5746–5756. doi: 10.1128/mcb.24.13.5746-5756.2004.

Shoelson, S. E. *et al.* (1993) 'Specific phosphopeptide binding regulates a conformational change in the PI 3-kinase SH2 domain associated with enzyme activation', *EMBO Journal*, 12(2), pp. 795–802. doi: 10.1002/j.1460-2075.1993.tb05714.x.

Sierecki, E. *et al.* (2010) 'Discovery of Small Molecule Inhibitors of the PH Domain Leucine-Rich Repeat Protein Phosphatase (PHLPP) by Chemical and Virtual Screening', *Journal of Medicinal Chemistry*, 53(19), pp. 6899–6911. doi: 10.1021/jm100331d.

Silver, L. M., Nadeau, J. and Klein, J. (1998) 'High sequence similarity within ras exons 1 and 2 in different mammalian species and phylogenetic divergence of the ras gene family', *Mammalian Genome*, 9(1), pp. 214–219. doi: 10.1007/BF00350840.

Simanshu, D. K., Nissley, D. V. and McCormick, F. (2017) 'RAS Proteins and Their Regulators in Human Disease', *Cell*. Elsevier, 170(1), pp. 17–33. doi: 10.1016/j.cell.2017.06.009.

Simon, J. A. and Schreiber, S. L. (1995) 'Grb2 SH3 binding to peptides from Sos: evaluation of a general model for SH3-ligand interactions', *Chemistry and Biology*, 2(1), pp. 53–60. doi: 10.1016/1074-5521(95)90080-2.

Sindhu, C. B. *et al.* (2021) 'Hydroxychloroquine', *Journal of Skin and Sexually Transmitted Diseases*, 3(1), pp. 33–39. doi: 10.25259/JSSTD.

Singh, A. *et al.* (2009) 'A Gene Expression Signature Associated with "K-Ras Addiction" Reveals Regulators of EMT and Tumor Cell Survival', *Cancer Cell*. Elsevier Ltd, 15(6), pp. 489–500. doi: 10.1016/j.ccr.2009.03.022.

Singh, A. and Settleman, J. (2009) 'Oncogenic K-ras "addiction" and synthetic lethality', *Cell Cycle*, 8(17), pp. 2676–2677. doi: 10.4161/cc.8.17.9336.Oncogenic.

Skolnik, E. Y. and Margolis, B. (1994) 'Activation of Ras by receptor tyrosine kinases', *Journal of the American Society of Nephrology*, 5(6), pp. 1288–1299.

Slack-Davis, J. K. *et al.* (2003) 'PAK1 phosphorylation of MEK1 regulates fibronectin-stimulated MAPK activation', *Journal of Cell Biology*, 162(2), pp. 281–291. doi: 10.1083/jcb.200212141.

Smith, A. J. *et al.* (2016) 'PHLPP negatively regulates cell motility through inhibition of Akt activity and integrin expression in pancreatic cancer cells', *Oncotarget*, 7(7), pp. 7801–7815.

Smith, G. *et al.* (2010) 'Activating K-Ras mutations outwith "hotspot" codons in sporadic colorectal tumours – implications for personalised cancer medicine', *British Journal of Cancer*, 102(4), pp. 693–703. doi: 10.1038/sj.bjc.6605534.

Smith, M. J., Neel, B. G. and Ikura, M. (2013) 'NMR-based functional profiling of RASopathies and oncogenic RAS mutations', *Proceedings of the National Academy of Sciences of the United States of America*, 110(12), pp. 4574–4579. doi: 10.1073/pnas.1218173110.

Spencer-Smith, R. *et al.* (2017) 'Inhibition of RAS function through targeting an allosteric regulatory site', *Nature Chemical Biology*. Nature Publishing Group, 13(1), pp. 62–68. doi: 10.1038/nchembio.2231.

Spoerner, M. *et al.* (2001) 'Dynamic properties of the Ras switch I region and its importance for binding to effectors', *Proceedings of the National Academy of Sciences of the United States of America*, 98(9), pp. 4944–4949. doi: 10.1073/pnas.081441398.

Stephen, A. G. *et al.* (2014) 'Dragging ras back in the ring', *Cancer Cell*. Elsevier Inc., 25(3), pp. 272–281. doi: 10.1016/j.ccr.2014.02.017.

Stephens, L. R. *et al.* (1997) 'The Gβγ/sensitivity of a PI3K is dependent upon a tightly associated adaptor, p101', *Cell*, 89(1), pp. 105–114. doi: 10.1016/S0092-8674(00)80187-7.

Stephens, R. M. *et al.* (2017) 'Tumor RAS gene expression levels are influenced by the Mutational status of RAS genes and both Upstream and Downstream RAS Pathway genes', *Cancer Informatics*, 16, pp. 1–10. doi: 10.1177/1176935117711944.

Stokoe, D. *et al.* (1992) 'Identification of MAPKAP kinase 2 as a major enzyme responsible for the phosphorylation of the small mammalian heat shock proteins', *FEBS Letters*, 313(3), pp. 307–313.

Stokoe, D. *et al.* (1994) 'Activation of Raf as a result of recruitment to the plasma membrane',

Science, 264(5164), pp. 1463–1467. doi: 10.1126/science.266.5192.1792-a.

Stokoe, D. *et al.* (1997) 'Dual role of phosphatidylinositol-3,4,5-trisphosphate in the activation of protein kinase B', *Science*, 277(5325), pp. 567–570. doi: 10.1126/science.277.5325.567.

Stolze, B. *et al.* (2014) 'Comparative analysis of KRAS codon 12, 13, 18, 61, and 117 mutations using human MCF10A isogenic cell lines', *Scientific Reports*, 5, p. 8535. doi: 10.1038/srep08535.

Stoscheck, C. M. and King, L. E. (1986) 'Role of Epidermal Growth Factor in Carcinogenesis', *Cancer Research*, 46(3), pp. 1030–1037.

Stoyanov, B. *et al.* (1995) 'Cloning and characterization of a G protein-activated human phosphoinositide-3 kinase', *Science*, 269(5224), pp. 690–693. doi: 10.1126/science.7624799.

Streb, H. *et al.* (1983) 'Release of Ca2+ from a nonmitochondrial intracellular store in pancreatic acinar cells by inositol-1,4,5-trisphosphate', *Nature*, 306(5938), pp. 67–69. doi: 10.1038/306067a0.

Sturm, O. E. *et al.* (2010) 'The mammalian MAPK/ERK pathway exhibits properties of a negative feedback amplifier', *Science Signaling*, 3(153), p. ra90. doi: 10.1126/scisignal.2001212.

Sun, W. *et al.* (2001) 'MEKK2 Associates with the Adapter Protein Lad/RIBP and Regulates the MEK5-BMK1/ERK5 Pathway', *Journal of Biological Chemistry*. Â© 2001 ASBMB. Currently published by Elsevier Inc; originally published by American Society for Biochemistry and Molecular Biology., 276(7), pp. 5093–5100. doi: 10.1074/jbc.M003719200.

Sun, X. *et al.* (2019) 'Protacs: Great opportunities for academia and industry', *Signal Transduction and Targeted Therapy*. Springer US, 4(64). doi: 10.1038/s41392-019-0101-6.

Sweeney, G. *et al.* (1999) 'An inhibitor of p38 mitogen-activated protein kinase prevents insulin-stimulated glucose transport but not glucose transporter translocation in 3T3-L1 adipocytes and L6 myotubes', *Journal of Biological Chemistry*. Â© 1999 ASBMB. Currently published by Elsevier Inc; originally published by American Society for Biochemistry and Molecular Biology., 274(15), pp. 10071–10078. doi: 10.1074/jbc.274.15.10071.

Sylvestersen, K. B. *et al.* (2011) 'Fgf9 signalling stimulates Spred and Sprouty expression in embryonic mouse pancreas mesenchyme', *Gene Expression Patterns*. Elsevier B.V., 11(1–2), pp. 105–111. doi: 10.1016/j.gep.2010.10.001.

Szwed, A., Kim, E. and Jacinto, E. (2021) 'Regulation and metabolic functions of mTORC1 and mTORC2', *Physiological reviews*, 101(3), pp. 1371–1426. doi: 10.1152/physrev.00026.2020.

Taieb, J. *et al.* (2017) 'Adjuvant FOLFOX +/- cetuximab in full RAS and BRAF wildtype stage III colon

cancer patients', *Annals of Oncology*, 28(4), pp. 824–830. doi: 10.1093/annonc/mdw687.

Takeda, K. *et al.* (2001) 'Critical role of Rho-Kinase and MEK/EFK pathways for angiotensin II-induced plasminogen activator inhibitor type-1 gene expression', *Arteriosclerosis, Thrombosis, and Vascular Biology*, 21(5), pp. 868–873. doi: 10.1161/01.ATV.21.5.868.

Takishima, K. *et al.* (1991) 'Epidermal growth factor (EGF) receptor T669 peptide kinase from 3T3-L1 cells is an EGF-stimulated "MAP" kinase', *PNAS*, 88(6), pp. 2520–2524.

Tan, Y. *et al.* (1996) 'FGF and stress regulate CREB and ATF-1 via a pathway involving p38 MAP kinase and MAPKAP kinase-2', *EMBO Journal*, 15(17), pp. 4629–4642. doi: 10.1002/j.1460-2075.1996.tb00840.x.

Tanoue, T. *et al.* (2000) 'A conserved docking motif in MAP kinases common to substrates, activators and regulators', *Nature Cell Biology*, 2(2), pp. 110–116. doi: 10.1038/35000065.

Tartaglia, M. *et al.* (2001) 'Mutations in PTPN11, encoding the protein tyrosine phosphatase SHP-2, cause Noonan syndrome', *Nature Genetics*, 29(4), pp. 465–468. doi: 10.1038/ng772.

Tartaglia, M. *et al.* (2007) 'Gain-of-function SOS1 mutations cause a distinctive form of Noonan syndrome', *Nature Genetics*, 39(1), pp. 75–80. doi: 10.1038/ng1939.

Tassin, T. C. *et al.* (2015) 'Regulation of ERK kinase by MEK1 kinase inhibition in the brain', *Journal of Biological Chemistry*, 290(26), pp. 16319–16329. doi: 10.1074/jbc.M115.654897.

Temko, D. *et al.* (2018) 'The effects of mutational processes and selection on driver mutations across cancer types', *Nature Communications*, 9(1), p. 1857. doi: 10.1038/s41467-018-04208-6.

Terai, K. and Matsuda, M. (2005) 'Ras binding opens c-Raf to expose the docking site for mitogen-activated protein kinase kinase', *EMBO Reports*, 6(3), pp. 251–255. doi: 10.1038/sj.embor.7400349.

Terrell, E. M. and Morrison, D. K. (2019) 'Ras-Mediated Activation of the Raf Family Kinases', *Cold Spring Harbor Perspectives in Medicine*, 9(1), pp. 1–14. doi: 10.1101/cshperspect.a033746.

Therrien, M. *et al.* (1996) 'KSR modulates signal propagation within the MAPK cascade', *Genes and Development*, 10(21), pp. 2684–2695.

Thuerauf, D. J. *et al.* (1998) 'p38 mitogen-activated protein kinase mediates the transcriptional induction of the atrial natriuretic factor gene through a serum response element: A potential role for the transcription factor ATF6', *Journal of Biological Chemistry*. Â© 1998 ASBMB. Currently published by Elsevier Inc; originally published by American Society for Biochemistry and Molecular Biology., 273(32), pp. 20636–20643. doi: 10.1074/jbc.273.32.20636.

Tian, X. *et al.* (2002) 'PDK1 mediates growth factor-induced Ral-GEF activation by a kinase-independent mechanism', *EMBO Journal*, 21(6), pp. 1327–1338. doi: 10.1093/emboj/21.6.1327.

Ting, P. Y. *et al.* (2015) 'Tyrosine phosphorylation of RAS by ABL allosterically enhances effector binding', *FASEB Journal*, 29(9), pp. 3750–3761. doi: 10.1096/fj.15-271510.

To, M. D. *et al.* (2013) 'Interactions between wild-type and mutant Ras genes in lung and skin carcinogenesis', *Oncogene*, 32(34), pp. 4028–4033. doi: 10.1038/onc.2012.404.

Tong, L. *et al.* (1989) 'Structural differences between a ras oncogene protein and the normal protein', *Nature*, 337(6202), pp. 90–93. doi: 10.1038/337090a0.

Torii, S. *et al.* (2004) 'Sef is a spatial regulator for Ras/MAP kinase signaling', *Developmental Cell*, 7(1), pp. 33–44. doi: 10.1016/j.devcel.2004.05.019.

Tournier, C. *et al.* (1997) 'Mitogen-activated protein kinase kinase 7 is an activator of the c-jun nh2-terminal kinase', *Proceedings of the National Academy of Sciences of the United States of America*, 94(14), pp. 7337–7342. doi: 10.1073/pnas.94.14.7337.

Tournier, C. (2013) 'The 2 Faces of JNK Signaling in Cancer', *Genes and Cancer*, 4(9–10), pp. 397–400. doi: 10.1177/1947601913486349.

Tovell, H. and Newton, A. C. (2021) 'PHLPPing the balance : restoration of protein kinase C in cancer', *Biochemical Journal*, 478(2), pp. 341–355.

Trahey, M. and McCormick, F. (1987) 'A cytoplasmic protein stimulates normal N-ras p21 GTPase, but does not affect oncogenic mutants', *Science*, 238(4826), pp. 542–545. doi: 10.1126/science.2821624.

Tran, E. *et al.* (2016) 'T-Cell Transfer Therapy Targeting Mutant KRAS in Cancer', *New England Journal of Medicine*, 375(23), pp. 2255–2262. doi: 10.1056/nejmoa1609279.

Tran, N. H. and Frost, J. A. (2003) 'Phosphorylation of Raf-1 by p21-activated Kinase 1 and Src Regulates Raf-1 Autoinhibition', *Journal of Biological Chemistry*. Â© 2003 ASBMB. Currently published by Elsevier Inc; originally published by American Society for Biochemistry and Molecular Biology., 278(13), pp. 11221–11226. doi: 10.1074/jbc.M210318200.

Tran, N. H., Wu, X. and Frost, J. A. (2005) 'B-Raf and Raf-1 Are Regulated by Distinct Autoregulatory Mechanisms', *Journal of Biological Chemistry*. Â© 2005 ASBMB. Currently published by Elsevier Inc; originally published by American Society for Biochemistry and Molecular Biology., 280(16), pp. 16244–16253. doi: 10.1074/jbc.M501185200.

Traverse, S. *et al.* (1992) 'Sustained activation of the mitogen-activated protein (MAP) kinase cascade may be required for differentiation of PC12 cells. Comparison of the effects of nerve growth factor and epidermal growth factor', *Biochemical Journal*, 288(2), pp. 351–355. doi: 10.1042/bj2880351.

Traverse, S. *et al.* (1994) 'EGF triggers neuronal differentiation of PC12 cells that overexpress the EGF receptor', *Current Biology*, 4(8), pp. 694–701. doi: 10.1016/S0960-9822(00)00154-8.

Tsai, F. D. *et al.* (2015) 'K-Ras4A splice variant is widely expressed in cancer and uses a hybrid membrane-targeting motif', *Proceedings of the National Academy of Sciences of the United States of America*, 112(3), pp. 779–784. doi: 10.1073/pnas.1412811112.

Tse, J. C. and Kalluri, R. (2007) 'Mechanisms of metastasis: Epithelial-to-mesenchymal transition and contribution of tumor microenvironment', *Journal of Cellular Biochemistry*, 101(4), pp. 816–829. doi: 10.1002/jcb.21215.

Tsukumo, Y., Naito, M. and Suzuki, T. (2020) 'Influence of EGFR-activating mutations on sensitivity to tyrosine kinase inhibitors in a KRAS mutant non-small cell lung cancer cell line', *PLoS ONE*, 15(3), pp. 7–14. doi: 10.1371/journal.pone.0229712.

Türei, D. *et al.* (2021) 'Integrated intra- and intercellular signaling knowledge for multicellular omics analysis', *Molecular Systems Biology*, 17(3), pp. 1–16. doi: 10.15252/msb.20209923.

Türei, D., Korcsmáros, T. and Saez-Rodriguez, J. (2016) 'OmniPath: Guidelines and gateway for literature-curated signaling pathway resources', *Nature Methods*. Nature Publishing Group, 13(12), pp. 966–967. doi: 10.1038/nmeth.4077.

Tzivion, G., Luo, Z. and Avruch, J. (1998) 'A dimeric 14-3-3 protein is an essential cofactor for Raf kinase activity', *Nature*, 394(6688), pp. 88–92. doi: 10.1038/255243a0.

Übel, C. *et al.* (2013) 'Establishing the role of tyrosine kinase 2 in cancer', *OncoImmunology*, 2(1), pp. 1–9. doi: 10.4161/onci.22840.

Ullrich, A. and Schlessinger, J. (1990) 'Signal transduction by receptors with tyrosine kinase activity', *Cell*, 61(2), pp. 203–212. doi: 10.1016/0092-8674(90)90801-K.

Umanoff, H. *et al.* (1995) 'The murine N-ras gene is not essential for growth and development', *Proceedings of the National Academy of Sciences of the United States of America*, 92(5), pp. 1709–1713. doi: 10.1073/pnas.92.5.1709.

Ussar, S. and Voss, T. (2004) 'MEK1 and MEK2, different regulators of the G1/S transition', *Journal of*

Biological Chemistry. Â© 2004 ASBMB. Currently published by Elsevier Inc; originally published by American Society for Biochemistry and Molecular Biology., 279(42), pp. 43861–43869. doi: 10.1074/jbc.M406240200.

Vakana, E. *et al.* (2017) 'LY3009120, a panRAF inhibitor, has significant anti-tumor activity in BRAF and KRAS mutant preclinical models of colorectal cancer', *Oncotarget*, 8(6), pp. 9251–9266. doi: 10.18632/oncotarget.14002.

Valluet, A. *et al.* (2010) 'B-raf alternative splicing is dispensable for development but required for learning and memory associated with the hippocampus in the adult mouse', *PLoS ONE*, 5(12), p. e15272. doi: 10.1371/journal.pone.0015272.

Van, Q. N. *et al.* (2021) 'Ras nanoclusters: Dynamic signaling platforms amenable to therapeutic intervention', *Biomolecules*, 11(3), p. 337. doi: 10.3390/biom11030377.

Vantaggiato, C. *et al.* (2006) 'ERK1 and ERK2 mitogen-activated protein kinases affect Ras-dependent cell signaling differentially', *Journal of Biology*, 5(5), p. 14. doi: 10.1186/jbiol38.

Vetter, I. R. and Wittinghofer, A. (2001) 'The guanine nucleotide-binding switch in three dimensions', *Science*, 294(5545), pp. 1299–1304. doi: 10.1126/science.1062023.

Vido, M. J. *et al.* (2018) 'BRAF Splice Variant Resistance to RAF Inhibitor Requires Enhanced MEK Association', *Cell Reports*. ElsevierCompany., 25(6), pp. 1501-1510.e3. doi: 10.1016/j.celrep.2018.10.049.

Villanueva, J. *et al.* (2010) 'Acquired resistance to BRAF inhibitors mediated by a RAF kinase switch in melanoma can be overcome by cotargeting MEK and IGF-1R/PI3K', *Cancer Cell*. Elsevier Inc., 18(6), pp. 683–695. doi: 10.1016/j.ccr.2010.11.023.

Vinay, D. S. *et al.* (2015) 'Immune evasion in cancer: Mechanistic basis and therapeutic strategies', *Seminars in Cancer Biology*. Elsevier Ltd, 35, pp. S185–S198. doi: 10.1016/j.semcancer.2015.03.004.

Viskochil, D. *et al.* (1990) 'Deletions and a Translocation Gene at the Neurofibromatosis Interrupt a Cloned Type 1 Locus', *Cell*, 62(1), pp. 187–192.

Vivanco, I. (2014) 'Targeting molecular addictions in cancer', *British Journal of Cancer*. Nature Publishing Group, 111(11), pp. 2033–2038. doi: 10.1038/bjc.2014.461.

Vivanco, I. and Sawyers, C. L. (2002) 'The phosphatidylinositol 3-kinase-AKT pathway in human cancer', *Nature Reviews Cancer*, 2(7), pp. 489–501. doi: 10.1038/nrc839.

Vojtek, A. B., Hollenberg, S. M. and Cooper, J. A. (1993) 'Mammalian Ras interacts directly with the

serine/threonine kinase raf', *Cell*, 74(1), pp. 205–214. doi: 10.1016/0092-8674(93)90307-C.

Volmat, V. *et al.* (2001) 'The nucleus, a site for signal termination by sequestration and inactivation of p42/p44 MAP kinases', *Journal of Cell Science*, 114(19), pp. 3433–3443.

De Vos, A. M. *et al.* (1988) 'Three-dimensional structure of an oncogene protein: Catalytic domain of human c-H-ras p21', *Science*, 239(4842), pp. 888–893. doi: 10.1126/science.2448879.

Walker, C., Mojares, E. and Del Río Hernández, A. (2018) 'Role of extracellular matrix in development and cancer progression', *International Journal of Molecular Sciences*, 19(10), p. 3028. doi: 10.3390/ijms19103028.

Walker, E. H. *et al.* (1999) 'Structural insights into phosphoinositide 3-kinase catalysis and signalling', *Nature*, 402(6759), pp. 313–320.

Wallace, M. R. *et al.* (1990) 'Type 1 Neurofibromatosis Gene : Identification of a Large Transcript Disrupted in Three NF1 Patients', *Science*, 249(4965), pp. 181–186.

Walsh, J. H. *et al.* (1991) 'Autocrine growth factors and solid tumor malignancy', *Western Journal of Medicine*, 155(2), pp. 152–163.

Wang, B. *et al.* (2019) 'MYH9 promotes growth and metastasis via activation of MAPK/AKT signaling in colorectal cancer', *Journal of Cancer*, 10(4), pp. 874–884. doi: 10.7150/jca.27635.

Wang, C. *et al.* (2014) 'The concordance between RNA-seq and microarray data depends on chemical treatment and transcript abundance', *Nature Biotechnology*, 32(9), pp. 926–932. doi: 10.1038/nbt.3001.

Wang, L. *et al.* (2017) 'Overexpression of G protein-Coupled receptor GPR87 promotes pancreatic cancer aggressiveness and activates NF-KB signaling pathway', *Molecular Cancer*. Molecular Cancer, 16(61). doi: 10.1186/s12943-017-0627-6.

Wang, T. *et al.* (2017) 'Gene Essentiality Profiling Reveals Gene Networks and Synthetic Lethal Interactions with Oncogenic Ras', *Cell*. Elsevier, 168(5), pp. 890-903.e15. doi: 10.1016/j.cell.2017.01.013.

Wang, X., Destrument, A. and Tournier, C. (2007) 'Physiological roles of MKK4 and MKK7: Insights from animal models', *Biochimica et Biophysica Acta - Molecular Cell Research*, 1773(8), pp. 1349–1357. doi: 10.1016/j.bbamcr.2006.10.016.

Wang, Z., Gerstein, M. and Snyder, M. (2009) 'RNA-Seq: a revolutionary tool for transcriptomics', *Nature Reviews Genetics*, 10(1), pp. 57–63.

Warren, B. A. (1966) 'The ultrastructure of capillary sprouts induced by melanoma transplants in the golden hamster', *Journal of the Royal Microscopical Society*, 86(2), pp. 177–187. doi: 10.1111/j.1365-2818.1966.tb05336.x.

Wartmann, M. *et al.* (1997) 'Negative modulation of membrane localization of the Raf-1 protein kinase by hyperphosphorylation', *The Journal of Biological Chemistry*. Â© 1997 ASBMB. Currently published by Elsevier Inc; originally published by American Society for Biochemistry and Molecular Biology., 272(7), pp. 3915–3923. doi: 10.1074/jbc.272.7.3915.

Waters, S. B. *et al.* (1996) 'Insulin and Epidermal Growth Factor Receptors Regulate Distinct Pools of Grb2-SOS in the Control of Ras Activation', *Journal of Biological Chemistry*. Â© 1996 ASBMB. Currently published by Elsevier Inc; originally published by American Society for Biochemistry and Molecular Biology., 271(30), pp. 18224–18230. doi: 10.1074/jbc.271.30.18224.

Weber, C. K. *et al.* (2000) 'Mitogenic signaling of Ras is regulated by differential interaction with Raf isozymes', *Oncogene*, 19(2), pp. 169–176. doi: 10.1038/sj.onc.1203261.

Weber, C. K. *et al.* (2001) 'Active ras induces heterodimerization of cRaf and BRaf', *Cancer Research*, 61(9), pp. 3595–3598.

Weis, K. (2003) 'Regulating access to the genome: Nucleocytoplasmic transport throughout the cell cycle', *Cell*, 112(4), pp. 441–451. doi: 10.1016/S0092-8674(03)00082-5.

Weiss, R. H., Maga, E. A. and Ramirez, A. L. (1998) 'MEK inhibition augments Raf activity, but has variable effects on mitogenesis, in vascular smooth muscle cells', *American Journal of Physiology*, 274(6), pp. C1521-1529.

Weiss, W. A., Taylor, S. S. and Shokat, K. M. (2007) 'Recognizing and exploiting differences between RNAi and small-molecule inhibitors', *Nature Chemical Biology*, 3(12), pp. 739–744. doi: 10.1038/nchembio1207-739.Recognizing.

Wellbrock, C., Karasarides, M. and Marais, R. (2004) 'The RAF proteins take centre stage', *Nature Reviews Molecular Cell Biology*, 5(11), pp. 875–885. doi: 10.1038/nrm1498.

Welsch, M. E. *et al.* (2017) 'Multivalent Small-Molecule Pan-RAS Inhibitors', *Cell*. Elsevier, 168(5), pp. 878-889.e29. doi: 10.1016/j.cell.2017.02.006.

Wennerberg, K., Rossman, K. L. and Der, C. J. (2005) 'The Ras superfamily at a glance', *Journal of Cell Science*, 118(5), pp. 843–846. doi: 10.1242/jcs.01660.

Westermarck, J. *et al.* (2001) 'p38 Mitogen-Activated Protein Kinase-Dependent Activation of Protein

Phosphatases 1 and 2A Inhibits MEK1 and MEK2 Activity and Collagenase 1 (MMP-1) Gene Expression', *Molecular and Cellular Biology*, 21(7), pp. 2373–2383. doi: 10.1128/mcb.21.7.2373-2383.2001.

Westermark, B. and Heldin, C. -H (1985) 'Similar action of platelet-derived growth factor and epidermal growth factor in the prereplicative phase of human fibroblasts suggests a common intracellular pathway', *Journal of Cellular Physiology*, 124(1), pp. 43–48. doi: 10.1002/jcp.1041240108.

White, M. A. *et al.* (1996) 'A role for the Ral guanine nucleotide dissociation stimulator in mediating Ras-induced transformation', *Journal of Biological Chemistry*. Â© 1996 ASBMB. Currently published by Elsevier Inc; originally published by American Society for Biochemistry and Molecular Biology., 271(28), pp. 16439–16442. doi: 10.1074/jbc.271.28.16439.

Whitehead, R. H. *et al.* (1985) 'A colon cancer cell line (LIM1215) derived from a patient with inherited nonpolyposis colorectal cancer', *Journal of the National Cancer Institute*, 74(4), pp. 759–765.

Whitman, M. *et al.* (1988) 'Type I phosphatidylinositol kinase makes a novel inositol phospholipid, phosphatidylinositol-3-phosphate', *Nature*, 332, pp. 644–646.

Whitmarsh, A. J. and Davis, R. J. (1996) 'Transcription factor AP-1 regulation by mitogen-activated protein kinase signal transduction pathways', *Journal of Molecular Medicine*, 74(10), pp. 589–607. doi: 10.1007/s001090050063.

Whyte, D. B. *et al.* (1997) 'K- and N-Ras are geranylgeranylated in cells treated with farnesyl protein transferase inhibitors', *Journal of Biological Chemistry*. Â© 1997 ASBMB. Currently published by Elsevier Inc; originally published by American Society for Biochemistry and Molecular Biology., 272(22), pp. 14459–14464. doi: 10.1074/jbc.272.22.14459.

Wiese, S. *et al.* (2001) 'Specific function of B-Raf in mediating survival of embryonic motoneurons and sensory neurons', *Nature Neuroscience*, 4(2), pp. 137–142.

Wilhelm, B. T. and Landry, J. R. (2009) 'RNA-Seq-quantitative measurement of expression through massively parallel RNA-sequencing', *Methods*. Elsevier Inc., 48(3), pp. 249–257. doi: 10.1016/j.ymeth.2009.03.016.

Williams, J. G. *et al.* (2000) 'Elucidation of binding determinants and functional consequences of Ras/Raf-cysteine-rich domain interactions', *Journal of Biological Chemistry*. Â© 2000 ASBMB. Currently published by Elsevier Inc; originally published by American Society for Biochemistry and

Molecular Biology., 275(29), pp. 22172–22179. doi: 10.1074/jbc.M000397200.

Willumsen, B. M. *et al.* (1984) 'The p21 ras C-terminus is required for transformation and membrane association', *Nature*, 310, pp. 583–586.

Witkiewicz, A. K. *et al.* (2015) 'Whole-exome sequencing of pancreatic cancer defines genetic diversity and therapeutic targets', *Nature Communications*. Nature Publishing Group, 6, p. 6744. doi: 10.1038/ncomms7744.

Wojnowski, L. *et al.* (1997) 'Endothelial apoptosis in Braf-deficient mice', *Nature Genetics*, 16(3), pp. 293–297.

Wojnowski, L. *et al.* (1998) 'Craf-1 protein kinase is essential for mouse development', *Mechansims of Development*, 76(1–2), pp. 141–149.

Wojnowski, L. *et al.* (2000) 'Overlapping and specific functions of Braf and Craf-1 proto-oncogenes during mouse embryogenesis', *Mechansims of Development*, 91(1–2), pp. 97–104.

Wolchok, J. D. *et al.* (2017) 'Overall Survival with Combined Nivolumab and Ipilimumab in Advanced Melanoma', *New England Journal of Medicine*, 377(14), pp. 1345–1356. doi: 10.1056/nejmoa1709684.

Wolfman, A. *et al.* (1993) 'Complexes of Ras.GTP with Raf-1 and Mitogen-Activated Protein Kinase Kinase', *Science*, 260(5114), pp. 1658–1661.

Wolfman, A. (2001) 'Ras isoform-specific signaling: location, location, location', *Science's STKE*, 2001(96), p. pe2.

Wolpin, B. M. *et al.* (2014) 'Phase II and Pharmacodynamic Study of Autophagy Inhibition Using Hydroxychloroquine in Patients With Metastatic Pancreatic Adenocarcinoma', *The Oncologist*, 19(6), pp. 637–638. doi: 10.1634/theoncologist.2014-0086.

Wortzel, I. and Seger, R. (2011) 'The ERK cascade: Distinct functions within various subcellular organelles', *Genes and Cancer*, 2(3), pp. 195–209. doi: 10.1177/1947601911407328.

Wu, J. *et al.* (1993) 'Inhibition of the EGF-activated MAP kinase signaling pathway by adenosine 3',5'-monophosphate', *Science*, 262(5136), pp. 1065–1069. doi: 10.1126/science.7694366.

Wu, X. *et al.* (1996) 'Selective activation of MEK1 but not MEK2 by A-Raf from epidermal growth factor-stimulated Hela cells', *Journal of Biological Chemistry*, 271(6), pp. 3265–3271. doi: 10.1074/jbc.271.6.3265.

Wu, Y., Chen, Z. and Ullrich, A. (2003) 'EGFR and FGFR signaling through FRS2 is subject to negative feedback control by ERK1/2', *Biological Chemistry*, 384(8), pp. 1215–1226.

Wunderlich, W. *et al.* (2001) 'A novel 14-kilodalton protein interacts with the mitogen-activated protein kinase scaffold MP1 on a late endosomal/lysosomal compartment', *Journal of Cell Biology*, 152(4), pp. 765–776. doi: 10.1083/jcb.152.4.765.

Wynn, M. L. *et al.* (2011) 'Kinase inhibitors can produce off-target effects and activate linked pathways by retroactivity', *BMC Systems Biology*. BioMed Central Ltd, 5(1), p. 156. doi: 10.1186/1752-0509-5-156.

Xing, H., Kornfeld, K. and Muslin, A. J. (1997) 'The protein kinase KSR interacts with 14-3-3 protein and Raf', *Current Biology*, 7(5), pp. 294–300.

Xu, F. *et al.* (2020) 'Roles of the PI3K/AKT/mTOR signalling pathways in neurodegenerative diseases and tumours', *Cell and Bioscience*. BioMed Central, 10(1), pp. 1–12. doi: 10.1186/s13578-020-00416-0.

Xu, S. *et al.* (1997) 'Differential regulation of mitogen-activated protein/ERK kinase (MEK)1 and MEK2 and activation by a Ras-independent mechanism', *Molecular Endocrinology*, 11(11), pp. 1618–1625. doi: 10.1210/mend.11.11.0010.

Yachis, M. *et al.* (1994) 'Feedback regulation of mitogen-activated protein kinase kinase kinase activity of c-Raf-1 by insulin and phorbol ester stimulation', *Journal of Biological Chemistry*, 269(22), pp. 15756–15761. doi: 10.1016/S0021-9258(17)40745-9.

Yadav, V. *et al.* (2012) 'Reactivation of mitogen-activated protein kinase (MAPK) pathway by FGF receptor 3 (FGFR3)/Ras mediates resistance to vemurafenib in human B-RAF V600E mutant melanoma', *Journal of Biological Chemistry*. Â© 2012 ASBMB. Currently published by Elsevier Inc; originally published by American Society for Biochemistry and Molecular Biology., 287(33), pp. 28087–28098. doi: 10.1074/jbc.M112.377218.

Yamaguchi, A. *et al.* (1997) 'An Eps homology (EH) domain protein that binds to the Ral-GTPase target, RalBP1', *Journal of Biological Chemistry*. Â© 1997 ASBMB. Currently published by Elsevier Inc; originally published by American Society for Biochemistry and Molecular Biology., 272(50), pp. 31230–31234. doi: 10.1074/jbc.272.50.31230.

Yamaji, M. *et al.* (2017) 'Novel ATP-competitive Akt inhibitor afuresertib suppresses the proliferation of malignant pleural mesothelioma cells', *Cancer Medicine*, 6(11), pp. 2646–2659. doi: 10.1002/cam4.1179.

Yamashita, H. *et al.* (2015) 'Oligomerization-function relationship of EGFR on living cells detected by the coiled-coil labeling and FRET microscopy', *Biochimica et Biophysica Acta - Biomembranes*. Elsevier B.V., 1848(6), pp. 1359–1366. doi: 10.1016/j.bbamem.2015.03.004.

Yan, C. and Theodorescu, D. (2018) 'RAL GTpases: Biology and potential as therapeutic targets in cancer', *Pharmacological Reviews*, 70(1), pp. 1–11. doi: 10.1124/pr.117.014415.

Yang, A. and Kimmelman, A. C. (2014) 'Inhibition of autophagy attenuates pancreatic cancer growth independent of TP53/TRP53 status', *Autophagy*, 10(9), pp. 1683–1684. doi: 10.1158/2159-8290.CD-14-0362.

Yang, J. *et al.* (2011) 'Mechanism of Isoprenylcysteine Carboxyl Methylation from the Crystal Structure of the Integral Membrane Methyltransferase ICMT', *Molecular Cell*. Elsevier Inc., 44(6), pp. 997–1004. doi: 10.1016/j.molcel.2011.10.020.

Yang, M. H. *et al.* (2012) 'Regulation of RAS oncogenicity by acetylation', *Proceedings of the National Academy of Sciences of the United States of America*, 109(27), pp. 10843–10848. doi: 10.1073/pnas.1201487109.

Yang, S. *et al.* (2011) 'Pancreatic cancers require autophagy for tumor growth', *Genes and Development*, 25(7), pp. 717–729. doi: 10.1101/gad.2016111.

Yang, S. H. *et al.* (1998) 'Differential targeting of MAP kinases to the ETS-domain transcription factor Elk-1', *EMBO Journal*, 17(6), pp. 1740–1749. doi: 10.1093/emboj/17.6.1740.

Yang, S. H., Sharrocks, A. D. and Whitmarsh, A. J. (2003) 'Transcriptional regulation by the MAP kinase signaling cascades', *Gene*, 320(1–2), pp. 3–21. doi: 10.1016/S0378-1119(03)00816-3.

Yang, X. *et al.* (2006) 'Sprouty Genes Are Expressed in Osteoblasts and Inhibit Fibroblast Growth Factor-Mediated Osteoblast Responses', *Calcified Tissue International*, 78(4), pp. 233–240. doi: 10.1007/s00223-005-0231-4.

Yao, Z. and Seger, R. (2004) 'The molecular mechanism of MAPK/ERK inactivation', *Current Genomics*, 5, pp. 385–393. doi: 10.2174/1389202043349309.

Yao, Z. and Seger, R. (2009) 'The ERK signaling cascade-views from different subcellular compartments', *BioFactors*, 35(5), pp. 407–416. doi: 10.1002/biof.52.

Yeh, C. H. *et al.* (2020) 'Loss of FBXW7-mediated degradation of BRAF elicits resistance to BET inhibitors in adult T cell leukemia cells', *Molecular Cancer*. Molecular Cancer, 19(1), pp. 1–13. doi: 10.1186/s12943-020-01254-x.

Yeh, C. H., Bellon, M. and Nicot, C. (2018) 'FBXW7: A critical tumor suppressor of human cancers', *Molecular Cancer*. Molecular Cancer, 17(1), pp. 1–19. doi: 10.1186/s12943-018-0857-2.

Yen, I. *et al.* (2018) 'Pharmacological Induction of RAS-GTP Confers RAF Inhibitor Sensitivity in KRAS Mutant Tumors', *Cancer Cell*. Elsevier Inc., 34(4), pp. 611-625.e7. doi: 10.1016/j.ccell.2018.09.002.

Yin, Q. *et al.* (2019) 'K27-linked ubiquitination of BRAF by ITCH engages cytokine response to maintain MEK-ERK signaling', *Nature Communications*. Springer US, 10(1), p. 1870. doi: 10.1038/s41467-019-09844-0.

Yin, X. L. *et al.* (2002) 'Identification of interaction between MEK2 and A-Raf-1', *Biochimica et Biophysica Acta - Molecular Cell Research*, 1589(1), pp. 71–76. doi: 10.1016/S0167-4889(01)00188-4.

Yu, J. *et al.* (1998) 'Regulation of the p85/p110 Phosphatidylinositol 3'-Kinase: Stabilization and Inhibition of the p110α Catalytic Subunit by the p85 Regulatory Subunit', *Molecular and Cellular Biology*, 18(3), pp. 1379–1387. doi: 10.1128/mcb.18.3.1379.

Yu, W. *et al.* (1998) 'Regulation of the MAP kinase pathway by mammalian Ksr through direct interaction with MEK and ERK', *Current Biology*, 8(1), pp. 56–64.

Yu, X. *et al.* (2002) 'Ligand-independent dimer formation of epidermal growth factor receptor (EGFR) is a step separable from ligand-induced EGFR signaling', *Molecular Biology of the Cell*, 13(7), pp. 2547–2557. doi: 10.1091/mbc.01-08-0411.

Yusoff, P. *et al.* (2002) 'Sprouty2 inhibits the Ras/MAP kinase pathway by inhibiting the activation of Raf', *Journal of Biological Chemistry*. Â© 2002 ASBMB. Currently published by Elsevier Inc; originally published by American Society for Biochemistry and Molecular Biology., 277(5), pp. 3195–3201. doi: 10.1074/jbc.M108368200.

Zarubin, T. and Han, J. (2005) 'Activation and signaling of the p38 MAP kinase pathway', *Cell Research*, 15(1), pp. 11–18. doi: 10.1038/sj.cr.7290257.

Zeng, M. *et al.* (2020) 'Exploring Targeted Degradation Strategy for Oncogenic KRAS G12C', *Cell Chemical Biology*, 27(1), pp. 19–31. doi: 10.1016/j.chembiol.2019.12.006.

Zerial, M. and McBride, H. (2001) 'Rab proteins as membrane organizers', *Nature Reviews Molecular Cell Biology*, 2(2), pp. 107–117. doi: 10.1038/35052055.

Zhang, F. *et al.* (1994) 'Atomic structure of the MAP kinase ERK2 at 2.3 Å resolution', *Nature*, 367(6465), pp. 704–711. doi: 10.1038/367704a0.

Zhang, J. *et al.* (2020) 'The Functional Effects of Key Driver KRAS Mutations on Gene Expression in

Lung Cancer', *Frontiers in Genetics*, 11(17), pp. 1–8. doi: 10.3389/fgene.2020.00017.

Zhang, K. *et al.* (1991) 'Heterogeneous amino acids in Ras and Rap1A specifying sensitivity to GAP proteins', *Science*, 254(5038), pp. 1630–1634. doi: 10.1126/science.1749934.

Zhang, M., Jang, H. and Nussinov, R. (2019) 'The mechanism of PI3Kα activation at the atomic level', *Chemical Science*, 10(12), pp. 3671–3680. doi: 10.1039/c8sc04498h.

Zhang, X. *et al.* (2006) 'An Allosteric Mechanism for Activation of the Kinase Domain of Epidermal Growth Factor Receptor', *Cell*, 125(6), pp. 1137–1149. doi: 10.1016/j.cell.2006.05.013.

Zhang, Z. *et al.* (2001) 'Wildtype Kras2 can inhibit lung carcinogenesis in mice', *Nature Genetics*, 29(1), pp. 25–33. doi: 10.1038/ng721.

Zhang, Z. *et al.* (2010) 'Dual specificity phosphatase 6 (DUSP6) is an ETS-regulated negative feedback mediator of oncogenic ERK signaling in lung cancer cells', *Carcinogenesis*, 31(4), pp. 577–586. doi: 10.1093/carcin/bgq020.

Zhao, H. *et al.* (2015) 'Roles of palmitoylation and the KIKK membrane-targeting motif in leukemogenesis by oncogenic KRAS4A', *Journal of Hematology & Oncology*. Journal of Hematology & Oncology, 8(132). doi: 10.1186/s13045-015-0226-1.

Zhao, S. *et al.* (2014) 'Comparison of RNA-Seq and microarray in transcriptome profiling of activated T cells', *PLoS ONE*, 9(1), p. e78644. doi: 10.1371/journal.pone.0078644.

Zhao, Y. and Jensen, O. N. (2009) 'Modification-specific proteomics: Strategies for characterization of post-translational modifications using enrichment techniques', *Proteomics*, 9(20), pp. 4632–4641.

Zheng, C. F. and Guan, K. L. (1993) 'Cloning and characterization of two distinct human extracellular signal- regulated kinase activator kinases, MEK1 and MEK2', *Journal of Biological Chemistry*. Â© 1993 ASBMB. Currently published by Elsevier Inc; originally published by American Society for Biochemistry and Molecular Biology., 268(15), pp. 11435–11439. doi: 10.1016/s0021-9258(18)82142-1.

Zhou, J. *et al.* (2018) 'TAK1 mediates excessive autophagy via p38 and ERK in cisplatin-induced acute kidney injury', *Journal of Cellular and Molecular Medicine*, 22(5), pp. 2908–2921. doi: 10.1111/jcmm.13585.

Zhou, S. *et al.* (1993) 'SH2 domains recognize specific phosphopeptide sequences', *Cell*, 72(5), pp. 767–778. doi: 10.1016/0092-8674(93)90404-E.

Zhou, T. *et al.* (2006) 'Docking Interactions Induce Exposure of Activation Loop in the MAP Kinase

ERK2', *Structure*, 14(6), pp. 1011–1019. doi: 10.1016/j.str.2006.04.006.

Zhou, Y., Gorfe, A. A. and Hancock, J. F. (2021) 'RAS Nanoclusters Selectively Sort Distinct Lipid Headgroups and Acyl Chains', *Frontiers in Molecular Biosciences*, 8, p. 686338. doi: 10.3389/fmolb.2021.686338.

Zimmermann, S. and Moelling, K. (1999) 'Phosphorylation and regulation of Raf by Akt (protein kinase B)', *Science*, 286(5445), pp. 1741–1744. doi: 10.1126/science.286.5445.1741.

Zocche, D. M. *et al.* (2015) 'Global impact of KRAS mutation patterns in FOLFOX treated metastatic colorectal cancer', *Frontiers in Genetics*, 6(MAR), pp. 1–7. doi: 10.3389/fgene.2015.00116.